
**Pacific Northwest
National Laboratory**

Operated by Battelle for the
U.S. Department of Energy

Interim Report:

**100-NR-2 Apatite Treatability Test:
Low-Concentration Calcium-Citrate-
Phosphate Solution Injection for In Situ
Strontium-90 Immobilization**

M.D. Williams	B.N. Bjornstad
B.G. Fritz	R.D. Mackley
D.P. Mendoza	D.R. Newcomer
M.L. Rockhold	J.E. Szecsody
P.D. Thorne	V.R. Vermeul
Y. Xie	

July 2008



Prepared for the U.S. Department of Energy
under Contract DE-AC05-76RL01830

DISCLAIMER

This report was prepared as an account of work sponsored by an agency of the United States Government. Neither the United States Government nor any agency thereof, nor Battelle Memorial Institute, nor any of their employees, makes **any warranty, express or implied, or assumes any legal liability or responsibility for the accuracy, completeness, or usefulness of any information, apparatus, product, or process disclosed, or represents that its use would not infringe privately owned rights.** Reference herein to any specific commercial product, process, or service by trade name, trademark, manufacturer, or otherwise does not necessarily constitute or imply its endorsement, recommendation, or favoring by the United States Government or any agency thereof, or Battelle Memorial Institute. The views and opinions of authors expressed herein do not necessarily state or reflect those of the United States Government or any agency thereof.

PACIFIC NORTHWEST NATIONAL LABORATORY
operated by
BATTELLE
for the
UNITED STATES DEPARTMENT OF ENERGY
under Contract DE-AC05-76RL01830

Printed in the United States of America

Available to DOE and DOE contractors from the
Office of Scientific and Technical Information, P.O. Box 62, Oak Ridge, TN 37831;
prices available from (615) 576-8401.

Available to the public from the National Technical Information Service,
U.S. Department of Commerce, 5285 Port Royal Rd., Springfield, VA 22161



This document was printed on recycled paper.

Interim Report:

**100-NR-2 Apatite Treatability Test:
Low-Concentration Calcium-Citrate-
Phosphate Solution Injection for In Situ
Strontium-90 Immobilization**

M.D. Williams	B.N. Bjornstad
B.G. Fritz	R.D. Mackley
D.P. Mendoza	D.R. Newcomer
M.L. Rockhold	J.E. Szecsody
P.D. Thorne	V.R. Vermeul
Y. Xie	

July 2008

Prepared for
the U.S. Department of Energy
under Contract DE-AC05-76RL01830

Pacific Northwest National Laboratory
Richland, Washington 99352

Summary

Efforts to reduce the flux of strontium-90 (^{90}Sr) to the Columbia River from past-practice liquid waste disposal sites have been underway since the early 1990s in the 100-N Area at the Hanford Site. Termination of all liquid discharges to the ground in 1993 was a major step toward meeting this goal. However, ^{90}Sr adsorbed on aquifer solids beneath the liquid waste disposal sites and extending beneath the near-shore riverbed remains a continuing source to groundwater and the Columbia River. Researchers realized from the onset that the initial pump-and-treat system was unlikely to be an effective long-term solution because of the geochemical characteristics of ^{90}Sr ; subsequent performance monitoring has substantiated this theory. Accordingly, the first *Comprehensive Environmental Response, Compensation, and Liability Act of 1980* (CERCLA) 5-year review re-emphasized the need to pursue alternative methods to reduce impacts on the Columbia River.¹

Following an evaluation of potential ^{90}Sr treatment technologies and their applicability under 100-NR-2 hydrogeologic conditions, U.S. Department of Energy, Fluor Hanford, Inc. (FH), Pacific Northwest National Laboratory, and the Washington State Department of Ecology agreed the long-term strategy for groundwater remediation at the 100-N Area will include apatite sequestration as the primary treatment, followed by a secondary treatment—or polishing step—if necessary (most likely phytoremediation). Since then, the agencies have worked together to agree on which apatite-sequestration technology has the greatest chance of reducing ^{90}Sr flux to the Columbia River at a reasonable cost. In July 2005, aqueous injection, (i.e., the introduction of apatite-forming chemicals into the subsurface) was endorsed as the interim remedy and selected for field testing. Studies are in progress to assess the efficacy of in situ apatite formation by aqueous solution injection to address both the vadose zone and the shallow aquifer along the 91 m (300 ft) of shoreline where ^{90}Sr concentrations are highest. This report describes the field testing of the shallow aquifer treatment that was funded by FH.

A low-concentration, apatite-forming solution was injected into the shallow aquifer in 10 injection wells during fiscal years 2006 and 2007, and performance monitoring is underway. The low-concentration, apatite-forming solution consists primarily of calcium chloride, trisodium citrate, and sodium phosphate. The objective of the low-concentration Ca-citrate- PO_4 injections is to stabilize the ^{90}Sr in the aquifer at the test site, to be followed by high-concentration injections to provide for long-term ^{90}Sr treatment. Two pilot test sites at the east and west ends of the barrier, which are equipped with extensive monitoring well networks, were used for the initial injections to develop the injection design for the remaining portions of the barrier. Based on a comparison of hydraulic and transport response data at the two pilot test sites, it was determined the apparent permeability contrast between the Hanford and Ringold Formations was significantly less over the upstream portion of the barrier, allowing for treatment of the entire Hanford/Ringold Formation screened interval with a single-injection operation at the high-river stage. Because of a larger contrast over the downstream portion of the barrier, wells screened only across the contaminated portion of the Ringold Formation will be installed before future injections to allow for better treatment efficiency and coverage.

¹ *Comprehensive Environmental Response, Compensation, and Liability Act*. 1980. Public Law 96-510, as amended, 94 Stat. 2767, 42 USC 9601 et seq.

Analysis of the operational and early monitoring results of the pilot tests were used to modify the injection solution composition, injection volumes, and operational parameters. A tracer injection test and the first pilot apatite injection test were conducted at the upstream end of the barrier in the spring of 2006 during high-river stage conditions. A second pilot test was conducted at the downstream end of the barrier in September 2006 during low-river stage conditions. Injections in the 10 barrier wells were conducted during two phases: the first in February-March 2007, which was supposed to target low-river stage conditions but resulted in both low- and high-river stage conditions, and a second phase in June-July 2007 during high-river stage conditions.

River stage during the barrier injection was an important parameter in the depth interval treated and treatment efficiency. River stage along this section of the Columbia River is controlled by the rate of discharge at Priest Rapids Dam, located approximately 29 km (18 mi) upstream of the 100-N Area. Initially, researchers theorized that conducting injections during low-river stage would provide treatment in the Ringold Formation, while injections during high-river stage would provide treatment in the Hanford formation. For the upstream portion of the barrier, the contrast between permeability in the Hanford and Ringold Formations was sufficiently small that injections at high-river stage alone were successful in treating both the Hanford and Ringold Formations. However, for the downstream portion of the barrier, multiple injections did not provide complete treatment. High-river stage conditions provided a hydraulic barrier that contained the injection solution in the Hanford formation, allowing adequate treatment. Unfortunately, it appeared that injections conducted during low-river stage were of limited success in providing adequate treatment in the Ringold Formation. The large contrast in permeability between the Hanford and Ringold Formations along the downstream portion of the barrier resulted in the loss of a significant portion of the injection volume to the relatively thin saturated Hanford formation interval, associated shoreline seeps, and limited treatment of the Ringold Formation.

Design specifications for the barrier installation stipulated that the chemical concentrations should be at least 50% of injection concentration 6 m (20 ft) from each injection well. This specification is considered a sufficient radial extent of treatment to provide overlap of treatment between injection wells. While monitoring points were not installed between injection wells outside the pilot test sites, monitoring was conducted in adjacent injection wells during treatment operations. Because no monitoring wells were available at a 6 m (20 ft) radial distance to assess the extent of treatment, arrival data from adjacent injection wells (9-m [30-ft] spacing) were used as an indicator. To account for the increase in radial distance to this monitoring point, the phosphate-concentration metric for arrival at adjacent injection wells was reduced to 20% to 30% of the injection concentration (from 50% at a 6-m [20-ft] distance). Based on this injection-performance metric, phosphate concentrations measured in adjacent, fully screened injection wells indicated generally satisfactory treatment. However, data from available Ringold Formation monitoring wells indicated treatment of the Ringold Formation over the downstream portion of the barrier (where Hanford/Ringold Formation permeability contrast is larger) was not as effective.

Temporary increases in strontium and ^{90}Sr were expected during the low-concentration Ca-citrate- PO_4 field injection tests, which were designed based on bench-scale laboratory studies with low-concentration formulation and sediments from the 100-N Area. The observed increases in ^{90}Sr concentration are caused by the higher ionic strength of the solution and increases in calcium concentration resulting from this process. Concentrations are expected to decline over time (months, years) as the ^{90}Sr is incorporated through initial precipitation and adsorption/slow incorporation into the apatite, and as the reagent plume dissipates.

The ^{90}Sr concentrations in monitoring wells at the first pilot test site, conducted in the spring of 2006, showed an average increase in peak ^{90}Sr concentrations of 8.4 times the average baseline measurements at the site measured earlier in the year. Based on these results and additional laboratory measurements, the Ca-citrate- PO_4 injection concentrations were revised with lower calcium and citrate concentrations (2.5 times) for the second pilot test conducted in the fall of 2006. Average peak ^{90}Sr concentrations following the second pilot test injection were significantly lower than the first pilot test (3.8 times the average baseline ^{90}Sr concentrations) while still targeting the same level of apatite formation. The injection formulation was revised again following the second pilot test with further decreases in calcium and citrate concentrations, and a ~ 4 times increase in the phosphate concentration to maximize the apatite precipitate mass and minimize the initial ^{90}Sr increase. This final low-concentration formulation was used for the barrier well injections conducted in 2007. Monitoring of ^{90}Sr concentrations at the two pilot test sites in 2007 using the final low-concentration formulation showed average peak increases of 2.8 times the baseline average ^{90}Sr at the first pilot test site and 2.3 times the baseline average ^{90}Sr at the second test site.

The ^{90}Sr concentrations in groundwater along the Columbia River at the 100-N Area show significant temporal variability based on measurements from aquifer tubes and compliance monitoring wells installed prior to the apatite treatability test. Additionally, there is a general spatial trend in ^{90}Sr concentrations in the aquifer along the river, with the highest concentrations existing over the central/downstream portion of the barrier, and concentrations decreasing from this high in both the upstream and downstream directions. Because of the short time between the installation of compliance, injection, and pilot test monitoring wells at the 100-N Area apatite treatability test site and the Ca-citrate- PO_4 injections (started at the site in the spring of 2006), there were insufficient data from these wells to establish baseline conditions for ^{90}Sr . Therefore, baseline ^{90}Sr ranges were developed for the injection and compliance wells at the treatability test site based on gross beta concentrations from nearby aquifer tubes and limited preinjection ^{90}Sr monitoring from the treatability test wells.

The ^{90}Sr , gross beta, and SpC monitoring data available for inclusion in this interim report (up to and including samples collected on November 14, 2007) showed post-treatment increases in these values at the injection wells, compliance wells, and aquifer tubes. However, this initial spike in ^{90}Sr concentration was followed by a generally decreasing trend at all injection well locations. Longer-term post-treatment ^{90}Sr concentrations at most injection well locations showed that levels were maintained near or below the low end of the estimated range in baseline ^{90}Sr concentrations, indicating the low-concentration treatments likely had an impact on aqueous ^{90}Sr concentrations within the treatment zone. Additional monitoring that encompasses the full extent of seasonal variability in Columbia River stage would be required to fully assess the effectiveness of the low-concentration treatments. Note also that wells screened only in the Hanford formation at the pilot test sites have been dry since shortly after the 2007 injections. Monitoring in these Hanford formation-screened wells will resume after the river stage increases in the spring of 2008. Because high-concentration injections will be conducted during the upcoming spring/summer high-river stage period, continued assessment of the effectiveness of the low-concentration treatments cannot be continued after these injections commence. Attention will shift instead to performance assessment of high-concentration treatments, which is the primary objective of the apatite treatability studies.

Longer-term, post-treatment ^{90}Sr concentrations in the compliance monitoring wells and river tubes have generally remained high relative to baseline ranges, although values had started to drop by the end of the monitoring period. Elevated ^{90}Sr concentrations were well correlated with elevated SpC values,

indicating elevated ^{90}Sr concentrations are likely associated with impacts from residual high-ionic strength injection solutions. Compliance monitoring wells and river tubes are located outside the primary treatment zone and therefore are expected to take additional time for ^{90}Sr concentrations to decline to treatment zone levels.

The objectives of the field treatability testing, as stated in the treatability test plan (DOE/RL 2006), is to address the following:²

- Will apatite precipitate in the target zone?
- Does the apatite result in reducing ^{90}Sr in groundwater?
- Given a fixed well spacing of 9 m (30 ft), what is the optimal injection volume per well for installation of a 91-m (300-ft) barrier wall?

As anticipated, the objectives outlined in the treatability test plan were not fully met during this initial, low-concentration treatment phase of the project. Injections using a higher-concentration chemical formulation will be required to fully assess the first two objectives. However, injection volume requirements for installation of the 91-m (300-ft) PRB were determined.

² DOE/RL – U.S. Department of Energy, Richland Operations Office. 2006. *Strontium-90 Treatability Test Plan for 100-NR-2 Groundwater Operable Unit*. DOE/RL-2005-96, Rev. 0, U.S. Department of Energy, Richland Operations Office, Richland, Washington.

Acknowledgements

The authors would like to acknowledge the support of Fluor Hanford, Inc. personnel during the planning, field site preparation, and field testing operations for the subject treatability test. We specifically thank Vern Johnson, Deb Alexander, Robert Edrington, Russ Fabre, Roger Fichter, Kurt Lenkersdorfer, Mike Neville, and Chuck Rambo. We would also like to acknowledge the support of Pacific Northwest National Laboratory staff, including John Fruchter, who provided a thorough technical peer review; Hope Matthews, Sheila Bennett, and Mike Parker who provided document editing and text processing support; and programmatic oversight support from Mike Thompson at the U. S. Department of Energy, Richland Operations Office. Funding for this treatability study was provided by Fluor Hanford, Inc.

Acronyms and Abbreviations

ACS	American Chemical Society
AWLM	Automated Water Level Data Monitoring
bgs	below ground surface
CERCLA	<i>Comprehensive Environmental Response, Compensation, and Liability Act of 1980</i>
DO	dissolved oxygen
DOE	U.S. Department of Energy
DOE-RL	U.S. Department of Energy, Richland Operations Office
Ecology	Washington State Department of Ecology
EDS	energy dispersive spectroscopy
FH	Fluor Hanford, Inc.
FTIR	Fourier transform infrared
FY	fiscal year
gpm	gallons/minute
HEIS	Hanford Environmental Information System
HP	horsepower
HRTEM	high-resolution transmission electron microscopy
IC	ion chromatography
ICP-OES	inductively coupled plasma-optical emission spectroscopy
ID	inside diameter
ISE	ion-selective electrodes
LWDF	liquid waste disposal facility
ORP	oxidation-reduction potential
OU	operable unit
PNNL	Pacific Northwest National Laboratory
PRB	permeable reactive barriers
PRD	Priest Rapid Dam
PVC	polyvinyl chloride
QC	quality control
RACS	Remediation and Closure Science (Project)
SEM	scanning electronic microscope

SNL	Sandia National Laboratories
SpC	specific conductance
STOMP	Subsurface Transport Over Multiple Phases
TEM	transmission electron microscope
USB	universal serial bus
WIDS	Waste Information Data System
XRD	X-ray powder diffraction

Measurements

°C	degrees Centigrade
cfs	cubic feet per second
cfu	colony forming units?
CI	curie, curies
cm	centimeter
ft	foot, feet
g	gram, grams
gal	gallon, gallons
hr	hour, hours
in.	inch, inches
kg	kilogram, kilograms
km	kilometer, kilometers
L	liter, liters
m	meter, meters
mg	milligram, milligrams
mi	mile, miles
min	minute, minutes
mM	millimolar, millimolars
Mo	month, months
mol	mole, moles
pCi	picocurie
ppm	parts per million
yd	yard, yards

Contents

Summary	iii
Acknowledgements	vii
Acronyms and Abbreviations	ix
1.0 Introduction	1.1
1.1 Background	1.2
1.2 Strontium-90 Immobilization with Apatite	1.7
1.3 Subsurface Apatite Placement by Solution Injection	1.7
1.4 Site Description	1.8
1.4.1 Geology	1.8
1.4.2 Hydrogeology	1.8
1.4.3 Groundwater-River Interaction	1.10
1.5 Nature and Extent of Strontium-90 Contamination	1.10
1.6 Field Testing Approach	1.14
2.0 Treatment Technology Description	2.1
2.1 General Characteristics of Apatite	2.1
2.2 Apatite Placement in the Subsurface	2.3
2.3 Mass of Apatite Needed for Hanford 100-N Area	2.4
2.4 Strontium and Strontium-90 Incorporation Rate into Apatite	2.5
2.5 Strontium-90 Initial Mobilization and Sequential Injection Strategy	2.7
2.6 Calcium Citrate-Phosphate Solutions	2.8
2.6.1 Solution for Field Pilot Test #1	2.8
2.6.2 Solution for Field Pilot Test #2	2.8
2.6.3 Solution for Field Injections #3 to #18	2.8
2.7 Other Chemical Effect Issues	2.9
2.7.1 Diesel-Related Chemical Effects	2.9
2.7.2 Water Quality Impacts	2.10
2.7.3 Creation of a New Buried Waste Site	2.10
3.0 Aqueous Injection Bench Studies	3.1
3.1 Sequential Injection of Ca-Citrate-PO ₄ to Form Apatite and Sequester Strontium-90	3.1
3.1.1 Citrate Biodegradation Rate	3.2
3.1.2 Characterization of Apatite Precipitate	3.4
3.2 Initial Low Ca-Citrate-PO ₄ Concentration Injection Experiments	3.5
3.2.1 Laboratory Support Experiments for Field Injection #1	3.5
3.2.2 Laboratory Support Experiments for Field Injection #2	3.7
3.2.3 Laboratory Support Experiments for Field Injections #3 to #18	3.8
3.3 Techniques for Measuring Barrier Performance at Field Scale	3.12

3.4	Long-Term Strontium-90 Incorporation Mass and Rate into Apatite	3.14
3.5	Additional Injections to Increase In Situ Apatite Mass	3.18
4.0	100-N Apatite Site Setup	4.1
4.1	Well Installation	4.1
4.1.1	2005 Characterization Well Installation	4.2
4.1.2	Early 2006 Well Installation – Injection, Performance Monitoring, and Pilot Test #1 Monitoring Wells	4.3
4.1.3	Late 2006 Well Installation – Pilot Test #2 Monitoring Wells	4.7
4.1.4	Updated Geologic Cross Section	4.7
4.2	Aquifer Tubes	4.8
4.3	Site Setup	4.9
4.3.1	Site Utilities	4.10
4.3.2	Injection Equipment	4.10
4.3.3	Pressure Monitoring	4.12
4.4	Aqueous Sampling and Analysis	4.12
5.0	100-N Apatite Pilot Field Tests	5.1
5.1	Tracer Test at Pilot Test Site #1	5.1
5.1.1	Tracer Test Description	5.2
5.1.2	Tracer Test Results and Discussion	5.5
5.2	Pilot Test #1	5.11
5.2.1	Flow Rates and Pressures	5.12
5.2.2	Injection Monitoring/Radial Extent	5.15
5.2.3	Post-Injection Processes	5.22
5.2.4	General Water Quality	5.23
5.2.5	Strontium-90 Monitoring	5.26
5.3	Pilot Test #2	5.30
5.3.1	Flow Rates and Pressures	5.30
5.3.2	Injection Monitoring/Radial Extent	5.30
5.3.3	Post-Injection Processes	5.39
5.3.4	General Water Quality	5.39
5.3.5	Strontium-90 Monitoring	5.44
6.0	Design Analysis for Barrier Installation	6.1
6.1	Design Objectives and Considerations	6.1
6.2	Pre-Pilot Test Injection Design	6.3
6.2.1	Tracer Test Injection Design at Pilot Test Site # 1	6.4
6.2.2	Volume Estimate for Pilot Test Site #1 Ca-Citrate-PO ₄ Injection	6.4
6.2.3	Volume Estimate for Pilot Test #2 Ca-Citrate-PO ₄ Injection	6.5
6.3	Barrier Emplacement Design (Post-Pilot Testing)	6.6
6.3.1	Pilot Test Site #2 Model	6.6
6.3.2	Pilot Test Site #1 Model	6.13

6.3.3	Winter 2007 Injection Design	6.14
6.3.4	June/July 2007 Injection Design	6.16
6.4	Post-Barrier Injection Design Revisions/Recommendations	6.16
7.0	100-N Area Low-Concentration Barrier Injections	7.1
7.1	Barrier Installation	7.1
7.2	Assessment of Lateral Regent Coverage	7.6
7.3	Hydrogeologic Differences Along Barrier Length	7.9
8.0	100-N Apatite Low-Concentration Injection Performance Monitoring	8.1
8.1	Estimation of Baseline Strontium-90 Concentrations	8.2
8.1.1	Available Data	8.2
8.2	Field Test Performance – Pilot Test Sites	8.16
8.2.1	Field Test Performance – Pilot Test Site #1	8.17
8.2.2	Field Test Performance – Pilot Test #2 Site	8.19
8.3	Field Test Performance – Injection Wells	8.19
8.4	Field Test Performance – Compliance Wells	8.25
8.5	Field Test Performance – Aquifer Tubes	8.34
9.0	Summary, Conclusions, and Path Forward	9.1
9.1	Summary and Conclusions	9.1
9.2	Path Forward	9.4
10.0	References	10.1
	Appendix A – Arrival Curves for Low-Concentration Treatment – March and June 2007	A.1
	Appendix B – Pilot Test Performance Monitoring Figures	B.1
	Appendix C – Well Information for Pilot Test #2 Site	C.1

Figures

1.1	Index Map for the Hanford Site, South-Central Washington.....	1.3
1.2	100-N Area Groundwater Monitoring Wells	1.4
1.3	Aquifer Tubes, Seep Wells, and Monitoring Wells on 100-N Shoreline Showing Location of Apatite Barrier	1.5
1.4	Test Site Location Aerial Photo in 2003	1.6
1.5	100-N Area Site Conceptual Model in Cross Section.....	1.9
1.6	100-N Area Water Table Map, April 2006	1.11
1.7	Average ⁹⁰ Sr Concentrations in 100-N Area, Upper Part of Unconfined Aquifer	1.12
1.8	⁹⁰ Sr Distributions Along 100-N Area Shoreline, September 2006.....	1.13
1.9	⁹⁰ Sr Profiles from Three Boreholes Along 100-N Area Apatite Treatability Test Site.....	1.15
1.10	100-N Area Apatite Treatability Test Plan Site Map	1.16
2.1	Cation and Anion Substitution in Apatite	2.1
2.2	⁹⁰ Sr Aqueous and Ion Exchangeable Fraction in 100-N Area Sediments with No Apatite Addition and with Ca-citrate-PO ₄ Solution Addition to Form Apatite	2.2
3.1	⁸⁵ Sr Desorption in a One-Dimensional Column with Ca-Citrate-PO ₄ Injection	3.2
3.2	Citrate Biodegradation in Aerobic System and Anaerobic System	3.3
3.3	Characterization of Nanocrystalline Apatite Formed in Hanford Site Sediment by Microbially Mitigated Ca-Citrate Degradation in the Presence of Aqueous Phosphorous: TEM, XRD, FTIR, and EDS	3.4
3.4	Citrate Mineralization and Depth in Five Boreholes Showing Trend of Mineral.....	3.6
3.5	Injection of 2 mM Ca, 5 mM Citrate, and 2.2 mM PO ₄ into a 1-m Sediment Column.....	3.8
3.6	1-m-Long One-Dimensional Column Experiment with the Injection of 1 mM Ca, 2.5 mM Citrate, and 10 mM PO ₄ with Results of PO ₄ , Calcium, Sodium, and Strontium Breakthrough.....	3.9
3.7	Simulation of One-Dimensional Injection of a Ca-Citrate-PO ₄ Solution	3.11
3.8	Scanning Electron Microbe Images of a Single Apatite Crystal.....	3.14
3.9	Strontium Uptake from Groundwater Suspension of 0.34 g/L Apatite and 20 g/L Sediment at 82°C with Solid-Phase Apatite Added and Ca-Citrate-PO ₄ Solution Added.....	3.15
3.10	Strontium Uptake from Sediment/Apatite Systems Showing Sorbed + Incorporated Fraction and Incorporated Only	3.16
3.11	Strontium Incorporation Rates Calculated from Uptake Experiments.....	3.17
3.12	⁹⁰ Sr Breakthrough in Sequential Low- and High-Concentration Ca-Citrate-PO ₄ Injections in One-Dimensional Columns.....	3.19
4.1	Photograph Showing Location of the 100-N Area Apatite Treatability Test Along the Columbia River	4.1
4.2	Pilot Test Site #1	4.2
4.3	Pilot Test Site #2	4.3
4.4	Geologic Cross Section Updated Based on 2005 Characterization Wells	4.4
4.5	Specific Capacity of the Apatite Barrier Injection Wells.....	4.6

4.6	Geologic Cross Section Updated Based on Data Collected During Installation of Injection and Compliance Monitoring Wells in 2006	4.8
4.7	Components of the Screen Portion of an Aquifer Tube Used During Installation.....	4.9
4.8.	Apatite Chemical Delivery Systems Along the 100-N Area Shoreline	4.10
4.9	Schematic Drawing of Skid for Apatite Delivery System	4.11
4.10	Apatite Delivery System Skid 2.....	4.12
5.1	Columbia River Stage and Timing of 100-N Area Pilot Tests.....	5.2
5.2	Columbia River Stage and Timing for 100-N Area Tracer Test.....	5.2
5.3	Bromide Tracer Test at Pilot Test #1 Showing the Flow Rates, Duration, and Total Volumes Injected into Injection Well IW-3	5.4
5.4	Bromide Tracer Concentration Breakthrough Curves for Wells Completed in the Hanford Formation.....	5.6
5.5	Bromide Tracer Concentration Breakthrough Curves for Wells Completed in the Ringold Formation	5.7
5.6	Radial Transport Analytic Solution for 100-N Area Tracer Test.....	5.8
5.7	Buildup and Recovery of Water Levels During the Bromide Tracer Test.....	5.11
5.8	Columbia River Stage and Timing for 100-N Area Pilot Test #1 Showing Injection Period	5.12
5.9	Apatite Pilot Test #1 Test Flow Rates; Dilution = River Water, Feed 1= Mix 1, Feed 2 = Mix 2	5.13
5.10	Relative Columbia River Stage and Priest Rapids Dam Discharge During Apatite Pilot Test #1	5.14
5.11	Water Level Monitoring in Wells During Apatite Pilot Test #1 Conducted in May/June 2006	5.15
5.12	Apatite Pilot Test #1 Injection – Specific Conductance, PO ₄ , and Calcium Breakthrough Curves in Hanford Formation	5.16
5.13	Apatite Pilot Test #1 Injection – Specific Conductance, PO ₄ , and Calcium Breakthrough Curves in Ringold Formation.....	5.18
5.14	Summary of Specific Conductance and Phosphate in Monitoring Wells at End of Pilot Test #1 Injection and ~1 Week Later	5.20
5.15	Summary of Calcium Measurements in Monitoring Wells Showing Baseline, 1 Day and 8 Days after the Injection	5.21
5.16	Apatite Pilot Test #1 Injection Dissolved Oxygen and Oxidation-Reduction Potential for Selected Monitoring Wells	5.23
5.17	Columbia River Stage and Specific Conductance Measurements After Pilot Test #1.....	5.24
5.18	⁹⁰ Sr and ^{89/90} Sr Concentrations Before and 5 Months After Pilot Test #1 Injection.....	5.28
5.19	Calcium and ^{89/90} Sr Ratios at Pilot Test #1 Injection; Data from July and October 2006 and May and June 2007.....	5.29
5.20	Columbia River Stage and Timing for 100-N Area Pilot Test #2.....	5.31
5.21	Apatite Pilot Test #2 Flow Rates.....	5.33
5.22	Water Level Monitoring in Hanford Formation Wells During Apatite Pilot Test #2	5.33
5.23	Water Level Monitoring in Ringold Formation Wells During Apatite Pilot Test #2	5.34

5.24	Apatite Pilot Test #2 Injection – Specific Conductance, PO ₄ , and Calcium Breakthrough Curves in Hanford Formation	5.35
5.25	Apatite Pilot Test #2 Injection – Specific Conductance, PO ₄ , and Calcium Breakthrough Curves in Ringold Formation.....	5.37
5.26	Apatite Pilot Test #2 Injection – Citrate, Formate, and Dissolved Oxygen Breakthrough Curves in Hanford Formation	5.40
5.27	Apatite Pilot Test #2 Injection – Citrate, Formate, and Dissolved Oxygen Breakthrough Curves in Ringold Formation.....	5.42
5.28	Normalized Breakthrough Curves for Well P2-R-3.....	5.46
5.29	⁹⁰ Sr measurements following September 2006 Pilot Test #2.....	5.47
6.1	Well Spacing and Plume Overlap Design for 100-N Area Apatite Barrier	6.2
6.2	Monthly Average River Stage at 100-N Area from RS-1 for 1994 to 2004	6.2
6.3	Earth Vision Cross-Section Transect Location	6.7
6.4	Earth Vision Cross Section	6.7
6.5	STOMP Model Cross Section and Zonations for Pilot Test Site #2	6.8
6.6	Columbia River Stage and Flow for 2006 at the 100-N Area.....	6.9
6.7	Detailed Columbia River Stage and Flow for 2006 Pilot Test #2 at 100-N Area	6.10
6.8	Hydraulic Head Results of Pilot Test #2 Model Fit.....	6.12
6.9	Bromide Results of Pilot Test #2 Model Fit	6.13
6.10	Phosphate Results of Pilot Test #2 Model Fit.....	6.14
6.11	Phosphate Results of Pilot Test #2 Injection Test with Volume Extended to 140,000 gal.....	6.15
7.1	Location and Relative Discharge Rate of Springs During Injection	7.5
7.2	Treatment Efficiency Around Well 199-N-137 During March 2007 Injection	7.8
7.3	Treatment Efficiency Around 199-N-138 (Pilot Test Site #1 During June 2007 Injection	7.8
7.4	Arrival Curves for Wells Adjacent to Injection Well.....	7.10
7.5	Arrival Curves for Wells Adjacent to 199-N-136 During the June 2007 Injection in Well 199-N-136	7.10
7.6	Arrival Curves for Wells Adjacent to Well 199-N-142 During March and June Injections in Well 199-N-142	7.11
8.1	Spatial Coordinate Transform	8.3
8.2	Temporal Variation in Pretreatment Observations for Aquifer Tubes and Temporal Variation in Pretreatment Observations for Injection/Compliance Wells.....	8.8
8.3	Temporal Variation in Pretreatment Observations (monthly binned) for Aquifer Tubes and Temporal Variation in Pretreatment Observations (monthly binned) for Injection/Compliance Wells	8.9
8.4	Spatial Variation.....	8.10
8.5	Data Ranges Extracted for Aquifer Tubes and Compliance Wells and Estimated for Injection Wells	8.10
8.6	Histogram of Strontium Concentrations in Table 8.6	8.13
8.7	Calculated Variogram and Variogram Model.....	8.14

8.8	Temporal Variation of the Estimated Pretreatment ⁹⁰ Sr Concentrations at the Injection/ Compliance Along with Measured Concentrations at Aquifer Tubes NS-3A and NVP2	8.15
8.9	The Notched Box Plot of the Kriged Pretreatment ⁹⁰ Sr Concentration at Each Injection Well	8.15
8.10	Interpolated Ranges, Estimated CIs, and Measurements of Baselines of the Injection Wells	8.16
8.11	⁹⁰ Sr Performance Monitoring Plots for Pilot Test #1 Injection Well 199-N-138	8.18
8.12	Calcium, Phosphate, and Specific Conductance Performance Monitoring Plots for Pilot Test #1 Injection Well 199-N-138	8.18
8.13	⁹⁰ Sr Performance Monitoring Plots for Pilot Test #2 Injection Well 199-N-137	8.20
8.14	Calcium, Phosphate, and Specific Conductance Performance Monitoring Plots for Pilot Test #2 Injection Well 199-N-137	8.20
8.15	⁹⁰ Sr Performance Monitoring Plots for Injection Well 199-N-136	8.21
8.16	⁹⁰ Sr Performance Monitoring Plots for Injection Well 199-N-139	8.21
8.17	⁹⁰ Sr Performance Monitoring Plots for Injection Well 199-N-140	8.22
8.18	⁹⁰ Sr Performance Monitoring Plots for Injection Well 199-N-141	8.22
8.19	⁹⁰ Sr Performance Monitoring Plots for Injection Well 199-N-142	8.23
8.20	⁹⁰ Sr Performance Monitoring Plots for Injection Well 199-N-143	8.23
8.21	⁹⁰ Sr Performance Monitoring Plots for Injection Well 199-N-144	8.24
8.22	⁹⁰ Sr Performance Monitoring Plots for Injection Well 199-N-145	8.24
8.23	Calcium, Phosphate, and Specific Conductance Performance Monitoring Plots for Injection Well 199-N-136	8.26
8.24	Calcium, Phosphate, and Specific Conductance Performance Monitoring Plots for Injection Well 199-N-139	8.26
8.25	Calcium, Phosphate, and Specific Conductance Performance Monitoring Plots for Injection Well 199-N-140	8.27
8.26	Calcium, Phosphate, and Specific Conductance Performance Monitoring Plots for Injection Well 199-N-141	8.27
8.27	Calcium, Phosphate, and Specific Conductance Performance Monitoring Plots for Injection Well 199-N-142	8.28
8.28	Calcium, Phosphate, and Specific Conductance Performance Monitoring Plots for Injection Well 199-N-143	8.28
8.29	Calcium, Phosphate, and Specific Conductance Performance Monitoring Plots for Injection Well 199-N-144	8.29
8.30	Calcium, Phosphate, and Specific Conductance Performance Monitoring Plots for Injection Well 199-N-145	8.29
8.31	⁹⁰ Sr Performance Monitoring Plots for Compliance Well 199-N-122	8.30
8.32	⁹⁰ Sr Performance Monitoring Plots for Compliance Well 199-N-123	8.30
8.33	⁹⁰ Sr Performance Monitoring Plots for Compliance Well 199-N-146	8.31
8.34	⁹⁰ Sr Performance Monitoring Plots for Compliance Well 199-N-147	8.31
8.35	Calcium, Phosphate, and Specific Conductance Performance Monitoring Plots for Compliance Well 199-N-122	8.32

8.36	Calcium, Phosphate, and Specific Conductance Performance Monitoring Plots for Compliance Well 199-N-123	8.32
8.37	Calcium, Phosphate, and Specific Conductance Performance Monitoring Plots for Compliance Well 199-N-146	8.33
8.38	Calcium, Phosphate, and Specific Conductance Performance Monitoring Plots for Compliance Well 199-N-147	8.33
8.39	Gross Beta and Specific Conductance for Aquifer Tubes.....	8.34

Tables

2.1	Apatite Mass and Change in ⁹⁰ Sr Mobilization.....	2.4
2.2	⁹⁰ Sr Sorption Fraction in Field System Containing Sediment and Apatite	2.5
2.3	Composition of Calcium Citrate-Phosphate Solutions Used for Field Injections.....	2.9
3.1	Calculated Strontium Uptake Rates in Apatite-Laden Sediment for a 30-ft-wide Barrier.....	3.17
3.2	Sequential Treatments of ⁹⁰ Sr-Laden Sediment with Fraction ⁹⁰ Sr Uptake and Efficiency.....	3.18
3.3	⁹⁰ Sr Mass Balance for Low-, then High-Ca-Citrate-PO ₄ Injections in One-Dimensional Columns	3.19
4.1	Early 2006 Well Identification and Drilling Date Summary	4.5
4.2	Small-Diameter Pilot Test Site #1 Monitoring Well Construction Summary.....	4.5
4.3	Small-Diameter Pilot Test Site #2 Monitoring Well Construction Summary.....	4.7
4.4	Pilot Test Site Aquifer Tube Construction Summary	4.9
4.5	Apatite Pilot Test Sampling Requirements	4.13
4.6	Analytical Requirements.....	4.13
5.1	Summary of Apatite Pilot Test #1 Bromide Tracer Injection Test	5.3
5.2	Injection and Monitoring Well Summary for Pilot Test Site #1	5.3
5.3	Summary of Apatite Pilot Test #1 Injection Test.....	5.13
5.4	Summary of Phosphate and Specific Conductance in Selected Monitoring Wells for Pilot Test #1 Injection Test.....	5.19
5.5	Summary of Field Parameters in Selected Monitoring wells at Pilot Test #1 Injection Test Site.....	5.25
5.6	Summary of Anions in Selected Monitoring Wells at Pilot Test #1 Injection Test Site.....	5.25
5.7	Summary of Selected Metals and ⁹⁰ Sr at Pilot Test #1 Injection Test Site	5.26
5.8	Summary of Baseline and Peak ⁹⁰ Sr Concentrations After Injections at Pilot Test Site #1.....	5.29
5.9	Summary of Apatite Pilot Test #2.....	5.31
5.10	Injection and Monitoring Well Summary for the Pilot Test Site #2	5.32
5.11	Summary of Phosphate and Specific Conductance in Selected Monitoring Wells for Pilot Test #2 Injection Test.....	5.39

5.12	Summary of Field Parameters at Pilot Test #2 Injection Test Site.....	5.44
5.13	Summary of Selected Anions at Pilot Test #2 Injection Test Site	5.45
5.14	Summary of Selected Metals and ⁹⁰ Sr at Pilot Test #2 Injection Test Site	5.45
5.15	Summary of Baseline and Peak ⁹⁰ Sr Concentrations After Injections at Pilot Test Site #2.....	5.46
6.1	Injection Volume Estimates for Tracer Test Planning.....	6.4
6.2	100-N Pilot Test #2 Preliminary Parameter Estimation Results	6.11
7.1	100-N Area Low-Concentration Apatite Injection Summary	7.2
7.2	Design Specified Chemical Concentrations of Injection Solution.....	7.2
7.3	Injection Concentrations and Total Chemical Mass Injected During the March 2007 Apatite Barrier Formation Injections	7.3
7.4	Injection Concentrations and Total Chemical Mass Injected During the June 2007 Apatite Barrier Formation Injections	7.4
7.5	River Stage During the March 2007 Injections and the 7-Day Reaction Period, as Measured at the 100-N Area River Stage Gauge	7.4
7.6	River Stage During the June 2007 Injections and 7-Day Reaction Period.....	7.4
7.7	Comparison of Treatment Efficiency at Wells Adjacent to Injection Wells During FY 2007 Injections.....	7.7
8.1	Pretreatment Baseline ⁹⁰ Sr Measurements Identified for Injection and Compliance Monitoring Wells	8.4
8.2	Name and Coordinates of Aquifer Tubes.....	8.5
8.3	Pretreatment Baseline ⁹⁰ Sr Measurements Identified for Aquifer Tubes	8.5
8.4	Distance of Each Well to the Origin Along the Regression Line Parallel to the Apatite Barrier.....	8.7
8.5	Data Ranges Extracted for Aquifer Tubes and Compliance Wells and Linearly Interpolated for Injections Wells.....	8.11
8.6	Data Retained for Variogram Analysis and Kriging Estimation.....	8.12
8.7	Kriged Estimate of Pretreatment ⁹⁰ Sr Concentrations for Each Month at the 10 Injection Wells	8.14
8.8	The Mean and 95% Confidence Interval of the Mean of the Kriged Pretreatment ⁹⁰ Sr Concentration (pCi/L) at Each Injection Well	8.14

1.0 Introduction

Efforts to reduce the flux of strontium-90 (^{90}Sr) to the Columbia River from past-practice liquid waste disposal sites have been underway since the early 1990s in the 100-N Area at the Hanford Site (Figures 1.1 and 1.2). Termination of all liquid discharges to the ground by 1993 was a major step toward meeting this goal. However, ^{90}Sr adsorbed on aquifer solids beneath the liquid waste disposal sites and extending to beneath the near-shore riverbed remains a continuing source to groundwater and the Columbia River.

The remedy specified in the 100-NR-1/2 Interim Action Record of Decision (Ecology 1999) included operation of a pump-and-treat system, as well as a requirement to evaluate alternative ^{90}Sr treatment technologies. Researchers recognized from the onset that the pump-and-treat system was unlikely to be an effective long-term treatment method because of the geochemical characteristics of ^{90}Sr , the primary contaminant of concern. Subsequent performance monitoring has substantiated this expectation. Accordingly, the first *Comprehensive Environmental Response, Compensation, and Liability Act of 1980* (CERCLA) 5-year review re-emphasized the need to pursue alternative methods to reduce impacts on the Columbia River.

With the presentation of the *Evaluation of ^{90}Sr Treatment Technologies for the 100 NR-2 Groundwater Operable Unit*¹ at the December 8, 2004, public meeting, U.S. Department of Energy (DOE), Fluor Hanford, Inc. (FH), Pacific Northwest National Laboratory (PNNL), and the Washington State Department of Ecology (Ecology) agreed that the long-term strategy for groundwater remediation at the 100-N Area will include apatite sequestration as the primary treatment, followed by a secondary treatment—or polishing step—if necessary (most likely phytoremediation). Since then, the agencies have worked together to agree on which apatite sequestration technology has the greatest chance of reducing ^{90}Sr flux to the Columbia River at a reasonable cost. In July 2005, aqueous injection, (i.e., the introduction of apatite-forming chemicals into the subsurface) was endorsed as the interim remedy and selected for field testing. Studies are in progress to assess the efficacy of in situ apatite formation by aqueous solution injection to address both the vadose zone and the shallow aquifer along the 91 m (300 ft) of shoreline where ^{90}Sr concentrations are highest (see Figures 1.2 to 1.4).

A low-concentration, apatite-forming solution was injected into the shallow aquifer in 10 injection wells during fiscal year (FY) 2006 and 2007, and performance monitoring is underway. The low-concentration, apatite-forming solution consists primarily of calcium chloride, trisodium citrate, and sodium phosphate. The objective of the low-concentration Ca-citrate- PO_4 solution injections is to stabilize the ^{90}Sr in the aquifer at the test site, to be followed by high-concentration injections to provide for long-term ^{90}Sr treatment. Two pilot test sites at the east and west ends of the barrier, which are equipped with extensive monitoring well networks, were used for the initial injections to develop the injection design for the remaining portions of the barrier. A detailed discussion of objectives and technical approach for these field activities is provided in a project-specific treatability test plan (DOE/RL 2006).

¹ Fluor Hanford, Inc. and CH2M HILL Hanford Group. 2004. *Evaluation of Strontium-90 Treatment Technologies for the 100-NR-2 Groundwater Operable Unit*. Letter Report available online at http://www.washingtonclosure.com/projects/endstate/risk_library.html#narea.

The objective of the field treatability testing, as stated in the treatability test plan (DOE/RL 2006), is to address the following:

- Will apatite precipitate in the target zone?
- Does the apatite result in reducing ^{90}Sr in groundwater?
- Given a fixed well spacing of 9 m (30 ft), what is the optimal injection volume per well for installation of a 91-m (300-ft) barrier wall?

The first two questions are not addressed in this interim report for the low Ca-citrate- PO_4 injections, but will be addressed from analysis of sediment samples collected from coreholes within the treatment zone and performance groundwater monitoring following the high-concentration Ca-citrate- PO_4 injections scheduled to begin in 2008. Injection volumes for the fixed 9.1-m (30-ft) spacing injection wells to create the barrier were determined based on the field-sampling results of the low-concentration Ca-citrate- PO_4 injections described in Section 7 of this report. In addition to the injection volumes, recommendations were made for installation of injection wells targeting only the lower portion of the contaminated zone for improved and more efficient reagent coverage for the downstream section of the barrier. These additional wells are planned to be installed in the winter and spring of 2008. Higher-concentration Ca-citrate- PO_4 solution injections are planned for FY 2008.

This report describes the technology, laboratory development, and field testing of a saturated zone injection approach using low-concentration Ca-citrate- PO_4 solutions at the 100-N Area for the treatment of ^{90}Sr contamination in situ. The studies presented in this report were funded by FH.

Section 2.0 of this report describes the general characteristics of apatite and mineral apatite; the aqueous injection technique; potential chemical effects of this treatment; and the testing that has been done using this technology. Section 3.0 describes bench tests conducted at Sandia National Laboratories and at PNNL to demonstrate the feasibility of aqueous injection, and to quantify various processes involved in the technology. Section 4.0 presents site setup and initial characterization for the 91-m (300-ft) long barrier at 100-N Area, and Section 5.0 describes pilot field testing with detailed short-term monitoring results. Section 6.0 contains the design analysis, and Section 7.0 describes the barrier installation injections of the revised low-concentration, apatite-forming solution. Section 8.0 contains the longer-term performance monitoring results, Section 9.0 the summary and path forward, and Section 10.0 provides the cited references.

1.1 Background

The Hanford Site is a DOE-owned site located in southeastern Washington State near Richland, Washington (Figure 1.1). The 100-N Area is located along the Columbia River and includes the 100-N Reactor, a DOE nuclear reactor previously used for plutonium production.

Operation of the 100-N Area nuclear reactor required the disposal of bleed-and-feed cooling water from the reactor's primary cooling loop, the spent fuel storage basins, and other reactor-related sources. Two crib and trench liquid waste disposal facilities (LWDFs) were constructed to receive these waste streams, and disposal consisted of percolation into the soil. The first LWDF (1301-N/116-N-1 shown in Figure 1.2) was constructed in 1963, about 244 m (800 ft) from the Columbia River (Figure 1.2).

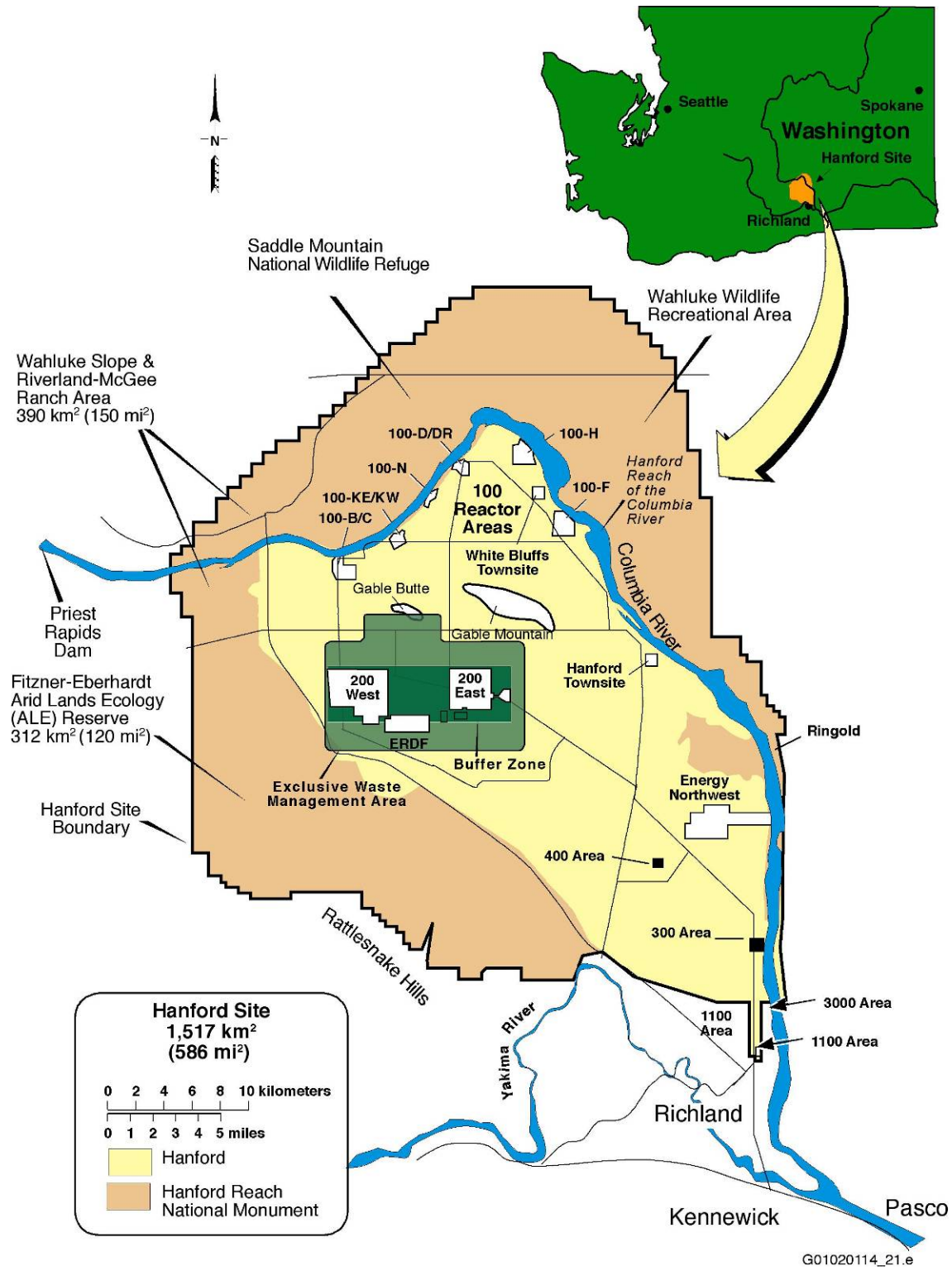
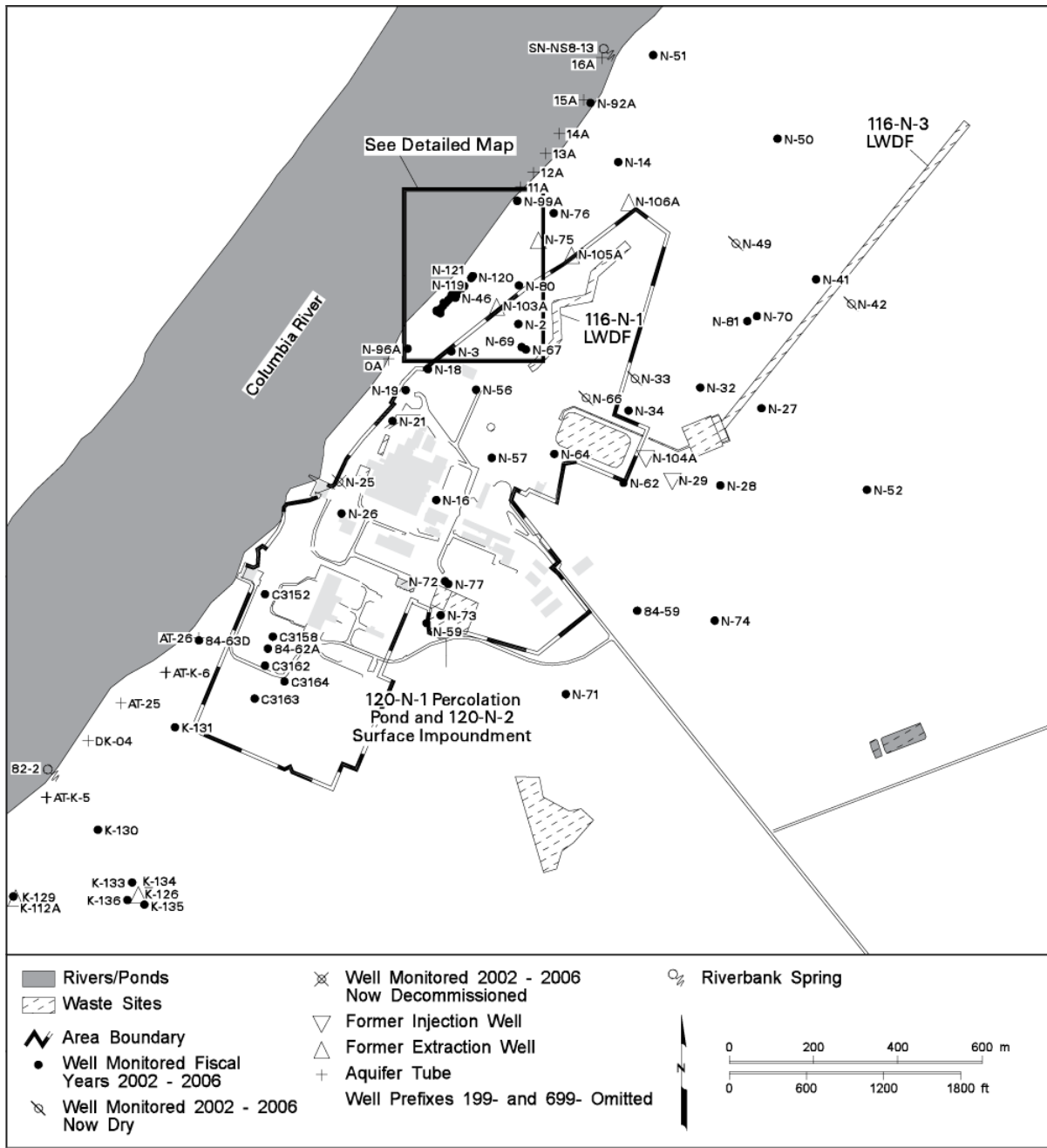


Figure 1.1. Index Map for the Hanford Site, South-Central Washington. The 100-N Area is located on the northern portion of the site along the Columbia River.



can_gwf06_151 February 14, 2007 5:08 PM

Figure 1.2. 100-N Area Groundwater Monitoring Wells (from Hartman et al. 2007). Detailed map is shown in Figure 1.3.



Figure 1.4. Test Site Location Aerial Photo in 2003. The 1301-N Crib has been backfilled since this photo was taken.

Liquid discharges to this LWDF contained radioactive fission and activation products, including ^{60}Co , ^{137}Cs , ^{90}Sr , and tritium. Minor amounts of hazardous wastes such as sodium dichromate, phosphoric acid, lead, and cadmium were also part of the waste stream. When ^{90}Sr was detected at the shoreline, disposal at the first LWDF was terminated and a second crib and trench (1325-N LWDF/116-N-3) was constructed farther inland in 1983. Discharges to 1325-N stopped in 1991. The LWDFs have been excavated to remove the most highly contaminated soil and backfilled.

A more complete history of groundwater contamination at the 100-N Area is provided in *Hanford 100-N Area Remediation Options Evaluation Summary Report* (TAG 2001).² In summary, as a result of wastewater disposal practices, soils beneath the LWDF were contaminated from the surface sediments to the lower boundary of the unconfined aquifer. A portion of the contaminants migrated to the Columbia River via groundwater. To address contamination in the 100-N Area, it was divided into two operable units (OUs). The 100-NR-1 OU contains all the source waste sites located within the main industrial area around the 100-N Reactor and the Hanford Generating Plant, and includes the LWDF surface sediments and shallow subsurface soil. The 100-NR-2 OU contains the contaminated groundwater and aquifer.

Hartman et al. (2007) described remediation activities in the 100-N Area related to the groundwater contamination which are summarized below. As part of the source waste site remediation, contaminated soil was removed from 116-N-1 LWDF (see Figure 1.2) to a depth of ~4.6 m from 2002 to 2005 and was backfilled with clean soil in 2006. Contaminated soil was also excavated and removed from 116-N-3 LWDF to a depth of ~4.6 m from 2000 to 2003 and backfilled with clean soil in 2004 and 2005. From 1995 to 2006, a groundwater pump-and-treat system for ^{90}Sr began operating in the 100-N Area under a

² Technical Advisory Group (TAG). 2001. *Hanford 100-N Area Remediation Options Evaluation Summary Report*.

CERCLA interim action for the 100-NR-2 OU. This pump-and-treat system was put on cold standby in 2006 because it did not meet the remedial action objectives. DOE is testing alternative groundwater remediation methods for ^{90}Sr in the 100-N Area, which includes the apatite PRB treatability testing described in this report.

1.2 Strontium-90 Immobilization with Apatite

Apatite [$\text{Ca}_{10}(\text{PO}_4)_6(\text{OH})_2$] is a natural calcium-phosphate mineral occurring primarily in the Earth's crust as phosphate rock. It is also a primary component in the teeth and bones of animals. Apatite minerals sequester elements into their molecular structures via isomorphic substitution, whereby elements of similar physical and chemical characteristics replace calcium, phosphate, or hydroxide in the hexagonal crystal structure (Hughes et al. 1991; Spence and Shi 2005). Apatite has been used for remediation of other metals, including uranium (Arey et al. 1999; Fuller et al. 2002, 2003; Jeanjean et al. 1995), lead (Bailliez et al. 2004; Mavropoulos et al. 2002; Ma et al. 1995), plutonium (Moore et al. 2005), and neptunium (Moore et al. 2003). Because of the extensive substitution into the general apatite structure, over 350 apatite minerals have been identified (Moelo et al. 2000). Strontium incorporation into apatite has also been previously studied (Smiciklas et al. 2005; Rendon-Angeles et al. 2000). Apatite minerals are very stable and practically insoluble in water (Tofe 1998; Wright 1990; Wright et al. 2004). The solubility product of hydroxyapatite is about 10^{-44} , while quartz crystal, which is considered the most stable mineral in the weathering environment, has a solubility product (K_{sp}) of 10^{-4} (Geochem Software 1994). Strontiapatite, $\text{Sr}_{10}(\text{PO}_4)_6(\text{OH})_2$, which is formed by the complete substitution of calcium by strontium (or ^{90}Sr), has a K_{sp} of about 10^{-51} , another 10^7 times less soluble than hydroxyapatite (Verbeeck et al. 1977). The substitution of strontium for calcium in the crystal structure is thermodynamically favorable, and will proceed provided the two elements coexist. Strontium substitution in natural apatites is as high as 11%, although dependent on available strontium (Belousova et al. 2002). Synthetic apatites have been made with up to 40% strontium substitution for calcium (Heslop et al. 2005). The mechanism (solid-state ion exchange) of strontium substitution for calcium in the apatite structure has been previously studied at elevated temperature (Rendon-Angeles et al. 2000), but low-temperature aqueous rates under Hanford Site groundwater conditions (i.e., calcium /strontium ratio of 220/1) have not.

1.3 Subsurface Apatite Placement by Solution Injection

The method of emplacing apatite in subsurface sediments at the 100-N Area is to inject an aqueous solution containing a Ca-citrate complex and Na-phosphate. Citrate is needed to keep calcium in solution long enough (days) to inject into the subsurface; a solution containing Ca^{2+} and phosphate only will rapidly form mono- and di-calcium phosphate, but not apatite (Andronescu et al. 2002; Elliott et al. 1973, Papargyris et al. 2002). Relatively slow biodegradation of the Ca-citrate complex (days) allows sufficient time for injection and transport of the reagents to the areas of the aquifer where treatment is required. As Ca-citrate is degraded (Van der Houwen and Valsami-Jones 2001; Misra 1998), the free calcium and phosphate combine to form amorphous apatite. The formation of amorphous apatite occurs within a week and crystalline apatite forms within a few weeks. Citrate biodegradation rates in 100-N Area sediments (water saturated) at temperatures from 10° to 21°C (aquifer temperature 15° to 17°C) over the range of citrate concentrations to be used (10 to 100 mM) have been determined experimentally and simulated with a first-order model (Bailey and Ollis 1986; Brynhildsen and Rosswall 1997). In addition, the microbial biomass has been characterized with depth and position along the shoreline, and the relationship between biomass and the citrate biodegradation rate determined. Because 100-N Area

injections typically use river water (~90 to 95%) with concentrated chemicals, microbes in the river water are also injected, which results in a somewhat more uniform citrate biodegradation rate in different aquifer zones.

Emplacement of apatite precipitate by a solution injection has significant advantages over other apatite emplacement technologies for application at the 100-N Area. The major advantage is minimal disturbance of the subsurface (both vadose and saturated zone) because this technology only requires injection wells (for groundwater remediation) or a surface infiltration gallery (for vadose zone treatment), in contrast with excavation of the riverbank for trench-and-fill emplacement of solid-phase apatite. Other apatite emplacement technologies were also considered for the 100-N Area (DOE/RL 2006), including pneumatic injection of solid apatite and vertical hydrofracturing for apatite emplacement, both as a permeable reactive barrier (PRB) and grout curtain. Although each technology has advantages and disadvantages, the Ca-citrate-PO₄ injection technology was chosen because it appears to provide the most economic emplacement methodology to treat ⁹⁰Sr in the near-shore sediments. A limitation of all of these apatite technologies is that the ⁹⁰Sr is not removed from the sediment until radioactive decay occurs because it is incorporated into the apatite crystalline structure.

1.4 Site Description

1.4.1 Geology

Stratigraphic units of significance at the 100-N Area include the following:

- Elephant Mountain Member of the Columbia River Basalt Group
- Ringold Formation
- Hanford formation.

The Elephant Mountain Member is an extensive basalt unit that underlies the fluvial-lacustrine deposits of the Ringold Formation and glaciofluvial deposits of the Hanford formation. The unconfined aquifer at the 100-N Area near the shoreline is composed of gravels and sands of the Hanford and Ringold Formations, as shown in Figure 1.5. The Ringold Formation is composed of several lithologic facies; of most interest at the 100-N Area is Ringold Unit E, which forms the unconfined aquifer beneath the Hanford formation, and the Ringold Upper Mud Unit, which forms the base of the unconfined aquifer.

1.4.2 Hydrogeology

The uppermost stratigraphic unit in the 100-N Area is the Hanford formation, which consists of uncemented and clast-supported pebble, cobble, and boulder gravel with minor sand and silt interbeds. The matrix in the gravel is composed mostly of coarse-grained sand, and an open-framework texture is common. For most of the 100-N Area, the Hanford formation extends from ground surface to just above the water table, 5.8 to 24.5 m (19 to 77 ft) in thickness. However, some channels of Hanford formation gravels extend below the water table.

The uppermost Ringold stratum at the 100-N Area is Unit E, consisting of variably cemented pebble to cobble gravel with a fine- to coarse-grained sand matrix. Sand and silt interbeds may also be present. Unit E forms the unconfined aquifer in the 100-N Area and is approximately 12 to 15 m (39 to 49 ft) thick. The base of the aquifer is situated at the contact between Ringold Unit E and the underlying, much less transmissive, silty strata referred to locally as the Ringold Upper Mud, approximately 60 m (197 ft) thick.

The Hanford formation is much more transmissive than the underlying Ringold Unit E; however, due to geologic heterogeneity, the hydraulic conductivity in both units is highly variable. Typical values of 15.2 and 182 m/day (50 and 597 ft/day) have been used for modeling purposes for the Ringold and Hanford Units, respectively.³

Figure 1.5 depicts a cross section of the Hanford and upper Ringold Units in the near-river environment. As illustrated in Figure 1.5, the aquifer outcrops into the Columbia River channel and the high-river stage rises into the Hanford formation.

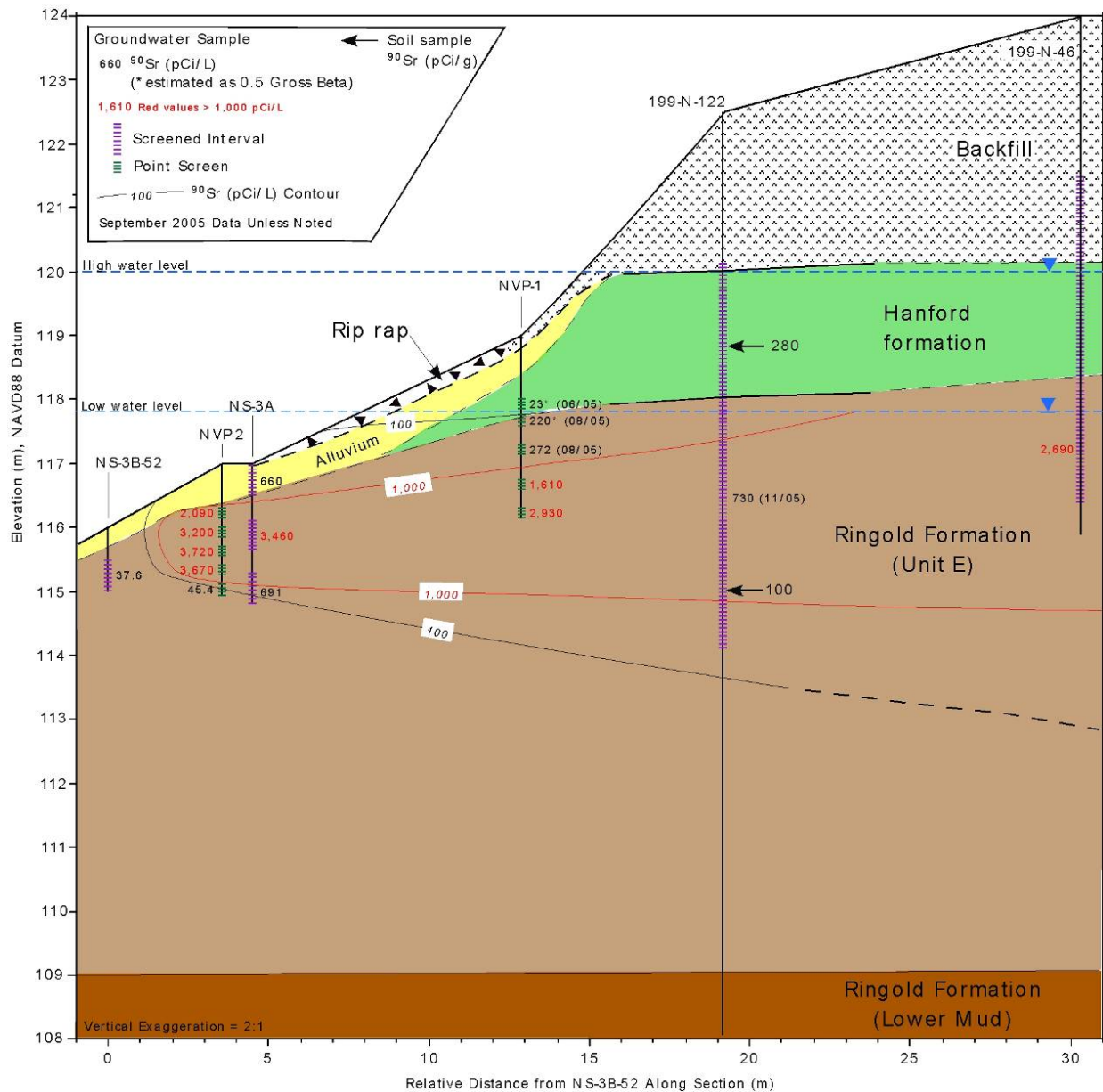


Figure 1.5. 100-N Area Site Conceptual Model in Cross Section

³ Connelly MP. 2001. *Strontium-90 Transport in the Near-River Environment at the 100-N Area*. Innovative Treatment and Remediation Demonstration Program, HydroGeoLogic, Reston, Virginia.

Groundwater flows primarily in a north-northwesterly direction most of the year and discharges to the Columbia River, as shown in Figure 1.6, a local water table map constructed using April 2006 water-level data. The groundwater gradient varies from 0.0005 to 0.003. Near the LWDF facilities, average groundwater velocities are estimated to be between 0.03 and 0.6 m/day (0.1 and 2 ft/day), where 0.3 m/day (1 ft/day) is generally considered typical (DOE/RL 2006). However, groundwater flows near the river are significantly influenced by both diurnal and seasonal variability in Columbia River stage.

1.4.3 Groundwater-River Interaction

Fluctuations in river stage resulting from seasonal variations and daily operations of Priest Rapids Dam (PRD), located 29 km (18 mi) upstream of 100-N Area, have a significant effect on groundwater flow direction, hydraulic gradient, and groundwater levels near the river. The volume of water moving in and out of the unconfined aquifer on both a daily and seasonal basis is an order of magnitude greater than groundwater flowing as a result of the regional hydraulic gradient. In addition, with the changing direction of groundwater flow, pore-water velocities near the river may exceed 10 m/day (32.8 ft/day).⁴ During the high-river stage, river water moves into the bank and mixes with groundwater. The zone of mixing is restricted to within tens of meters of the shoreline. During low-river stage, this bank storage water drains back into the river and may be observed as springs along the riverbank. Springs, seeps, and subsurface discharge along the riverbank are the primary pathway of 100-N Area groundwater contaminants to the Columbia River. Additional details on the extent of seasonal and daily changes in river stage at the site from PRD discharge are provided in Sections 5.0 and 6.0.

1.5 Nature and Extent of Strontium-90 Contamination

Groundwater at the 100-N Area has been contaminated with various radionuclides and nonionic and ionic constituents. Contaminants of concern in the 100-NR-2 Operable Unit include ⁹⁰Sr, tritium, nitrate, sulfate, petroleum hydrocarbons, manganese, and chromium (Hartman et al. 2007). Of primary concern is the presence of ⁹⁰Sr in the groundwater and the discharge of ⁹⁰Sr to the Columbia River via groundwater (Figures 1.7 and 1.8). The ⁹⁰Sr is more mobile than many other radiological contaminants found at the site (exceptions include tritium, ⁹⁹Tc, and ¹²⁹I) and because of its chemical similarity to calcium, it bioaccumulates in plants and animals. With a half-life of 28.6 years, it will take approximately 300 years for the ⁹⁰Sr concentrations present in the subsurface at 100-N Area to decay to below current drinking water standards.

The zone of ⁹⁰Sr-contaminated soils resulting from 30 years of wastewater discharge to the LWDFs includes the portions of the vadose zone that were saturated during discharge operations, and the underlying aquifer, which extends to the Columbia River (Figure 1.5). During operations, a groundwater mound approximately 6 m (20 ft) high was created. Not only was the water table raised into more transmissive Hanford Site sediments, but steeper hydraulic gradients were created, increasing the groundwater flow rate toward the river. While the 100-N Reactor was operating, riverbank seepage was pronounced. Since then, the number of springs and seeps has decreased in proportion to the decrease in artificial recharge caused by the wastewater disposal.

⁴Connelly MP. 1999. *Groundwater-River Interaction in the Near River Environment at the 100-N Area*. Innovative Treatment and Remediation Demonstration Program, HydroGeoLogic, Reston, Virginia.

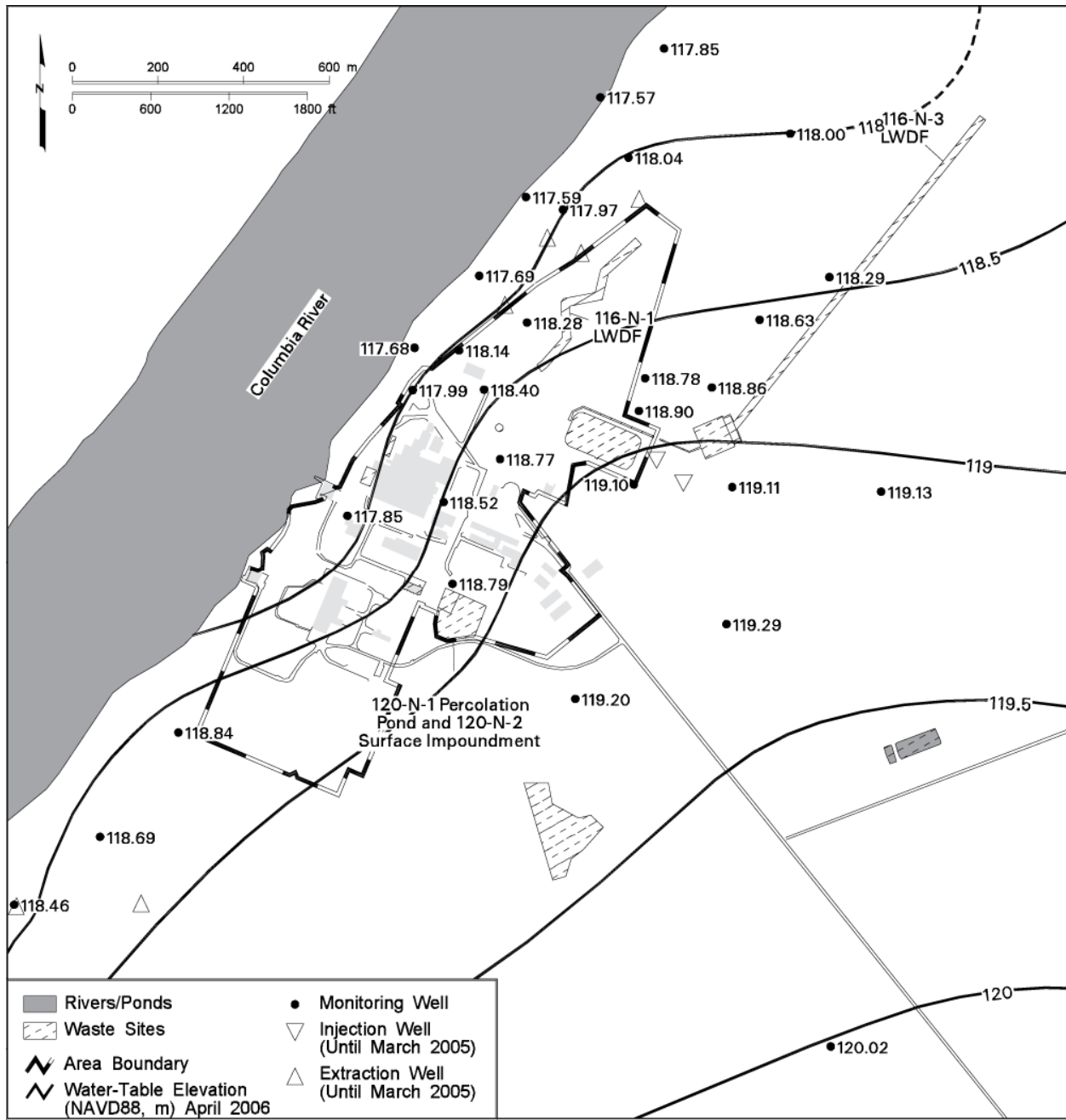


Figure 1.6. 100-N Area Water Table Map, April 2006 (from Hartman et al. 2007)

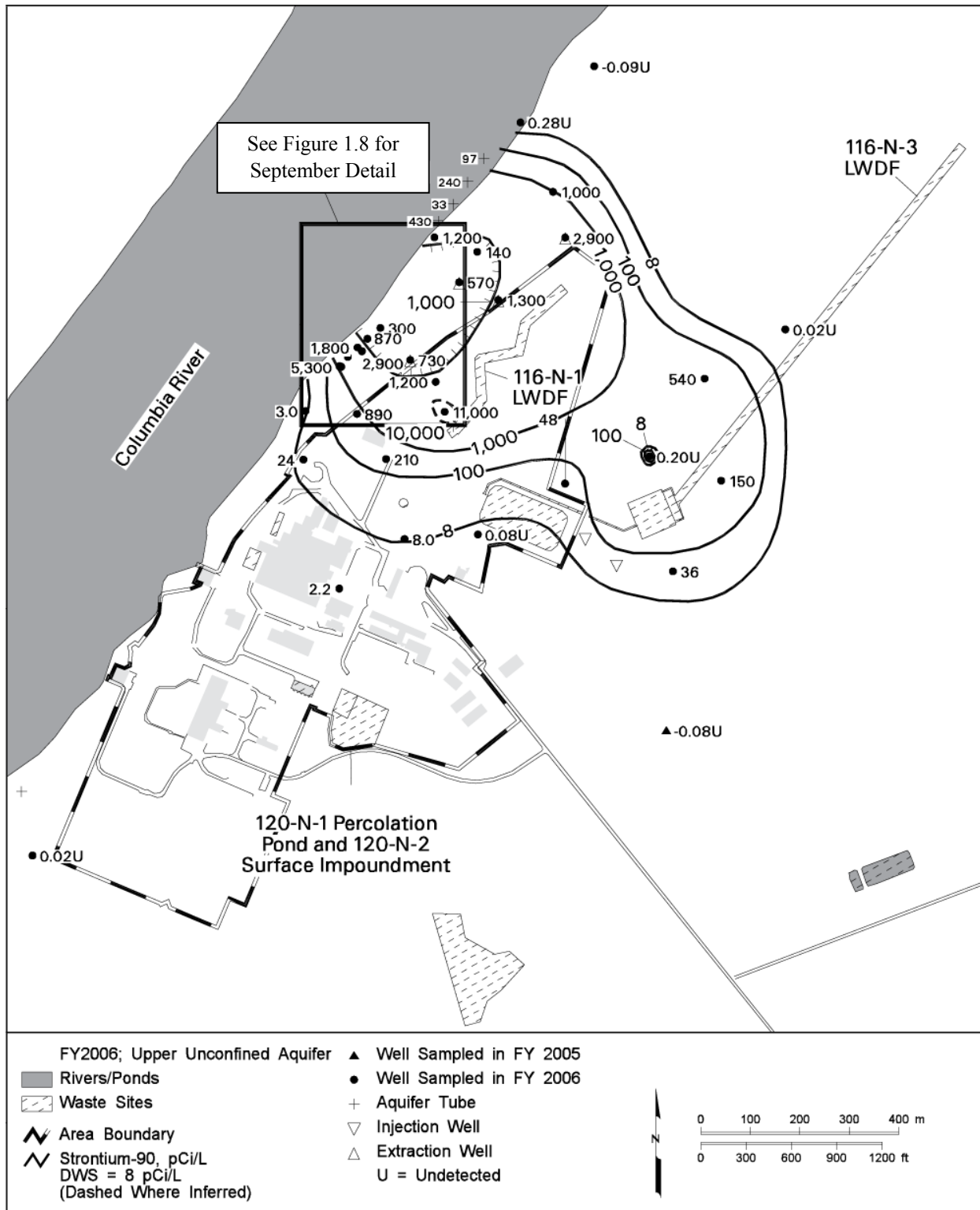
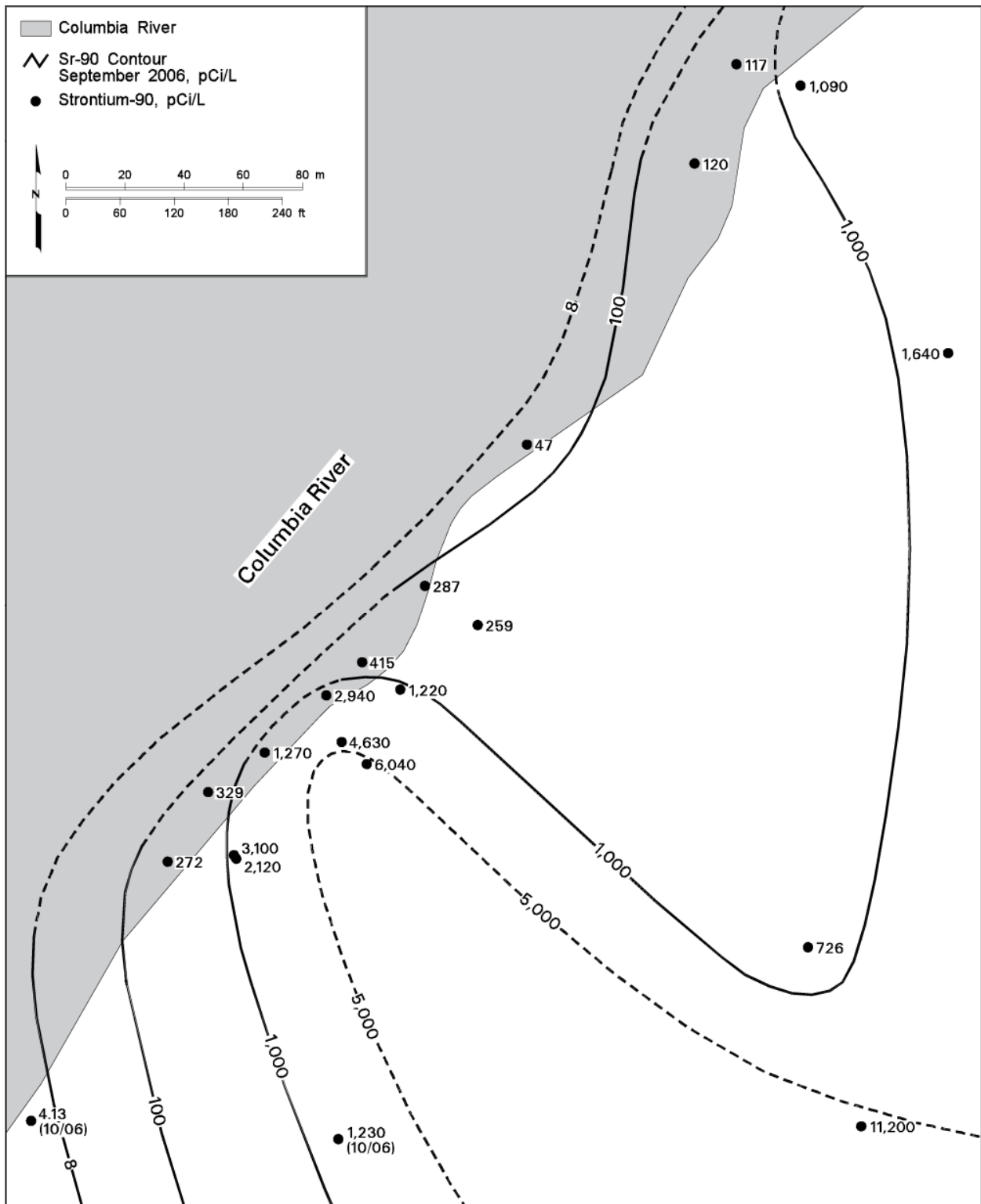


Figure 1.7. Average ^{90}Sr Concentrations in 100-N Area, Upper Part of Unconfined Aquifer (from Hartman et al. 2007)



can_gwf06_156 February 14, 2007 8:48 AM

Figure 1.8. ⁹⁰Sr Distributions Along 100-N Area Shoreline, September 2006 (from Hartman et al. 2007)

The majority of the 1500 curies (Ci) of ^{90}Sr remaining in the unsaturated and saturated zones in the 100-N Area as of 2003 (DOE/RL 2004) is present in the vadose zone above the aquifer. An estimated 72 Ci of ^{90}Sr are contained in the saturated zone, and approximately 0.8 Ci are in the groundwater. Data from soil borings collected along the riverbank indicate that ^{90}Sr concentrations in soil reach a maximum near the mean water table elevation and then decrease with depth (BHI 1995) (see Figures 1.3, 1.8, and 1.9). This vertical contaminant distribution will also be reflected in depth-discrete groundwater concentration data. Because ^{90}Sr has a much greater affinity for sediment than for water (high K_d), its rate of transport in groundwater to the river is considerably slower than the actual groundwater flow rate. The relative velocity of ^{90}Sr to groundwater is approximately 1:100. Under current conditions, approximately 0.14 to 0.19 Ci are released to the Columbia River from the 100-N Area annually (TAG 2001).⁵

In 1995, the ^{90}Sr groundwater plume extended approximately 400 m (1300 ft) along the length of the Columbia River between the 1000 picocuries per liter (pCi/L) contours, and approximately 800 m (2600 ft) between the 8 pCi/L (drinking water standard) contours.^{6,7} The highest concentrations along the shoreline were observed between wells 199-N-94 and 199-N-46. An area of “preferential flow” was identified in the *Technical Reevaluation of the N-Springs Barrier Wall* (BHI 1995) that encompasses 199-N-94, 199-N-95, and 199-N-46. Because of an erosional feature in the Ringold Unit, the Hanford formation dips below the water table at this location, forming a more transmissive flow path between the disposal crib and the Columbia River (Figure 1.5).

N-Springs data from 1985 to 1991 show significantly higher concentrations of ^{90}Sr in seep wells NS-2, NS-3, and NS-4 compared to the adjacent springs upstream and downstream (Figure 1.8) (BHI 1995). Well NS-3 and the neighboring monitoring wells 199-N-46 and 199-N-8T have currently and historically shown the highest ^{90}Sr concentrations along the shoreline, with concentrations as high as 15,000 pCi/L observed at 199-N-46 (TAG 2001; DOE/RL 2004). Recent clam data collected for the ecological risk assessment show the highest concentrations of ^{90}Sr in clams were observed along the approximately 90 m (300 ft) of riverbank that encompasses wells NS-1, NS-2, NS-3 and NS-4 (see NS-galvanized tube locations in Figure 1.3, which are located near the associated seep well). The previous N-Springs, aquifer tube, groundwater, and clam data (DOE/RL 2006) all indicate that treating the 91 m (300 ft) of shoreline near well 199-N-46 will address the highest concentration portion, if not the majority, of the near-shore ^{90}Sr contamination. The targeted length of shoreline is approximately between wells NS-1 and NS-4, as shown in Figure 1.3.

1.6 Field Testing Approach

The objective of the low-concentration, apatite-forming solution injections is to provide an initial, limited capacity treatment that acts to stabilize the ^{90}Sr residing within the treatment zone, while minimizing ^{90}Sr mobilization due to the injection of high-ionic strength solutions. This will be followed by high-concentration injections to provide for long-term ^{90}Sr treatment.

⁵ Technical Advisory Group (TAG). 2001. *Hanford 100-N Area Remediation Options Evaluation Summary Report*.

⁶ Connelly MP. 1999. *Groundwater-River Interaction in the Near River Environment at the 100-N Area*. Innovative Treatment and Remediation Demonstration Program, HydroGeoLogic, Reston, Virginia.

⁷ Innovative Treatment and Remediation Demonstration Program (ITRD). 2001. *Hanford 100-N Area Remediation Options Evaluation Summary Report*. Office of Environmental Management, Subsurface Contaminants Focus Area, Sandia National Laboratories, Albuquerque, New Mexico.

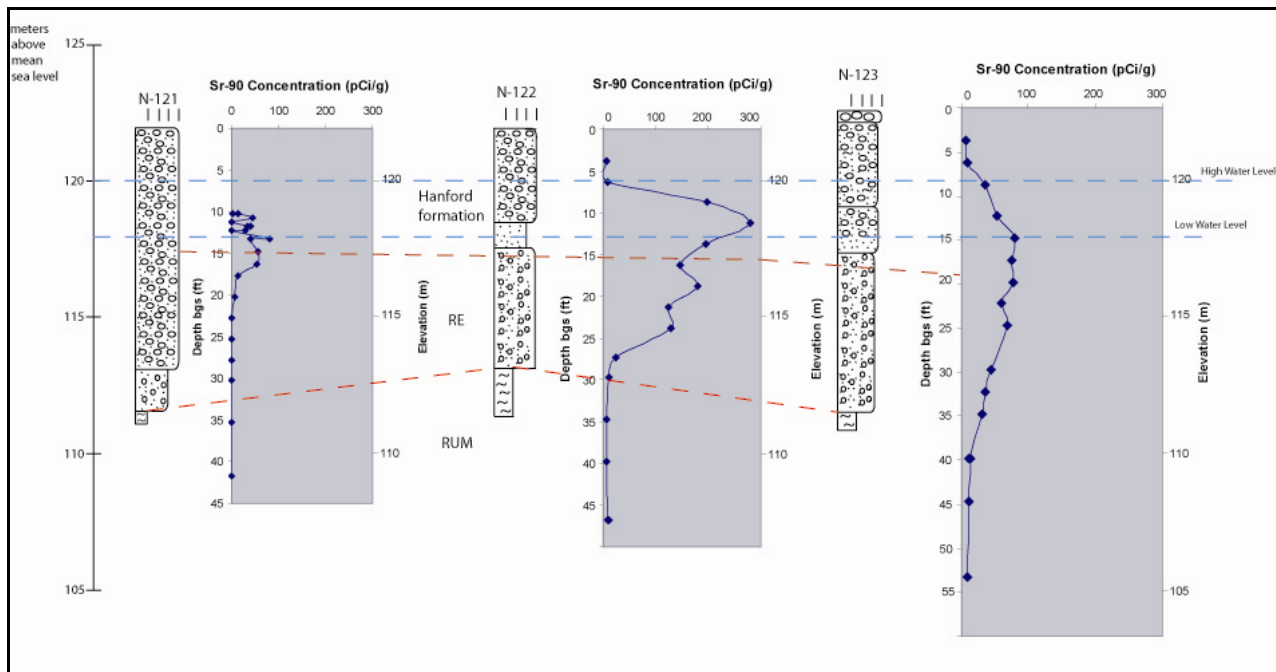


Figure 1.9. ^{90}Sr Profiles from Three Boreholes Along 100-N Area Apatite Treatability Test Site. See Figure 1.1 for borehole locations. Typical water level elevations range from approximately 118 to 120 m above mean sea level.

The injection solution causes temporary increases in aqueous ^{90}Sr concentrations, so this two-step approach—low-concentration injections, followed by high-concentration injections approximately 1 year later—was developed to minimize the ^{90}Sr peaks that occur for a relatively short period following treatment. Two pilot test sites at the east and west ends of the barrier, which are equipped with extensive monitoring well networks, were used for the initial injections to develop the injection design for the remaining portions of the barrier. Conducting pilot tests at both ends of the barrier help to assess differences in hydrogeologic conditions along the 91-m (300-ft) barrier length.

Injections at the treatability test site were timed during high- and low-river stage periods to focus treatment in different portions of the contaminated zone. During this phase of the testing, injection wells were screened across both the Hanford and upper portion of the Ringold Formations. Wells screened only across the contaminated portion of the Ringold Formation are planned for future injections for better efficiency and treatment coverage. Injections conducted during high-river stage periods targeted Hanford formation treatment as a result of the higher permeability of this formation relative the Ringold Formation. High-river stage injections were scheduled in an attempt to take advantage of the highest possible river stage conditions because contaminated sediments also exist above the mean water table elevation and vadose zone (Figure 1.9). The contaminated upper portion of the Ringold Formation is targeted during low-river stage periods to minimize reagent flux to the Hanford formation. As will be discussed in more detail in Section 5.0, based on results from the two pilot injection tests, permeability contrast between the Hanford and Ringold Formations was significantly less over the upstream portion of the barrier, allowing for treatment of the entire Hanford/Ringold screened interval with a single-injection operation at high-river stage.

Two initial characterization wells were installed at the 100-N Area apatite treatability test site in 2005 for detailed aquifer and sediment analysis, including depth-discrete ⁹⁰Sr measurements of the sediment (wells 199-N-122 and 199-N-123; see Figures 1.9 and 1.10). These wells are subsequently used for compliance monitoring. During 2006, 10 injection wells were installed at 9-m (30-ft) spacing intervals for emplacing the 91-m (300-ft) barrier, 17 performance monitoring wells were installed around the two pilot test sites (see Section 4.0), and two additional compliance monitoring wells were installed (199-N-146 and -147; see Figure 1.10).

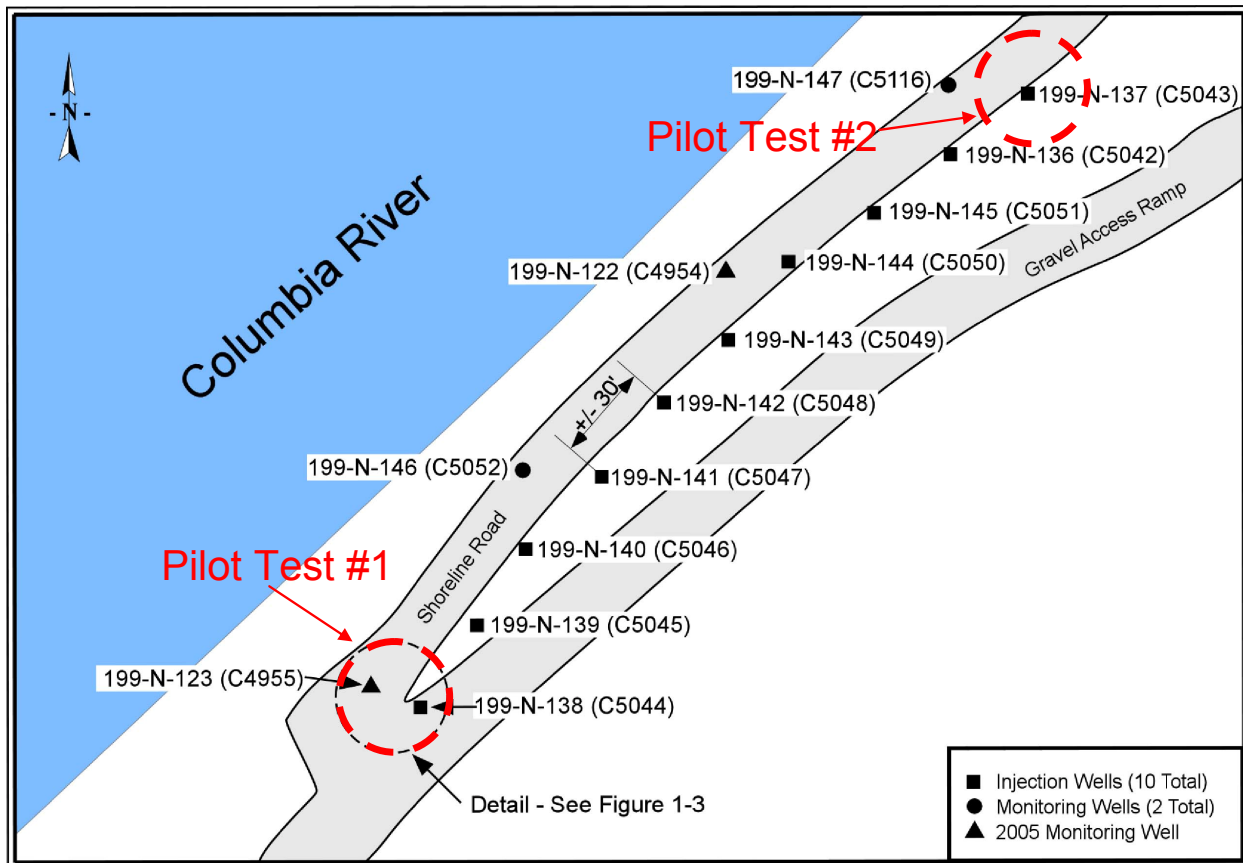


Figure 1.10. 100-N Area Apatite Treatability Test Plan Site Map

Analysis of the operational and early monitoring results of the pilot tests were used to modify the injection solution composition, injection volumes, and operational parameters. A tracer injection test and the first pilot apatite injection test (well 199-N-138) were conducted in the spring of 2006 during high-river stage conditions. A second pilot test at a different well (199-N-137) at the downstream end of the barrier was conducted in September 2006 during low-river stage conditions. Injections in the 10 barrier wells were conducted during two phases: the first in February-March 2007, which was supposed to target low-river stage conditions but resulted in both low- and high-river stage conditions, and a second phase in June-July of 2007 during high-river stage conditions.

2.0 Treatment Technology Description

All technologies considered for ^{90}Sr removal from groundwater at 100-NR-2 use apatite as the sequestering agent, differing only by emplacement method. This section describes apatite in general and the properties that make it a good sequestering agent; includes a description of the different forms of apatite commercially available, and that have been used in bench testing; and provides a detailed description of the aqueous injection technology.

2.1 General Characteristics of Apatite

Apatite [$\text{Ca}_{10}(\text{PO}_4)_6(\text{OH})_2$] is a natural calcium phosphate mineral occurring primarily in the Earth's crust as phosphate rock. It is also a primary component in the teeth and bones of animals. Apatite minerals sequester elements into their molecular structures via isomorphic substitution, whereby elements of similar physical and chemical characteristics replace calcium, phosphate, or hydroxide in the hexagonal crystal structure (Hughes et al. 1989; Spence and Shi 2005). Apatite has been used for remediation of other metals including uranium (Arey et al. 1999; Fuller et al. 2002, 2003; Jeanjean et al. 1995), lead (Bailliez et al. 2004; Mavropoulos et al. 2002; Ma et al. 1995), plutonium (Moore et al. 2005), and neptunium (Moore et al. 2003). Because of the extensive substitution into the general apatite structure (Figure 2.1), over 350 apatite minerals have been identified (Moelo et al. 2000). Strontium incorporation into apatite has also been previously studied (Smiciklas et al. 2005; Rendon-Angeles et al. 2000). Apatite minerals are very stable and practically insoluble in water (Tofe 1998; Wright 1990; Wright et al. 2004). The solubility product of hydroxyapatite is about 10^{-44} , while quartz crystal, which is considered the most stable mineral in the weathering environment, has a solubility product (K_{sp}) of 10^{-4} (Geochem Software 1994). Strontiapatite, $\text{Sr}_{10}(\text{PO}_4)_6(\text{OH})_2$, which is formed by the complete substitution of calcium by strontium (or ^{90}Sr), has a K_{sp} of about 10^{-51} , another 10^7 times less soluble than hydroxyapatite (Verbeeck et al. 1977). The substitution of strontium for calcium in the crystal structure is thermodynamically favorable, and will proceed provided the two elements coexist. Strontium substitution in natural apatites is as high as 11%, although dependent on available strontium (Belousova et al. 2002). Synthetic apatites have been made with up to 40% strontium substitution for calcium (Heslop et al. 2005). The mechanism (solid-state ion exchange) of strontium substitution for calcium in the apatite structure has been previously studied at elevated temperatures (Rendon-Angeles et al. 2000), but low-temperature aqueous rates under Hanford Site groundwater conditions (i.e., calcium/strontium ratio of 220/1) have not.

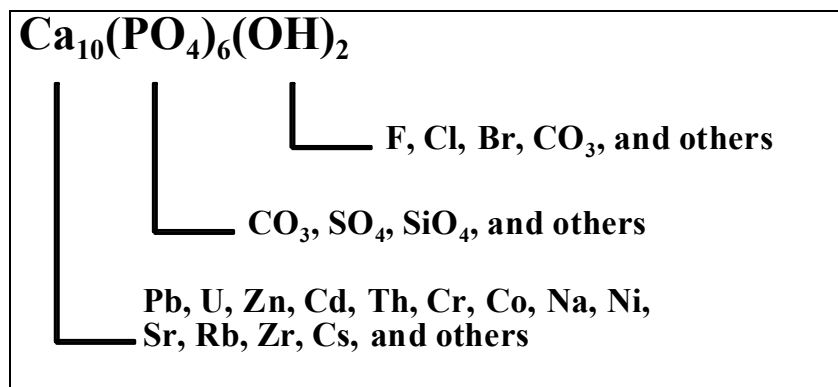


Figure 2.1. Cation and Anion Substitution in Apatite

Apatite can remove soluble strontium and ^{90}Sr from groundwater both during and after its formation:

- Via precipitation of strontium in solution with PO_4 anion (Figure 2.2, < 300 hr). Precipitation directly from solution, or homogeneous nucleation, generally occurs only at very high metal concentrations; that is, greater than 10 parts per million (ppm). However, apatite will act as a seed crystal for the precipitation of metal phosphates at much lower concentrations (Ma et al. 1995). The apatite itself serves as a small but sufficient source of phosphate to solution, and with low concentrations of cations such as strontium or calcium, heterogeneous nucleation occurs on the surface of the apatite seed crystal (Lower et al. 1998). Over time, the precipitated metals are sequestered into the apatite crystal matrix.

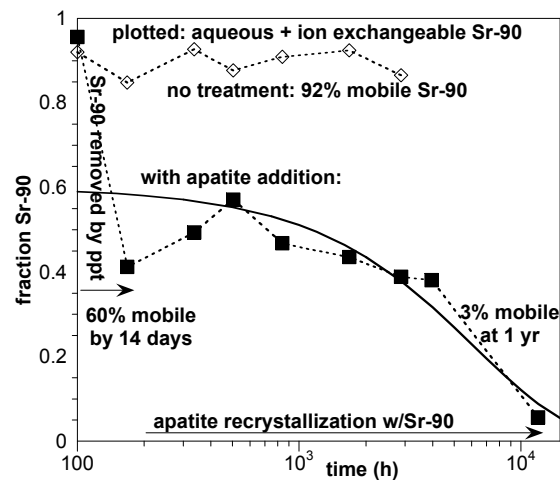


Figure 2.2. ^{90}Sr Aqueous and Ion Exchangeable Fraction in 100-N Area Sediments with No Apatite Addition (diamonds) and with Ca-citrate-PO_4 Solution Addition (squares) to Form Apatite

- Via substitution of strontium into the structure of mineral apatite. Strontium and calcium are both alkaline Earth metals with a 2^+ charge, and both compete for the same lattice sites in the apatite structure (Figure 2.2, time of months to years). Because calcium is more prevalent in the Earth's crust, it is more common in apatite. However, the substitution of strontium for calcium in the crystal structure is thermodynamically favorable, and in the presence of high enough concentrations, strontium will replace calcium.

Although the rate of metal incorporation into the apatite crystal lattice can be relatively slow (on the order of months to years), the precipitation reaction is nearly instantaneous on the molecular scale. Initially, the precipitate formed is amorphous apatite; however, within several days it will transform into a more stable apatite crystal.

Note that stable strontium and other competing cations in groundwater, especially the divalent transition metals (e.g., cadmium, zinc, iron, lead, manganese, etc.), can also be incorporated in the apatite structure. The average concentrations of stable strontium and competing cations present in groundwater will dictate the mass of apatite needed for long-term sequestration. Recent experiments measuring strontium incorporation in apatite from a solution containing only calcium and strontium to groundwater (containing all transition metals) found no difference in the strontium uptake mass (Szecsody et al. 2007, Figure 6.6b).

The effect of competing cation concentrations is to reduce the in situ apatite longevity for a given mass loading. To achieve a desired longevity (e.g., a 300-year period during which most of the ^{90}Sr will have decayed), loading must be increased to account for the competing cation effect.

2.2 Apatite Placement in the Subsurface

Vertical hydrofracture and air injection could be used to emplace solid mineral apatite particles into the subsurface, while in aqueous injection, apatite is precipitated in situ from chemical precursors in aqueous form. The advantage of aqueous injection is that it has the potential to create a larger treatment zone surrounding the point of injection than the other technologies. Various placement technologies have been previously evaluated and described in a project-specific treatability test plan (DOE/RL 2006).

The method of emplacing apatite in subsurface sediments at the 100-N Area is to inject an aqueous solution containing a Ca-citrate complex and Na-phosphate. Citrate is needed to keep calcium in solution long enough (days) to inject into the subsurface; a solution containing Ca^{2+} and phosphate only will rapidly form mono- and di-calcium phosphate, but not apatite (Andronescu et al. 2002; Elliot et al. 1973; Papargyris et al. 2002). Relatively slow biodegradation of the Ca-citrate complex (days) allows sufficient time for injection and transport of the reagents to the areas of the aquifer where treatment is required. As Ca-citrate is degraded (Van der Houwen et al. 2001; Misra 1996), the free calcium and phosphate combine to form amorphous apatite. The formation of amorphous apatite occurs within a week and crystalline apatite forms within a few weeks. Citrate biodegradation rates in Hanford 100-N Area sediments (water saturated) at temperatures from 10°C to 21°C (aquifer temperature 15–17°C) over the range of citrate concentrations to be used (10 to 100 mM) have been determined experimentally and simulated with a first-order model (Bailey and Ollis 1986; Bynhildsen and Rosswall 1997). In addition, the microbial biomass has been characterized with depth and position along the Columbia River shoreline, and the relationship between biomass and the citrate biodegradation rate determined, as described in the results section (see Szecsody et al. 2007, Section 5.1). Because Hanford 100-N Area injections typically use river water (~90–95%) with concentrated chemicals, microbes in the river water are also injected, which results in a somewhat more uniform citrate biodegradation rate in different aquifer zones.

The specific steps of this remediation technology are as follows:

- Injection of Ca- PO_4 -citrate solution (with a Ca-citrate solution complex)
- In situ biodegradation of citrate resulting in apatite $[\text{Ca}_6(\text{PO}_4)_3(\text{OH})_2]$ precipitation and coprecipitation of ^{90}Sr in pore fluid and solids in the treatment zone
- Adsorption of ^{90}Sr by the apatite surface (new ^{90}Sr migrating into the treated zone from upgradient sources)
- Apatite recrystallization with ^{90}Sr substitution for calcium (permanent)
- Radioactive decay of ^{90}Sr to ^{90}Y to ^{90}Zr .

Emplacement of apatite precipitate by a solution injection has significant advantages over other apatite emplacement technologies for application at the Hanford 100-N Area. The major advantage is minimal disturbance of the subsurface (both vadose and saturated zone) because this technology only requires injection wells (for groundwater remediation) or a surface infiltration gallery (for vadose zone

treatment), in contrast with excavation of the riverbank for trench-and-fill emplacement of solid-phase apatite. Other apatite emplacement technologies were also considered for the 100-N Area (DOE/RL 2006), which included pneumatic injection of solid apatite, and vertical hydrofracturing for apatite emplacement. Although each technology has advantages and disadvantages, the Ca-citrate-PO₄ injection technology was chosen because it provides the most economic emplacement methodology to treat ⁹⁰Sr in the near-shore sediments. A weakness of all of these apatite technologies is the ⁹⁰Sr is not removed from the sediment until radioactive decay occurs, as the ⁹⁰Sr is incorporated into the apatite crystalline structure. For the remedy, a solution such as the one presented in Table 2.1, is prepared and then injected into the formation. As indigenous microorganisms degrade the citrate (this is an easily metabolized carbon source), the resulting increase in free calcium will result in precipitation of calcium phosphate solids in the aquifer. If successful, the net effect of the treatment would be to decrease contaminant flux to the Columbia River by sequestering ⁹⁰Sr within the treatment zone.

Table 2.1. Apatite Mass and Change in ⁹⁰Sr Mobilization

System	Injected PO ₄ (mM)	g Apatite/ g Sediment	Predicted ^(a) ⁹⁰ Sr (pCi/L) w/Sorption only	Predicted ^(a) ⁹⁰ Sr (pCi/L) w/Incorporation
Groundwater	0.0	0.0	1000	1000
Field inj. #1, #2	2.4	9E-5	999	165
Field inj. #3-10	10	3.8E-4	974	44
Max. single inj.	24	9E-4	928	18
300-yr capacity	90	3.4E-3	767	4

(a) Assumptions: 1000 pCi/L initially in groundwater; Sr/sediment Kd = 25 cm³/g, Sr/apatite = 1370 cm³/g, 10% Sr substitution for Ca in apatite.

2.3 Mass of Apatite Needed for Hanford 100-N Area

Two factors control the amount of apatite needed to sequester ⁹⁰Sr in the Hanford 100-N Area. First, from a mass-balance viewpoint, a specific amount of apatite is needed that will remove all strontium and ⁹⁰Sr from groundwater over the next 300 years (i.e., 10 half lives of ⁹⁰Sr decay, half-life 29.1 years). This calculation is dependent on the crystal substitution of strontium for calcium in apatite. If 10% substitution is assumed, then 1.7 mg of apatite is sufficient to sequester strontium and ⁹⁰Sr from the estimated 3300 pore volumes of water that will flow through an apatite-laden zone. This calculation assumes an average groundwater flow rate of 0.3 m/day (1 ft/day) and a 10-m (32-ft)-thick apatite-laden barrier. The 1.7-mg apatite/g of sediment does occupy some pore space in the aquifer, which has an average field porosity of 20%. Given crystal lattice dimensions of 9.3A by 6.89 A (assume a cylinder of dimensions 7.5E-21 cm³/atom), the 1.7 mg apatite/g sediment would occupy 13.6% of the pore space, so there should be some decrease in permeability.

The second factor that would control the amount of apatite needed to sequester ⁹⁰Sr is the rate of incorporation. This PRB concept of apatite solids in the aquifer is viable only if the natural groundwater flux rate of strontium and ⁹⁰Sr (1.36 x 10⁻⁶ mmol strontium/day/cm²) is slower than the removal rate of strontium and ⁹⁰Sr by apatite. If the groundwater flow rate is too high, even highly sorbing Sr and ⁹⁰Sr could advect through the apatite-laden zone more quickly than it is removed. The way to circumvent this issue is to have additional apatite in the groundwater system (i.e., greater than the amount needed from the mass balance calculation above) to essentially remove ⁹⁰Sr at an increased rate. Based on experience in the 100-D Area, where partially reduced sediment is slowly removing chromate (and nitrate), seasonal

fluctuations in the river level lead to specific times of year when flow in the aquifer exceeds the chromate removal rate of the reduced sediment. Therefore, numerous experiments have been conducted in this study to clearly define the rate at which strontium and ^{90}Sr is incorporated into the crystal structure of apatite.

Because strontium and ^{90}Sr interact with apatite by two processes (sorption by ion exchange and incorporation into sediment), the effect of adding a small amount of apatite to sediment and the subsequent change in both sorption and incorporation can be calculated (Table 2.1). These calculations assume no $\text{Sr}/^{90}\text{Sr}$ is incorporated into apatite during the initial precipitation (experiments show 25 to 40% incorporated).

These calculations show that even though the strontium sorption to apatite is very high ($K_d = 1370 \text{ cm}^3/\text{g}$ or 55 times greater than to sediment), because the mass of apatite is so small (as precipitate in pore space of sediment), the resulting sorption of strontium and ^{90}Sr onto apatite/sediment is small. The net effect is that right after apatite is placed in sediment (i.e., weeks), there will be little observed decrease in the ^{90}Sr . However, over months strontium and ^{90}Sr are slowly removed, and the amount of incorporation (10% crystal substitution of strontium for calcium in apatite is assumed in these calculations) is fairly significant. Even the 2.4 mM of PO_4 injected in field injections 1 and 2 should eventually result in an 8 times decrease in the ^{90}Sr concentration (after 6–12 months). This small amount of apatite will be exhausted after a few years, so additional apatite would be needed. A sequential low-concentration injection, followed by a 6-12 month wait, then one or more high-concentration injections are proposed (as described in Section 2.5) to emplace enough apatite for 300 years of capacity but minimize the initial desorption of ^{90}Sr in the injection zone. Strontium and ^{90}Sr sorption in field systems containing sediment only (no apatite) have 99.2% of the strontium sorbed on the surface by ion exchange (Table 2.2, line 1). With the amount of apatite precipitated from field injections #3 to #18 (10 mM PO_4 injected, 0.38 mg apatite/g sediment, line 2, Table 2.2), 97.2% of the strontium is now sorbed on the sediment and 2% on the apatite, even though on an equal per gram basis, strontium sorbs 55 times more strongly on apatite. With the final field design amount of apatite emplaced (3.4 mg apatite/g sediment), 17% of the strontium would sorb to apatite (line 3, Table 2.2).

Table 2.2. ^{90}Sr Sorption Fraction in Field System Containing Sediment and Apatite

System/Mass								Ion Exchange Equilibrium		
System	#	Kd, apa (cm^3/g)	Kd, sed (cm^3/g)	Apatite Mass (g)	Sediment Mass (g)	Vol (mL)	Fraction Aqueous	Fraction Sorbed on Apatite	Fraction Sorbed on Sediment	Fraction Sorbed Total
Sr/sed only	1	1350	25	0	1.0	0.2	0.0079	0.0000	0.9921	0.9921
Sr/sed/apatite	2	1350	25	0.00038	1.0	0.2	0.0078	0.0200	0.9723	0.9922
Sr/sed/apatite	3	1350	25	0.0038	1.0	0.2	0.0066	0.1691	0.8243	0.9934

2.4 Strontium and Strontium-90 Incorporation Rate into Apatite

Because Sr^{2+} and ^{90}Sr behave essentially the same as Ca^{2+} , some strontium and ^{90}Sr are incorporated in apatite during the initial precipitation. Thermodynamically strontiapatite [$\text{Sr}_{10}(\text{PO}_4)_6(\text{OH})_2$, $K_{sp} = 10^{-51}$] is favored relative to hydroxyapatite [$\text{Ca}_{10}(\text{PO}_4)_6(\text{OH})_2$, $K_{sp} = 10^{-44}$]. However, the more rapid the apatite precipitation is, the calcium/strontium ratio in the crystalline structure will simply reflect the calcium/strontium ratio in the solution. Therefore, while it is relatively easy to make 40% strontium-substituted apatite from a solution containing 40% strontium, the Hanford Site groundwater calcium/strontium ratio

is 220:1. Results in this report show that the amount of strontium substitution into apatite during the initial precipitation is far greater than 0.4% (1/220) and is generally in the 30 to 40% range, so it reflects the influence of thermodynamics on the slow precipitation.

Once solid-phase apatite is precipitated, strontium and ^{90}Sr will additionally be incorporated into the apatite structure by solid-phase dissolution/recrystallization, as described below. The initial step in this process is strontium and ^{90}Sr sorption to the apatite surface. Results in this study show this sorption is quite strong ($K_d = 1370 \pm 439 \text{ L/kg}$) or 55 times stronger affinity than to sediment ($K_d = 24.8 \pm 0.4 \text{ L/kg}$). The rate of metal incorporation into the apatite crystal lattice can be relatively slow, on the order of days to years (LeGeros et al. 1979, 1991; Vukovic et al. 1998; Moore et al. 2003, 2005). While there have been several studies of this strontium-substitution rate into apatite (Hill et al. 2004; Lazic and Vukovic 1991; Raicevic et al. 1996; Heslop et al. 2005; Koutsoukos and Nancollas 1981), geochemical conditions differ from the application in groundwater at the 100-N Area. However, in the presence of soluble phosphates, apatite acts as a seed crystal for the precipitation of metal phosphates (Vukovic et al. 1998). Homogeneous nucleation (precipitation directly from solution) will generally not occur except at very high-metal concentrations; e.g., greater than 10 ppm. However, at low concentrations of the substituting cation (such as calcium) and in the presence of small amounts of phosphate and a seed crystal of apatite, heterogeneous nucleation occurs on the surface of the apatite seed crystal (Lower et al. 1998). The apatite itself serves as a small, but sufficient source of phosphate to solution, and thus perpetuates the precipitation reaction. Over time, the precipitated metals are sequestered into the apatite crystal matrix. The mechanism (solid-state ion exchange) of strontium substitution for calcium in the apatite structure has been studied at elevated temperatures (Rendon-Angeles et al. 2000), but low-temperature aqueous rates under Hanford Site groundwater conditions (i.e., calcium/strontium ratio of 220/1) have not been studied.

The amount of ^{90}Sr incorporation into solid-phase apatite has been characterized in previous studies by various methods. The most reliable types of studies that prove the phenomena use pure apatite in a solution containing a specific strontium concentration, and the apatite solid phase is analyzed for percent strontium substitution by 1) dissolution and aqueous strontium or ^{90}Sr analysis, or 2) electron microprobe with energy dispersive spectroscopy (EDS) or elemental detection of strontium. Analysis of the remaining strontium and ^{90}Sr aqueous concentration in an apatite/water system is insufficient to determine if $\text{Sr}/^{90}\text{Sr}$ has been incorporated into apatite. However, if the $\text{Sr}/^{90}\text{Sr}$ aqueous concentration and ion-exchangeable strontium concentrations are analyzed, the remaining $\text{Sr}/^{90}\text{Sr}$ must be incorporated into the apatite structure.

Therefore, sequential extractions of selected chemical extraction were used to remove ion-exchangeable ^{90}Sr , organic-bound ^{90}Sr , carbonate-bound ^{90}Sr , and remaining (residual) ^{90}Sr . Both strontium and ^{90}Sr were analyzed in extractions to determine whether the strontium was retained differently from the ^{90}Sr . It was expected that strontium was geologically incorporated into many different sediment minerals (Belousova et al. 2002), so they should be more difficult to remove than ^{90}Sr , which was recently added to the systems. The ion-exchangeable extraction consisted of adding 0.5M KNO_3 to the sediment sample for 16 hours (Amrhein and Suarez 1990). The organic-bound extraction conducted after the ion-exchangeable extraction consisted of 0.5M NaOH for 16 hours (Sposito et al. 1982). The carbonate-bound extraction conducted after the organic-bound extraction consisted of adding 0.05M Na_3EDTA for 6 hours (Sposito et al. 1983a,b; Steefel 2004). The residual extraction conducted after the carbonate-bound extraction consisted of adding 4M HNO_3 at 80°C for 16 hours (Sposito et al. 1983a,b).

Apatite dissolution rates are highest at low pH (Chairat et al. 2004), so this extraction is expected to remove ^{90}Sr that is incorporated into the apatite.

2.5 Strontium-90 Initial Mobilization and Sequential Injection Strategy

Because ~90% of the Sr and ^{90}Sr in the 100-N Area sediments is held by ion exchange, any solution that is injected into the aquifer (or infiltrating into the vadose zone) that has a higher ionic strength relative to groundwater (11.5 mM) and/or proportionally higher percentage of divalent cations will cause strontium and ^{90}Sr to desorb from sediments. At the 100-N Area pH (~7.8), the strontium Kd value is ~15 L/kg, or an approximate retardation factor of 125 (i.e., ~99% of the strontium and ^{90}Sr mass is sorbed). As described in the pilot testing section (Section 5.0) of this report, injection of a low concentration of the Ca-citrate- PO_4 (4, 10, 2.4) solution results in a ~10 times increase in strontium and ^{90}Sr aqueous concentration. Injection of a much higher-concentration Ca-citrate- PO_4 (40, 100, 24) solution results in about a 50-times increase in strontium and ^{90}Sr aqueous concentration. Injection of a Ca-citrate- PO_4 solution at the field scale will mobilize some strontium and ^{90}Sr in the injection zone (~3% of the sorbed ^{90}Sr mass for a low Ca-citrate- PO_4 concentration injection), and less ^{90}Sr for the zone that the spent solution migrates through. As described in Section 2.3, a total mass of ~1.7 mg apatite per gram of sediment is needed (assuming 10% strontium substitution for calcium in apatite) to sequester ^{90}Sr for 300 years (i.e., ~10 half lives of the ^{90}Sr decay with a half-life of 29.1 years). This mass of apatite is equivalent to injections totaling 90 mM PO_4 .

To emplace the total amount of phosphate needed to achieve sufficient ^{90}Sr sequestration capacity and minimize ^{90}Sr mobilization during the injections, a sequential injection strategy can be used. Injection of a low concentration of the Ca-citrate- PO_4 (1, 2.5, 10) solution will cause a small increase in the strontium and ^{90}Sr during the weeks of emplacement (~5 times increase in aqueous concentration). Over the time scale of 6 to 12 months, most of the ^{90}Sr in the injection zone will be incorporated into the apatite structure. This relatively low-concentration injection has some capacity to incorporate ^{90}Sr but insufficient capacity to sequester ^{90}Sr that is upgradient of this apatite-laden zone and slowly migrating toward the Columbia River over the next 300 years. After the time interval to sequester the local ^{90}Sr in the injection zone, then one or more higher concentration Ca-citrate- PO_4 (1, 25, 100, for example) can be injected with minimal ^{90}Sr mobilization. These sequential experiments have been successfully conducted in the laboratory, and should work at the field scale for a system with a downgradient injection zone (where apatite is emplaced) with most of the ^{90}Sr mass upgradient of the apatite-laden zone. One zone that would be difficult to manage at the field scale is the aquifer zone downgradient of the injection zone (i.e., between the injection wells and the Columbia River). If the low-concentration Ca-citrate- PO_4 injections are designed such that the solution is leaching out into the river, then apatite precipitate should occur all the way to the riverbank sediments, and there will be an initial ~5 times increase in aqueous ^{90}Sr and a subsequent decrease (over months) in aqueous ^{90}Sr . However, if the low-concentration injections do not reach the river edge, there will be ^{90}Sr mass in the near-river sediment held only by ion exchange (i.e., zone where the solution did not reach). Later high-concentration injections will mobilize this ^{90}Sr , resulting in high ^{90}Sr peak concentrations in groundwater for a short period of time while the injected/spent solution slowly leaches out into the river. This result may be mitigated to some extent by the presence of Coyote willows along the riverbank (i.e., the active bioremediation), which if emplaced for the first few years during the apatite injections, could limit ^{90}Sr transport into the river.

2.6 Calcium Citrate-Phosphate Solutions

This technology uses a Ca-citrate-PO₄ solution that does not precipitate until the citrate is biodegraded. The composition of this solution has changed over time, reflecting: 1) increasing utilization of available Ca²⁺ from groundwater (and on ion exchange sites) rather than injecting all the Ca²⁺ needed, and 2) minimizing strontium and ⁹⁰Sr ion-exchange release from sediments upon injection. Initially, the solution composition did not reflect utilization of Ca²⁺ from groundwater or ion-exchange sites, so the solution injected for field injection #1 used a higher concentration of calcium chloride [[CaCl₂*2H₂O] and trisodium citrate [HOC(COONa)(CH₂COONa)²*2H₂O] compared to later injections. When combined, the solution at this low concentration is stable for days, depending on whether microbes are present in the makeup water (i.e., citrate biodegrades).

2.6.1 Solution for Field Pilot Test #1

The field injections of 227,000 to 529,800 L (60,000 to 140,000 gal) (each) delivered the solution to each well using concentrated mixtures of calcium chloride and trisodium citrate (called solution 1, in one tanker truck) and a second solution of the phosphates and nitrate (called solution 2, in a second tanker truck), and Columbia River water. The maximum concentration that can be used also depends on the makeup of the water. In a laboratory setting with deionized water, a 80 mM Ca, 200 mM citrate, and 50 mM PO₄ solution is stable for ~12 hours at room temperature. Stability of the solutions utilized at the field scale was tested in the laboratory, and solution 1 (56 mM Ca, 140 mM citrate) and solution 2 (28 mM phosphates and 14 mM nitrate) mixed up in deionized water were stable at 4°C for 7 days (Table 2.3). The mixture of phosphates defines the final pH of 7.5. The solutions were refrigerated to minimize microbial growth. The mixing of solution 1, solution 2, and Columbia River water is done at the well head continuously during injection. This Ca-citrate-PO₄ (4, 10, 2.4) solution has an ionic strength of 99.5 mM, which is 8.6 times that of groundwater.

2.6.2 Solution for Field Pilot Test #2

Based on laboratory experiments described in Szecsody et al. (2007) and results from the first pilot-scale field test, the solution composition was reduced to half of the calcium chloride and half of the sodium citrate concentrations, given the significant amount of calcium available from exchanging off of the sediments. In addition, it was determined that less nitrogen was needed (and as ammonium rather than nitrate) for biodegradation, so diammonium phosphate was used instead of multiple sodium phosphates and separate ammonium nitrate. This Ca-citrate-PO₄ (2, 5, 2.4) solution has an ionic strength of 60.7 mM, which resulted in less strontium and ⁹⁰Sr ion exchange during injection, compared with the solution used in field injection #1.

2.6.3 Solution for Field Injections #3 to #18

Further laboratory experiments described in Szecsody et al. (2007) and results from the second pilot-scale field test showed apatite precipitation would occur with even lower calcium chloride and sodium citrate injection concentrations. Because significantly more PO₄ mass was needed for the ultimate capacity of 300 years to sequester ⁹⁰Sr than the 2.4 mM PO₄ (see background section), the solutions used in field injections 3 to 18 had 10 mM PO₄, or four times that of field injections #1 and #2. Laboratory experiments showed that the initial strontium and ⁹⁰Sr ion exchange would be about the same as field pilot test #2. An additional change was to decrease the amount of ammonium due to the ion-exchange affinity.

While the major divalent cations (Ca^{2+} , Mg^{2+} , Sr^{2+}) had roughly the same ion-exchange affinities, the monovalent cations differed. Na^+ had half the affinity of Ca^{2+} , but both K^+ and NH_4^+ had significantly higher affinities relative to Na^+ . Therefore, there is less ion exchange if Na^+ is used instead of NH_4^+ .

Table 2.3. Composition of Calcium Citrate-Phosphate Solutions Used for Field Injections

Name (conc. in mmol/L)	Composition ^(a)	pH	Max. Solubility ^(b)	Ionic str. (mM)	Field Use
Ca-citrate- PO_4 (4, 10, 2.4)	Solution 1: 4.0 mM calcium chloride 10 mM trisodium citrate Solution 2: 2.0 mM disodium phosphate 0.4 mM sodium phosphate 1.0 mM ammonium nitrate	7.5 ± 0.1	56 mM 140 mM 28 mM 14 mM	99.5	Field injection #1
Ca-citrate- PO_4 (2, 5, 2.4)	Solution 1: 2.0 mM calcium chloride 5.0 mM trisodium citrate Solution 2: 2.4 mM diammonium phosphate 1.0 mM sodium bromide	8.0 ± 0.1	40 mM 100 mM 480 mM 200 mM	60.7	Field injection #2
Ca-citrate- PO_4 (1, 2.5, 10)	Solution 1: 1.0 mM calcium chloride 2.5 mM trisodium citrate Solution 2: 8.1 mM disodium phosphate 1.4 mM sodium phosphate 0.5 mM diammonium phosphate 1.0 mM sodium bromide	7.8± 0.1	48 mM 120 mM 526 mM 91 mM 32 mM 65 mM	84.5	Field injections #3 to #18 (2/07 to 4.07)
100-N Area groundwater	1.3 mM Ca, 0.2 mM K, 0.54 mM Mg, 1.1 mM Na, 0.60 mM Cl 0.69 mM SO_4 2.72 mM HCO_3	7.7-8.3		11.5	
(a) Concentrations listed are for the final mix of solutions 1 + 2.					
(b) Tested solubility in complete solution.					

2.7 Other Chemical Effect Issues

Bench tests conducted in previous years (described in Section 3.0) were conducted to evaluate in situ apatite formation and its effectiveness, identify any unintended consequences, and address concerns raised during public briefings and workshops.

2.7.1 Diesel-Related Chemical Effects

A large diesel spill occurred just upstream from the ^{90}Sr plume area during the 1960s. As much as 0.3 m (1 ft) of floating product was observed in nearby monitoring wells in the past (e.g., 199-N-18). Currently, only a thin film of free product remains; however, elevated dissolved iron (up to 24,000 $\mu\text{g/L}$) and depleted oxygen occurs in well N-18, indicating reducing conditions in the aquifer impacted by the diesel spill. Also, depleted oxygen and elevated iron in shallow aquifer tubes near the shoreline in front of the past spill area were found during summer 2005. A question was raised during the October 2005 public workshop on possible effects of the diesel and related degradation byproducts on the proposed apatite treatment remedy.

One possible impact considered was competition of the dissolved iron for the sequestration sites in the emplaced apatite. Although this is theoretically possible, the specific impact of dissolved iron on apatite performance has not been evaluated. However, a monitoring well (199-N-96A) located near the riverbank at the center of the past diesel spill site indicates a maximum dissolved iron concentration of ~100 µg/L occurred in the past with less than 50 µg/L in 2005. Thus, it is unlikely that dissolved iron concentrations in the proposed treatment zone will be higher than in well 199-N-96A. Laboratory studies will be needed to evaluate the long-term implications of diesel and potentially elevated dissolved iron. (Note: Dissolved iron, both ferrous and ferric, were measured in purge water samples from new wells 199-N-122 and 199-N-123 during a vertical velocity profile test in December 2005. All samples were less than 10 µg/L)

2.7.2 Water Quality Impacts

The chemical byproducts from the apatite precipitation process include simple salts (sodium and calcium chloride) and small amounts of agricultural-type chemicals (sodium phosphate and ammonium nitrate) and any remaining unreacted calcium citrate. The initial field tests were conducted using more dilute solutions (nominally 0.01 molar) than used for initial laboratory studies (~0.1 molar). Thus, a conservative approach will be used during the initial field treatability testing. The array of existing aquifer tubes at the shoreline covering the planned 91-m (300-ft) treatment zone will be used to monitor concentrations of reaction products. Dilution by river water is expected to greatly reduce the salt concentrations at the river-riverbed interface. The nonhazardous nature of these food (e.g., citrate) and agricultural-type chemicals are highly unlikely to have a negative impact on the near-shore biota. The residual chemical plume from the treatment zone will occur as a temporary pulse that will dissipate and mix with river water in the stream bank storage zone and as it discharges through the riverbed gravels. Citrate biodegradation during these injections will result in temporary reducing conditions at the site. The reducing conditions will result in decreased dissolved oxygen (DO) concentrations and increases in redox-sensitive trace metal concentrations (e.g., iron, manganese, and aluminum). These concentrations are expected to return to baseline conditions after the injection plumes dissipate. Evaluation of the monitoring data from the aquifer tubes will be used to guide future treatment regimes and injection protocol.

2.7.3 Creation of a New Buried Waste Site

Long-term accumulation of ⁹⁰Sr by the apatite emplaced along the shoreline could be considered creation of a new buried waste site along the Columbia River. The objective of the sequestration barrier is to fix the migrating ⁹⁰Sr in place and thereby reduce the flux to the near-shore zone. Accumulation of ⁹⁰Sr in the treated zone represents trading continued exposure of near-shore biota for fixation of the contaminant where it is not in contact with biota. One important mitigating factor is the shoreline along the central portion of the ⁹⁰Sr plume is protected with rip-rap and is therefore protected from major erosional events. Thus, it is highly unlikely the buried apatite could be eroded, even under extreme hydrologic event scenarios.

In addition, the shoreline is already contaminated with ⁹⁰Sr so it is not really a question of creating a new buried waste site. The only difference will be the capture of ⁹⁰Sr in aquifer pore fluid that passes through the barrier and remains in the treatment zone until it decays to insignificant amounts. For example, the total amount currently estimated in the aquifer is about 0.8 Ci. If this amount is captured in the volume of aquifer sediment treated by the in situ apatite PRBs, the resulting average concentration would be approximately 200 pCi/g (for a 91-m [300-ft] barrier emplacement). This concentration is not

much higher than concentrations currently observed in shoreline sediments. Considering decay, there would be less than 20 pCi/g left in 100 years, which is near the cleanup standard. The issue of whether this constitutes a new waste site that needs a Waste Information Data System (WIDS) designation can be evaluated, if necessary, for the final remedy.

3.0 Aqueous Injection Bench Studies

This section describes the laboratory-scale studies that were conducted to investigate remediation of ^{90}Sr in 100-N Area sediments using a Ca-citrate- PO_4 solution to form apatite precipitate, which incorporates the ^{90}Sr in its structure (Szecsody et al. 2007). In situ apatite formation by this technology occurs by 1) injection of Ca- PO_4 -citrate solution (with a Ca-citrate solution complex), and 2) in situ biodegradation of citrate, which slowly releases the calcium required for apatite [$\text{Ca}_5(\text{PO}_4)_3(\text{OH})$] precipitation (amorphous, then crystalline). Because the injection solution has a higher ionic strength than groundwater, some strontium and ^{90}Sr desorption from sediment occurs (i.e., ^{90}Sr in groundwater increases during injections). Therefore, a primary objective of these laboratory studies is to develop a method to deliver sufficient apatite into subsurface sediments but minimize ^{90}Sr initial mobility. This can be accomplished by sequential injections of low-, then high-concentration Ca-citrate- PO_4 solutions. Injection of a low-concentration Ca-citrate- PO_4 solution results in minimal ^{90}Sr mobilization (groundwater ^{90}Sr concentration increases <6 times relative to preinjection concentration), but results in a small amount of precipitate that, over the course of a year, will incorporate ^{90}Sr in the immediate injection area. After most of the ^{90}Sr is incorporated, one or more high-concentration Ca-citrate- PO_4 solution injections can then be used to increase the apatite mass in the subsurface but have minimal increase in ^{90}Sr groundwater concentration.

Laboratory results are organized in the following sections:

- 3.1, “Sequential Injection of Ca-Citrate- PO_4 to Form Apatite and Sequester ^{90}Sr ”
- 3.2, “Initial Low Ca-Citrate- PO_4 Concentration Injection Experiments”
- 3.3, “Techniques for Measuring Barrier Performance at Field Scale”
- 3.4, “Long Term ^{90}Sr Incorporation Mass and Rate into Apatite”
- 3.5, “Additional Injections to Increase In Situ Apatite Mass.”

3.1 Sequential Injection of Ca-Citrate- PO_4 to Form Apatite and Sequester Strontium-90

Small one-dimensional column experiments were conducted to measure the amount of ^{90}Sr mobilized by injection of a Ca-citrate- PO_4 solution compared to Hanford Site groundwater. Batch studies showed that strontium (and ^{90}Sr) $K_d = 25.96 \pm 0.89 \text{ cm}^3/\text{g}$ in Hanford Site groundwater (<4-mm size fraction of 100-N Area composite sediment). For a baseline of strontium behavior in sediments, two one-dimensional columns were used in which ^{85}Sr was added to the sediment and allowed to equilibrate for several days; injection of Hanford groundwater resulted in a K_d of 11.8 and 9.1 cm^3/g (i.e., $R_f = 61$ and 47.6, respectively; one is shown in Figure 3.1a). In comparison, injecting a low-concentration Ca-citrate- PO_4 solution (10 mM citrate, Figure 3.1b) caused initial peaking desorption of ^{85}Sr , and a higher concentration Ca-citrate- PO_4 solution (70-mM citrate, Figure 3.1c) caused a higher ^{85}Sr peak and greater mass to be eluted. Ninety days after the 10-mM citrate (Ca-citrate- PO_4) treatment, 53% of the ^{85}Sr was incorporated into apatite and did not elute (i.e., Figure 3.1d versus 3.1b). This mass of elution (47% of the ^{85}Sr) was the same after 125 days (after the 10-mM citrate treatment), and 70-mM citrate (Ca-citrate- PO_4) was injected (Figure 3.1e), which shows that sequential low, then high-concentration injections of Ca-citrate- PO_4 can be used to minimize the initial ^{90}Sr mobility but still deliver sufficient PO_4 to form enough

apatite for long-term ^{90}Sr sequestration. There are limitations in these small experiments, with the sample collection size somewhat large relative to the breakthrough shape of the peak, so some of the peak shape is lost.

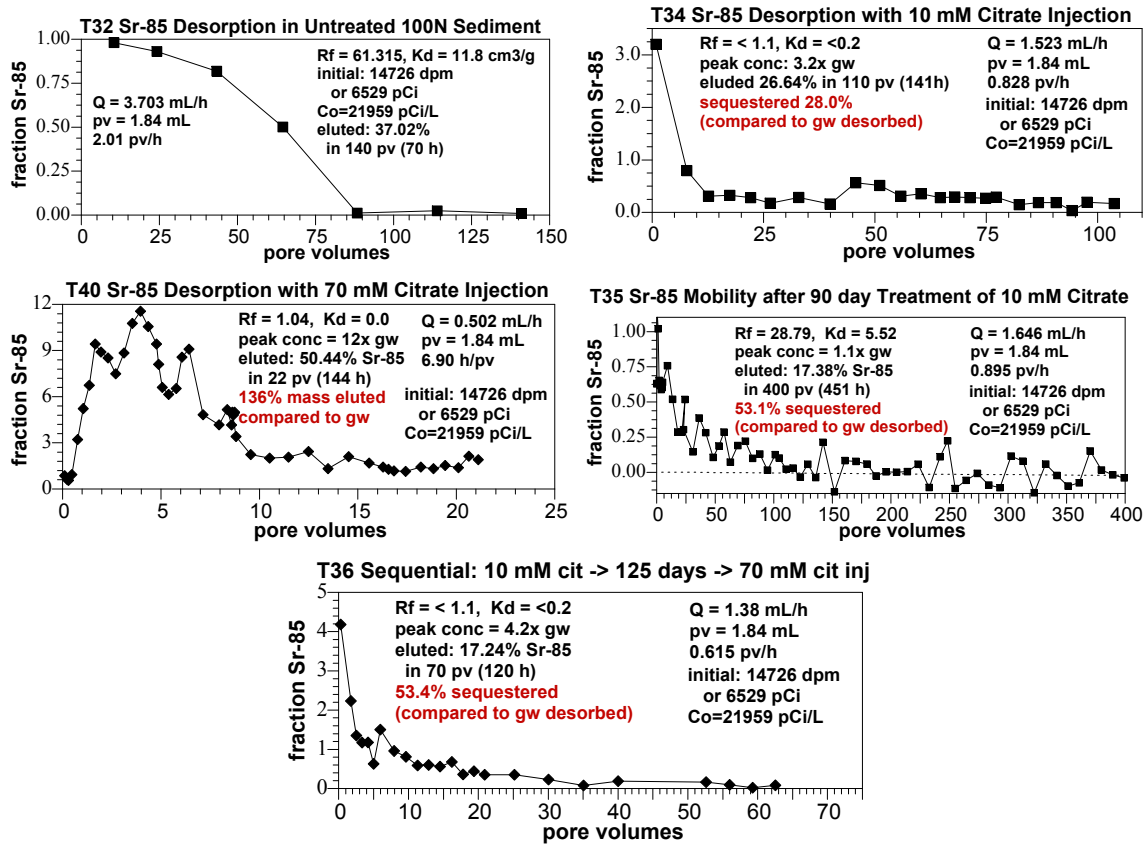
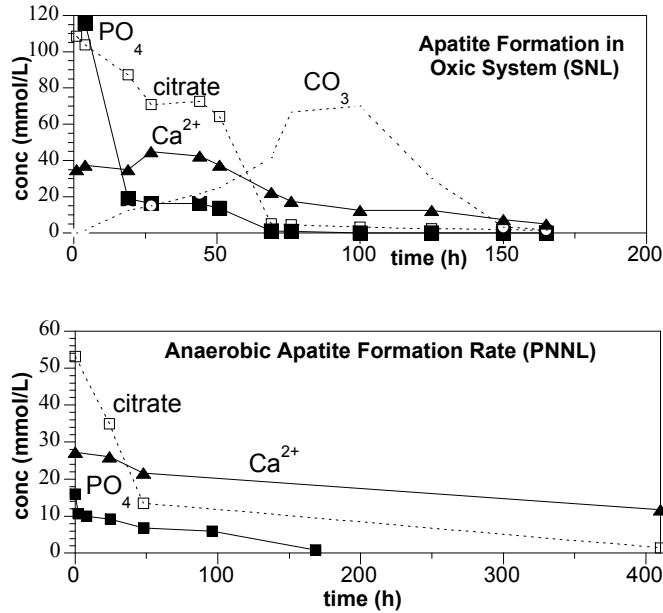


Figure 3.1. ^{85}Sr Desorption in a One-Dimensional Column with Ca-Citrate- PO_4 Injection

Subsequent experiments use significantly larger (0.9-m to 6-m [3- to 20-ft]) columns to minimize this problem. The general nature of the breakthrough curve shape is shown with a higher concentration ^{85}Sr initial peak and a higher concentration injection of Ca-citrate- PO_4 .

3.1.1 Citrate Biodegradation Rate

The first step in apatite formation from injection of Ca-citrate- PO_4 solution is the biodegradation of citrate. Citrate is used to complex calcium during injection (to prevent immediate precipitation of mono- and di- Ca-PO_4) and to control the precipitation process, which appears to lead to a more uniform apatite precipitate. This may be associated with the citrate increasing biomass and microbes nucleating apatite. Within a few days of Ca-citrate- PO_4 solution contact with sediment, biodegradation of the citrate occurs in both aerobic and anaerobic environments (Figure 3.2). Upon citrate biodegradation in aerobic (Figure 3.2a) and anaerobic systems (Figure 3.2b), the aqueous Ca^{2+} and PO_4 decrease, forming apatite and other Ca-PO_4 precipitates which, over several weeks, recrystallize into apatite. In aerobic systems, citrate is mineralized (i.e., forms CO_2 as shown in Figure 3.2b), whereas in an anaerobic environment, citrate degrades to some lower molecular weight organic acids (acetate, formate).



SNL = Sandia National Laboratories.

Figure 3.2. Citrate Biodegradation in a) Aerobic System and b) Anaerobic System

Citrate biodegradation is more rapid in an anaerobic environment, which is expected to occur in most groundwater injections, but both aerobic and anaerobic citrate biodegradation is expected to occur during solution infiltration. Citrate biodegradation rates determined from experiments conducted at different temperature and citrate concentration indicate that initial field injections (10 mM citrate, 15°C) should have a half-life of ~50 h. At higher concentrations, the citrate biodegradation rate slows.

Citrate biodegradation depends on subsurface microbial activity, and there should be a direct correlation between the microbial biomass and the citrate biodegradation rate. As expected, microbial biomass in 100-N Area wells decreased significantly with depths from 10^8 cells/g at 1.8-m (6-ft) depth to 10^5 cells/g at a 7.6-m (25-ft) depth to $<10^3$ cells/g at a 12-m (40-ft) depth (Szecsody et al. 2007, Figure 5.64). However, the citrate mineralization rate decreased only 1 order of magnitude for the 5 order of magnitude decrease in biomass, indicating influence of another process. The likely cause of the relative uniformity of the citrate biodegradation rate may be caused by the biomass of microbes injected. In field injection experiments, 5% concentrated Ca-citrate-PO₄ chemicals (by volume) are injected with 95% river water (by volume), and the 10^7 cfu/mL in the river water (in sediment equivalent to 2×10^6 cfu/g) varies from an insignificant amount of mass relative to the 10^8 cfu/g (shallow sediment) to a significant amount of mass for deep sediment (with 10^4 cfu/g). Microbes attach by multiple and dynamic mechanisms, so when injected are not evenly distributed in the subsurface (or during infiltration). For these simple batch laboratory experiments, the biomass in the infiltration water is evenly distributed throughout the sediment. The net result is the citrate mineralization rate and extent (i.e., fraction CO₂ produced) decreased only slightly with depth, as shown by rates observed for sediments at specific depth intervals in five different boreholes. The citrate mineralization rate was also investigated in depth composites from 10 different 100-N Area wells, which did not show significant variation (citrate mineralization half-life average 250 ± 114 h, range 133 h to 472 h), indicating there should be no significant trends with lateral distance along the injection barrier. At aquifer temperature, the citrate biodegradation rate averages 0.014/h (half life ~50 h), and would decrease up to an order of magnitude at a 12-m (40-ft) depth (generally beyond the

typical injection depth). The conclusion of the citrate mineralization studies is there will be relatively uniform citrate degradation observed in field-scale injection at different locations and at different depths.

3.1.2 Characterization of Apatite Precipitate

Previous studies have used multiple characterization techniques employed to assess the crystal chemistry of the apatite formed by the microbial digestion of Ca-citrate in sediments. These techniques (and others) were used in this study to assess both the apatite purity formed, but additionally the amount of organic carbon in the apatite (due to the presence of microbial biomass), inorganic carbon, and the mass of apatite in sediment (generally present at low concentrations). Previous studies showed that high-resolution transmission electron microscopy (HRTEM) and X-ray powder diffraction (XRD) were used to assess apatite crystallinity and to document the transformation from an amorphous calcium phosphate to nanocrystalline apatite. EDS and Fourier transform infrared (FTIR) spectroscopy were used to analyze the chemical constituents. Blade-like crystals in an amorphous matrix are approximately 0.1 μm in size (Figure 3.3, upper left). This was consistent with the observed broad overlapping peaks in the XRD pattern at 2 microns of approximately 32° , a typical characteristic of poorly crystallized apatite (Figure 3.3, upper right; Waychunas 1988; Nancollas and Mohan 1970; Hughes and Rakovan 2002).

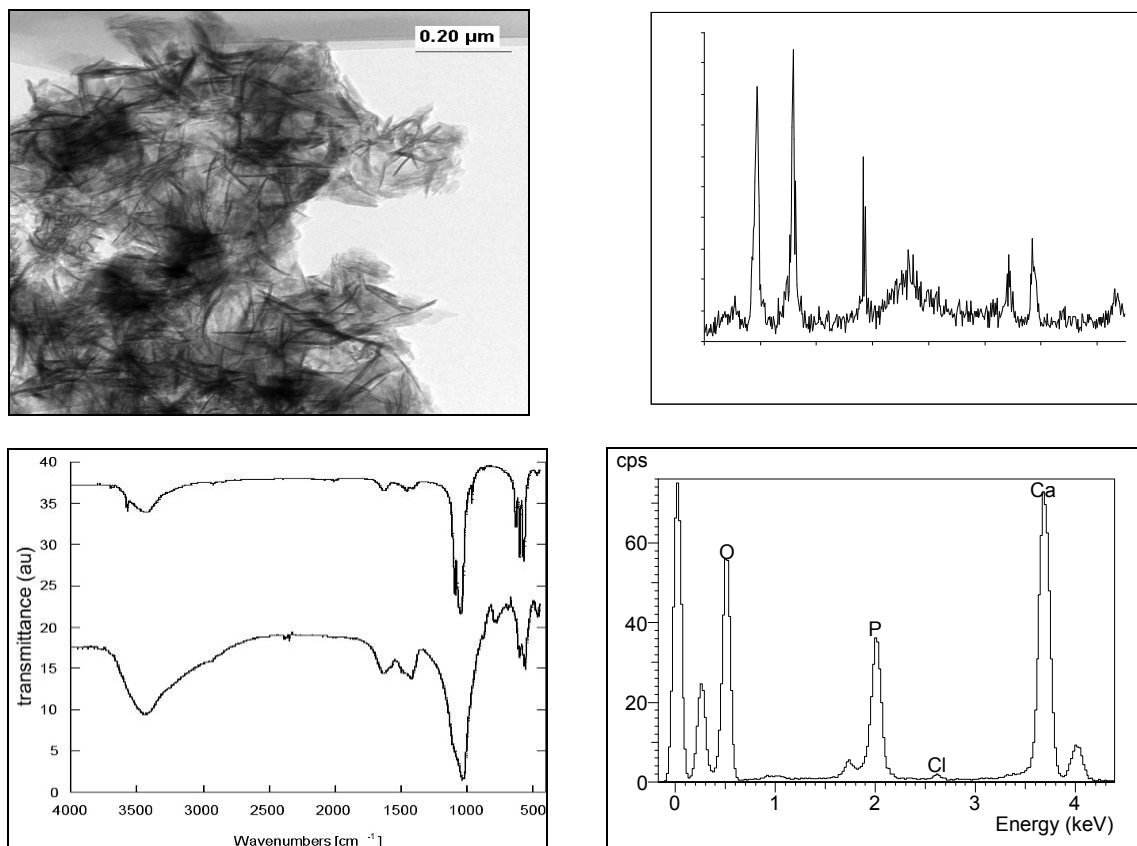


Figure 3.3. Characterization of Nanocrystalline Apatite Formed in Hanford Site Sediment by Microbially Mitigated Ca-Citrate Degradation in the Presence of Aqueous Phosphorous: a) TEM, b) XRD, c) FTIR, and d) EDS

The remaining peaks in the XRD correspond to components of the sediment. FTIR spectra are given for pure hydroxyapatite (top spectrum) produced by precipitation and heat treatment at 700°C and

calcium phosphate precipitates in 100-N Area sediment after 1 month (bottom spectrum). The lower resolution of the PO_4^- bands confirms the lower crystallinity of the sample, as observed by both HRTEM and XRD. The bands at 1455 cm^{-1} and 879 cm^{-1} indicate the presence of carbonate in the apatite structure. The transmission electron microscope (TEM)-EDS spectrum identifies calcium and phosphate as the major components with a stoichiometric apatite ratio of approximately 5:3.

3.2 Initial Low Ca-Citrate- PO_4 Concentration Injection Experiments

Laboratory one-dimensional flow experiments were conducted to predict behavior that would be observed at the field scale for the field injections of specific Ca-citrate- PO_4 solutions. The composition of the solution was modified over time from an initial formula that is the stoichiometric ratio of components needed to form apatite (used for field injection #1), to a calcium-deficient formulation to utilize some calcium desorbed from sediment (used for field injection #2), and finally to a calcium-deficient formulation with additional PO_4 that still minimizes initial ^{90}Sr mobilization (used for field injections #3 to #18). Although some small-scale (i.e., 10 to 20 cm [4 to 8 in.] in length) one-dimensional flow experiments had already been conducted, the initial “snow plow” (peaking) effect of ion exchange upon breakthrough was difficult to accurately sample with these very small columns, so 100-cm (3.2-ft) and 6-m (20-ft)-long columns were used to more accurately represent a 6- to 9-m (20- to 30-ft)-radius field injection. Additional field support experiments were conducted to accomplish the following:

1. Quantify the stability of the Ca-citrate and Na- PO_4 tanker trucks at high concentration and low temperatures.
2. Quantify the relationship between specific conductance (SpC) and solution of the two separate tanker trucks and the mix.
3. Quantify the relationship between solution density and solution concentration.
4. Quantify the amount of interference of citrate on field PO_4 measurement as described in Szecsody et al. (2007).

3.2.1 Laboratory Support Experiments for Field Injection #1

Several one-dimensional column experiments of 0.9- to 6-m (3- to 20-ft) length were conducted to quantify geochemical changes that would occur in Hanford Site sediments with a low concentration of Ca-citrate- PO_4 (4, 10, 2.4 mM; see Table 2.2 for complete description) injection. The 1-m, one-dimensional column experiment results (Figure 3.4) show nearly identical behavior to the 100-cm (3.3-ft)-long column to the 6-m (20-ft)-long column (not shown). Both calcium and strontium breakthroughs were nearly unretarded (at 1.0 pore volume) with peaking behavior of 10-11 times groundwater concentrations (i.e., so ^{90}Sr is expected, on average, to peak at 10 times groundwater concentration in the field injection #1). The average ^{90}Sr initial peak was 10.5 times and varied from 3 times to 25 times. Citrate breakthrough was unretarded ($R_f = 1.0$) with no initial peak, and PO_4 breakthrough was retarded, with the PO_4 retardation factor varying with injection velocity. Phosphate sorbs to sediment within minutes, but one or more phosphate phases begin to precipitate within hours and continue to precipitate for hundreds of hours. Injection of a PO_4 -containing solution would, therefore, show both retardation and mass loss, although the retardation (i.e., reversible) should be mainly caused by sorption, because mass loss alone would not cause any retardation.

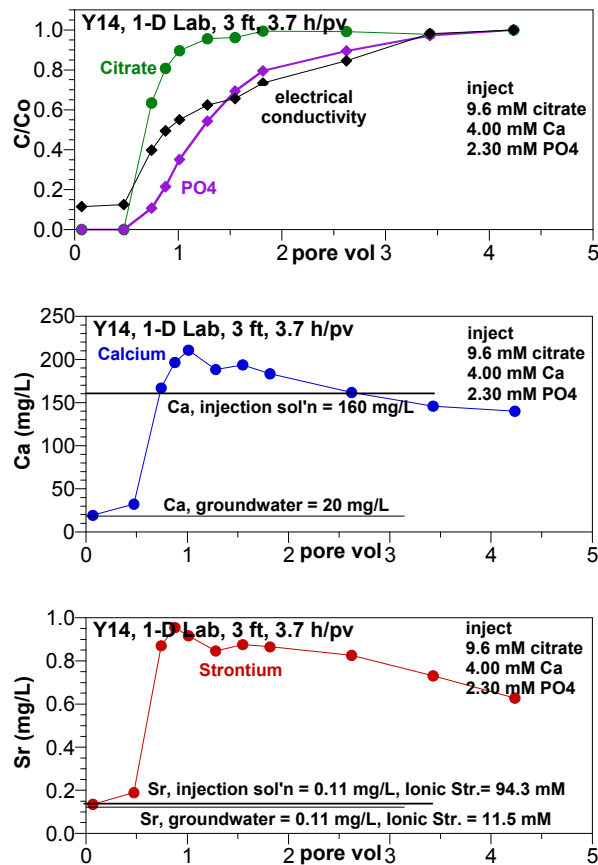


Figure 3.4. Citrate Mineralization and Depth in Five Boreholes Showing Trend of Mineral

The phosphate retardation observed in the 1-m (3.3-ft) column (Figure 3.4, $R_f = 2.1$, residence time in column 3.3 hours) was slightly smaller than observed in the experiment with the 6-m (20-ft)-long column ($R_f = 4.5$, residence time 4.5 hours), as there was less reaction time to sorb the PO_4 .

Additional 1-m (3.3-ft) column experiments were conducted after injection #1 in which Ca-citrate concentration was decreased relative to PO_4 (next section). The composition of the solution used for field injection #1 was as follows:

- 10 mM trisodium citrate [$HOC(COONa)(CH_2COONa)_2 \cdot 2H_2O$] fw 294.1 g/mol
 - granular more soluble than powdered
 - reagent grade (quality) for citrate: USP/FCC (lower grades contain up to 5 ppm heavy metals)
- 2.0 mM disodium phosphate [Na_2HPO_4], fw 141.96 g/mol
 - reagent grade (quality): certified American Chemical Society (ACS) grade (lower grades can contain extra NaOH, which is only a small problem, and changes pH and ionic strength)
- 0.4 mM sodium phosphate [NaH_2PO_4], fw 119.98 g/mol
 - reagent grade (quality): certified ACS grade (lower grades can contain 8 ppm arsenic and 10 ppm heavy metals)

- 1.0 mM ammonium nitrate [NH₄NO₃], fw 80.04 g/mol
 - granular
 - reagent grade (quality): certified ACS
- 4.0 mM calcium chloride, [CaCl₂*2H₂O], fw 147.02 g/mol
 - reagent grade (quality): certified ACS (lower grades can contain 20 ppm lead).

3.2.2 Laboratory Support Experiments for Field Injection #2

The original Ca-citrate-PO₄ formulation provides for the exact proportions of chemicals needed to precipitate apatite [Ca₁₀(PO₄)₆(OH)₂], with a Ca/PO₄ molar ratio of 10/6 and a Ca/citrate ratio of 4/10 (i.e., enough citrate to complex Ca²⁺). Citrate has an additional role of inhibiting the immediate formation of Ca-PO₄ precipitates. With this Ca-citrate-PO₄ formulation, the resulting calcium and strontium and ⁹⁰Sr solution concentration peaked at 10 times groundwater concentration, then maintained 1.6 times greater than the injection solution because of ion exchange (i.e., the high sodium concentration injected displaced some Ca/Sr off sediment ion-exchange sites). For field injection #2, this formulation was modified to inject the same amount of phosphate but less Ca-citrate to use Ca²⁺ desorbing from sediment. The net effect is still forming the same mass of apatite but with less initial peaking ⁹⁰Sr behavior in groundwater.

Five additional 1-m column experiments were conducted, varying the Ca-citrate concentration (keeping PO₄ concentration constant at 2.4 mM) to measure the peaking calcium and strontium behavior. The citrate concentration was varied from 5 to 10 mM (and maintaining a Ca/citrate ratio of 4/10). Results of one experiment with 2 mM calcium and 5 mM citrate (Figure 3.5, formulation used in field injection #2) show the obvious effect of ion exchange; injection of a lower ionic strength solution results in less calcium and strontium desorption from the sediment. The calcium and strontium peak concentration of 5-7 times for the 2 mM Ca injection (ionic strength 62 mM), and 7-9 times for the 4.6 mM Ca injection (ionic strength 79 mM). The laboratory PO₄ breakthrough was relatively invariant with solution concentration (Rf 2.0 to 2.7). The composition of the solution used for field injection #2 was as follows:

- 5.0 mM trisodium citrate [HOC(COONa)(CH₂COONa)₂*2H₂O] fw 294.1 g/mol
 - granular is more soluble than powdered reagent grade (quality) for the citrate: USP/FCC (lower grades contain up to 5 ppm heavy metals)
- 2.0 mM calcium chloride, [CaCl₂*2H₂O], fw 147.02 g/mol reagent grade (quality): certified ACS (lower grades can contain 20 ppm lead)
- 2.4 mM diammonium phosphate [(NH₄)₂ H PO₄] fw 132.1 g/mol (also called ammonium phosphate dibasic) pH 8.0 ± 0.1 reagent grade (>98%)
- 1.0 mM sodium bromide (tracer, 80 mg/L Br⁻ or 103 mg/L NaBr, fw 103 g/mol).

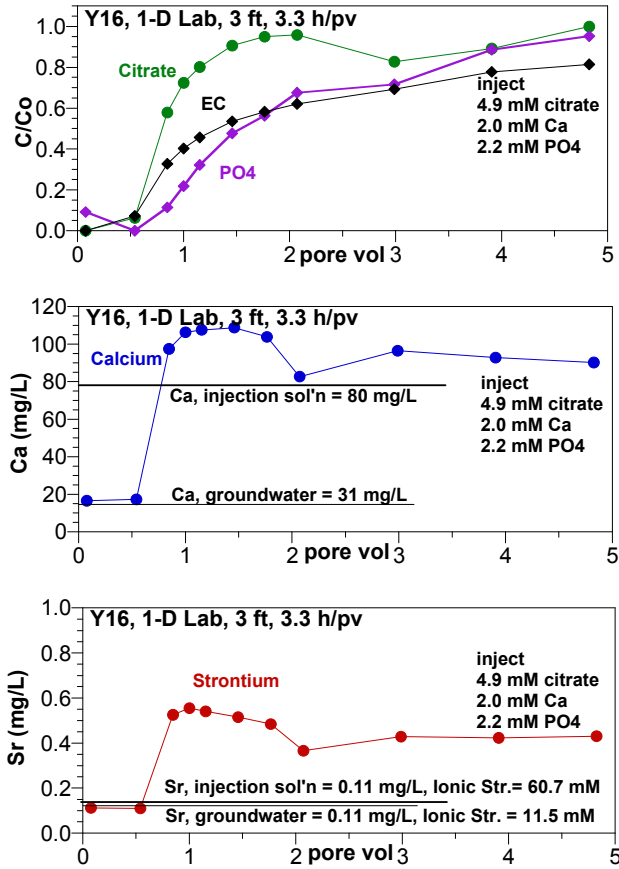


Figure 3.5. Injection of 2 mM Ca, 5 mM Citrate, and 2.2 mM PO₄ (experiment Y16) into a 1-m (3.3-ft) Sediment Column

3.2.3 Laboratory Support Experiments for Field Injections #3 to #18

Field injection #1 had an initial ⁹⁰Sr increase of 10.5 times (range 0 to 25 times), the average of which was predicted from strontium and calcium peaking breakthrough in laboratory experiments (10 times to 11 times increase relative to groundwater). Field injection #2 had an initial ⁹⁰Sr increase of 3.3 times (range 0 to 6.2 times), which was slightly smaller than predicted from laboratory experiments (4.5 times to 6 times). Calculations of the mass of apatite needed to lower the ⁹⁰Sr concentration (Table 2.1) show that additional PO₄ needs to be injected, so the objective of laboratory experiments before field injection #3 was to alter the injection formulation to maintain <6 times increase in ⁹⁰Sr concentration, but inject a greater mass of PO₄.

Two different approaches were considered: 1) increasing the PO₄ and decreasing the Ca-citrate (solution used for field injections #3 to #18), and 2) injecting PO₄ only. The column experiments conducted paralleled field systems with the following: 1) rapid injection of the Ca-citrate-PO₄ solution for 24 hours, and 2) slow groundwater injection for the next 30 days. This enabled collection of strontium and calcium mobility data both during the initial peak, and allowed additional time to collect data in which groundwater had flowed into the solution-treated sediment zone. The series of experiments are described in Szecsody et al. (2007), with one experiment described that used the solution that was used in field injections #3 to #18 (Figure 3.6).

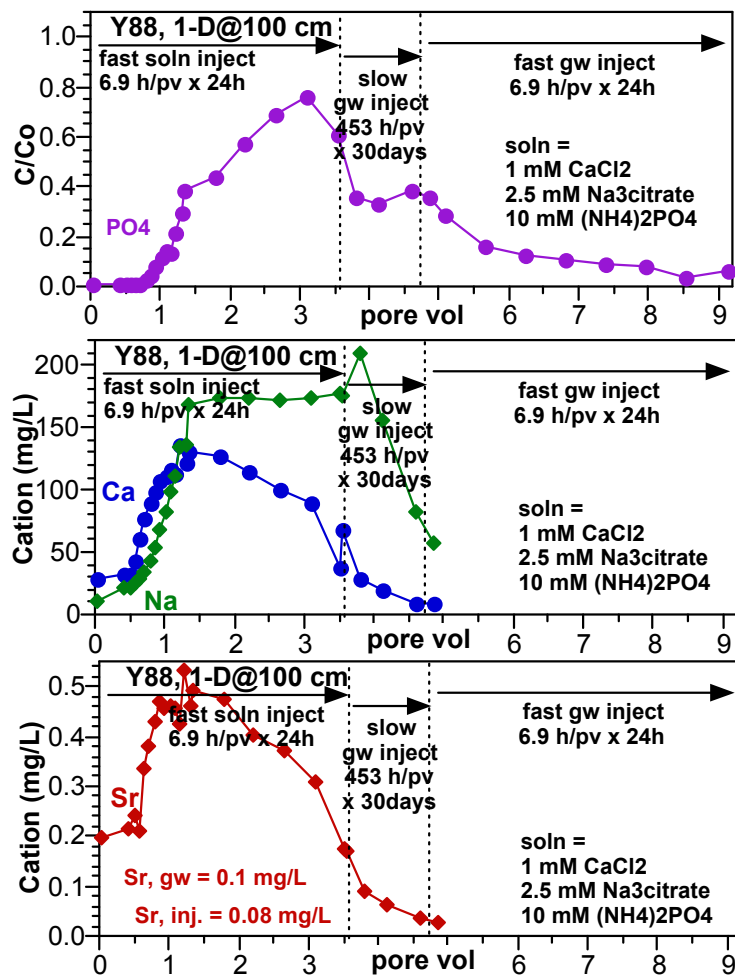


Figure 3.6. 1-m-Long One-Dimensional Column Experiment (Y88) with the Injection of 1 mM Ca, 2.5 mM Citrate, and 10 mM PO₄ with Results of PO₄, Calcium, Sodium, and Strontium Breakthrough

In a 1-m (3.3-ft)-long column experiment (Y88, Figure 3.6), 10 mM PO₄ was injected with 1 mM calcium and 2.5 mM citrate, so the injection solution was significantly deficient in calcium (16.7 mM needed to form apatite with 10 mM of PO₄). Solution injection in this experiment resulted in a strontium peak (24 hour) at 4.7 times groundwater and calcium peak (24 hours) at 4.5 times groundwater. By 30 days, the aqueous strontium concentration was 0.28 times groundwater and calcium was 0.43 times groundwater. Phosphate breakthrough reached 76% of injection concentration with a retardation factor of 1.7. The total PO₄ mass balance at 32 days showed that 29% of the PO₄ injected precipitated in the column (0.61 mg of 2.66 mg injected). The percent precipitate is somewhat artificial, an artifact of the limited volume of the column. At the field scale, essentially all injected PO₄ would precipitate. This column (from experiment Y88) is being stored to allow further strontium sequestration by the apatite and will be injected with a high Ca-citrate-PO₄ concentration solution at a future date.

Simulation of the injection of a Ca-citrate-PO₄ solution (1, 2.5, 10 mM) over a 31-day period (Figure 3.7) also shows general agreement between the data and simulation of the multiple breakthrough

species. Details on these simulations are described in Szecsody et al. (2007) and use the STOMP (Subsurface Transport Over Multiple Phases) code developed by PNNL (White and Oostrom 2006) with a reactive transport network developed for Ca-citrate-PO₄ studies. The reactive transport model in these simulations account for the observed increase in aqueous ⁹⁰Sr in groundwater during the first few hours of Ca-citrate-PO₄ (generally caused by cation-exchange reactions) injection and subsequent citrate biodegradation, apatite formation, and only strontium removal by precipitation with apatite. The reactions included 1) strontium, calcium, magnesium, sodium, potassium, NH₄ ion exchange; 2) metal-OH, -CO₃, -PO₄, and -citrate aqueous speciation; 3) citrate biodegradation; and 4) solids apatite, CaCO₃, and SrCO₃, which was 42 reactions with 51 species.

In this experiment, the Ca-citrate-PO₄ solution was injected at a rapid rate to achieve a 6.9-hour residence time for a total of 24 hours or 3.5 pore volumes (similar to a field injection), followed by a 30-day slow flow rate injection of groundwater with a 453-hour residence time. This solution is similar in major component concentrations to field injections #3 to #18, but differs in the fact that this laboratory experiment used 20 mM NH₄⁺, whereas the field injection used 17.6 mM Na⁺ and 1.0 mM NH₄⁺, to limit both N for microbes and also limit Ca²⁺ and Sr²⁺ ion exchange.

The experimental data show Ca²⁺ (third panel, Figure 3.7) and Sr²⁺ (first panel) concentrations during initial solution breakthrough at 5 to 10 hours, peaking at ~6 times the equilibrium groundwater concentration as well matched by the simulation. Phosphate breakthrough lags (green line, second panel), but apatite precipitation starts to occur in the 10- to 100-hour time frame, then decreases in extent. The final change that occurs in the system is at 800 hours, when the large Na⁺ pulse is eluted out of the system as a result of the slow groundwater injection and Sr²⁺ and Ca²⁺ decrease, largely (in this case) due to ion exchange onto the sediment (not precipitation). The composition of the solution used for field injections #3 to #18 was as follows:

- 2.5 mM trisodium citrate [HOC(COONa)(CH₂COONa)₂*2H₂O] FW 294.1 g/mol (also called sodium citrate dihydrate, ACS registry 6132-04-3)
 - granular is more soluble than powdered
 - reagent grade (quality) or equivalent for the citrate: USP/FCC (lower grades contain up to 5 ppm heavy metals).
- 1.0 mM calcium chloride, [CaCl₂], FW 110.98 g/mol
 - reagent grade (quality) or equivalent: certified ACS, ACS registry 10043-52-4 (lower grades can contain 20 ppm lead).
- 8.1 mM disodium hydrogenphosphate [Na₂HPO₄], FW 141.96 g/mol
 - also called disodium phosphate, anhydrous
 - reagent grade (quality) or equivalent: certified ACS, ACS registry 7558-79-4 (lower grades can contain extra NaOH, which is only a small problem, and changes pH and ionic strength).
- 1.4 mM sodium dihydrogenphosphate [NaH₂PO₄], FW 119.98 g/mol, also called monosodium phosphate, anhydrous
 - reagent grade or equivalent: certified ACS grade, ACS registry 7558-80-7 (lower grades can contain 8 ppm arsenic and 10 ppm heavy metals).

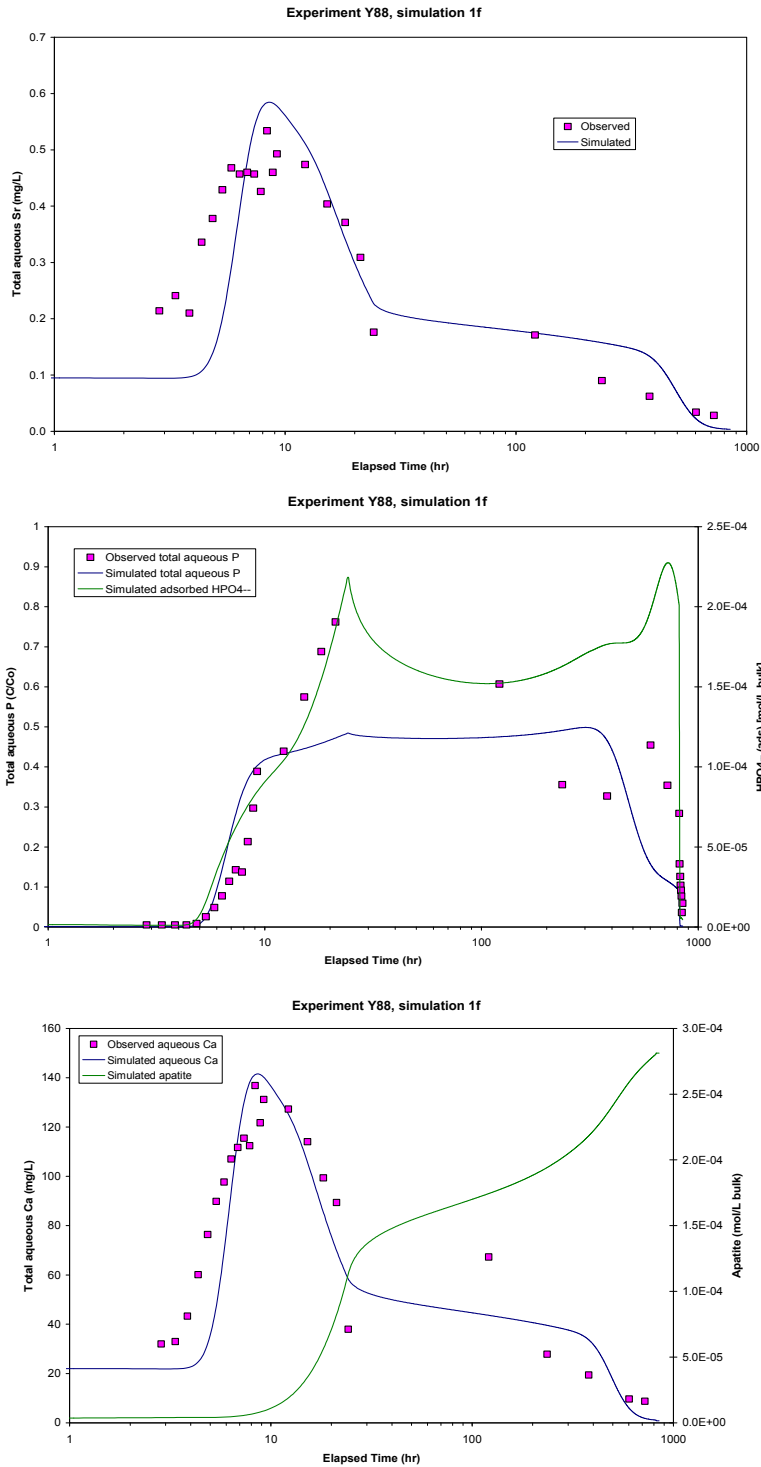


Figure 3.7. Simulation of One-Dimensional Injection of a Ca-Citrate-PO₄ Solution (experiment Y88, similar to field #3 to 18)

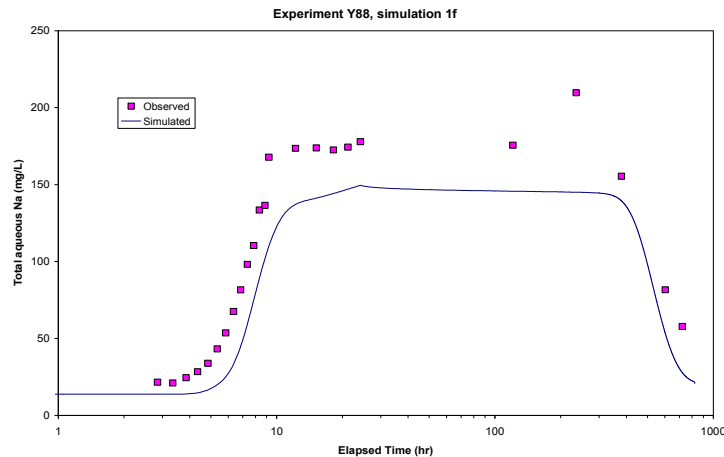


Figure 3.7. (contd)

- 0.5 mM diammonium hydrogenphosphate $[(\text{NH}_4)_2\text{HPO}_4]$, FW 132.1 g/mol
 - also called diammonium phosphate
 - granular is more soluble than powdered.
 - reagent grade (quality) or equivalent: certified ACS, ACS registry 7783-28-0.
- 1.0 mM sodium bromide $[\text{NaBr}]$, FW 102.90 g/mol
 - reagent grade (quality) or equivalent: certified ACS, ACS registry 7647-15-6.

3.3 Techniques for Measuring Barrier Performance at Field Scale

Monitoring groundwater ^{90}Sr concentrations over time will be used to assess the field-scale performance of the zones injected with the Ca-citrate- PO_4 solution to determine if ^{90}Sr is being sequestered (uptake into apatite structure). Unfortunately, ^{90}Sr is not an ideal contaminant to assess change using *aqueous* concentration measurements because most (99%+) of the ^{90}Sr mass is on the solid phase the actual assessment needs to characterize ^{90}Sr adsorbed to sediment, adsorbed to apatite, or sequestered. In contrast, chromate (under Hanford Site alkaline conditions at pH 8), which exhibits nearly no sorption, can be successfully monitored through a PRB by just aqueous concentration measurements. With Ca-citrate- PO_4 solution injections, initial precipitation of apatite within a week or two will remove some localized ^{90}Sr , as shown in Figure 2.2. Over a longer period of time (months, years), ^{90}Sr will be incorporated into the apatite structure (Figure 2.2, >300 hours). Although ^{90}Sr sorption is strong onto the apatite surface, even with a significant amount of apatite emplaced in sediment (Table 2.2, lines 2, 3) the amount of ^{90}Sr in aqueous solution remains about the same at ~0.8%. Therefore, aqueous ^{90}Sr measurements are only useful to assess initial apatite precipitation removing localized ^{90}Sr over a short-time scale (<1 month), but long-term removal (years) needs to be assessed with downgradient monitoring. Flow reversals in groundwater (i.e., toward or from the Columbia River) will make it more difficult to assess barrier performance.

Techniques are needed to assess the difference between adsorbed ^{90}Sr and incorporated ^{90}Sr . Core samples of sediment in the apatite-laden zone are the most useful, and can be used to characterize the amount of apatite present (as described below) and the amount of ^{90}Sr incorporated in apatite. Although core sampling and analysis provides definitive results, other field techniques could be used.

A small-volume injection/withdrawal or injection only test (approximately 1135 L [300 gal]) of a specified ionic-strength solution (e.g., a Ca-citrate-PO₄ solution) could be used to cause localized desorption of calcium and strontium. This type of test would show if ⁹⁰Sr is still 99% held on the sediment surface by ion exchange (natural sediment; see Table 2.2, line 1), or partially by ion exchange and partially sequestered into apatite. A high ion-exchange solution desorbs ⁹⁰Sr held only by ion exchange (does not dissolve apatite). The added advantage of injecting a Ca-citrate-PO₄ solution is that the characteristics of the desorption amount are well known, and the long-term effects are beneficial (just provides a small amount of additional apatite). There are limitations of the push/pull method, in that only the adsorbed ⁹⁰Sr is quantified. Probing a well in a field system (open system with no mass balance) will likely show constant adsorbed ⁹⁰Sr over time, regardless of the amount of ⁹⁰Sr sequestered (i.e., would not be useful). Sequential push/pull field experiments with groundwater, Ca-citrate-PO₄ solution, followed by a weak acid solution (described below) would be useful because the weak acid solution would dissolve apatite, releasing ⁹⁰Sr. Unfortunately, this technique (i.e., weak acid solution injection) would have a destructive effect on the barrier because it would remove a portion of the apatite. Therefore, core sampling and destructive analysis of cores appears to be the best method to fully assess both apatite placement and ⁹⁰Sr incorporation into apatite. Multilevel sampling in wells could be useful to assess ⁹⁰Sr breakthrough in different formations (i.e., Ringold/Hanford) or subunits within formations and locations where additional apatite is needed.

Different experimental techniques were used to identify the small amount of apatite precipitate that results from Ca-citrate-PO₄ injection into sediments. Field injections #1 and #2 (2.4 mM PO₄) should have ~0.1 mg apatite/g of sediment, whereas field injections #3 to #18 (10 mM PO₄) should have 0.4 mg apatite/g of sediment (Table 2.1). The final 300-year design capacity should have 3.4 mg apatite/g of sediment. Techniques that have been used and are being developed for this project include the following:

1. XRD
2. scanning electron microscope with EDS and elemental detectors (Figure 3.8)
3. acid dissolution of the sediment and phosphate measurement (i.e., aqueous PO₄ extraction)
4. fluorescence of substituted apatites.

Results of these techniques are described below. Additional characterization techniques were used on the apatite precipitate to determine specific properties that included 1) Brunauer-Emmett-Teller surface area (Summer 2000), 2) FTIR scan to determine apatite crystallinity and change in crystallinity upon strontium substitution, and 3) organic and inorganic carbon analysis. Some of these techniques overlap in application to determine the amount of strontium substitution in the apatite.

While the electron microprobe shows that very small concentrations of apatite can be quantitatively identified, the cost of the process is significant, as is the time to process the samples. An example (Figure 3.8) shows 0.016 mg apatite/g of sediment with an EDS detector clearly identifying apatite precipitate outside mineral grains. One method involves aqueous measurement of phosphate after the apatite was dissolved in acidic solution, which does not have the low detection limits of the electron microprobe (Figure 3.8). Field injections #1 and #2, which resulted in a calculated 0.1 mg apatite/g of sediment, are likely not detectable, but field injections #3 to #18 (calculated 0.4 mg apatite/g sediment) are likely detectable. A third method of measuring added apatite in sediment investigated was fluorescence scans. While pure hydroxyapatite does not fluoresce, apatites with fluorine or carbonate substitution do fluoresce. This method is still in development; its ability to measure low concentrations of substituted apatite has yet to be determined.

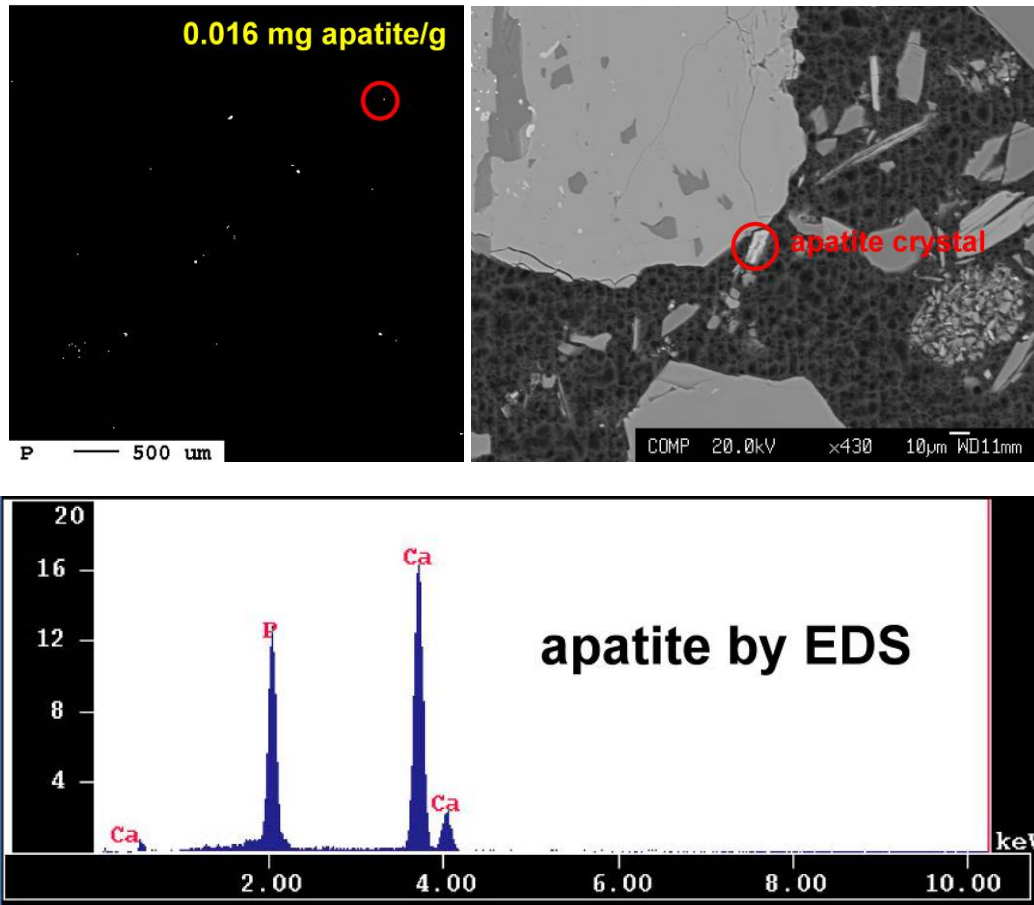


Figure 3.8. Scanning Electron Microbe Images of a Single Apatite Crystal

The amount of ^{90}Sr incorporation into apatite can be quantified by sequential chemical extractions on the sediment/apatite mixture (i.e., high-ionic strength solution to desorb ^{90}Sr , then 4M HNO_3 acid dissolution to dissolve the apatite, as described in Section 3.4).

3.4 Long-Term Strontium-90 Incorporation Mass and Rate into Apatite

For this technology to be effective, sufficient apatite needs to be emplaced in sediments to incorporate strontium and ^{90}Sr for 300 years (approximately 10 half-lives of ^{90}Sr), and the rate of incorporation needs to exceed the natural groundwater flux rate of strontium in the 100-N Area. The ^{90}Sr is incorporated into apatite by two mechanisms: during initial precipitation of apatite (time scale of a period of days) and slow recrystallization of strontium-laden apatite (time scale of months to years). The initial incorporation (Figure 3.9b, black triangles and circles) occurs within days and typically incorporates a fraction of the ^{90}Sr mass equal to the fraction calcium uptake in apatite (i.e., calcium and strontium and ^{90}Sr behave similarly). The ^{90}Sr incorporation rate into solid-phase apatite is observed at times scales of months by the following:

1. additional decrease in aqueous ^{90}Sr (Figure 3.9a, red triangles)
2. decrease in adsorbed ^{90}Sr on sediment (Figure 3.9a, purple circles)
3. decrease in ^{90}Sr sorbed on apatite (Figure 3.9a, blue diamonds)
4. increased ^{90}Sr in apatite (Figure 3.9a, green triangles and Figure 3.9b, black triangles and circles).

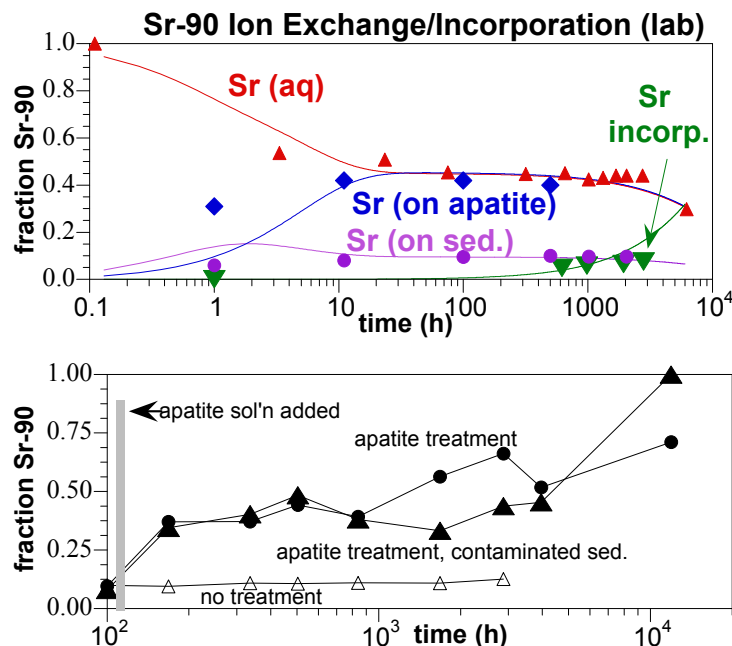


Figure 3.9. Strontium Uptake from Groundwater Suspension of 0.34 g/L Apatite and 20 g/L Sediment at 82°C with a) Solid-Phase Apatite Added and b) Ca-Citrate-PO₄ Solution Added. Model fit consists of Ca-Na-Sr ion exchange on sediment, Ca-Na-Sr ion exchange on apatite, and Sr incorporation within the apatite structure.

Simulation of Ca-Sr-Na ion exchange in sediment, Ca-Sr-Na ion exchange on apatite, and strontium incorporation in apatite was conducted to quantify the incorporation rate in this specific laboratory system (Figure 3.9a, lines), then simulate the field system with a much higher sediment to water ratio. The field scenario simulation using the total apatite needed in the field showed the same time scale for ⁹⁰Sr incorporation into apatite as the laboratory experiment (Figure 3.9a). The reason for this lack of change is the relative time scales of ion-exchange reactions versus the incorporation reaction being 5 to 6 orders of magnitude different. In contrast, if the ion exchange and incorporation reaction rates were only an order of magnitude different (i.e., coupled), then the ion-exchange reaction would slow the apparent incorporation rate.

The amount of ⁹⁰Sr uptake during the initial apatite precipitation phase varies with the type of solution (Figure 3.10a). For the Ca-citrate-PO₄ (1, 2.5, 10 mM) solution used in injections #3 to #18, several laboratory experiments show this uptake should be ~60% of the ⁹⁰Sr mass by 30 days (Figure 3.6), which includes both ⁹⁰Sr sorbed and incorporated in apatite. Over the long term (months), the amount of ⁹⁰Sr uptake resulting from apatite recrystallization with ⁹⁰Sr incorporation varies with the calcium and strontium ratio (Figures 3.10a and b).

Uptake mass in long-term studies consisted of a specific mass of sediment/apatite exposed to the equivalent of 350 pore volumes of a ⁹⁰Sr-laden solution (diamonds, Figure 3.10). In contrast, uptake mass in short-term studies consisted of the sediment/apatite exposed to the equivalent of 3 pore volumes of ⁹⁰Sr-laden solution (triangles, Figure 3.10). By 1 month, ⁹⁰Sr total uptake was 95 to 99% (Figure 3.10a, triangles), with 18 to 25% incorporation into apatite (i.e., during initial precipitation, Figure 3.10b, triangles). The remaining fraction of ⁹⁰Sr uptake was held onto apatite/sediment surfaces by ion

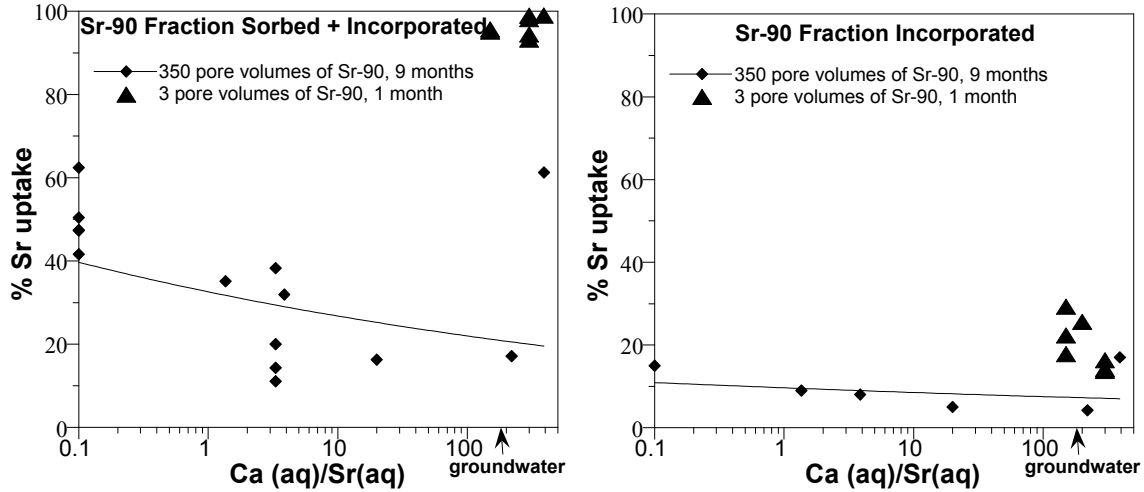


Figure 3.10. Strontium Uptake from Sediment/Apatite Systems Showing (l) Sorbed + Incorporated Fraction and (r) Incorporated Only

exchange. These batch studies were conducted at near-field sediment to water ratios and represent what should occur to the ^{90}Sr in the Ca-citrate- PO_4 injection zone. Experiments conducted at very low sediment to water ratios (diamonds, Figure 3.10) represent uptake of 350 pore volumes of ^{90}Sr -laden water by apatite. The total ^{90}Sr uptake (Figure 3.10a) decreased with increasing calcium and strontium ratios, which was mainly caused simply by less sorbed ^{90}Sr on the surface. The ^{90}Sr fraction incorporated into apatite (by 9 months) varied from 3 to 18% (of the 350 pore volumes of ^{90}Sr -laden water).

It is unclear if there was a relationship between increasing calcium and strontium ratio and decreasing ^{90}Sr uptake. The ionic strength had less effect on strontium incorporation because strontium adsorption on apatite was more highly correlated with divalent cation concentration. The rate-limiting step in strontium incorporation appears to be solid-phase diffusion, based on the low activation energy (11.3 kJ/mol) derived from temperature studies. Experiments are in progress to measure the strontium profile with depth using an electron microprobe to prove if diffusion is the rate-limiting step. As described in Table 2.1, 3.4 mg of apatite per gram of sediment is needed to incorporate ^{90}Sr for 300 years, assuming 10% strontium substitution for calcium in the apatite structure. Experiments showed measured strontium or ^{90}Sr fraction substitution for calcium in apatite by 9 months varied from 1 to 16.3%. FTIR scans showed that strontium was indeed substituting into apatite (i.e., crystal structure did not change, or other strontium phases were not present). Factors that increased the amount (and rate) of strontium substitution for calcium in apatite included 1) less crystalline/more substituted initial apatite structure, and 2) presence of citrate during initial apatite precipitation. Field-scale apatite precipitation in sediments is expected to be less crystalline, so there should be greater strontium substitution. There was not a clear trend between higher aqueous Ca^{2+} (such as in groundwater) and strontium substitution.

The ^{90}Sr incorporation rate into solid-phase apatite (not including more rapid incorporation during initial precipitation) averaged $2.7 \pm 2.6 \times 10^{-5} \text{ h}^{-1}$ (half-life 1080 days, $1.42 \times 10^{-8} \text{ mg Sr/day/mg apatite}$, Figure 3.11, Table 3.1) for sediment/water systems containing 350 pore volumes of ^{90}Sr -laden water.

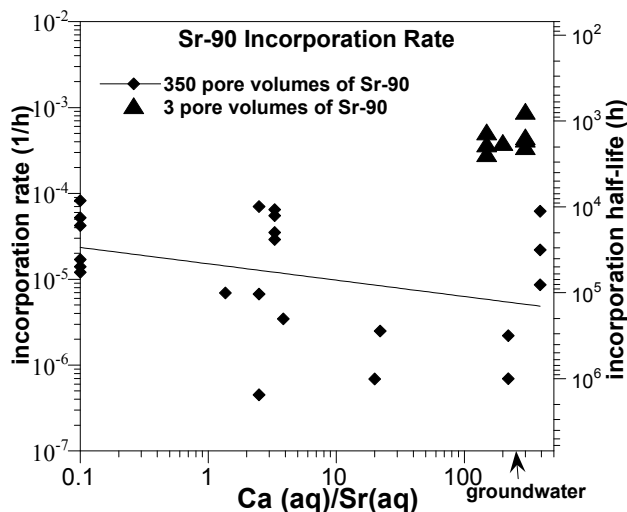


Figure 3.11. Strontium Incorporation Rates Calculated from Uptake Experiments

Table 3.1. Calculated Strontium Uptake Rates in Apatite-Laden Sediment for a 30-ft-wide Barrier

Scenario	Barrier Diameter (ft)	Apatite Mass (mg apa/g sed)	Apatite Total Mass (g/cm ² cross sect)	Sr Uptake Rate (mmol Sr/d/cm ²)
During initial ppt (1 mo), inj. #3-18 apatite	30	0.38	0.619	5.5E-04
During initial ppt (1 mo), final apatite	30	3.4	5.53	4.9E-03
Solid phase incorp. (9 mo), inj #3-18 apatite	30	0.38	0.619	8.8E-06
Solid phase incorp. (9 mo), final apatite	30	3.4	5.53	7.8E-05
Natural Sr flux rate toward river ^(a)	--	--	--	1.36E-06

(a) Assumes 0.1 mg/L Sr, $K_d = 14 \text{ cm}^3/\text{g}$, porosity 0.20, bulk density 1.78 g/cm^3 , 1 ft/day groundwater flow rate.

This long-term, solid-phase ⁹⁰Sr incorporation rate was used to calculate the strontium uptake rate in a 9-m (30-ft)-wide (diameter) apatite barrier to compare with the natural groundwater flux rate of strontium. For the field scenario of current injections #3 to #18 (i.e., 10 mM PO₄ injected or 0.34 mg apatite/g sediment), the strontium uptake rate was 8.8×10^{-6} mmol strontium/day/cm². This strontium incorporation rate into apatite was 6.5 times greater than the average natural strontium groundwater flux rate (1.4×10^{-6} mmol Sr day⁻¹ cm⁻², assuming 0.3-m [1-ft]/day groundwater flow rate). This indicates strontium would be sequestered in the apatite-laden zone for the *average* strontium groundwater flux rate, but zones of higher groundwater flux (10 to 100 times) would exceed the barrier uptake rate for this low apatite loading (0.34 mg apatite/g sediment). In addition, this low apatite loading would also not be able to incorporate strontium and ⁹⁰Sr for 300 years. From a mass balance perspective, approximately 3.4 mg apatite per gram of sediment is needed to incorporate strontium and ⁹⁰Sr for 300 years (assumes 10% Sr substitution for calcium in apatite). At this higher apatite loading, the strontium uptake rate during initial precipitation (5×10^{-3} mmol Sr day⁻¹ cm⁻²) is 3600 times more rapid than the average strontium groundwater flux rate, and the strontium uptake rate during solid-phase incorporation (7.8×10^{-5} mmol Sr day⁻¹ cm⁻²) is 57 times more rapid than the average strontium groundwater flux rate; therefore, the barrier will effectively remove all strontium except in extreme high-groundwater flow conditions.

3.5 Additional Injections to Increase In Situ Apatite Mass

Experiments were conducted to test the efficiency of ^{90}Sr uptake by sequential injections of different phosphate solutions to increase the amount of apatite in the sediment. These experiments were conducted for a relatively short time period (2–5 weeks), so ^{90}Sr incorporation represents only the initial incorporation during apatite precipitation. The baseline case was sequentially low, followed by high concentration injection of Ca-citrate- PO_4 solutions (lines 6 and 7, Table 3.2), which showed 14.2% ^{90}Sr incorporated at 2 weeks (after just the low-concentration injection, line 6), and 29.3% incorporation after 2 weeks of the subsequent high-concentration injection. Over this relatively short-time period, not all of the high-concentration solution had precipitated, so the efficiency of ^{90}Sr uptake (mmol strontium uptake per mmol of PO_4 injected) did not increase.

Table 3.2. Sequential Treatments of ^{90}Sr -Laden Sediment with Fraction ^{90}Sr Uptake and Efficiency

PO ₄ Application Description	PO ₄ total (mM)	Sr-90 incorporation in apatite			Sr/Ca incorp.
		mass fraction	half-life (h)	incorp. efficiency Sr/PO ₄ (mM/mM)	
Sequential PO₄, then Ca-citrate-PO₄					
1) 8.34 mM PO ₄ , 1 week	8.34	0.141	770	0.0017	1.052
2) Ca-Cit-PO ₄ (14-35-8.38 mM) 4 weeks	16.7	0.21	1850	0.0013	0.955
Citrate-PO₄ only (no Ca addition)					
Cit-PO ₄ (10-2.4 mM) 3 weeks	2.4	0.163	1980	0.0068	1.216
Sequential Ca-citrate-PO₄, then PO₄					
1) Ca-Cit-PO ₄ (7-17.5-4.19) 2 weeks	4.2	0.137	1610	0.0033	0.725
2) 8.38 mM PO ₄ 3 weeks	12.6	0.178	2390	0.0014	0.844
Sequential low conc., high conc. Ca-citrate-PO₄					
1)*Ca-Cit-PO ₄ (1-2.5-10 mM) 2weeks	10	0.142	1520	0.0014	1.543
2) Ca-Cit-PO ₄ (28-70-16.8 mM) 2 weeks	26.8	0.293	1330	0.0011	1.724
Ca-citrate-PO₄ only (high conc.)					
Ca-Cit-PO ₄ (28-70-16.75) 5 weeks	16.8	0.256	1780	0.0015	0.672

Alternative single-injection scenarios considered included injection of PO_4 alone, citrate- PO_4 alone (no calcium), and high-concentration Ca-citrate- PO_4 solution. Of these *single*-injection scenarios, there was little difference in ^{90}Sr uptake fraction and incorporation efficiency, except that the incorporation efficiency of the citrate- PO_4 solution (no calcium) was much higher. Sequential injection schemes considered included injecting PO_4 first, then Ca-citrate- PO_4 and Ca-citrate- PO_4 first, then PO_4 . Of these sequential injection scenarios, the amount of ^{90}Sr incorporation was nearly the same, but incorporation efficiency was greater for solutions containing citrate. In general, injection solutions containing citrate and PO_4 appeared more efficient at ^{90}Sr uptake over the 5-week-long experiments than PO_4 -only solutions.

A sequential low- then high-concentration Ca-citrate- PO_4 solution was injected into a set of three small columns (in series), with destructive sampling. After the low-concentration injection and 32 additional days, 29% of the ^{90}Sr was incorporated in apatite (Table 3.3, line 3). The subsequent high-concentration injection (Figure 3.12b) eluted 14.1% of the ^{90}Sr . The subsequent 90-day waiting period is in progress before destructive sampling of this column is conducted to measure ^{90}Sr incorporated in apatite. Additional experiments, which are ongoing, are needed to quantify the long-term ^{90}Sr uptake rates for these different sequential solution applications, along with ^{90}Sr mobilization that results from these high-concentration injections.

Table 3.3. ^{90}Sr Mass Balance for Low-, then High-Ca-Citrate- PO_4 Injections in One-Dimensional Columns

Event	Sr-90 Mass Balance (%)				Total (uCi)
	Aqueous	Ion Exch.	In Apatite	Eluded	
1. Sr-90/sed. equilibrium	0.70%	99.30%			0.1908
2. low conc. inject (4, 10, 2.4 mM)				5.6%	0.1801
3. 32 d wait, gw inject	0.06%	70.9%	29.0%	1.3%	0.1778
4. high conc. inject (28,79,17 mM)				14.1%	0.1527
5. 90 d wait, gw inject (in progress)					

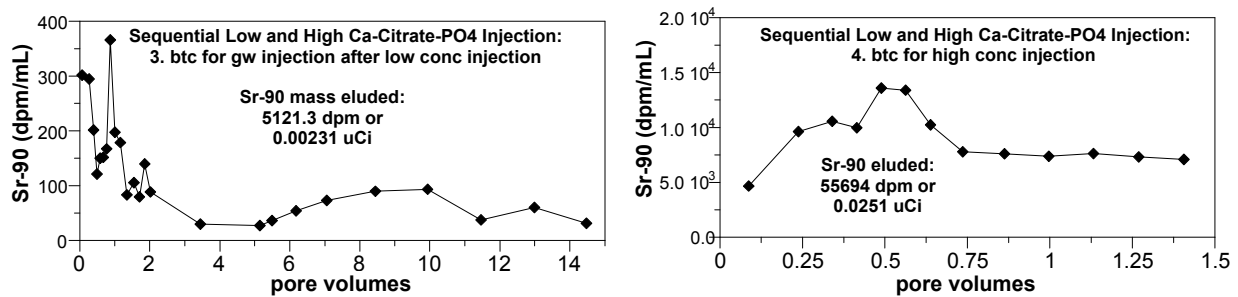


Figure 3.12. ^{90}Sr Breakthrough in Sequential Low- and High-Concentration Ca-Citrate- PO_4 Injections in One-Dimensional Columns

In summary, laboratory-scale experiments have demonstrated that injection of different Ca-citrate- PO_4 solutions into 100-N Area subsurface sediments results in citrate biodegradation and subsequent formation of microcrystalline apatite. Both ^{90}Sr uptake mass and uptake rate were quantified to assess the viability of a long-term PRB. Some ^{90}Sr uptake occurs during the initial apatite precipitation phase (20 to 60%), especially if divalent-poor Ca-citrate- PO_4 solutions are injected. Solid-phase substitution of strontium (and ^{90}Sr) for calcium in the apatite structure occurs due to higher thermodynamic stability of strontium-laden apatite. This solid-phase ^{90}Sr incorporation is slow (months to years) but more rapid than the natural groundwater migration rate of strontium, so from a rate perspective should form an effective PRB. From a ^{90}Sr mass perspective, targeted apatite content would provide sufficient apatite mass to uptake strontium (and ^{90}Sr) for 300 years (10 half-lives of ^{90}Sr decay) assuming 10% strontium substitution for calcium in apatite (measured strontium substitution for calcium in apatite varied from 1 to 16.3% at 9 months), with greater substitution for poorly crystalline apatite (expected at field scale). Because most laboratory experiments were focused on relatively low-concentration Ca-citrate- PO_4 solutions, additional experiments are needed to determine the most efficient method of sequential injections to increase the amount of apatite precipitation needed to prevent migration of ^{90}Sr in the 100-N Area aquifer toward the Columbia River. Additional experiments evaluating several chemical formulations and their impact on this sequential injection approach are ongoing.

4.0 100-N Apatite Site Setup

This section describes site injection/monitoring well and aquifer tube installation, operational and monitoring equipment setup, and aqueous sampling/analysis methods/requirements for the apatite treatability test (see Figures 4.1 and 1.10). Two initial characterization wells were installed at the 100-N Area apatite treatability test site in 2005 for detailed aquifer and sediment analysis, including depth-discrete ^{90}Sr measurements of the sediment. These wells were also identified as downgradient compliance monitoring wells. During 2006, 10 injection wells were installed to support installation of the 91-m (300-ft) barrier, 8 performance monitoring wells were installed at pilot test site #1 (199-N-138), 9 performance monitoring wells were installed at pilot test site #2 (199-N-137), and 2 additional compliance monitoring wells were installed. A tracer injection test and the first pilot apatite injection test (well 199-N-138) were conducted in spring 2006 during high-river stage conditions. Pilot test #2 was conducted in September 2006 at 199-N-137, which is located on the downstream end of the barrier, during low-river stage conditions.



Figure 4.1. Photograph Showing Location of the 100-N Area Apatite Treatability Test Along the Columbia River

4.1 Well Installation

This section presents details of the well design, drilling, sampling, well construction, and development. Figures 1.10, 4.2, and 4.3 show the locations of the large-diameter injection wells and smaller-diameter monitoring wells that were installed during the three drilling campaigns described in the following sections.

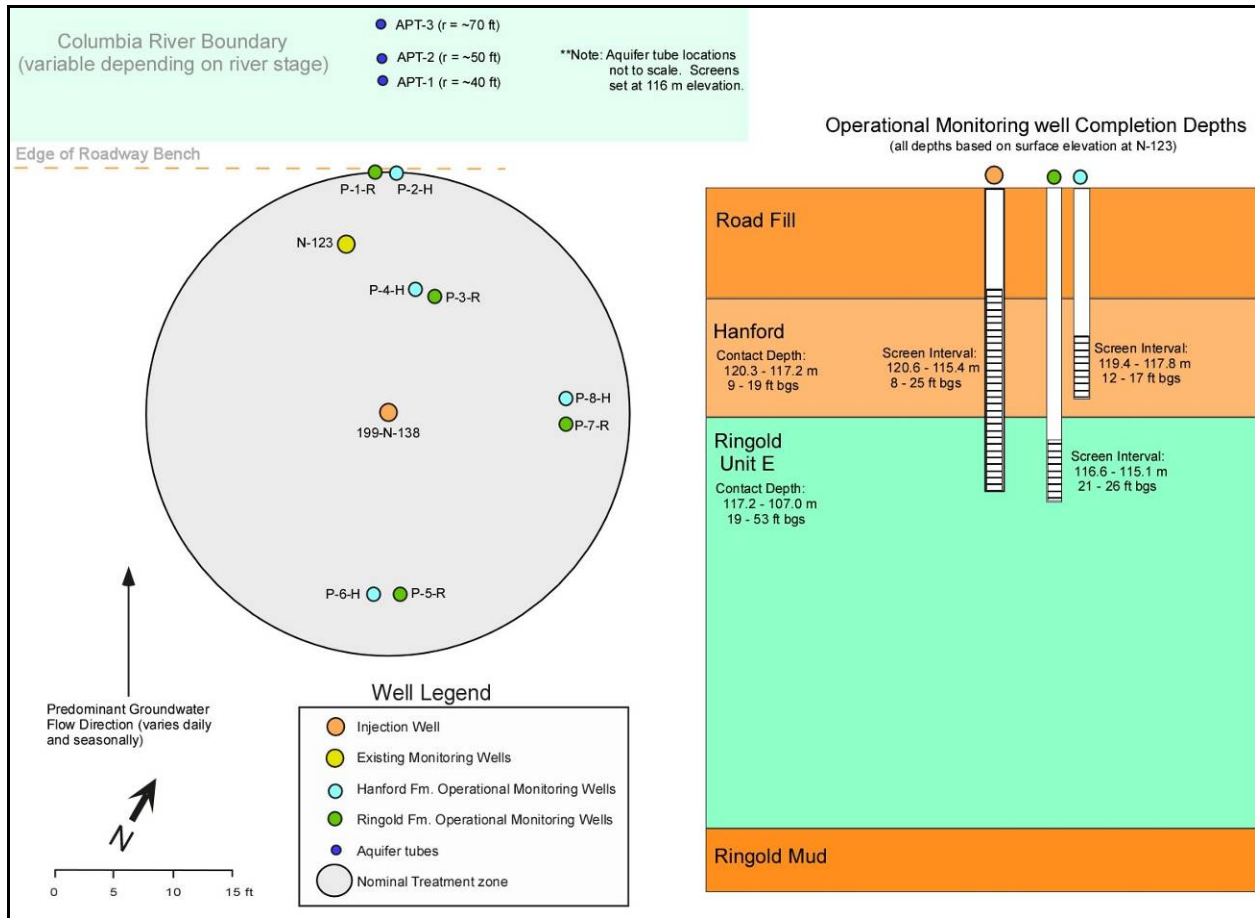


Figure 4.2. Pilot Test Site #1 (Around Well 199-N-138). Prefix 199- omitted from well names.

4.1.1 2005 Characterization Well Installation

Two boreholes (199-N-122 and 199-N-123, Figure 1.10) were drilled in FY 2005 to provide hydrogeologic and geochemical characterization data needed for the pilot test and overall barrier emplacement design analysis. These wells are designated as compliance monitoring wells for the barrier. They are 15-cm (6-in.)-inside-diameter (ID) wells installed using cable tool drilling with 6-m- (20-ft)-long, 20-slot screens. The screen depth intervals for the wells are 2.1 to 8.2 m (7 to 27 ft) below ground surface (bgs) for well 199-N-122 and 3 to 9 m (10 to 30 ft) bgs for well 199-N-123. A geologic cross section running along the proposed barrier alignment is illustrated in Figure 4.4. This cross section was constructed based on hydrogeologic information obtained during the installation of these wells and from geologic logs from previous well installations. The zone designated as the Hanford formation contains a significant amount of reworked Ringold Formation materials; this effect was more evident at the well 199-N-123 location. Both of the boreholes were completed as downgradient performance assessment monitoring wells. As the boreholes were advanced, continuous core samples were collected and submitted for grain-size analysis, microbial characterization, and determination of ^{90}Sr concentration with depth. The results of the ^{90}Sr soil profiles with depth are shown in Figure 1.9. These data were used to determine the injection well screened interval for subsequent well installations. Based on the data in Figure 1.9, a 5.2-m (17-ft)-thick treatment zone was selected from 2.1 to 8.2 m (7 to 27 ft) bgs.

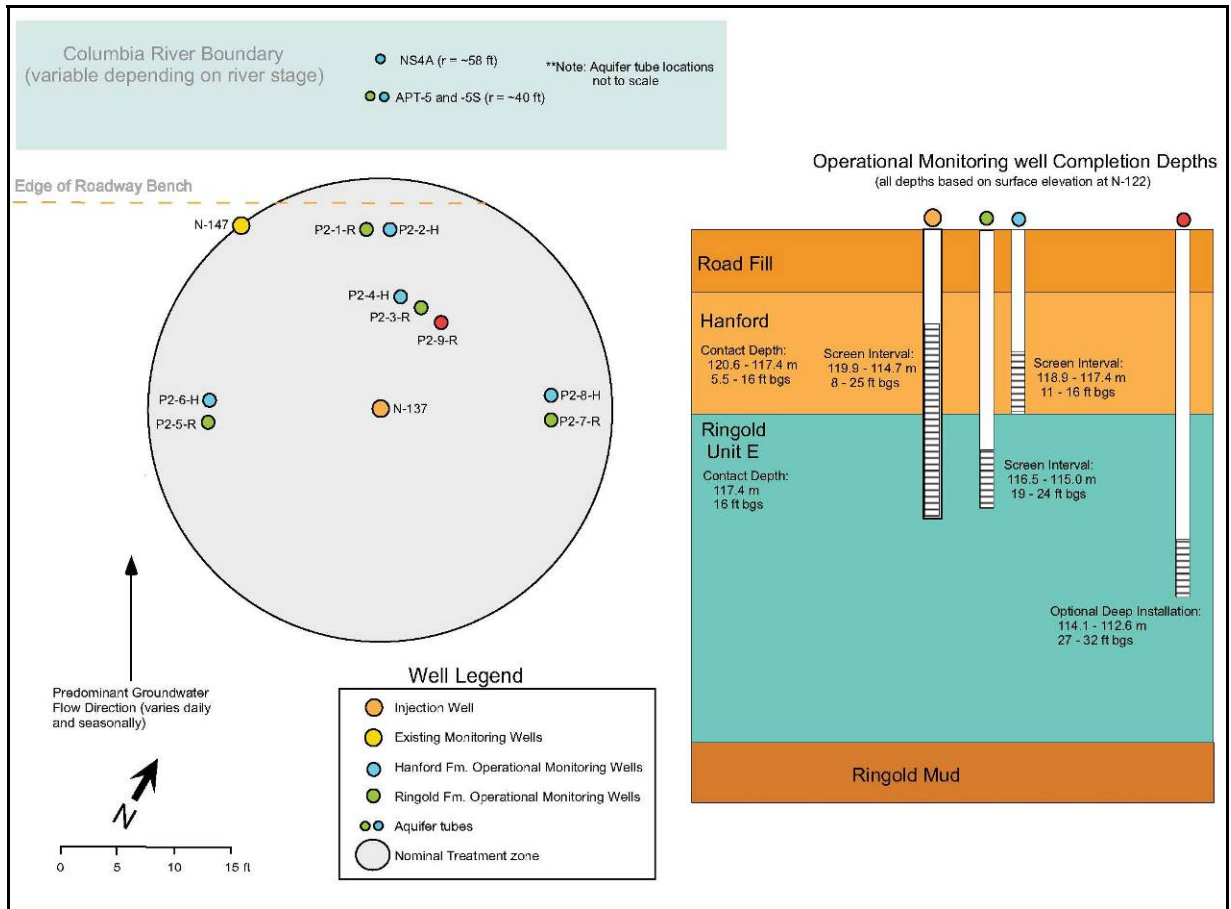


Figure 4.3. Pilot Test Site #2 (Around Well 199-N-137). Prefix 199- omitted from well names.

4.1.2 Early 2006 Well Installation – Injection, Performance Monitoring, and Pilot Test #1 Monitoring Wells

This section is a summary of *Borehole Summary Report for 100-NR-2 Treatability Test Wells* (FH 2006), which provides detailed documentation of the well installations including field-generated records, field activities during drilling, and well construction of both monitoring and injection wells. Well drilling for installation of the initial injection and monitoring wells was conducted at the site from January-March 2006. This drilling campaign resulted in the installation of 10 injection wells, 2 additional compliance monitoring wells, and 8 small-diameter wells for monitoring the pilot test site #1. These wells are listed in Table 4.1 and discussed in more detail below.

After all the wells were completed, the top of the well casing was cut off slightly below ground surface and then fitted with a slip-on well cap. The surface completion comprised a flush-mount, water-tight monument surrounded by a concrete surface seal that extended below grade. A brass survey marker with the well identification number, name, and completion date was installed in the concrete surface.

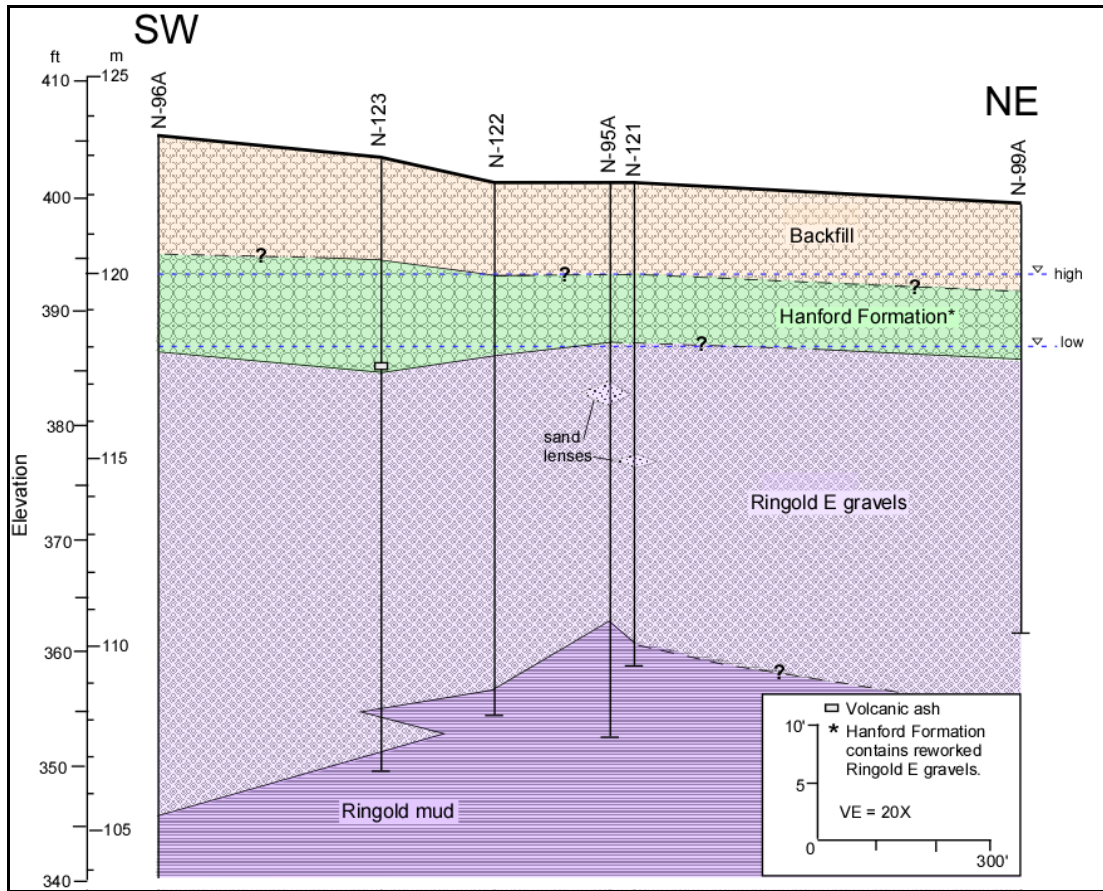


Figure 4.4. Geologic Cross Section Updated Based on 2005 Characterization Wells. Prefix 199- omitted from well names.

4.1.2.1 Injection Wells

Ten injection wells, 199-N-136 to 199-N-145, were installed using cable tool drilling along the road at N-Springs at 30-ft spacing along the road (see Figure 1.10 and Table 4.1). The injection wells are 15-cm (6-in.)-ID stainless steel with 5.2-m (17-ft)-long, 20-slot screens. The screened interval for the injection wells was from 2.1 to 7.3 m (7 to 24 ft) bgs based on the depth interval of ⁹⁰Sr contamination measured in soil samples from the 2005 characterization wells shown in Figure 1.9.

4.1.2.2 Compliance Monitoring Wells

Two additional compliance monitoring wells, 199-N-146 and 199-N-147, were also installed during this period using the cable-tool drilling rig while it was available at the site (see Figure 1.10 and Table 4.1). Construction for these compliance monitoring wells was the same as the injection wells (15-cm [6-in.]-ID stainless steel with 5.2-m [17-ft]-long, 20-slot screen). The monitoring wells also were equipped with sampling pumps.

4.1.2.3 Pilot Test Site #1 Small-Diameter Monitoring Wells

Eight small-diameter operation monitoring wells were also installed at the first pilot test site (around well 199-N-138; see Figure 4.2) during January 2006 using a hydraulic hammer unit (Table 4.1). These

small-diameter wells were constructed from 3.2-cm (1.25-in.)-ID polyvinyl chloride (PVC) with 1.5-m (5-ft) screened intervals (10-slot). The wells were installed in pairs in shallow 3.7 to 5.2 m (12 to 17 ft) bgs and deep 6.4 to 7.9 m (21 to 26 ft) bgs completions, as shown in Table 4.2. The wells are used to monitor the extent of the injected apatite solution during the first pilot test at different radial distances in both the upper (Hanford) and lower (Ringold) Formation portions of the targeted treatment zone. In addition to the assigned Hanford Site well name, a project-specific well identifier that provides indication of the interval sampled (i.e., Hanford or Ringold Formation) is shown in Table 4.2.

Table 4.1. Early 2006 Well Identification and Drilling Date Summary

Well Name	Well ID	Drilling Date 2006		Purpose	Ecology Well Tag
		Start	Finish		
199-N-126	C5032	1-09	1-10	SM	ALC-201
199-N-127	C5033	1-10	1-10	SM	ALC-202
199-N-128	C5034	1-11	1-12	SM	ALC-203
199-N-129	C5035	1-12	1-12	SM	ALC-204
199-N-130	C5036	1-12	1-13	SM	ALC-205
199-N-131	C5037	1-13	1-13	SM	ALC-206
199-N-132	C5038	1-10	1-11	SM	ALC-207
199-N-133	C5039	1-11	1-11	SM	ALC-208
199-N-136	C5042	3-20	3-22	I	ALC-220
199-N-137	C5043	3-23	3-27	I	ALC-221
199-N-138	C5044	1-30	2-06	I	ALC-211
199-N-139	C5045	2-07	2-10	I	ALC-212
199-N-140	C5046	2-10	2-15	I	ALC-213
199-N-141	C5047	2-16	2-22	I	ALC-214
199-N-142	C5048	2-28	3-02	I	ALC-216
199-N-143	C5049	3-02	3-07	I	ALC-217
199-N-144	C5050	3-07	3-14	I	ALC-218
199-N-145	C5051	3-14	3-17	I	ALC-219
199-N-146	C5052	2-23	2-27	CM	ALC-215
199-N-147	C5116	3-28	3-30	CM	ALC-222

CM = Compliance monitoring well.
I = Injection well.
SM = Small-diameter monitor well.

Table 4.2. Small-Diameter Pilot Test Site #1 Monitoring Well Construction Summary

Well Name	Project Well ID	Drill Depth (ft bgs)	Screen Interval (ft bgs)	Completion Design
199-N-126	P-1-R	28.8	27.3-22.3	Deep – Ringold Completion
199-N-127	P-2-H	18.2	17.7-12.7	Shallow – Hanford Completion
199-N-128	P-3-R	28.5	26.6-21.6	Deep – Ringold Completion
199-N-129	P-4-H	18.0	17.1-12.1	Shallow – Hanford Completion
199-N-130	P-5-R	30.0	27.5-22.2	Deep – Ringold Completion
199-N-131	P-6-H	19.0	17.5-12.5	Shallow – Hanford Completion
199-N-132	P-7-R	29.5	27.2-22.2	Deep – Ringold Completion
199-N-133	P-8-H	19.0	17.7- 12.7	Shallow – Hanford Completion

bgs = Below ground surface.

4.1.2.4 Well Development

Well development of the treatability test injection wells (199-N-136 to 199-N-145) was conducted in April 2006; results from these well development activities are provided in FH (2006, Table 2-4). Each small diameter, pilot test site monitoring well was surged repeatedly with an appropriately sized surge block and pumped to clarity with a peristaltic pump. Development of these small diameter wells was performed by FH personnel (results are not included in FH 2006).

Development data of the injection wells show there is a distinct difference in drawdown of the upstream injection wells between 199-N-138 and 199-N-142 (see Figure 1.10) and the downstream injection wells between 199-N-143 and 199-N-137. Specific capacity for each injection well was calculated based on pressure response to developmental pumping (FH 2006, Table 2-4) and is shown in Figure 4.5. Specific capacity is the quantity of water a well can produce per unit of drawdown and can be used to compare the relative transmissivity of the aquifer and injection wells. While specific capacity is not directly proportional to hydraulic conductivity, it is an indicator of both hydraulic conductivity and well efficiency. The specific capacity on the downstream half of the barrier is 10 to 30 times higher than the upstream portion of the barrier. These differences were also observed during the injections at the pilot test site #1 at the upstream end of the barrier that had a higher injection mound than pilot test site #2.

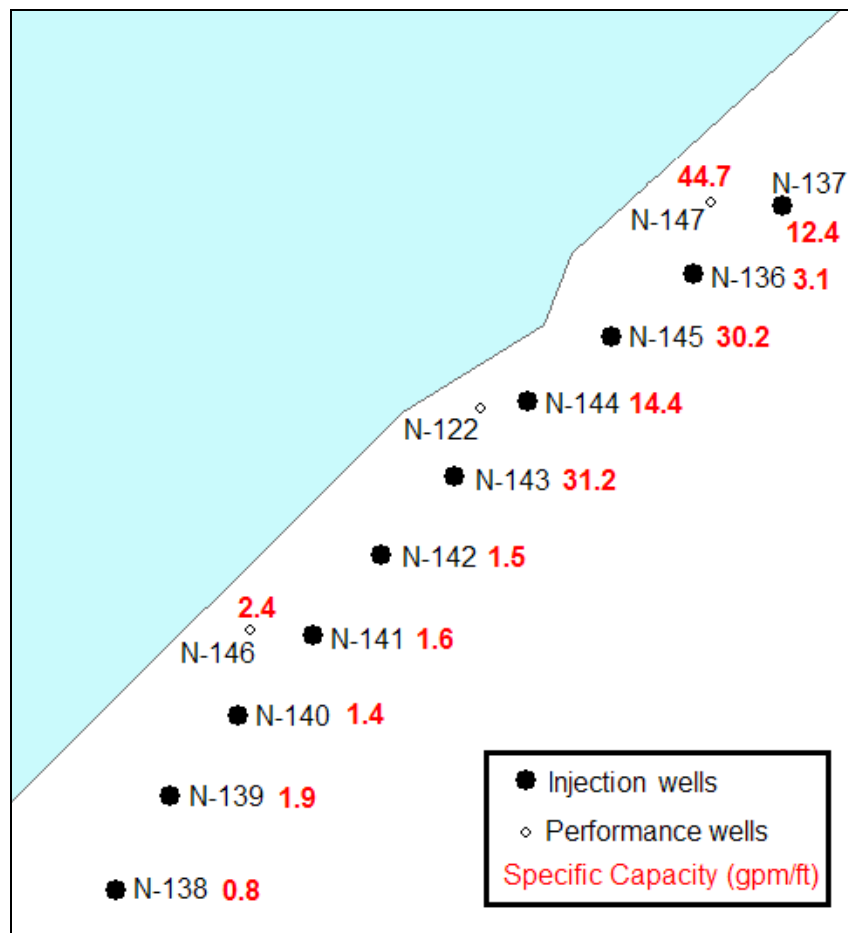


Figure 4.5. Specific Capacity (gal/min/ft) of the Apatite Barrier Injection Wells (calculated from FH 2006, Table 2-4). Prefix 199- omitted from well names.

4.1.3 Late 2006 Well Installation – Pilot Test #2 Monitoring Wells

Nine 5-cm (2-in.)-ID PVC monitoring wells were installed around the second pilot test site (well 199-N-137) between September 18 to September 20, 2006 (see Figure 4.3), using sonic drilling. These monitoring wells included shallow (screen from 3.4 to 4.6 m [11 to 15 ft] bgs in the Hanford formation) and deep completions (screen interval from 5.8 to 7.3 m [19 to 24 ft] bgs in the Ringold Formation). An additional well was also installed deeper in the Ringold Formation (screen interval from 8.5 to 10 m [28 to 33 ft] bgs) below the targeted treatment zone. Well construction summary sheets and survey coordinates for the Pilot Test Site #2 monitoring wells are included in Appendix C. Correlation between the Hanford Site well name and project-specific well identifier is shown in Table 4.3. These wells were used to monitor the extent of the injected apatite solution during the second pilot test at different radial distances in both the upper (Hanford) and lower (Ringold) Formation portions of the targeted treatment zone. There were no sediment samples collected or analyzed as part of this well installation effort.

Table 4.3. Small-Diameter Pilot Test Site #2 Monitoring Well Construction Summary

Well Name	Project Well ID	Completion Design
199-N-148	P2-1-R	Deep – Ringold Completion
199-N-149	P2-2-H	Shallow – Hanford Completion
199-N-151	P2-3-R	Deep – Ringold Completion
199-N-150	P2-4-H	Shallow – Hanford Completion
199-N-156	P2-5-R	Deep – Ringold Completion
199-N-155	P2-6-H	Shallow – Hanford Completion
199-N-154	P2-7-R	Deep – Ringold Completion
199-N-153	P2-8-H	Shallow – Hanford Completion
199-N-152	P2-9-R	Deeper Ringold completion

4.1.4 Updated Geologic Cross Section

Data from the two borehole summary reports for the 2005 and 2006 drilling (FH 2005, 2006) were used to update the geologic cross section along the 100-N Area apatite barrier. A southwest-to-northeast cross section through the 100-N Area is presented in Figure 4.6. Because the texture of the sediments between the upper stratigraphic units (Ringold Unit E, Hanford formation, and backfill) is so similar (i.e., sandy gravel), it may be difficult to distinguish between these units. Furthermore, the boundaries between these units are not discrete, but instead often grade into one another as a result of the sediment reworking and mixing during deposition.

The characteristics used to differentiate these units include a combination of often-subtle variations in 1) basalt content, 2) sorting, 3) color, 4) roundness, 5) consolidation, and 6) weathering (DOE/RL 2002). Some of these diagnostic properties (e.g., consolidation, sorting, and roundness) are destroyed during the drilling process, so inspection of drill cuttings may not provide a clear indication of stratigraphic boundaries. For this reason, intact drill cores (with accompanying high-resolution photographs) provide the best and most representative samples for distinguishing subtle differences between the units.

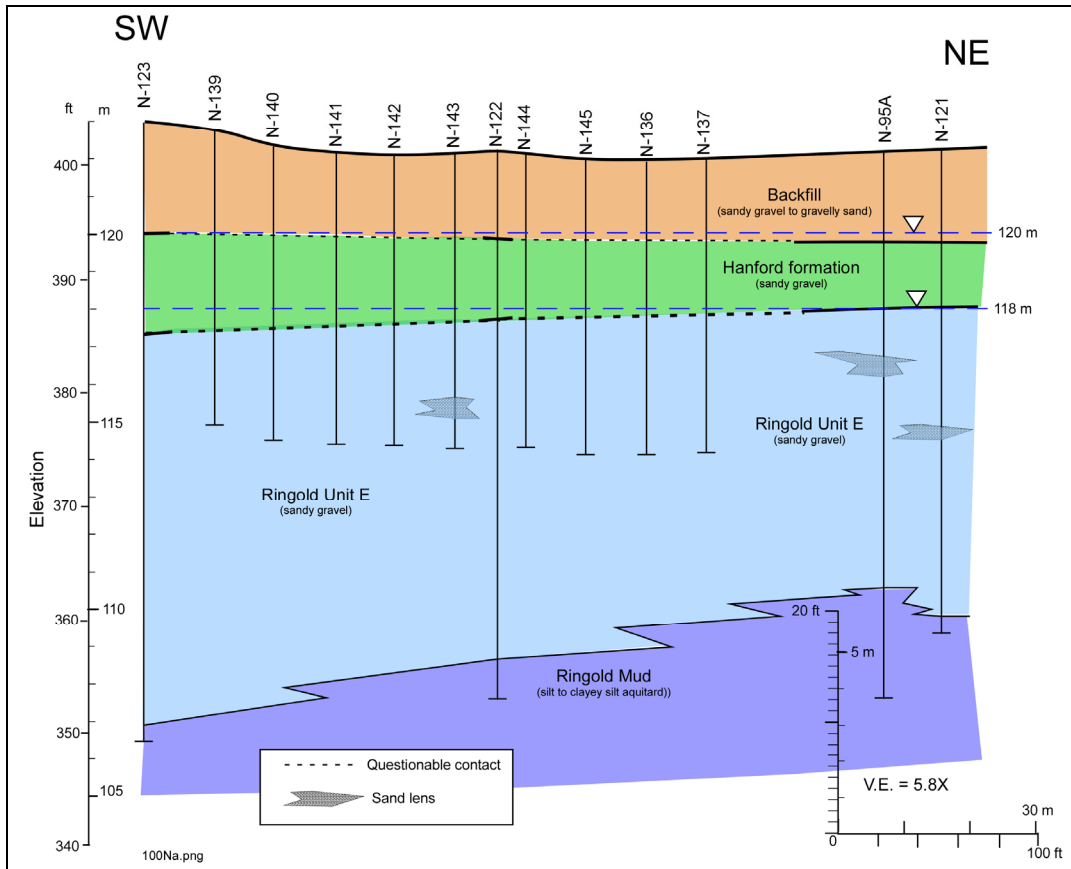


Figure 4.6. Geologic Cross Section Updated Based on Data Collected During Installation of Injection and Compliance Monitoring Wells in 2006. Prefix 199- omitted from well names.

The quality of the noncore samples and log descriptions coming from the injection and compliance monitoring wells installed in 2006 are inferior to the core samples collected from characterization wells drilled in 2004 (199-N-121, 199-N-122, and 199-N-123); therefore, the contacts based on the characterization wells were used as the baseline for the developed cross section. Contacts for the intervening wells in the cross section are simple straight lines, which connect the contacts for the core holes. Contact depths for the injection and compliance monitoring wells identified on geologist logs are highly variable, and as a result show considerable relief along contacts, which is probably not realistic. Therefore, using contacts from the characterization wells alone is believed to provide the best available estimation.

4.2 Aquifer Tubes

Between June 2005 and August 2006, 33 aquifer tubes were installed along the 100-N Area shoreline in support of the Remediation Task of the Remediation and Closure Science (RACS) Project. Figure 4.7 is a picture of an aquifer tube installed to better characterize the ^{90}Sr plume. During the apatite pilot testing, some of these tubes were used as sampling locations to examine the efficiency of the apatite injection. An additional five tubes were installed to directly support this test. The aquifer tubes used by this test were located along the river shore between the apatite barrier and river (Figure 1.3).

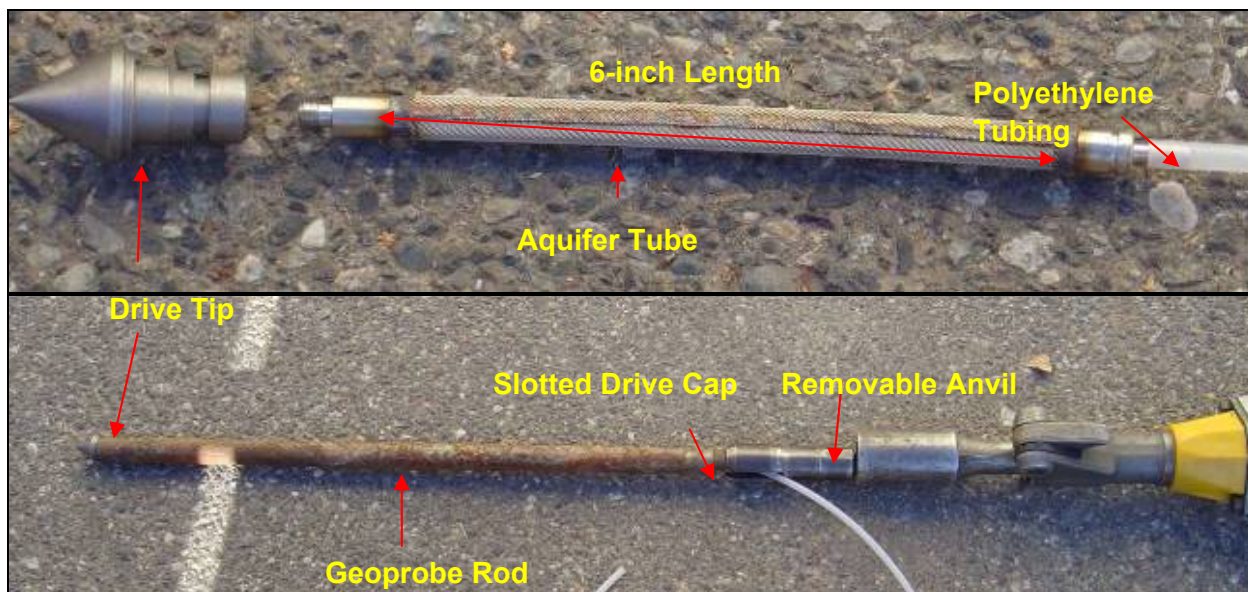


Figure 4.7. Components of the Screen Portion of an Aquifer Tube Used During Installation

The sampling port for each aquifer tube is 15-cm (6-in.) long, 7.6-mm (0.3-in.) in diameter, with an 80-mesh stainless-steel screen (Geoprobe, Salina, Kansas). Polyethylene tubing was attached to one end of the screen; the other end was mated with a hardened-steel drive tip (Figure 4.7). The polyethylene tubing was run up the shoreline above the high water mark where sampling took place. Table 4.4 lists the aquifer tubes that were used for sampling along with screened depths. Installation procedures can be found in Mendoza et al. (2007).

Table 4.4. Pilot Test Site Aquifer Tube Construction Summary

Aquifer Tube Name	Well ID	Screen Top Elevation (m amsl)
AT-1	C5269	116.2
AT-2	C5270	116.4
AT-3	C5271	116.2
AT-5	C5386	116.2
AT-5S	Na	117.7

amsl = Above mean sea level.
 NA = Not available, pending assignment.

4.3 Site Setup

This section includes a description of the site utilities, monitoring equipment, analytical equipment, injection equipment, and the integration of these components into the operational systems required to conduct this test at the 100-NR-2 OU located along the Columbia River. Figure 4.8 shows a picture of the field site with the injection equipment and sampling trailer. FH provided all injection equipment and the delivery monitoring components associated with these field tests. PNNL provided and operated all required sampling equipment during and immediately after the injections. FH provided equipment and personnel for longer-term post injecting performance assessment monitoring.

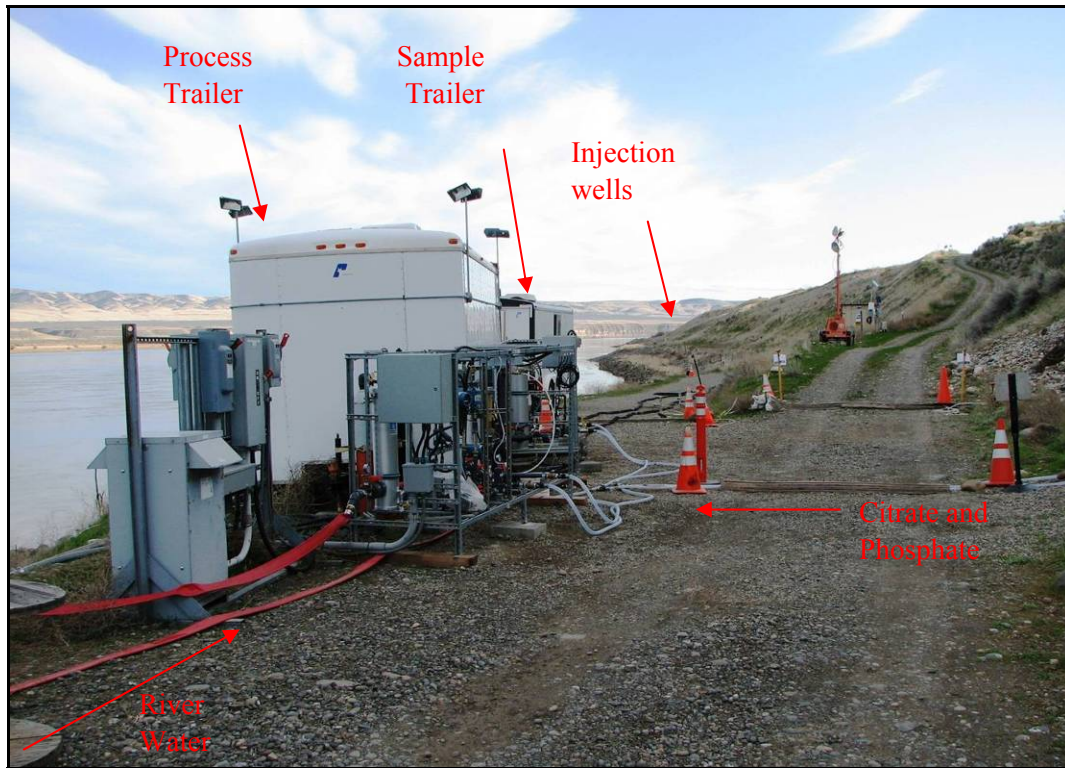


Figure 4.8. Apatite Chemical Delivery Systems Along the 100-N Area Shoreline

4.3.1 Site Utilities

Site utility requirements for this apatite injection include access to power, a water supply, and wastewater disposal. A substantial amount of water was needed to make up the injection solutions. At the test site, Columbia River water was used to dilute the apatite chemical solution, which consisted of two simultaneous injections, a citrate, and phosphate solution. These solutions were purchased and brought to the site premixed in 18,900-L (5000-gal) tanker trucks. A diesel generator was used to operate the site facilities, which included a mobile laboratory trailer, an injection monitoring process trailer, and the injection/monitoring equipment. Ancillary equipment was also powered via the generator.

During sampling, purge water was collected in a 1135-L (300-gal) purge tank during the test. FH was responsible for the disposal of this purge water.

4.3.2 Injection Equipment

Two skids were used for the injection of the apatite solution. A schematic and a picture of the injection equipment are shown in Figures 4.9 and 4.10, respectively. Each skid used a 10-cm (4-in.) submersible pump (A.Y. McDonald Mfg. Co., 7.5 horsepower [HP]) to carry the process water from the Columbia River to the skids, where it went through an in-line filter to remove any debris. The river flow rates ranged from 40–60 gpm during the testing, depending on the head buildup in the wells, and were controlled by an adjustable frequency drive (Allen-Bradley Rockwell Automation, 10 HP) and measured with an in-line flow meter (Rosemount Division, Emerson Process Management, 8732 C). The two citrate and phosphate solutions were gravity fed (height of ~23 m [~75 ft]), or in some cases, additional line pressure was provided by an in-line centrifugal booster pump from the tanker trucks to the skids. The

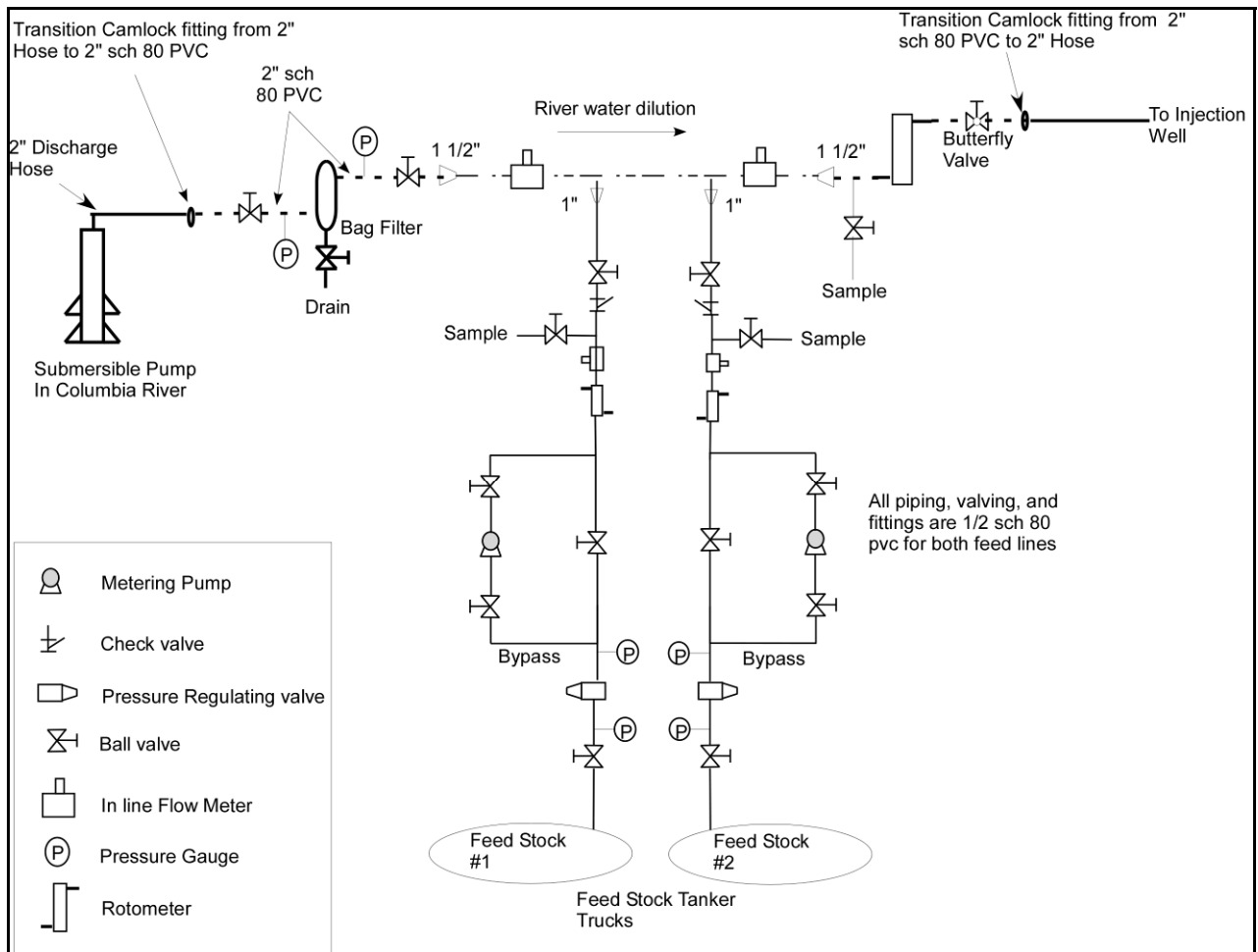


Figure 4.9. Schematic Drawing of Skid for Apatite Delivery System

flow rates were controlled with ball valves and monitored with two instruments; an in-line flow meter (Rosemount, 8732 C) and a rotometer (F44750LH-12, BlueWhite Industries). After the two solutions were mixed with the river water, an additional in-line flow meter (8732 C, Rosemount) was used to measure the total flow along with a rotometer (F452100LHN, BlueWhite Industries). The data for the in-line flow meters were recorded with universal serial bus (USB) style 4-20 mA data loggers (EasyLogger EL-USB-4) and recorded at 1-minute intervals. From the skid, 5-cm (2-in.) Goodyear® hose with camlock fittings was run to each injection well.¹ Pressure gauges were outfitted on the filter housing and on the apatite solution lines. These gauges provided pressure monitoring for the filters and gave an indication of the tanker level or potential clogging.

¹ Goodyear is a registered trademark of the Goodyear Tire & Rubber Company.

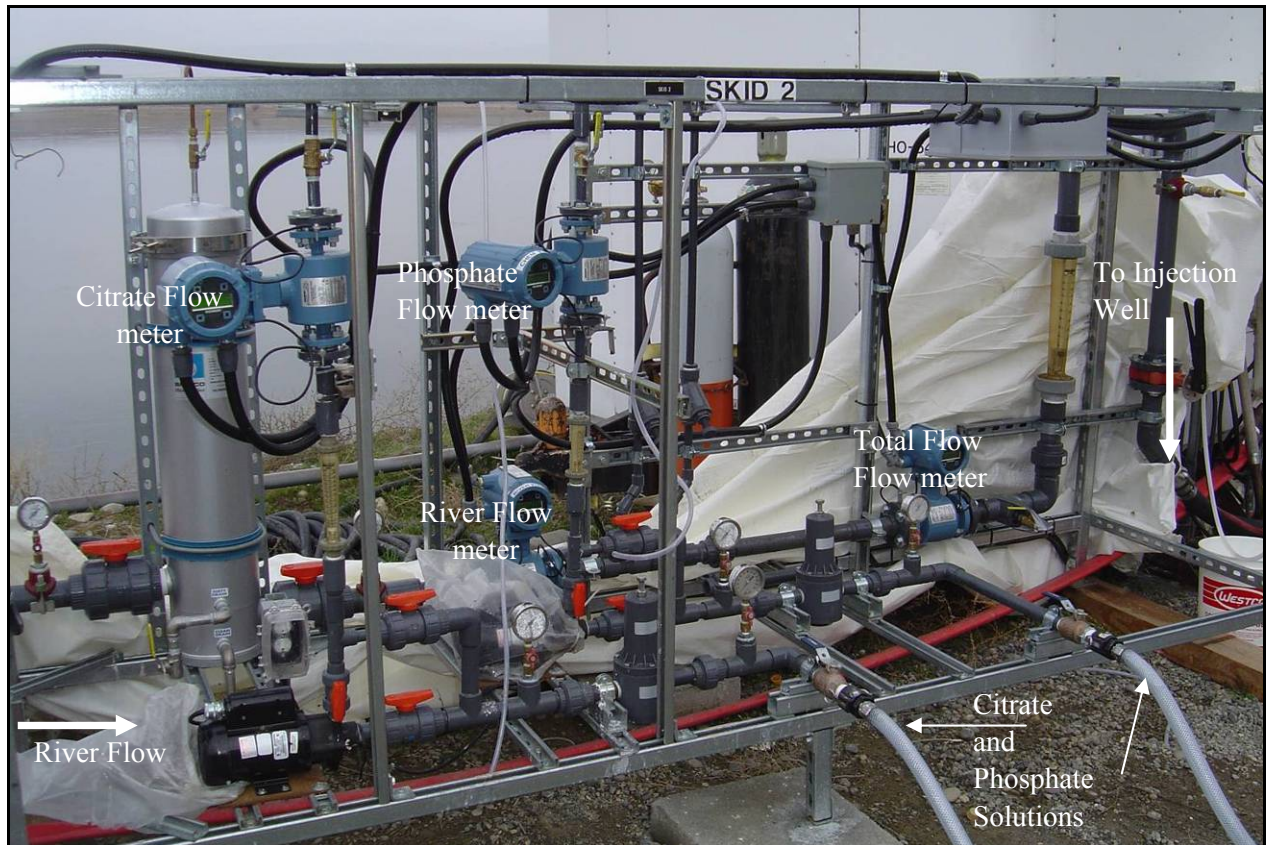


Figure 4.10. Apatite Delivery System Skid 2. An identical skid was used in parallel with this skid to deliver the phosphate and citrate solutions to the injection wells. All control of the solution mixing and delivery was performed on the skid.

4.3.3 Pressure Monitoring

Water levels in the wells were monitored with a hermit and level troll (In-Situ, Inc.) pressure transducers and data loggers. Depending on availability, pressure transducers were installed in the injection well, adjacent wells, and available nearby monitoring wells. Typical data logger rates were 1 minute.

4.4 Aqueous Sampling and Analysis

Aqueous samples were collected using either a peristaltic pump (E/S portable sampler, Cole Parmer, Illinois) or 12-V electric submersible pump (ProPurge™ Mini-Typhoon, Marton Geotechnical Services, United Kingdom) during the pilot testing and barrier installation. A dedicated pump and/or sample line tubing was installed in each well. Field parameters were measured for each sample using a handheld ultrameter (Model 6P, Myron L Company, California) or an MP-20 flow cell (QED Environmental Systems, Inc., Michigan). Specific conductance, oxidation reduction potential, temperature, DO, and pH were measured in the field (Table 4.5). Aqueous samples were collected in the field trailer for offsite analyses of other parameters. Table 4.5 lists the analytic sampling requirements for the parameters, container volume, and preservation methods required for the required offsite analyses; Table 4.6 lists parameters, analytic methods, and detection limits for aqueous analytes.

Table 4.5. Apatite Pilot Test Sampling Requirements

Parameter	Media/ Matrix	Volume/ Container	Preservation	Hold Time
Major Cations/metals: Al, As, B, Ba, Bi, Ca, Co, Fe, K, Mg, Mn, Ni, Zn, Zr, P, Sr, Na, Si, S, Sb	Water	20 mL plastic vial	Filtered (0.45 µm), HNO ₃ to pH <2	60 days
Anions: Cl ⁻ , Br ⁻ , SO ₄ ²⁻ , PO ₄ ³⁻ , NO ₂ ⁻ , NO ₃ ⁻	Water	20 mL plastic vial	Cool 4°C	45 days
Small molecular weight organic acids: Citrate, Formate	Water	20 ml plastic via	Filtered (0.22 µm) Sodium azide or freeze	20 days
⁹⁰ Sr	Water	1 L plastic bottle	Filtered (0.45 µm), HNO ₃ TO PH <2	60 days
^{89/90} Sr	Water	1 L plastic bottle	Filtered (0.45 µm), HNO ₃ TO PH <2	60 days
pH	Water	Field Measurement	N/A	N/A
Specific Conductance	Water	Field Measurement	N/A	N/A
Dissolved Oxygen	Water	Field Measurement	N/A	N/A
Oxidation-Reduction Potential	Water	Field Measurement	N/A	N/A
Temperature	Water	Field Measurement	N/A	N/A

N/A = Not applicable.

Table 4.6. Analytical Requirements

Parameter	Analysis Method	Detection Limit or Range	Typical Precision/ Accuracy	QC Requirements
Major cations/metals: Al, As, B, Ba, Bi, Ca, Co, Fe, K, Mg, Mn, Ni, Zn, Zr, P, Sr, Na, Si, S, Sb	ICP-OES, EPA Method 6010B	1 mg/L to 0.1 mg/L, depending on cation	±10%	Daily calibration; blanks and duplicates and matrix spikes at 10% level per batch of 20.
Anions: Cl ⁻ , Br ⁻ , SO ₄ ²⁻ , PO ₄ ³⁻ , NO ₂ ⁻ , NO ₃ ⁻	Ion chromatography, EPA Method 300.0A. or equivalent	1 mg/L	±15%	Daily calibration; blanks and duplicates at 10% level per batch of 20.
Small molecular weight organic acids: citrate and formate	Ion chromatography, AGG-IC-001 (based on EPA Method 300.0A)	1 mg/L	±15%	Daily calibration; blanks and duplicates at 10% level per batch of 20.
⁹⁰ Sr	Separation followed by gross alpha/beta via liquid scintillation	75 pCi/L	±15%	Daily calibration; blanks and duplicates at 10% level per batch of 20.
^{89/90} Sr	Liquid scintillation	25 pCi/L	±10%	1 blank spike and 1 matrix spike per analytical batch.
pH	pH electrode	(2 to 12 units)	± 0.2 pH unit	User calibrate per manufacturer directions.
Specific conductance	Electrode	(0 to 100 mS/cm)	± 1% of reading	User calibrate per manufacturer directions.
Dissolved oxygen	Membrane electrode	(0 to 20 mg/L)	± 0.2 mg/L	User calibrate per manufacturer directions.
Oxidation-reduction potential	Electrode	(-999 to 999 mV)	±20 mV	User calibrate per manufacturer directions.
Temperature	Thermocouple	(-5 to 50°C)	± 0.2°C	Factory calibration.

ICP-OES = Inductively coupled plasma-optical emission spectroscopy.
QC = Quality control.

Samples of the injection solution and raw feed stock were collected at the injection skid. Injection solution field parameters were routinely monitored throughout the injection and samples for laboratory analysis were collected at the beginning, middle, and end of each injection. All skid samples were collected in 500-mL polyethylene bottles. The skid samples were then taken to the laboratory trailer where they were divided into multiple bottles for the various analyses (see Table 4.5).

5.0 100-N Apatite Pilot Field Tests

This section describes the pilot field testing of low-concentration apatite forming (i.e., Ca-citrate-PO₄) solutions that was conducted at the 100-N Area treatability test site for the in situ sequestration of ⁹⁰Sr over a 91-m (300-ft)-long PRB (see Figure 1.10). The objective of the low-concentration Ca-citrate-PO₄ solution injections is to stabilize the existing ⁹⁰Sr before injecting high-concentration Ca-citrate-PO₄ solutions. The ionic strength of the injection solution, particularly divalent ions such as calcium, causes desorption of ⁹⁰Sr from the sediments, resulting in increased aqueous ⁹⁰Sr concentrations. Low-concentration injections limited this temporary increase in ⁹⁰Sr concentration by stabilizing existing ⁹⁰Sr adsorbed to sediments within the treatment zone so that subsequent higher-concentration apatite solution injections could then be accomplished without large ⁹⁰Sr concentration increases (see Section 2.5).

Field testing for the 100-N Area apatite treatability test consisted of two phases: initial pilot injection tests at two locations, followed by development of and injection design and subsequent barrier emplacement operation at eight additional well locations, providing for initial low-concentration treatment of the 91-m (300-ft)-long PRB. The monitoring well layout design for the pilot test sites consisted of a number of two-well sets, one completed in the Hanford formation and one in the Ringold Formation, at various radial distances and directions from the injection wells.

A tracer injection test and the first pilot Ca-citrate-PO₄ injection test were conducted at the upstream end of the barrier (well 199-N-138; see Figure 1.10 and 4.2) in spring 2006 during high-river stage conditions. A second pilot test at a different well (199-N-137; see Figure 4.3) at the opposite (downstream) end of the barrier was conducted in September 2006 during low river stage conditions. The tracer test was conducted to help determine injection volumes and rates, in addition to testing of the site injection/monitoring systems. The timing of these tests, along with the Columbia River stage at 100-N Area, is shown in Figure 5.1. As discussed in Section 3.2, the injection formula was revised for the second pilot test based on results monitoring of the first pilot test and additional laboratory work. The injection formula was revised again after the second pilot test for the remaining barrier well injections. Low-concentration Ca-citrate-PO₄ solutions were injected into nine wells in February and March 2007 during both high- and low-river stage conditions. Six additional injections occurred in June and July 2007 during high river stage conditions for wells that were treated during low-river stage conditions in February and March. Detailed field test instructions containing injection chemical composition, injection volumes and rates, and sampling requirements were prepared before these field tests. These tests are described in the following sections.

5.1 Tracer Test at Pilot Test Site #1

A conservative tracer test using a sodium bromide solution was conducted at the pilot test site #1 (well 199-N-138) on May 3, 2006, during relatively high-river stage conditions, as shown in Figures 5.1 and 5.2. The objectives of the tracer test, which were developed to aid in designing the apatite treatment injection test, included estimating the radial extent of injected solution, assessing spatial variability (heterogeneities) in the aquifer, testing field equipment, refining field operations, and determining sampling protocols.

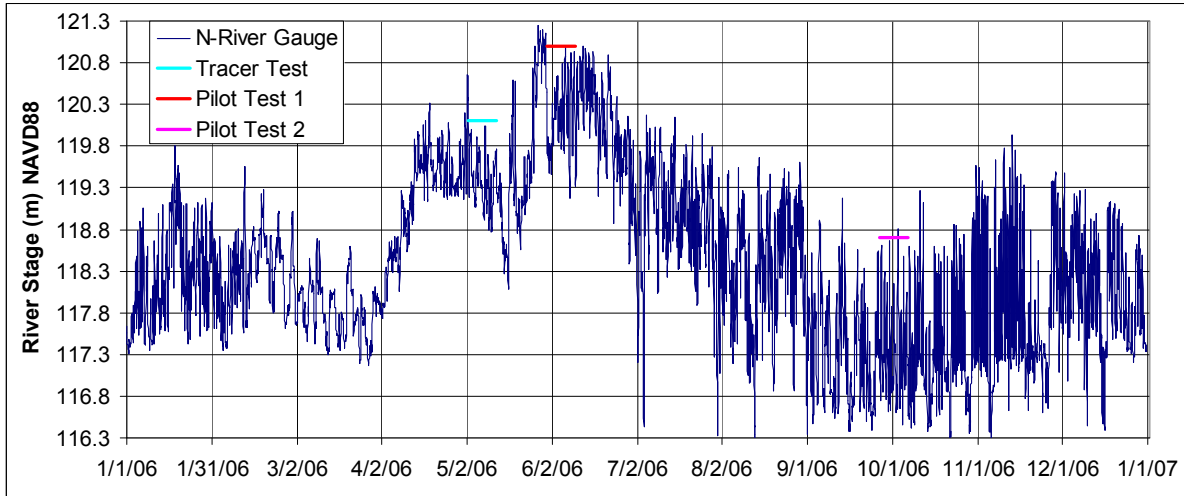


Figure 5.1. Columbia River Stage and Timing of 100-N Area Pilot Tests. Timing shown for the tests is from the start of the injection period plus 10 days.

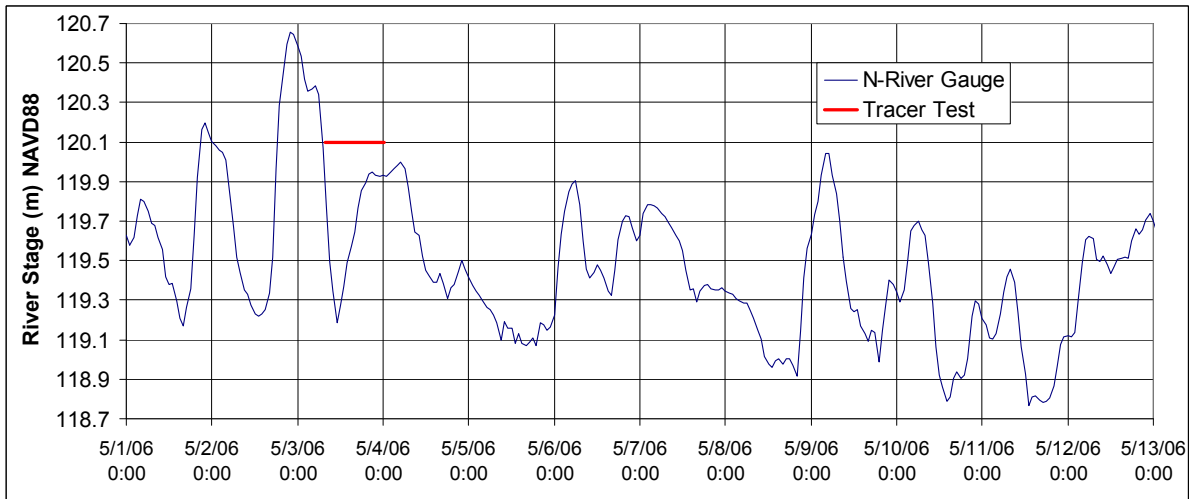


Figure 5.2. Columbia River Stage and Timing for 100-N Area Tracer Test. Tracer test timing shows the injection period.

5.1.1 Tracer Test Description

The tracer test was conducted by injecting a solution containing a conservative, non-reactive tracer (Br^-) into a central injection well (IW-3, well 199-N-138 as shown in Figure 1.10) and monitoring for arrival response in surrounding wells (Figure 4.2). Bromide concentrations were measured in the injection stream and the eight surrounding monitoring wells to determine the arrival times and extent of the tracer plume. Table 5.1 summarizes the operational parameters of the tracer test. Table 5.2 provides well summary information for the injection and monitoring wells at pilot test site #1, including well screen intervals, casing material and diameter, drilling methods, and radial distance of the monitoring wells from the injection well (as shown in Figure 4.2).

Table 5.1. Summary of Apatite Pilot Test #1 Bromide Tracer Injection Test (May 3, 2006)

Test Parameter	Value
Tracer Mass	11.7 kg (25.7 lb) of sodium bromide (NaBr)
Concentrated Tracer Solution Volume	2432 gal
Total Injection Rate	40 gal per min
Concentrated Tracer Injection Rate	3.5 gpm
River Water Injection Rate	36.5 gpm
Injection Concentration	86.5 mg/L Br ⁻
Injection Duration	695 min. (11.6 hr)
Total Tracer Injection Volume	27,800 gal
Additional River Water Injection following Tracer	12,200 gal at 40 gpm for 305 min. (5.08 hr)

Table 5.2. Injection and Monitoring Well Summary for Pilot Test Site #1 (FH 2005)

Apatite Project Well ID	Hanford Site Well Name	Radial Distance from Injection Well (ft)	Drilling Method	Well Diameter (in.) and material	Screen Interval (ft bgs) and Formation
IW-3	199-N-138	0 Injection Well	Cable Tool	6.0 Stainless Steel	24.8 to 7.8 Hanford and Ringold
P-1-R	199-N-126	19.5	Hydraulic Hammer	1.25 PVC	27.3 to 22.3 Ringold
P-2-H	199-N-127	19.3	Hydraulic Hammer	1.25 PVC	17.7 to 12.7 Hanford
P-3-R	199-N-128	9.7	Hydraulic Hammer	1.25 PVC	26.6 to 21.6 Ringold
P-4-H	199-N-129	9.7	Hydraulic Hammer	1.25 PVC	17.1 to 12.1 Hanford
P-5-R	199-N-130	15.2	Hydraulic Hammer	1.25 PVC	27.5 to 22.2 Ringold
P-6-H	199-N-131	15.1	Hydraulic Hammer	1.25 PVC	17.5 to 12.5 Hanford
P-7-R	199-N-132	15.1	Hydraulic Hammer	1.25 PVC	27.2 to 22.2 Ringold
P-8-H	199-N-133	15.2	Hydraulic Hammer	1.25 PVC	17.7 to 12.7 Hanford

A concentrated sodium bromide (NaBr) solution was prepared in a ~2600-gal tank and diluted in-line during the injection to the required concentration using filtered water pumped from the Columbia River. The volume of concentrated NaBr solution prepared was 9205 L (2432 gal) with 11.7 kg of NaBr. Injection rates were maintained at 3.5 gpm for the concentrated NaBr solution and 36.5 gpm for the pumped river water, resulting in an injection concentration of 86.5 mg/L Br⁻. The NaBr solution was injected into the aquifer through the injection well (IW-3, well 199-N-138) at 151 L/minute (40 gpm for 11.6 hours, yielding an injection volume of 105,200 L (27,800 gal). Due to the low-tracer concentrations measured in some of the more distant wells (see discussion in tracer tests results below), the injected tracer plume was followed by additional filtered river water to push the tracer plume farther radially. The filtered river water was injected at a rate of 151 L/minute (40 gpm for 5.08 hours (305 minutes), resulting in an additional injection volume of 46,170 L (12,200 gal). The total injection volume was 151,400 L (40,000 gal) was injected over a duration of 16.7 hr (1000 min). Flow rates during the test were monitored using in-line turbine flow meters and recorded in a field log book (see Figure 5.3).

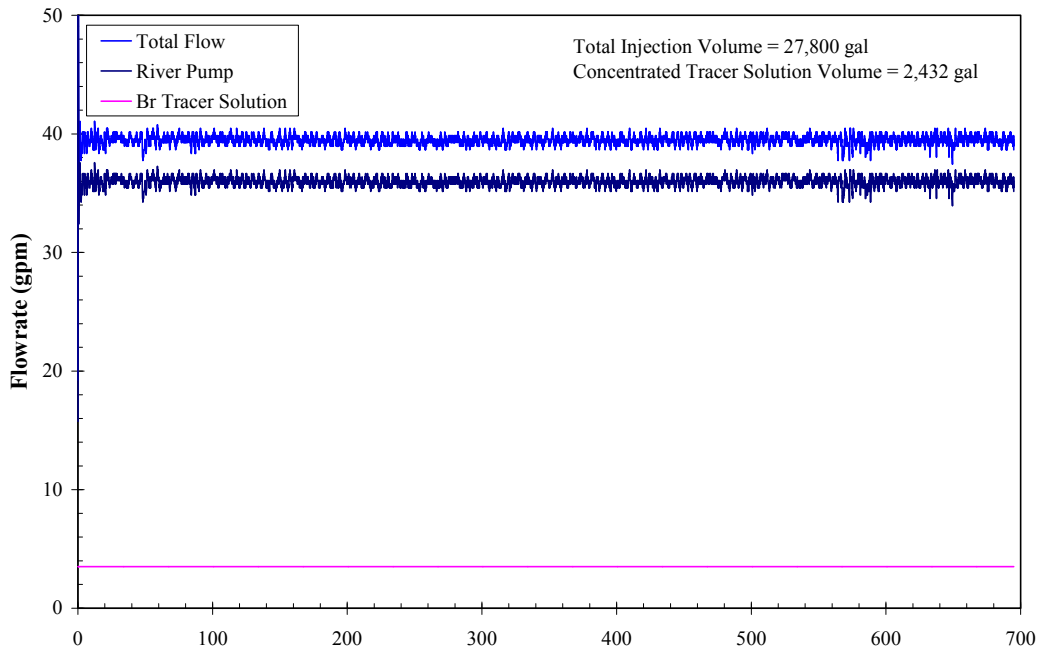


Figure 5.3. Bromide Tracer Test at Pilot Test #1 Showing the Flow Rates, Duration, and Total Volumes Injected into Injection Well IW-3. An additional 12,200 gal of Columbia River water was injected following the tracer at 40 gpm for 305 minutes.

Bromide concentrations were measured using down-hole ion-selective electrodes (ISE) at five selected monitoring wells and the measurements were recorded using a single data logger. Four of the wells with ISEs were completed in the Hanford formation, and the other was completed in the Ringold Formation. The ISEs were calibrated before and after the tracer injection test using prepared calibration standards over the range of bromide concentrations encountered during the test. The measurement frequency during the tracer injection test ranged from 1 minute during the early part of the test to 10 minutes during the latter part of the test. In the mobile laboratory, an ISE was installed in the sampling manifold for in-line bromide measurements during collection of aqueous samples from all monitoring wells. A separate data logger was used for displaying these measurements in real time.

Aqueous samples were collected from the injection stream and the surrounding monitoring wells to determine the extent of the tracer plume during the test. Samples were collected at the sampling manifold in the mobile laboratory, and a subset was submitted to an analytical laboratory for bromide analysis by ion chromatography (IC). During each sampling event, SpC and temperature were measured using an in-line electrode in the sampling manifold. The SpC electrode was calibrated just before the tracer injection test began. Two hundred aqueous samples were collected during the injection portion of the test, with 87 additional samples collected in the week following the injection. Of the 287 aqueous samples collected, 210 were submitted for laboratory Br⁻ analysis by IC. Selection of these samples was based on field measurements of Br⁻ concentrations obtained using the in-line and down-hole Br⁻ ISEs.

To account for differences between bench-top and down-hole conditions that may impact probe calibration, the down-hole Br⁻ ISE calibration curve for each electrode was adjusted based on a linear regression of the IC data collected from a given monitoring well with the corresponding Br⁻ ISE measurement. Down-hole Br⁻ ISE data was omitted for two wells (P-2-H and P-6-H) for the injection and early post-injection period (elapsed time = 1700 minutes) because of the erratic behavior of these probes during this time period. Some erroneous spikes in Br⁻ ISE values were also removed for time periods when the sampling pumps were turned on.

5.1.2 Tracer Test Results and Discussion

Analysis (IC) of samples collected from the injection stream indicates that the average bromide injection concentration was 89.4 mg/L Br⁻. This concentration is close to the concentration of 86.5 mg/L Br⁻, calculated based on the mass of NaBr used, tank concentration, and flow rate data. Figure 5.4 shows the tracer breakthrough curves for the wells completed in the Hanford formation, and Figure 5.5 shows the breakthrough curves for wells completed in the Ringold Formation.

Indication that some wells were just starting to see tracer arrival at the end of the planned 700-minute tracer injection (P-1-R, P-5-R, and P-8-H) resulted in a decision to inject Columbia River water for an additional 300 minutes to increase the radial extent of the injected tracer. This increase in injection volume was sufficient to produce tracer arrivals in these wells (Figures 5.4 and 5.5) that allowed for a quantitative evaluation of arrival response.

5.1.2.1 Hanford Formation Tracer Test Results

For wells completed in the Hanford formation, the tracer breakthrough curves show variability in arrival times and peak concentrations that are not well-correlated with radial distance from the injection well (Figure 5.4). The tracer arrived in well P-6-H (4.6-m [15.1-ft] inland from the injection well) within 30 minutes of the tracer injection. This well also showed a rapid decrease in tracer concentrations when the injection concentration was switched to river water at $t \sim 700$ minutes. For well P-8-H at a similar distance from the injection well ($r = 15.2$ ft), the tracer didn't arrive until approximately $t = 800$ minutes. The initial tracer arrival in well P-6-H was sooner than in well P-4-H, which is closer to the injection well. The tracer began arriving at well P-4-H ($r = 10$ -ft) at approximately $t = 160$ minutes. Initial tracer arrival at the farthest monitoring well, P-2-H at $r = 19.3$ ft, was earlier than in P-8-H, which is at $r = 15.2$ ft.

As discussed previously, because of the low Br⁻ concentrations in wells P-8-H and P-2-H at the end of the planned tracer injection (105,200 L [27,800 gal]), the injection continued with 87,000 L (23,000 gal) of river water to push the tracer plume out farther radially (Figure 5.4). This additional river water was helpful in establishing the initial arrival curve of tracer at well P-8-H. Bromide concentrations in well P-2-H did not increase significantly during this additional injection period. Concentrations decreased during the river water-only injection for the wells that had significant tracer arrivals earlier in the test (wells P-6-H and P-4-H).

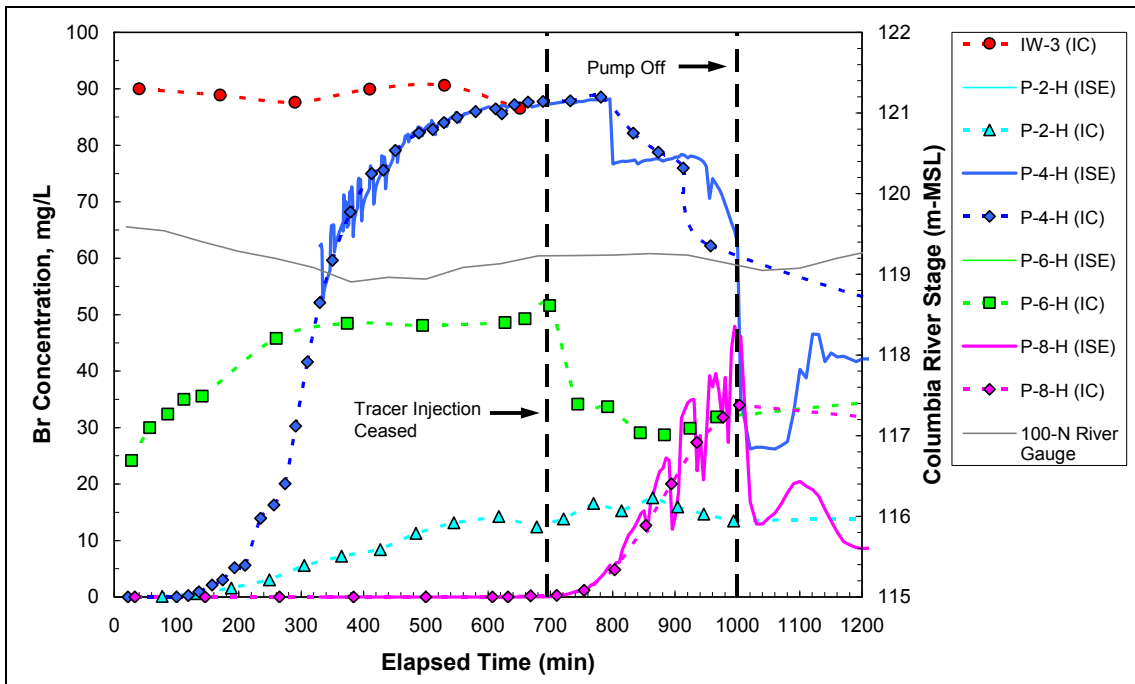
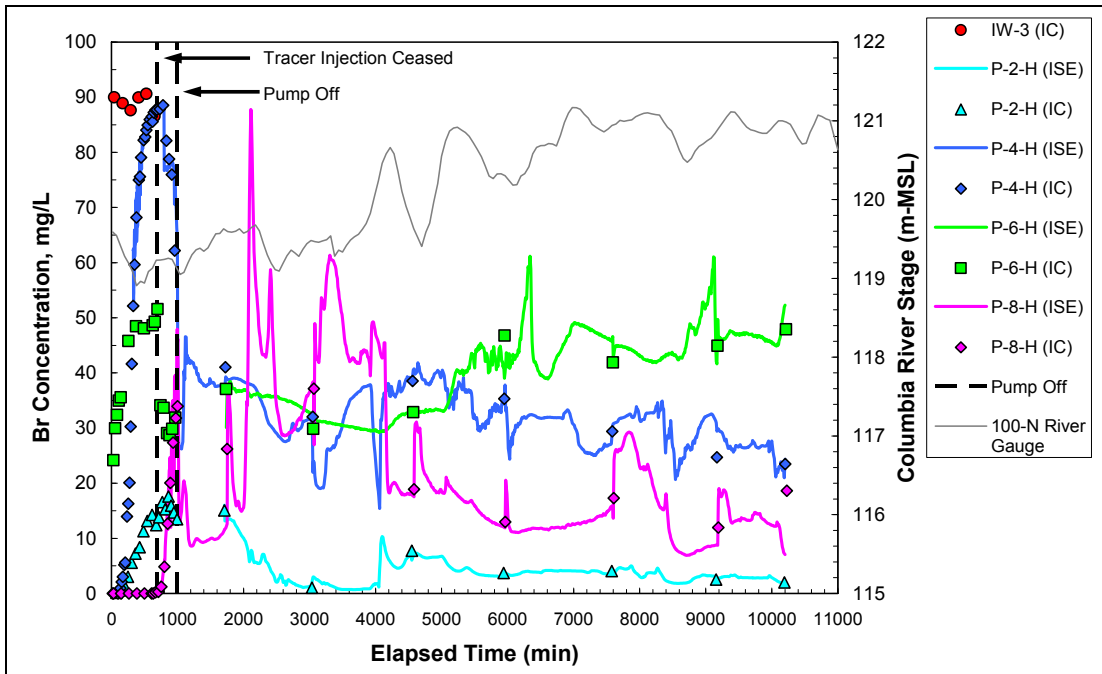


Figure 5.4. Bromide Tracer Concentration Breakthrough Curves for Wells Completed in the Hanford Formation

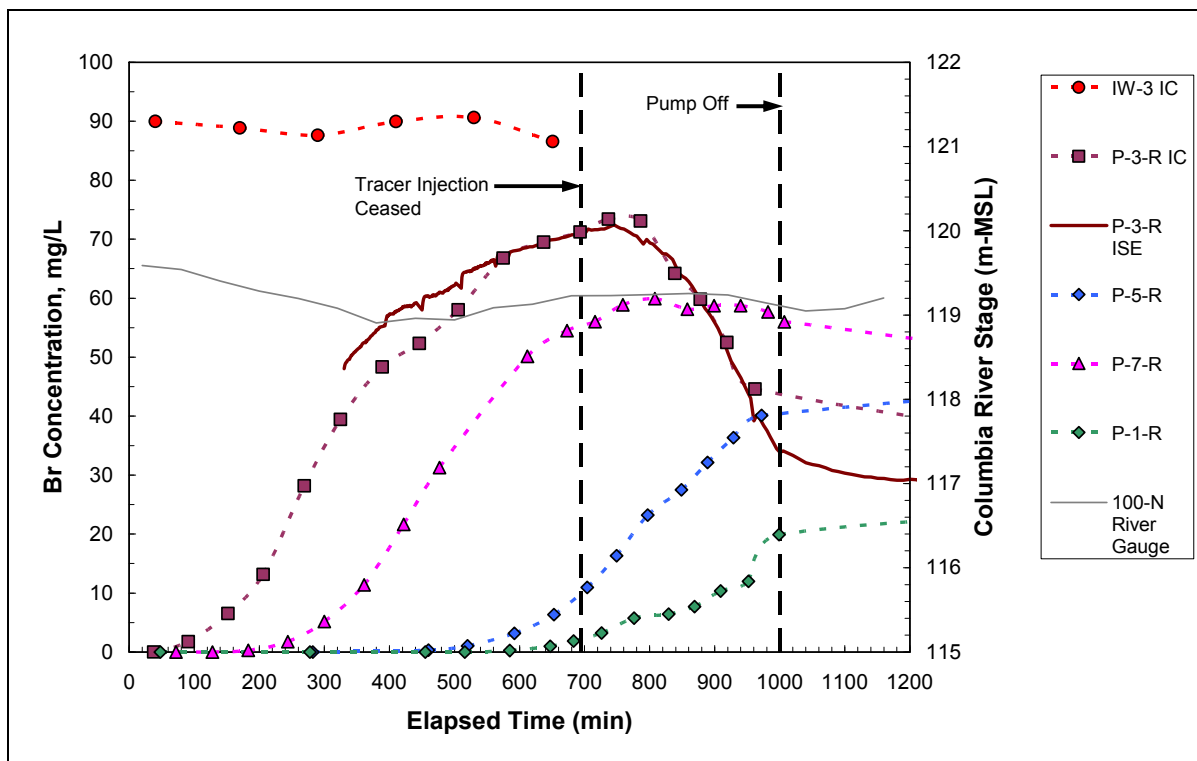
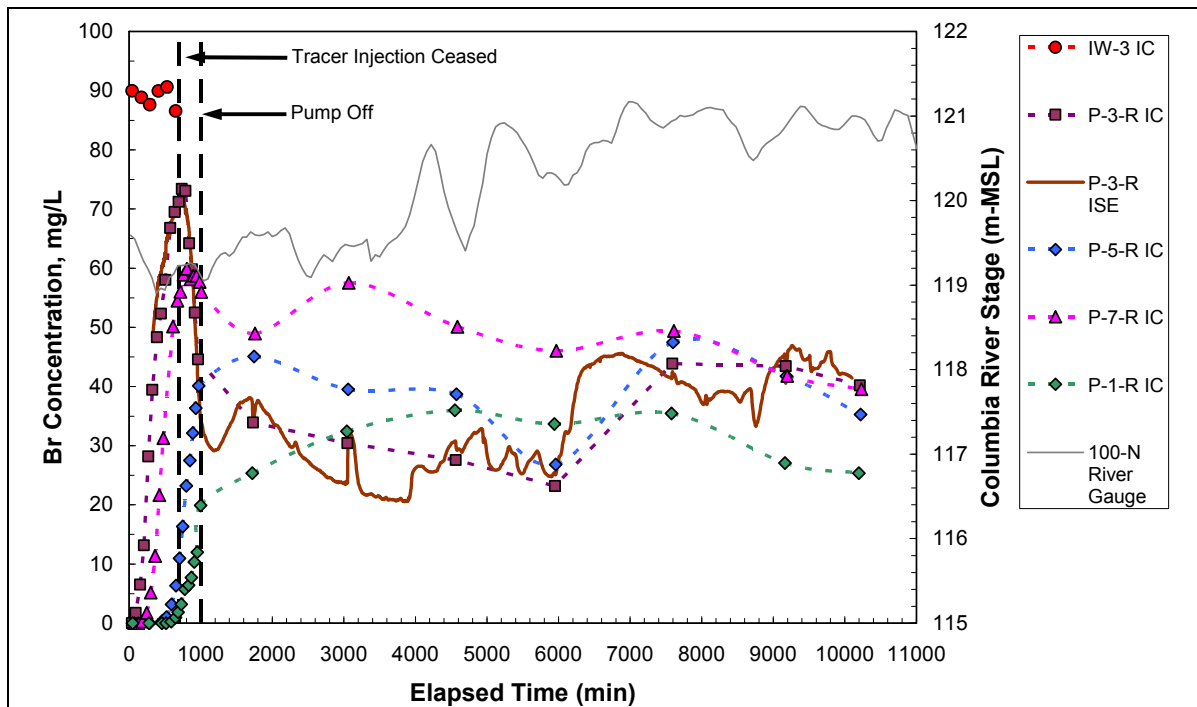


Figure 5.5. Bromide Tracer Concentration Breakthrough Curves for Wells Completed in the Ringold Formation

The shape of the tracer breakthrough curves in the Hanford formation, as shown in Figure 5.4, also provide some qualitative information on heterogeneities in the formation. The curve for well P-4-H has a classic sigmoidal shape for advection/dispersion in a homogeneous radial flow field with the change in

concentration symmetrical above and below the $C/C_0 = 0.5$ level. Tracer concentrations in this well also reached levels close to the injection concentrations. Tracer concentrations for the well with the fastest arrival, P-6-H, level off quickly at concentrations significantly below the injection value. This behavior may indicate the well screen intersects multiple permeability zones within the formation, some with faster and others with slower connections to the injection well. The other well at the 4.6-m (15-ft) radial distance in the Hanford formation, P-8-H, had a much later arrival; however, the increase in tracer concentrations was sharper and showed a more regular homogeneous breakthrough curve response (although the test ended while the concentrations were still increasing in the well). Tracer concentrations were detected relatively early for the 6-m (20-ft) radial distance well, P-2-H, in the Hanford formation; however, the concentrations did not increase significantly for the remainder of the injection test. The shape of the tracer breakthrough curve for well P-2-H was indicative of significant heterogeneities.

Figure 5.6 shows the analytic solution for the nominal case of the tracer test in a homogeneous/isotropic aquifer at radial distances similar to the monitoring wells at the pilot test site #1. This is a single-layer model with a uniform aquifer 4.8-m (15.7-ft) thick (no distinction between Hanford and Ringold Formations). The aquifer thickness was determined using the elevation at the bottom of the injection well screen and the river stage during the tracer test. The porosity was set at 21%, an average value in Hanford and Ringold Formation gravels. The tracer breakthrough curve for the well at a 3.0-m (9.7-ft) radial distance in the Hanford formation is shown in Figure 5.4 for comparison. The measured tracer data for well P-4-H was slower than predicted by the analytic solution at the 3.0-m (9.7-ft) radial distance. This slower arrival in this direction could be explained by much faster arrivals seen in the Hanford formation at the opposite inland 4.6-m (15-ft) direction (well P-6-H), indicating a much greater permeability zone in this area.

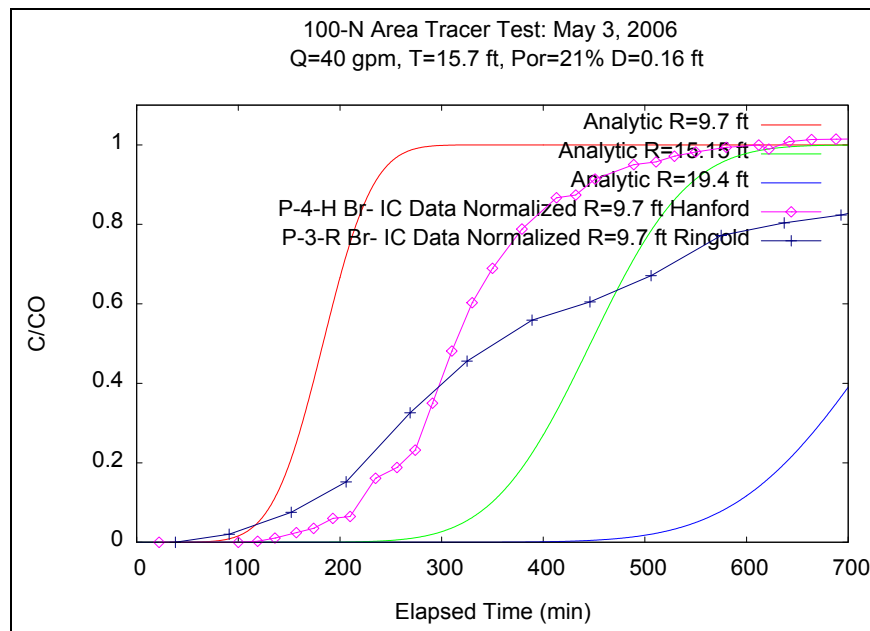


Figure 5.6. Radial Transport Analytic Solution for 100-N Area Tracer Test (Hoopes and Harleman 1967). Br- results from well P-2-H (Q =injection rate, T =aquifer thickness, POR =porosity (Hanford/Ringold mean used), D =longitudinal dispersivity).

5.1.2.2 Ringold Formation Tracer Test Results

Tracer arrival times and peak concentrations for wells completed in the Ringold Formation correlated with radial distance from the injection well during the tracer injection test ($t < 1000$ minutes) (Figure 5.5). Monitoring wells closer to the injection well showed earlier arrival times and higher peak concentrations than wells farther away from the injection well.

A comparison of the tracer breakthrough at the 3-m (9.7-ft) radial distance monitoring well in the Ringold Formation (P-3-R) is shown in Figure 5.6, along with the analytic model results for the nominal case and the tracer breakthrough curve from the adjacent Hanford formation well (P-4-H). Similar to the well in the Hanford formation, the Ringold Formation well at this distance is also slower than the predicted arrival from the nominal case. Initial tracer arrivals were faster in the Ringold Formation well than the Hanford formation well; however, the increase in tracer concentrations in this well was slower for the remainder of the injection test (greater dispersion).

The two 4.6-m (15-ft) radial distance wells in the Ringold Formation, P-5-R and P-7-R, had very different arrival times, as shown in Figure 5.5, with the tracer arrival faster in the eastern well (P-7-R) compared to the inland well (P-5-R).

5.1.2.3 Post-Injection Tracer Monitoring

Tracer concentrations were monitored for 1 week at the pilot test site #1 following the tracer injection, as shown in Figures 5.4 and 5.5 for the Hanford and Ringold Formations, respectively. The plume shape at the end of the injection period was complicated as a result of heterogeneities and the river water with no tracer that was injected at the end of the test.

Tracer concentrations in the Hanford formation during the post-injection monitoring period showed significant variations. Except for well P-2-H, which is closest to the Columbia River in the Hanford formation, there were still significant tracer concentrations in the aquifer at the end of this 1-week post-injection period. No overall trend is apparent in the tracer plume from these data. Tracer concentrations from the well on the eastern edge of the plume, P-8-H, did show an increase, followed by a decrease in concentrations during this time. There was an increase in the average river stage during this period, as shown in Figure 5.4. However, the range in river-stage changes that occurred within a 1-day period was greater than the change in the mean.

Tracer concentrations in the Ringold Formation wells changed relatively slowly from the concentrations at the end of the injection period and were leveling off at concentrations close to half the injection concentration by the end of the 1-week post-injection monitoring period.

5.1.2.4 Comparison of Hanford and Ringold Formation Tracer Test Results

Overall, there was more variation in tracer arrivals in the Hanford formation than the Ringold Formation (see Figures 5.4 and 5.5), but there was no systematic increase in arrival time in the Hanford formation compared to the Ringold Formation. This would be expected if the permeability contrast between the formations was much larger. The effect of the range of permeability heterogeneities at pilot test site #1 site within the Hanford formation was greater than the overall contrast in permeabilities between the Hanford and Ringold Formations. While the fastest arrival time was at a Hanford formation well (P-6-H), there was a Hanford/Ringold well pair in which the tracer arrival at the Ringold Formation

well was faster than the Hanford well (P-7-R and P-8-H). Well inefficiency (i.e., skin effects) in the injection well may also have minimized the impact of the Hanford/Ringold formation permeability contrast on the proportioning of injection flux between these two formations.

Tracer arrivals in the 3-m (9.7-ft) radial distance wells (P-4-H and P-3-R in Figure 5.6) in the Hanford and Ringold Formations showed tracer concentrations measured slightly earlier in the Ringold well than the Hanford well. After the initial tracer arrival, concentrations increased faster in the Hanford well, resulting in an earlier 50% concentration arrival at this location. The Ringold well tracer breakthrough curve at 3 m (9.7 ft) was more dispersed than the Hanford well, and the curve was asymmetrical around the 50% tracer concentration.

Comparing the breakthrough curves at the 4.6-m (15-ft) radial distance wells, tracer arrivals in the Ringold wells were faster in the eastern well (P-7-R) compared to the inland well (P-5-R). This was the reverse of the relative order of tracer arrivals in the 4.6-m (15-ft) radial wells in the Hanford formation (see Figure 5.4). Tracer concentrations in the 4.6-m (15-ft) radial distance wells at the end of the injection test were higher at the Ringold wells than the Hanford wells. Additionally, Hanford well P-8-H had the slowest arrival of any of the 4.6-m (15-ft) radial wells, but the fastest arrival was the other Hanford well (P-6-H).

Although initial arrivals of the tracer at the 5.8-m (19-ft) monitoring wells in the Hanford and Ringold Formations (P-2-H and P-1-R) were different, the tracer concentrations in these wells were similar by the end of the injection (elapsed = 1000 min). However, both had relatively low concentrations (~15 to 20% of the injection concentration).

5.1.2.5 Water Level Monitoring

The buildup of water levels in the injection and monitoring wells during the bromide tracer test followed by recovery are shown in Figure 5.7. The water levels in the injection well raised significantly during the test, ~3 m (~9.8 ft), and were within 0.98 to 0.49 m (3.2 to 1.6 ft) of the ground surface during the 151-L/minute (40 gpm) injection. Water levels in the monitoring wells showed a much lower buildup (i.e., <0.1 m [0.33 ft]) and were more strongly influenced by the change in the Columbia River stage. The observed pressure response is consistent with a significant positive skin impacting the efficiency of injection well 199-N-138. The efficiency of this well limited the rate at which the tracer solution could be injected and, as indicated above, may have minimized the impact of the Hanford/Ringold permeability contrast on the proportioning of injection flux between these two formations.

5.1.2.6 Injection Volume for Pilot Test #1 – High-River Stage Periods

Results from the tracer injection test were used to estimate the volume of apatite-forming solutions that would be required to achieve the required radial extent of treatment during pilot test #1. Because of the heterogeneous nature of the observed tracer arrival responses, a quantitative estimate of effective porosity for the treatment volume was not possible. However, tracer arrival did provide both a measure of the degree of formational heterogeneities, and a direct indication of the volume of aquifer that would be interrogated for a given volume of tracer solution injected. This information was incorporated into an injection design analysis (see Section 6.0) that was used to determine operational parameters for pilot test #1.

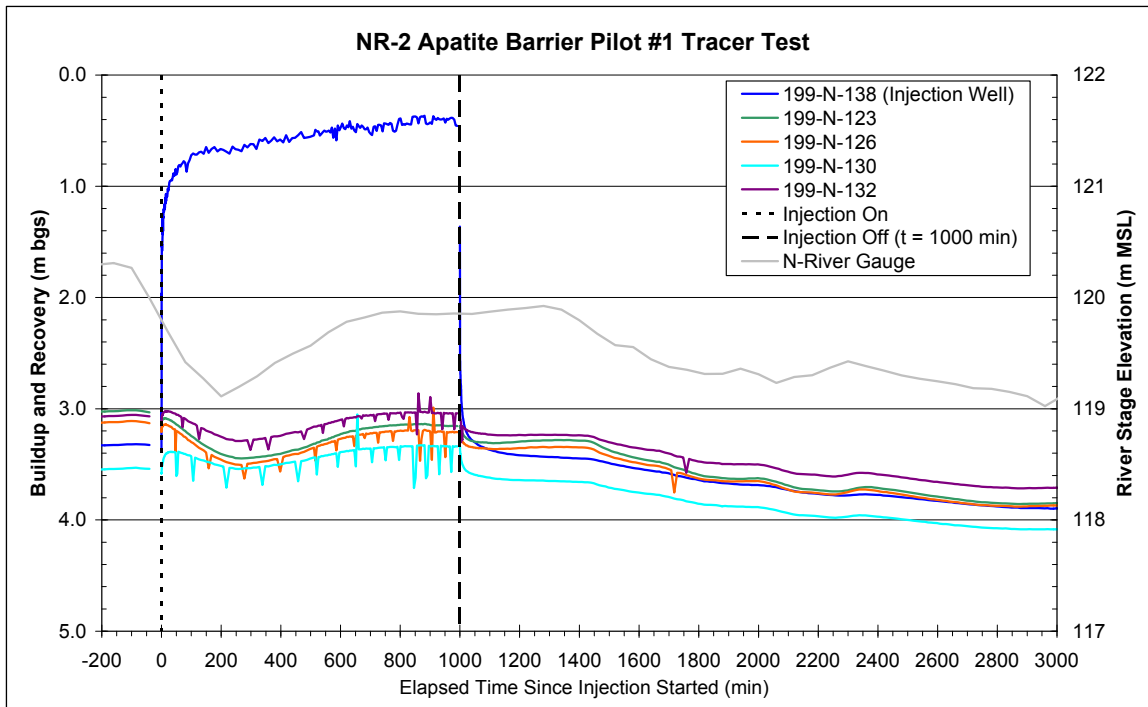


Figure 5.7. Buildup and Recovery of Water Levels During the Bromide Tracer Test

5.2 Pilot Test #1

The first apatite pilot injection test was conducted at well 199-N-138 (see Figures 1.10 and 4.2) from May 31 to June 1, 2006, during high-river stage conditions (see Figures 5.1 and 5.8). The test configuration involved injecting approximately 367,000 L (97,000 gal) of reagent over 35.4 hours. Injection rates ranged from 227 to 151 L/min (60 to 40 gpm), as shown in Figure 5.9. The initial higher injection rates resulted in over-pressurization of the well seal and associated seepage at the injection wellhead, so the injection rates were reduced for the remainder of the injection (227 L/min [60 gpm] for ~4 hr, 190 L/min (50 gpm) for ~11 hr, 151 L/min (40 gpm) for ~20 hr). Extensive aqueous sampling was conducted on the injection stream and monitoring wells during the test. Daily to weekly monitoring of the 11 monitoring wells at the site was conducted after the injection for the first month, with less frequent sampling afterward. The test occurred during the high-river stage to target the uppermost portion of the Hanford formation aquifer. This high-river stage was maintained during June 2006.

The low-concentration apatite formula for pilot test #1 is shown in Table 5.3. Formula development details are provided in Section 2.6 and Table 3.2. The injection chemicals were delivered in concentrated form in four tanker trucks to the test site based on the solubility of the mixture, and to keep the calcium and phosphate mixtures separate before injection. Two tanker trucks arrived at the site at the start of the test followed by the next two trucks, which arrived later in the test. The maximum solubility and stability of these chemical mixtures were determined in the laboratory and described in Szecsody et al. (2007, Table 5.11). The composition of the injection formula for subsequent pilot testing and barrier installation evolved during the field testing and are described in Section 2.6.

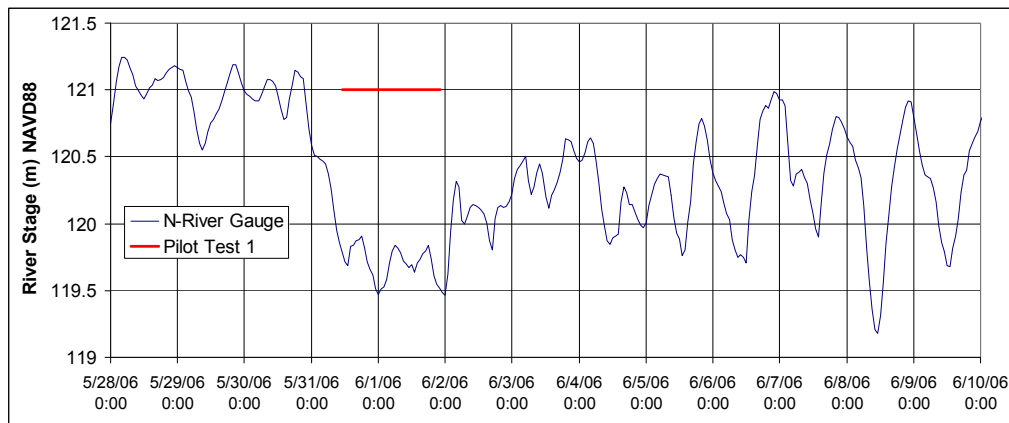


Figure 5.8. Columbia River Stage and Timing for 100-N Area Pilot Test #1 Showing Injection Period

For pilot test #1, a 454,000-L (120,000-gal) injection volume was planned, but only 367,000 L (97,000 gal) were injected for the test. During the injection, a precipitate was noticed in one of the calcium-citrate tankers (Mix 1) that caused the feed line to clog. The injection was switched over to the second Mix 1 tanker and no more precipitate was detected for the remainder of the test. The injection was stopped early from this loss of mass, yielding a total injection volume of 367,000 L (97,000 gal). As a result, only a portion of the total tanker truck volumes shown in Table 5.3 (32,500 L [8600 gal] and 28,400 L [7500 gal] of Mix 1 and Mix 2, respectively) was injected. The precipitate was caused by the supplier mixing the concentrated trisodium citrate and calcium chloride solutions (see Table 5.3) together prior to diluting with water for shipment. The order of dissolving and mixing of the chemicals by the supplier was changed for subsequent injections, which eliminated this problem.

Operational monitoring data during the injection showed good coverage radially in both the Hanford and Ringold Formations (see upper and lower zone well-pair locations in Figure 4.2). This is caused by the relatively small contrast in hydraulic properties between the Hanford and Ringold Formations at this location, but also may have been controlled to some extent by skin effects around the injection well. The operational monitoring also showed preferential flow inland (toward monitoring well P-6-H) during the injection with faster and higher concentration arrivals in these wells, indicating a higher hydraulic conductivity zone in the Hanford formation in this direction. This observed response is consistent with the arrival response observed during the tracer injection test.

5.2.1 Flow Rates and Pressures

Flow rates for the two concentrated feed solutions, dilution water, and the total injection stream rates are shown in Figure 5.9. The injection rates for the two concentrated solutions (Mix 1 and Mix 2) were set based on the liquid volumes in the separate tankers delivered to the test site. River water was pumped at the site for diluting the concentrated solutions to the target injection concentrations. The initial injection rate for the test was 227 L/min (60 gpm) but the rate was decreased twice during the test due to over-pressurization of the well seal and associated seepage at the injection wellhead. The first decrease occurred 4.3 hours into the test when the rate was reduced to 189 L/min (50 gpm) and the second decrease occurred after 15.1 hours of injection when the rate was again reduced to 151 L/min (40 gpm). The 151 L/min (40 gpm) rate was sustained for the remainder of the test (Figure 5.9). The total injection duration was 35.4 hours with a total injection volume of 367,000 L (97,000 gal) (see Table 5.3).

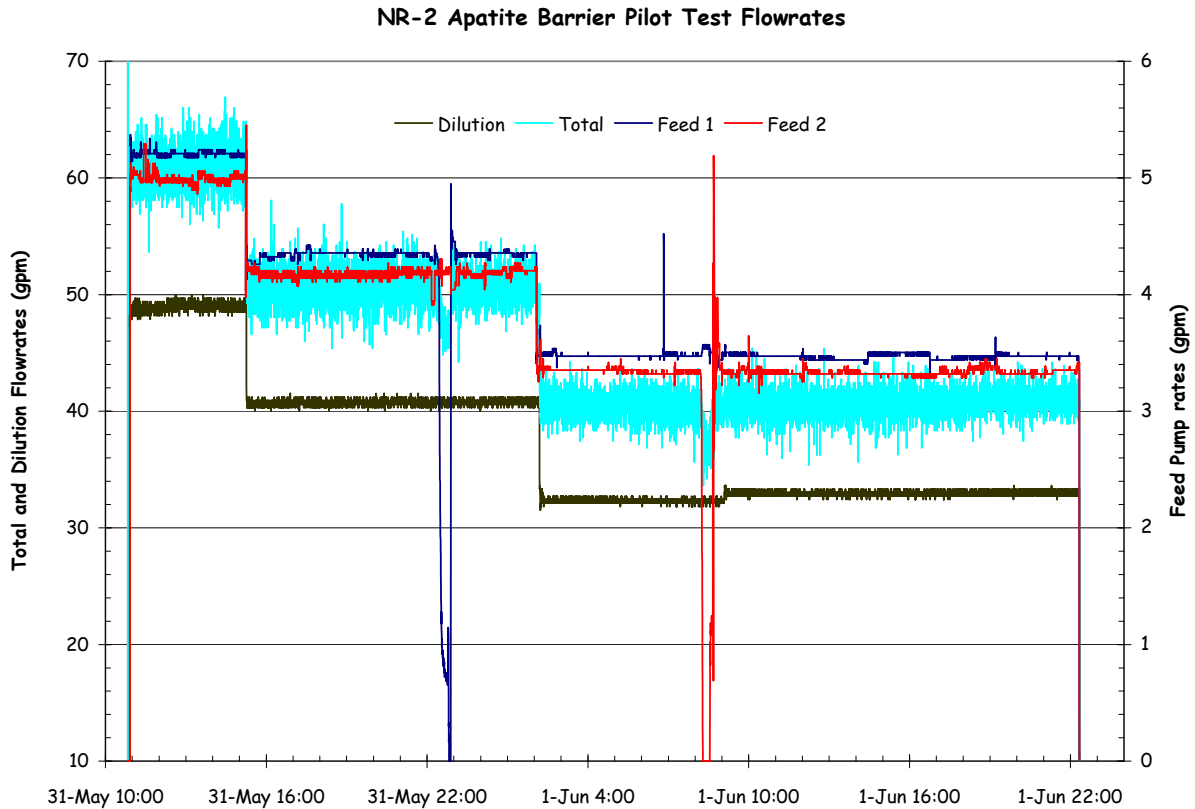


Figure 5.9. Apatite Pilot Test #1 (2006) Test Flow Rates; Dilution = River Water, Feed 1= Mix 1 (Ca-citrate), Feed 2 = Mix 2 (phosphate)

Table 5.3. Summary of Apatite Pilot Test #1 Injection Test

Test Parameter	Value
Injection volume	97,000 gal (injection was stopped early – 120,000 gal were planned)
Injection concentrations (target)	10 mM trisodium citrate 4.0 mM calcium chloride (160 mg/L Ca) 2.0 mM disodium phosphate (190 mg/L PO ₄) 0.4 mM sodium phosphate (38 mg/L PO ₄) 1.0 mM ammonium nitrate
Tanker truck 1 (mix 1) volume/mass	10,400 gal 1336 kg trisodium citrate 267 kg calcium chloride
Tanker truck 2 (mix 2) volume/mass	10,050 gal 129 kg disodium phosphate 22 kg sodium phosphate 36 kg ammonium nitrate
Total injection rate	~60, 50, and 40 gpm (rates lowered during test in 3 steps)
Tanker 1 (mix 1) injection rate	5.2, 4.4, and 3.5 gpm
Tanker 2 (mix 2) injection rate	5.0, 4.2, and 3.3 gpm
Injection rate pumped from river	49, 41, and 33 gpm
Injection duration	35.4 hr (May 31 to June 1, 2006)

As mentioned above, the supply line from the first Mix 1 (Ca-Citrate) tanker clogged 11.8 hours into the injection because of the precipitate at the tank bottom. The injection was switched over to the second tanker of Mix 1 for the remainder of the test. The total volume of the pilot test #1 injection was less than planned (367,000 L [97,000 gal] versus 454,000 L [120,000 gal]) because of the loss of chemicals from this first Mix #1 tanker. The first Mix #2 (phosphate) tanker was empty 21.9 hours into the injection and the second Mix #2 tanker was used for the rest of the test. Remaining chemicals in the first Mix #1 tanker with precipitate and the unused portion in the second Mix #2 tanker was returned to the supplier.

The relative Columbia River stage was monitored during the test (Figure 5.10) with a separate pressure transducer installed in the river near the pilot test site. The river stage fluctuated over (0.43 m (1.4 ft)) during the injection. Columbia River discharge measured at Priest Rapids Dam (PRD) is also shown on Figure 5.10 and ranged from 4560 to 5440 m³/sec (161,000 to 192,000 ft³/sec) during the pilot test #1 injection. The discharge and river stage was higher during the week following the pilot test. This plot also shows the time lag between operational changes at the dam and river-stage fluctuations at the test site, with a mean lag time of approximately 75 min in this example.

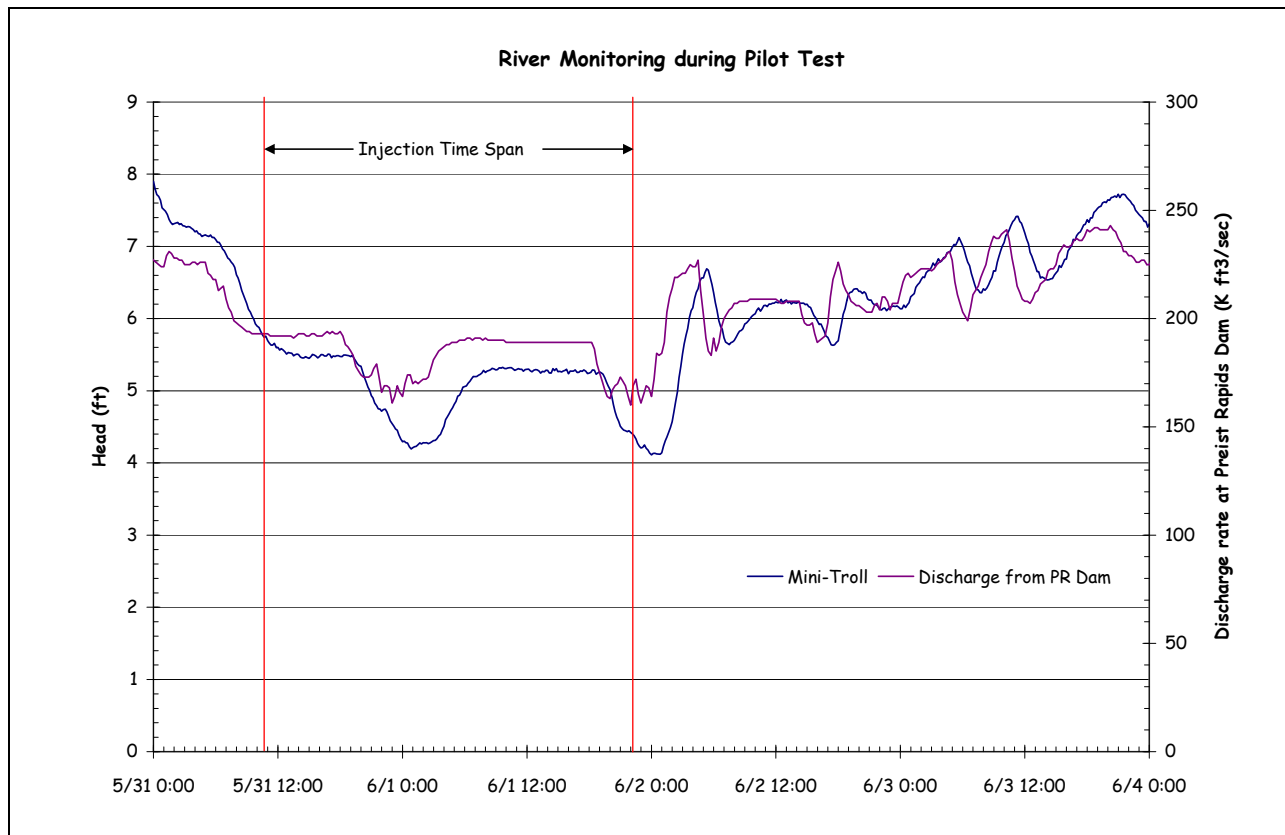


Figure 5.10. Relative Columbia River Stage and Priest Rapids Dam Discharge During Apatite Pilot Test #1 (2006). Mini-troll is a pressure transducer installed in the river near the pilot test site.

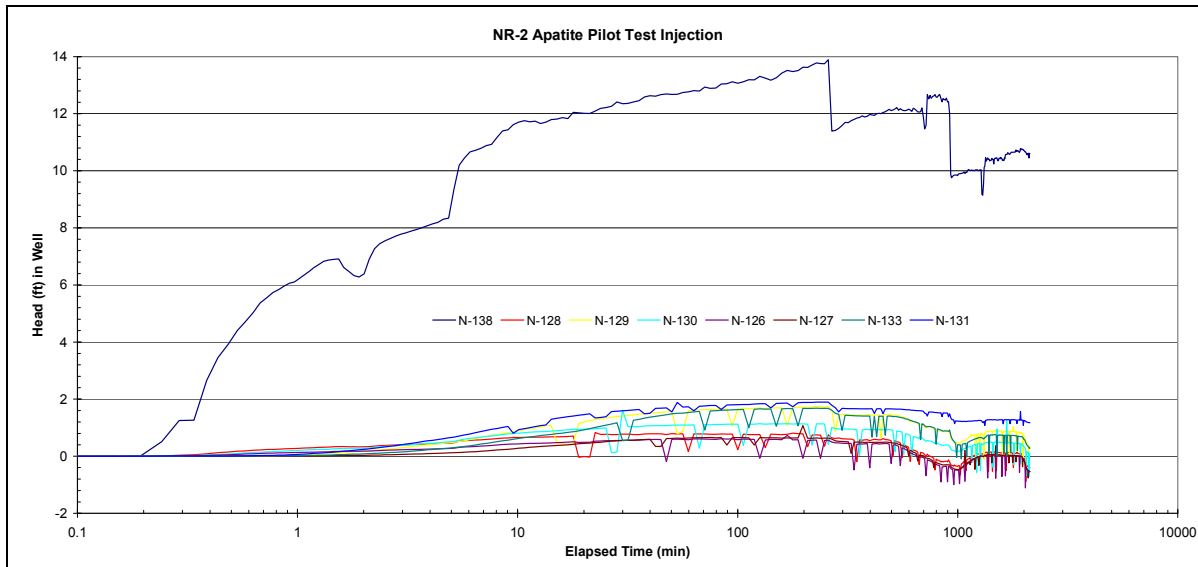


Figure 5.11. Water Level Monitoring in Wells During Apatite Pilot Test #1 Conducted in May/June 2006 (see Table 5.2 for pilot test monitoring well IDs). Prefix 199- omitted from well names.

The injection mound is shown in Figure 5.11 for the injection well and surrounding monitoring wells. Based on results of the tracer injection test (Section 5.1), the excessive pressure buildup was observed in the injection well relative to that observed in the surrounding formation, indicating poor well efficiency (i.e., skin effects) for this injection well. The two step drops in the pressure buildup in the injection well seen in Figure 5.11 around $t = 258$ min (4.3 hr) and $t=906$ min (15.1 hr) resulted from reductions in the injection rate during the test (from 227 L [60 gpm] to 189 L (50 gpm) and then 151 L/min [40 gpm]). The water table mounding in the surrounding monitoring wells, out to 5.9 m (19.5 ft), was less than 0.6 m (2 ft) of buildup, as shown in Figure 5.11. The smallest pressure buildup was measured in well P-1-R, which would be expected because this is the farthest monitoring well screened in the Ringold Formation. The largest pressure buildup was in P-6-H (a 4.6-m (15-ft) radial distance well screened in the Hanford formation, which also had the fastest tracer and solute arrivals) and P-4-H, which is the closest monitoring well screened in the Hanford formation ($r=9.7$ ft). Pressure buildup in the other 4.6-m (15-ft) radial distance monitoring well in the Hanford formation (P-8-H) was delayed but reached the levels seen in well P-4-H. Decreases in the pressure buildup in the monitoring wells approximately $t=500$ min elapsed time in the test (Figure 5.14) were caused by a drop in the Columbia River stage (Figure 5.10).

5.2.2 Injection Monitoring/Radial Extent

Groundwater measurements of SpC and phosphate during the pilot test #1 injection, and for approximately 2 weeks following the injection, are shown for the Hanford formation (i.e., shallow) monitoring wells in Figure 5.12 and the Ringold Formation (deeper) monitoring wells in Figure 5.13. SpC measurements represent a generalized average of the movement of the Ca-citrate- PO_4 mixture injected. Calcium measurements from selected samples submitted for major cation analyses are also shown in these figures. Table 5.4 and Figure 5.14 summarize the SpC measurements and phosphate concentrations for each monitoring well near the end of the injection period and approximately 1 week following the injection.

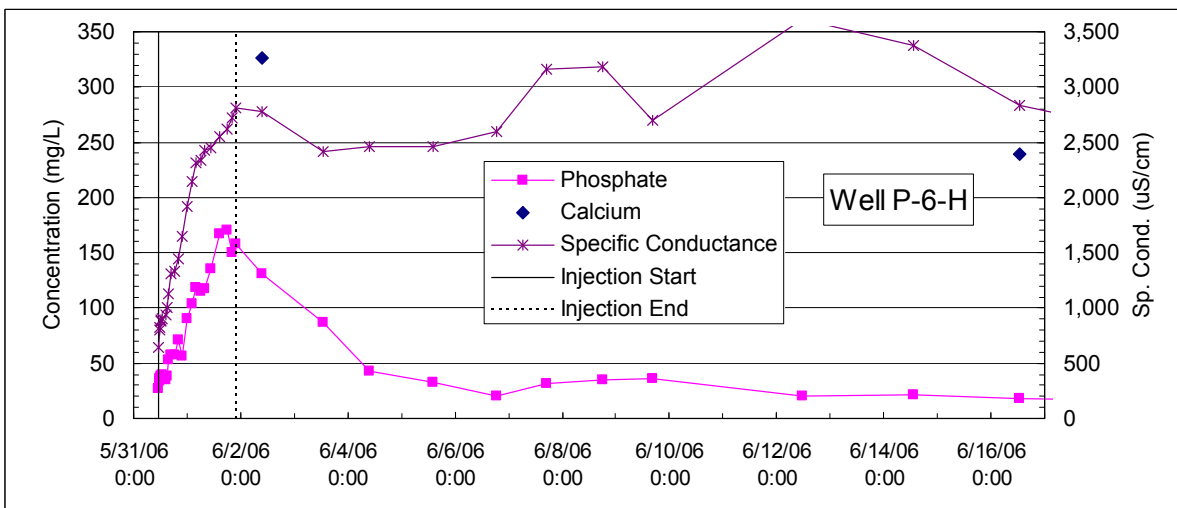
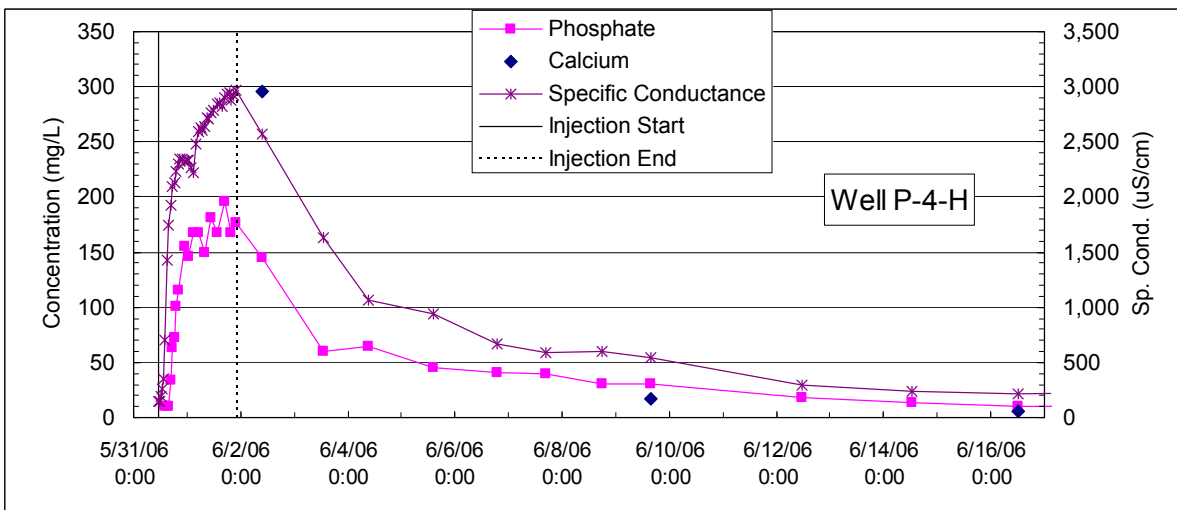
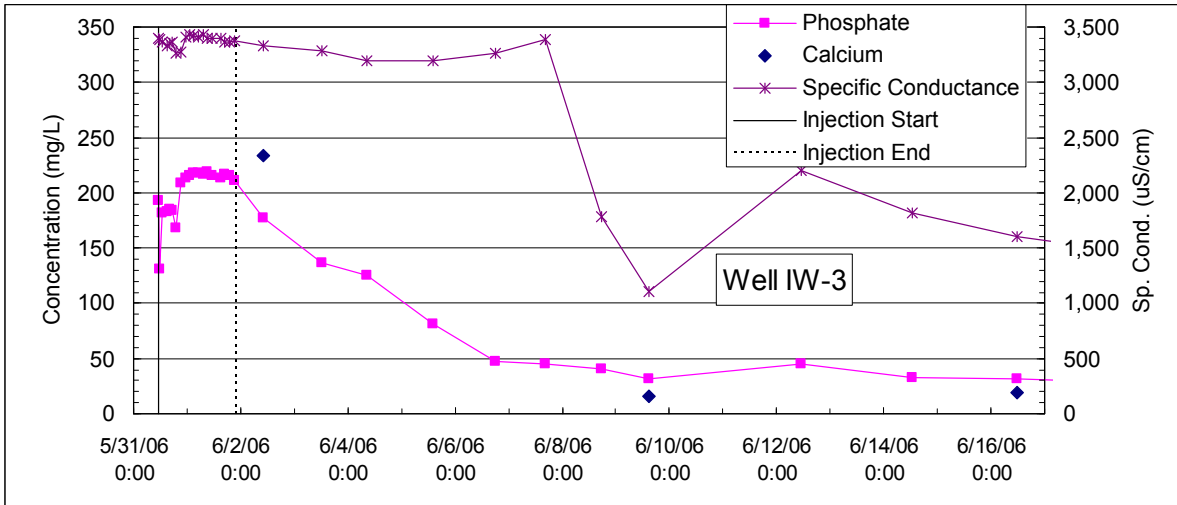


Figure 5.12. Apatite Pilot Test #1 Injection – Specific Conductance, PO₄, and Calcium Breakthrough Curves in Hanford Formation

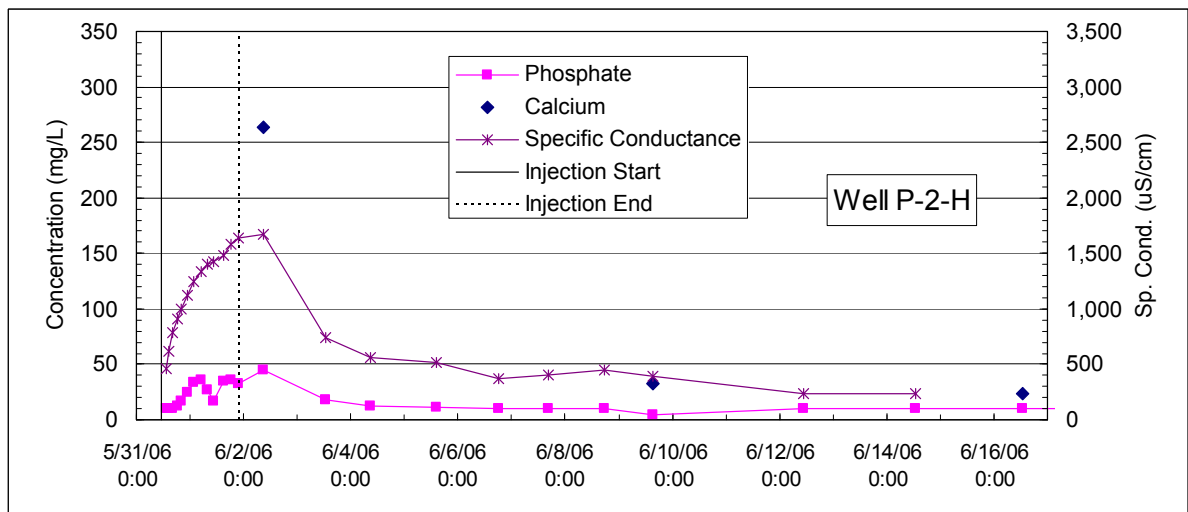
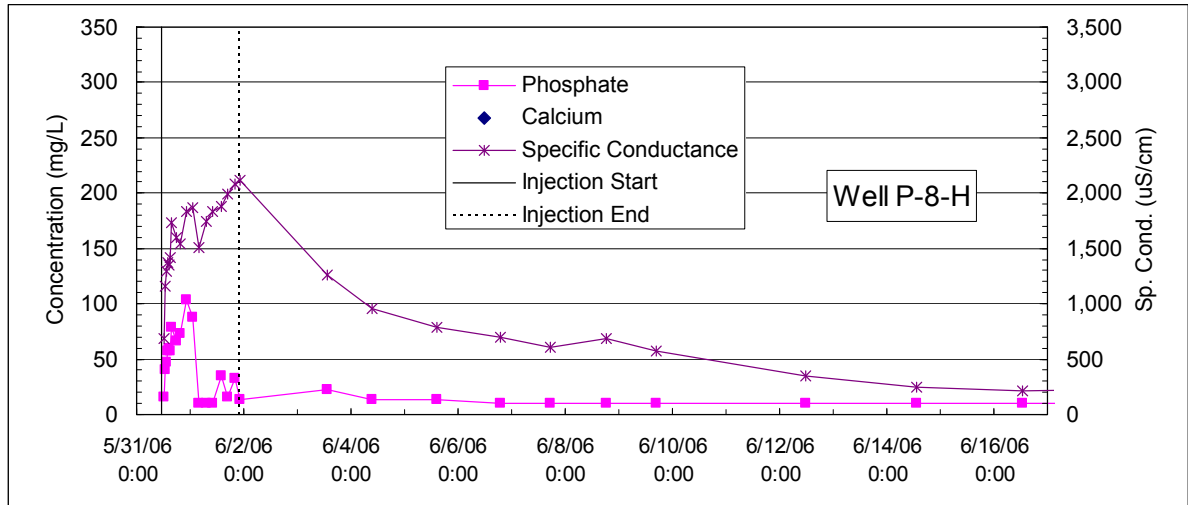


Figure 5.12. (contd)

Baseline SpC measurements at the site, collected on April 26, 2006, prior to the tracer test, ranged from 160 to 237 $\mu\text{S}/\text{cm}$. Significant variability in the SpC measurements in wells near the river is caused by river water/groundwater mixing with river water SpC values typically around 140 $\mu\text{S}/\text{cm}$ and higher values for groundwater. SpC measurements for selected wells further inland in the 100-N Area (199-N-2, 199-N-34, and 199-N-64), which would have less influence from river water mixing had values between 350 to 550 $\mu\text{S}/\text{cm}$ since 2002. Relative arrivals of SpC in the monitoring wells during the injection were similar to the results from the bromide tracer test (Section 5.1.2). The SpC of the injection solution is significantly greater than background values (e.g., ~ 3300 $\mu\text{S}/\text{cm}$ for the pilot test #1 injection). SpC measurements are not conservative due to sorption of phosphate, ion exchange of cations and citrate biodegradation reactions, but are useful for monitoring the injection plume extent. In the Hanford formation (Figure 5.12), the fastest initial arrivals were in well P-6-H with well P-4-H having the highest concentrations at the end of the injection period.

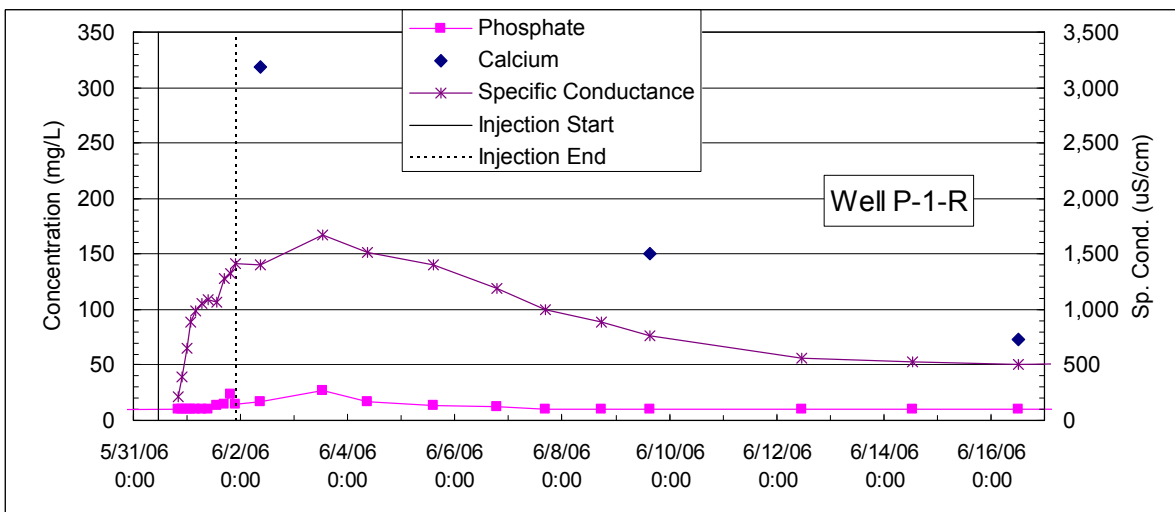
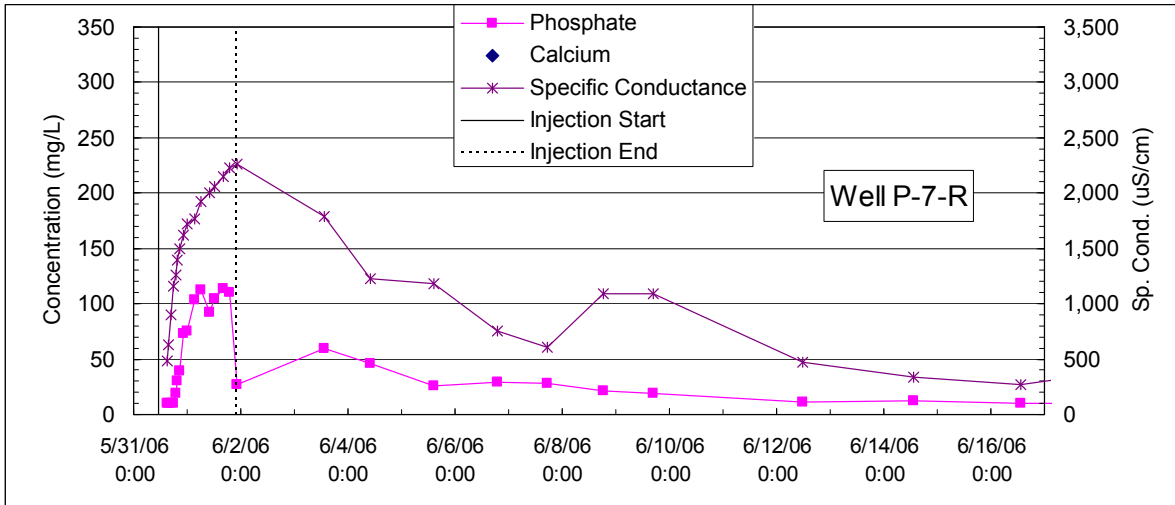


Figure 5.13. (contd)

Table 5.4. Summary of Phosphate and Specific Conductance in Selected Monitoring Wells for Pilot Test #1 Injection Test. Percentage of final injection concentrations shown in parentheses.

Apatite Project Well ID	End of Injection		1 Week after	
	SpC (µS/cm)	PO ₄ (mg/L)	SpC (µS/cm)	PO ₄ (mg/L)
IW-3	3380 (100%)	211 (100%)	1107 (33%)	31 (15%)
P-1-R	1410 (42%)	15 (7%)	765 (23%)	11 (5%)
P-2-H	1640 (49%)	32 (15%)	398 (12%)	4 (2%)
P-3-R	2560 (76%)	135 (64%)	1367 (40%)	9 (4%)
P-4-H	2970 (88%)	176 (84%)	544 (16%)	30 (14%)
P-5-R	2090 (62%)	46 (22%)	2020 (60%)	11 (5%)
P-6-H	2810 (83%)	158 (75%)	2700 (80%)	36 (17%)
P-7-R	2230 (66%)	111 (53%)	1096 (32%)	20 (9%)
P-8-H	2080 (62%)	33 (16%)	574 (17%)	10 ^(a) (5%)

(a) Estimated from field PO₄ measurements. All others are from IC analysis.

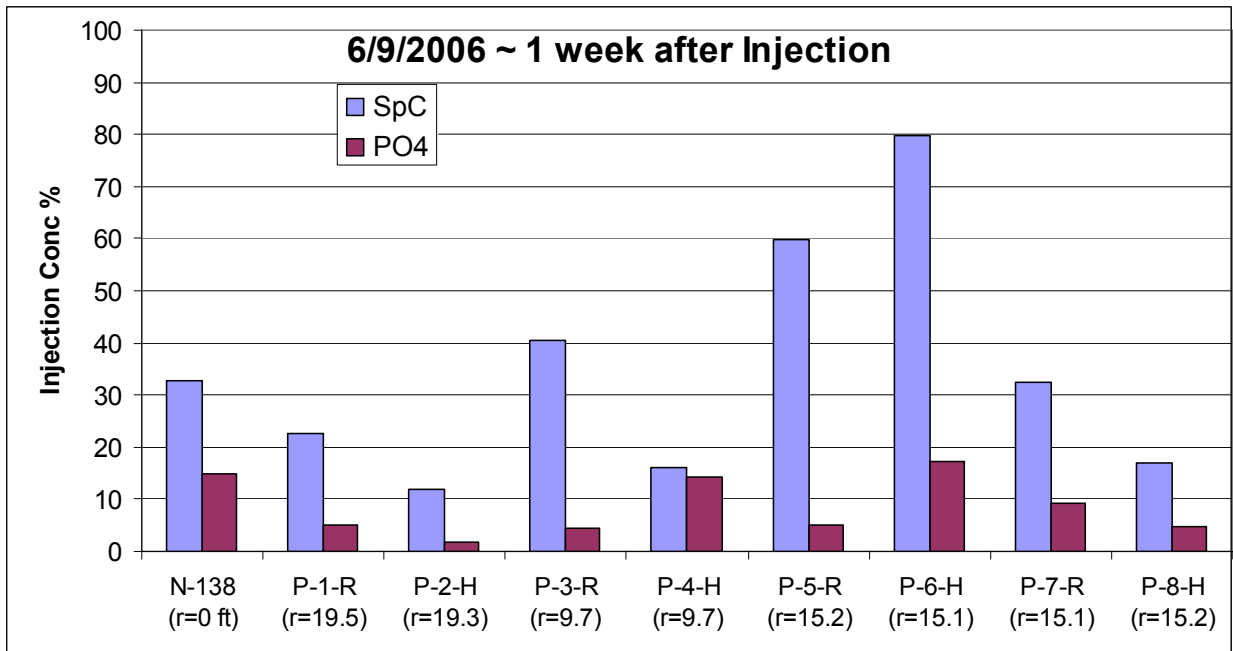
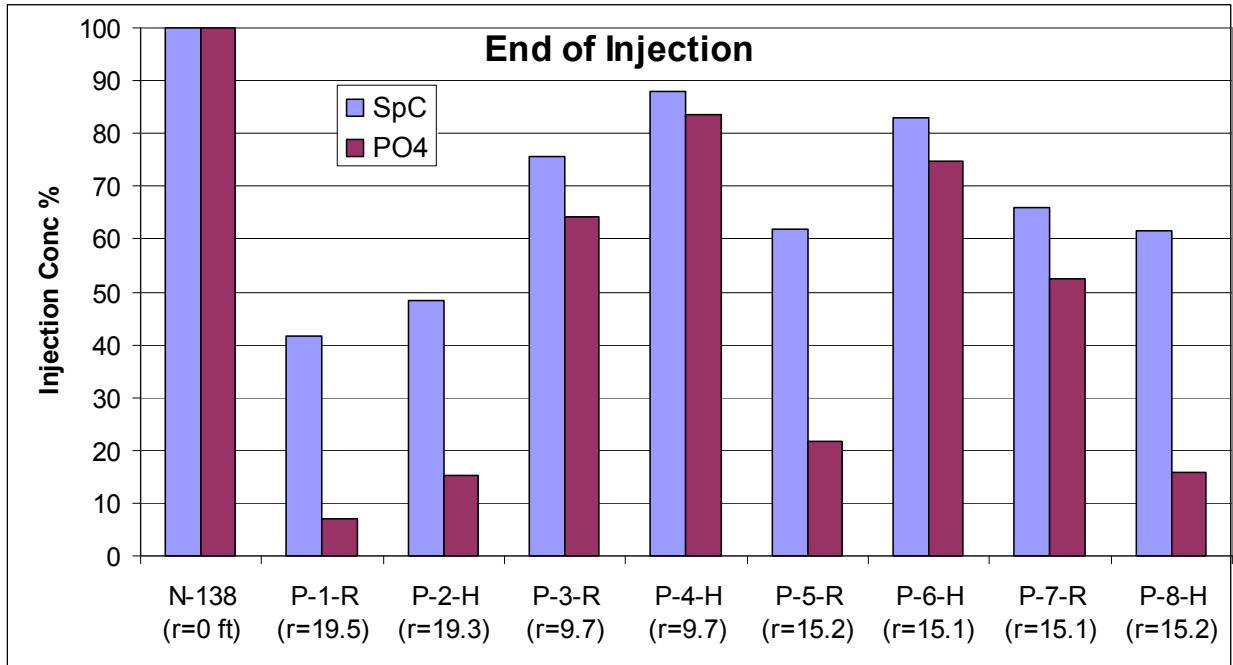


Figure 5.14. Summary of Specific Conductance and Phosphate in Monitoring Wells at End of Pilot Test #1 Injection (June 1, 2006) and ~1 Week Later (June 9, 2006). Concentrations are shown as a percentage of the injection concentration. The “r” is radial distance from the injection well in feet.

In the Ringold Formation (Figure 5.13), SpC arrivals were correlated with radial distance (unlike the Hanford formation monitoring wells) with the closest well, P-3-R, having the fastest arrival and the farthest well, P-1-R, having the slowest arrival and lowest concentration at the end of the injection period.

For the 4.6 m (15-ft) radial distance wells in the Ringold Formation, arrivals were faster for P-7-R than P-5-R (the same as the tracer test ranking). At the end of the injection period, relative SpC measurements in the monitoring wells ranged from 42% (in the 6-m [20-ft] radial monitoring well in the Ringold Formation) to 88% (in the closest monitoring well in the Hanford formation) as shown in Table 5.4. Specific conductance measurements decreased to a range of 12% to 80% 1 week following the injection.

Baseline phosphate measurements at selected wells at the pilot #1 test site were below detection limits of (<0.206 mg/L). Phosphate measurements during the injection were lower than the SpC measurements at the monitoring wells relative to injection values due to sorption and reactions. The percent concentrations of phosphate for the monitoring wells are shown in Table 5.4 and Figure 5.14. At the end of the injection, phosphate concentrations in the monitoring ranged from 7% (in the 6-m [20-ft] radial monitoring well in the Ringold Formation) to 84% (in the closest monitoring well in the Hanford formation). Phosphate concentrations decreased faster than the SpC measurements 1 week after the injection with relative concentrations ranging from 2 to 17%.

The average baseline calcium measurements from selected wells at the pilot test site #1 was 25 mg/L (April 26, 2006), as shown in Figure 5.15. Calcium concentrations in selected inland wells in the 100-N Area (199-N-2, 199-N-34, and 199-N-64), with less influence from river water mixing, had concentrations from 50 to 80 mg/L since 2002. Calcium concentrations for the injection solution for pilot test #1 are estimated at 160 mg/L, based on the design concentration and chemical mass delivered to the site.

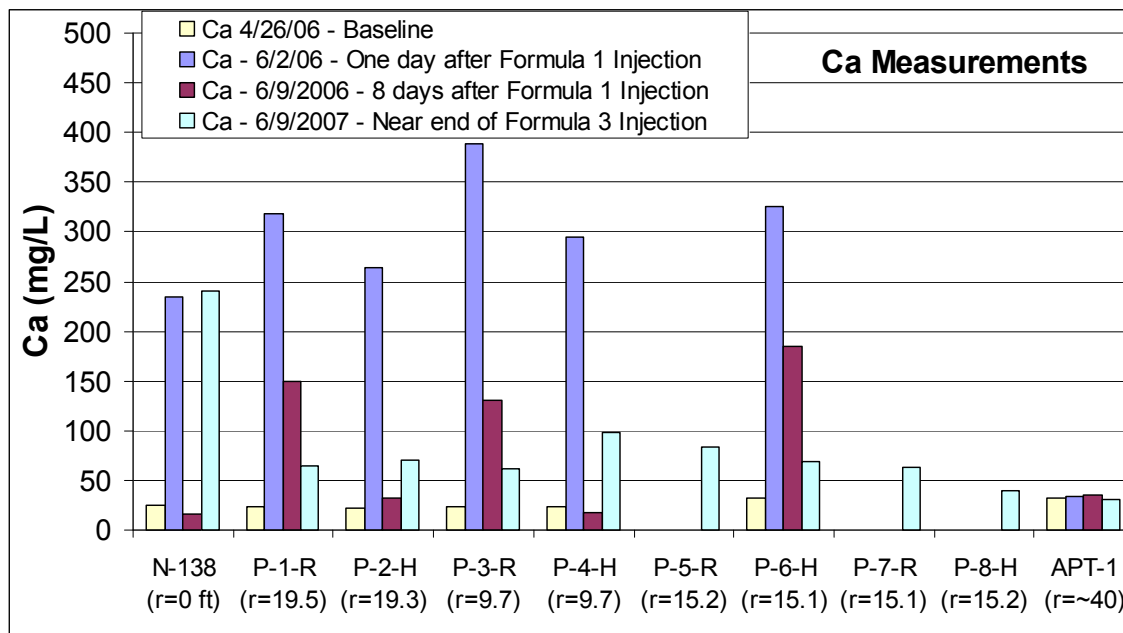


Figure 5.15. Summary of Calcium Measurements in Monitoring Wells Showing Baseline, 1 Day (June 2, 2006) and 8 Days (June 9, 2006) after the Injection. Analysis was conducted on a selected subset of wells. Injection concentration was estimated at 160 mg/L based on design concentration/chemical mass. The “r” is radial distance from the injection well in feet.

Calcium concentrations measured in a subset of wells 1 day after the end of the pilot test #1 injection were significantly above the injection concentration, as shown in Figure 5.15. This occurred due to a

fraction of the calcium held on the sediment by ion exchange desorbing due to the high-ionic strength injection solution (i.e., being replaced by the high sodium in the injection solution). These data are also shown in Figures 5.12 and 5.13, along with the SpC and phosphate measurements for the monitoring wells. Calcium concentrations decreased to baseline levels in the injection well and two of the Hanford formation monitoring wells 8 days after the injection, and were still elevated in one Hanford formation well and the two Ringold Formation wells (Figure 5.15). The trends follow the relative increases in SpC in these wells, with the higher calcium values in wells with significantly elevated SpC during this time (compare with Figure 5.14).

Because of a problem with the preservation technique used for samples collected for citrate analyses during this test, no citrate results were available. An improved preservation technique, as shown in Table 4.5, was used during subsequent field testing activities. Laboratory tests injecting this solution into one-dimensional sediment columns showed initial SpC breakthrough generally represents citrate breakthrough (see Figure 5.16 in Szecsody et al. [2007]). Phosphate adsorption to sediment results in a lag (retardation) in laboratory and field tests. This PO₄ sorption is slow (i.e., hours to reach equilibrium), so greater retardation is observed in the field with slower injection rates, which allows for greater sediment-PO₄ contact time.

5.2.3 Post-Injection Processes

Citrate biodegradation creates reducing conditions in the aquifer by initially utilizing available DO as an electron acceptor. There is little reductive capacity in the injected zone because iron oxides are not reduced (i.e., the reduced zone is temporary, as oxygen-laden water is advected into the injected zone). DO concentrations and oxidation-reduction potential (ORP) measurements are shown for two wells during and after the pilot test #1 injection in Figure 5.16. For the pilot test #1, DO concentrations were significantly decreased by the next sampling after the end of the injection (~11 hours) and decreased further over the next day (Figure 5.16). ORP measurements also decreased over a 1-week period following the injection. The DO and ORP measurements remained low for most of the wells at the site in June 2006 following the test except for significant increases for well P-2-H (the well closest to the river within the Hanford formation). The reducing conditions established in the aquifer increased some redox-sensitive trace metal concentrations of iron, manganese, and aluminum. Trace metal concentration changes are summarized in Section 5.2.4, along with a discussion of longer-term monitoring results.

Groundwater flow directions after the injection can be inferred from SpC measurements in the monitoring wells, as shown in Figures 5.12 and 5.13. The near-river monitoring wells, P-1-R and P-2-H, show a decreasing SpC trend flowing toward the injection until approximately 2 weeks later, when the trend reverses with increasing SpC. A similar SpC trend is seen in the other two monitoring wells between the injection well and the river (P-3-R and P-4-H), and the two monitoring wells adjacent to the injection well (P-7-R and P-8-H). The two monitoring wells on the inland side of the injection well (P-5-R and P-6-H) show an opposite trend with SpC measurements increasing for 10 to 26 days following the injection and then decreasing with faster response in the Hanford formation monitoring well. The interpretation of these trends is that the high-river stage following the injection caused inflow from the river with the injection plume initially migrating in an inland direction. When the river stage dropped later in June 2006, the injection plume drift reversed direction toward the river. Figure 5.17 shows this SpC trend for a longer monitoring period, along with the river stage, for Hanford and Ringold Formation wells inland from the injection well (P-6-H and P-5-R) and between the injection well and the river (P-4-H and P-3-R).

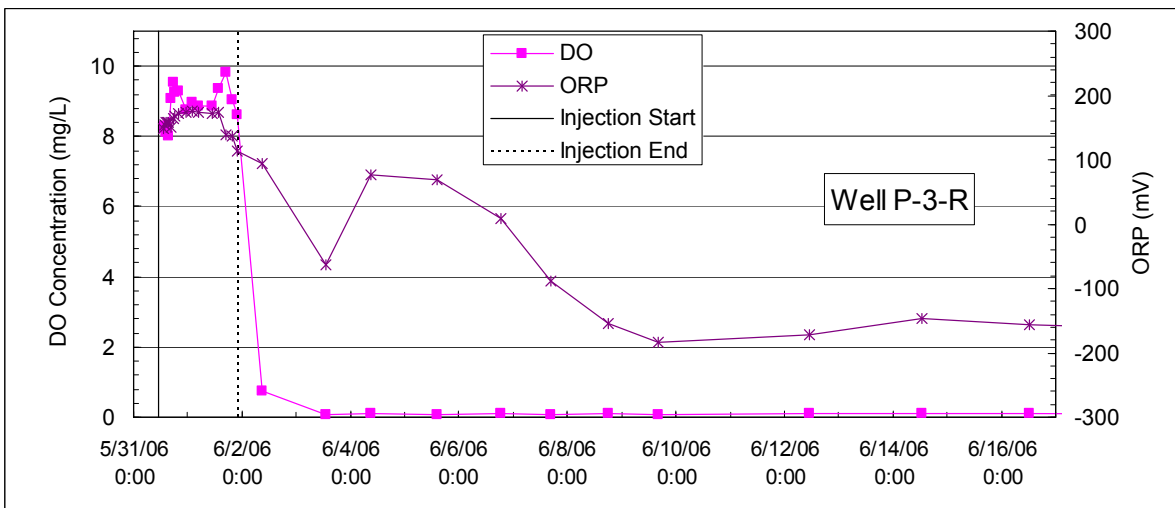
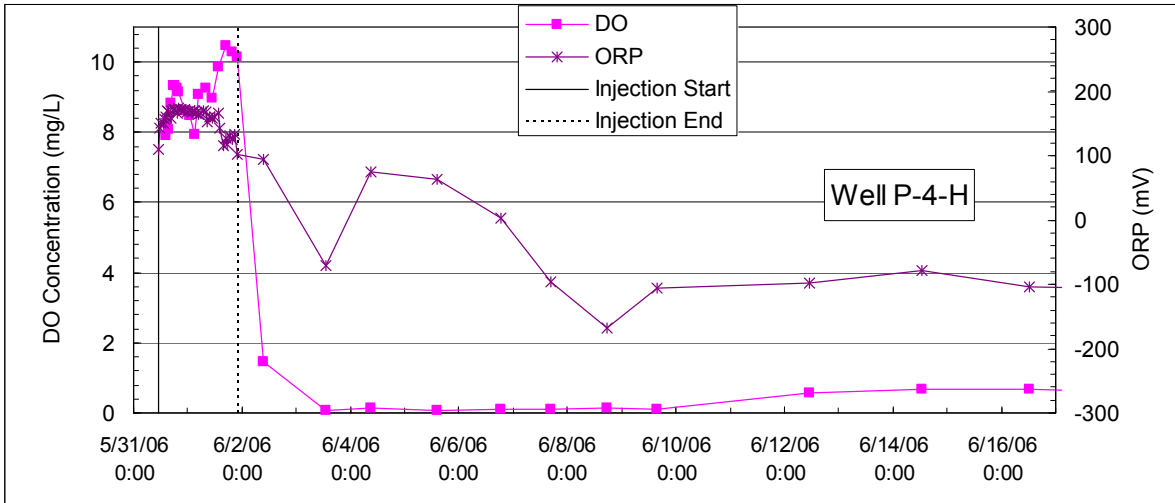


Figure 5.16. Apatite Pilot Test #1 Injection Dissolved Oxygen and Oxidation-Reduction Potential for Selected Monitoring Wells. Results for other monitoring wells were similar.

5.2.4 General Water Quality

Water quality parameters at the site were collected prior to testing at the site to establish baseline conditions during the pilot injection test #1 to monitor the injection process, and following the test for assessing the impact the process had on water quality. A subset of six wells was selected for water quality monitoring at the test site: P-2-H, P-4-H, P-6-H, P-1-R, P-3-R, and APT-1. Shorter-term water quality is assessed in this section. Results of longer-term monitoring at the site are provided in Section 8.0, followed by a discussion of ⁹⁰Sr concentrations in Section 5.2.5.

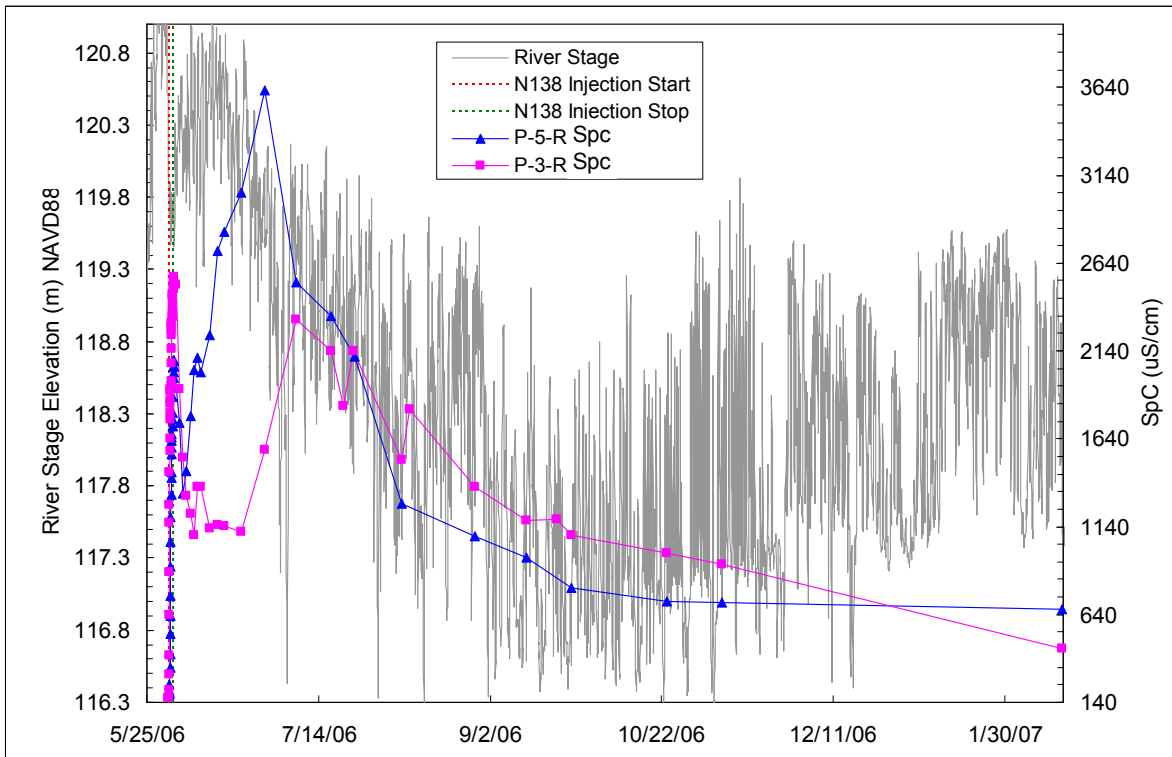
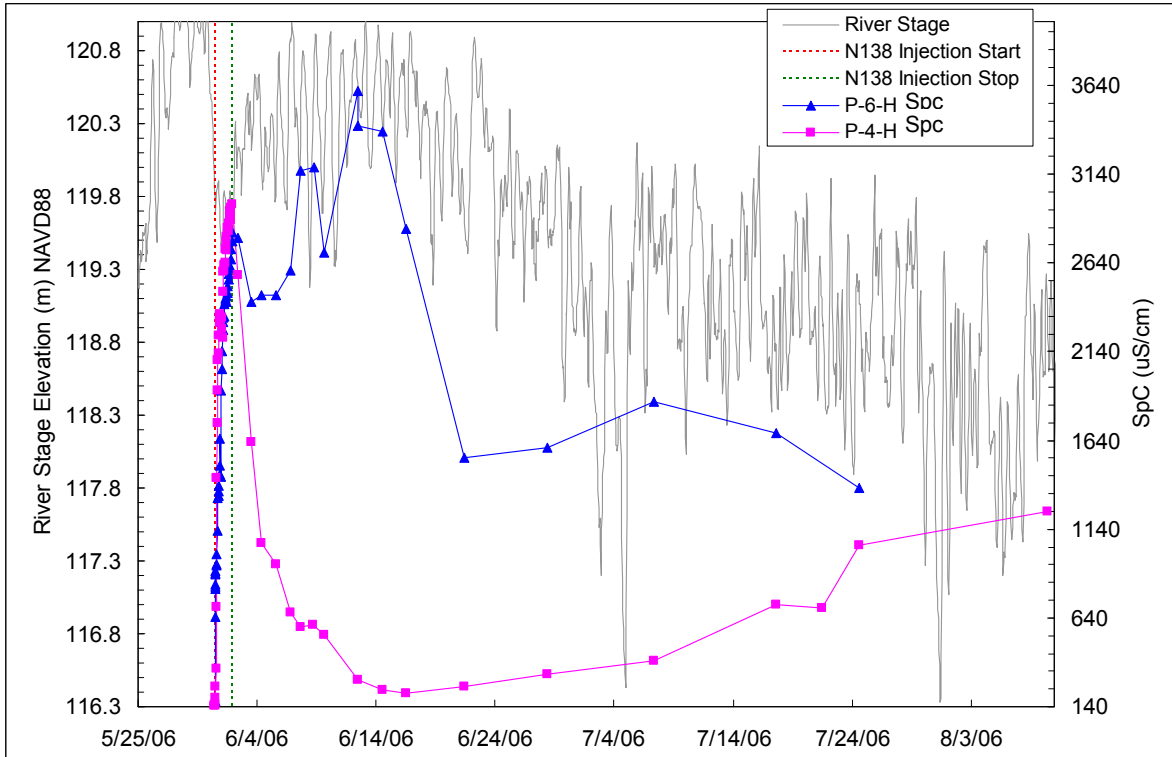


Figure 5.17. Columbia River Stage and Specific Conductance Measurements After Pilot Test #1. Upper figure shows two wells in the Hanford formation; lower figure shows two wells in the Ringold Formation (with a longer monitoring period).

Water quality parameters are described in three categories: field parameters, anions, and trace metals. Summary tables are provided for these in Tables 5.5 through 5.7.

Table 5.5. Summary of Field Parameters in Selected Monitoring wells at Pilot Test #1 Injection Test Site. Baseline field parameters were collected immediately prior to the pilot test #1 injection on May 31, 2006 (after the tracer test at the site). Monitoring wells are P-2-H, P-4-H, P-6-H, P-1-R, P-3-R, and APT-1.

	SpC ($\mu\text{S}/\text{cm}$)	DO (mg/L)	ORP (mV)	Temp. ($^{\circ}\text{C}$)	pH
<i>Baseline Conditions</i>					
Minimum	149	5.9	160	13.0	7.64
Maximum	210	9.1	181	15.9	7.93
Average	174	8.2	170	13.8	7.73
<i>Conditions Near End of Injection</i>					
Minimum	211	0.8	73	13.0	7.51
Maximum	2780	7.2	107	15.4	7.91
Average	1859	4.0	94	14.2	7.71
<i>Conditions ~1 Month After Injection</i>					
Minimum	276	0.04	-198	14.6	7.21
Maximum	1600	1.9	-54	18.4	8.00
Average	780	0.6	-141	15.9	7.64

Table 5.6. Summary of Anions in Selected Monitoring Wells at Pilot Test #1 Injection Test Site. Baseline anions samples were collected from the site prior to the tracer test on April 26, 2006. Monitoring wells are P-2-H, P-4-H, P-6-H, P-1-R, P-3-R, and APT-1.

Conditions	Anions			
	Chloride (mg/L)	Formate (mg/L)	PO ₄ (mg/L)	Citrate (mg/L)
<i>Baseline Conditions</i>				
Minimum	1.12	<0.820	<0.206	<0.500
Maximum	4.66	<0.820	<0.206	<0.500
Average	1.97	<0.820	<0.206	<0.500
<i>Conditions Near End of Injection</i>				
Minimum	0.760	<0.8	<1.1	<0.5
Maximum	401	380	145	1848
Average	265	124	80	571
<i>Conditions ~1 Month After Injection</i>				
Minimum	3.73	<8.2	<10.6	<50
Maximum	113	<8.2	<10.6	<50
Average	42.2	<8.2	<10.6	<50
Drinking Water Standard	250			

Table 5.7. Summary of Selected Metals and ⁹⁰Sr at Pilot Test #1 Injection Test Site. Baseline samples for metals and ⁹⁰Sr were collected from the site before the tracer test and apatite pilot test #1 on April 26, 2006. Monitoring wells are P-2-H, P-4-H, P-6-H, P-1-R, P-3-R, APT-1.

Conditions	Metals					⁹⁰ Sr (pCi/L)
	Al (mg/L)	Ca (mg/L)	Fe (mg/L)	Mn (mg/L)	Na (mg/L)	
<i>Baseline Conditions</i>						
Minimum	<0.030	22.7	0.006	0.001	2.5	314
Maximum	<0.030	32.9	0.011	0.006	3.7	895
Average	<0.030	26.4	0.008	0.004	3.0	660
<i>Conditions Near End of Injection</i>						
Minimum	<0.030	33.2	0.007	0.047	3.8	907
Maximum	11.1	388	2.2	0.245	704	7829
Average	7.60	271	1.1	0.134	410	5404
<i>Conditions ~1 Month After Injection</i>						
Minimum	<0.075	6.68	0.006	0.008	2.7	32
Maximum	0.850	144	0.73	6.5	224	4483
Average	0.204	59.8	0.25	2.2	70	1652
Drinking Water Standard	0.05 to 0.2 Secondary		0.3 Secondary	0.05 Secondary		8

Table 5.5 summarizes the field parameters (SpC, DO, ORP, temperature, and pH) at the site for baseline conditions, near the end of the injection, and 1 month following the injection. Comparing the results from 1 month following the injection to baseline conditions, the pilot test #1 resulted in increases in SpC from the residual chemicals in the aquifer and a significant reduction in DO concentrations and ORP from biodegradation of citrate. Measurements of pH at the site before and after the test were similar; however, the range was slightly larger 1 month following the test (as shown in Table 5.5).

A comparison of anion measurements at the test site are shown in Table 5.6. Pilot test #1 increased chloride, phosphate, and citrate concentrations at the site test due to the reagent composition (see Table 5.3). Formate forms as a degradation product of citrate and was detected following the injection. Concentrations of these anions were lower 1 month after the injection. Citrate and formate measurements in Table 5.6 should be viewed as minimum concentrations due to analytical uncertainties associated with sample preservation problems.

A summary of selected metals at the site are shown in Table 5.7. Sodium concentrations were above baseline conditions due to the reagent composition (Table 5.3). Calcium concentrations were elevated from the injection solution and from desorption of existing calcium from the sediments (ion exchange from the injection solution and complexation with citrate). Redox-sensitive trace metals (e.g., aluminum, iron, and manganese) showed an increase in concentrations following the injection because of reducing conditions created by biodegradation of citrate.

5.2.5 Strontium-90 Monitoring

Figure 5.18 shows ⁹⁰Sr concentrations at pilot test site #1 for a subset of the monitoring wells at the site that were selected for long-term monitoring with baseline values and results up to 5 months after the

injection test. Baseline conditions were measured in these wells before the tracer and apatite injection tests at the site. Following the injection, ^{90}Sr concentrations at the test site increased significantly above baseline values. Highest concentrations occurred immediately after the injection test for most wells with concentrations generally decreasing toward the end of this period. The monitoring wells in this subset (as shown in Figure 5.18) that were screened in the Hanford formation were not sampled after July 2006 because these wells were dry during low-river stage conditions. Peak ^{90}Sr concentrations in the pilot test #1 monitoring wells are summarized in Table 5.8 for the period following the first apatite injection (June 2006) and prior to the second apatite injection at this site (June 2007). Peak ^{90}Sr concentrations in these monitoring wells were on average 8.4 times the mean baseline ^{90}Sr value at the site; observed peaks ranged from 1.1 to 16.5 times the baseline value.

Table 5.8 also shows the peak ^{90}Sr concentrations after the second injection at pilot test site #1 conducted in June 2007 (see Section 8.0 for description). The injection formula was revised for pilot test #2 conducted in September 2006 (described in Section 5.3) and was revised again for the 2007 barrier well injections. The objective of these formula revisions was to reduce the temporary increase in ^{90}Sr by reducing the ionic strength of the injection solution and specifically the amount of calcium (both by lowering the injection calcium and citrate concentration that forms Ca-complexes). Phosphate concentrations were increased during these revisions. Changes in the injection concentrations were first tested in laboratory experiments prior to the field tests (see Sections 2.6 and 3.2). The peak ^{90}Sr concentrations with the revised barrier formulation in 2007 was much lower than measured during pilot test #1 as shown in Table 5.8. Some of the decrease in peak ^{90}Sr concentrations following the 2007 injection at the pilot test site #1 may be attributed to apatite that formed during the first injection in this site in 2006.

Initial increases in ^{90}Sr were caused by desorption and ion-exchange reactions from the injection solution, particularly calcium (Szecsody et al. 2007). As discussed in Section 5.2.2, aqueous calcium concentrations in the aquifer were greater than the injection solution concentration due to citrate complexation and desorption of existing calcium from the sediment. Laboratory one-dimensional columns showed calcium and strontium peaking at ~ 10 times natural aqueous calcium and strontium values due to the injection solution, and the field test average approximated this increase. This increase is temporary because citrate degrades (over weeks), and calcium and strontium precipitate out with PO_4 , forming apatite. A plot of calcium versus $^{89/90}\text{Sr}$ concentrations from the pilot test site #1 monitoring wells in Figure 5.19 shows the relationship between increased concentrations of these constituents. The injection formula was changed for later injections at the treatability test site based on laboratory tests to minimize the initial increase in ^{90}Sr by decreasing the calcium and citrate concentrations in the injection solution, and utilize more calcium from sediment to combine with PO_4 and still form a sufficient mass of apatite precipitate. Results from pilot test site #2, as discussed in the following section, had a lower increase in the ^{90}Sr concentrations following the Ca-citrate- PO_4 injection.

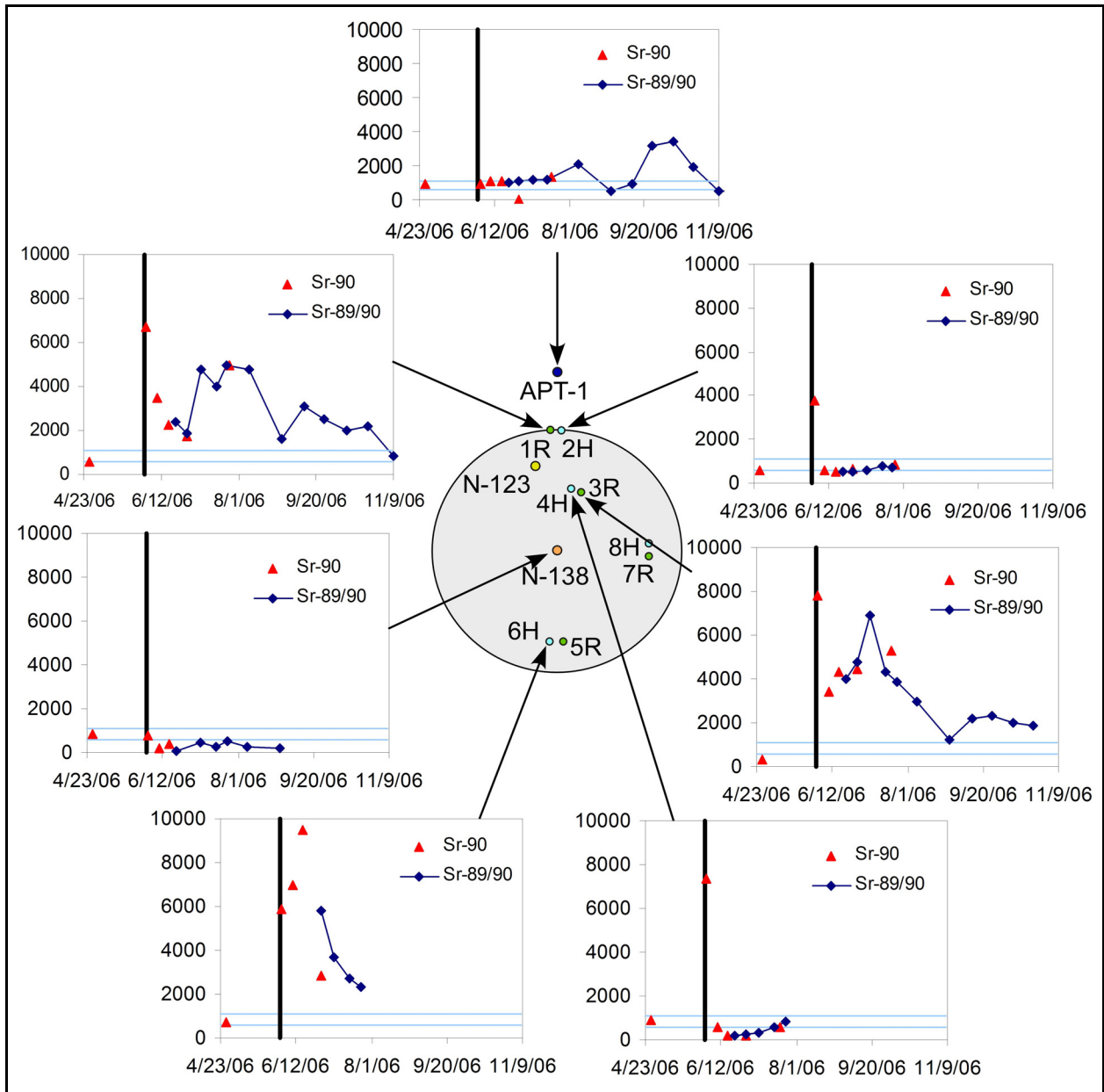


Figure 5.18. ^{90}Sr and $^{89/90}\text{Sr}$ Concentrations (pCi/L) Before and 5 Months After Pilot Test #1 Injection. Wells were selected from a subset of the monitoring wells that had baseline ^{90}Sr values. Hanford formation wells were not sampled (because they were dry) following July 2006. Vertical line denotes injection timing and horizontal lines represent the estimated minimum and maximum baseline concentrations at the pilot test site (see Section 8.0).

Table 5.8. Summary of Baseline and Peak ⁹⁰Sr Concentrations After Injections at Pilot Test Site #1 (N-138)

Well	Baseline		5/31/06 N-138 Inject Formula 1 (4,10,2.4) Post Inj Peak		6/8/2007 N-138 Inject Formula 3 (1,2.5,10) Post Inj Peak		Ratios			
	Sr pCi/L	Date	Sr pCi/L	Date	Sr pCi/L	Date	Formula 1 Peak / Mean Baseline	Formula 1 Peak / Baseline	Formula 3 Peak / Mean Baseline	Formula 3 Peak / Baseline
N-138	811	4/26/2006	801	6/2/2006	480	10/19/2007	1.10	0.99	0.66	0.59
N-123	1,040	4/12/2006	2,720	8/8/2006	1,480	9/7/2007 ^a	3.75	2.62	2.04	1.42
APT-1	877	4/26/2006	3,400	10/9/2006	1,400	7/13/2007	4.68	3.88	1.93	1.60
P-1-R	570	4/26/2006	6,696	6/2/2006	2,500	7/8/2007	9.22	11.75	3.44	4.39
P-2-H	574	4/26/2006	3,735	6/2/2006	1,400	6/20/2007	5.14	6.51	1.93	2.44
P-3-R	314	4/26/2006	7,829	6/2/2006	1,600	10/19/2007	10.78	24.93	2.20	5.10
P-4-H	895	4/26/2006	7,365	6/2/2006	2,600	7/13/2007	10.14	8.23	3.58	2.91
P-5-R			11,000	6/28/2006	5,000	10/19/2007	15.15		6.88	
P-6-H	729	4/26/2006	9,482	6/16/2006	1,400	7/8/2007	13.06	13.01	1.93	1.92
P-7-R			12,000	7/17/2006	3,000	11/14/2007	16.52		4.13	
P-8-H			2,100	7/24/2006	1,100	7/8/2007	2.89		1.51	
Mean	726		6,103		1,996		8.40	8.99	2.75	2.54

Color Key

Sr-90

WSCF - Total beta radiostromtium

^aData flagged with Q qualifier

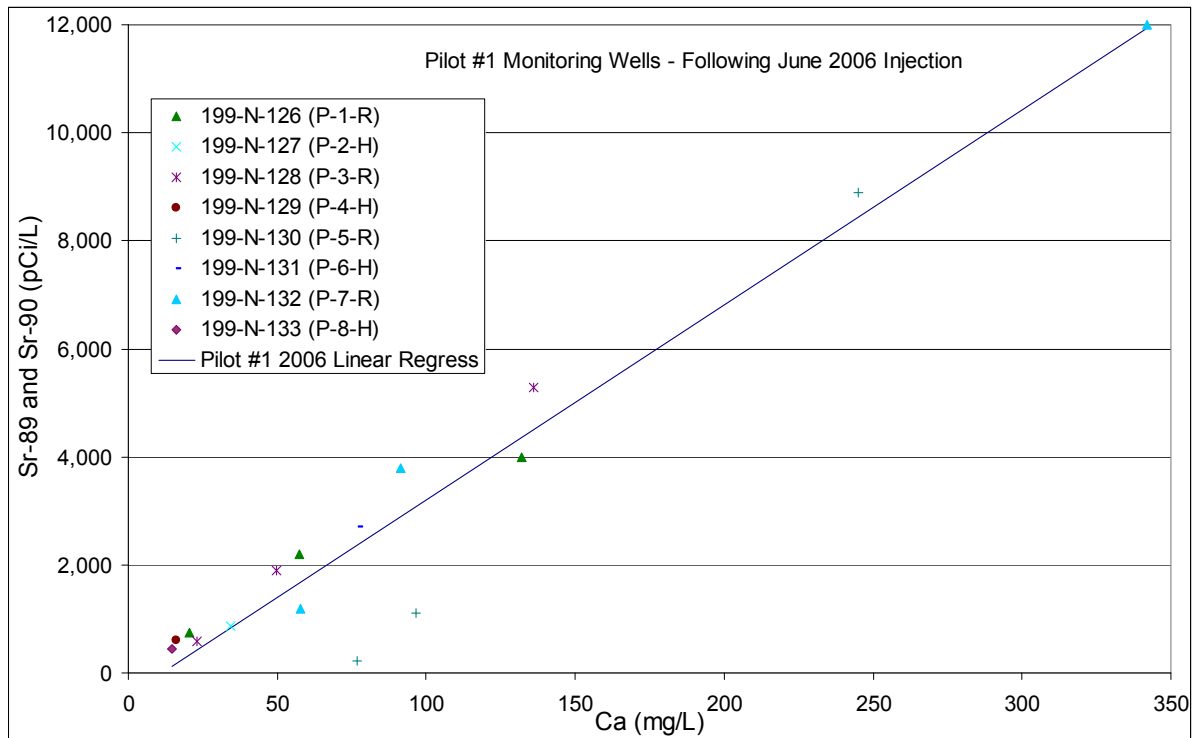


Figure 5.19. Calcium and ^{89/90}Sr Ratios at Pilot Test #1 Injection; Data from July and October 2006 and May and June 2007 (prior to second injection at pilot test site #1)

5.3 Pilot Test #2

A second Ca-citrate-PO₄ pilot injection test was conducted at the downstream end of the treatability test barrier at well 199-N-137 (see Figures 1.10 and 4.3) on September 27 and 28, 2006, during low-river stage conditions (see Figure 5.20). Table 5.9 provides an operational summary of this test. The reagent formulation for this test was modified based on monitoring results of the first test and additional laboratory studies (see Section 2.6 and Table 2.3). The Ca-citrate-PO₄ formulation used in pilot test #1 was the stoichiometric proportions of calcium and PO₄ needed to form apatite. In pilot test #2, half as much calcium was injected (same PO₄ concentration was injected) as sufficient calcium ion exchanged off sediment surfaces to form the apatite. The concentrations for the second test are shown in Table 5.9. The objective of this modification in the concentrations (compare Tables 5.3 and 5.9) was to lower the excess calcium to minimize the increase in ⁹⁰Sr concentrations. Some nitrate (i.e., ammonium nitrate) was also removed from the formulation to slow down the biodegradation rate of citrate. The injection chemicals were delivered in concentrated form in two tanker trucks to the site to keep the calcium and phosphate separate prior to injection. The maximum solubility and stability of these chemical mixtures were determined in the laboratory and described in Szecsody et al. (2007, Section 5.3.2). Test operations, monitoring, and short-term water quality impacts are described in the following sections.

5.3.1 Flow Rates and Pressures

The total volume injected for pilot test #2 Ca-citrate-PO₄ test was 228,600 L (60,400 gal) in 24 hours. Flow rates for the two concentrated feed solutions, dilution water, and the total injection stream rates are shown in Figure 5.21. The injection rates for the two concentrated solutions (Mix 1 and Mix 2) were set based on the liquid volumes in the separate tankers delivered to the site. River water was pumped at the site for diluting the concentrated solutions to the target injection concentrations. The injection rate was started at 303 L/min (80 gpm) and was reduced to 151 L/min (40 gpm) after approximately 3 hours (see Figure 5.21) because monitoring data of field parameters showed the injection plume was appearing more rapidly in the Hanford formation, and the objective of the test was to target the Ringold Formation. Reducing the injection rate was intended to reduce the elevation of the injection mound into the Hanford formation and thus reduce the amount of reagent flux in the Hanford formation relative to the Ringold Formation. Figures 5.22 and 5.23 show the injection mound for the injection well and monitoring wells during the test. Decreasing the injection rate to 151 L/min (40 gpm) decreased the head in the injection well by approximately 1.5 m (4.9 ft) and initially decreased the heads in the monitoring wells by 0.3 to 0.4 m (0.98 to 1.3 ft). However, the heads measured in the monitoring wells increased toward the middle of the test due to increases in the river stage (see Figure 5.20).

5.3.2 Injection Monitoring/Radial Extent

Figures 5.24 and 5.25 show the SpC, phosphate, and calcium breakthrough curves for the monitoring wells at pilot test site #2 for the Hanford and Ringold Formation wells. A summary of the SpC and phosphate concentrations in the monitoring wells at the end of the injection is provided in Table 5.11. Citrate breakthrough curves are shown in Figure 5.26 and 5.27. Overall, arrivals in the Hanford formation wells were much faster and the ending injection concentrations were greater than in the adjacent Ringold Formation wells. Significant concentrations of phosphate, citrate, and calcium were also seen in the adjacent injection well (199-N-136 at a 9.1-m [30-ft] distance) most likely caused by rapid transport in the

Hanford formation. The greater difference between the Hanford and Ringold Formation arrivals at pilot test site #2, compared to pilot test site #1, is caused by a greater contrast in the relative permeability of these formations at the pilot test site #2.

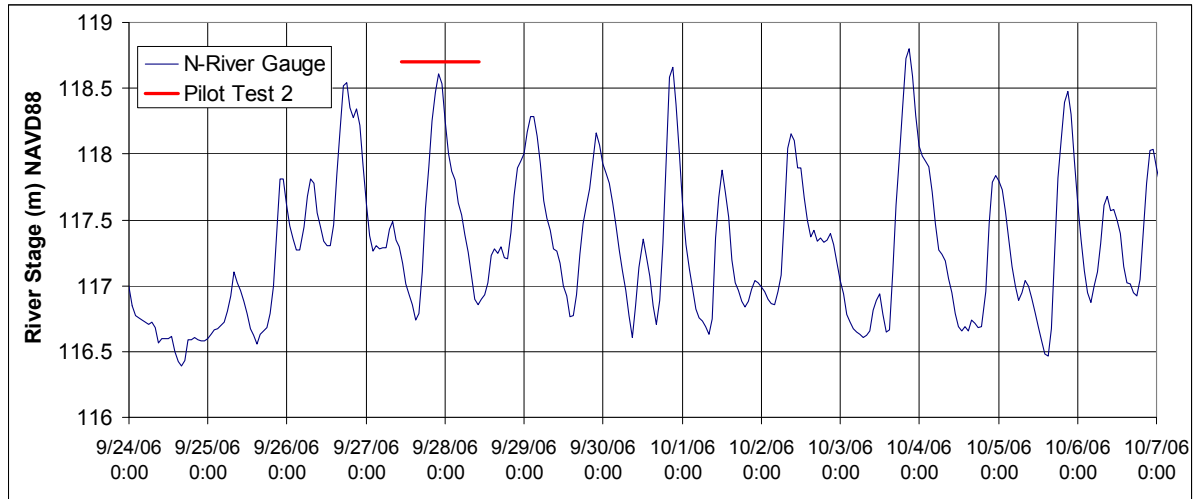


Figure 5.20. Columbia River Stage and Timing for 100-N Area Pilot Test #2. Pilot test #2 timing shows the injection period.

Table 5.9. Summary of Apatite Pilot Test #2 (September 27 and 28, 2006)

Test Parameter	Value
Injection Volume	60,400 gallons
Injection Concentrations (Target)	5.0 mM tri-sodium citrate 2.0 mM calcium chloride 2.4 mM diammonium phosphate 1.0 mM sodium bromide
Tanker Truck 1 (Mix 1) Volume / Mass	2500 gallons 735 lbs (334 kg) tri-sodium citrate 147 lbs (66.8 kg) calcium chloride
Tanker Truck 2 (Mix 2) Volume / Mass	2500 gallons 158 lbs (71.8 kg) diammonium phosphate 51 lbs (23.2 kg) sodium bromide
Total Injection Rate	~80 to 40 gpm
Tanker 1 Injection Rate	~3.1 to 1.7 gpm
Tanker 2 Injection Rate	~3.3 to 1.7 gpm
Injection Rate Pumped from River	~74 to 37 gpm
Injection Duration	23.6 hr (September 27 to September 28, 2006)

Monitoring of the aquifer tube APT-5 during this pilot test, as shown in Figure 5.25 and Table 5.11 (located approximately 12 m [40 ft] from the injection well; see Figure 4.3), had a slight impact during the injection period. Concentrations increased in APT-5 following the injection due to plume drift toward the Columbia River.

Well P2-9-R, which is screened below the 199-N-137 injection screen, was installed to determine if the injection plume spreads out deeper in the Ringold Formation (see Figure 4.3). As shown in

Figure 5.25 and Table 5.11, there was some impact in this zone below the injection screen but it was much less than observed in other Ringold Formation wells at a similar radial distance (compare to P2-3-R). Concentrations increased in well P2-9-R following the injection, possibly caused by fluid density effects.

Table 5.10. Injection and Monitoring Well Summary for the Pilot Test Site #2

Apatite Project Well ID	Hanford Site Well Name	Radial Distance from Injection Well (ft)	Drilling Method	Well Diameter (inches) and Material	Screen Interval (ft bgs) and Formation
199-N-137	199-N-137	0 Injection Well	Cable Tool	6.0 Stainless Steel	24.0 to 7.0 Hanford and Ringold
P2-1-R	199-N-148	15.2	Sonic	2.0 PVC	24 to 19, Ringold
P2-2-H	199-N-149	15.2	Sonic	2.0 PVC	16 to 11, Hanford
P2-3-R	199-N-151	10.2	Sonic	2.0 PVC	24 to 19, Ringold
P2-4-H	199-N-150	9.6	Sonic	2.0 PVC	16 to 11, Hanford
P2-5-R	199-N-156	15.5	Sonic	2.0 PVC	24 to 19, Ringold
P2-6-H	199-N-155	14.9	Sonic	2.0 PVC	16 to 11, Hanford
P2-7-R	199-N-154	15.1	Sonic	2.0 PVC	24 to 19, Ringold
P2-8-H	199-N-153	15.3	Sonic	2.0 PVC	16 to 11, Hanford
P2-9-R	199-N-152	10.8	Sonic	2.0 PVC	33 to 28, deeper Ringold

Calcium concentrations in the monitoring wells, shown in Figures 5.24 and 5.25, were greater than the injection concentration (well 199-N-137) because of desorption from the sediment and complexation with citrate. Calcium concentrations were greater in wells farther from the injection well that had longer travel times/path lengths than closer wells. Calcium concentrations were also much greater in the Ringold Formation than in the adjacent Hanford formation wells.

Field-scale retardation factors are influenced by groundwater velocities, which can override sorption and/or reaction kinetics, and formation heterogeneities yielding significant variability in the fine-grained sediment fraction that is important in controlling the sorption/reactions. As an example of relative retardation factors for the major injection constituents, Figure 5.28 shows normalized breakthrough curves for bromide, citrate, SpC, and phosphate during the injection period for well P2-3-R. Bromide and citrate breakthrough curves are relatively symmetrical in this example with the citrate arrival slightly retarded ($R_f \sim 1.2$) compared to bromide, which is a conservative solute. Although the SpC and phosphate breakthrough curves are asymmetrical around the 50% concentration level, they did achieve concentrations greater than 50% that enabled estimation of retardation factors for the early arrivals. With these qualifications, retardation factors estimated based on the 50% concentrations were ~ 1.3 for SpC and ~ 3.0 for phosphate. SpC arrivals are asymmetrical because it measures a mixture of species with different sorption and reaction characteristics. One reason for the asymmetry in the phosphate arrivals is due to precipitation reactions that can result in the concentration leveling off at a value less than the injection concentration. Accounting for reductions in phosphate concentrations caused by precipitation reactions would result in a lower estimate of the retardation factor (i.e., a lower peak value yields a faster 50% arrival time). Retardation estimates for calcium are complicated by desorption of calcium from the sediments, yielding concentrations at the monitoring wells in excess of the injected values.

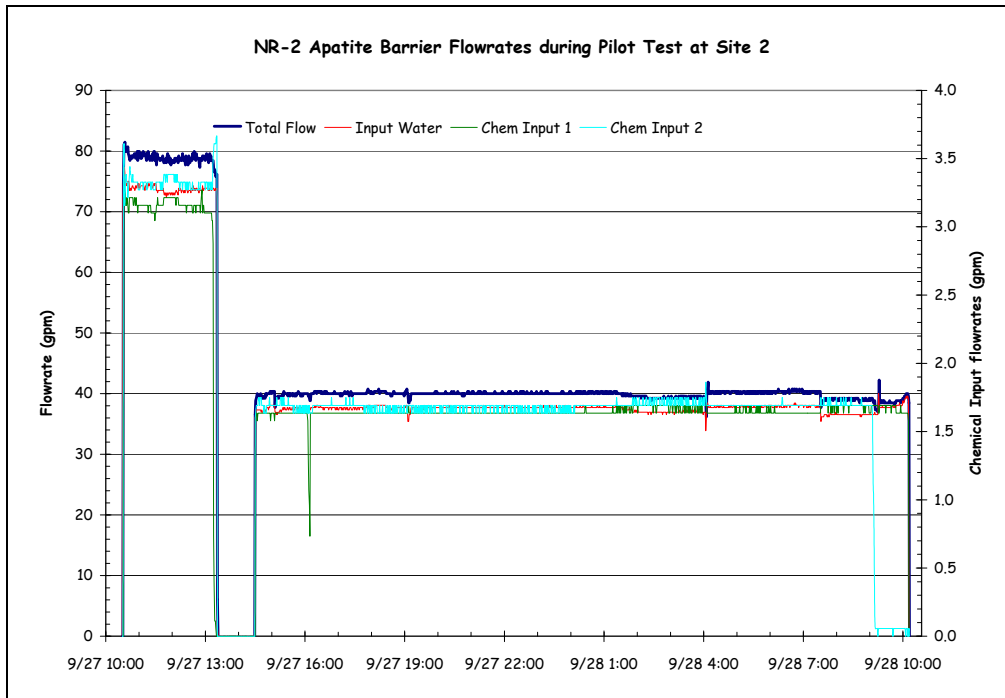


Figure 5.21. Apatite Pilot Test #2 (2006) Flow Rates. Chem input 1 = Mix 1 (Ca-citrate). Chem input 2 = Mix 2 (phosphate).

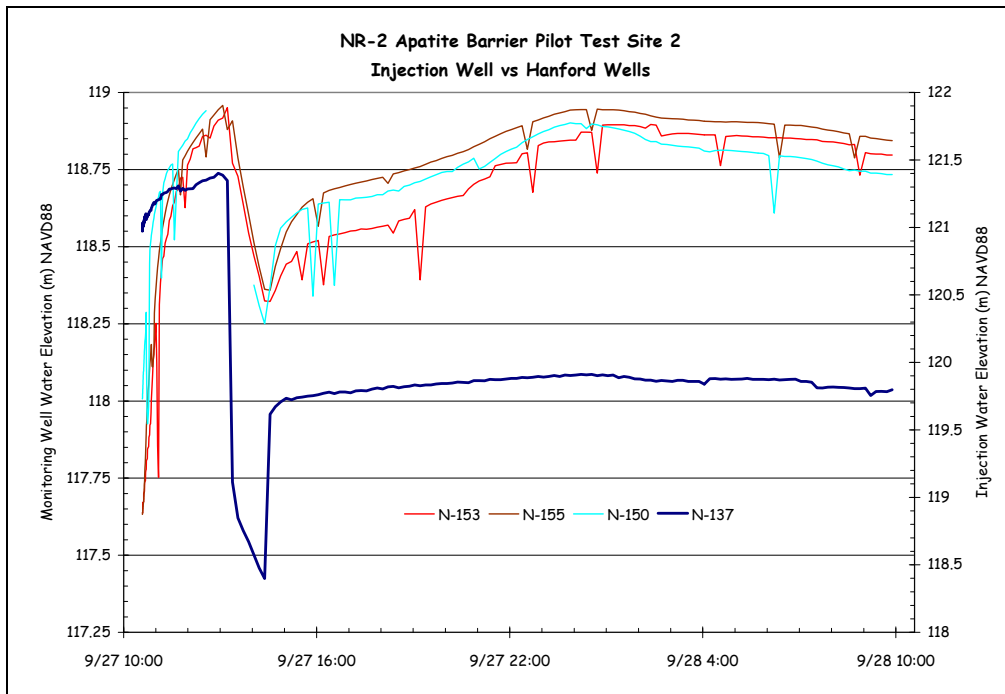


Figure 5.22. Water Level Monitoring in Hanford Formation Wells During Apatite Pilot Test #2 (2006). Prefix 199- omitted from well names.

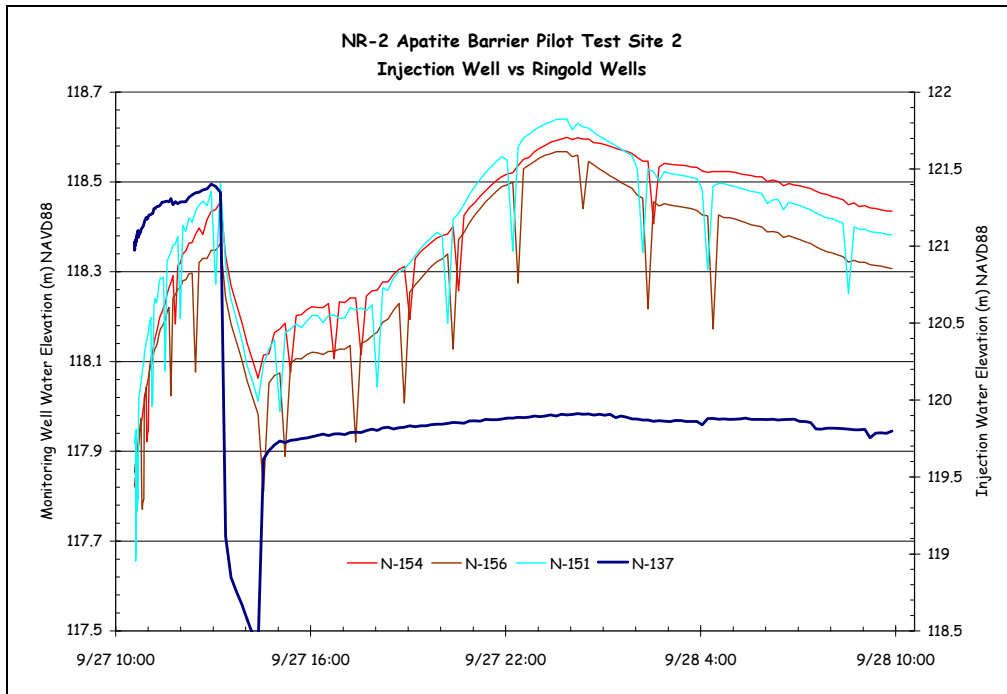


Figure 5.23. Water Level Monitoring in Ringold Formation Wells During Apatite Pilot Test #2 (2006). Prefix 199- omitted from well names.

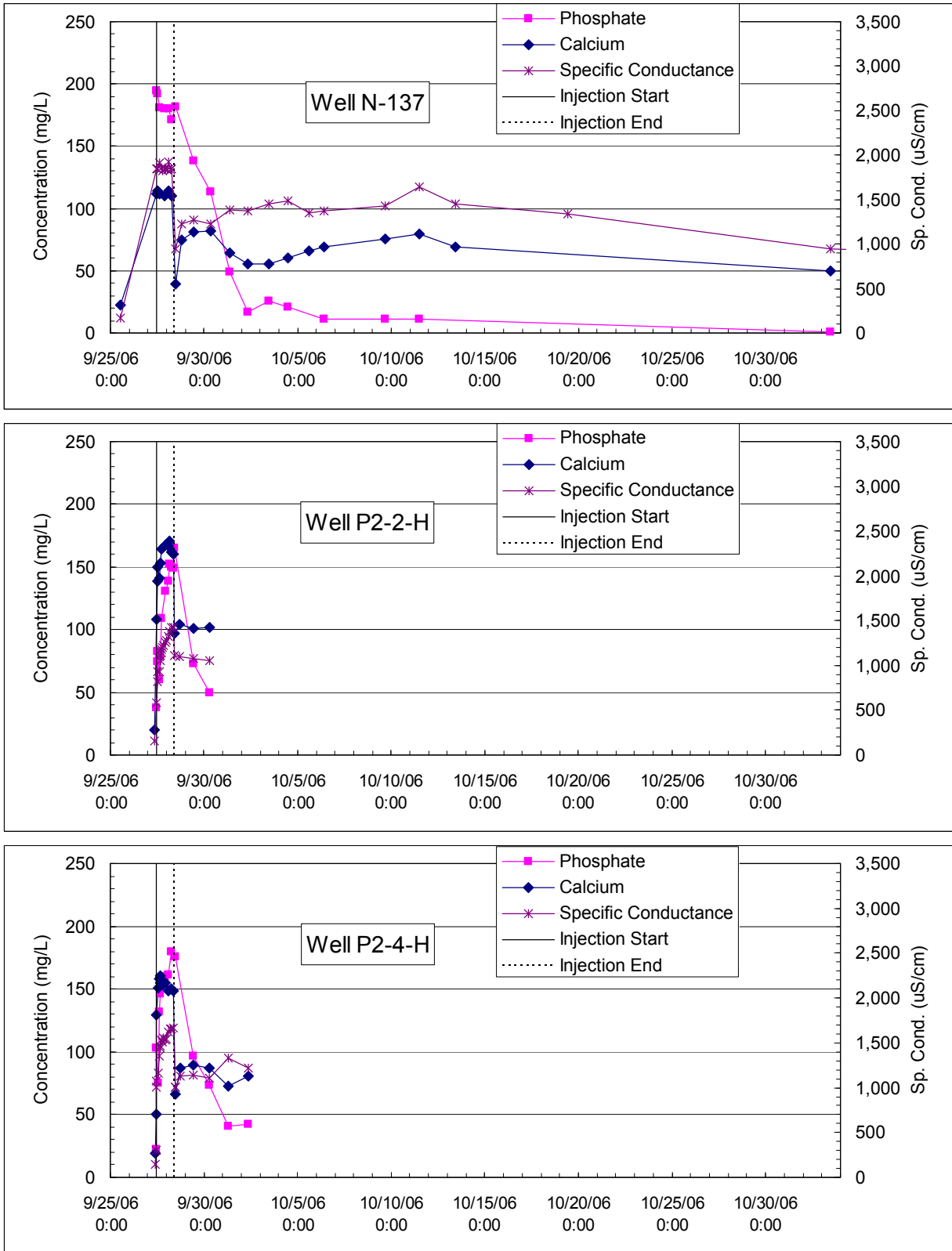


Figure 5.24. Apatite Pilot Test #2 Injection – Specific Conductance, PO₄, and Calcium Breakthrough Curves in Hanford Formation. Hanford formation wells went dry in late September/early October.

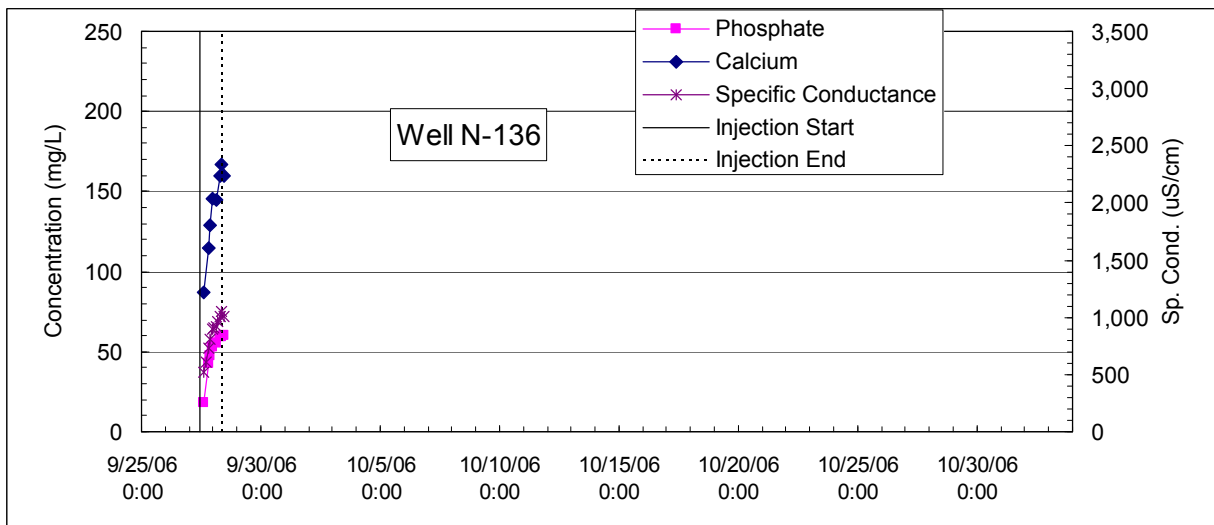
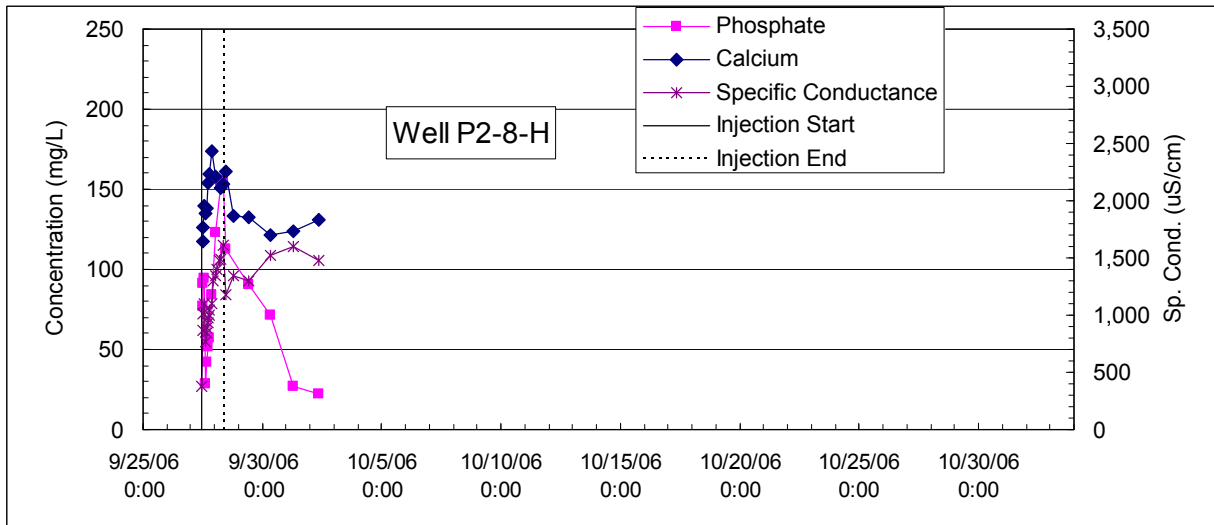
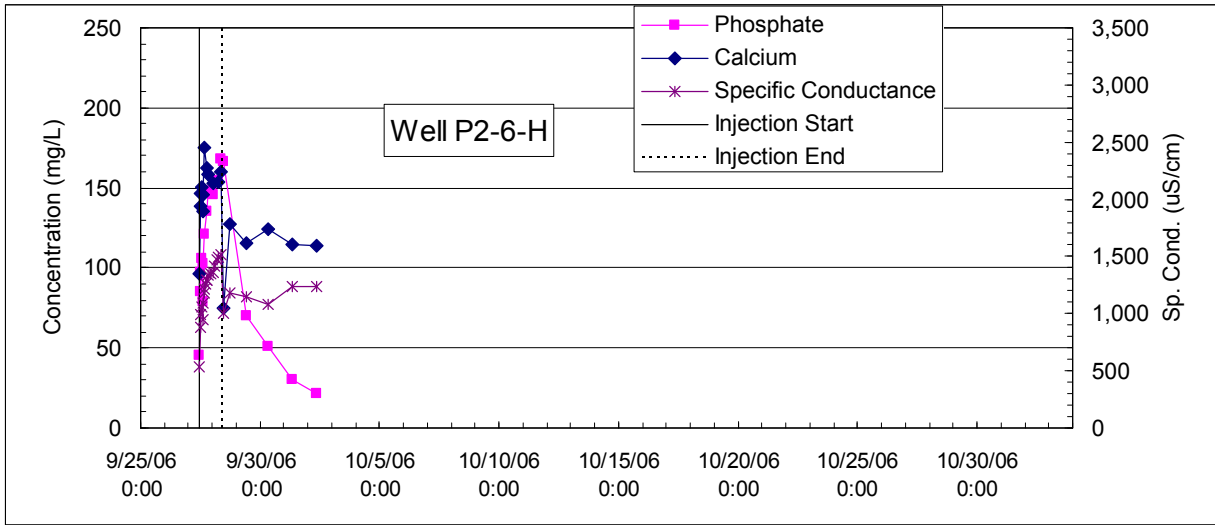


Figure 5.24. (contd)

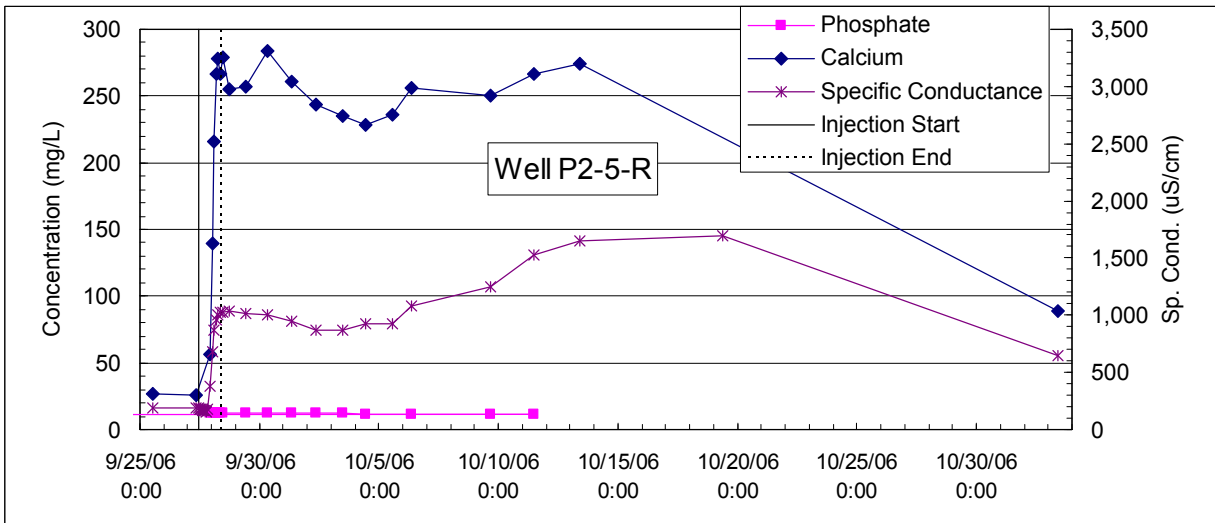
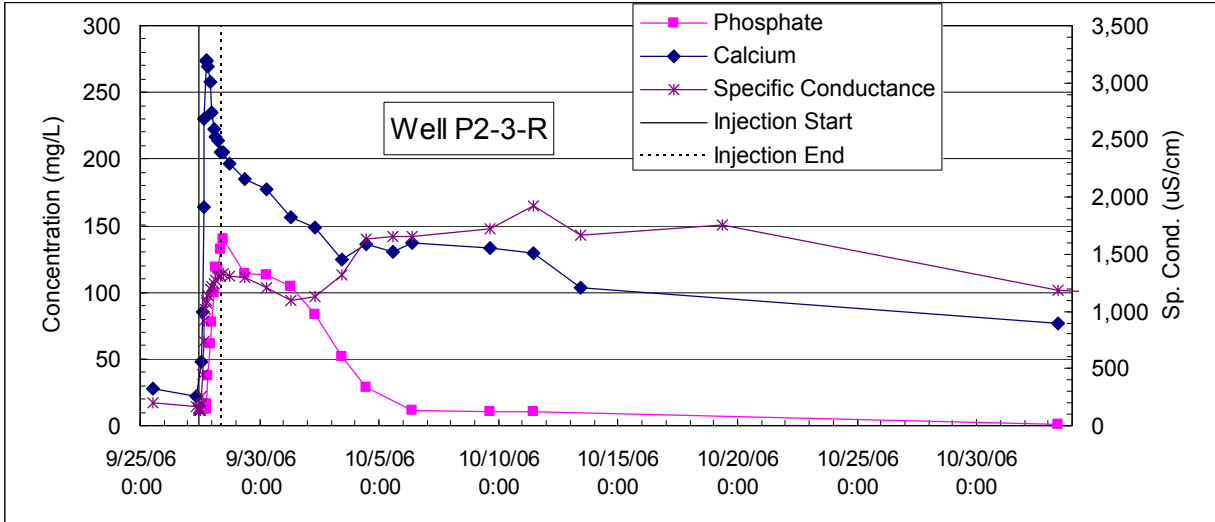
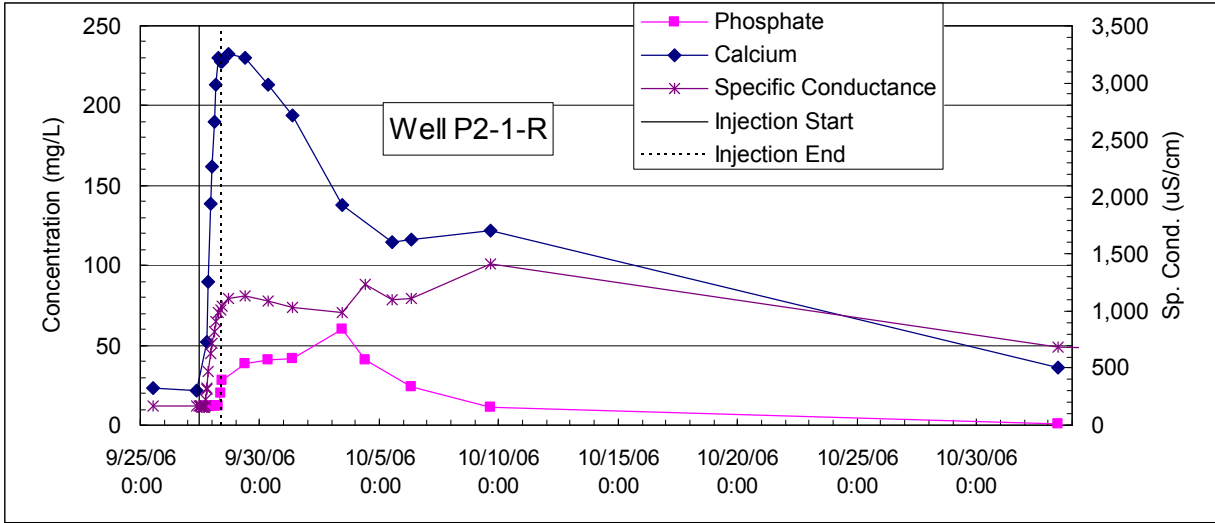


Figure 5.25. Apatite Pilot Test #2 Injection – Specific Conductance, PO₄, and Calcium Breakthrough Curves in Ringold Formation

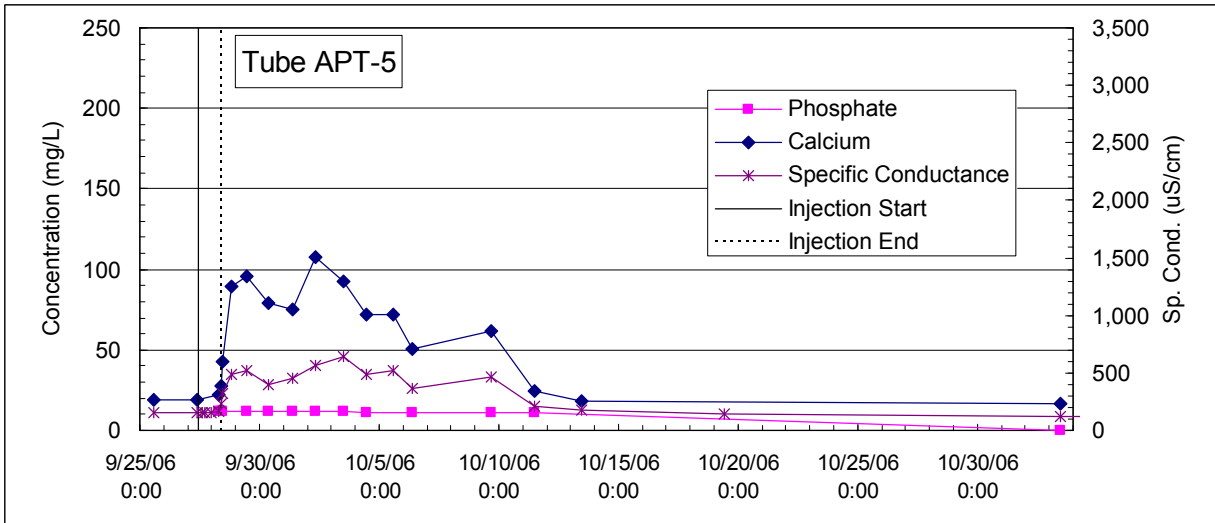
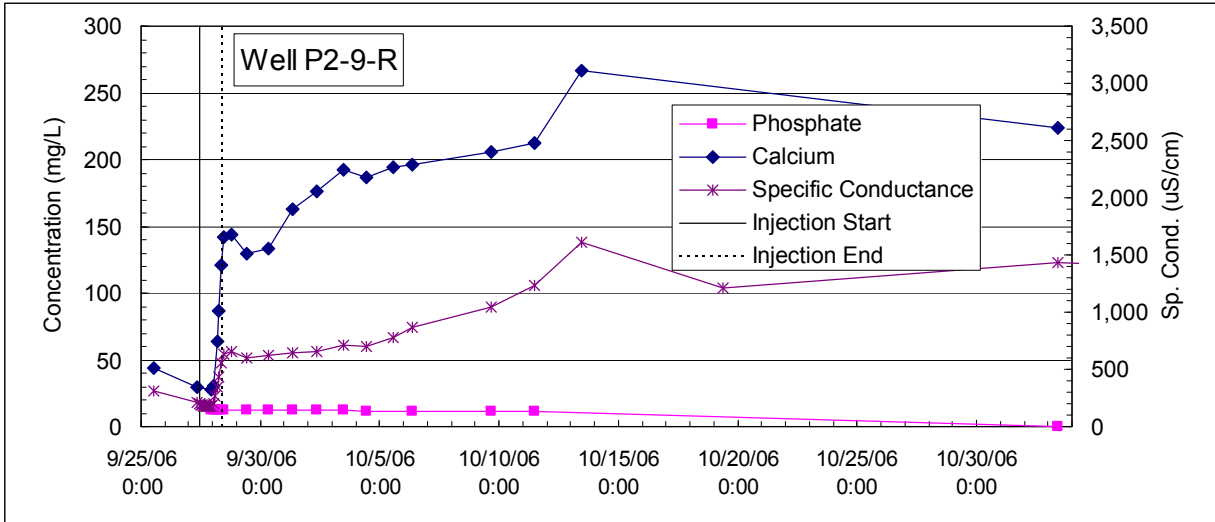
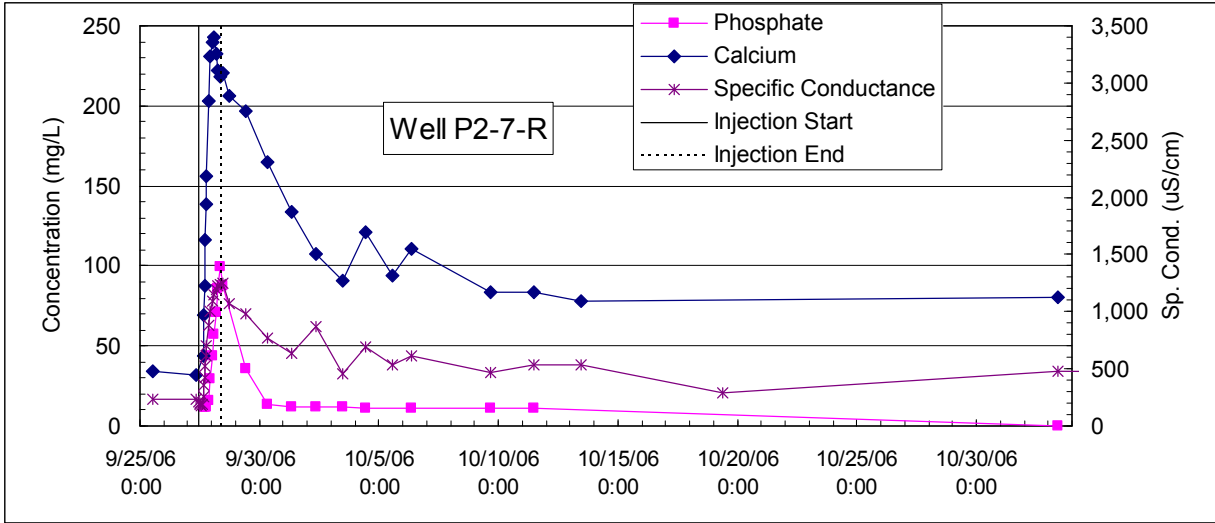


Figure 5.25. (contd)

Table 5.11. Summary of Phosphate and Specific Conductance in Selected Monitoring Wells for Pilot Test #2 Injection Test. Percentage of mean injection concentrations are shown in parentheses.

Apatite Project Well ID	End of Injection Next Sampling after 9/28/06 10:10		8 Days after Injection 10/6/06	
	SpC ($\mu\text{S}/\text{cm}$)	PO_4 (mg/L)	SpC ($\mu\text{S}/\text{cm}$)	PO_4 (mg/L)
199-N-137	943 (51%)	182 (99%)	1377 (74%)	<11 (6%)
P2-1-R	1040 (56%)	<28 (15%)	1112 (60%)	24 (13%)
P2-2-H	1111 (60%)	165 (90%)	Dry	Dry
P2-3-R	1326 (71%)	140 (77%)	1650 (89%)	12 (6%)
P2-4-H	1009 (54%)	176 (96%)	Dry	Dry
P2-5-R	1028 (55%)	<12 (7%)	1078 (58%)	<11 (6%)
P2-6-H	1004 (54%)	166 (91%)	Dry	Dry
P2-7-R	1243 (67%)	87 (48%)	611 (33%)	<11 (6%)
P2-8-H	1177 (63%)	113 (62%)	Dry	Dry
P2-9-R	638 (34%)	<12 (7%)	864 (47%)	<11 (6%)
APT-5	318 (17%)	<12 (7%)	363 (20%)	<11 (6%)
199-N-136	1004 (54%)	60 (33%)	N/A	N/A

5.3.3 Post-Injection Processes

Following the Ca-citrate- PO_4 injection, a number of important reactions occur as the plume drifts with the ambient groundwater flow (although with varying degrees of sorption as discussed in previous sections). The important reactions involve the biodegradation of citrate, which complexes with calcium, and the precipitation of amorphous Ca-phosphate phases. The biodegradation of citrate creates reducing conditions that lowers the ORP and DO.

Citrate concentrations following the injection are shown in Figures 5.26 and 5.27. These measurements show that citrate is mostly gone within 1 to 2 weeks following the injection. DO concentrations decrease rapidly after the injection within a few days to a week. Formate, a reaction product of citrate degradation, is measured above detection limits during the same time period (Figures 5.26 and 5.27).

Phosphate concentrations decrease faster than the decrease in SpC following the injection as shown in Figures 5.24 and 5.25. This faster decrease in phosphate relative to SpC is evidence of phosphate reactions occurring because SpC can be used as a gross indicator for injection plume drift. The relative decrease in phosphate and SpC, 8 days after the injection, is calculated in Table 5.11.

5.3.4 General Water Quality

Field parameters measured at pilot test site #2 are summarized for baseline conditions prior to the Ca-citrate- PO_4 injection, near the end of the injection, and approximately 1 month following the injection in Table 5.12. One month following the injection, SpC, and pH values are still elevated above baseline values with DO and ORP below baseline values.

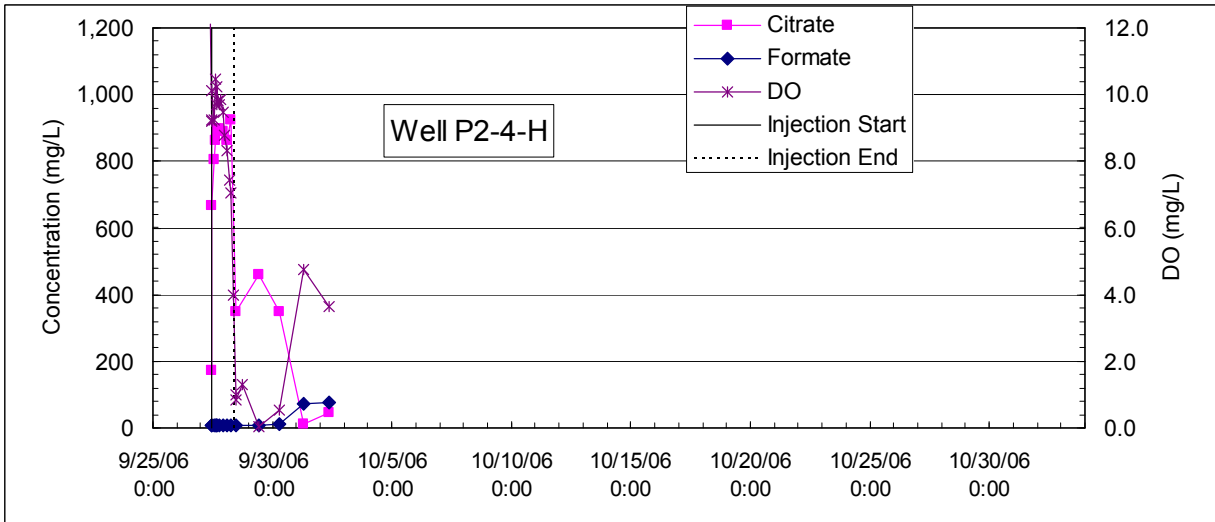
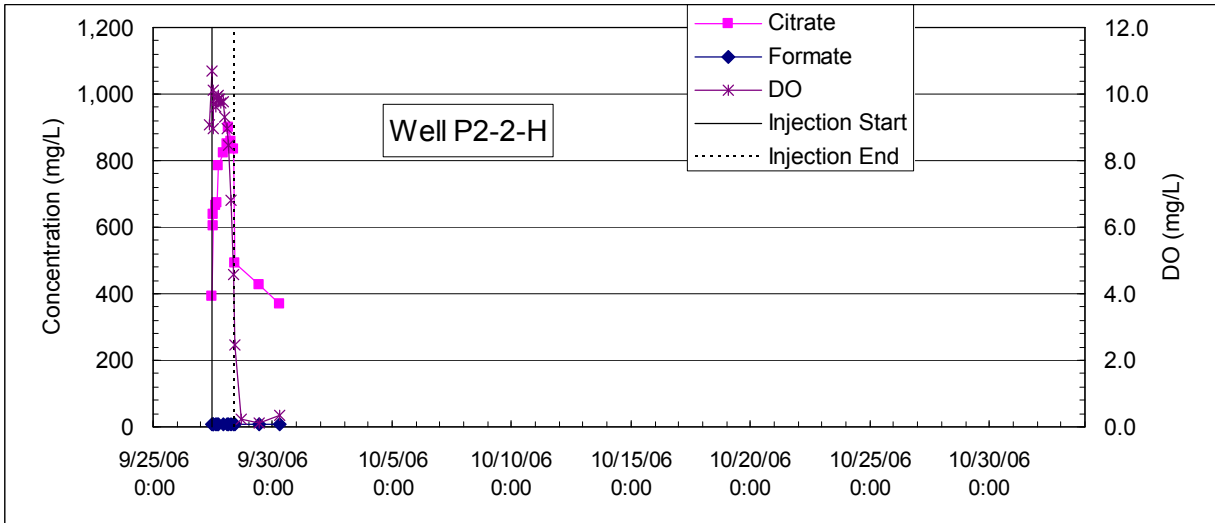
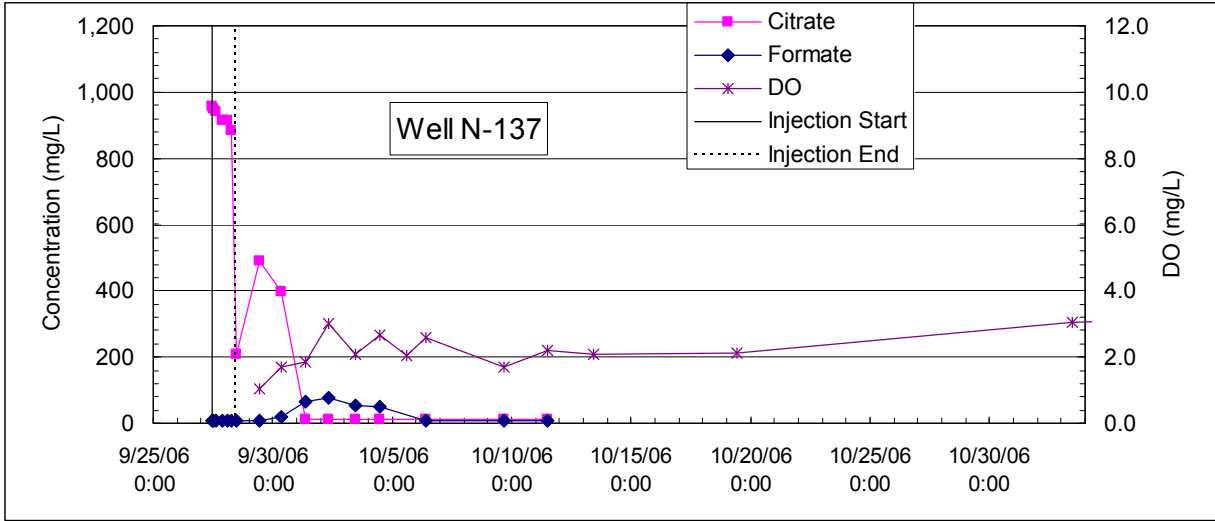


Figure 5.26. Apatite Pilot Test #2 Injection – Citrate, Formate, and Dissolved Oxygen Breakthrough Curves in Hanford Formation. Hanford wells were dry in late September/early October.

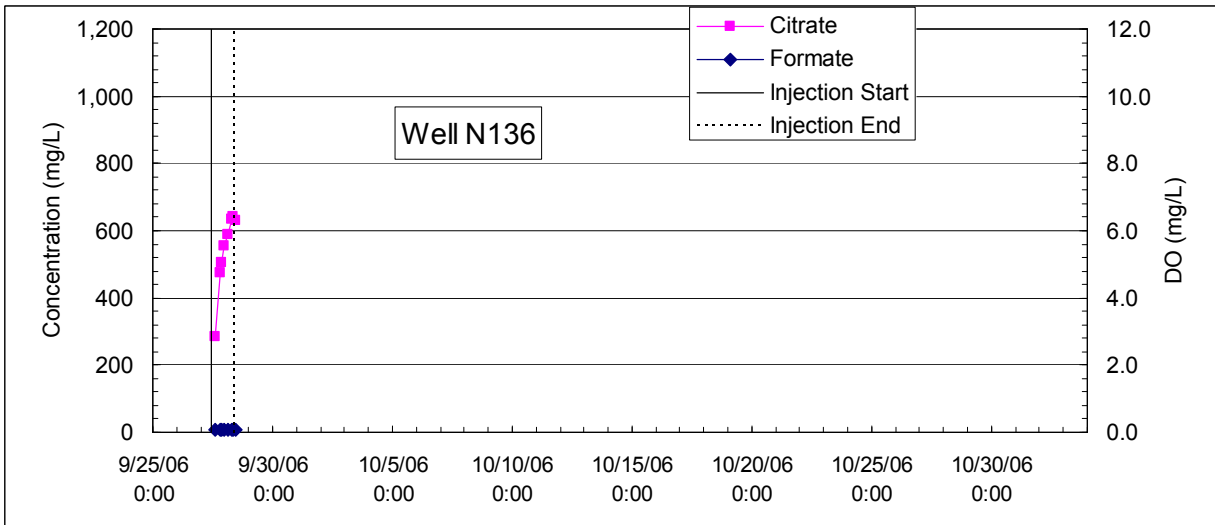
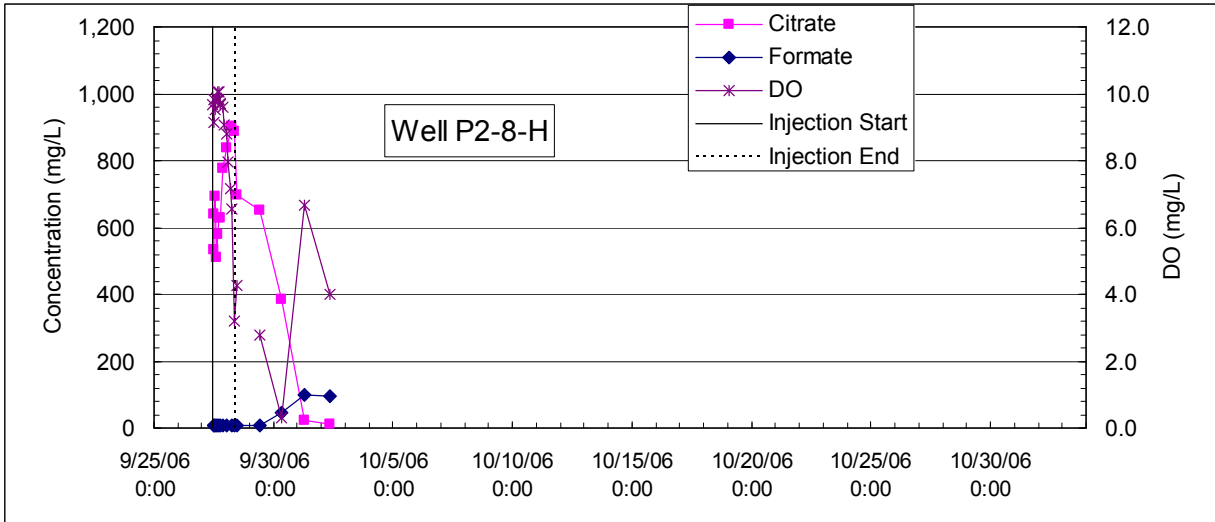
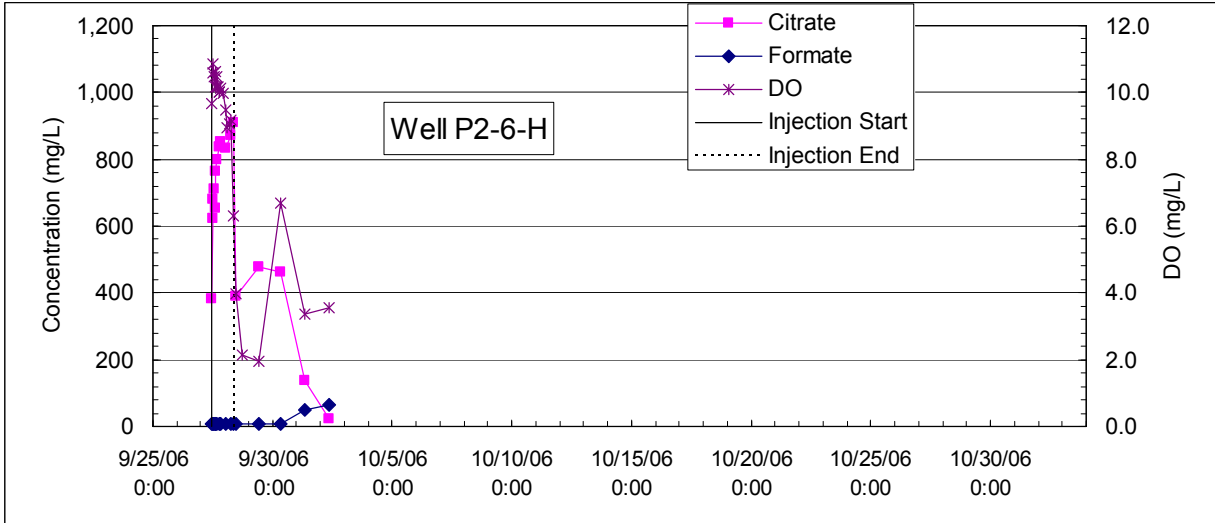


Figure 5.26. (contd)

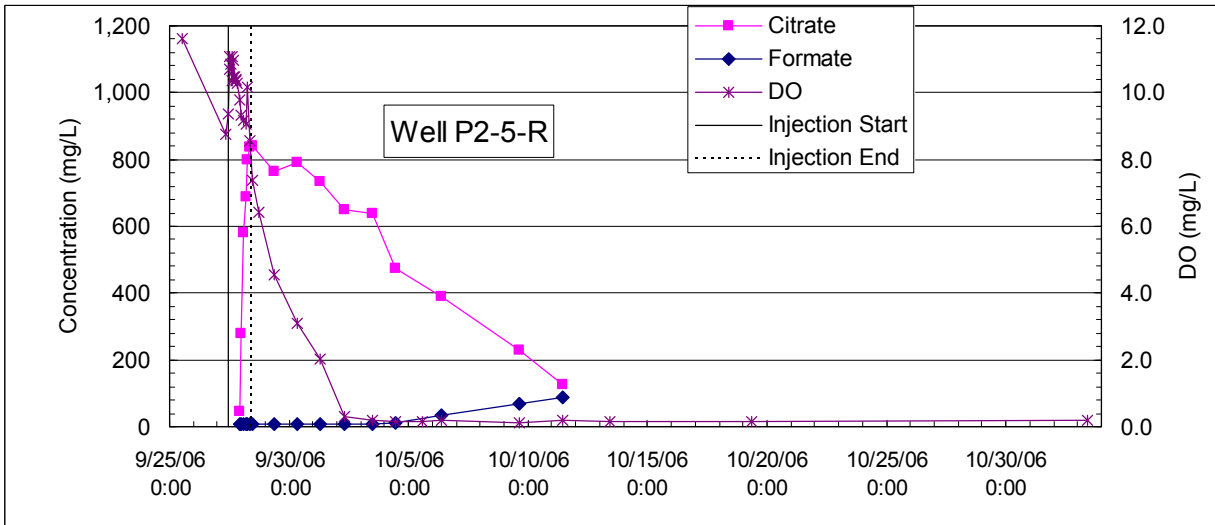
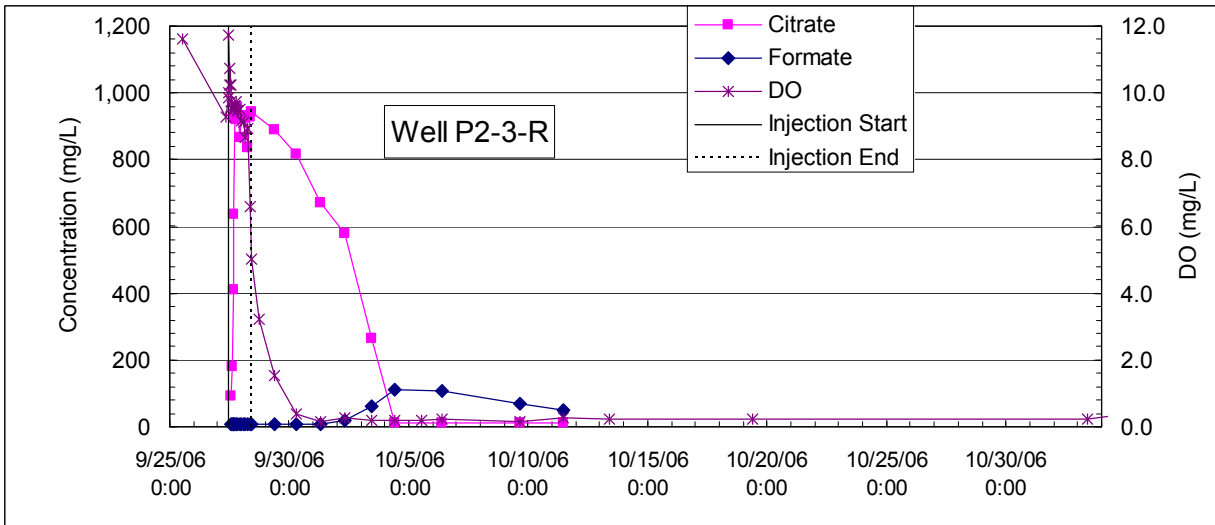
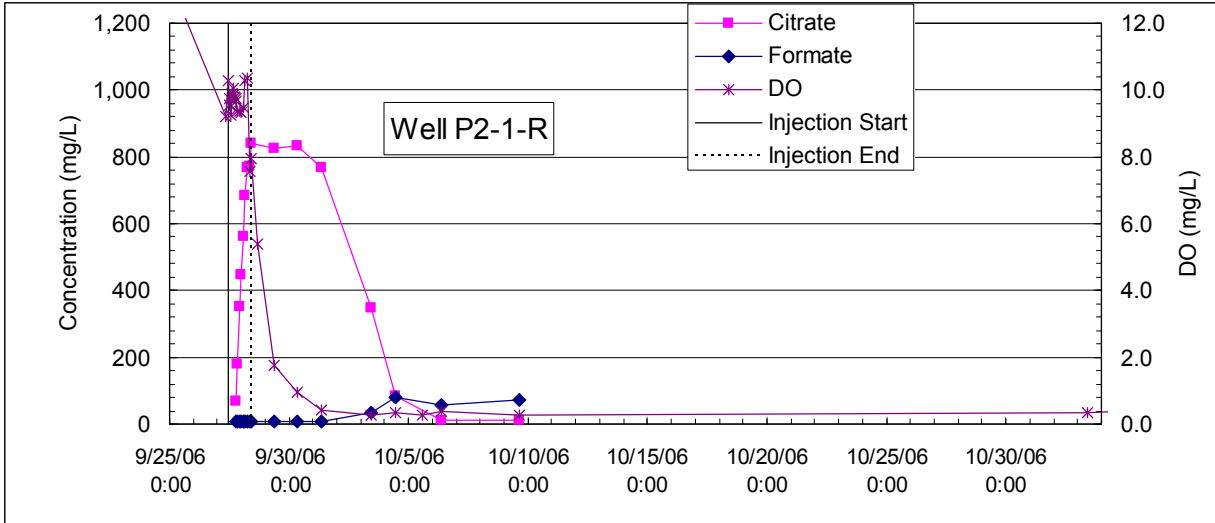


Figure 5.27. Apatite Pilot Test #2 Injection – Citrate, Formate, and Dissolved Oxygen Breakthrough Curves in Ringold Formation

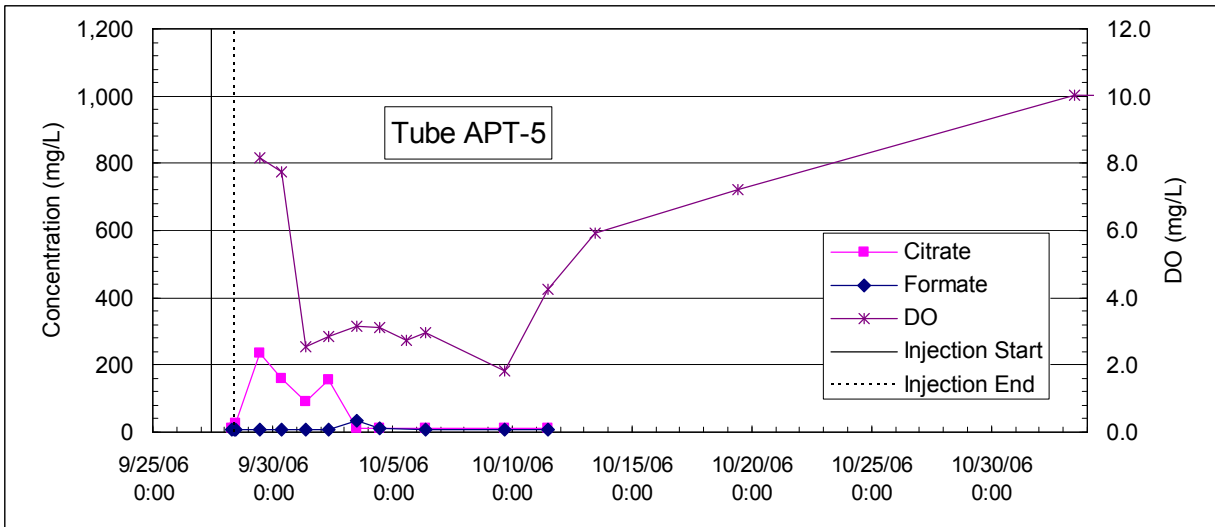
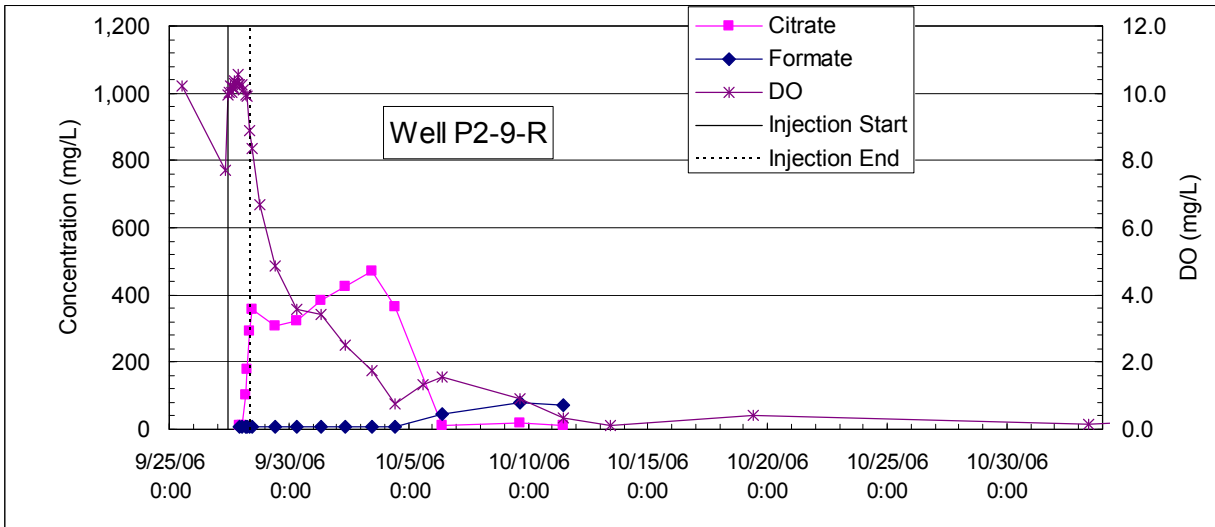
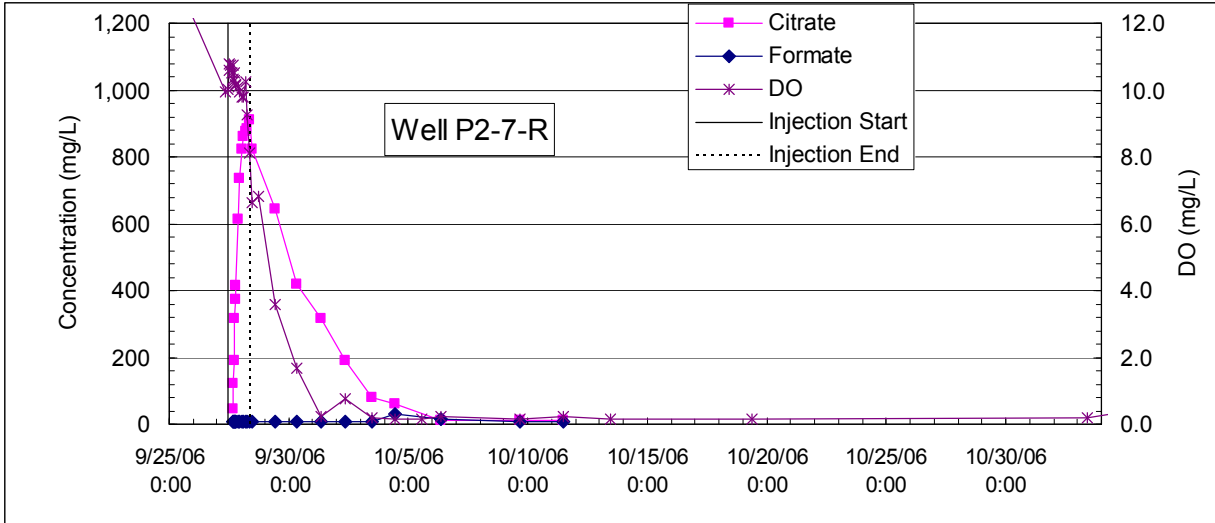


Figure 5.27. (contd)

Table 5.12. Summary of Field Parameters at Pilot Test #2 Injection Test Site. Monitoring wells are P2-2-H, P2-4-H, P2-1-R, P2-3-R, P2-5-R, P2-7-R, P2-9-R, and APT-5. Hanford formation wells were dry ~1 month after the injection.

Baseline Conditions	Field Parameters				
	SpC ($\mu\text{S}/\text{cm}$)	DO (mg/L)	ORP (mV)	Temp. ($^{\circ}\text{C}$)	pH
Minimum	146	7.7	55	14.37	6.62
Maximum	315	13	210	19.60	8.05
Average	192	10	122	16.05	7.57
<i>Conditions Near End of Injection</i>					
Minimum	232	4.0	144	14.70	7.36
Maximum	1670	8.9	182	18.70	7.95
Average	1058	6.9	163.4	16.75	7.64
<i>Conditions ~1 Month After Injection</i>					
Minimum	119	0.1	-194	12.38	7.76
Maximum	1431	10	46	16.83	8.77
Average	757	1.8	-122	15.41	8.33

Baseline measurements for selected anions were not measured prior to the test, but concentrations of phosphate, citrate, and formate were significantly reduced from injection concentrations 1 month after the test, as shown in Figures 5.26 and 5.27 and summarized in Table 5.13. Chloride concentrations were elevated by the injection solution (see Table 5.9) but were below drinking water standards (Table 5.13).

A summary of baseline and post-injection concentrations of trace metals is shown in Table 5.14. As noted above, biodegradation of citrate creates reducing conditions that causes an increase in redox-sensitive trace metals (i.e., aluminum, iron, and manganese). Concentrations of these trace metals remain elevated above baseline conditions 1 month after the test while the reducing conditions persist. Calcium and sodium concentrations, components of the injection solution as shown in Table 5.9, remain elevated at the site 1 month following the injection (see Table 5.14).

Assessment of baseline and post-injection measurements of this test are complicated by the monitoring wells in the Hanford formation that went dry shortly after the injection. Monitoring of the wells at pilot test site #2 is continuing with longer-term water quality results discussed in Section 8.0.

5.3.5 Strontium-90 Monitoring

Concentrations of ^{90}Sr increased at pilot test site #2 following the injection due to the increases in ionic strength and calcium from the Ca-citrate- PO_4 injection solution. The injection solution was revised for the September 2006 pilot test #2 after analysis of results from the June 2006 pilot test #1 (see Section 5.2.5) and additional laboratory analysis (see Section 2.6 and Table 2.3). Peak ^{90}Sr increases during pilot test #2 (see Table 5.15), relative to the mean baseline ^{90}Sr concentrations at the site, were significantly less than for pilot test #1. The mean peak ^{90}Sr increase at the site was 3.8 times the mean baseline concentrations, with a range of 0.7 to 9.2 times the baseline, and occurred within a month of the September 2006 Ca-citrate- PO_4 injection. Laboratory one-dimensional columns indicated strontium and calcium should peak at ~5 times groundwater concentration with this injection formulation. Concentrations of ^{90}Sr and $^{89/90}\text{Sr}$ at selected monitoring wells at the test site are shown in Figure 5.29. This figure shows the measurements prior to the February/March 2007 injections at the treatability test site, along with a baseline ^{90}Sr range around the 199-N-137 injection well (see Section 8.0 for a discussion on the determination of the baseline ^{90}Sr range at the treatability test site).

Table 5.13. Summary of Selected Anions at Pilot Test #2 Injection Test Site. Note: baseline anions were not measured at pilot test site #2. Monitoring wells are P2-2-H, P2-4-H, P2-1-R, P2-3-R, P2-5-R, P2-7-R, P2-9-R, and APT-5. Hanford formation wells were dry ~1 month after the injection.

Conditions Near End of Injection	Anions			
	Chloride (mg/L)	Formate (mg/L)	PO ₄ (mg/L)	Citrate (mg/L)
Minimum	20.1	<7.0	<12.0	<10.0
Maximum	182	<7.0	180	926
Average	142	<7.0	77.0	689
<i>Conditions 1 Month After Injection</i>				
Minimum	1.3	NA	<0.14	NA
Maximum	140	NA	3.5	NA
Average	62	NA	1.3	NA
Drinking Water Standard	250	--	--	--
NA = Not applicable.				

Table 5.14. Summary of Selected Metals and ⁹⁰Sr at Pilot Test #2 Injection Test Site. Monitoring wells are P2-2-H, P2-4-H, P2-1-R, P2-3-R, P2-5-R, P2-7-R, P2-9-R, and APT-5. Hanford formation wells were dry ~1 month after the injection.

Baseline Conditions	Metals					
	Al (mg/L)	Ca (mg/L)	Fe (mg/L)	Mn (mg/L)	Na (mg/L)	⁹⁰ Sr (pCi/L)
Minimum	<0.040	18.9	0.004	0.006	2.00	605
Maximum	<0.074	43.3	0.017	0.085	2.90	1900
Average	<0.042	26.0	0.007	0.041	2.39	1176
<i>Conditions Near End of Injection</i>						
Minimum	<0.500	28.0	0.006	0.017	2.69	NA
Maximum	9.00	266	0.807	0.412	378	NA
Average	4.43	172	0.324	0.179	176	NA
<i>Conditions ~1 Month After Injection</i>						
Minimum	<0.037	17.0	0.033	0.013	5.0	440
Maximum	<0.037	224	0.63	6.0	217	5800
Average	<0.037	87.2	0.19	3.1	79	2690
Drinking Water Standard	0.05 to 0.2 Secondary	--	0.3 Secondary	0.05 Secondary	--	8
NA = Not applicable.						

Table 5.15. Summary of Baseline and Peak ⁹⁰Sr Concentrations After Injections at Pilot Test Site #2 (199-N-137)

Well	Baseline		9/27/06 N-137 Inject Formula 2 (2,5,2.4) Post Inj Peak		3/20/2007 N-137 Inject Formula 3 (1,2.5,10) Post Inj Peak		Ratios			
	Sr pCi/L	Date	Sr pCi/L	Date	Sr pCi/L	Date	Formula 2 Peak / Mean Baseline	Formula 2 Peak / Baseline	Formula 3 Peak / Mean Baseline	Formula 3 Peak / Baseline
N-137	1,842	9/25/2006	4,002	10/27/2006	500	8/10/2007	3.25	2.17	0.41	0.27
N-147	1,220	9/18/2006	942	2/15/2007	3,000	3/23/2007	0.77	0.77	2.44	2.46
APT-5	932	9/25/2006	2,657	10/5/2006	1,100	10/19/2007	2.16	2.85	0.89	1.18
P2-1-R	1,857	9/27/2006	11,320	9/28/2006	6,800	4/6/2007 ^a	9.20	6.10	5.53	3.66
P2-2-H	605	9/27/2006	1,804	9/28/2006			1.47	2.98		
P2-3-R	1,900	9/25/2006	8,800	10/19/2006	3,800	3/23/2007	7.16	4.63	3.09	2.00
P2-4-H	867	9/27/2006	1,768	9/28/2006			1.44	2.04		
P2-5-R	728	9/25/2006	4,574	10/13/2006	2,600	3/26/2007	3.72	6.28	2.11	3.57
P2-6-H			5,050	9/28/2006			4.11			
P2-7-R	1,295	9/25/2006	4,330	9/28/2006	2,200	8/23/2007	3.52	3.34	1.79	1.70
P2-8-H			3,535	9/28/2006			2.87			
P2-9-R	1,053	9/25/2006	6,721	10/13/2006	2,900	8/23/2007	5.46	6.38	2.36	2.75
Mean	1,230		4,625		2,863		3.76	3.76	2.33	2.20

Color Key

Sr-90

WSCF - Total beta radiostrontium

^aData Flagged with F Qualifier

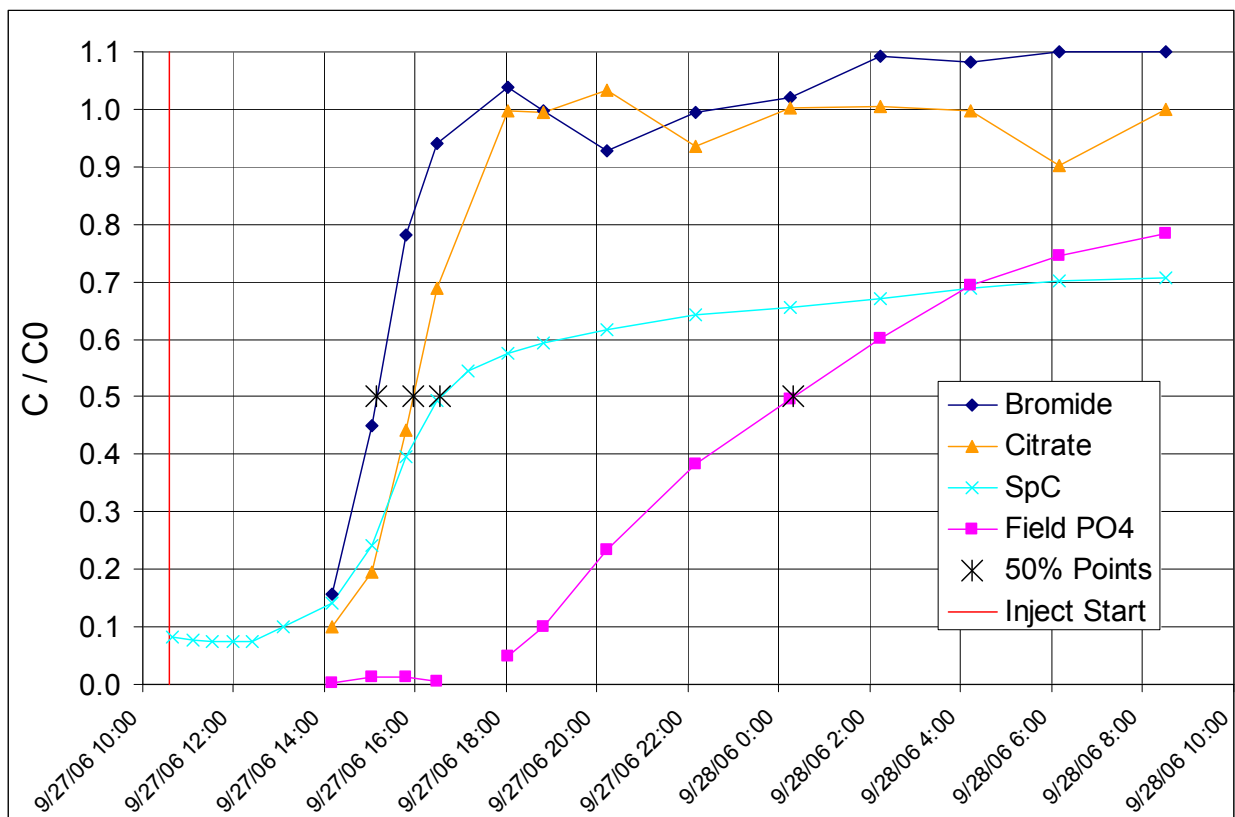


Figure 5.28. Normalized Breakthrough Curves for Well P2-R-3

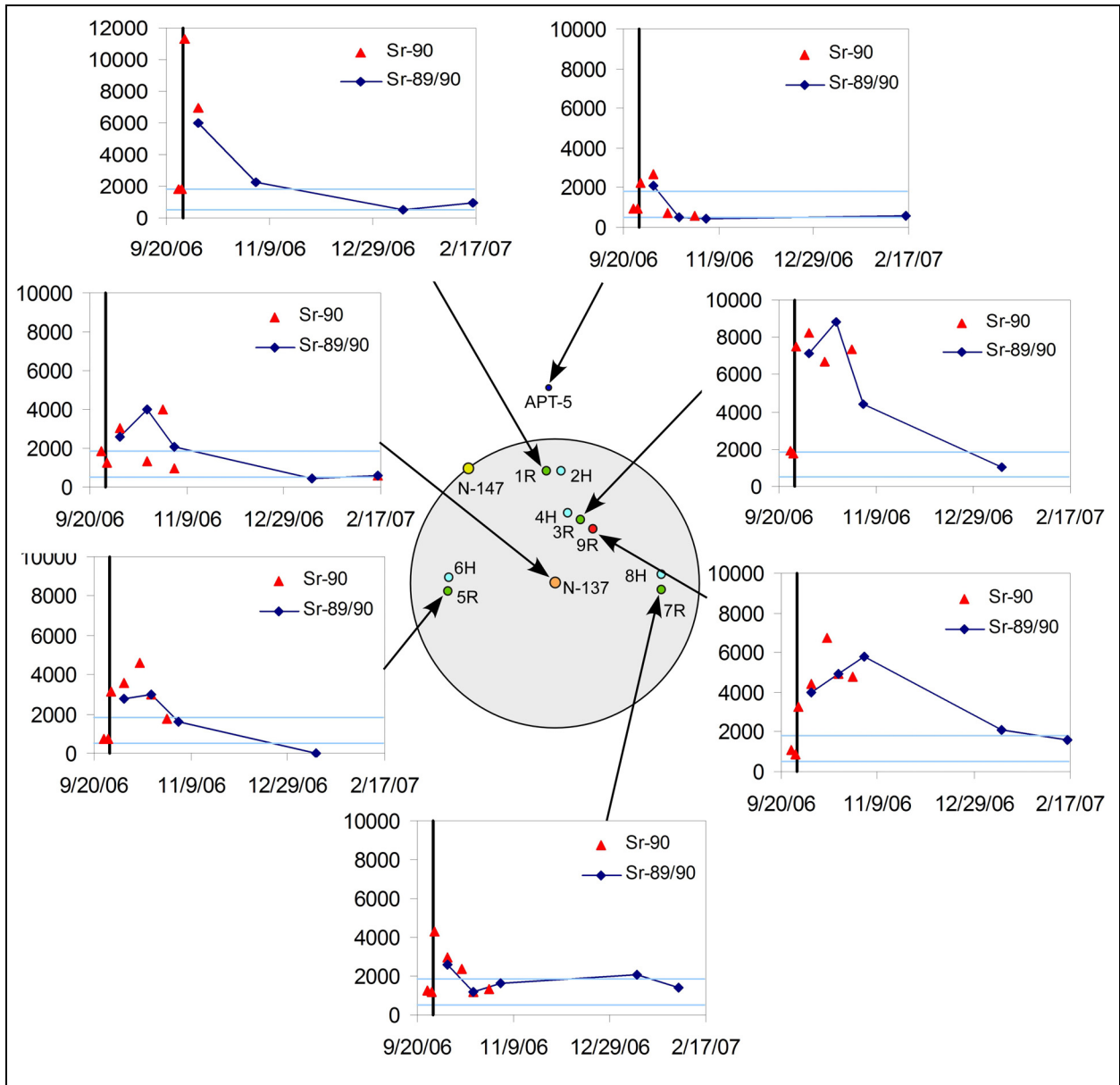


Figure 5.29. ^{90}Sr measurements (pCi/L) following September 2006 Pilot Test #2. Vertical line denotes injection timing and horizontal lines represent the estimated minimum and maximum baseline concentrations at the pilot test site (see Section 8.0).

Table 5.15 also shows the short-term ^{90}Sr monitoring results at pilot test site #2 following the March 20, 2007, injection during high-river stage conditions. The Ca-citrate- PO_4 injection formulation was revised again for this injection with further reductions in the calcium and citrate concentrations and an increase in the phosphate concentration. As shown in Table 5.15, peak ^{90}Sr concentrations following the March 2007 injection were less than the peak observed after the September 2006 injection. These differences can be attributed to the change in the injection concentrations and potential effects of apatite formation from the first injection at the test site. Longer-term monitoring at the site is discussed in Section 8.0.

6.0 Design Analysis for Barrier Installation

This section describes the design analysis approach for low-concentration Ca-citrate-PO₄ solution injections for the initial formation of a 91-m (300-ft) PRB. The 100-N Area apatite barrier design involves determining injection timing, injection volumes, and rates required to create a continuous barrier for an injection well spacing of 9.1 m (30 ft) (Figure 1.10). The primary basis for the emplacement design is from measurements collected during the injections at the two pilot test sites located at opposite ends of the barrier. Numerical models were used for guidance during design of these pilot tests and to explore other emplacement options.

6.1 Design Objectives and Considerations

The treatability test design provides operational specifications for the injection and monitoring wells, including injection volumes, injection rates, reaction period duration, and the sampling/analysis requirements. The targeted treatment zone and the injection well screens span two different hydrostratigraphic units: the higher permeability Hanford formation in the upper portion of the treatment zone, and the lower permeability Ringold Formation in the lower portion of the treatment zone. Injection timing is important relative to the Columbia River stage for two reasons: 1) injections conducted during high-river stage conditions provides for treatment of Hanford formation sediments, which is the most contaminated portion of the profile (see Figure 1.9); and 2) injections conducted during low-river stage conditions target treatment in the lower portion of the treatment zone within the lower-permeability Ringold Formation.

The overlapping injection design schematic is shown in Figure 6.1, which requires significant injection concentrations (i.e., >50%) at a radial distance of 6.1 m (20 ft) from the injection wells to provide adequate coverage. This overlap was specified to provide for a minimum barrier width and to reduce the chances of gaps in the barrier between the injection wells. The injection volumes are important in achieving this overlap with fixed 9.1-m (30-ft) spacing between the injection wells. While larger injection volumes will provide for better coverage, factors to be considered for the injection volumes are cost and operational time. In addition to efficiency, with the immediate proximity of the apatite treatability test to the Columbia River, the potential exists for reagent and reaction products to enter the river. This is particularly true for treatment of the Hanford formation, with its higher relative groundwater velocities, at low-river stage when the gradients are directed toward the river. Heterogeneities in the formations can also create highly conductive channels toward the river.

Injection rates in the design were initially specified to be as high as practical under the field conditions to reduce the injection time requirements, and to potentially override any kinetic sorption rates that could limit the radial extent of phosphate. As discussed in more detail (Section 6.2), injection rates were lowered for injections targeting the lower portion of the treatment zone during low-river stage conditions on the downstream portion of the barrier to minimize injection mounding in the upper, more permeable, portion of the treatment.

Following the Ca-citrate-PO₄ injection, up to 2 weeks is required for citrate degradation to occur and amorphous Ca-phosphate phase precipitate to form based on bench-scale laboratory studies. During this period, the injected reagent plume drifts with the ambient groundwater flow. The timing of the injections relative to the river stage is important in determining the direction and amount of plume drift that occurs.

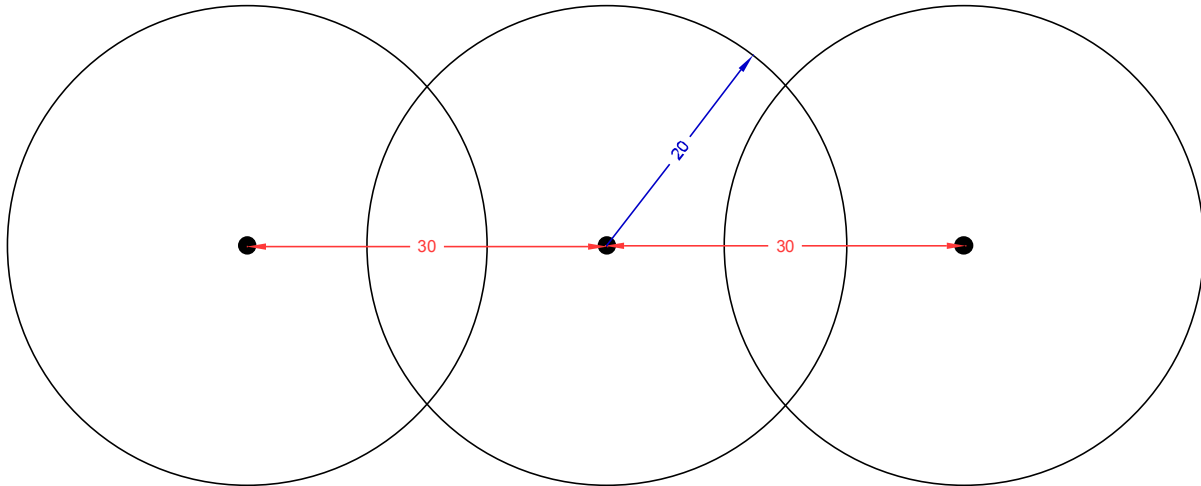


Figure 6.1. Well Spacing and Plume Overlap Design for 100-N Area Apatite Barrier (lengths in ft)

Timing of the injection relative to river stage conditions is also a critical factor for treating the targeted portion of the aquifer because of the strong influence of the river stage on the water table elevation, and the groundwater flow directions and velocities. The river stage is very dynamic, with large hourly, daily, weekly, and seasonal variations. Injections during periods of relatively high-river stage will enable treatment of the upper portion of the aquifer. Injections during low-river stage target the Ringold Formation with less reagent loss to the upper, more permeable, Hanford formation. Although the timing and extent of the large seasonal variations in the Columbia River stage changes from year to year depending on weather conditions and dam operations, hourly measurements from the RS-1 river stage recorder at the 100-N Area for the years 1994 through 2004 show a high-river stage season typically from April to July and a low-river stage season typically from September to November (Figure 6.2). During seasonal high-river stage conditions, groundwater flow is predominantly directed inland. Groundwater flow is predominantly directed toward the river during low-river stage conditions.

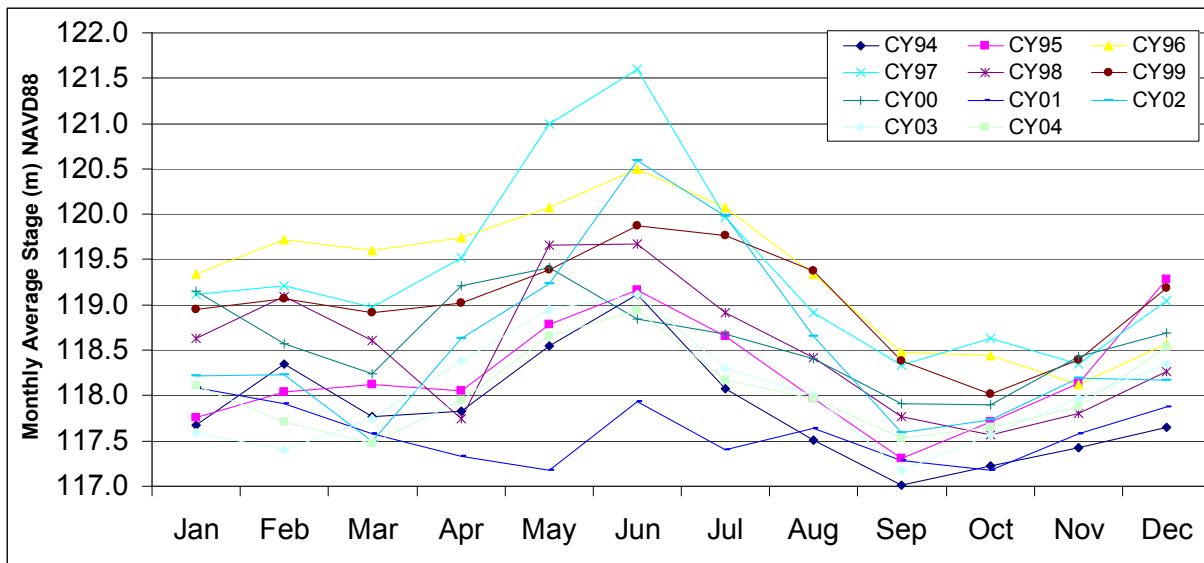


Figure 6.2. Monthly Average River Stage at 100-N Area from RS-1 for 1994 to 2004. Averages were calculated from hourly measurements; elevations are NAVD 1988 Datum.

Numerical models for the 100-N Area pilot test sites were developed, as described in Section 6.2, and continue to be refined based on results from bench- and field-scale testing activities. These models have been used to assist in the determination of operational parameters for the injections, aid in the interpretation of the field test operational results, and estimate hydraulic properties. Numerical models are used for estimating hydraulic properties because the application of standard analytical methods based on type curve matching techniques are problematic at the 100-N Area treatability test site because of continuous river stage fluctuations and injection wells that are screened across multiple hydrostratigraphic layers (i.e., Hanford and partial Ringold Formation). In addition to aiding in the injection operational parameters (i.e., volumes, rates), a preliminary evaluation of hydraulic properties was conducted based on numerical model fits of field test data collected to date. As part of the injection design analysis for the upcoming high-concentration barrier injection, this preliminary evaluation will be revisited and data collected at the end of the high-concentration Ca-citrate-PO₄ injections planned to start in 2008 will be used to determine whether the apatite formation process caused any changes in aquifer permeability. Pressures and arrival data collected during the various injection operations will be compared to assess any changes in permeability associated with emplacement of the apatite PRB.

The design analysis approach, which evolved during the treatability testing lifecycle, can be divided into three distinct periods. The first period involved preinjection design for determining volumes and rates for conducting the tracer test and the first Ca-citrate-PO₄ injections at the two pilot test sites in 2006. The second design period incorporated results from the pilot field tests into numerical models that were used to refine the injection design for low- and high-river stage barrier emplacement injections (initial low-concentration treatment only) during early 2007. Lastly, analysis of these injection results were used for refining the design and developing recommendations for the high-concentration Ca-citrate-PO₄ injections planned for 2008. These analyses are described in the following sections.

6.2 Pre-Pilot Test Injection Design

Previous unpublished numerical modeling studies were conducted that capture the dynamics of the near-river setting at the 100-N Area.¹ These simulations used the STOMP computer code, which was developed by PNNL for simulating subsurface flow and transport in the aquifer and vadose zone (White and Oostrom 2000, 2006). Initial simulations for designing the tracer and pilot test #1 used the 100-N Area cross-section model developed in these earlier studies with the material properties (hydraulic conductivity, porosity, dispersivity, and soil characteristics).¹ Tracer pulses were simulated along the road with this two-dimensional, cross-section model at different river stages to investigate plume drift near the river. Preliminary results from these efforts are described in DOE/RL (2006). As described in Section 6.2.1, these simulations were updated to reflect revised topography, geology, and material properties based on the site characterization activities that were conducted as part of this treatability test and the Remediation Closure and Science Project. One significant difference resulting from inclusion of this new site characterization data is the much lower hydraulic conductivity values for the Hanford formation compared to the values used in the earlier modeling studies.

¹ Connelly MP, CR Cole, and MD Williams. 1997. *Bank Storage Modeling at the 100-N Area*. Pacific Northwest National Laboratory for CH2M HILL Hanford Group, Richland, Washington.

Connelly MP. 1999. *Groundwater-River Interaction in the Near River Environment at the 100-N Area*. Innovative Treatment and Remediation Demonstration Program, HydroGeoLogic, Reston, Virginia.

Connelly MP. 2001. *Strontium-90 Transport in the Near-River Environment at the 100-N Area*. Innovative Treatment and Remediation Demonstration Program, HydroGeoLogic, Reston, Virginia.

6.2.1 Tracer Test Injection Design at Pilot Test Site # 1

Following well installation and baseline sampling at pilot test site #1, a NaBr tracer test was conducted at the site (described in Section 5.1) to determine injection volumes required for the low-concentration Ca-citrate-PO₄ injection, test the field injection equipment, and refine sampling procedures. This test was conducted at relatively high-river stage conditions in May 2006 (see Figures 5.1 and 5.2). The injection volume for this test was estimated based on the aquifer thickness and porosity estimates for both the Hanford formation and upper portion of the Ringold Formation that is screened by the injection well (i.e., the screened interval of the injection well; see Figure 4.2), as required to achieve sufficient concentrations at a 6.1-m (20-ft) radial extent. The entire thickness of the Hanford formation at the site was used from the bottom of the road fill to the Hanford/Ringold formation contact. These volume estimates are shown in Table 6.1 for various radial distances. An analytic solution for radial transport in a homogeneous and isotropic aquifer (Hoopes and Harleman 1967), as described in Section 5.2, was also used to help determine sample collection frequency during the test.

Table 6.1. Injection Volume Estimates for Tracer Test Planning

		radius (ft):	5	10	15	20	25	30
		radius (m):	1.52	3.05	4.57	6.10	7.62	9.14
Pilot #1 Test Site	Aquifer Thickness (m)	porosity	Volume (gal)					
Hanford - High river stage (road fill to H/R contact)	3.1	0.24	1,434	5,736	12,907	22,946	35,853	51,628
Ringold (H/R contact to bottom of Injection Well)	1.77	0.18	614	2,456	5,527	9,826	15,353	22,108
Total Volume			2,048	8,193	18,434	32,772	51,206	73,736

Based on these estimates, a ~110,000-L (~30,000-gal) injection volume was specified for the tracer test. Field screening of bromide concentrations conducted during the test in the site trailer, as described in detail in Section 5.1, showed this injection volume was not achieving significant tracer arrivals in many of the monitoring wells; therefore, the test was extended with an additional volume of river water to push the tracer plume out farther radially (see Table 5.1). Heterogeneities at the pilot test site #1 had a large impact of the tracer arrivals with very quick tracer arrivals detected in monitoring wells in the inland direction and much slower arrivals toward the Columbia River and in the downstream direction. The final injection volume for the tracer test, including the extended river water, was 150,000 L (40,000 gal). Analysis of the preliminary test results showed this injection volume was insufficient for adequate coverage and that a larger volume would be required for the low-concentration Ca-citrate-PO₄ injection.

6.2.2 Volume Estimate for Pilot Test Site #1 Ca-Citrate-PO₄ Injection

Shortly after the tracer injection test at pilot test site #1, the first low-concentration Ca-citrate-PO₄ injection was planned for the pilot test site #1 later in May 2006 during high-river stage conductions. Analysis of the preliminary tracer test results showed relatively low tracer concentrations at the 4.6-m (15-ft) radial distance well pair in the downstream direction (P-7-R and P-8-H) and the 6.1-m (20-ft) radial distance well pair toward the river (P-1-R and P-2-H). Final results of this test, using laboratory

analysis of aqueous samples collected during the test, are shown in Figures 5.4 and 5.5. These slower responses were offset by much faster responses in the inland direction in the Hanford formation (P-6-H).

The injection volume used in the tracer test was significantly increased for the first pilot test Ca-citrate-PO₄ injection to ensure adequate reagent was injected out to a 6.1-m (20-ft) radial distance. It was difficult to extrapolate the larger volumes needed for the Ca-citrate-PO₄ from the volumes used in the tracer test because of the observed heterogeneous arrival responses and many of the monitoring wells not having reached 50% breakthrough during the test. Larger volumes were also needed, given the unknown amount of field-scale sorption and reactions of phosphate with this injection mixture. The tracer test results are only applicable for conservative, nonsorbing species. Therefore, to be conservative, a 454,000-L (120,000-gal) volume was specified for this next injection at pilot test site #1. Smaller volumes could be used for subsequent injections if this volume was too large based on detailed monitoring during the test.

Results of the pilot test #1 Ca-citrate-PO₄ injection are described in Section 5.2. Precipitation problems that occurred in the chemical tanker trucks that delivered the reagent to the site necessitated this injection be stopped early due to plugging in the chemical feed lines. Because of these problems, the actual injection volume that was used in the test was 367,000 L (97,000 gal) (see Table 5.3), 19% less than the 454,000 L (120,000 gal) specified.

6.2.3 Volume Estimate for Pilot Test #2 Ca-Citrate-PO₄ Injection

For low-river stage Ca-citrate-PO₄ injection at pilot test site #2 in September 2006 targeting the Ringold Formation, a 227,000-L (60,000-gal) injection volume was specified. This volume was estimated based on half of the high-river stage injection volume specified for the pilot test #1 injection. The Ca-citrate-PO₄ injection formulation was changed for this injection to lower the calcium concentrations and thus reduce the ⁹⁰Sr increases measured from the first pilot test injection at pilot test site #1 (see Section 5.3).

Based on the pilot test #2 operational monitoring results from September 2006, the 227,000-L (60,000-gal) injection volume was insufficient for treating the Ringold Formation because of excessive reagent going into the Hanford formation (see detailed results of pilot test #2 in Section 5.3). The injection rates were reduced during the test to lower the mounding and reduce the amount of reagent loss to the Hanford formation. The injection volumes needed for sufficient coverage of the Ringold Formation at low-river stage could not be easily extrapolated directly from test results. As described in the following section, a numerical model was developed for pilot test site #2 using data from the injection test to estimate hydraulic and transport properties to better estimate volumes needed during low-river stage to treat the lower portion of the treatment zone (i.e., within the Ringold Formation).

6.3 Barrier Emplacement Design (Post-Pilot Testing)

Numerical models were developed for treatability test injection design analysis based on earlier numerical modeling studies (DOE/RL 2006),² site characterization conducted as part of this treatability study, and the results of the pilot tests. Significant differences between the two test sites required development of two site-specific models representing conditions at both ends of the barrier.

To support the construction of numerical models, an EarthVision GIS database of the Hanford Site was refined and updated based on detailed well logs and additional wells from the 100-N Area. One past limitation was that the topographic data were insufficient to resolve the road and bank near the Columba River at N-Springs. A new topographic survey was conducted by PNNL in September 2005 that provided detailed elevations around the 100-N Area apatite barrier that includes the river shore and road, and extends inland to include the bluff. This revised topography was incorporated into the EarthVision database. The transect location for one cross-section through the EarthVision database showing the hydrostratigraphy around the site is shown in Figures 6.3 and 6.4.

These simulations use the STOMP computer code (White and Oostrom 2000, 2006). The EarthVision hydrostratigraphy is sampled at finite difference STOMP model node locations to determine the hydrostratigraphic unit for each node.

The initial pilot test simulation development focused on the pilot test site #2 based on the need to estimate the injection volumes required for low-river stage injections targeting the Ringold Formation. This model is described and preliminary results of the pilot test site #1 model, which is still under development, are discussed.

6.3.1 Pilot Test Site #2 Model

The injection model for pilot test site #2 was developed based on a two-dimensional x-z cross section that was replicated and projected into three dimensions in the y-direction out to 100 m (328 ft) for simulating injections. A half-well symmetry was used to reduce the model domain. The extent of the two-dimensional cross section extends over a 400-m (1300-ft) length, from approximately the center of the river to inland well 199-N-67, as shown in Figure 6.3. Figure 6.4 shows the hydrostratigraphy along the cross section.

The Hanford and Ringold Formation contact for this cross section was adjusted to fit the specific pilot test #2 injection well 199-N-137 elevation (NAVD88) of 117.4 m (385 ft), along with road fill added to 2.7 m (9 ft) below the road surface (119.7 m elevation). The hydrostratigraphy sampled onto the STOMP finite difference grid along the shoreline and road is shown in Figure 6.5. The hydrostratigraphy was simplified by lumping the Hanford formation gravel and sand units shown in the cross section in

² Connelly MP, CR Cole, and MD Williams. 1997. *Bank Storage Modeling at the 100-N Area*. Pacific Northwest National Laboratory for CH2M HILL Hanford Group, Richland, Washington.

Connelly MP. 1999. *Groundwater-River Interaction in the Near River Environment at the 100-N Area*. Innovative Treatment and Remediation Demonstration Program, HydroGeoLogic, Reston, Virginia.

Connelly MP. 2001. *Strontium-90 Transport in the Near-River Environment at the 100-N Area*. Innovative Treatment and Remediation Demonstration Program, HydroGeoLogic, Reston, Virginia.

Figure 6.4 into a single Hanford formation gravel/sand unit. Most of these subunits were identified above the water table in the Hanford formation. Lumping was also done for the Ringold Formation sand and gravel units.



Figure 6.3. Earth Vision Cross-Section Transect Location

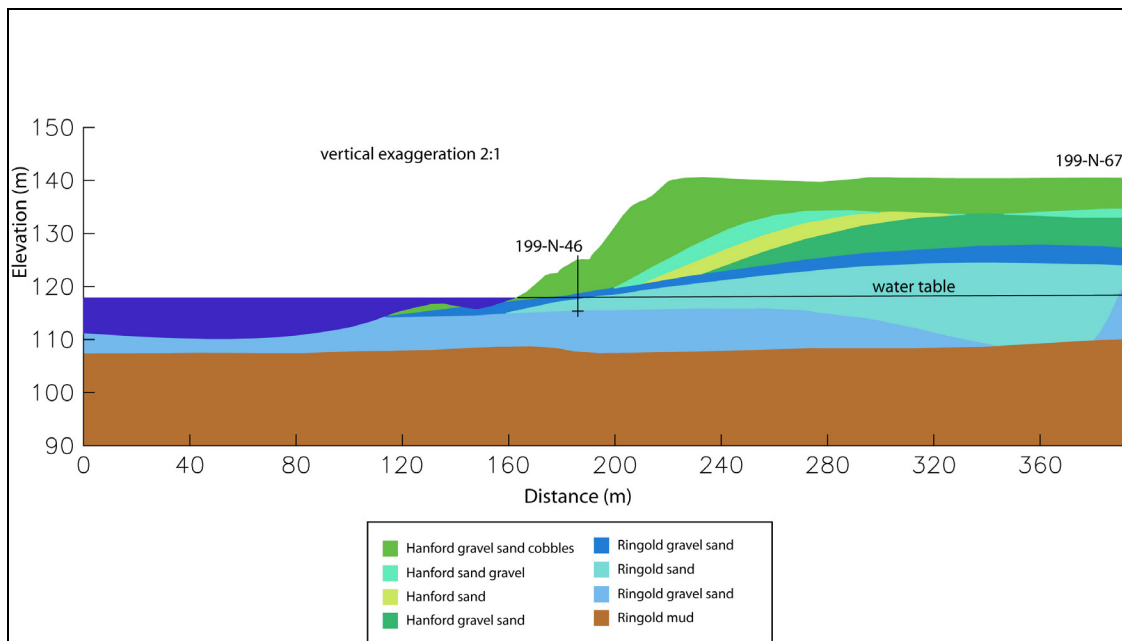


Figure 6.4. Earth Vision Cross Section (see Figure 6.3 for transect location)

The finite difference grid, a portion of which is shown in Figure 6.5, is 238 by 15 by 52 nodes in the x, y, and z directions, respectively, yielding 192,780 total nodes with 156,675 active nodes. The grid spacing is variable with refinement around the shoreline and injection area at 0.25 m (0.82 ft) spacing vertically and horizontally.

Boundary conditions on the northern portion of the model use hourly river-stage measurements applied to the river bottom surface obtained from the Columbia River stage recorder RS-1 in the 100-N Area. These data were extracted from the Hanford Virtual Library, Automated Water Level Data Monitoring (AWLM) module. Water level data for well 199-N-67 were used for the southern model boundary. Hourly water level data were available for well 199-N-67 but high-resolution data were not required given its damped response to river-stage fluctuations.

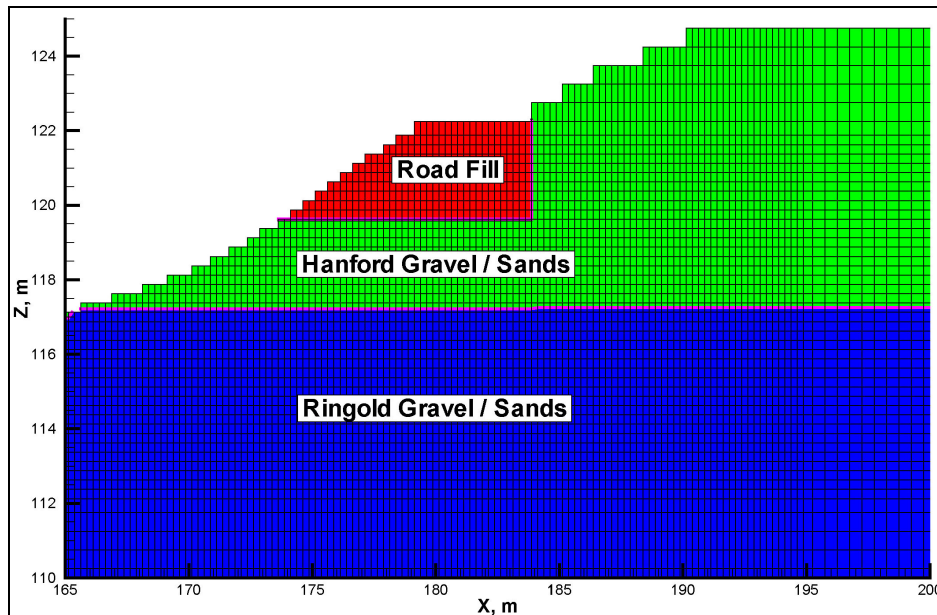
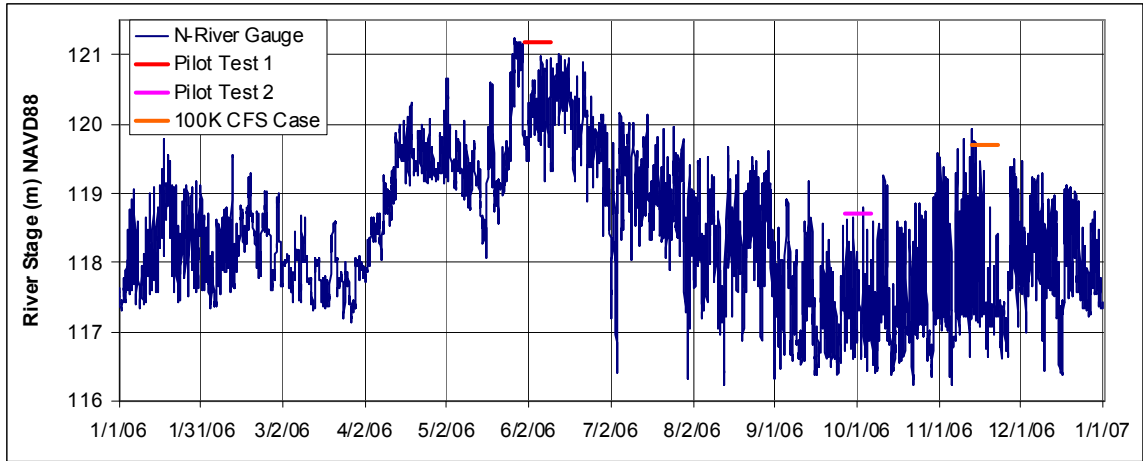


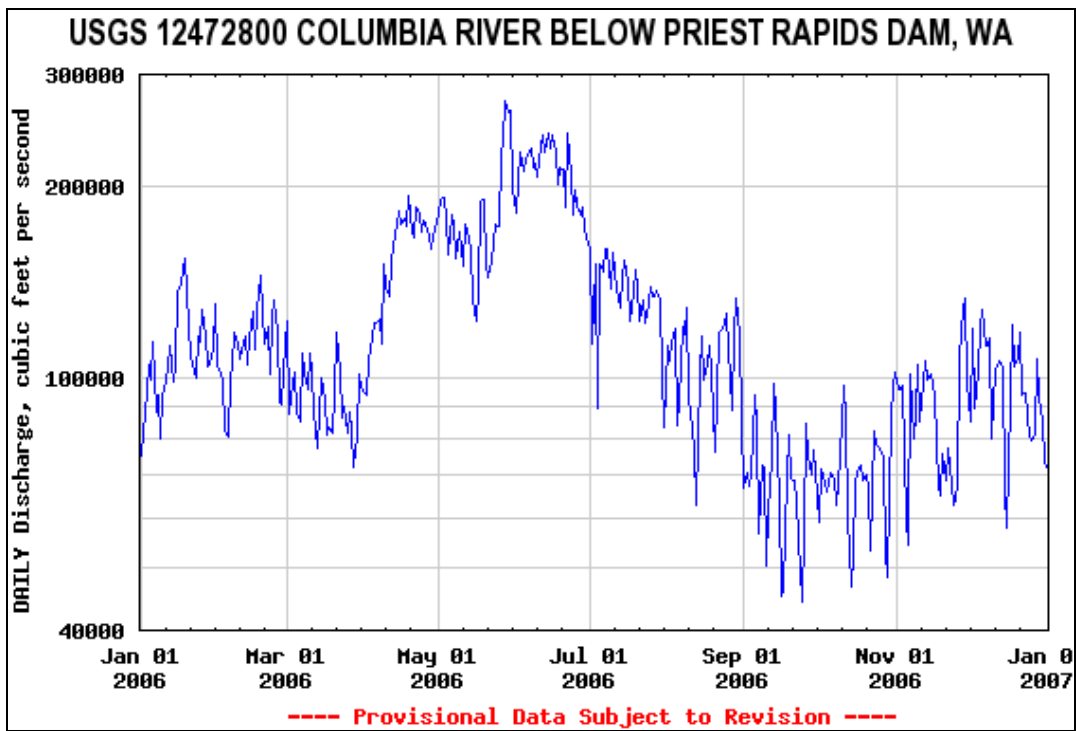
Figure 6.5. STOMP Model Cross Section and Zonations for Pilot Test Site #2. This is a partial view of the cross section showing near-shore details along the road (see Figure 6.3 for transect location).

Simulations were developed to fit pilot test #2 for estimating hydraulic and transport parameters for the field tests. The Columbia River stage and river flow below PRD for 2006, along with the timing of pilot test #2, are shown in Figures 6.6 and 6.7. Field data used in the development and comparison of the simulation results included injection rates, water levels in the injection and surrounding monitoring wells, and bromide and phosphate breakthrough curves at the monitoring wells. The monitoring wells for this test were installed at upper and lower zone pairs (i.e., Hanford and Ringold Formations), and at different radial distances and directions from the injection well (see well layout in Figure 4.3 and Table 5.10).

A trial-and-error manual parameter estimation process was used. Interim simulation results were inspected and the parameters were adjusted based on the comparison of simulated with measured values of hydraulic heads, bromide, and phosphate for the pilot test #2. This simulation involved injection over a well screen that spanned the two hydrostratigraphic units, as shown in Figure 4.3. Bromide was simulated as a conservative tracer.

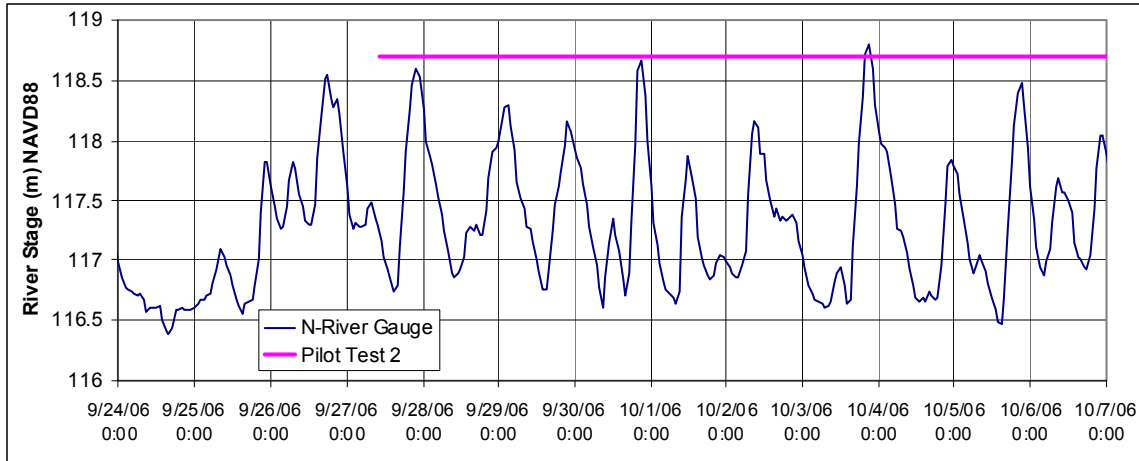


A

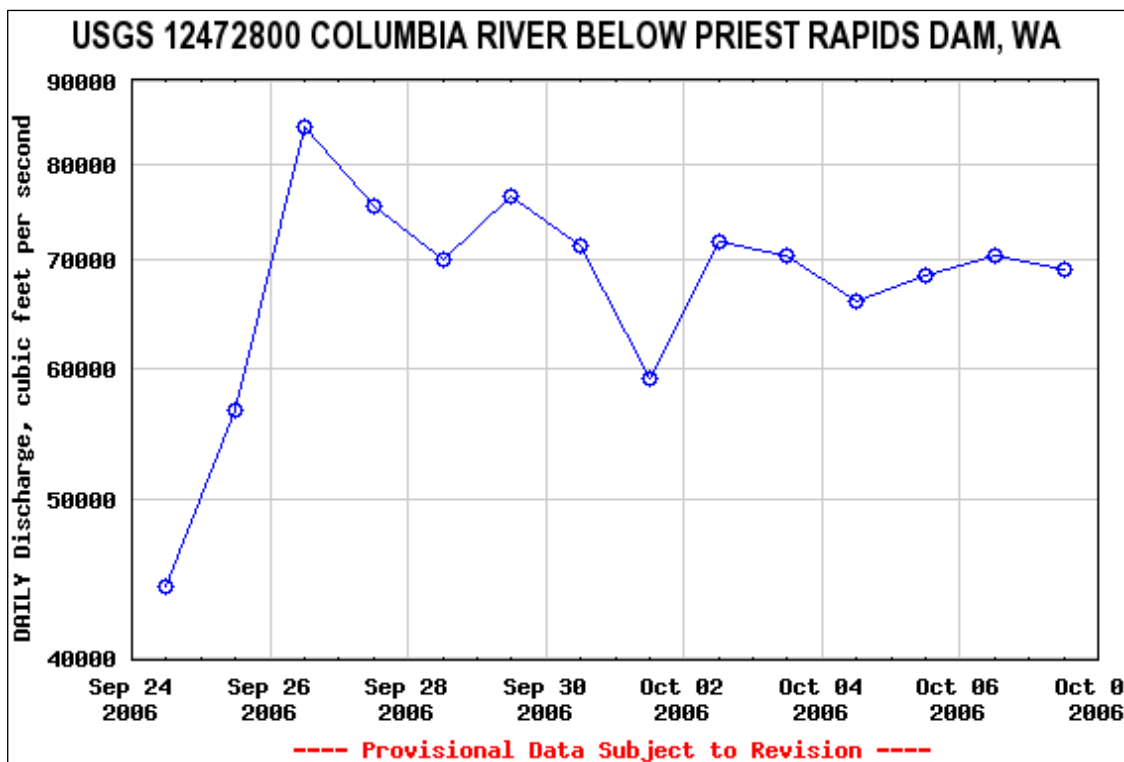


B

Figure 6.6. Columbia River Stage (a) and Flow (b) for 2006 at the 100-N Area. The river stage and timing of the first two pilot tests are also shown. River stage data are from the Hanford Virtual Library, Automated Water Level Network Data Viewing module.



A



B

Figure 6.7. Detailed Columbia River Stage (a) and Flow (b) for 2006 Pilot Test #2 at 100-N Area. The river stage and timing of the first two pilot tests are also shown. River-stage data from Hanford Virtual Library, Automated Water Level Network Data Viewing module.

Phosphate transport was simulated using a linear isotherm (K_d). Parameters estimated during this fitting process include the hydraulic conductivity of the Hanford and Ringold Formations (K_{xy} and anisotropy), dispersivity, and phosphate K_d .

Porosity values were specified based on physical property measurements from sediment samples collected from the characterization boreholes drilled in 2005 (199-N-122 and 199-N-123). Average porosities were calculated from core samples collected near the middle of the split-spoon samples (B-cores) because there was evidence of significant sample disturbance and partial recovery in the

samples collected near the bottom (D-cores). A total porosity value for the Hanford formation was calculated from a mean of all the total porosity measurements from these two boreholes, which resulted in an estimate of 24% (the mean value for each borehole was similar). A total porosity value of 18% for the Ringold Formation was calculated from the mean for well 199-N-123. The Ringold Formation mean for well 199-N-122 was slightly higher at 21%; however, the higher porosity values were below the targeted treatment zone. Effective porosities in the model were set to the same values as the total porosities.

This fitting process involved numerous iterations for specifying values for the two hydrostratigraphic layers because adjustments in the hydraulic properties of one unit would change how the injection flux was proportioned between both units. Final hydraulic property values were determined based on a visual inspection of the fit of both the hydraulic head and solute breakthrough data. In some cases, a good fit could not be achieved for both; in these cases, the fit for the solutes was favored over the hydraulic heads. Additionally, measurements for wells at similar radial distances but oriented in different directions had slightly different responses (e.g., well P2-5-R and P2-7-R). However, no spatial zonation was developed in this model to account for these differences (i.e., only a single value is specified for each parameter in the Ringold Formation unit) so parameters were selected with simulated results that fit between these different responses at the same radial distance. Breakthrough curves for the conservative tracer, Br⁻, were fit first before adjusting Kds for the phosphate breakthrough match.

The number of runs for parameter estimation was limited by the simulation execution time. The three-dimensional flow and transport simulations of the pilot test #2 took approximately 3 days per run on a dual-processor Xeon (Pentium 4, ranging from 3.2 to 3.6 GHz) Linux workstations.

The parameters from this estimation process are shown in Table 6.2. Comparison of the simulated results using these values with the measurements for the hydraulic head data are shown in Figure 6.8, for the bromide tracer in Figure 6.9, and for phosphate in Figure 6.10. These parameters may be updated from additional runs with this model using field data from subsequent injections at the pilot test site #2.

Table 6.2. 100-N Pilot Test #2 Preliminary Parameter Estimation Results

Parameter	Hanford Formation Gravel / Sand	Ringold Formation Gravel / Sand
Hydraulic Conductivity	K _{xy} = 29 m/day K _z = 2.9 m/day	K _{xy} = 9 m/day K _z = 0.9 m/day
Porosity (not estimated in modeling)	24%	18%
Dispersivity	Longitudinal = 0.2 m Transverse = 0.04 m	Longitudinal = 0.2 m Transverse = 0.04 m
Phosphate K _d	K _d = 0.13 cm ³ /g	K _d = 0.13 cm ³ /g

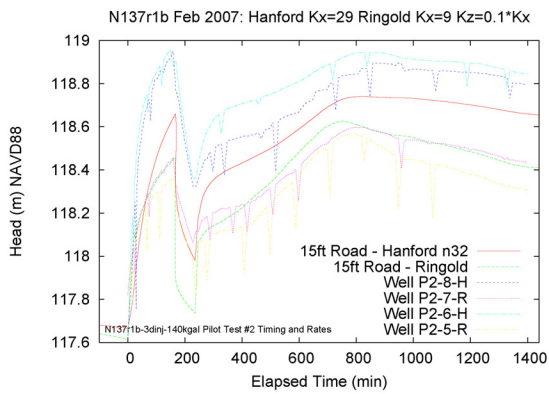
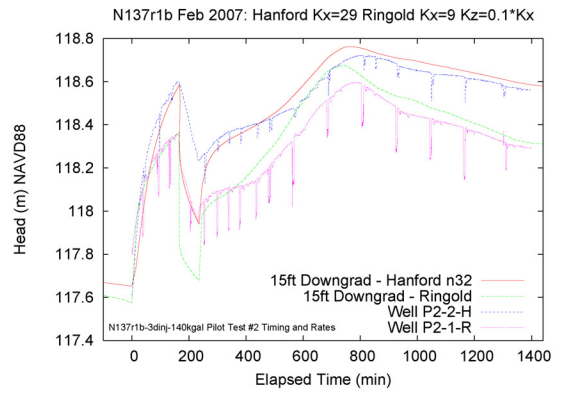
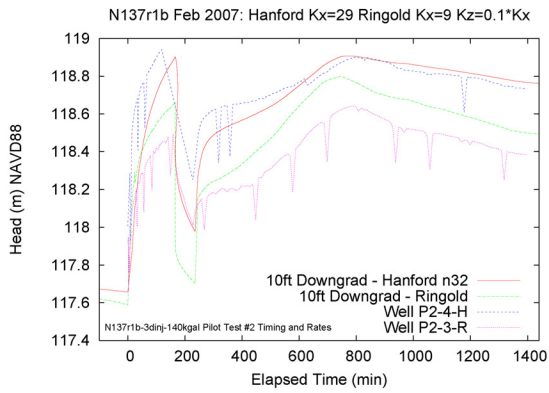


Figure 6.8. Hydraulic Head Results of Pilot Test #2 Model Fit. Simulation results are the first two lines on each plot at differing radial distances followed by well measurements at these distances.

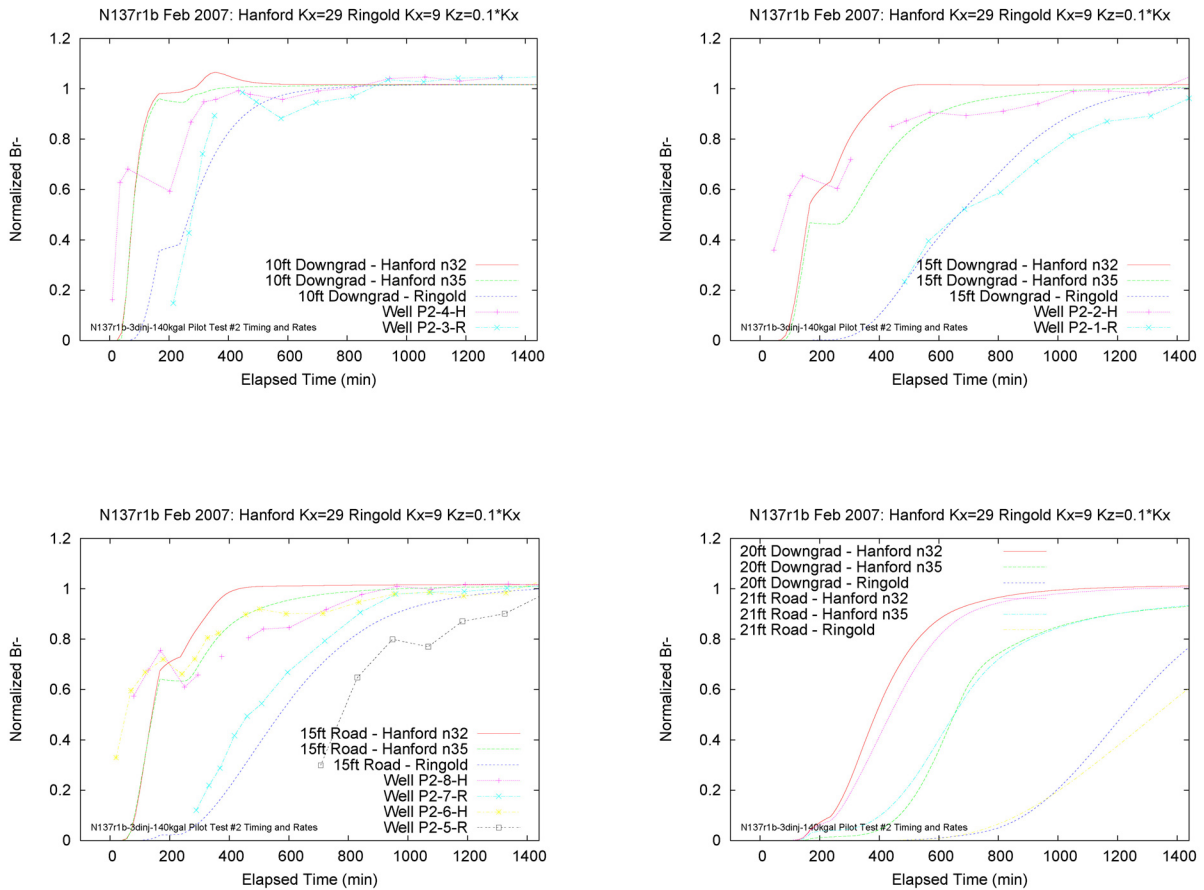


Figure 6.9. Bromide Results of Pilot Test #2 Model Fit. Simulation results (shown as lines) at differing radial distances are followed by measurements from wells at similar radial distances (shown with both lines and symbols).

6.3.2 Pilot Test Site #1 Model

A numerical model is being developed for pilot test site #1. The construction of this model was similar to the pilot test site #2 model described in the previous section (i.e., three-dimensional domain created by replicating a two-dimensional cross section, half-well symmetry, and the inland and river boundaries). Major differences between these models are the elevation of the Hanford/Ringold formation contact that was based on geologists' logs at the pilot test sites, a lower permeability contrast between the Hanford and Ringold Formations, and the addition of a high hydraulic conductivity zone within the Hanford formation that was created based on the monitoring results during the tracer test (see Section 5.1). The high-hydraulic conductivity zone within the Hanford formation was created on the inland side of the injection well for fitting the fast tracer arrival times seen at monitoring well P-6-H.

Hydraulic property estimates for pilot test site #1 need to include values for the High-K zone in the Hanford formation, in addition to the values for the rest of the Hanford formation and the Ringold Formation. The monitoring results of the tracer and first Ca-citrate- PO_4 injection at pilot test site #1

showed the contrast between the hydraulic conductivity of the Hanford (not including the High-K zone) and Ringold formations is lower than for pilot test site #2. This was observed in the differences in relative arrivals between the Hanford and Ringold Formation monitoring wells at the two pilot test sites. It is unknown how much of this apparent reduction in permeability contrast is associated with the relatively extreme well inefficiency observed in these wells (see discussion in Sections 4.0 and 5.0). The specific capacity of the injection well at pilot test site #1 was much less than that of pilot test site #2 (see Figure 4.5).

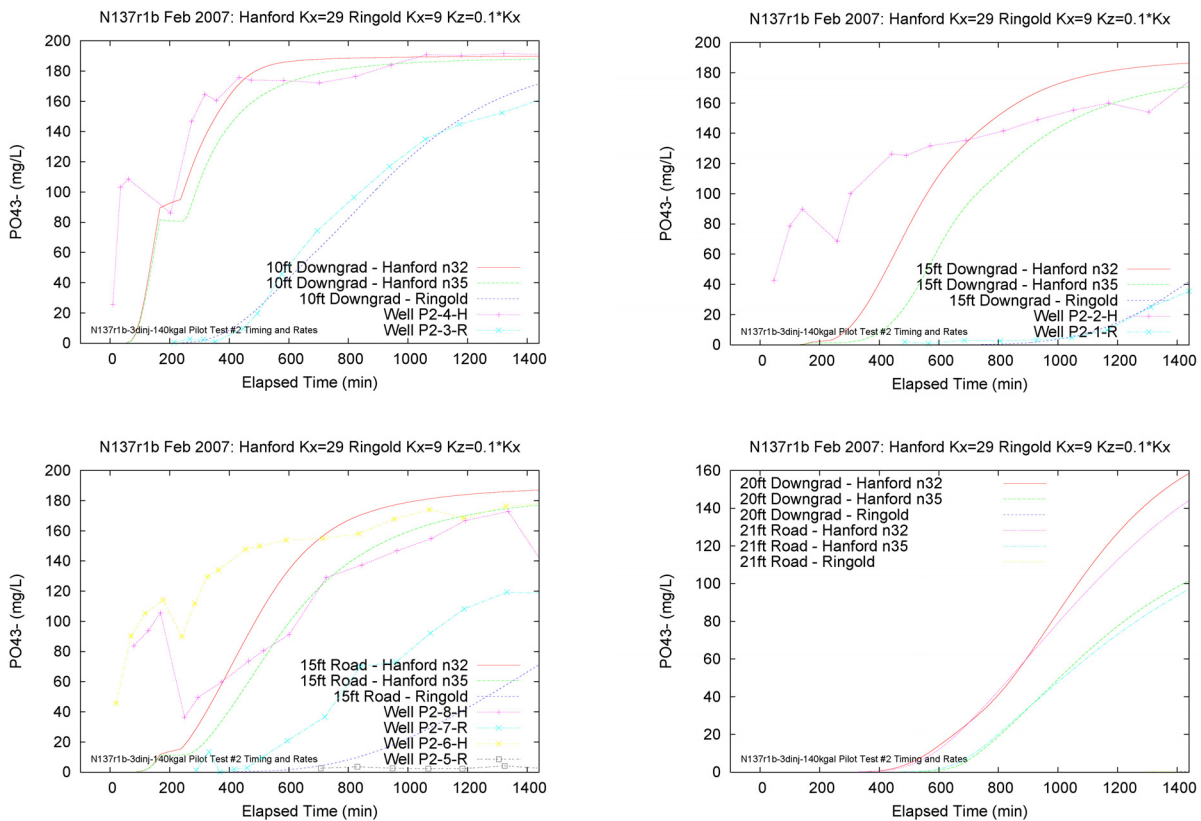


Figure 6.10. Phosphate Results of Pilot Test #2 Model Fit. Simulation results (shown as lines) at differing radial distances are followed by measurements from wells at similar radial distances (shown with both lines and symbols).

Preliminary hydraulic property estimates for pilot test site #1 were developed based on fitting the results of the tracer test. Hydraulic conductivity estimates in the xy direction for the High-K Hanford formation zone was 200 m/day (656 ft/day), 12 m/day (39 ft/day) for the rest of the Hanford formation, and 10 m/day (33 ft/day) for the Ringold Formation. The vertical hydraulic conductivity values were set to 1/10 for the horizontal value. These estimates will be updated based on additional pilot test site #1 model simulations using data from the tracer test and Ca-citrate-PO₄ injections at the site.

6.3.3 Winter 2007 Injection Design

Barrier emplacement injections were conducted in 9 of the 10 barrier injection wells in February and March 2007. Because river stage conditions varied over this period to outside the expected range, these injections resulted in both targeted treatment of the Ringold Formation (during low-stage conditions) and combined Hanford/Ringold formation treatments in the upstream wells (see discussion is Section 7.0).

Pilot test site #1 was not targeted for treatment to continue post-injection monitoring from the spring 2006 injection at this site. Injection volume estimates for these low-river stage injections, 530,000 L (140,000 gal), were developed based on simulations with pilot test site #2. The Ca-citrate-PO₄ injection concentrations were revised again for these injections with an increase in the phosphate concentration and decreases in the calcium and citrate based on analysis of the September 2006 pilot test #2 operational and monitoring results and additional laboratory experiments.

Simulations were conducted with the pilot test site #2 model (described in Section 6.3.1) using the same hydraulic properties and timing as the September 2006 pilot test site #2 Ca-citrate-PO₄ injection. Columbia River flow conditions over this time period are shown in Figure 6.7 (~70,000 cfs). The injection was extended with this model, using the lower rate of 151 L/min (40 gpm) that was used for the later part of pilot test #2 to determine the volume required to achieve ~50% phosphate concentrations at a 6.1-m (20-ft) radial distance. The injection volume estimate based on this method was 530,000 L (140,000 gal) (3500 minutes elapsed injection time), as shown in Figure 6.11 (see 20-ft and 21-ft phosphate concentrations in the Ringold Formation).

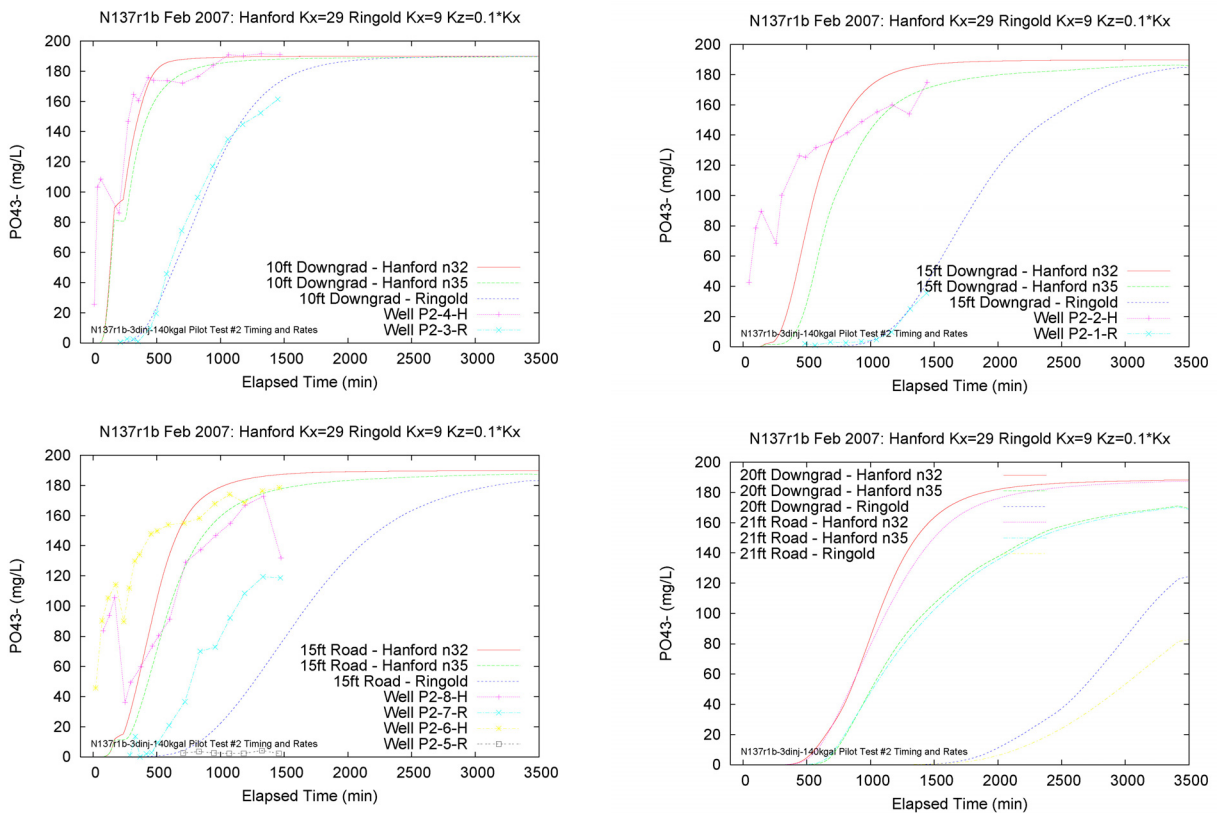


Figure 6.11. Phosphate Results of Pilot Test #2 Injection Test with Volume Extended to 140,000 gal. Simulation results (shown as lines) at differing radial distances are followed by measurements from wells at similar radial distances (shown with both lines and symbols)

Simulations were also conducted with the pilot test site #2 model during different river stage conditions to determine the effect on injection volumes required for Ringold Formation treatment. In addition to the ~70,000-cfs case shown in Figure 6.11, cases were run at very high-river stage conditions with the timing of the May/June 2006 pilot test #1 injection and at an intermediate river stage period

(100,000 cfs) as shown in Figure 6.6. Simulated phosphate concentrations after 530,000 L (140,000 gal) of injection were between 30 to 45% of the injection concentration at a 6.1-m (20-ft) radial distance in the Ringold Formation for the 100,000 cfs case. These concentrations were approximately 30% lower than the ~70,000-cfs case as shown in Figure 6.11. For the very high-river stage during the June 2006 pilot test #1, simulated phosphate concentrations after 530,000 L (140,000 gal) of injection were between 18 to 37% of the injection concentration at a 6.1-m (20-ft) radial distance in the Ringold Formation.

As discussed in Section 7.0, the Columbia River stage increased earlier than expected in March 2007 (see Figure 6.2) so that some of these injections occurred during high-river stage conditions instead of the planned low-river stage. Additionally, springs appeared during some of these injections from high hydraulic conductivity channels in the Hanford formation, resulting in potential poor reagent coverage in these cases. One injection was stopped shortly after it started due to excessive seepage; this seepage loss is discussed in more detail in Section 7.0.

6.3.4 June/July 2007 Injection Design

A second injection campaign was conducted in June and July of 2007. These injections were initially intended for high-river stage treatment of all the barrier injection wells; however, some of these wells were treated during high-river stage conditions in March 2007 because of the early seasonal rise in the Columbia River stage. Thus, these injections targeted the wells that were not injected at high-river stage during the earlier injections of 2007. This injection campaign also included another injection at pilot test site #1. The Ca-citrate-PO₄ formulation during these injections was the same as the winter 2007 injections.

Planning for these high-river stage injections also accounted for differences in the hydraulic conductivity along the barrier determined through site characterization, pilot test injections, and the winter 2007 injections. Based on these observations, the barrier can be divided into two distinct portions with an upstream portion between wells 199-N-138 to 199-N-141 and a downstream portion between wells 199-N-142 to 199-N-137. The upstream portion of the barrier is characterized by pilot test site #1 and the downstream portion is characterized by pilot test site #2. The upstream portion has a much lower well-specific capacity (as shown in Figure 4.5) than the downstream portion. The hydraulic conductivity contrast between the Hanford and Ringold Formations is lower in the upstream portion than the downstream portion based on relative arrivals in these units at the pilot test sites and estimates from numerical modeling fits. The bulk hydraulic conductivity in the Hanford formation (ignoring the larger-scale heterogeneities) is lower in the upstream portion compared to the downstream portions. Estimates of the hydraulic conductivity of the Ringold Formation are similar for both portions of the barriers.

For the upstream portion of the barrier, 378,500-L (100,000-gal) injection volumes were specified for treating the Hanford formation during high-river stage. For the downstream portion, a lower injection volume of 227,000 L (60,000 gal) was specified because there would be less reagent loss to the Ringold Formation due to the greater contrast in the Hanford/Ringold hydraulic conductivity. The June/July 2007 injections are described in Section 7.0.

6.4 Post-Barrier Injection Design Revisions/Recommendations

Operational monitoring results from the pilot sites and barrier well injections (described in Sections 5.0 and 7.0) showed that large injection volumes targeting the Ringold Formation in the

downstream portion of the barrier were inefficient, and coverage was not complete because of the springs that appeared and the earlier than usual high-river stage in 2007. PNNL scientists recommended that injection wells screened only over the contaminated portion in the Ringold Formation be installed between the existing injection wells in the downstream portion of the barrier. These wells would significantly reduce the injection volumes required to treat the Ringold Formation, reduce the loss from springs that formed during these injections, and also remove the low-river stage timing constraint for treatment of these wells. The installation of these Ringold-only injection wells is planned for the winter of 2008.

With this new well configuration including the Ringold Formation-only wells, the injection design for the high-concentration Ca-citrate-PO₄ planned for 2008 can be divided into two sections based on the upstream and downstream portions of the barrier. For the upstream portion of the barrier, which has injection wells spanning both the Hanford and Ringold Formation treatment zone, single large-volume injections (~454,000 L [~120,000 gal]) are required during high-river stage conditions for treating both the Hanford and Ringold Formations. Both units can be targeted simultaneously due to the relatively low contrast in hydraulic conductivity between these units. For the downstream portion of the barrier, which includes injection wells spanning both units and the Ringold-only injection wells, two injection operations, each with lower injection volumes (~227,000 L [~60,000 gal] each), will be required. The injection wells spanning both the Hanford and Ringold Formations need to be injected during high-river stage to treat the Hanford formation portion of the aquifer. The Ringold-only injection wells can be injected at any time.

The design analysis is continuing to refine the volumes needed for the planned 2008 injections. Work will continue on analysis of results from previous injections, and monitoring data collected during the first Ringold Formation-only screened injection will be analyzed to determine treatment volume requirements for these wells.

7.0 100-N Area Low-Concentration Barrier Injections

The section describes the low-concentration apatite solution injections conducted as the initial phase of treatment emplacement for a 91-m (300-ft)-long apatite PRB. After the pilot tests and additional laboratory studies were conducted (described in Sections 2.0, 3.0, and 5.0), the injection formula was modified for the remaining barrier well injections. The general injection design, as described in detail in Section 6.0, is for a combination of low- and high-river stage injections to target the ⁹⁰Sr-contaminated portion of the Hanford and Ringold Formations. Different injection volumes were needed during the low- and high-river stage injections. Additionally, differences in injection volumes were required for the upstream and downstream portions of the barrier due to differences in the hydraulic conductivity contrast between the Hanford and Ringold Formations (see Sections 4.1.2 and 6.3.2).

During these injections, it was determined that low-river stage injections were not needed for the upstream portion of the barrier because adequate coverage of reagent was also achieved in the Ringold Formation during the high-river stage injections. This more uniform distribution of treatment was caused by a relatively low apparent contrast in Hanford/Ringold formation hydraulic conductivity at these locations, as determined based on pilot test #1 results. Conversely, the larger hydraulic conductivity contrast between the Hanford and Ringold Formations in the downstream portion of the barrier resulted in the need for larger injection volumes during low-river stage conditions to adequately treat the Ringold Formation. Springs appeared during some of these injections, which resulted in termination of one injection after only 4 hours due to excessive seepage loss. Injection wells screened only in the Ringold Formation for the downstream portion of the barrier are needed for better coverage in this area, and will be installed before additional injections at the barrier. These Ringold-only injection wells should result in increased treatment efficiency by requiring smaller injection volumes to target the contaminated zone in the upper portion of the Ringold Formation.

Apatite injections were conducted in nine wells in February and March 2007 during both low- and high-river stage conditions. Six additional injections occurred in June and July of 2007 during high-river stage conditions for wells that had injections during low-river stage conditions in March. The apatite injections conducted at the 100-N Area are summarized in Table 7.1.

7.1 Barrier Installation

This initial phase of apatite barrier formation was accomplished by conducting 17 separate injections at the 10 barrier well locations (Table 7.1). Most wells were injected twice, per the two-phased injection strategy discussed above. Three different chemical formulations were used—one for the initial pilot test, a modified formulation for the second pilot test, and the final formulation for the barrier formation (Table 7.2).

The chemical mass injected, and the average concentration of the chemical treatment for each injection, was determined by monitoring concentrations within the injection well, monitoring flow rates of the injection stream and concentrated feed solutions, and measuring the undiluted chemical concentrations and volumes (see Section 4.3). After the chemical mass was injected, the average chemical concentration for each of the barrier formation injections was generally within 10% of the design specification (Tables 7.3 and 7.4). The injection volumes were typically lower than the design volumes.

Table 7.1. 100-N Area Low-Concentration Apatite Injection Summary. Table identifies purpose of injection, injection start date, river stage condition, formation treated, chemical formulation used, volume of solution injected, and the duration of the injection.^(a)

Well ID	First Treatment	Second Treatment
199-N-138	Pilot Test #1 5/31/06 – HR Hanford/Ringold – P1 Formulation 96,000 gal (35.4 hr)	Barrier Emplacement 6/8/07 – HR Hanford/Ringold – Barrier Formulation 89,900 gal (39 hr)
199-N-139	Barrier Emplacement 3/22/07 – HR Hanford/Ringold- Barrier Formulation 124,800 gal (53 hr)	<i>No follow-up treatment</i>
199-N-140	Barrier Emplacement 3/2/07 – LR Hanford/Ringold – Barrier Formulation 123,600 gal (57 hr)	Barrier Emplacement 7/10/07 – HR Hanford/Ringold – Barrier Formulation 82,700 gal (37 hr)
199-N-141	Barrier Emplacement 3/20/07 – HR Hanford/Ringold – Barrier Formulation 127,600 gal (54.5 hr)	<i>No follow-up treatment</i>
199-N-142	Barrier Emplacement 2/28/07 – LR Ringold – Barrier Formulation 129,900 gal (58 hr)	Barrier Emplacement 6/5/07 – HR Hanford – Barrier Formulation 55,900 gal (22 hr)
199-N-143	Barrier Emplacement 3/22/07 – HR Hanford – Barrier Formulation 131,600 gal (53 hr)	<i>No follow-up treatment</i>
199-N-144	Barrier Emplacement 3/2/07 – LR Ringold – Barrier Formulation 128,900 gal (57 hr)	Barrier Emplacement 6/5/07 – HR Hanford – Barrier Formulation 54,600 gal (22 hr)
199-N-145	Barrier Emplacement 2/28/07 – LR Ringold – Barrier Formulation 110,300 gal (53 hr)	Barrier Emplacement 7/10/07 – HR Hanford/Ringold – Barrier Formulation 55,600 gal (25 hr)
199-N-136	Barrier Emplacement 2/28/07 – LR Ringold – Barrier Formulation 9700 gal (4 hr)	Barrier Emplacement 6/5/07 – HR Hanford – Barrier Formulation 54,600 gal (22 hr)
199-N-137	Pilot Test #2 September 2006 – LR Ringold – P2 Formulation 60,000 gal (23.6 hr)	Barrier Emplacement 3/20/07 – HR Hanford – Barrier Formulation 134,500 gal (54.5 hr)

(a) HR= high-river stage, LR= low-river stage.

Table 7.2. Design Specified Chemical Concentrations of Injection Solution

Formulation	Citrate Concentration	Calcium Concentration	Phosphate Concentration
P1 Formulation – Pilot test #1	10 mM (1890 mg/L)	4 mM (160 mg/L)	2.4 mM (228 mg/L)
P2 Formulation – Pilot test #2	5 mM (945 mg/L)	2 mM (80 mg/L)	2.4 mM (228 mg/L)
Barrier Formulation	2.5 mM (473 mg/L)	1 mM (40 mg/L)	10 mM (950 mg/L)

Table 7.3. Injection Concentrations and Total Chemical Mass Injected During the March 2007 Apatite Barrier Formation Injections. Note that calcium design concentration includes calcium from the raw chemical feed (40 mg/L) and from the make-up water (17 mg/L). Solution injection rates were maintained at ~40 gpm during all injections.

Well Name	Total Solution injection volume (gal)	Average Injection Concentration (mg/L)			Total Chemical Injection Mass (kg)		
		Calcium	Citrate	Phosphate	Calcium	Citrate	Phosphate
199-N-139	124836	57.2	520	1069	27.0	238	528
199-N-140	123588	64.2	591	1032	30.0	274	494
199-N-141	127576	68.8	557	985	33.2	264	506
199-N-142	129923	64.3	540	987	31.5	256	493
199-N-143	131633	54.5	489	979	27.1	239	499
199-N-144	128888	61.8	559	1031	30.1	271	519
199-N-145	110297	62.3	549	1105	26.0	227	478
199-N-136	9669	68.6	600	1130	2.5	22	44
199-N-137	134505	65.3	504	936	33.2	253	495
Design Spec.	140000	57	473	950	30.2	250	503
	% Difference from design vol.	Percent difference from design specification concentration			Percent difference from design specification mass		
199-N-139	-11%	0.3	10	13	-11	-4.7	5.1
199-N-140	-12%	1%	25	8.6	-0.5	9.4	-1.6
199-N-141	-9%	21	18	3.7	10	5.6	0.6
199-N-142	-7%	13	14	3.9	4.3	2.3	-1.9
199-N-143	-6%	-4.3	3.5	3.1	-10	-4.3	-0.8
199-N-144	-8%	8	18	8.5	-0.2	8.3	3.4
199-N-145/ 199-N-136 comb	-14%	10	17	15	-5.6	-0.2	3.7
199-N-137	-4%	15	6.7	-1.4	10	1.2	-1.5

This occurred because the injections concentration was typically held slightly higher than the design specification, resulting in a slightly lower volume at a slightly higher concentration. Details of the pilot test injections are provided in Sections 5.2 and 5.3.

River stage during the barrier injection was an important parameter in the depth interval treated and the efficiency of treatment. River stage along this section of the Columbia River is controlled by the rate of discharge at PRD, located approximately 29 km (18 mi) upstream of the 100-N Area. Tables 7.5 and 7.6 show the Columbia River stage at the 100-N Area stage gauge, and the corresponding river discharge from PRD during the February/March and June/July 2007 injections. The initial plan, prior to pilot testing, was to conduct injections during low-river stage to provide treatment for the Ringold Formation, while injections during high-river stage would target Hanford formation treatment. For the upstream portion of the barrier, the contrast between permeability in the Hanford and Ringold Formations was sufficiently small that injections at high-river stage alone were successful in treating both the Hanford and Ringold Formations.

Table 7.4. Injection Concentrations and Total Chemical Mass Injected During the June 2007 Apatite Barrier Formation Injections. Note that calcium design concentration includes calcium from the raw chemical feed (40 mg/L) and from the makeup water (17 mg/L). Solution injection flow rate was maintained at ~40 gpm during all injections.

Well Name	Total Solution injection volume (gal)	Average Injection Concentration (mg/L)			Total Chemical Injection Mass (kg)		
		Calcium	Citrate	Phosphate	Calcium	Citrate	Phosphate
199-N-138	89,889	56.2	528	862	19.1	179	315
199-N-140	82,716	57.7	550	991	18.0	175	309
Design Spec.	100,000	57	473	950	21.6	179	359
199-N-142	55,911	57.6	570	1049	12.2	120	225
199-N-144	54,609	56.4	534	986	11.7	110	204
199-N-145	55,572	59.0	401	1063	12.4	97	225
199-N-136	54,609	56.4	534	986	11.7	110	204
Design Spec.	60,000	57	473	950	12.9	107	216
	% difference from design vol.	Percent difference from design specification concentration			Percent difference from design specification mass		
199-N-138	-10%	-1.5	12	-9.2	-12	0.0	-12
199-N-140	-17%	1.2	16	4.3	-17	-2.1	-14
199-N-142	-7%	1.0	20	10	-5.7	12	4.3
199-N-144	-9%	-1.0	13	3.8	-10	2.8	-5.4
199-N-145	-7%	3.5	-15	12	-3.9	-9.4	4.4
199-N-136	-9%	-1.0	13	3.8	-10	2.8	-5.4

Table 7.5. River Stage (and corresponding Priest River Dam discharge) During the March 2007 Injections and the 7-Day Reaction Period, as Measured at the 100-N Area River Stage Gauge

Well ID	River stage (m)			River Discharge (cfs)		
	Maximum	Minimum	Average	Maximum	Minimum	Average
199-N-136	119.36	117.30	118.14	117,000	76,900	100,682
199-N-137	120.42	118.19	119.43	196,000	127,000	161,818
199-N-139	120.59	117.42	119.53	223,000	131,000	174,000
199-N-140	119.36	117.30	117.98	112,000	76,900	96,445
199-N-141	120.42	118.19	119.43	196,000	127,000	161,818
199-N-142	119.36	117.30	118.14	117,000	76,900	100,682
199-N-143	120.59	117.42	119.53	223,000	131,000	174,000
199-N-144	119.36	117.30	117.98	112,000	76,900	96,445
199-N-145	119.36	117.30	118.14	117,000	76,900	100,682

Table 7.6. River Stage (and corresponding Priest River Dam discharge) During the June 2007 Injections and 7-Day Reaction Period

Well ID	Injection Start Date	River Stage (m)			River Discharge (cfs)		
		Maximum	Minimum	Average	Maximum	Minimum	Average
199-N-136	6/5/07	120.51	119.01	119.74	224,500	147,700	182,700
199-N-138	6/8/07	120.51	119.05	119.70	224,300	150,600	181,620
199-N-140	7/10/07	119.81	117.51	118.99	191,930	78,720	151,190
199-N-142	6/5/07	120.51	119.01	119.74	224,500	147,700	182,700
199-N-144	6/5/07	120.51	119.01	119.74	224,500	147,700	182,700
199-N-145	7/10/07	119.81	117.51	118.99	191,930	78,720	151,190

However, for the downstream portion of the barrier, multiple injections did not provide complete treatment. High-river stage conditions provided a hydraulic barrier that contained the injection solution in the Hanford formation, allowing adequate treatment. Unfortunately, injections during low-river stage had limited success in providing adequate extent of treatment in the Ringold Formation. The large contrast in permeability between the Hanford and Ringold Formations along the downstream portion of the barrier resulted in the loss of a significant portion of the injection volume to the saturated Hanford formation interval, associated shoreline seeps, and limited treatment of the Ringold Formation. As discussed earlier, Ringold-only injection wells will be required to provide a more effective treatment of this interval over the downstream portion of the barrier. Injections that occurred during a low-river stage (<118.5 m [388 ft]) were re-treated during June 2007 to provide treatment for the Hanford formation (Tables 7.5 and 7.6).

For injections conducted during periods of low-river stage, the injection solution was able to move through high-permeability zones within the lower portion of the Hanford formation (just above the Hanford/Ringold formation contact) and discharge directly to the Columbia River. This loss to the shoreline seeps resulted in a significant loss in treatment efficiency. The largest seeps that formed during barrier emplacement injections were located at the downstream portion of the barrier (Figure 7.1).

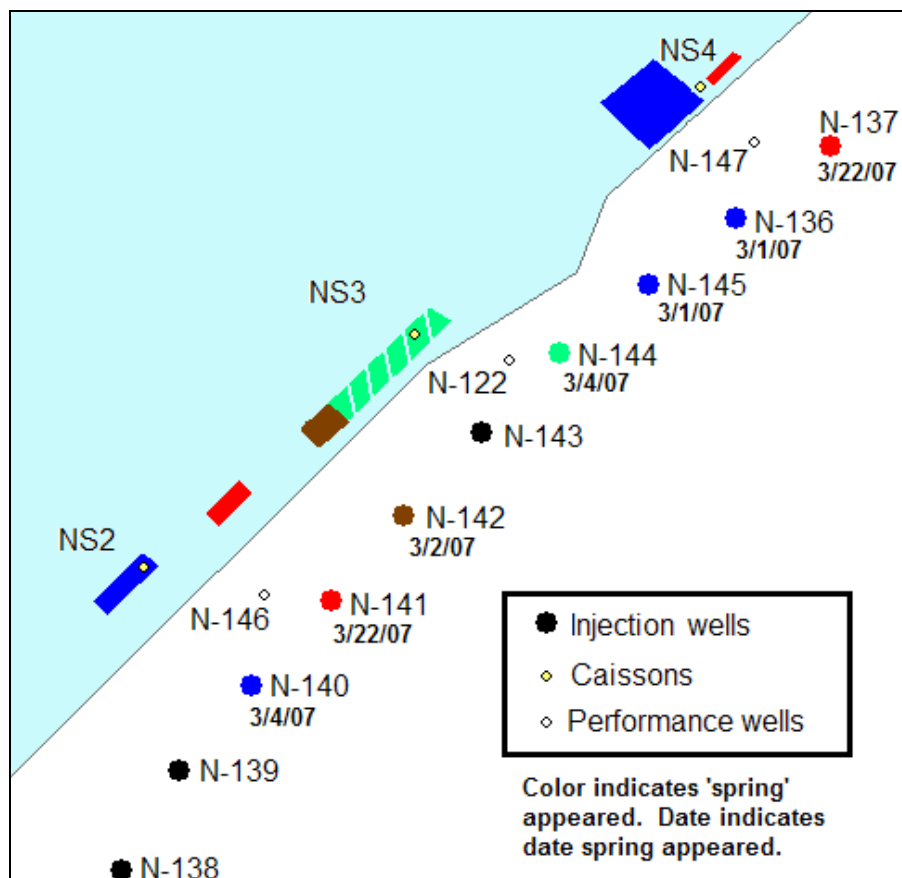


Figure 7.1. Location and Relative Discharge Rate of Springs During Injection. Spring locations are color coordinated to designate which wells were associated with which spring. Height of color block is qualitatively proportional to spring discharge rate. 199-well name prefix is omitted.

In general, seep locations were consistent with historical N-Spring locations reported during 100-N Reactor operations. Some of these springs occurred over very small areas, indicating the spring was caused by a high permeability feature of limited extent. The spring near monitoring well 199-N-147 appeared during the injection in 199-N-136. This injection was stopped after several hours and moved to well 199-N-145. Even after moving the injection, the spring continued to discharge injection solution to the river, though at a slower rate than during injections. Other springs occurred over a wide area, suggesting that a larger-scale high permeability feature led to formation of the spring. The injection wells where springs occurred are illustrated in Figure 7.1. The discharge from most springs found during injections consisted of virtually undiluted injection solutions, as indicated by SpC. No springs or seeps were observed during injections conducted at high-river stage conditions because all seep locations were underwater. No attempt was made to sample the submerged seeps at high-water stage due to the difficulties associated with both locating and sampling the features. It is possible that discharge of injection solution to the Columbia River occurred even during high-river stage conditions, although most likely at a significantly reduced rate.

7.2 Assessment of Lateral Regent Coverage

Design specifications for the barrier installation stipulated that the chemical concentrations should be at least 50% of injection concentration 6.1 m (20 ft) from each injection well. This is considered a sufficient radial extent of treatment to provide overlap of treatment between injection wells. While monitoring points were not installed between injection wells, monitoring was conducted in adjacent injection wells during treatment operations. Comparison of the SpC and phosphate concentrations relative to injection concentration provides an indication of treatment effectiveness at a radial distance of 6.1 m (20 ft) from the injection well (Table 7.7). Operational monitoring data during these injections in adjacent wells is shown in Appendix A. As expected, phosphate transport was somewhat retarded relative to the bulk solution (as indicated by SpC measurements). The SpC in adjacent wells was consistently closer to injection well values than the phosphate concentration. Thus, the phosphate concentration was considered a better indicator of treatment efficiency than SpC. Because no monitoring wells were available at a 6.1-m (20-ft) radial distance to assess the extent of treatment, arrival data from adjacent injection wells (9.1-m [30-ft spacing]) were used as an indicator. To account for the increase in radial distance to this monitoring point, the phosphate concentration metric for arrival at adjacent injection wells was reduced to 20% to 30% of the injection concentration (from 50% at a 6.1-m [20-ft] distance). Based on this injection performance metric, the phosphate concentration measured at wells adjacent to the injection indicated satisfactory treatment. The effectiveness of the injection was most questionable between injection wells 199-N-144 and 199-N-145. Concentrations measured along this portion of the barrier provide an example of hydraulic interference between adjacent injections. The July 2007 injections in wells 199-N-144 and 199-N-136 occurred simultaneously. Based on the phosphate concentrations measured in well 199-N-145 during these injections, it appears the two injection mounds created by simultaneous treatment of these closely spaced wells worked against each other, thus limiting flux between the two points of injection and, subsequently, treatment at well 199-N-145. Phosphate concentration in well 199-N-145 during the July 2007 injection was only 25% of the injection concentration. However, monitoring in well 199-N-144 during both the March and July 2007 injections in well 199-N-145 indicated adequate treatment of this portion of the barrier. This example illustrates the need for maintaining adequate spacing between active injection wells to ensure satisfactory treatment.

Table 7.7. Comparison of Treatment Efficiency at Wells Adjacent to Injection Wells During FY 2007 Injections

Injection Well	Upstream Well % of Injection Solution SpC	Upstream Well % of Injection Solution PO ₄ Concentration	Downstream Well % of Injection Solution SpC	Downstream Well % of Injection Solution PO ₄ Concentration
199-N-138 (June)	No upstream well	No upstream well	38% (@15 ft) ^(a) Hanford	21% (@15 ft) ^(a) Hanford
199-N-138 (June)	No upstream well	No upstream well	66% (@15 ft) Ringold	42% (@ 15 ft) Ringold
199-N-139 (March)	90%	83%	86% ^(b)	76% ^(b)
199-N-140 (March)	54%	38%	47%	40%
199-N-140 (July)	74% ^(b)	86% ^(b)	50%	34%
199-N-141 (March)	66%	39%	80%	56%
199-N-142 (February)	26%	16%	83%	85%
199-N-142 (June)	54%	33%	82%	74%
199-N-143 (March)	80% ^(b)	67% ^(b)	94% ^(b)	95% ^(b)
199-N-144 (March)	92% ^(b)	105% ^(b)	90%	85%
199-N-144 (June)	82%	74%	45% ^(c)	26% ^(c)
199-N-145 (February)	47%	34%	64% ^(b)	17% ^(b)
199-N-145 (July)	56%	37%	91% ^(b)	90% ^(b)
199-N-136 (June)	45% ^(c)	26% ^(c)	78%	70%
199-N-137 (March)	54%	25%	101% (@15 ft) Hanford	90% (@15 ft) Hanford
199-N-137 (March)	No Ringold well	No Ringold well	75% (@15 ft) Ringold	50% (@15 ft) Ringold
(a) Arrival was higher at mid-injection (80% SpC and phosphate).				
(b) Previous injections interfered with results at adjacent monitoring wells.				
(c) Interference from concurrent injections at wells 199-N-144 and 199-N-136.				

A more thorough evaluation of treatment efficiency can be conducted for injections in the two wells at the ends of the barrier. At these locations, additional monitoring points were installed as part of the pilot test injection monitoring network. During the March injection in well 199-N-137, the phosphate concentrations in the Hanford formation at the end of the test indicated good treatment. Phosphate concentrations 4.6 m (15 ft) from the injection well were 70 to 90% of the injection solution phosphate concentration (Figure 7.2). More than 6.1 m (20 ft) from the injection well, the aquifer tube installed in the Hanford formation (APT-5S) had a phosphate concentration 60% of the injection solution.

Treatment of the Ringold Formation was not as effective. The phosphate concentrations measured at wells P2-7-R and P2-3-R indicated some treatment; however, the other monitoring wells screened in the Ringold Formation showed much lower (or nondetectable) phosphate concentrations. Monitoring well P2-9-R was screened lower in the Ringold Formation (see Figure 4.3) than the other wells. Arrival data indicated that what treatment there was in the Ringold Formation was mostly limited to that interval targeted by the screen. However, over time some reagent was lost deeper in the formation.

The injection during June 2007 in well 199-N-138 indicated generally comparable treatment in both Hanford and Ringold Formations (Figure 7.3), although somewhat less extensive in the Ringold Formation. Results from this injection indicate that a larger volume should be specified for future injections in wells located within the upstream portion of the barrier.

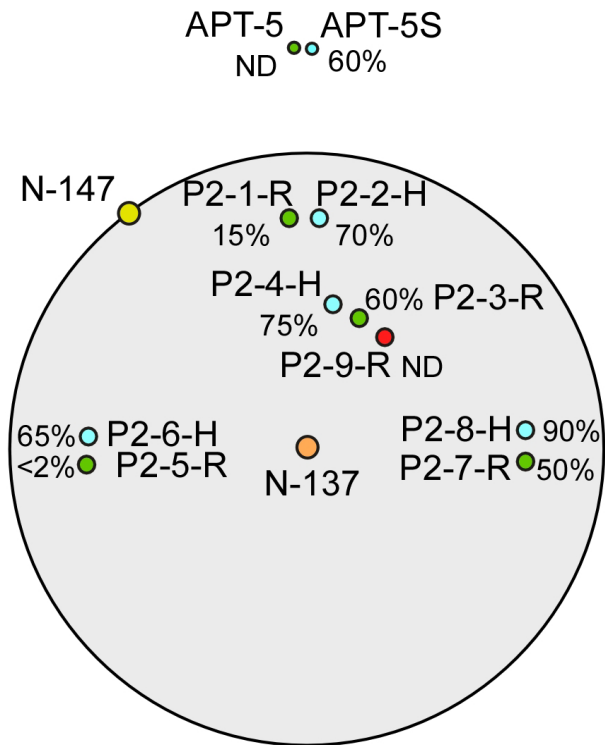


Figure 7.2. Treatment Efficiency Around Well 199-N-137 (Pilot Test Site #2) During March 2007 Injection. Final phosphate concentrations in monitoring wells reflected as percent of injection concentration. Shaded region shows ~20-ft radius. ND = No Data.

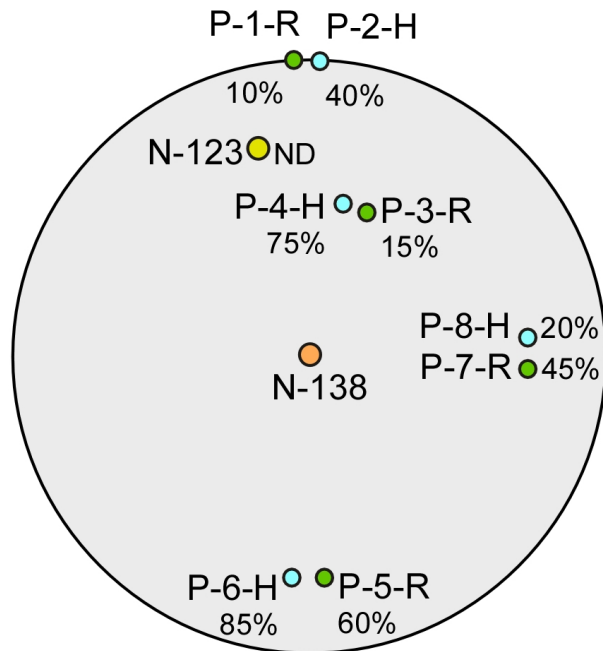


Figure 7.3. Treatment Efficiency Around 199-N-138 (Pilot Test Site #1) During June 2007 Injection. Final phosphate concentrations in monitoring wells reflected as percent of injection concentration. Shaded region shows ~20-ft radius. ND = No Data.

As indicated in Section 6.4, future injection volumes will be specified at 454,000 L (120,000 gal), which is a ~30% increase in volume from what was used during this injection. Consistent with pilot test #1, treatment of the Hanford formation appeared most effective north and south of the injection well, while treatment of the Ringold Formation appeared more effective east of the injection well. In fact, phosphate concentrations indicated that treatment of the Ringold Formation was more effective than treatment of the Hanford formation in that direction. Overall, this analysis supports the notion that effective treatment of both formations can be accomplished with the existing wells at the upstream portion of the barrier. Effective treatment along the downstream portion of the barrier will require injection wells screened only within the Ringold Formation.

7.3 Hydrogeologic Differences Along Barrier Length

During low-concentration treatment of the barrier, it was observed there were two distinct zones within the Hanford formation along the apatite barrier. The hydraulic conductivity of the Hanford formation appeared to be higher along the downstream half of the barrier, between wells 199-N-142 and 199-N-137. This was evident from the specific capacity estimates determined from drawdown response during well development (see Section 4.1.2), and from reagent arrivals in adjacent wells and the appearance of shoreline seeps during injection operations. The lower apparent hydraulic conductivity of the Hanford formation observed at pilot test site #1 (and assigned as representative of conditions over the upstream portion of the barrier) may be due in part to well inefficiency (i.e., skin effect) observed in these wells (see discussion in Sections 4.0 and 5.0).

While specific capacity cannot be directly related to hydraulic conductivity of the Hanford formation, it does provide an indication of the combined effects of formation permeability and well efficiency. The specific capacity on the downstream half of the barrier is 10 to 30 times higher than on the upstream portion of the barrier (see Figure 4.5). Given the consistent difference in specific capacity between the wells in the up and downstream portions of the barrier, it is apparent the downstream wells are in hydraulic communication with higher permeability materials than the upstream wells.

Another indicator of the relative difference in Hanford/Ringold formation permeability contrast over the upstream and downstream sections of the apatite barrier was provided by analysis of the arrival curves at wells adjacent to an injection well. Over the upstream portion of the barrier, the SpC of the adjacent wells increased gradually during the injection (Figure 7.4). Injections on the downstream portion of the barrier resulted in more rapid increases in SpC, which is indicative of a higher conductivity flow path (Figure 7.4).

Another example of this larger apparent permeability contrast between the Hanford and Ringold Formations is provided by the June 2007 injection in well 199-N-136. Partway between well 199-N-136 and 199-N-137, there was a well pair from the pilot test #2 well network. This well pair consisted of both a Hanford (PT-2-6H) and Ringold (PT-2-5R) monitoring point. The chemical arrival in the Hanford formation was consistent with the arrival monitored in the adjacent fully screened wells. However, there was no evidence of chemical arrival in the Ringold Formation (Figure 7.5).

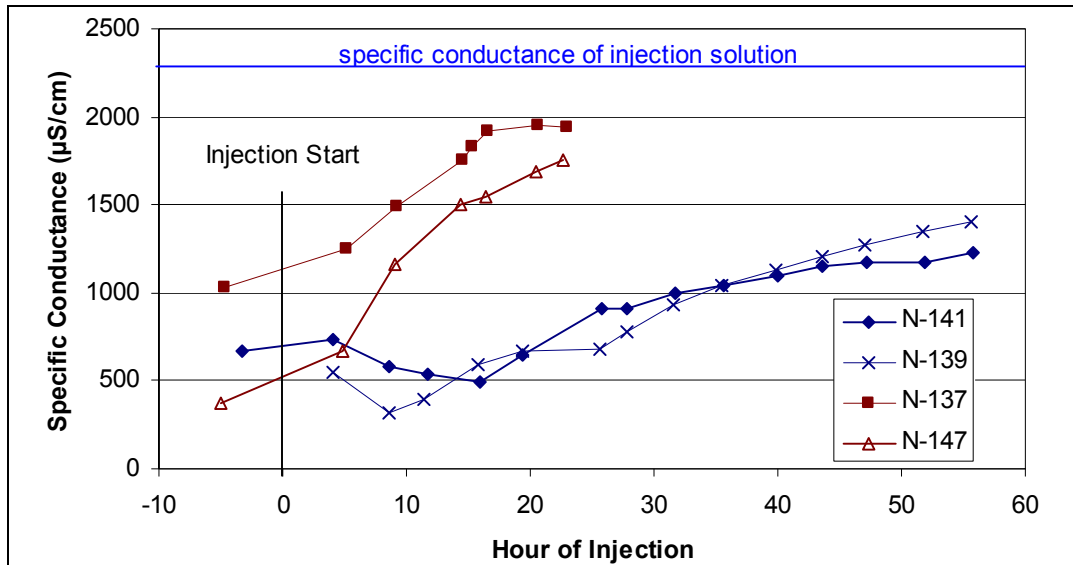


Figure 7.4. Arrival Curves for Wells Adjacent to Injection Well. Blue curves are for a March 2007 injection in well 199-N-140 (upstream portion of barrier). Red curves are for a June 2007 injection in well 199-N-136 (downstream portion of barrier). Prefix 199- omitted from well names.

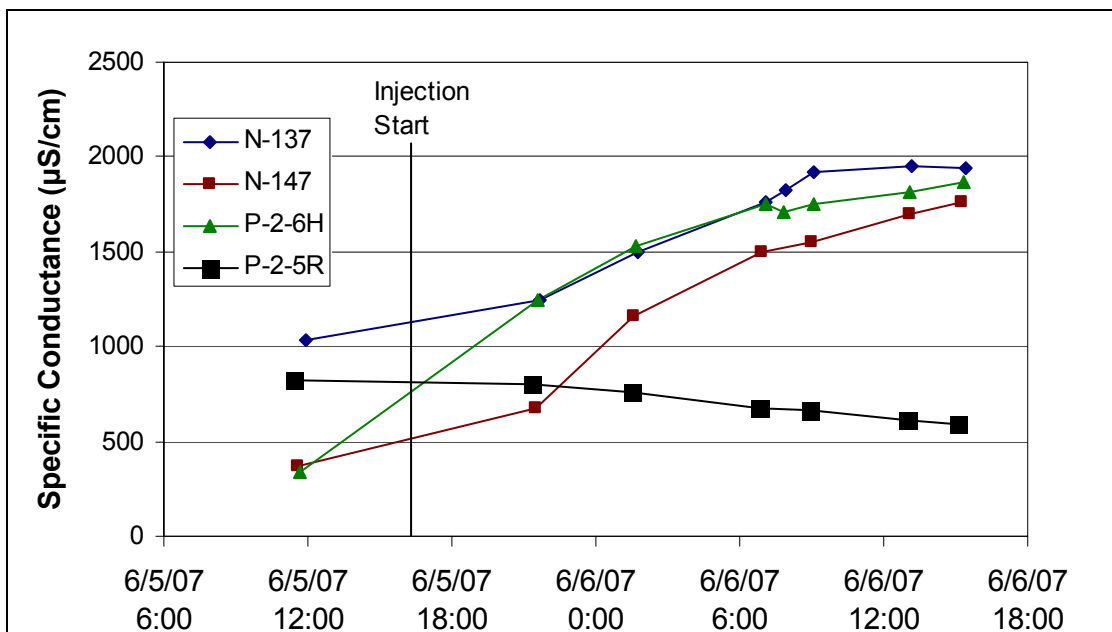


Figure 7.5. Arrival Curves for Wells Adjacent to 199-N-136 During the June 2007 Injection in Well 199-N-136. Prefix 199- omitted from well names.

Two injections in well 199-N-142 (March and June 2007) provide an example of a relatively asymmetric reagent transport distribution, which was exhibited to some degree at most of the injection well locations (see treatment efficiency estimates presented in Table 7.7). During both of these injections, much faster arrivals were observed in the downstream well (199-N-143) than in the upstream well (199-N-141) (Figure 7.6). This response indicates preferential flow in the downstream direction at this location. This effect was more pronounced during the low water (March 2007) injection.

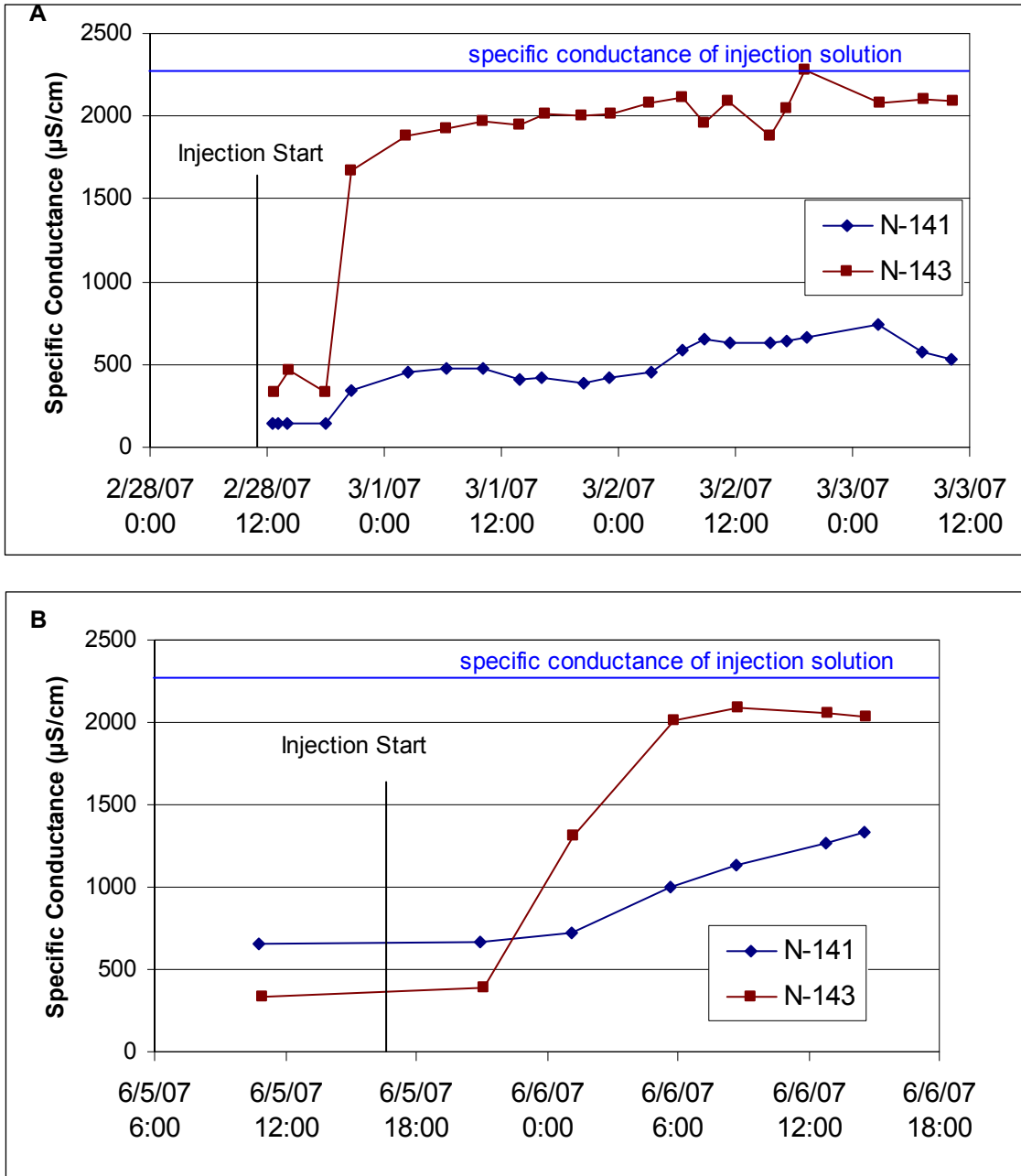


Figure 7.6. Arrival Curves for Wells Adjacent to Well 199-N-142 During March (A) and June (B) Injections in Well 199-N-142. Well 199-N-141 is upstream of 199-N-142; 199-N-143 is downstream.

8.0 100-N Apatite Low-Concentration Injection Performance Monitoring

The section describes the barrier performance following low-concentration apatite solution injections for the 91-m (300-ft) barrier. The objective of the low-concentration apatite solution injections is to stabilize the existing ^{90}Sr before injection of high-concentration apatite injections. The ionic strength of the injection solution, particularly divalent ions such as calcium, causes desorption of ^{90}Sr from the sediments resulting in temporary increased aqueous ^{90}Sr concentrations. Strontium-90 concentrations in groundwater along the Columbia River at the 100-N area show significant temporal variability based on measurements from aquifer tubes and long-term monitoring wells installed before the apatite treatability test. Additionally, there is a general spatial trend in ^{90}Sr concentrations in the aquifer along the river as shown in Figure 1.8. Because of the short time between the installation of compliance, injection, and pilot test monitoring wells at the 100-N Area apatite treatability test site and the Ca-citrate- PO_4 injections (started at the site in the spring of 2006), there were insufficient data from these wells to establish baseline ^{90}Sr ranges at the site. Therefore, baseline ^{90}Sr ranges were established for the injection and compliance wells at the treatability test site based on gross beta analysis from the aquifer tube monitoring and the limited preinjection monitoring from the treatability test wells.

Two different analytical methods and laboratories were used to measure ^{90}Sr as listed in Table 4.5 (^{90}Sr and $^{89/90}\text{Sr}$). The $^{89/90}\text{Sr}$ is reported in the Hanford Environmental Information System (HEIS) as “total beta radiostrontium.” Comparison of values from duplicate samples using these two different techniques yielded similar results. The results from these two different methods are indicated in the figures in this section. For simplicity, ^{90}Sr as referred to in the text includes both types of measurements (^{90}Sr and $^{89/90}\text{Sr}$). Additionally, Mendoza et al. (2007) has shown that aqueous gross beta measurements can directly correlate to aqueous ^{90}Sr concentrations around the 100-N Area shoreline with gross beta equal to two times the ^{90}Sr concentrations.

This section describes the data and methods used to establish a range of baseline ^{90}Sr concentrations for injection and compliance wells at the 100-N Area apatite treatability test site. The performance monitoring data available in February 2008 (which included the November 2007 sampling event) are provided in this section, which is organized by pilot test sites, barrier injection wells, compliance wells, and aquifer tubes. The performance monitoring data in this section include ^{90}Sr , calcium, phosphate, and specific conductance measurements.

Other performance measures for the 100-N apatite barrier include impact on general water quality (i.e., field parameters and trace metals), changes in aquifer permeability, and assessment of the amount of apatite formed from the field injections. Short-term monitoring results of field parameters and trace metals following the two pilot tests are described in Section 5.0. Analysis of longer-term field parameters and trace metal data will be included in the update of this interim report and/or in a separate report documenting results from high concentration treatment. Additionally, monitoring wells screened only in the Hanford formation at the pilot test sites have been dry since the June/July 2007 injections. Monitoring of these wells will resume when the river stage increases in spring 2008. Performance monitoring in the other wells is continuing with the results reported in subsequent reports. Because high-concentration injections will be conducted during the upcoming spring/summer high-river stage period, continued assessment of the effectiveness of the low-concentration treatments cannot be continued once these

injections commence. Attention will shift instead to performance assessment of the high-concentration treatments, which is the primary objective of the apatite treatability studies.

Changes in aquifer permeability from this process will also be assessed as part of the treatability test. Pressures and tracer arrivals monitored during the initial pilot injection tests will be compared to monitored values at the ending of high-concentration injections at the pilot test sites that are planned to begin in 2008. Numerical models developed for the pilot test sites will be used to estimate the hydraulic properties of these sites based on fitting the monitoring data collected during these tests.

Following the high Ca-citrate-PO₄ injections planned to begin in 2008, sediment samples will be collected from boreholes in the treatment zone (focused on the two pilot test sites) for laboratory analysis. These studies will be used to determine the quantity of apatite in the sediments achieved by the field injections and to estimate treatment longevity.

8.1 Estimation of Baseline Strontium-90 Concentrations

Only limited pretreatment data were available for the 10 apatite barrier injection wells, which made it difficult to establish baseline conditions for these wells, and therefore limited the ability to assess post-treatment performance data. However, more than a year of pretreatment data are available from downgradient aquifer tubes monitored as part of the Remediation and Closure Science Project (Mendoza et al. 2007) and one of the compliance monitoring wells installed in FY 2005 (others have a shorter data record but do provide some baseline information). In an attempt to use this previously collected data, a geostatistically based approach was implemented to estimate baseline conditions at the injection well locations based on the observed range in ⁹⁰Sr concentrations in these nearby aquifer tubes (Figure 8.1). Both spatial and temporal variability in ⁹⁰Sr concentration exists over the scale of the apatite barrier. The objective of this evaluation was to estimate the extent of temporal variability and the degree to which it varies spatially along the length of the barrier, to provide an improved understanding of baseline site conditions. This improved understanding of baseline conditions in turn allows for a more informed evaluation of the post-treatment performance assessment data collected to date.

Variogram analysis was conducted to assess and model the spatial variation. Available data were binned on a monthly basis, and the pretreatment concentration at the injection wells was estimated monthly using data from downgradient aquifer tubes, as well as available pretreatment observations in the compliance/injection wells. These data were collected separately for each month. Up to 12 monthly data collections were estimated by kriging with the use of the modeled variogram. Means and the 95% confidence intervals of the means were calculated.

8.1.1 Available Data

Injection and Compliance Wells: There are 10 injection wells (i.e., 199-N-138, 199-N-139, 199-N-140, 199-N-141, 199-N-142, 199-N-143, 199-N-144, 199-N-145, 199-N-136 and 199-N-137) and 4 compliance wells (199-N-123, 199-N-146, 199-N-122 and 199-N-147). After careful review of available data, a set of pretreatment observations were identified for the injection wells and compliance wells. Table 8.1 tabulates the 32 pretreatment data from the injection and compliance wells. Note there were no pretreatment observations available for 199-N-139 and 199-N-140. All other injection wells have a single pretreatment observation except for 199-N-137, which had two. Several more pretreatment observations were available for compliance wells 199-N-122 and 199-N-123.

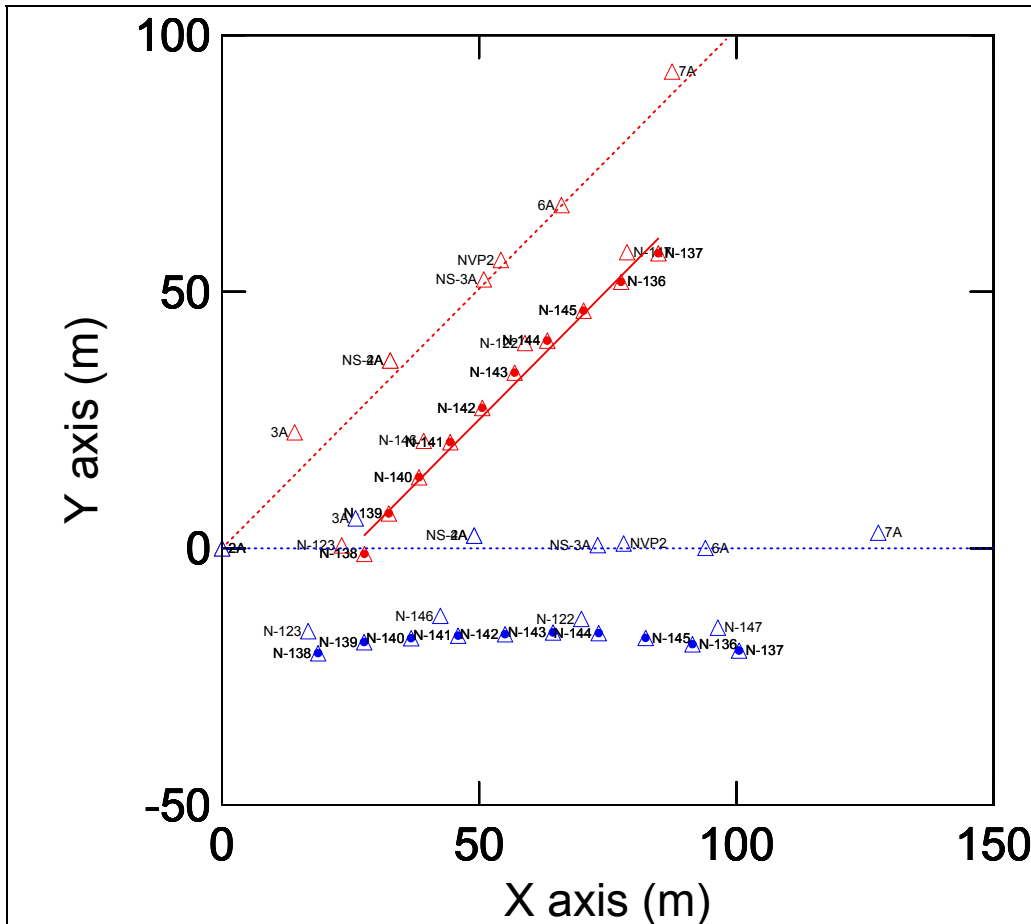


Figure 8.1. Spatial Coordinate Transform. Red symbols: wells in original coordinates relative to 2A. Solid red line: regression line based on the coordinates of 10 injection wells. This regression line defines the angle to be rotated. The dashed red line represents the x-axis that is rotated to the position shown as the dashed blue line. Blue symbols are well locations in the rotated coordinate system.

Aquifer Tubes: Gross beta concentration data, which has been shown to be directly correlated to ^{90}Sr concentration (Mendoza et al. 2007), from eight aquifer tubes (2A, 3A, 4A, 6A, 7A, NS-2A, NS-3A and NVP2, Figure 8.1) were evaluated for their usefulness in providing pretreatment ^{90}Sr baseline data. The selection of these aquifer tubes was based on their location relative to the apatite barrier and the depth interval sampled by the tube (116 m [380 ft] above mean sea level) was selected by Mendoza et al. (2007) to represent the highest concentration portion of the profile, and is the approximate contact between the Hanford/Ringold formations at the tube location. Data from these aquifer tubes were available from April 2004 to December 2007, with varying temporal coverage from tube to tube. A general cutoff for identifying pretreatment data in the aquifer tubes was prescribed as the initial injection test on well 199-N-137 at September 27, 2006. However, adjustment was made for aquifer tubes close to well 199-N-138, which had an initial injection on May 31, 2006. Table 8.2 lists the specification of pretreatment data retained from the aquifer tubes. After averaging the 24 duplicate observations on November 8, 2005, and the 2 duplicate observations on May 10, 2006, for NVP2, and the 2 duplicate observations on May 10, 2006 for NS-2A, and converting the gross beta to ^{90}Sr concentration (gross beta divided by two), a total of 102 pretreatment data were retained for the 8 aquifer tubes, as tabulated in Table 8.3.

Table 8.1. Pretreatment Baseline ⁹⁰Sr Measurements Identified for Injection and Compliance Monitoring Wells

Date/Time	Well Name	⁹⁰ Sr (pCi/L)	Easting (m) NAD83 (91) Datum	Northing (m) NAD83 (91) Datum
7/7/2006 11:00	199-N-136	1700.00	571337.18	149940.73
9/25/2006 13:24	199-N-137	1841.99	571344.43	149946.30
7/7/2006 13:38	199-N-137	875.00	571344.43	149946.30
4/26/06 9:24	199-N-138	811.24	571287.27	149887.72
7/10/2006 14:32	199-N-141	985.00	571303.97	149909.49
7/11/06 10:16	199-N-142	2200.00	571310.19	149916.16
7/11/2006 10:53	199-N-143	2050.00	571316.50	149923.04
7/11/06 11:54	199-N-144	1550.00	571322.83	149929.28
7/11/06 12:26	199-N-145	4450.00	571329.90	149935.11
11/28/2005 10:47	199-N-123	871.00	571282.86	149889.37
12/6/2005 11:48	199-N-123	745.00	571282.86	149889.37
1/16/2006 9:54	199-N-123	1180.00	571282.86	149889.37
1/31/2006 10:01	199-N-123	723.00	571282.86	149889.37
3/1/2006 12:20	199-N-123	857.00	571282.86	149889.37
4/12/2006 10:32	199-N-123	1040.00	571282.86	149889.37
11/28/2005 12:35	199-N-122	730.00	571318.48	149928.81
12/6/2005 13:07	199-N-122	1010.00	571318.48	149928.81
1/6/2006 12:07	199-N-122	657.00	571318.48	149928.81
5/18/2006 11:25	199-N-122	724.00	571318.48	149928.81
7/21/2006 8:57	199-N-122	2430.00	571318.48	149928.81
8/8/2006 9:52	199-N-122	2320.00	571318.48	149928.81
9/13/2006 10:13	199-N-122	4630.00	571318.48	149928.81
11/13/2006 10:42	199-N-122	1030.00	571318.48	149928.81
2/15/2007 13:18	199-N-122	942.00	571318.48	149928.81
7/11/2006 9:38	199-N-122	1150.00	571318.48	149928.81
6/13/2006 11:41	199-N-147	522.00	571338.34	149946.51
9/18/2006 11:50	199-N-147	1220.00	571338.34	149946.51
7/7/2006 12:20	199-N-147	685.00	571338.34	149946.51
6/13/2006 12:30	199-N-146	318.00	571298.80	149909.74
11/16/2006 9:22	199-N-146	882.00	571298.80	149909.74
2/15/2007 13:57	199-N-146	810.00	571298.80	149909.74
7/10/2006 15:12	199-N-146	665.00	571298.80	149909.74

The combined 134 pretreatment data from both aquifer tubes (Table 8.3) and injection/compliance wells (Table 8.1) were visually inspected for their temporal and spatial variations. For spatial variation, it was restricted to only consider the one-dimensional variation along the direction parallel to the injection barrier. To accomplish this, the following coordinate transformation was conducted. Coordinates of all wells/aquifer tubes relative to aquifer tube 2A were calculated. A regression line was established based on the relative coordinates of the 10 injection wells. The slope of the regression line established the rotation angle (about 45 degrees) for a new horizontal x axis with origin at 2A and parallel to the regression line passing through the 10 injection wells. All wells and aquifer tubes were projected to this new horizontal x axis. Figure 8.1 shows a sketch of this transformation, and Table 8.4 lists the distance of each well to the origin (aquifer tube 2A) along the regression line parallel to the apatite barrier.

Table 8.2. Name and Coordinates of Aquifer Tubes

Name	Easting (m) NAD83 (91) Datum	Northing (m) NAD83 (91) Datum	Comments
2A 116.0 m (screen top elev.)	571259.6	149888.8	Exclude data after 5/31/2006 (199-N-138). The first actually excluded is 6/6/2006.
3A 116.0 m (screen top elev.)	571273.7	149911.4	Exclude data after 5/31/2006 (199-N-138). The first actually excluded is 6/6/2006.
4A 116.0 m (screen top elev.)	571292.3	149925.4	Exclude data after 9/27/2006 (199-N-137). The first actually excluded is 3/15/2007.
6A 116.0 m (screen top elev.)	571325.6	149955.7	Exclude data after 9/27/2006 (199-N-137). The first actually excluded is 1/10/2007.
7A 116.0 m (screen top elev.)	571347.1	149981.7	Exclude data after 9/27/2006 (199-N-137). The first actually excluded is 3/14/2007.
NS-2A 116.1 m (screen top elev.)	571292.3	149925.4	No exclusion. Available data are between 4/9/2004 and 9/25/2006.
NS-3A 116.1 m (screen top elev.)	571310.5	149941.2	No exclusion. Available data are between 4/9/2004 and 11/1/2005.
NVP2 116.0 m (screen top elev.)	571313.8	149945	Exclude data after 9/27/2006 (199-N-137). The first actually excluded is 1/10/2007.

Table 8.3. Pretreatment Baseline ⁹⁰Sr Measurements Identified for Aquifer Tubes

Date/Time	Well Name	⁹⁰ Sr (pCi/L)	Date/Time	Well Name	⁹⁰ Sr
8/3/2005	2A	199.00	5/16/2005	NS-2A	1275.00
9/28/2005	2A	215.00	6/10/2005	NS-2A	1120.00
3/8/2006	2A	357.00	8/23/2005	NS-2A	1145.00
4/13/2006	2A	88.00	9/28/2005	NS-2A	1275.00
5/10/2006	2A	92.00	10/7/2005	NS-2A	1445.00
8/3/2005	3A	288.50	11/1/2005	NS-2A	1275.00
9/28/2005	3A	288.50	12/27/2005	NS-2A	1175.00
3/8/2006	3A	273.50	1/11/2006	NS-2A	1100.00
4/13/2006	3A	276.50	2/7/2006	NS-2A	1290.00
5/10/2006	3A	285.50	3/8/2006	NS-2A	1140.00
8/3/2005	4A	1040.00	4/13/2006	NS-2A	1380.00
9/28/2005	4A	1130.00	5/10/2006	NS-2A	1477.50
12/27/2005	4A	945.00	6/6/2006	NS-2A	1170.00

Table 8.3. (contd)

Date/Time	Well Name	⁹⁰ Sr (pCi/L)	Date/Time	Well Name	⁹⁰ Sr
1/11/2006	4A	935.00	7/20/2006	NS-2A	1105.00
2/7/2006	4A	1330.00	8/16/2006	NS-2A	1410.00
3/8/2006	4A	1040.00	9/25/2006	NS-2A	1555.00
4/13/2006	4A	965.00	4/9/2004	NS-3A	2930.00
5/10/2006	4A	875.00	6/9/2004	NS-3A	3855.00
6/6/2006	4A	985.00	8/16/2004	NS-3A	3115.00
7/20/2006	4A	1055.00	9/25/2004	NS-3A	2605.00
8/16/2006	4A	1075.00	10/29/2004	NS-3A	2855.00
9/25/2006	4A	1235.00	12/15/2004	NS-3A	2385.00
8/3/2005	6A	434.00	1/20/2005	NS-3A	2705.00
9/28/2005	6A	394.50	2/18/2005	NS-3A	2930.00
12/27/2005	6A	365.00	3/8/2005	NS-3A	2490.00
1/11/2006	6A	389.50	3/18/2005	NS-3A	2985.00
2/7/2006	6A	338.00	4/19/2005	NS-3A	3020.00
3/8/2006	6A	368.50	5/16/2005	NS-3A	4070.00
4/13/2006	6A	428.50	6/10/2005	NS-3A	4125.00
5/10/2006	6A	424.00	6/17/2005	NS-3A	4300.00
6/6/2006	6A	407.50	7/18/2005	NS-3A	4160.00
7/20/2006	6A	372.50	8/3/2005	NS-3A	3355.00
8/16/2006	6A	411.00	8/23/2005	NS-3A	3125.00
9/25/2006	6A	408.50	8/26/2005	NS-3A	2685.00
8/3/2005	7A	260.00	9/28/2005	NS-3A	3115.00
9/28/2005	7A	279.50	10/7/2005	NS-3A	3325.00
3/8/2006	7A	277.50	11/1/2005	NS-3A	2970.00
4/13/2006	7A	350.00	8/3/2005	NVP2	2525.00
5/10/2006	7A	383.00	9/28/2005	NVP2	2870.00
6/6/2006	7A	426.50	11/8/2005	NVP2	3513.96
9/25/2006	7A	266.50	12/27/2005	NVP2	2235.00
4/9/2004	NS-2A	1465.00	1/11/2006	NVP2	2560.00
6/9/2004	NS-2A	1460.00	2/7/2006	NVP2	2145.00
8/16/2004	NS-2A	1380.00	3/8/2006	NVP2	2115.00
9/25/2004	NS-2A	1340.00	4/13/2006	NVP2	1650.00
10/29/2004	NS-2A	1270.00	4/13/2006	NVP2	1515.00
12/15/2004	NS-2A	1050.00	5/10/2006	NVP2	1462.50
1/20/2005	NS-2A	1125.00	6/6/2006	NVP2	1240.00
2/18/2005	NS-2A	1125.00	7/20/2006	NVP2	2955.00
3/18/2005	NS-2A	1080.00	8/16/2006	NVP2	4285.00
4/19/2005	NS-2A	1060.00	9/25/2006	NVP2	2910.00

Figure 8.2 displays the time series and Figure 8.3 displays the monthly binned time series of the pretreatment observations in aquifer tubes and injection/compliance wells, respectively. Obvious temporal variations can be seen at NS-3A and NVP2. Figure 8.4 presents a plot of spatial variation of the pretreatment concentration by grouping data to each month and plotting against the distance from aquifer tube 2A along the projected line parallel to the barrier. As indicated in Figure 8.4, an obvious spatial pattern exists.

Table 8.4. Distance of Each Well to the Origin (Aquifer Tube 2A) Along the Regression Line Parallel to the Apatite Barrier (see Figure 8.1)

Well Name	Projected X (m)
199-N-136	91.47
199-N-137	100.52
199-N-138	18.68
199-N-139	27.63
199-N-140	36.76
199-N-141	45.90
199-N-142	55.02
199-N-143	64.35
199-N-144	73.24
199-N-145	82.35
199-N-146	42.45
199-N-147	96.39
199-N-122	69.84
199-N-123	16.75
2A	0.00
3A	25.99
4A	49.02
6A	93.98
7A	127.58
NS-2A	49.02
NS-3A	73.05
NVP2	78.07

Data variation ranges (i.e., minimum and maximum) at the aquifer tubes and the compliance wells were retrieved from the data in Tables 8.1 and 8.3 and plotted against the distance from the aquifer tube 2A in Figure 8.5 (minima shown in red-solid down triangle and maxima shown in blue-solid up triangle). Note the pretreatment data from the injection wells were used by assigning them to nearby river tubes/compliance wells as long as the distance is smaller than 10 m (33 ft). The minima and maxima at aquifer tube 4A and NS-2A were combined because they have the same projected distance to 2A and the smallest was used as the minima and the largest was used as the maxima. Data ranges at the injection well locations were estimated by linear interpolation to their location along the regression line, as shown in Figure 8.5 as the black open circles. Some pretreatment data from the injection wells was significantly higher than values from nearby river tubes and compliance wells, which resulted in interpolated maximum values at these locations that exceeded the bounds of the interpolated data range (e.g., July 11, 2006 at N145 with Sr=4450 and September 25, 2006, at 199-N-137 with Sr=1842). To address this inconsistency, a simple rule was applied that involved extending the data range to include these values whenever this condition occurred. Such estimations of data ranges considered the temporal and spatial variations of the nearby aquifer tubes and compliance wells. Table 8.5 lists the extracted data ranges for aquifer tubes and compliance wells along with the estimated data ranges for the injection wells.

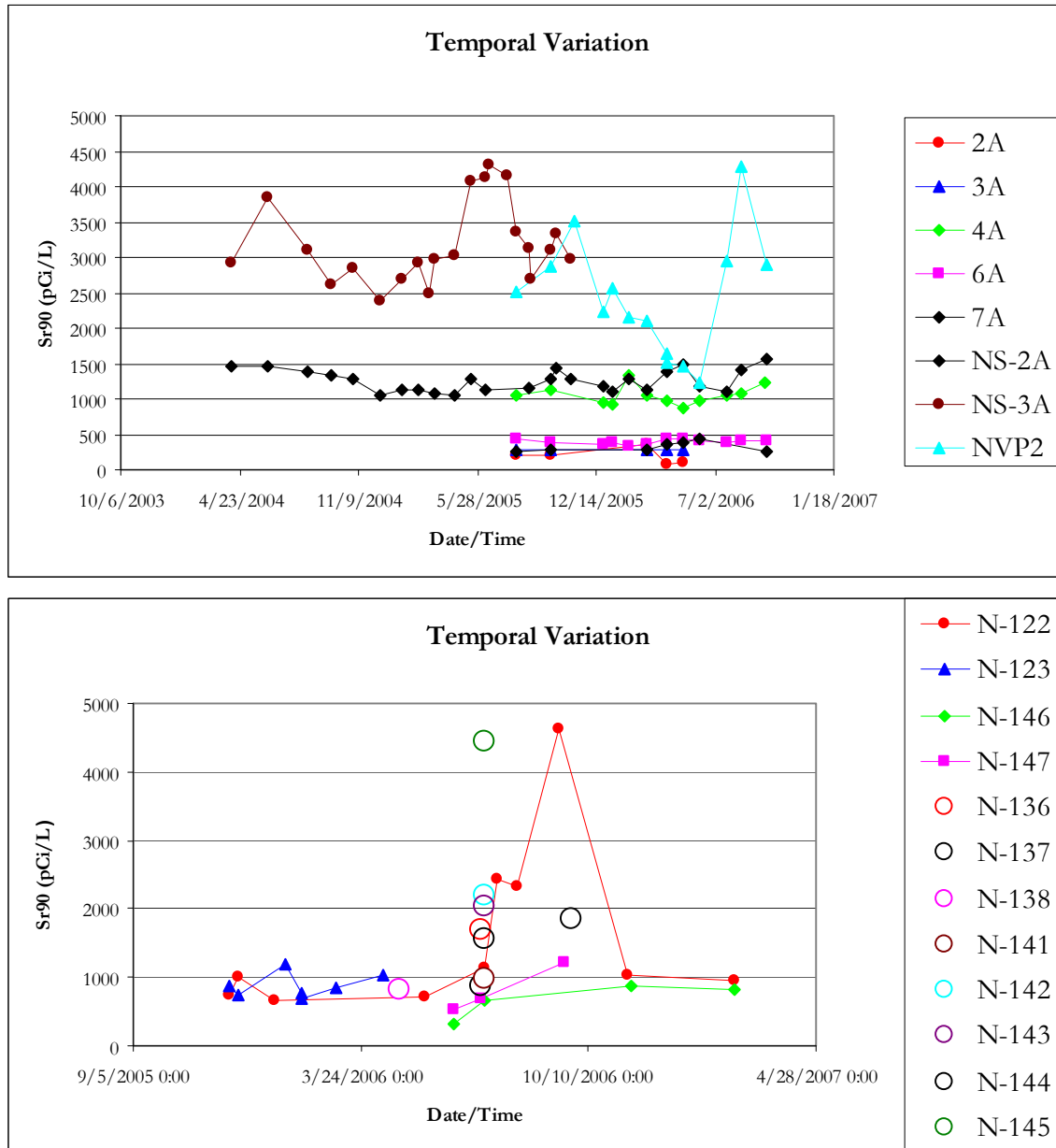


Figure 8.2. (a) Temporal Variation in Pretreatment Observations for Aquifer Tubes and (b) Temporal Variation in Pretreatment Observations for Injection/Compliance Wells. Prefix 199-omitted from well names.

Considering the spatial and temporal variation, researchers also decided to model the spatial variation through variogram analysis (ignoring possible spatial variation along the direction perpendicular to the barrier) and to bin the available data on the monthly basis (ignoring year-to-year variations), then to estimate the pretreatment concentration on each month at each injection well. Multiple data points resulting from binning of the data on a monthly basis were averaged to provide a single monthly value. The processed data set consisted of 90 data points, as tabulated in Table 8.6.

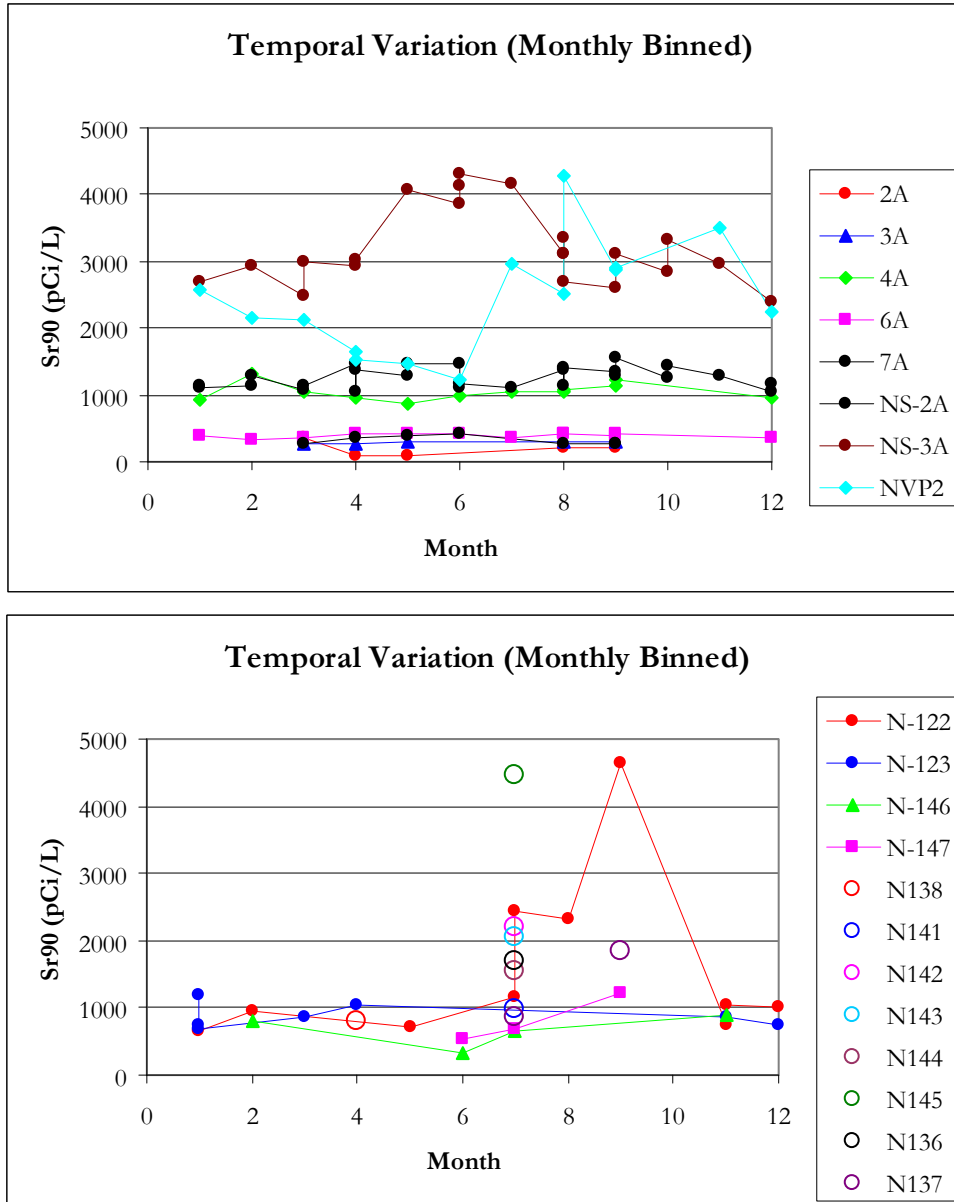


Figure 8.3. (a) Temporal Variation in Pretreatment Observations (monthly binned) for Aquifer Tubes and (b) Temporal Variation in Pretreatment Observations (monthly binned) for Injection/Compliance Wells. Prefix 199- omitted from well names.

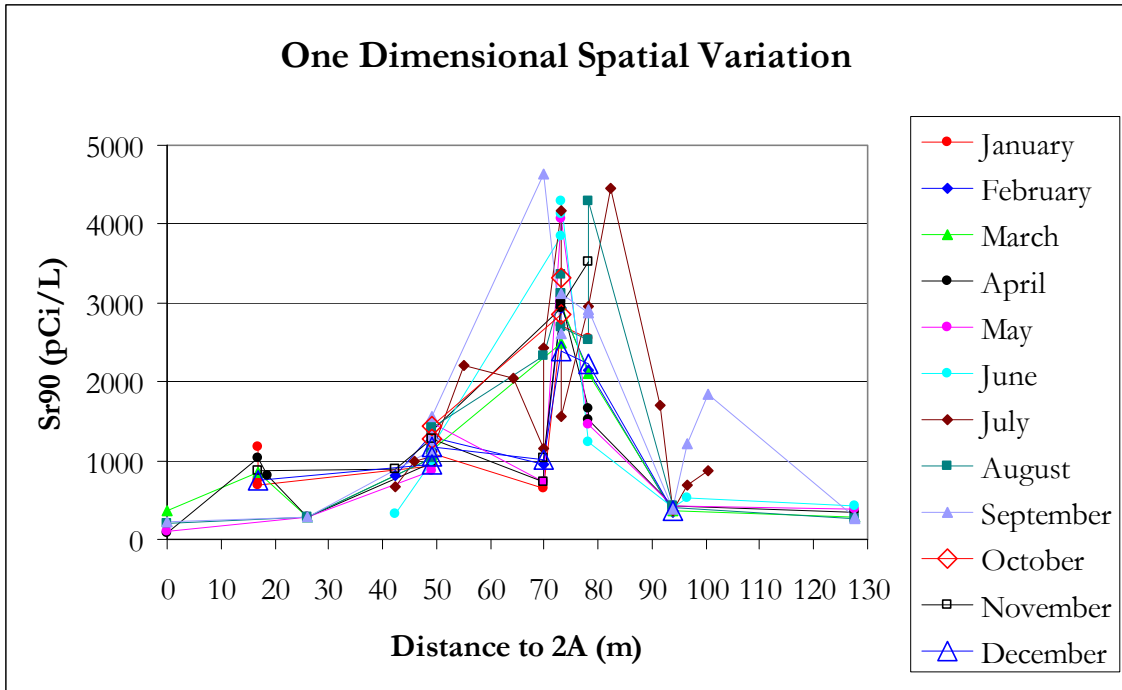


Figure 8.4. Spatial Variation

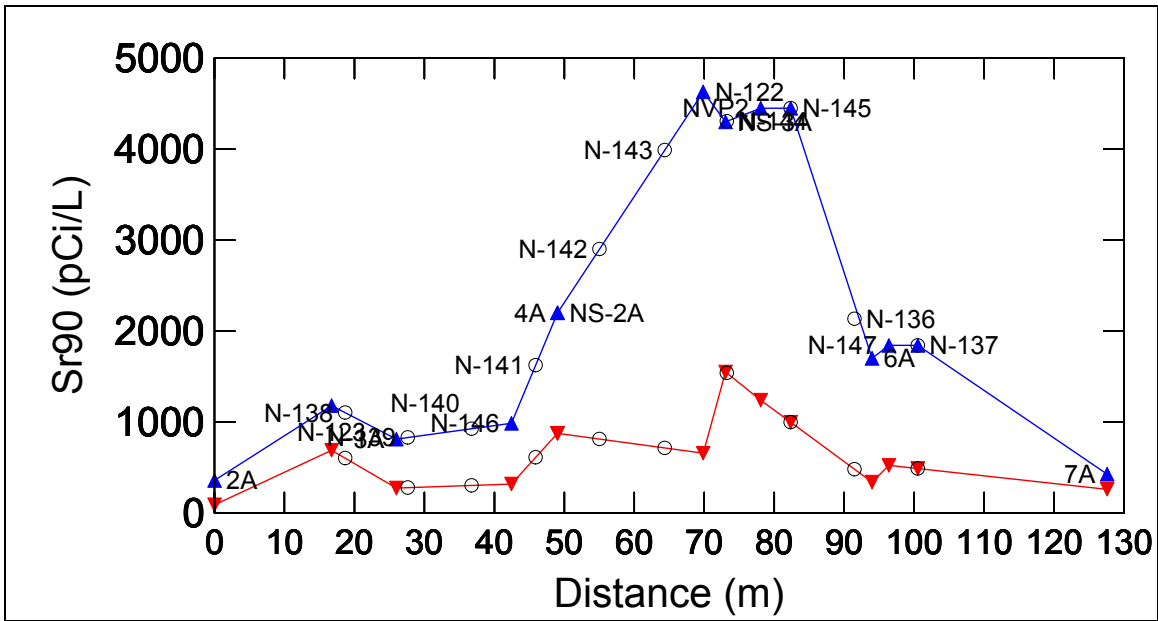


Figure 8.5. Data Ranges Extracted for Aquifer Tubes and Compliance Wells (minima shown in red-solid down triangle and line and maxima shown in blue-solid up triangle and line) and Estimated for Injection Wells (open black circles). Prefix 199- omitted from well names.

Table 8.5. Data Ranges (i.e., minimum and maximum) Extracted for Aquifer Tubes and Compliance Wells and Linearly Interpolated for Injections Wells (Note: 4A and NS-2A have the same projected X distance from 2A, and the smaller of the wells was used for the minimum and the larger of them was used for the maximum at that distance).

Well Name	Projected_X (m)	⁹⁰ Sr		Flag
		Minimum (pCi/L)	Maximum (pCi/L)	
2A	0.00	88.00	357.00	Extracted
199-N-123	16.75	689.00	1180.00	Extracted
199-N-138	18.68	602.33	1103.08	Interpolated
3A	25.99	273.50	811.24	Extracted
199-N-139	27.63	277.94	828.59	Interpolated
199-N-140	36.76	302.64	925.01	Interpolated
199-N-146	42.45	318.00	985.00	Extracted
199-N-141	45.90	610.93	1623.98	Interpolated
4A	49.02	875.00	2200.00	Extracted
NS-2A	49.02	875.00	2200.00	Extracted
199-N-142	55.02	812.18	2900.20	Interpolated
199-N-143	64.35	714.53	3988.71	Interpolated
199-N-122	69.84	657.00	4630.00	Extracted
NS-3A	73.05	1550.00	4300.00	Extracted
199-N-144	73.24	1538.47	4305.58	Interpolated
NVP2	78.07	1240.00	4450.00	Extracted
199-N-145	82.35	997.24	4450	Interpolated
199-N-136	91.47	480.34	2133.98	Interpolated
6A	93.98	338.00	1700.00	Extracted
199-N-147	96.39	522.00	1841.99	Extracted
199-N-137	100.52	487.30	1841.99	Interpolated
7A	127.58	260.00	426.50	Extracted

Figure 8.6 shows the histogram of the strontium concentrations and those after logarithm transformation. Researchers decided to perform variogram analysis and kriging estimation on the normal score transformed data (Deutsch and Journel 1998). The experimental variogram and the variogram model are shown in Figure 8.7.

Program *kt3d* in *gslib* (Deutsch and Journel 1998) was used for kriging. The kriging domain was specified to include a total of 8475 nodes to provide sufficient resolution to assure that estimates were available at the injection well locations. The data set in Table 8.6 was split into 12 subsets, one for each month with only data grouped at that month.

Table 8.7 presents the kriging estimates for each of the 10 injection wells. Estimates were missing when no nearby data could be found. The means and 95% confidence interval of the means were calculated based on the data in Table 8.7 and presented in Table 8.8. Figure 8.8 displays the temporal variation in the estimated pretreatment ⁹⁰Sr concentration at the injection well locations together with the measured data from NS-3A, NVP2. Figure 8.9 presents notched box plots of the kriged estimation listed in Table 8.7. Figure 8.10 show the combination of the estimated ranges of the pretreatment data (Table 8.5 and Figure 8.5, open-black circle), the kriging estimated 95% confidence interval of the mean

pretreatment data (Table 8.8, shown as light blue, open-upper triangle and pink open-down triangle), and the actual measured pretreatment data (Table 8.1, shown as red cross).

Table 8.6. Data Retained for Variogram Analysis and Kriging Estimation (red-framed numbers indicate averages were taken from multiple data points)

Projected X (m)	Month	Avg ⁹⁰ Sr (pCi/L)	Well Name	Date/Time	Projected X (m)	Month	Avg ⁹⁰ Sr (pCi/L)	Well Name	Date/Time
16.75	1	875.33	199-N-123	1/16/2006 9:54	42.45	7	665	199-N-146	7/10/2006 15:12
49.02	1	1053.33	4A	1/11/2006	45.90	7	985	199-N-141	7/10/2006 14:32
69.84	1	657	199-N-122	1/6/2006 12:07	49.02	7	1080	4A	7/20/2006
73.05	1	2705	NS-3A	1/20/2005	55.02	7	2200	199-N-142	7/11/2006 10:16
78.07	1	2560	NVP2	1/11/2006	64.35	7	2050	199-N-143	7/11/2006 10:53
93.98	1	389.5	6A	1/11/2006	69.84	7	1790	199-N-122	7/11/2006 9:38
42.45	2	810	199-N-146	2/15/2007 13:57	73.05	7	4160	NS-3A	7/18/2005
49.02	2	1248.33	4A	2/7/2006	73.24	7	1550	199-N-144	7/11/2006 11:54
69.84	2	942	199-N-122	2/15/2007 13:18	78.07	7	2955	NVP2	7/20/2006
73.05	2	2930	NS-3A	2/18/2005	82.35	7	4450	199-N-145	7/11/2006 12:26
78.07	2	2145	NVP2	2/7/2006	91.47	7	1700	199-N-136	7/7/2006 11:00
93.98	2	338	6A	2/7/2006	93.98	7	372.5	6A	7/20/2006
0.00	3	357	2A	3/8/2006	96.39	7	685	199-N-147	7/7/2006 12:20
16.75	3	857	199-N-123	3/1/2006 12:20	100.52	7	875	199-N-137	7/7/2006 13:38
25.99	3	273.5	3A	3/8/2006	0.00	8	199	2A	8/3/2005
49.02	3	1086.67	4A	3/8/2006	25.99	8	288.5	3A	8/3/2005
73.05	3	2737.50	NS-3A	3/8/2005	49.02	8	1210	4A	8/3/2005
78.07	3	2115	NVP2	3/8/2006	69.84	8	2320	199-N-122	8/8/2006 9:52
93.98	3	368.5	6A	3/8/2006	73.05	8	3070	NS-3A	8/16/2004
127.58	3	277.5	7A	3/8/2006	78.07	8	3405	NVP2	8/3/2005
0.00	4	88	2A	4/13/2006	93.98	8	422.5	6A	8/3/2005
16.75	4	1040	199-N-123	4/12/2006 10:32	127.58	8	260	7A	8/3/2005
18.68	4	811.24	199-N-138	4/26/06 9:24	0.00	9	215	2A	9/28/2005
25.99	4	276.5	3A	4/13/2006	25.99	9	288.5	3A	9/28/2005
49.02	4	1217.5	4A	4/13/2006	49.02	9	1307	4A	9/28/2005
73.05	4	2975	NS-3A	4/9/2004	69.84	9	4630	199-N-122	9/13/2006 10:13
78.07	4	1582.5	NVP2	4/13/2006	73.05	9	2860	NS-3A	9/25/2004
93.98	4	428.5	6A	4/13/2006	78.07	9	2890	NVP2	9/28/2005
127.58	4	350	7A	4/13/2006	93.98	9	401.5	6A	9/28/2005
0.00	5	92	2A	5/10/2006	96.39	9	1220	199-N-147	9/18/2006 11:50
25.99	5	285.5	3A	5/10/2006	100.52	9	1841.99	199-N-137	9/25/2006 13:24
49.02	5	1209.17	4A	5/10/2006	127.58	9	273	7A	9/28/2005
69.84	5	724	199-N-122	5/18/2006 11:25	49.02	10	1357.50	NS-2A	10/29/2004
73.05	5	4070	NS-3A	5/16/2005	73.05	10	3090.00	NS-3A	10/29/2004
78.07	5	1462.5	NVP2	5/10/2006	16.75	11	871	199-N-123	11/28/2005 10:47
93.98	5	424	6A	5/10/2006	42.45	11	882	199-N-146	11/16/2006 9:22
127.58	5	383	7A	5/10/2006	49.02	11	1275	NS-2A	11/1/2005
42.45	6	318	199-N-146	6/13/2006 12:30	69.84	11	880	199-N-122	11/28/2005 12:35
49.02	6	1183.75	4A	6/6/2006	73.05	11	2970	NS-3A	11/1/2005
73.05	6	4093.3333	NS-3A	6/9/2004	78.07	11	3513.96	NVP2	11/8/2005
78.07	6	1240	NVP2	6/6/2006	16.75	12	745	199-N-123	12/6/2005 11:48
93.98	6	407.5	6A	6/6/2006	49.02	12	1056.67	4A	12/27/2005
96.39	6	522	199-N-147	6/13/2006 11:41	69.84	12	1010	199-N-122	12/6/2005 13:07
127.58	6	426.5	7A	6/6/2006	73.05	12	2385	NS-3A	12/15/2004
					78.07	12	2235	NVP2	12/27/2005
					93.98	12	365	6A	12/27/2005

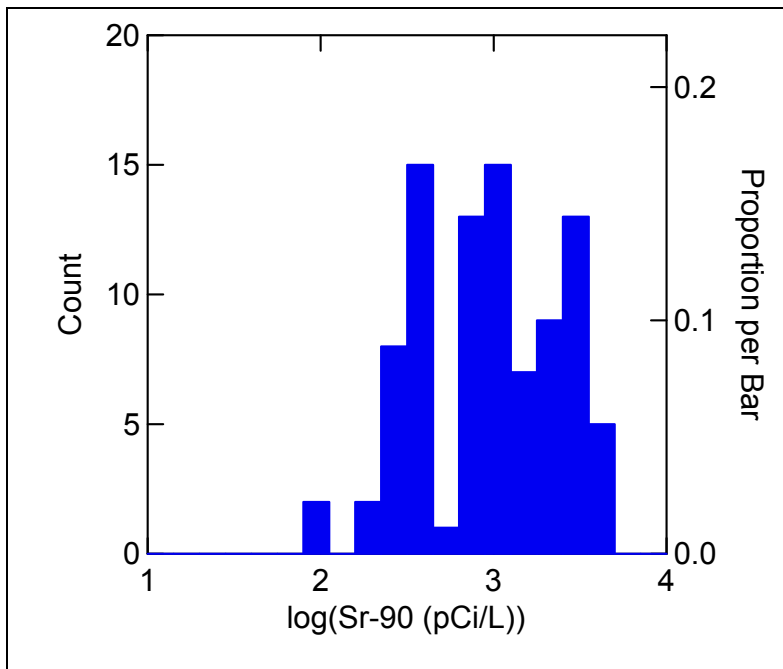
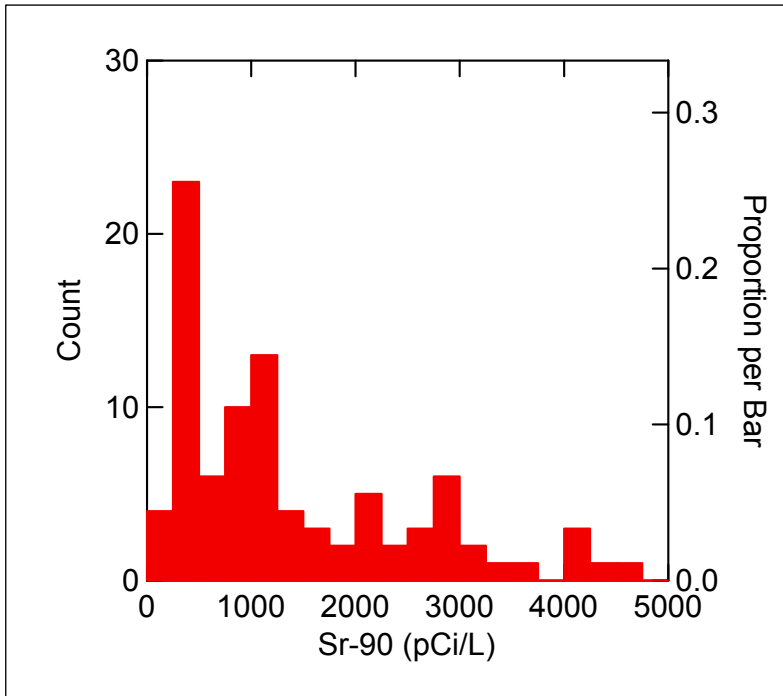


Figure 8.6. Histogram of Strontium Concentrations in Table 8.6

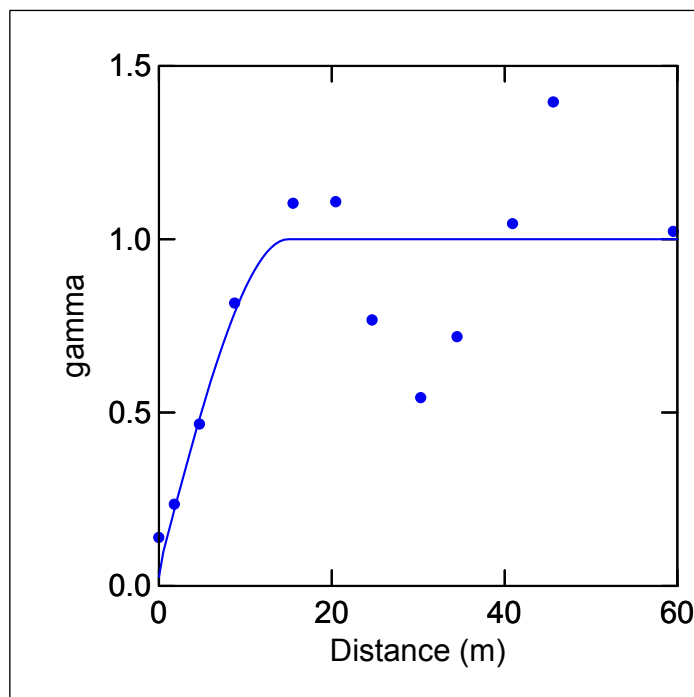


Figure 8.7. Calculated Variogram and Variogram Model

Table 8.7. Kriged Estimate of Pretreatment ⁹⁰Sr Concentrations (pCi/L) for Each Month at the 10 Injection Wells

Month	199-N-138	199-N-139	199-N-140	199-N-141	199-N-142	199-N-143	199-N-144	199-N-145	199-N-136	199-N-137
January					1081.98	834.50	2373.26	1353.57	658.04	
February			875.05	1046.67	1273.20	1054.54	2838.24	1211.84	398.16	
March	450.30	276.66	396.17	877.49	1298.88	2030.48	2718.15	1233.92	425.37	
April	811.23	281.40	520.51	991.88	1723.96	2320.85	2968.68	1218.43	810.42	
May	272.02		425.29	959.89	1257.69	858.83	3271.34	1071.06	759.29	
June			369.37	663.72	1634.66	2863.93	4042.85	1055.50	684.67	453.22
July		861.75	883.41	984.51	2200.12	2049.31	1549.83	4449.93	1698.17	875.01
August	275.64		500.03	1008.02	1566.72	2158.23	3038.70	2711.30	812.40	
September	276.26		660.63	1085.09	2366.50	4171.53	2931.30	2197.08	706.32	1842.18
October					2152.01	2861.35				
November		875.26	1013.00	1132.97	1316.33	1081.75	2955.01	2999.71	3087.40	
December					1209.17	1054.18	2273.30	1246.68	423.38	

Table 8.8. The Mean and 95% Confidence Interval of the Mean of the Kriged Pretreatment ⁹⁰Sr Concentration (pCi/L) at Each Injection Well

STATISTIC	199-N-138	199-N-139	199-N-140	199-N-141	199-N-142	199-N-143	199-N-144	199-N-145	199-N-136	199-N-137
N of cases	5	4	9	9	12	12	11	11	11	3
Mean	417.09	573.77	627.05	972.25	1590.10	1944.96	2814.61	1886.27	951.24	1056.80
95% CI Upper	706.51	1115.39	812.41	1077.59	1866.73	2597.18	3235.32	2621.08	1483.42	2825.77
95% CI Lower	127.66	32.14	441.69	866.91	1313.48	1292.74	2393.89	1151.47	419.06	-712.16

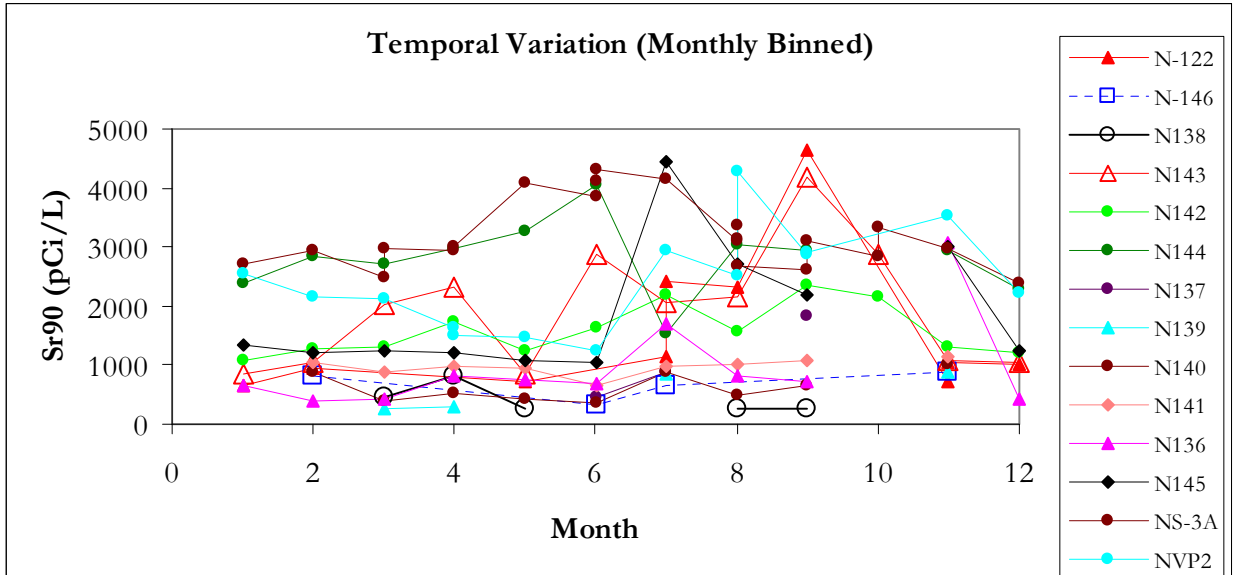


Figure 8.8. Temporal Variation of the Estimated Pretreatment ^{90}Sr Concentrations at the Injection/ Compliance Along with Measured Concentrations at Aquifer Tubes NS-3A and NVP2. Prefix 199- omitted from well names.

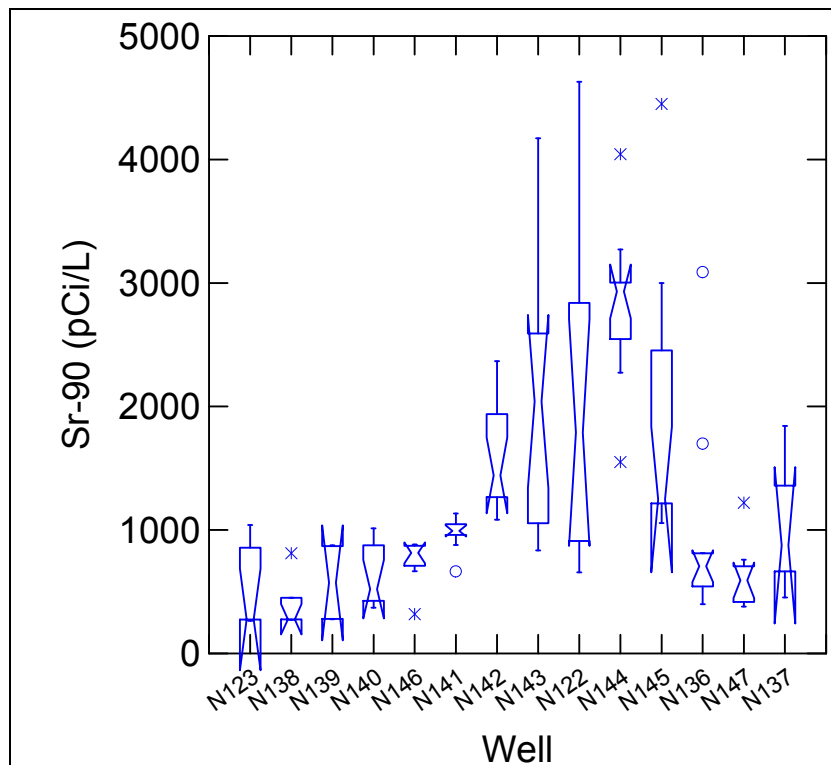


Figure 8.9. The Notched Box Plot of the Kriged Pretreatment ^{90}Sr Concentration at Each Injection Well (data shown in Table 8.6). The boxes are notched at the median value and return to full width at the upper and lower 95% confidence intervals. Prefix 199- omitted from well names.

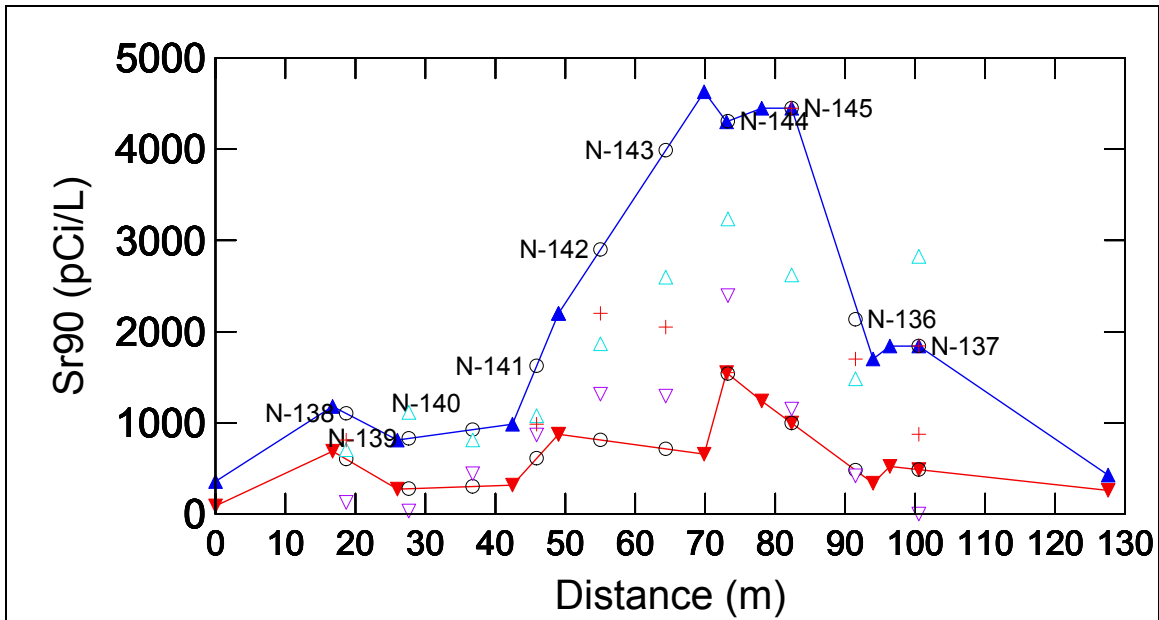


Figure 8.10. Interpolated Ranges (black-open circle, data in Table 8.5), Estimated CIs (light-blue, open-up triangle and pink open-down triangles for 95% CI upper and lower, respectively, data in Table 8.8), and Measurements (red cross, data in Table 8.1) of Baselines of the Injection Wells. Also shown are baseline data ranges for aquifer tubes and compliance wells (minima shown in red-solid down triangle, and line and maxima shown in blue-solid up triangle and line). Prefix 199- omitted from well names.

Note that several assumptions, as described above, were required to derive the means and their 95% confidence intervals using the selected approach. Subsequently, the data shown in Table 8.8 should not be used for strict statistical comparison, but rather to provide a general assessment of baseline ^{90}Sr concentrations at the injection well locations.

8.2 Field Test Performance – Pilot Test Sites

The pilot test site #1 consists of one injection well (199-N-138), eight monitoring wells (199-N-126 through 199-N-133), and one aquifer tube (APT-1). The pilot test site #2 consists of one injection well (199-N-137), nine monitoring wells (199-N-148 through 199-N-156), and one aquifer tube (APT-5). However, data from four of the nine pilot test site #2 monitoring wells are not described here because of a lack of data from these wells because of dry sampling conditions during low-river stage. Data gaps exist in the monitoring for other pilot test site wells that are screened only in the Hanford Formation when they are dry.

Detailed short-term monitoring results at the pilot test sites are described in Sections 5.2 for pilot test #1 and Section 5.3 for pilot test #2. These short-term results include field parameters, anions, and ^{90}Sr measurements. Longer-term monitoring results are provided below for ^{90}Sr and calcium, phosphate, and SpC.

8.2.1 Field Test Performance – Pilot Test Site #1

The pilot test #1 performance monitoring plots for ^{90}Sr and $^{89/90}\text{Sr}$ are shown in Figure 8.11 for the injection well and in Appendix B for the monitoring wells (B.2 through B.10). The minimum and maximum baseline range was determined for the injection well (199-N-138) from analysis of preinjection (i.e., 2004-2006) ^{90}Sr and gross beta concentration data from river aquifer tubes along the river shoreline (see preceding Section 8.1 and Table 8.5), and from the limited baseline data from the injection and compliance wells. This analysis for determining this baseline range assesses the spatial and temporal variability in concentrations. Because no long-term data are available to show the variability in concentrations over time for the pilot test site #1 wells, the range of 602 to 1103 pCi/L determined by the analysis for the injection well was assigned to all pilot test #1 wells. The ^{90}Sr data from five of six pilot test #1 wells and an aquifer tube for samples collected in April 2006, before the first injection at 199-N-138, show values that are within this assigned baseline range.

Immediately following the first injection on May 31 to June 1, 2006, ^{90}Sr concentrations in the pilot test #1 wells increased to a maximum ranging up to 7829 pCi/L on June 2, 2006 (see figures in Appendix B.1). Approximately 1 to 2 months after the first injection, concentrations appear to have increased a second time, reaching a maximum up to 12,000 pCi/L in one well (Figure B.7). Following this maximum, concentrations decreased significantly for 1 to 2 months and then continued to decrease before the second injection on June 8, 2007. No samples were collected from pilot test #1 monitoring wells for ^{90}Sr analyses during the March 22, 2007, injection at nearby well 199-N-139.

The pilot test #1 performance monitoring plots for calcium, phosphate, and SpC are shown in Figures 8.12 for the injection well and in Appendix B for the monitoring wells (B.12 through B.20). Complete datasets for these measurements have not been entered into HEIS or otherwise made available for use in this interim report. The plots indicate significant variability in SpC that coincides with increased ^{90}Sr concentrations following the first injection on May 31, 2006. Many of the plots indicate a double spike in SpC; one increase during the injection, and another increase approximately 1 to 2 months after the injection. These double spikes occur in the four wells that are completed in the Ringold Formation. SpC levels ranged up to 2970 $\mu\text{S}/\text{cm}$ during the injection (Figure B.14) and up to 3620 $\mu\text{S}/\text{cm}$ approximately 1 to 2 months after the injection (Figure B.15). All pilot test #1 wells also show an increase in calcium and phosphate concentrations during the May 31, 2006, injection.

Following the second injection on June 8-10, 2007, ^{90}Sr concentrations increased in some of the pilot test #1 wells, but did not increase to the levels observed during the previous May 31, 2006 injection. The most notable increase was observed at well 199-N-130 where ^{90}Sr concentrations reached 4000 pCi/L within approximately 1 month following the June 8 injection (Figure B.5). Phosphate showed a sharp increase in concentration during the June 8, 2007, injection followed by a steep drop in phosphate concentration after the injection. The maximum phosphate concentration observed during the injection was 856 mg/L in monitoring well 199-N-129 (Figure B.13). Calcium showed small increases in some of the wells during the June 8 injection, with a maximum of 156 mg/L in well 199-N-130 (Figure B.14). Specific conductance and other general parameter data are not yet available for pilot test #1 wells during the June 8, 2007 injection.

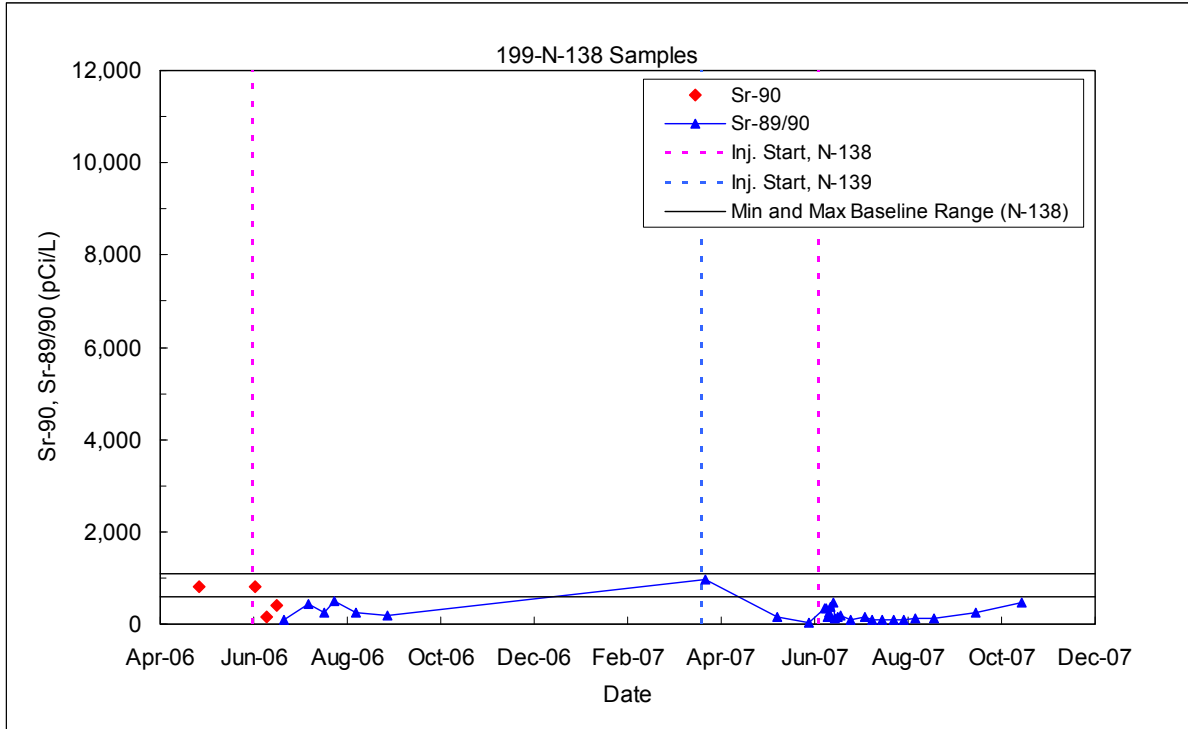


Figure 8.11. ^{90}Sr Performance Monitoring Plots for Pilot Test #1 Injection Well 199-N-138

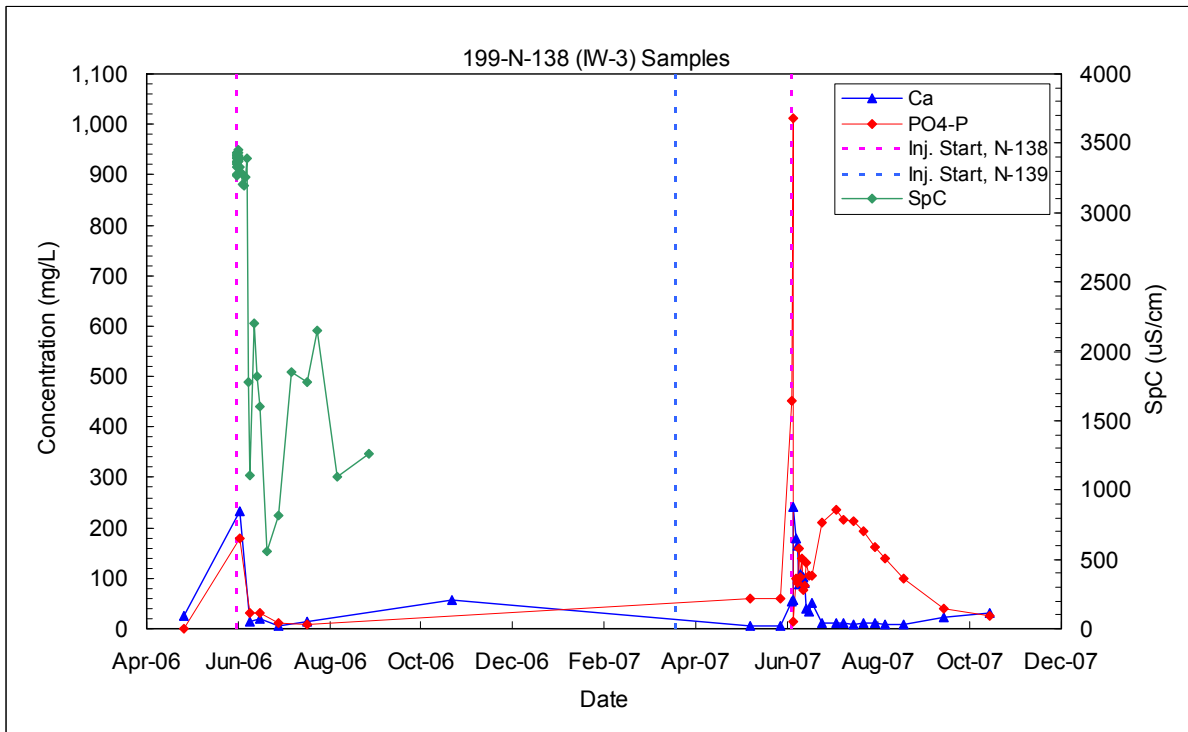


Figure 8.12. Calcium, Phosphate, and Specific Conductance Performance Monitoring Plots for Pilot Test #1 Injection Well 199-N-138

8.2.2 Field Test Performance – Pilot Test #2 Site

The pilot test #2 performance monitoring plots for ^{90}Sr are shown in Figure 8.13 for the injection well and in Appendix B for the monitoring wells (B.22 through B.27). The minimum and maximum baseline range was determined for the injection well (199-N-137) from the baseline analysis described previously in Section 8.1 (Table 8.5). Because no long-term data are available to show the variability in concentrations over time for the pilot test #2 wells, the range of 487 to 1842 pCi/L determined by the baseline analysis for the injection well were assigned to all pilot test #2 wells. The ^{90}Sr data from the pilot test #2 wells for samples collected in September 2006, before the first injection at 199-N-137, show values that are within this assigned baseline range.

Strontium-90 concentrations were impacted by the first injection at well 199-N-137 on September 27, 2006. Strontium-90 concentrations increased to levels above the baseline maximum, reaching ^{90}Sr levels as high as 11,320 pCi/L at well 199-N-148 (Figure B.22). During the second injection at well 199-N-137, $^{89/90}\text{Sr}$ concentrations responded to the injection and exceeded the baseline maximum, but generally at lower maximum levels than during the first injection at this well. The maximum ^{90}Sr concentration measured for the second injection was 6800 pCi/L in well 199-N-148 (Figure B.22). The plots show that ^{90}Sr concentrations did not respond significantly to injections at the adjacent well 199-N-136.

The pilot test #2 performance monitoring plots for calcium, phosphate, and SpC are shown in Figure 8.14 for the injection well and in Appendix B for the monitoring wells (B.29 through B.34). Complete datasets for these measurements have not been entered into HEIS or otherwise made available for use in this interim report. The plots indicate that calcium, phosphate, and SpC responded during both the September 27, 2006, and March 20, 2007, injections at pilot test site #2 injection well 199-N-137. The maximum phosphate concentrations were generally greater during the March 20, 2007, injection with a maximum of 733 mg/L in monitoring well 199-N-151 (Figure B.30). The maximum calcium concentration was 278 mg/L in monitoring well 199-N-156 during the first injection at well 199-N-137 (Figure B.33). SpC showed levels that reached a maximum of 2051 $\mu\text{S}/\text{cm}$ in monitoring well 199-N-154 (Figure B.32). SpC data are not yet available for the pilot test site #2 wells during the June 5, 2007, injection at adjacent well 199-N-136.

8.3 Field Test Performance – Injection Wells

In addition to the two pilot test site locations, eight additional injection wells located on 9.1-m (30-ft) spacing were used to treat the full 91-m (300-ft) barrier length. The injection well performance monitoring plots for ^{90}Sr are shown in Figures 8.11 and 8.13 for the pilot test injection wells, and Figures 8.15 through 8.22 for the remainder of the injection wells. The injection start times as indicated on each of these plots include the injection well and adjacent injection wells to show any potential impact on ^{90}Sr concentrations. The injection wells received one or two injections during the February-July 2007 period, as shown in Table 7.1.

The minimum and maximum baseline range was determined for each injection well from the baseline analysis described in Section 8.1 (Table 8.5). Strontium-90 data from all but two injection wells collected before the first injections occurred show values that are within these assigned baseline ranges. Two injection wells, 199-N-139 and 199-N-140, show preinjection $^{98/90}\text{Sr}$ values that exceed the assigned baseline range. Strontium-90 concentrations in these two wells, located close to pilot test site #1, were possibly impacted by the pilot test #1 injection that occurred in May-June 2006.

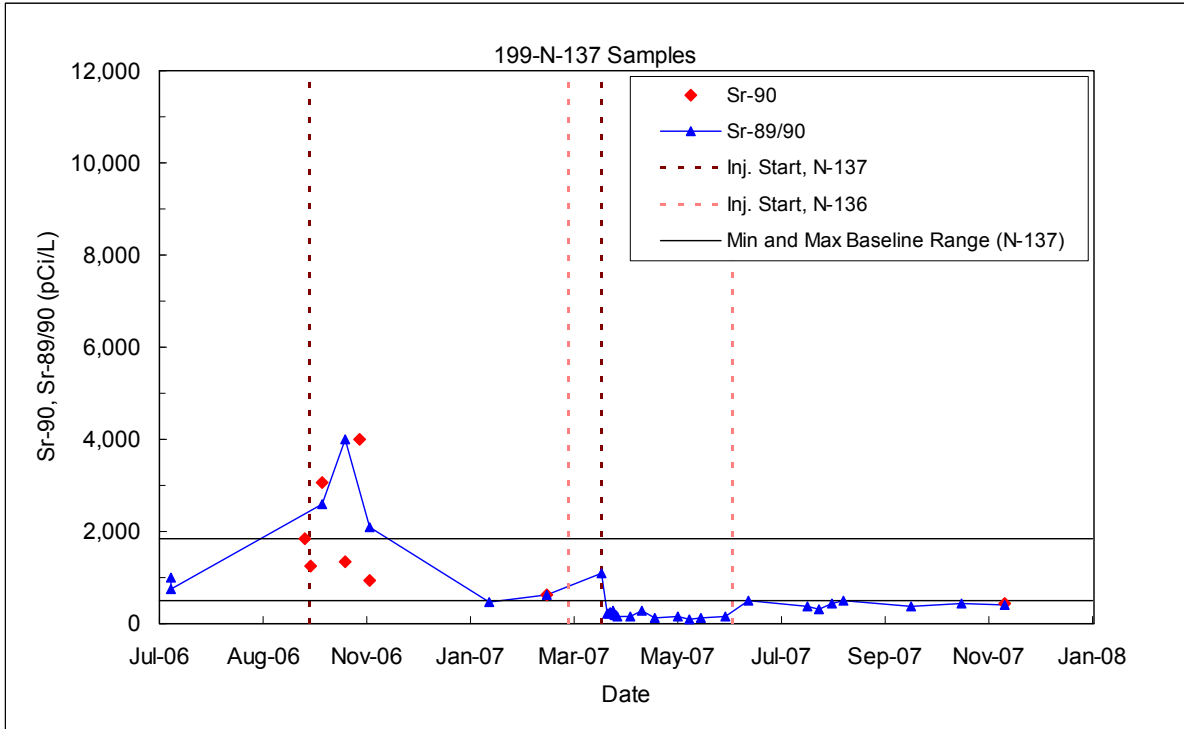


Figure 8.13. ^{90}Sr Performance Monitoring Plots for Pilot Test #2 Injection Well 199-N-137

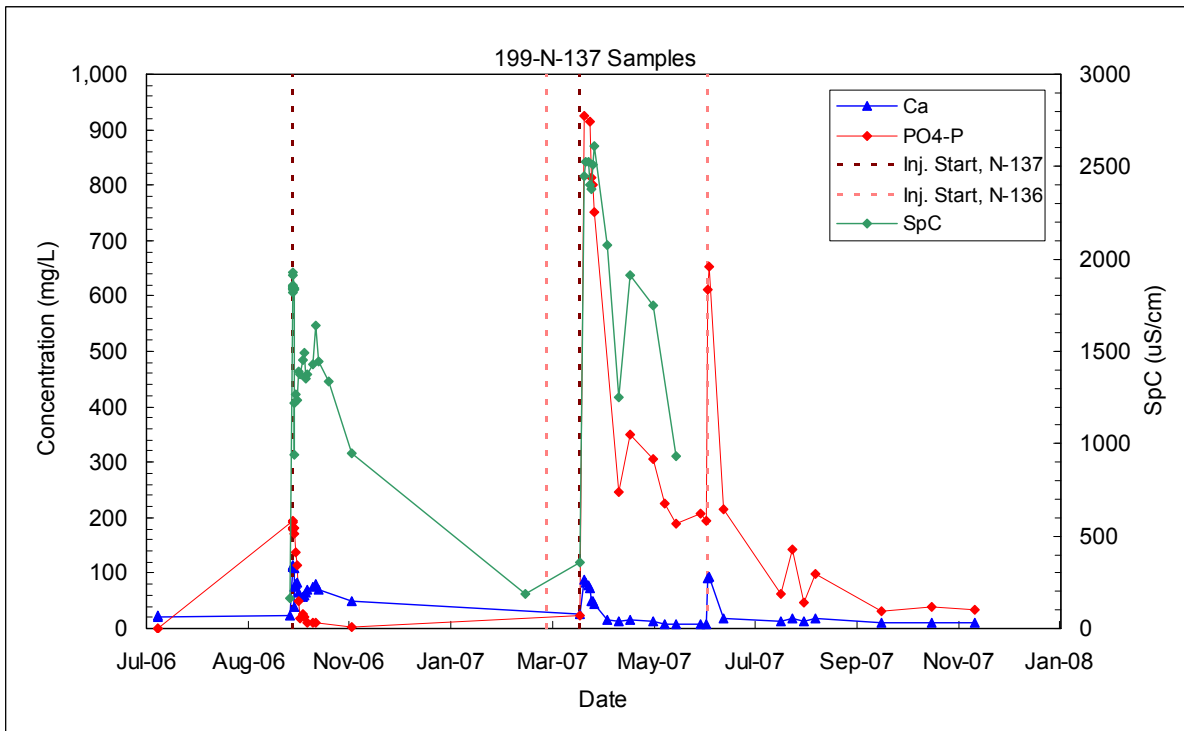


Figure 8.14. Calcium, Phosphate, and Specific Conductance Performance Monitoring Plots for Pilot Test #2 Injection Well 199-N-137

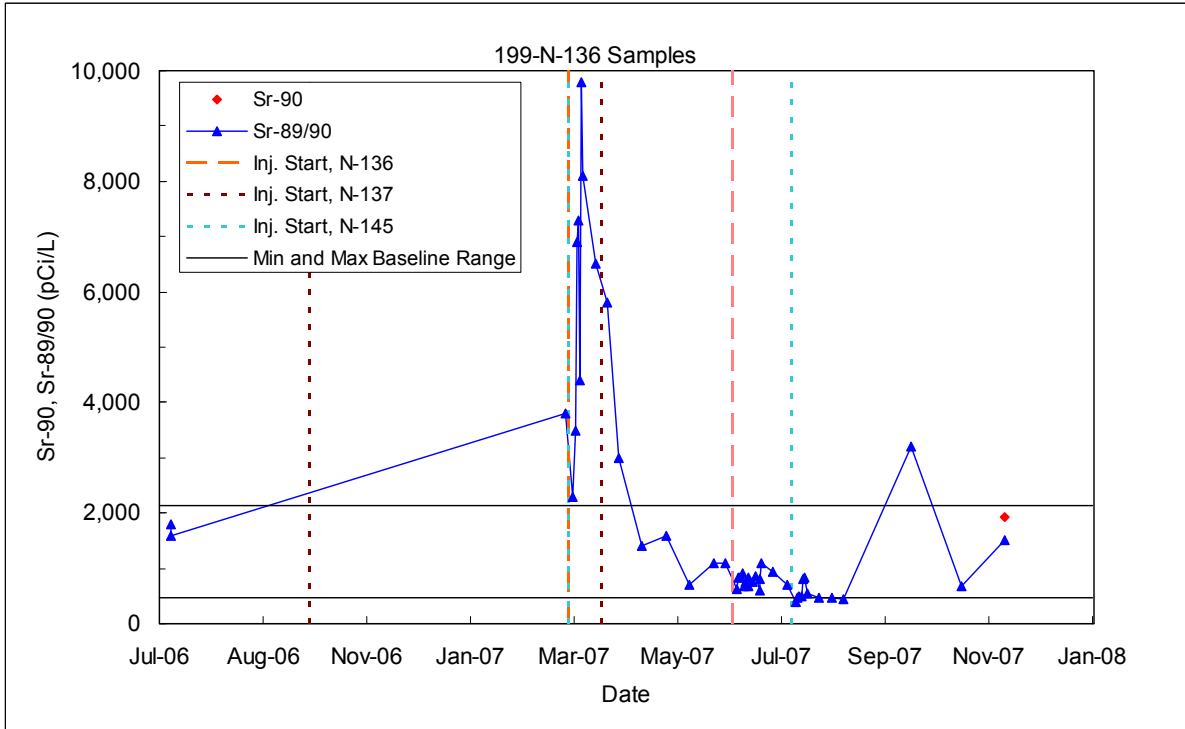


Figure 8.15. ⁹⁰Sr Performance Monitoring Plots for Injection Well 199-N-136

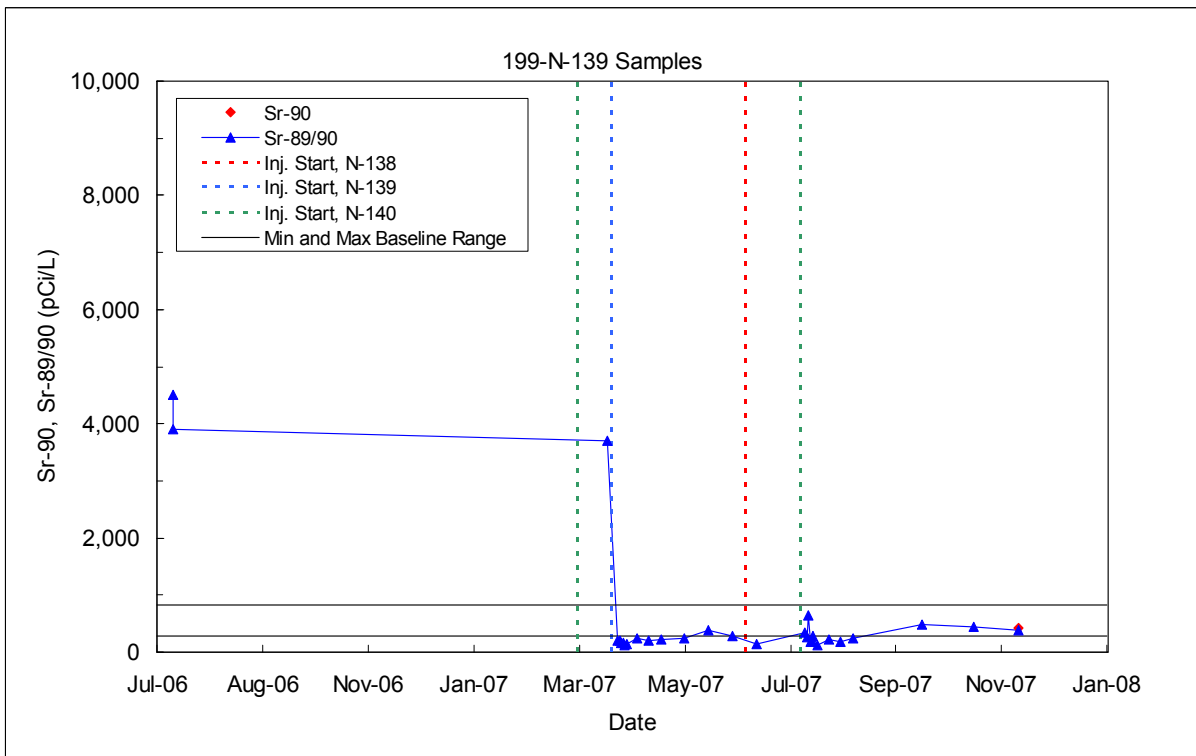


Figure 8.16. ⁹⁰Sr Performance Monitoring Plots for Injection Well 199-N-139

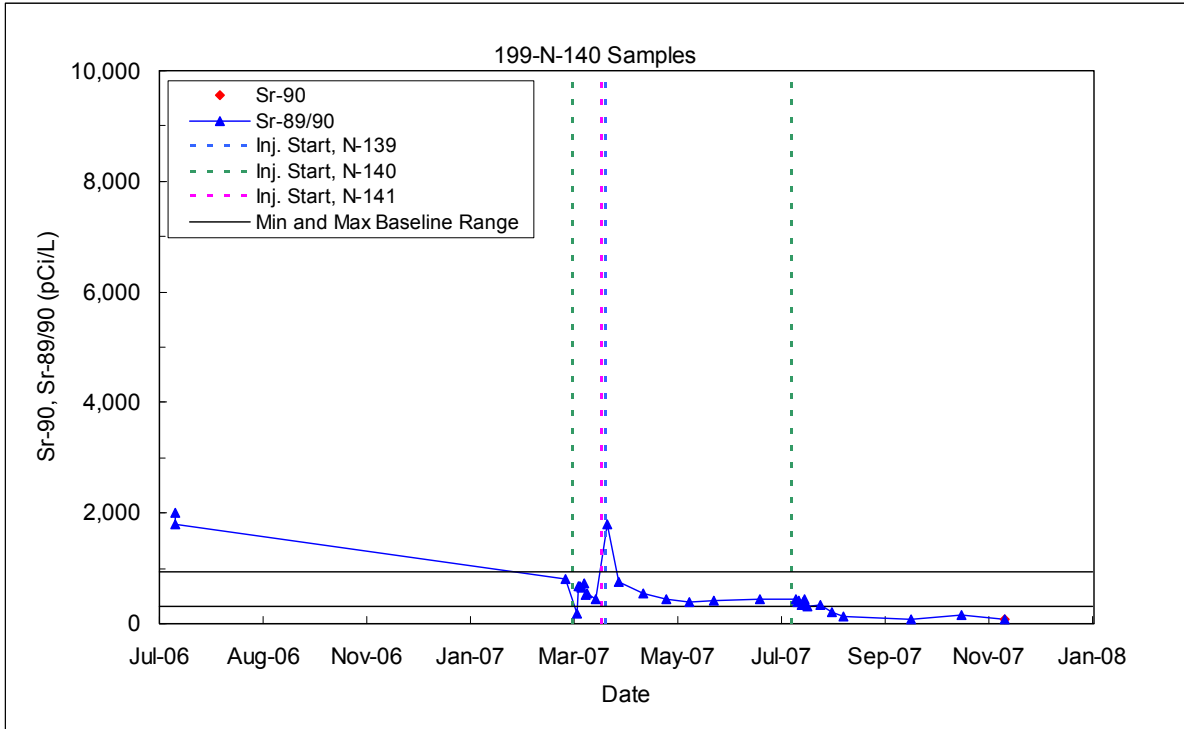


Figure 8.17. ^{90}Sr Performance Monitoring Plots for Injection Well 199-N-140

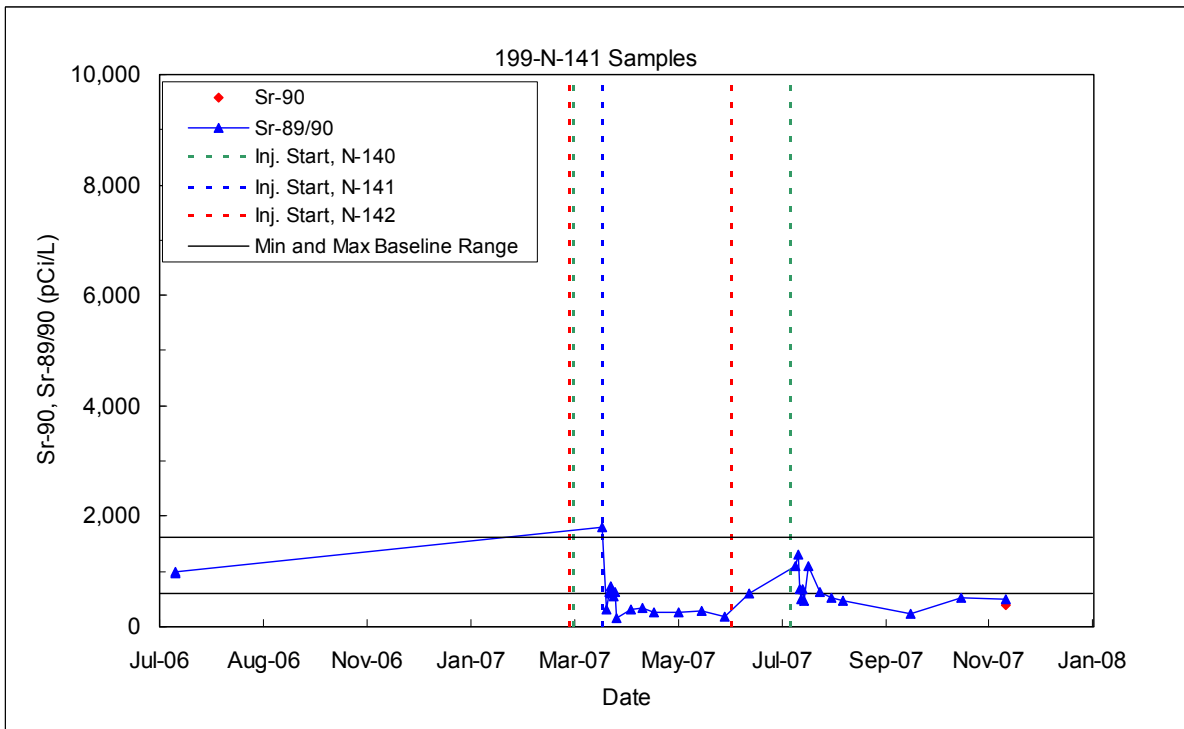


Figure 8.18. ^{90}Sr Performance Monitoring Plots for Injection Well 199-N-141

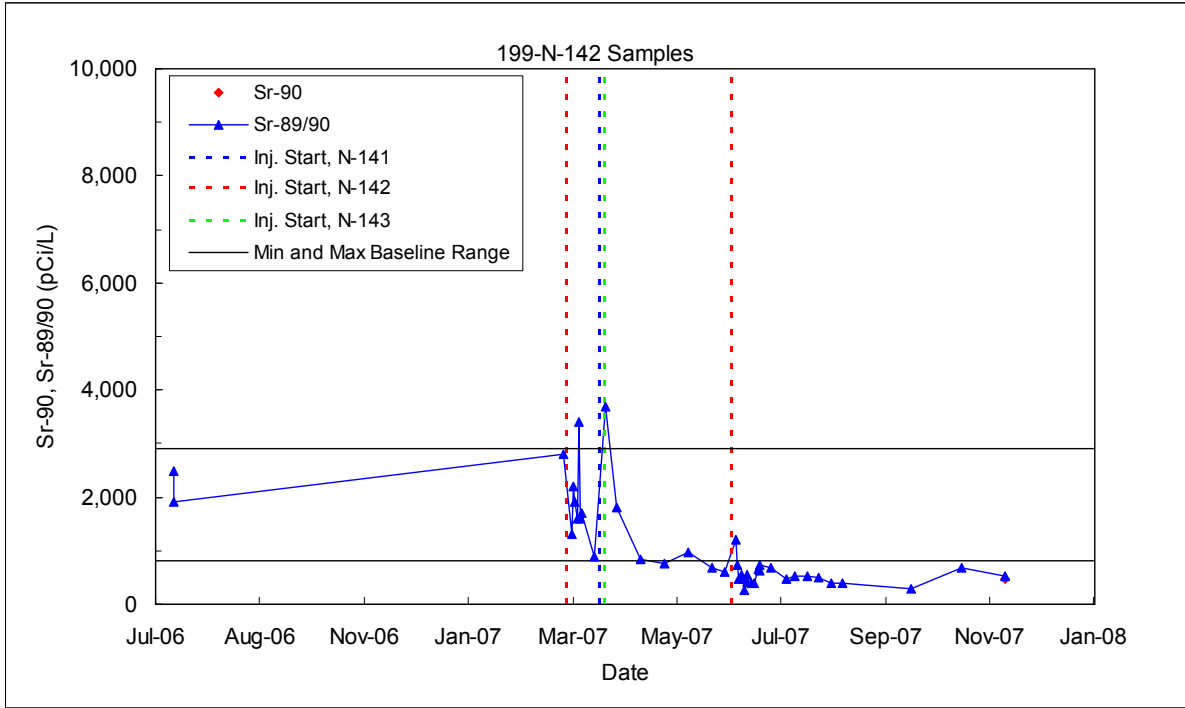


Figure 8.19. ⁹⁰Sr Performance Monitoring Plots for Injection Well 199-N-142

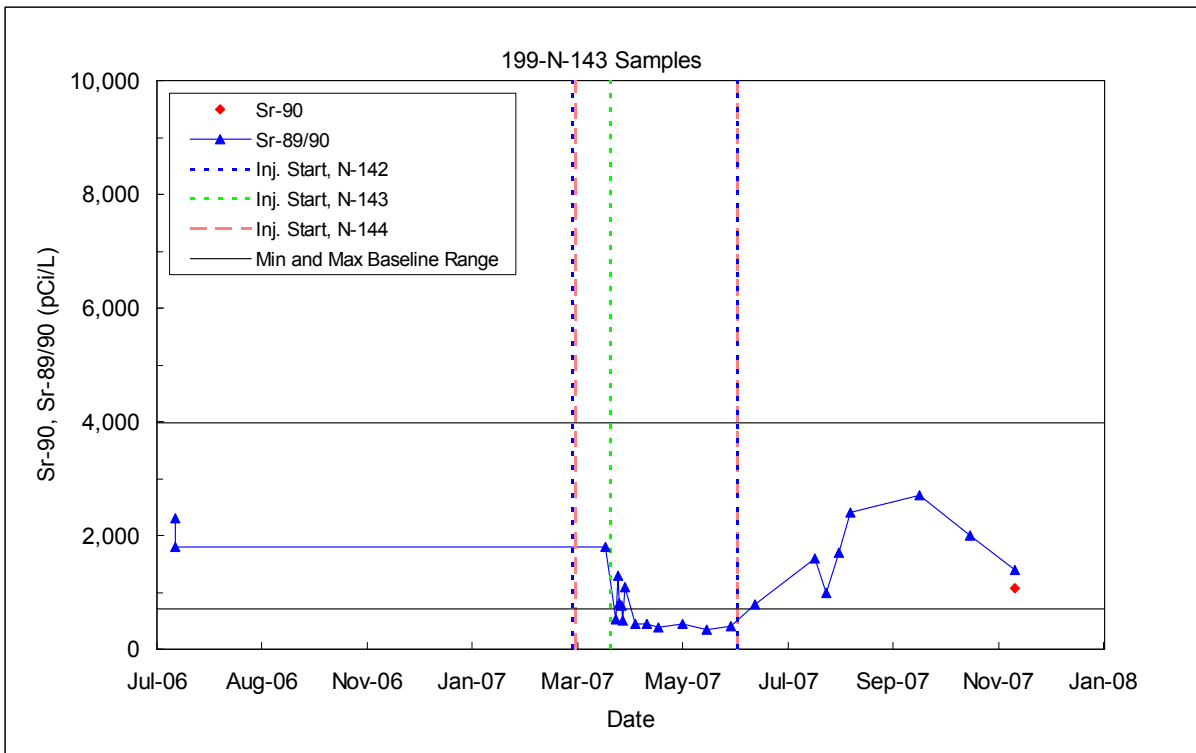


Figure 8.20. ⁹⁰Sr Performance Monitoring Plots for Injection Well 199-N-143

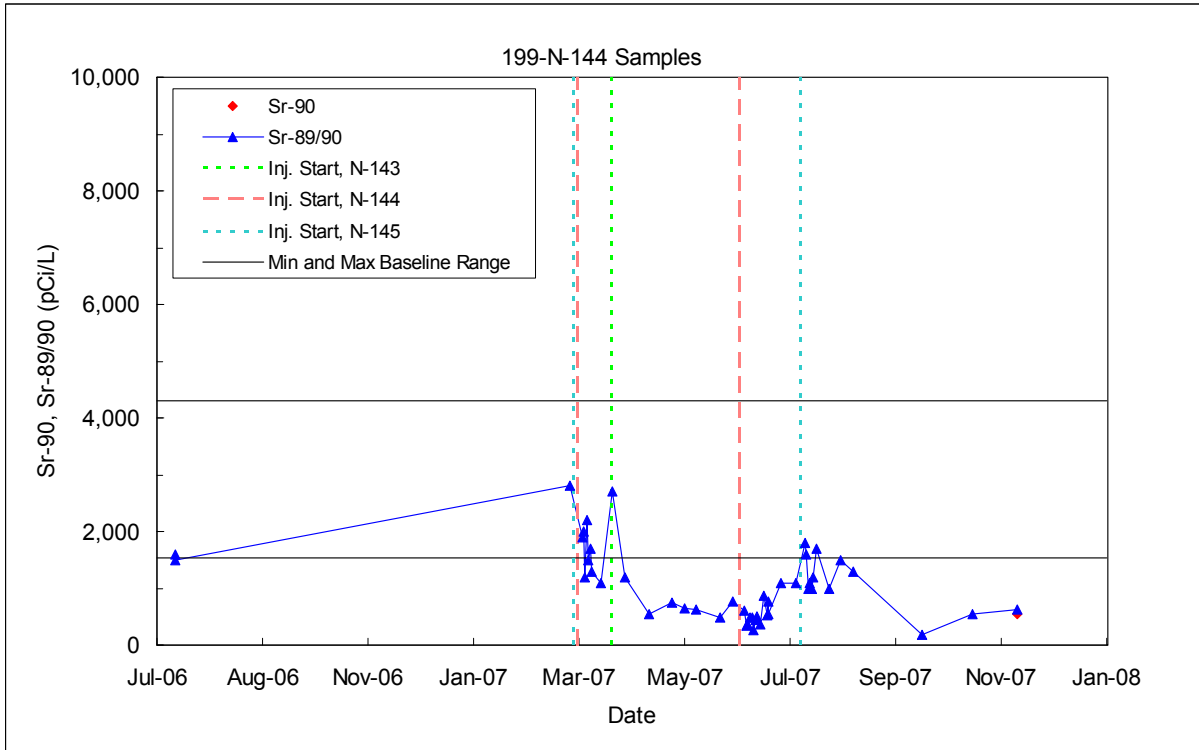


Figure 8.21. ⁹⁰Sr Performance Monitoring Plots for Injection Well 199-N-144

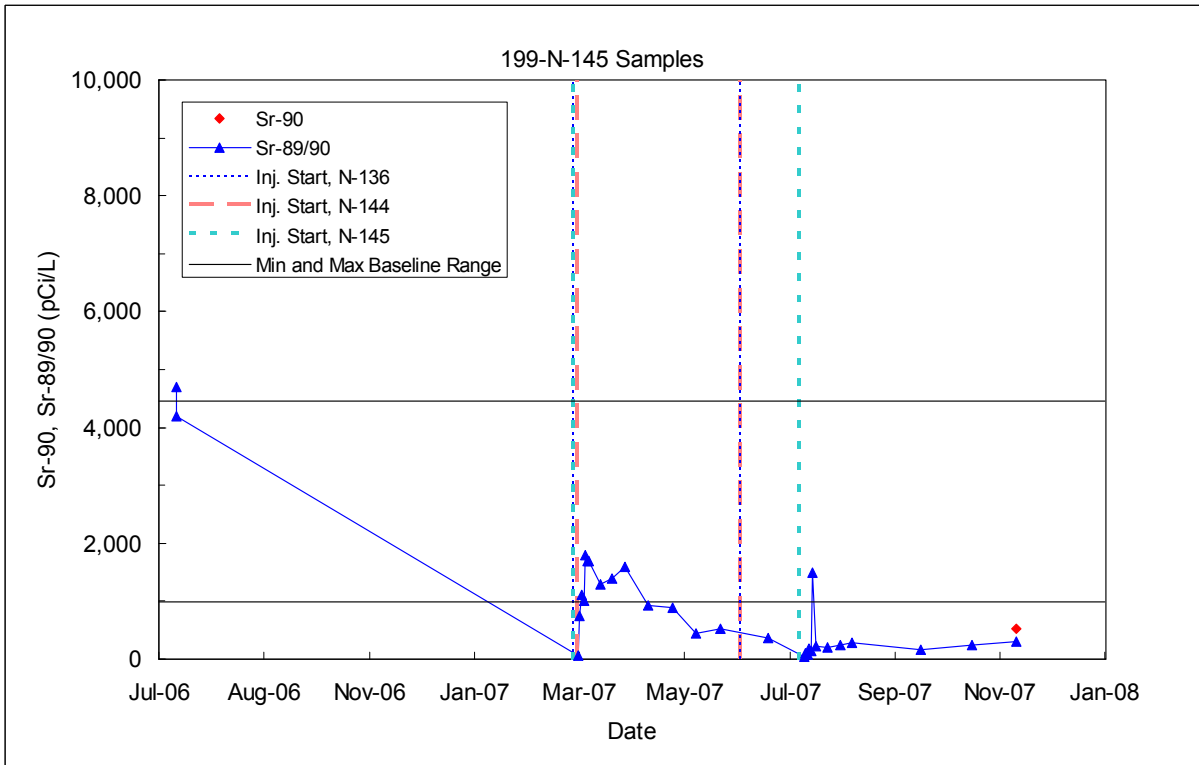


Figure 8.22. ⁹⁰Sr Performance Monitoring Plots for Injection Well 199-N-145

Strontium-90 concentrations showed the greatest increase during the February 28, 2007, injection at well 199-N-136 where a concentration spike exceeded the maximum baseline range, reaching a maximum of 9800 pCi/L (Figure 8.15). Other injection wells that showed an increase in ⁹⁰Sr concentrations to levels above the maximum baseline range during earlier injections include 199-N-140, 199-N-141, and 199-N-142 (Figures 8.17 through 8.19). During the later injections in June and July 2007, ⁹⁰Sr concentrations did not change significantly in response to the injections.

The injection well performance monitoring plots for calcium, phosphate, and SpC are shown in Figures 8.12 and 8.14 for the pilot test injection wells, and in Figures 8.23 through 8.30 for the remainder of the injection wells. The plots generally show large spikes in SpC and phosphate levels in response to all the injections during the February-July 2007 period, reaching maximum concentrations of 1090 mg/L in wells 199-N-142 and 199-N-145 (Figures 8.27 and 8.30, respectively). SpC reached maximum levels near or above 3000 μ S/cm. SpC data are not yet available for the later injections in June and July 2007. These plots also show that most injection wells were impacted by injections in adjacent injection wells as indicated by increases in SpC and in phosphate and calcium concentrations.

8.4 Field Test Performance – Compliance Wells

The compliance well performance monitoring plots for ⁹⁰Sr are shown in Figures 8.31 through 8.34. The minimum and maximum baseline range was determined for each compliance well from the baseline analysis described in Section 8.1 (Table 8.5). Preinjection ⁹⁰Sr data from the compliance wells show values within these assigned baseline ranges.

Strontium-90 concentrations in the compliance wells responded to injections that were initiated in March 2007 at adjacent injection wells. The most significant change in ⁹⁰Sr concentrations was at compliance well 199-N-146, where a maximum ⁹⁰Sr concentration of 5200 pCi/L was measured during the March 20, 2007, injection at well 199-N-141 (Figure 8.33). Significantly less change in ⁹⁰Sr concentration was measured for samples collected during the June and July 2007 injections at adjacent injection wells.

The compliance well performance monitoring plots for calcium, phosphate, and SpC are shown in Figures 8.35 through 8.38. Plots show that phosphate and SpC responded with spikes during injections at most of the adjacent injection wells. The maximum phosphate concentration was 888 mg/L in compliance well 199-N-122 during the June 5, 2007, injection at well 199-N-144 (Figure 8.35). The maximum SpC level was 2570 μ S/cm in compliance well 199-N-122 during the February 28, 2007 injection at well 199-N-144 (Figure 8.35). Calcium concentrations changed very little in the compliance wells in response to injections in the adjacent wells.

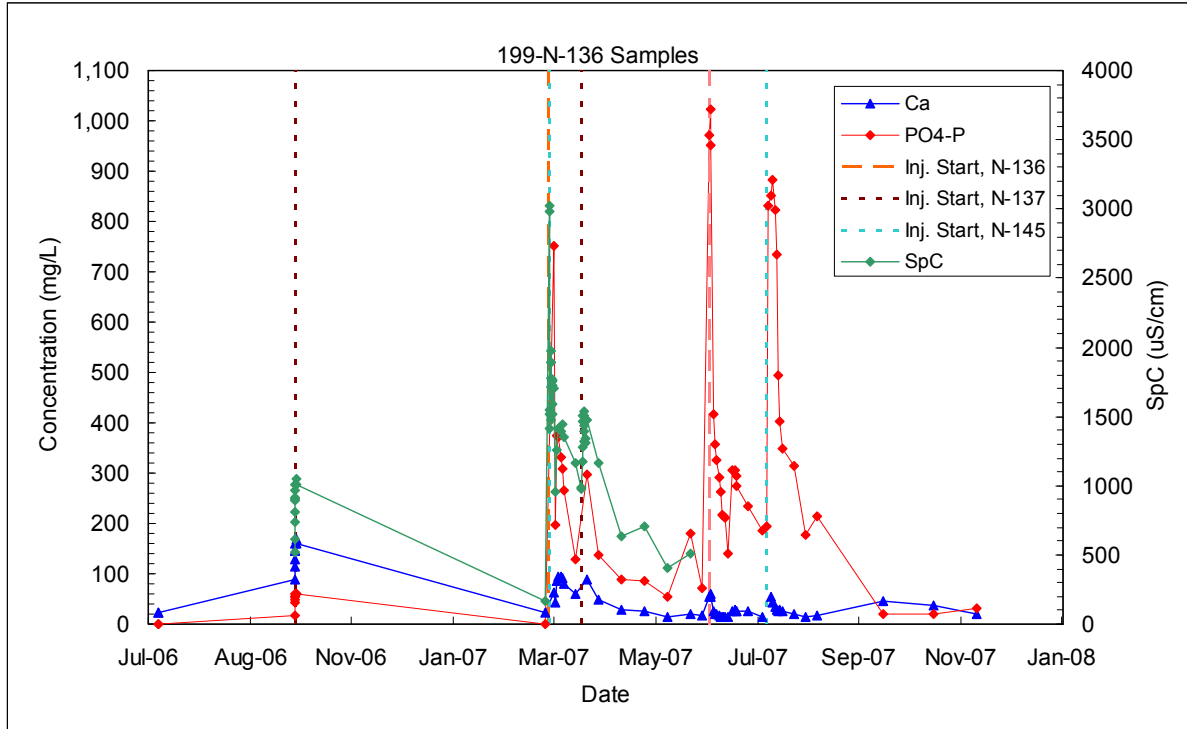


Figure 8.23. Calcium, Phosphate, and Specific Conductance Performance Monitoring Plots for Injection Well 199-N-136

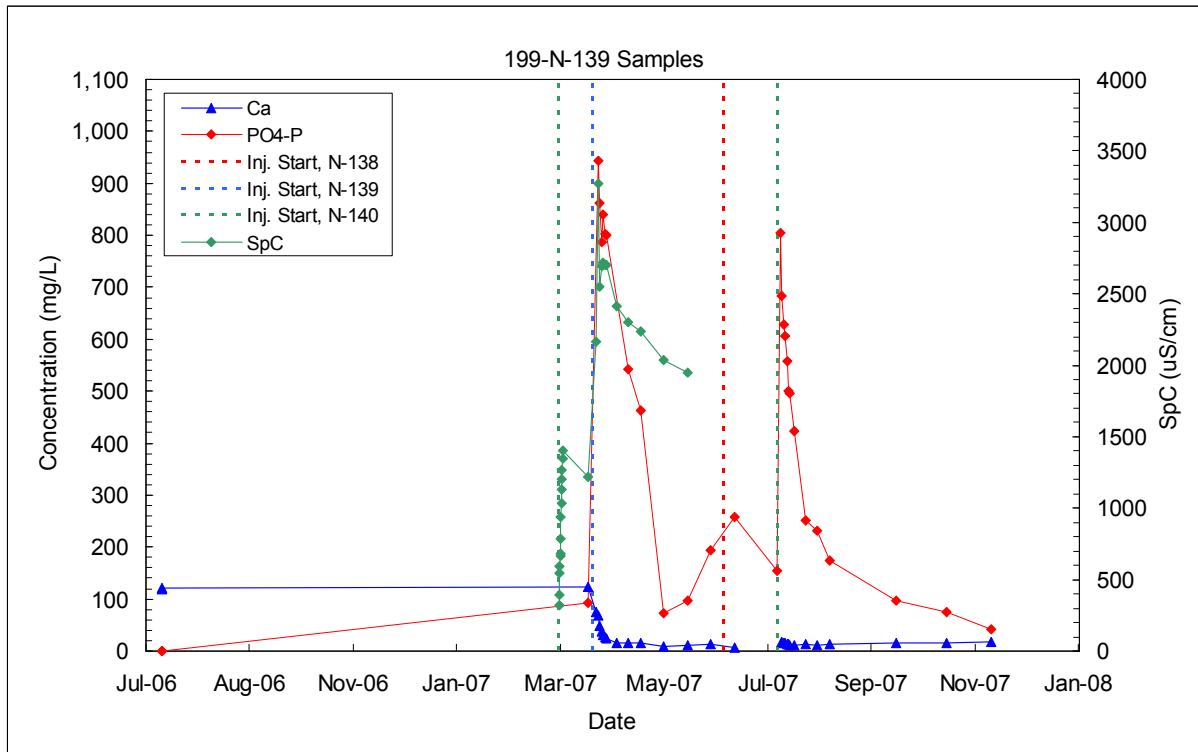


Figure 8.24. Calcium, Phosphate, and Specific Conductance Performance Monitoring Plots for Injection Well 199-N-139

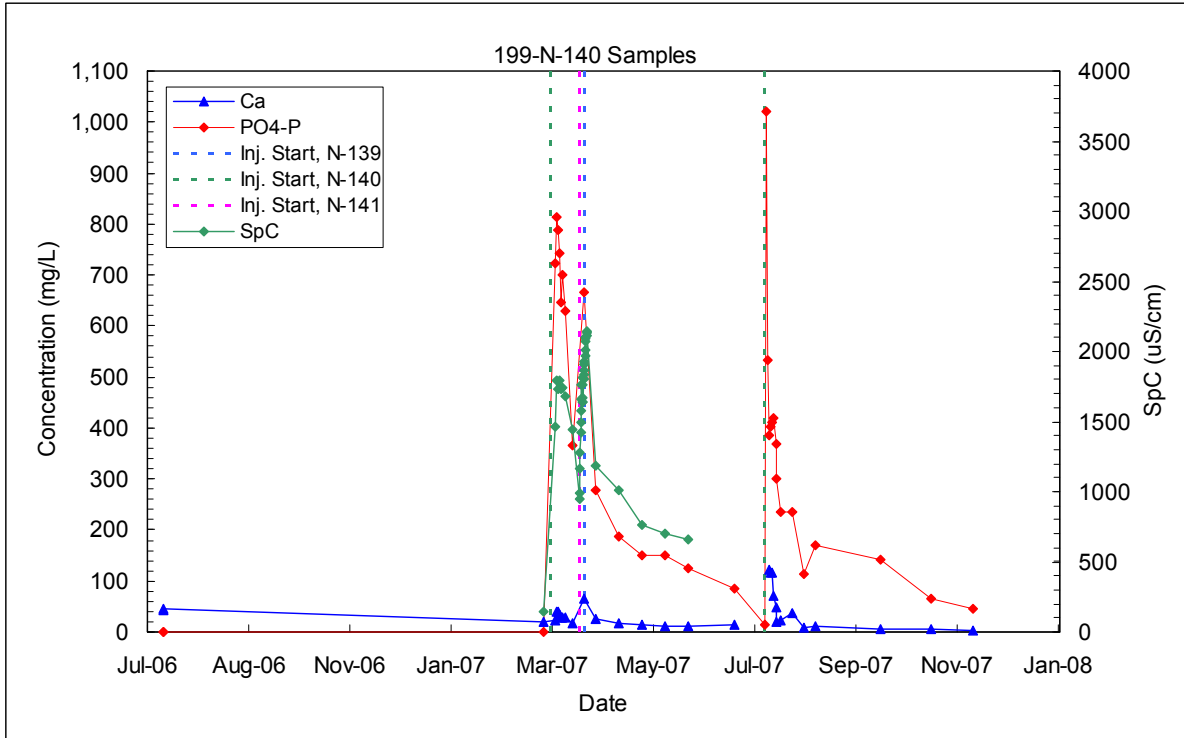


Figure 8.25. Calcium, Phosphate, and Specific Conductance Performance Monitoring Plots for Injection Well 199-N-140

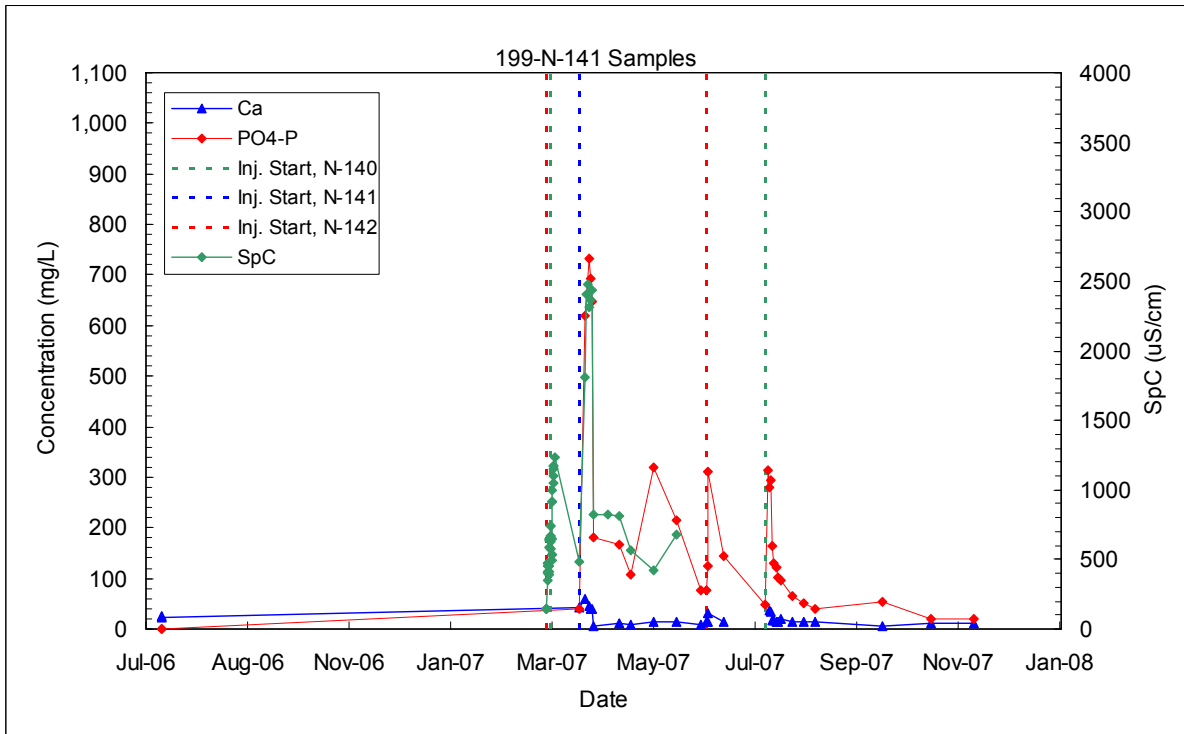


Figure 8.26. Calcium, Phosphate, and Specific Conductance Performance Monitoring Plots for Injection Well 199-N-141

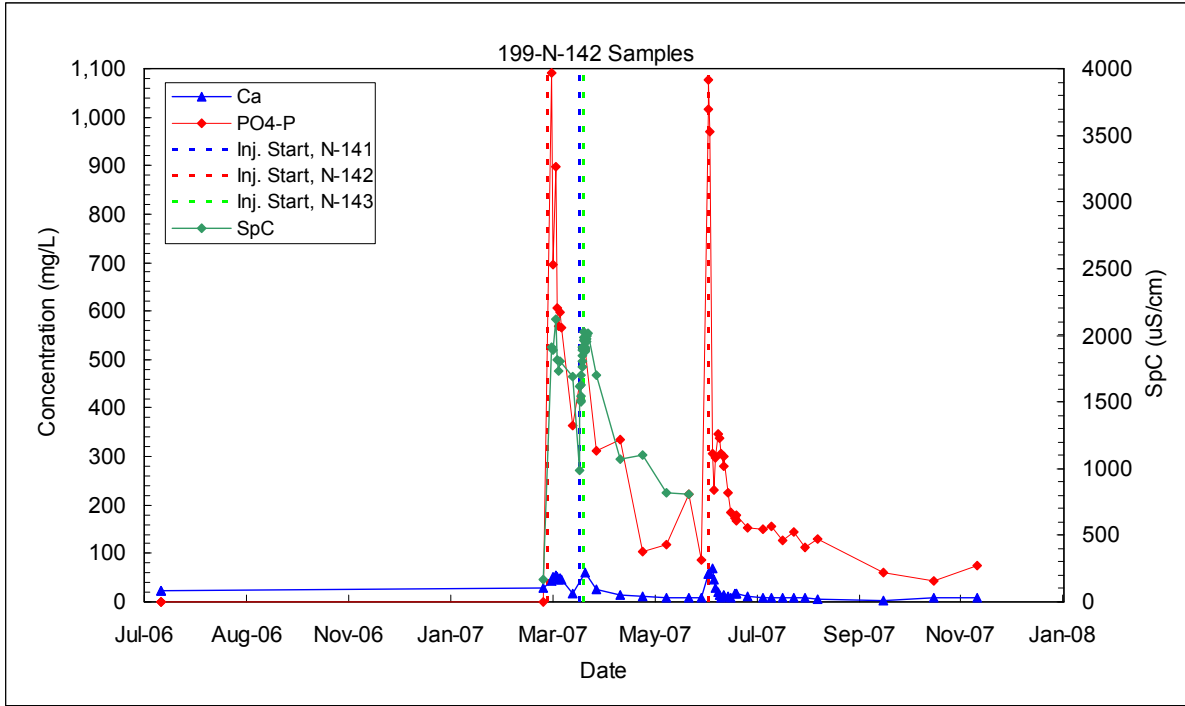


Figure 8.27. Calcium, Phosphate, and Specific Conductance Performance Monitoring Plots for Injection Well 199-N-142

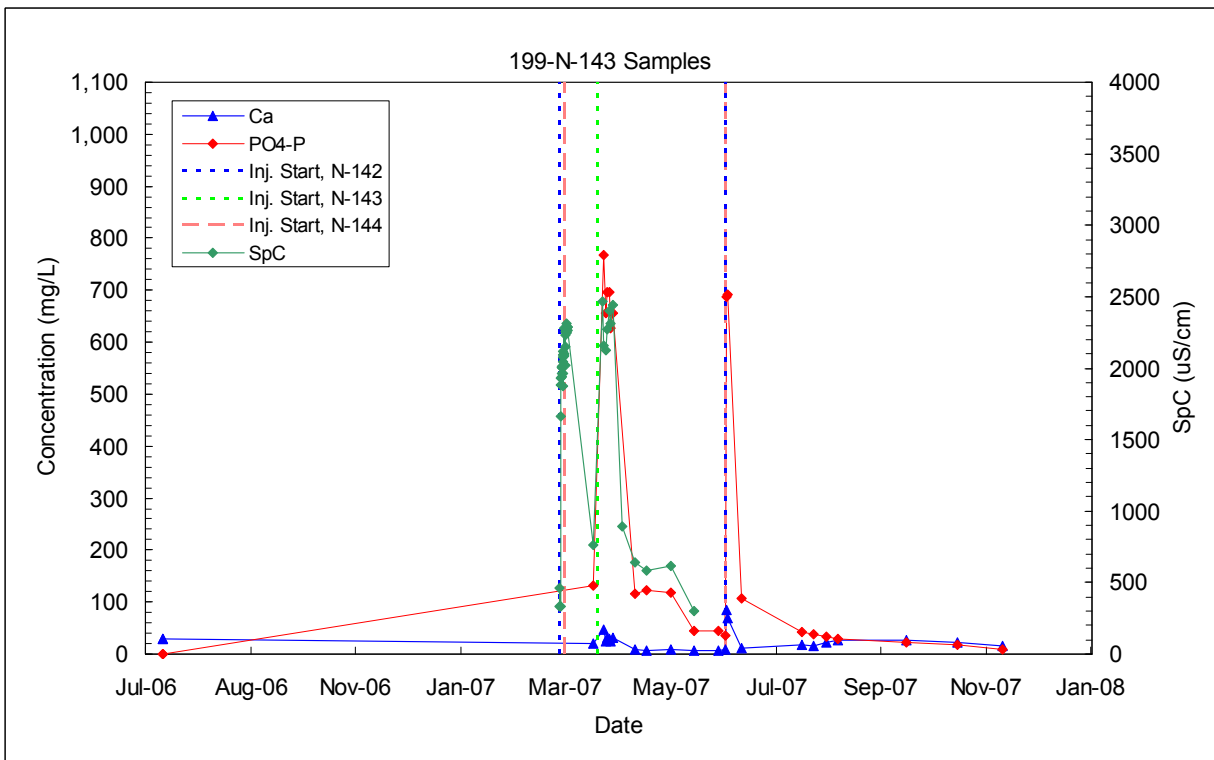


Figure 8.28. Calcium, Phosphate, and Specific Conductance Performance Monitoring Plots for Injection Well 199-N-143

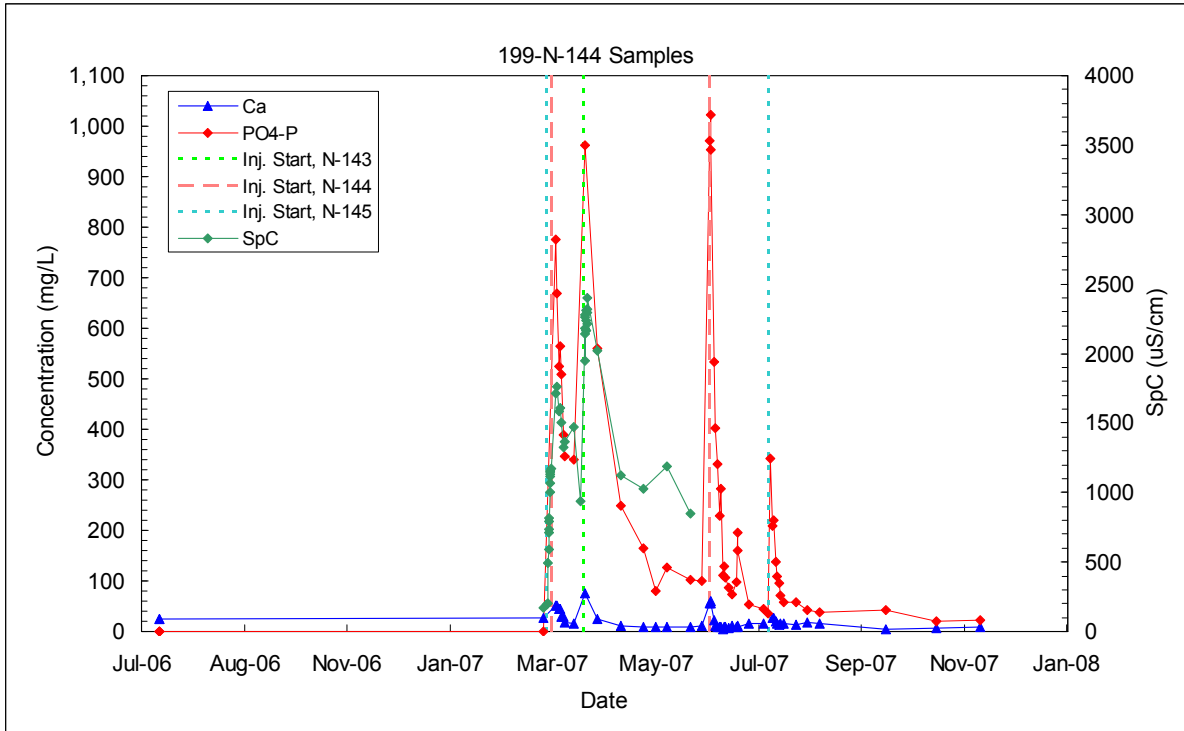


Figure 8.29. Calcium, Phosphate, and Specific Conductance Performance Monitoring Plots for Injection Well 199-N-144

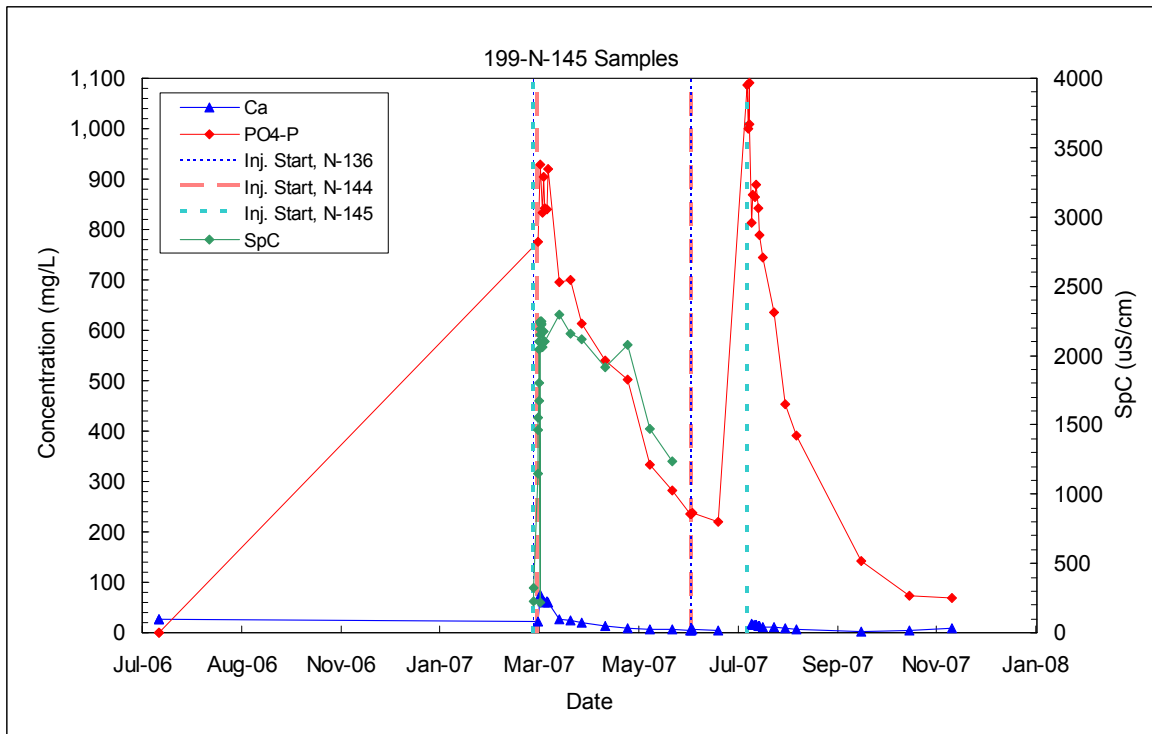


Figure 8.30. Calcium, Phosphate, and Specific Conductance Performance Monitoring Plots for Injection Well 199-N-145

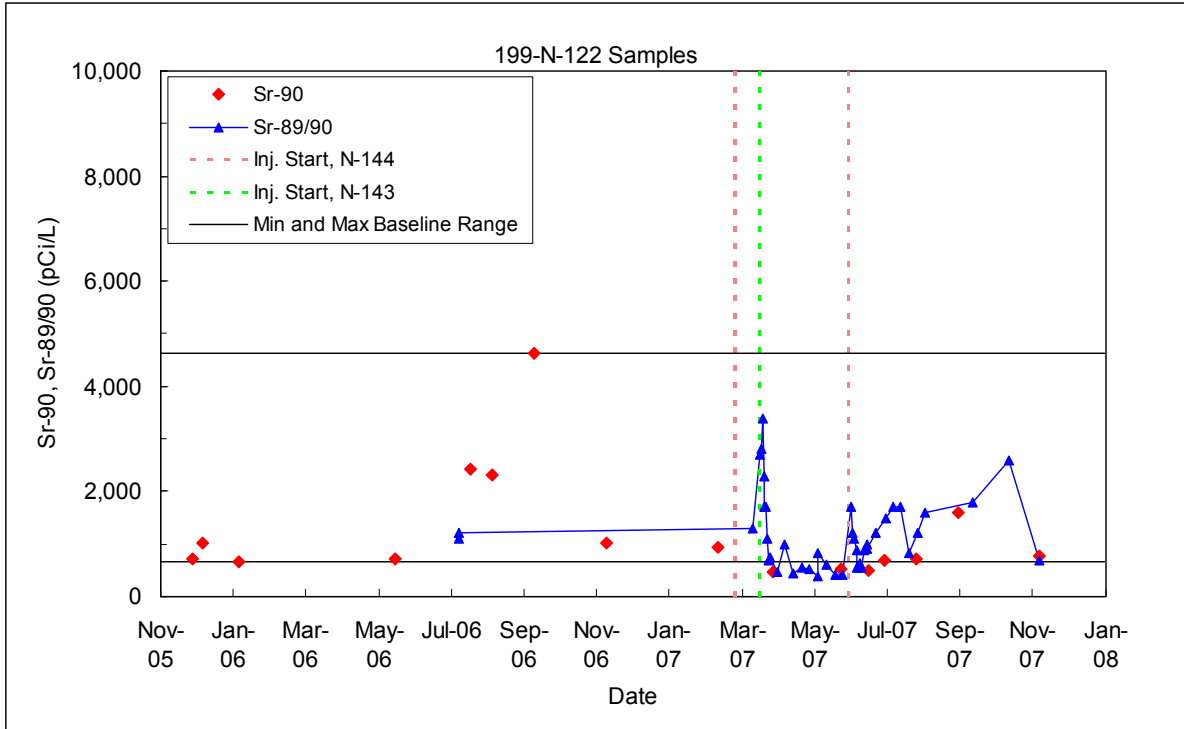


Figure 8.31. ⁹⁰Sr Performance Monitoring Plots for Compliance Well 199-N-122

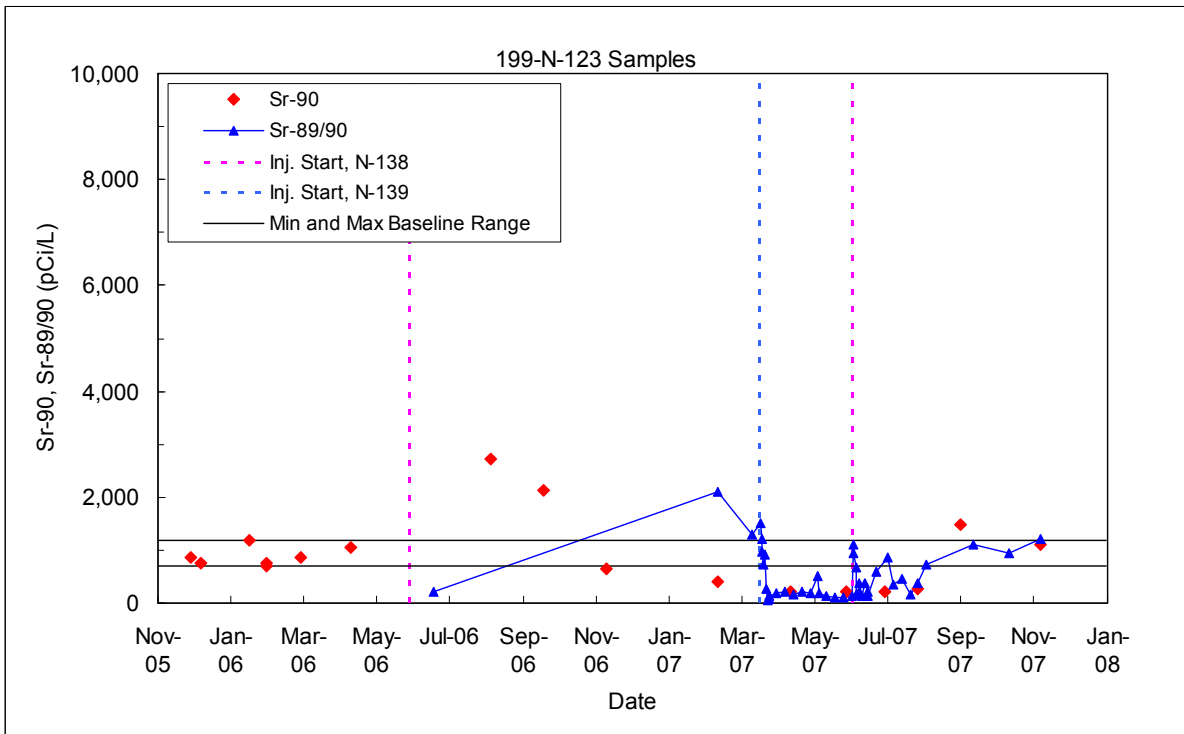


Figure 8.32. ⁹⁰Sr Performance Monitoring Plots for Compliance Well 199-N-123

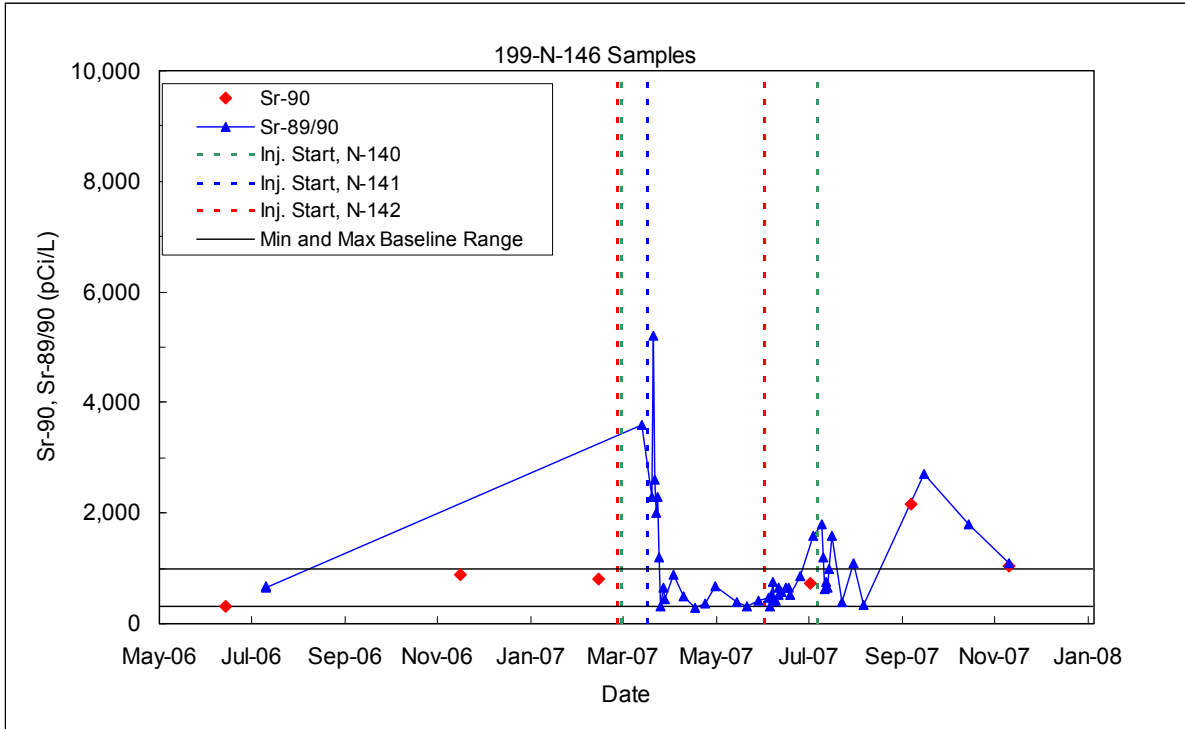


Figure 8.33. ^{90}Sr Performance Monitoring Plots for Compliance Well 199-N-146

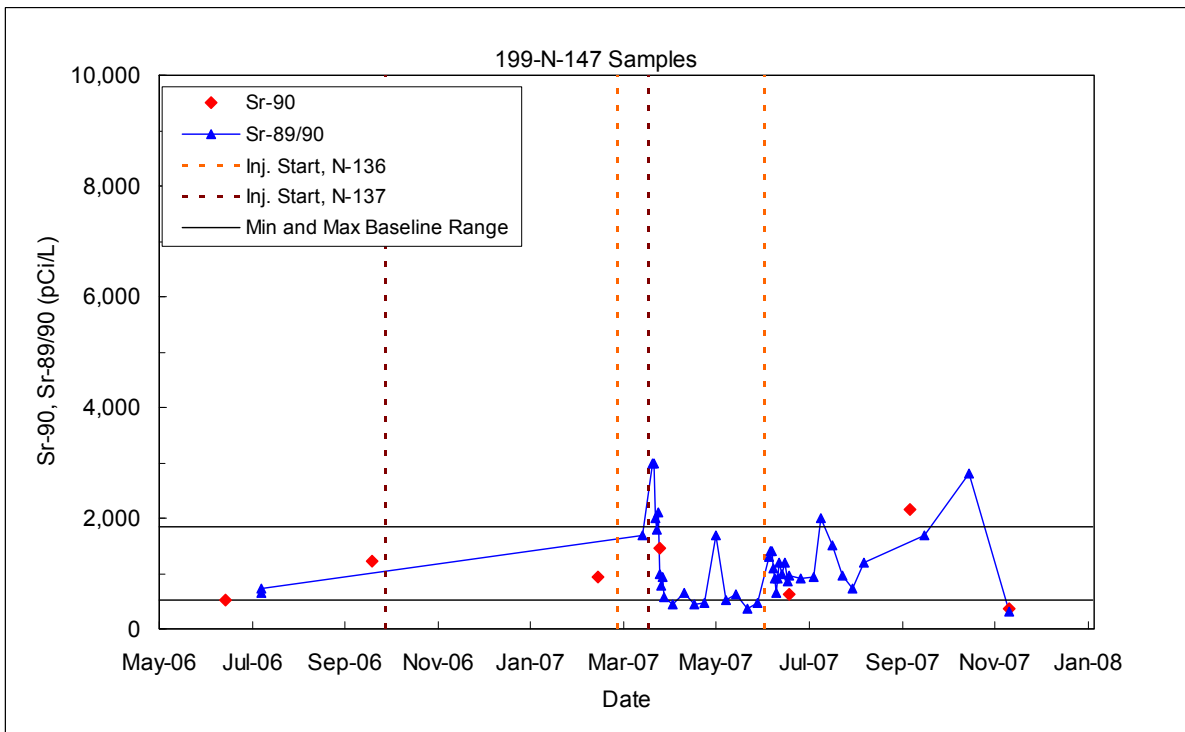


Figure 8.34. ^{90}Sr Performance Monitoring Plots for Compliance Well 199-N-147

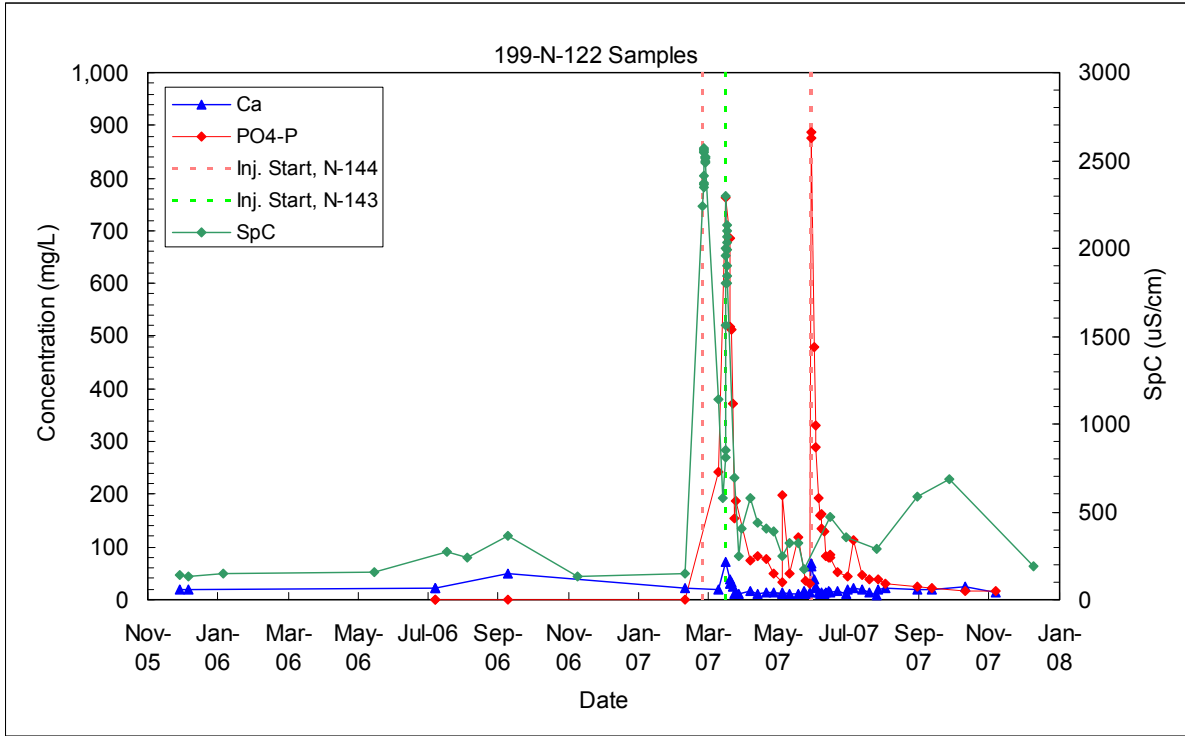


Figure 8.35. Calcium, Phosphate, and Specific Conductance Performance Monitoring Plots for Compliance Well 199-N-122

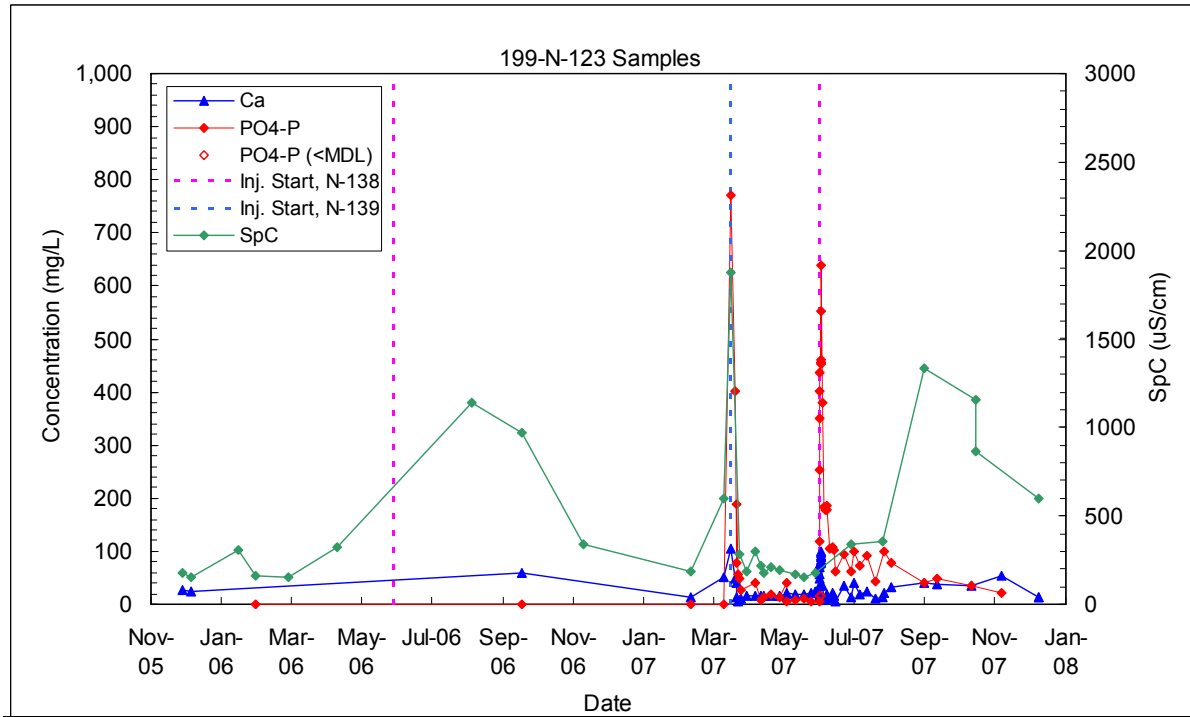


Figure 8.36. Calcium, Phosphate, and Specific Conductance Performance Monitoring Plots for Compliance Well 199-N-123

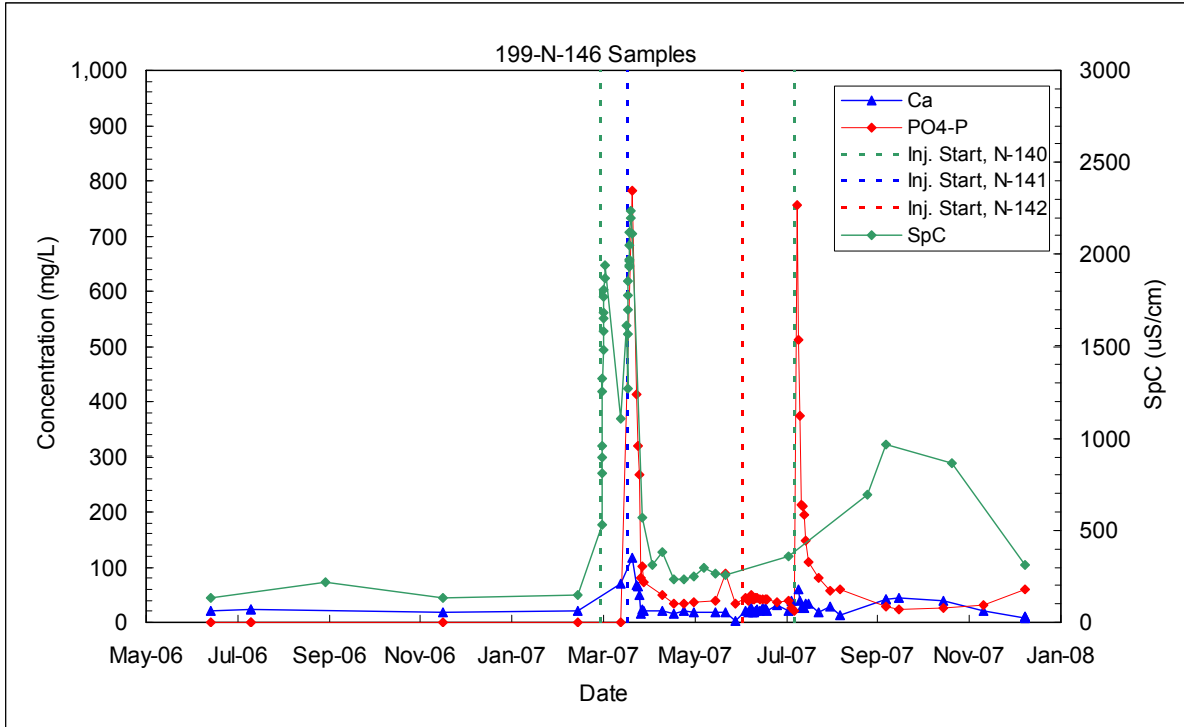


Figure 8.37. Calcium, Phosphate, and Specific Conductance Performance Monitoring Plots for Compliance Well 199-N-146

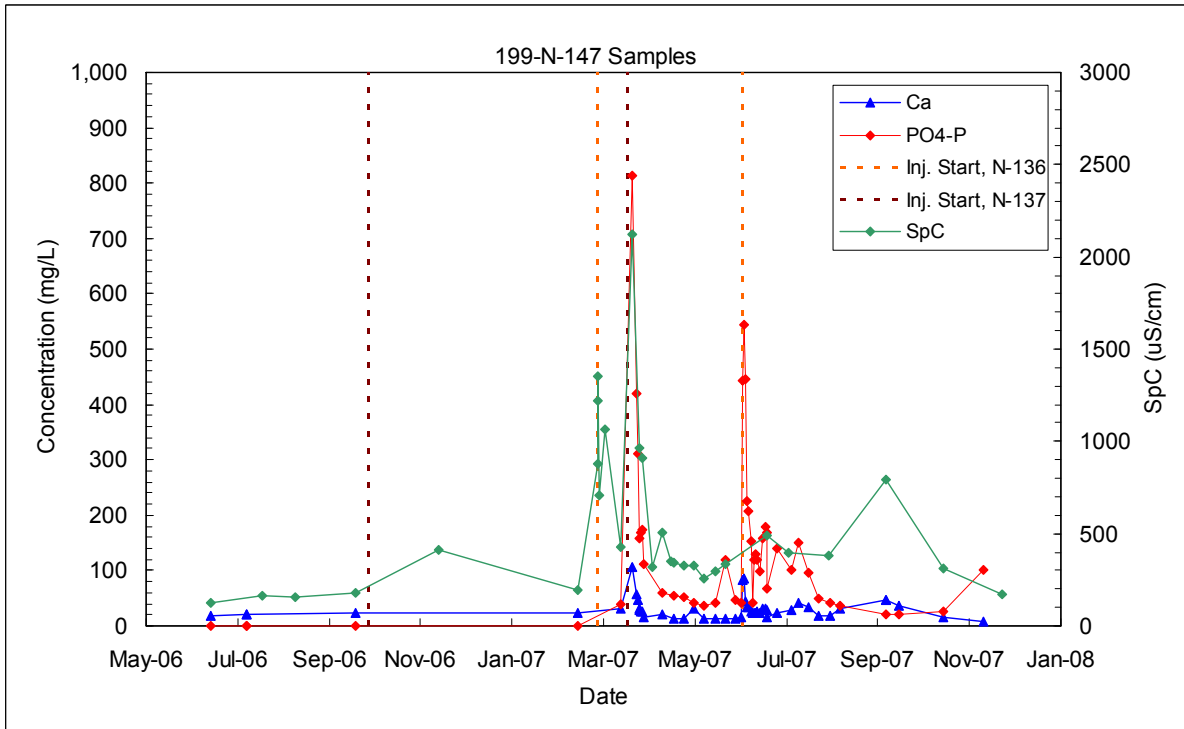


Figure 8.38. Calcium, Phosphate, and Specific Conductance Performance Monitoring Plots for Compliance Well 199-N-147

8.5 Field Test Performance – Aquifer Tubes

Figure 8.39 shows the gross beta and SpC for selected aquifer tubes near the apatite treatability test site (see Figures 8.1 and 1.3 for locations). These aquifer tubes were used for establishing baseline ^{90}Sr concentration ranges as described in Section 8.1. Aqueous ^{90}Sr concentrations can be estimated from gross beta measurements by dividing by 2 (see Mendoza et al. 2007). As shown in Figure 8.39, increases in SpC and gross beta in the aquifer tubes have occurred following Ca-citrate- PO_4 treatability test injections in 2006 and 2007. However, concentrations have decreased in some of the aquifer tubes in the latest available sampling data (later in 2007). Some of these aquifer tubes were removed prior to the field injections so they cannot be used for performance monitoring but are shown because they were used for the baseline range analysis. Performance monitoring results for two aquifer tubes that are part of the pilot test site monitoring (APT-1 and APT-5) are provided in Appendix B.

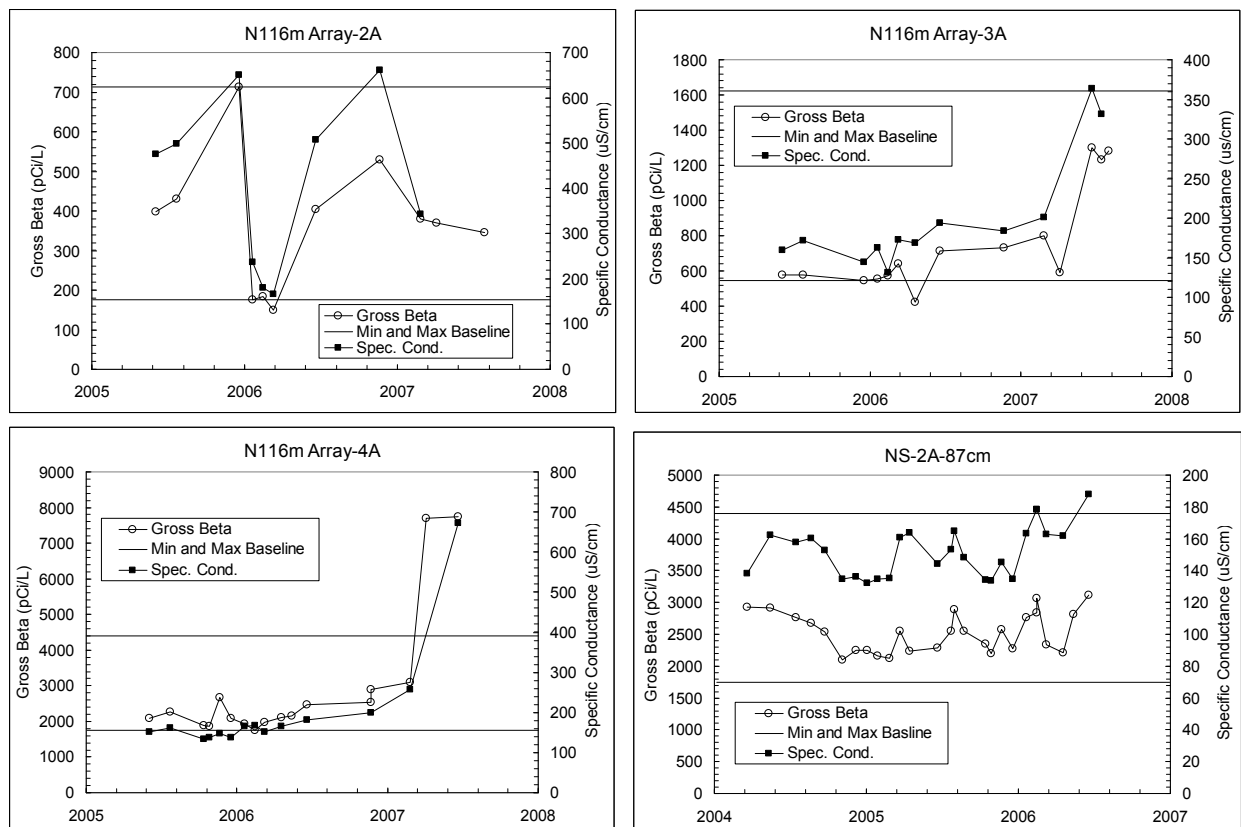


Figure 8.39. Gross Beta and Specific Conductance for Aquifer Tubes (data from HEIS dated February 2008). See Figures 8.1 and 1.3 for locations. Last data points (November 27, 2007, and December 11, 2007) were not shown for N116m Array-4A due to tube failure.

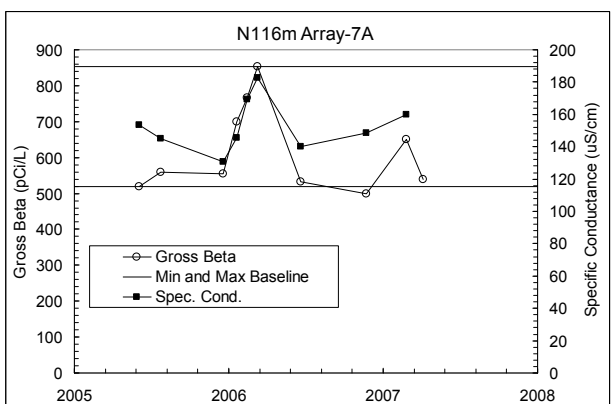
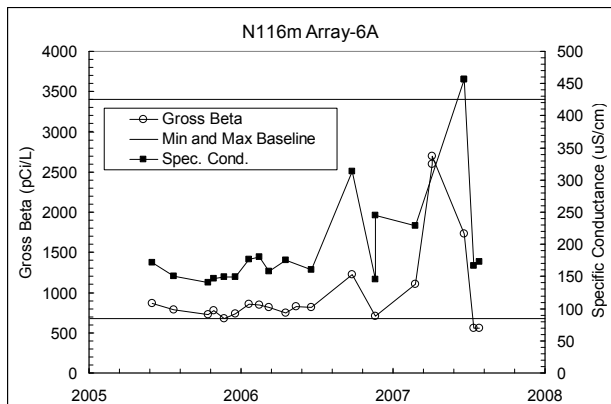
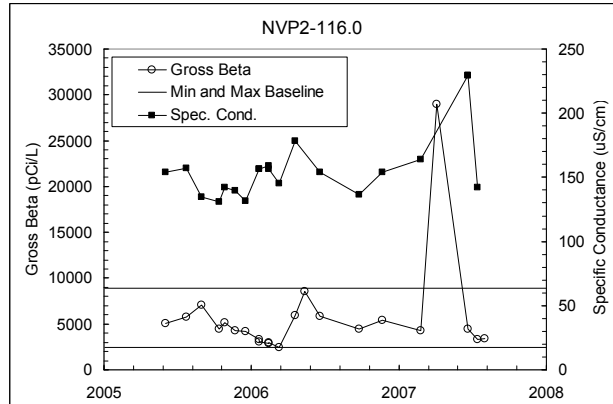
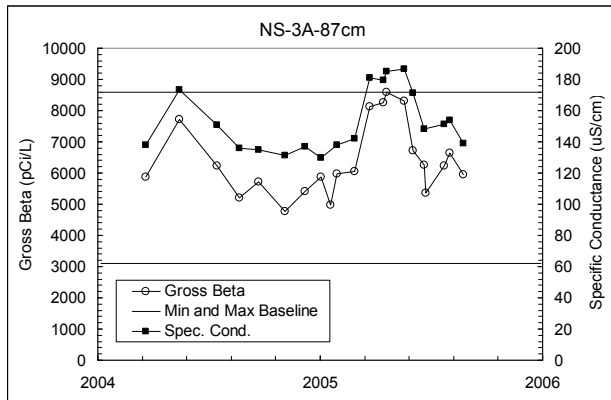


Figure 8.39. (contd)

9.0 Summary, Conclusions, and Path Forward

9.1 Summary and Conclusions

The objective of the low-concentration Ca-citrate-PO₄ solution injections is to stabilize the ⁹⁰Sr in the aquifer at the treatability test site in advance of the high-concentration injections that will provide for long-term ⁹⁰Sr treatment. Initially, two characterization wells were installed at the 100-N Area apatite treatability test site in 2005 for detailed aquifer and sediment analysis. The characterization included depth-discrete ⁹⁰Sr measurements of the sediment (see Figure 1.9). Following the characterization, two pilot test sites were installed at the east and west ends of the barrier (see Figures 1.10, 4.2, and 4.3). The test sites were equipped with extensive monitoring well networks, and were used for the initial injections to develop the injection design for the remaining portions of the barrier. During 2006, the following were installed at the 100-N apatite treatability test site: 10 injection wells for installation of the 91-m (300-ft) barrier; 8 monitoring wells around the first pilot test site; 9 monitoring wells around the second pilot test site; and 2 additional compliance monitoring wells.

A tracer injection test and the first pilot low-concentration Ca-citrate-PO₄ injection test (well N-138) were conducted in the spring 2006 during high-river stage conditions. A second pilot test at a different well (199-N-137) at the downstream end of the barrier was conducted in September 2006 during low-river stage conditions. The injection formula was revised for the second pilot test based on the monitoring of the results of the first pilot test and additional laboratory work. The injection formula was revised again following the second pilot-test for the remaining barrier well injections. The final low-concentration formulation consisted of 2.5 mM citrate, 1 mM calcium, and 10 mM phosphate. Low-concentration Ca-citrate-PO₄ injections were conducted in nine wells in March 2007, during both high- and low-river stage conditions. Six additional injections occurred in June and July of 2007, during high-river stage conditions, for wells that had injections during low-river stage in March. Performance monitoring is underway.

Based on a comparison of hydraulic and transport response data at the two pilot test sites, researchers determined the apparent permeability contrast between the Hanford and Ringold Formations was significantly less over the upstream portion of the barrier (between injection wells 199-N-138 and 199-N-141), allowing for treatment of the entire Hanford and Ringold Formations screened interval with a single-injection operation at high-river stage. Because of a larger contrast over the downstream portion of the barrier (between injection wells 199-N-142 and 199-N-137), researchers recommend that wells screened only across the contaminated portion of the Ringold Formation be installed before future injections to provide for better treatment efficiency and coverage.

River stage during the barrier injection was an important parameter in the depth interval treated and efficiency of treatment. River stage along this section of the river is controlled by the rate of discharge at PRD, located approximately 29 km (18 mi) upstream of the 100-N Area. Initially, it was theorized that conducting injections during low-river stage would provide treatment for the Ringold Formation, while injections during high-river stage target Hanford formation treatment. For the upstream portion of the barrier, the contrast between permeability in the Hanford and Ringold Formations was sufficiently small that injections at high-river stage alone were successful in treating both the Hanford and Ringold Formations. However, for the downstream portion of the barrier, multiple injections did not provide complete treatment. High-river stage conditions provided a hydraulic barrier that contained the injection

solution in the Hanford formation, allowing adequate treatment. Unfortunately, it appeared that injections conducted during low-river stage were of limited success in providing adequate extent of treatment in the Ringold Formation. The large contrast in permeability between the Hanford and Ringold Formations along the downstream portion of the barrier resulted in the loss of a significant portion of the injection volume due to the relatively thin saturated Hanford formation interval, associated shoreline seeps, and limited treatment of the Ringold Formation.

Design specifications for the barrier installation stipulated that the chemical concentrations should be at least 50% of injection concentration 6.1 m (20 ft) from each injection well. This is considered a sufficient radial extent of treatment to provide overlap of treatment between injection wells. While monitoring points were not installed between injection wells outside of the pilot test sites, monitoring was conducted in adjacent injection wells during treatment operations. Because no monitoring wells were available at a 6.1-m (20-ft) radial distance to assess the extent of treatment, arrival data from adjacent injection wells (9.1-m [30-ft] spacing) were used as an indicator. To account for the increase in radial distance to this monitoring point, the phosphate concentration metric for arrival at adjacent injection wells was reduced to 20% to 30% of the injection concentration (from 50% at a 6.1-m [20-ft] distance). Based on this injection performance metric, phosphate concentrations measured in adjacent fully screened injection wells indicated generally satisfactory treatment. However, data from available Ringold Formation monitoring wells indicated treatment of the Ringold Formation over the downstream portion of the barrier (where Hanford/Ringold formation permeability contrast is larger) was not as effective.

Temporary increases in Sr and ^{90}Sr were expected during field-scale low-concentration Ca-citrate- PO_4 injection tests, which were designed based on bench-scale laboratory studies with the low-concentration formulation and sediments from 100-N Area (see Sections 2 and 3). The observed increases in ^{90}Sr concentration are due to the higher ionic strength of the solution and increases in calcium concentration resulting from this process. Concentrations are expected to decline over time (months, years) as the ^{90}Sr is incorporated through initial precipitation and adsorption/slow incorporation into the apatite, and as the reagent plume dissipates.

^{90}Sr concentrations in monitoring wells at the first pilot test site, conducted in the spring of 2006, showed an average increase in peak ^{90}Sr concentrations of 8.4 times the average baseline measurements at the site measured earlier in the year (see Table 5.8). Based on these results and additional laboratory measurements, the Ca-citrate- PO_4 injection concentrations were revised with lower calcium and citrate concentrations (2.5 times) for the second pilot test, conducted in the fall of 2006. Average peak ^{90}Sr concentrations following the second pilot test injection were significantly lower than first pilot test (3.8 times the average baseline ^{90}Sr concentrations; see Table 5.15) while still targeting the same level of apatite formation. The injection formulation was revised again following the second pilot test with further decreases in calcium and citrate concentrations and a ~4 times increase in the phosphate concentration to maximize the apatite precipitate mass and minimize the initial ^{90}Sr increase. This final, low-concentration formulation was used for the barrier well injections conducted in 2007. Monitoring of ^{90}Sr concentrations at the two pilot test sites in 2007 using the final low-concentration formulation showed average peak increases of 2.8 times the baseline average ^{90}Sr concentration at the first pilot test site, and 2.3 times the baseline average ^{90}Sr concentration at the second pilot test site (see Tables 5.8 and 5.15).

Strontium-90 concentrations in groundwater along the Columbia River at the 100-N Area show significant temporal variability based on measurements from aquifer tubes and long-term monitoring

wells installed prior to the apatite treatability test. Additionally, there is a general spatial trend in ^{90}Sr concentrations in the aquifer along the river as shown in Figure 1.8 with the highest concentrations existing over the central/downstream portion of the barrier (between injection wells 199-N-142 and 199-N-136), and high concentrations decreasing in both the upstream and downstream directions. Due to the short time between the installation of compliance, injection, and pilot test monitoring wells at the 100-N Area apatite treatability test site and the Ca-citrate- PO_4 injections (started at the site in the spring of 2006), there were insufficient data from these wells alone to establish baseline ^{90}Sr ranges at the site. Therefore, baseline ^{90}Sr ranges were established for the injection and compliance wells at the treatability test site based on gross beta analysis from the aquifer tube monitoring and the limited preinjection monitoring from the treatability test wells. This analysis is discussed in Section 8.1 with the ^{90}Sr ranges determined for these wells shown in Table 8.5.

Strontium-90, gross beta, and SpC monitoring data available for inclusion in this interim report (up to and including samples collected on November 14, 2007) showed post-treatment increases in these values at the injection wells, compliance wells, and aquifer tubes (see Figures 8.11 through 8.39). However, this initial spike in ^{90}Sr concentration was followed by a generally decreasing trend at all injection well locations. Longer-term, post-treatment ^{90}Sr concentrations at most injection well locations showed that levels were maintained near or below the low end of the estimated range in baseline ^{90}Sr concentration, indicating that the low-concentration treatments likely did have an impact on aqueous ^{90}Sr concentrations within the treatment zone. Additional monitoring that encompasses the full extent of seasonal variability in Columbia River stage would be required to fully assess the effectiveness of the low-concentration treatments. It should also be noted that wells screened only in the Hanford Formation at the pilot test sites have been dry since shortly after the 2007 injections. Monitoring in these Hanford-screened wells will resume after the river stage increases in the spring of 2008. Because high-concentration injections will be conducted during the upcoming spring/summer high-river stage period, continued assessment of the effectiveness of the low-concentration treatments cannot be continued once these injections commence. Attention will shift instead to performance assessment of the high-concentration treatments, which is the primary objective of the apatite treatability studies.

Longer-term, post-treatment ^{90}Sr concentrations in the compliance monitoring wells and river tubes have generally remained high relative to baseline ranges, although values had started to drop by the end of the monitoring period. Elevated ^{90}Sr concentrations were well correlated with elevated SpC values, indicating that the elevated ^{90}Sr concentrations are likely associated with impacts from residual high-ionic strength injection solutions. Compliance monitoring wells and river tubes are located outside the primary treatment zone and therefore are expected to take additional time for ^{90}Sr concentrations to decline to treatment zone levels.

Longer-term monitoring of other water quality parameters (i.e., field parameters and trace metals) were not in HEIS or compiled for inclusion in this interim report. Shorter-term monitoring of field parameters and trace metals following the two pilot tests conducted in 2006 showed significant decreases in DO concentrations and ORP due to citrate biodegradation (see Tables 5.5 and 5.12). Redox-sensitive trace metals (e.g., iron, manganese, and aluminum) concentrations were increased above baseline values after the injections at the pilot test sites due to these reducing conditions (see Tables 5.7 and 5.14).

9.2 Path Forward

The objective of the field treatability testing, as stated in the test plan (DOE/RL 2006), is to address the following questions:

- Will apatite precipitate in the target zone?
- Does the apatite result in reducing ^{90}Sr in groundwater?
- Given a fixed well spacing of 9.1 m (30 ft), what is the optimal injection volume per well for installation of a 91-m (300-ft) barrier wall?

The first two questions listed above are not addressed in this interim report for the low Ca-citrate- PO_4 injections, but will be addressed from analysis of sediment samples collected from coreholes within the treatment zone and performance groundwater monitoring following the high-concentration Ca-citrate- PO_4 injections scheduled to begin in 2008. Injection volumes for the fixed 9.1 m (30-ft) spacing injection wells to create the barrier were determined based on the field sampling results of the low-concentration Ca-citrate- PO_4 injections described in this report. In addition to the injection volumes, researchers recommend installing injection wells that target only the lower portion of the contaminated zone, which would provide better and more efficient reagent coverage for the downstream section of the barrier. These additional wells are planned to be installed in the winter/spring of 2008.

Following the high concentration Ca-citrate- PO_4 injections planned to begin in 2008, sediment samples will be collected from boreholes in the treatment zone (focused on the two pilot test sites) for laboratory analysis. These studies will be used to determine the quantity of apatite in the sediments achieved by the field injections and to estimate the treatment longevity.

Strontium-90 performance monitoring of the treatability test site will begin after the final high concentration Ca-citrate- PO_4 injections are completed. Groundwater monitoring following these injections will also assess overall impacts on the water quality (e.g., field parameters, anions, and trace metals). Changes in aquifer permeability from this process will also be assessed as part of the treatability test. Pressures and tracer arrivals monitored during the initial pilot injection tests will be compared to monitored values at the ending high-concentration injections at the pilot test sites, which are planned to begin in 2008. Numerical models developed for the pilot test sites will be used to estimate the hydraulic properties of these sites based on fitting the monitoring data collected during these tests.

10.0 References

- Andronescu E, E Stefan, E Dinu, and C Ghitulica. 2002. "Hydroxyapatite Synthesis." *Key Engineering Materials*, 206-213:1595-1598.
- Arey JS, JC Seaman, and PM Bertsch. 1999. "Immobilization of Uranium in Contaminated Sediments by Hydroxyapatite Addition." *Environmental Science & Technology*, 33:337-342.
- Amrhein C and DL Suarez. 1990. "Procedure for Determining Sodium-Calcium Selectivity in Calcareous and Gypsiferous Soils." *Soil Science Society of America Journal*, 54:999-1007.
- Bailey JE and DF Ollis. 1986. *Biochemical Engineering Fundamentals*. McGraw-Hill Publishing Co., New York.
- Bailliez S, A Nzihou, E Beche, and G Flamant. 2004. "Removal of Lead by Hydroxyapatite Sorbent." *Process Safety and Environmental Protection*, 82:175-180.
- Bechtel Hanford, Inc. (BHI). 1995. *Technical Reevaluation of the N-Springs Barrier Wall*. BHI-00185 Rev. 0, Bechtel Hanford, Inc., Richland, Washington.
- Belousova EA, WL Griffin, SY O'Reilly, and NI Fisher. 2002. "Apatite as an Indicator Mineral for Mineral Exploration: Trace-Element Compositions and Their Relationship to Host Rock Type." *Journal of Geochemical Exploration*, 76:45-69.
- Brynhildsen L and T Rosswall. 1997. "Effects of Metals on the Microbial Mineralization of Organic Acids." *Water, Air, and Soil Pollution*, 94(1-2):45-57.
- Chairat C, EH Oelkers, S Kohler, N Harouiya, and JE Lartique. 2004. "An Experimental Study of the Dissolution Rates of Apatite and Britholite as a Function of Solution Composition and pH from 1-12." *Water-Rock Interaction*. Taylor & Francis Group, London, pp. 671-674.
- Deutsch and Journel. 1998. "GSLIB, Geostatistical Software Library and User's Guide, 2nd Ed.", Oxford University Press,
- DOE/RL. 2002. *Standardized Stratigraphic Nomenclature for Post-Ringold-Formation Sediments Within the Central Pasco Basin*. DOE/RL-2002-39, U.S. Department of Energy, Richland Operations Office, Richland, Washington.
- DOE/RL. 2004. *Calendar Year 2003 Annual Summary Report for the 100-HR-3, 100-KR-4, and 100-NR-2 Operable Unit (OU) Pump & Treat Operations*. DOE/RL-2004-21, Rev. 0, U.S. Department of Energy, Richland Operations Office, Richland, Washington.
- DOE/RL. 2006. *Strontium-90 Treatability Test Plan for 100-NR-2 Groundwater Operable Unit*. DOE/RL-2005-96, Rev. 0, U.S. Department of Energy, Richland Operations Office, Richland, Washington.

DOE/RL. 2007. *Aquatic and Riparian Receptor Impact Information for the 100-NR-2 Groundwater Operable Unit*. DOE/RL-2006-26, Rev. 0, U.S. Department of Energy, Richland Operations Office, Richland, Washington.

Elliot JC, PE Mackie, and RA Young. 1973. "Monoclinic Hydroxyapatite." *Science*, Vol. 180, pp. 1055-1057.

Fluor Hanford, Inc. (FH). 2005. *Borehole Summary Report for Wells 199-N-122 (C4954) and 199-N-123 (C4955); 100-NR-2 Operable Unit Rev 0*. WMP-27771, Fluor Hanford, Inc., Richland, Washington.

FH. 2006. *Borehole Summary Report for 100-NR-2 Treatability Test Wells 2006*. WMP-30078, Rev. 0, Fluor Hanford Inc., Richland, Washington.

Fuller CC, JR Bargar, and JA Davis. 2003. "Molecular-Scale Characterization of Uranium Sorption by Bone Apatite Materials for a Permeable Reactive Barrier Demonstration." *Environmental Science & Technology*, 37:4642-4649.

Fuller CC, JR Bargar, JA Davis, and MJ Piana. 2002. "Mechanisms of Uranium Interactions with Hydroxyapatite: Implications for Groundwater Remediation." *Environmental Science & Technology*, 36:158-165.

Geochem Software, Inc. (Geochem). 1994. *Mac MINTEQ-A2: Aqueous Geochemistry for the Macintosh*. Geochem Software, Inc., Reston, Virginia.

Hartman MJ, LF Morasch, and WD Webber. 2007. *Hanford Site Groundwater Monitoring for Fiscal Year 2006*. PNNL-16346, Pacific Northwest National Laboratory, Richland, Washington.

Heslop DD, Y Bi, AA Baig, M Otsuka, and WI Higuchi. 2005. "A Comparative Study of the Metastable Equilibrium Solubility Behavior of High-Crystallinity and Low-Crystallinity Carbonated Apatites Using Ph and Solution Strontium as Independent Variables." *Journal of Colloid and Interface Science*, 289:14-25.

Hill RG, A Stamboulis, RV Law, A Clifford, MR Towler, and C Crowley. 2004. "The Influence of Strontium Substitution in Fluorapatite Glasses and Glass-Ceramics." *Journal of Non-Crystalline Solids* 336:223-229.

Hoopes JA and DRF Harleman. 1967. "Dispersion in Radial Flow from a Recharge Well." *Journal of Geophysical Research*, Vol. 72, pp. 3595-3607.

Hughes JM, M Cameron, and KD Crowley. 1991. "Ordering of Divalent Cations in the Apatite Structure: Crystal Structure Refinements of Natural Mn- and Sr-bearing Apatite." *American Mineralogist*, Vol. 76(11-12):1857-1862.

Hughes JM and J Rakovan. 2002. "The Crystal Structure of Apatite, Ca₅(PO₄)₃(F,OH,Cl), in Phosphates: Geochemical, Geobiological and Materials Importance." *Reviews in Mineralogy and Geochemistry*, Vol. 48, pp. 1-12. Mineralogical Society of America, Washington, D.C.

Hydrogeologic, Inc. 1999. "Groundwater-River Interaction in the Near River Environment at the 100-N Area, Rev. 0." Prepared for Sandia National Laboratories by Hydrogeologic, Inc., Herndon, Virginia.

Hydrogeologic, Inc. 2001. "Strontium-90 Transport in the Near River Environment at the 100-N Area, Rev. 0." Hydrogeologic, Inc., Herndon, Virginia.

Innovative Treatment and Remediation Demonstration Program (ITRD). 2001. *Hanford 100-N Area Remediation Options Evaluation Summary Report*. Office Environmental Management, Subsurface Contaminants Focus Area, Sandia National Laboratories, Albuquerque, New Mexico.

Jeanjean J, JC Rouchaud, L Tran, and M Fedoroff. 1995. "Sorption of Uranium and Other Heavy Metals on Hydroxyapatite." *J. Radioanal. Nucl. Chem. Letters*, 201:529-539.

Koutsoukos PG and GH Nancollas. 1981. "Influence of Strontium Ion on the Crystallization of Hydroxylapatite from Aqueous-Solution." *Journal of Physical Chemistry*, 85:2403-2408.

Lazic S and Z Vukovic. 1991. "Ion-Exchange of Strontium on Synthetic Hydroxyapatite." *Journal of Radioanalytical and Nuclear Chemistry-Articles*, 149:161-168.

Legeros RZ, G Quirolgico, and JP Legeros. 1979. "Incorporation of Strontium in Apatite – Effect of pH." *Journal of Dental Research*, 58:169-169.

Lower SK, PA Maurice, SJ Traina, and EH Carlson. 1998. "Aqueous Lead Sorption by Hydroxylapatite: Applications of Atomic Force Microscopy to Dissolution, Nucleation and Growth Studies." *American Mineralogist*, Vol. 83, pp. 147-158.

Ma QY, SJ Traina, and TJ Logan. 1995. "In Situ Lead Immobilization by Apatite." *Environmental Science and Technology*, Vol. 27, pp. 1803-1810.

Mavropoulos E, AM Rossi, AM Costa, CAC Perez, JC Moreira, and M Saldanha. 2002. "Studies on the Mechanisms of Lead Immobilization by Hydroxyapatite." *Environmental Science & Technology*, 36:1625-1629.

Misra DN. 1998. "Interaction of Some Alkali Metal Citrates with Hydroxyapatite – Ion-Exchange Adsorption and Role of Charge Balance." *Colloids and Surfaces a-Physicochemical and Engineering Aspects*, 141:173-179.

Moelo Y, B Lasnier, P Palvadeau, P Leone, and F Fontan. 2000. "Lulzacite, Sr₂Fe₂+(Fe²⁺,Mg)(₂)Al-4(PO₄)(₄)(OH)(₁₀), a New Strontium Phosphate." *Comptes Rendus De L Academie Des Sciences Serie Ii Fascicule a-Sciences De La Terre Et Des Planetes*, Saint-Aubin-des-Chateaux, Loire-Atlantique, France, 330:317-324.

Mendoza DP, GW Patton, MJ Hartman, FA Spane, MD Sweeney, BG Fritz, TJ Gilmore, RD Mackley, BN Bjornstad, and RE Clayton. 2007. *Assessment of the Strontium-90 Contaminant Plume Along the Shoreline of the Columbia River at the 100-N Area of the Hanford Site*. PNNL-16894, Pacific Northwest National Laboratory, Richland, Washington.

Moore RC, K Holt, HT Zhao, A Hasan, N Awwad, M Gasser, and C Sanchez. 2003. "Sorptions of Np(V) by Synthetic Hydroxyapatite." *Radiochimica Acta*, 91:721-727.

Moore RC, M Gasser, N Awwad, KC Holt, FM Salas, A Hasan, MA Hasan, H Zhao, and CA Sanchez. 2005. "Sorptions of Plutonium(VI) by Hydroxyapatite." *Journal of Radioanalytical and Nuclear Chemistry*, 263:97-101.

Nancollas GH and MS Mohan. 1970. "The Growth of Hydroxyapatite Crystals." *Archives of Oral Biology*, 15(8):731-745.

Papargyris A, A Botis, and S Papargyri. 2002. "Synthetic Routes for Hydroxyapatite Powder Production." *Key Engineering Materials*, 206-213:83-86.

Raicevic S, Z Vukovic, TL Lizunova, and VF Komarov. 1996. "The Uptake of Strontium by Calcium Phosphate Phase Formed at Elevated pH." *Journal of Radioanalytical and Nuclear Chemistry-Articles*, 204:363-370.

Rendon-Angeles JC, K Yanagisawa, N Ishizawa, and S Oishi. 2000. "Effect of Metal Ions of Chlorapatites on the Topotaxial Replacement by Hydroxyapatite under Hydrothermal Conditions." *Journal of Solid State Chemistry*, 154:569-578.

Smiciklas I, A Onjia, and S Raicevic. 2005. "Experimental Design Approach in the Synthesis of Hydroxyapatite by Neutralization Method." *Separation and Purification Technology*, 44:97-102.

Spence RD and C Shi. 2005. *Stabilization and Solidification of Hazardous, Radioactive, and Mixed Wastes*. CRC Press, Boca Raton, Florida.

Sposito G, LJ Lund, and AC Chang. 1982. "Trace-Metal Chemistry in Arid-Zone Field Soils Amended with Sewage-Sludge. 1. Fractionation of Ni, Cu, Zn, Cd, and Pb in Solid-Phases." *Soil Science Society of America Journal*, 46:260-264.

Sposito G, KM Holtzclaw, C Jouany, and L Charlet. 1983a. "Cation Selectivity in Sodium – Calcium, Sodium – Magnesium, and Calcium – Magnesium Exchange on Wyoming Bentonite at 298-K." *Soil Science Society of America Journal* 47:917-921.

Sposito G, CS Levesque, JP Leclaire, and AC Chang. 1983b. Trace-Metal Chemistry in Arid-Zone Field Soils Amended with Sewage-Sludge. 3. Effect of Time on the Extraction of Trace-Metals." *Soil Science Society of America Journal* 47:898-902.

Steeffel CI. 2004. "Evaluation of the Field-Scale Cation Exchange Capacity of Hanford Sediments." *Water-Rock Interaction*, pp. 999-1002, Taylor & Francis Group, London.

Sumner, M. 2000. *Handbook of Soil Science*, CRC Press, p B-205.

Szecsody JE, CA Burns, RC Moore, JS Fruchter, VR Vermeul, MD Williams, DC Girvin, JP McKinley, MJ Truex, and JL Phillips. 2007. *Hanford 100-N Area Apatite Emplacement: Laboratory Results of Calcium Citrate-PO₄ Solution Injection and Sr-90 Immobilization in 100-N Sediments*. PNNL-16891, Pacific Northwest National Laboratory, Richland, Washington.

- Tofe AJ. 1998. "Chemical Decontamination Using Natural or Artificial Bone." US Patent 5,711,015.
- Van der Houwen JAM and AE Valsami-Jones. 2001. "The Application of Calcium Phosphate Precipitation Chemistry to Phosphorus Recovery: The Influence of Organic Ligands." *Environmental Technology*, 22:1325-1335.
- Vukovic Z, S Lazic, I Tutunovic, and S Raicevic. 1998. "On the Mechanism of Strontium Incorporation into Calcium Phosphates." *J. Serbian Chem. Soc.*, 63.5:387-393.
- Waychunas G. 1988. "Luminescence, X-ray Emission and New Spectroscopies." *Rev Mineral*. 18:638-698.
- Wright J. 1990. "Conodont Apatite: Structure and Geochemistry." *Biomineralization: Patterns, Processes and Evolutionary Trends*, J Carter (ed.), Van Nostrand Reinhold, New York.
- Wright J, KR Rice, B Murphy, and J Conca. 2004. "PIMS Using Apatite II™: How It Works To Remediate Soil and Water." *Sustainable Range Management*, RE Hinchee and B Alleman (eds.). Battelle Press, Columbus, Ohio. www.battelle.org/bookstore.
- Verbeeck RMH, M Hauben, HP Thun, and F Verbeeck. 1977. "Solubility and Solution Behaviour of Strontium Hydroxyapatite." *Z. Phys. Chem. (Wiesbaden)*, 108(2):203-215.
- Washington State Department of Ecology (Ecology). 1999. *Interim Remedial Action Record of Decision Declaration: Hanford 100 Area, Benton County, 100-NR-1 and 100-NR-2 Operable Units of the Hanford 100-N Area*. Washington State Department of Ecology, Olympia, Washington.
- White MD and M Oostrom. 2000. *Subsurface Transport Over Multiple Phase (STOMP): Theory Guide*. PNNL-11216, Pacific Northwest National Laboratory, Richland, Washington.
- White MD and M Oostrom. 2006. *Subsurface Transport Over Multiple Phases (STOMP): User's Guide Version 4.0*. PNNL-15782, Pacific Northwest National Laboratory, Richland, Washington.

Appendix A

Arrival Curves for Low-Concentration Treatment – March and June 2007

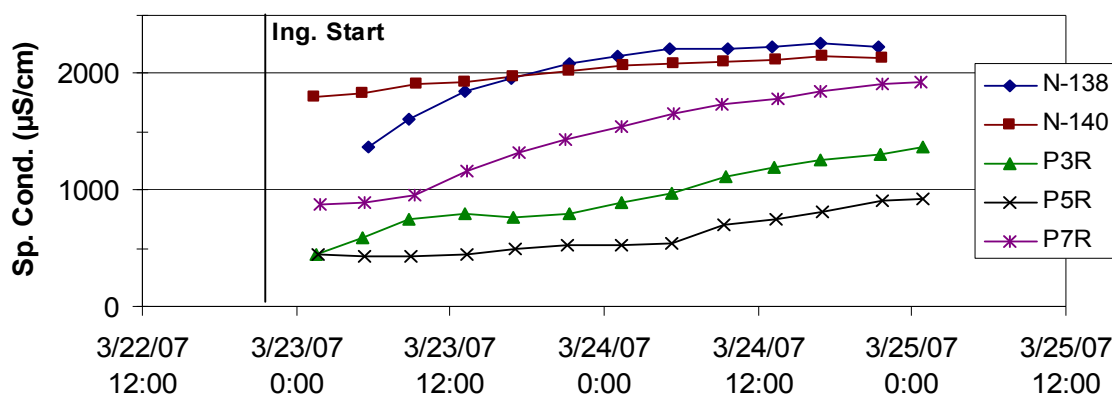
Appendix A

Arrival Curves for Low-Concentration Treatment – March and June 2007

Design specifications for the barrier installation stipulated that chemical concentrations would be 50% of injection concentration 6.1 m (20 ft) from each injection well. This is considered sufficient to provide overlap of barrier chemicals in between injection wells. While monitoring points were not installed between injection wells, monitoring was conducted in barrier wells adjacent to active injection wells. Periodic monitoring of the SpC in the monitoring wells adjacent to an injection well provided an indication of treatment effectiveness. This appendix provides plots for the SpC arrival at wells adjacent to injection wells. The actual phosphate concentrations over time were not measured over the course of the injection, but the timing and relative magnitude of the phosphate arrival could be expected to be similar to the increase in SpC, although somewhat dampened in magnitude and lagged in time.

March Injections

N-139 Injection Ringold Wells



N-139 Injection Hanford Wells

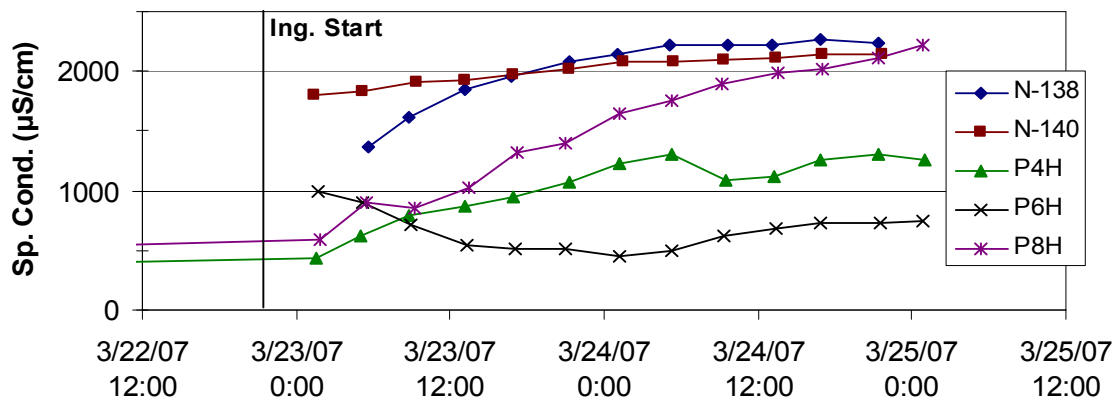


Figure A.1. Arrival Curves in Available Monitoring Wells During Treatment of 199-N-139

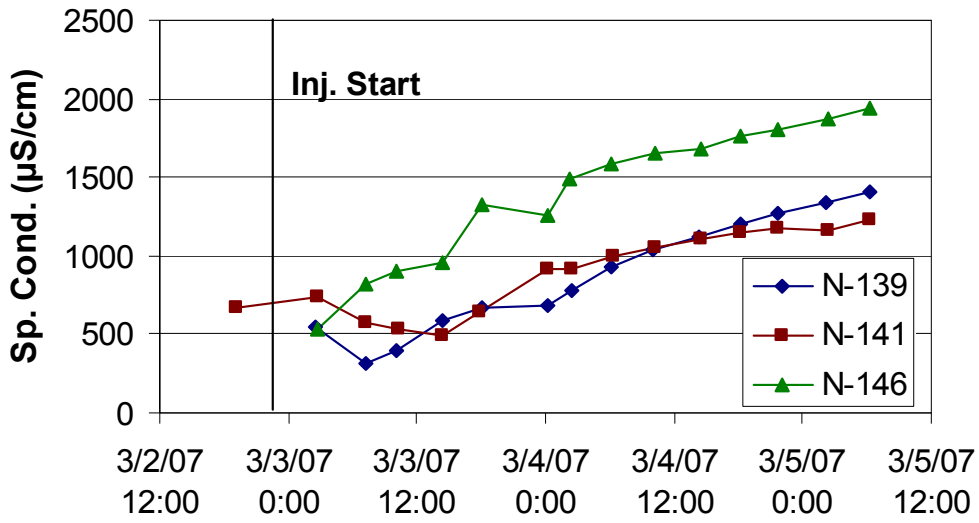


Figure A.2. Arrival Curves in Available Monitoring Wells During Treatment of 199-N-140

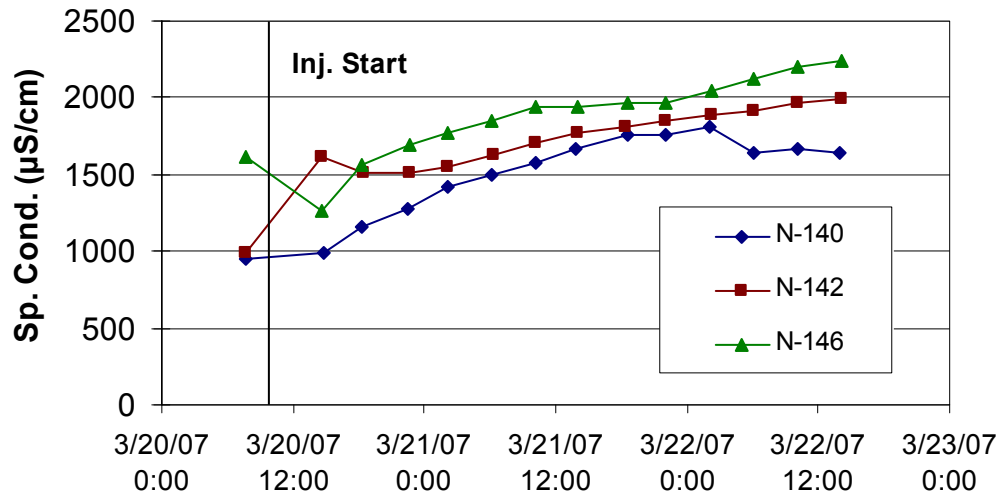


Figure A.3. Arrival Curves in Available Monitoring Wells During Treatment of 199-N-141

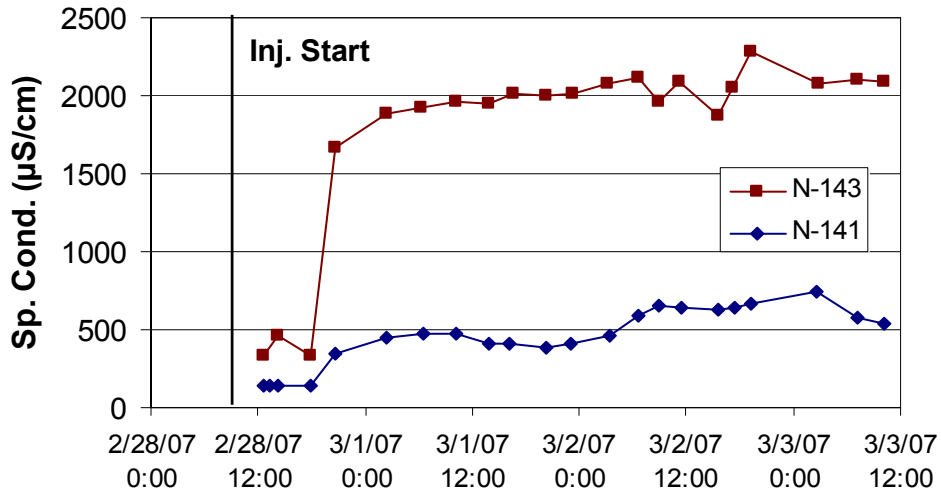


Figure A.4. Arrival Curves in Available Monitoring Wells During Treatment of 199-N-142

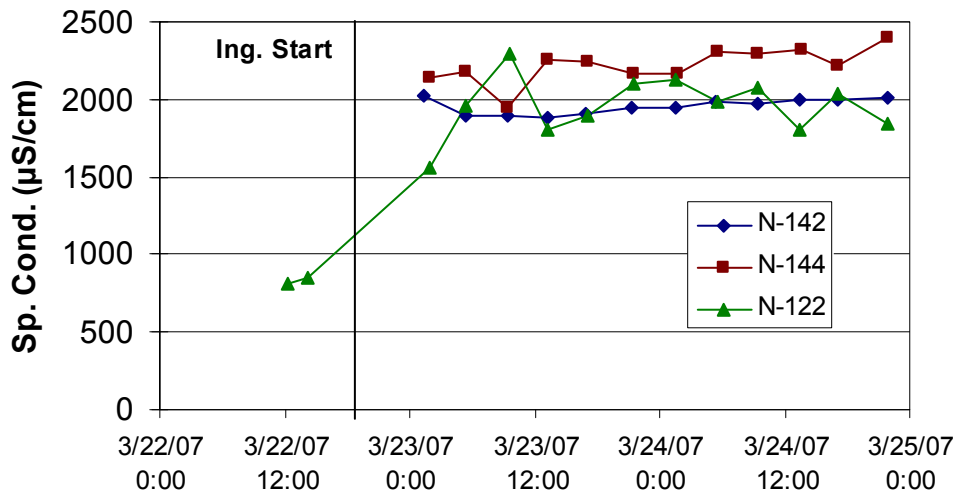


Figure A.5. Arrival Curves in Available Monitoring Wells During Treatment of 199-N-143

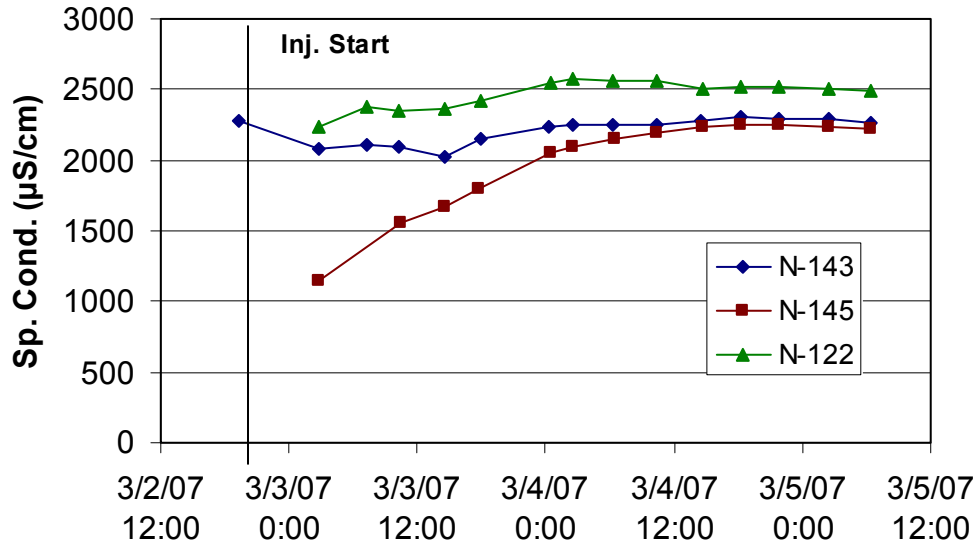


Figure A.6. Arrival Curves in Available Monitoring Wells During Treatment of 199-N-144

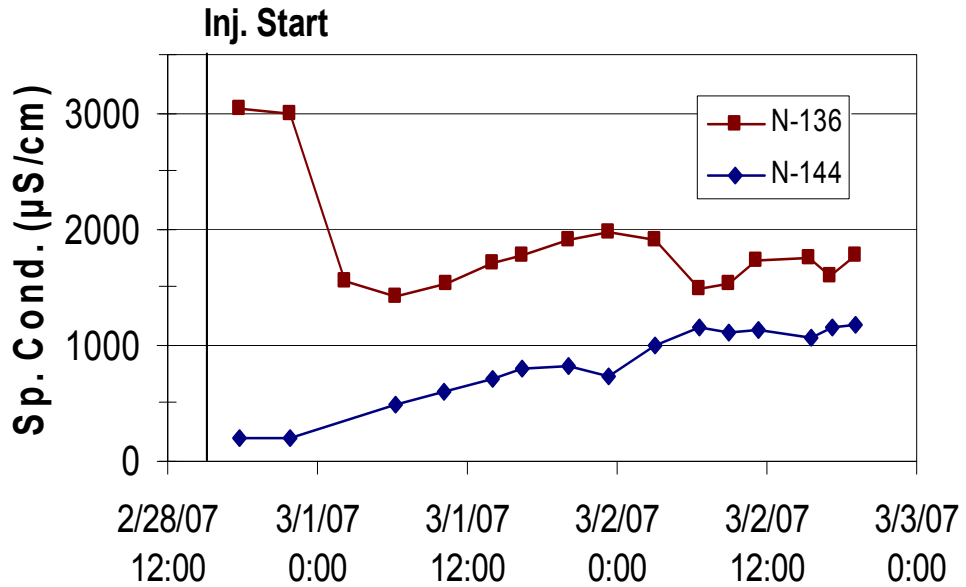


Figure A.7. Arrival Curves in Available Monitoring Wells During Treatment of 199-N-145

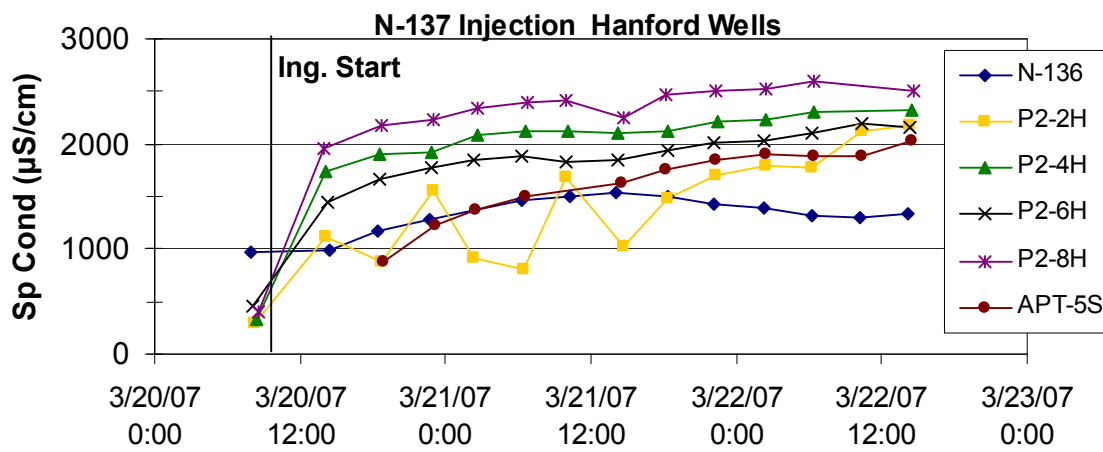
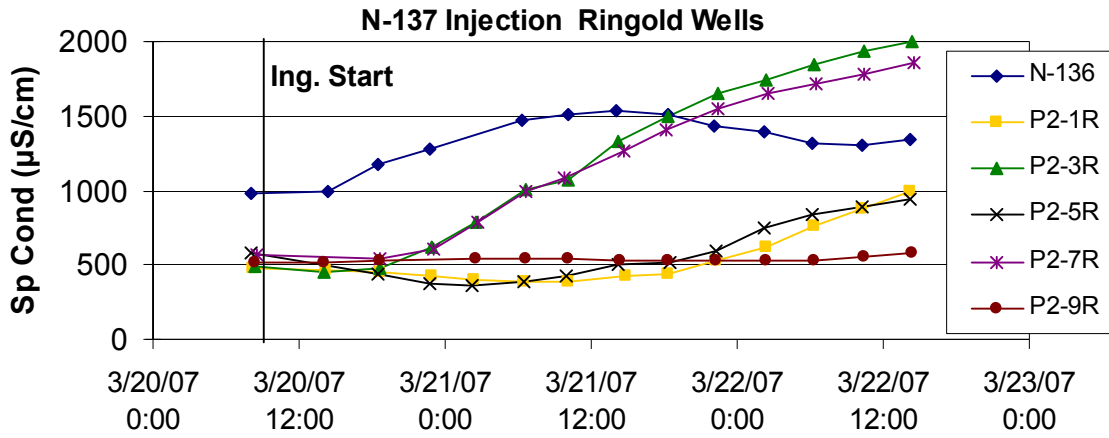


Figure A.8. Arrival Curves in Available Monitoring Wells During Treatment of 199-N-137

June Injections

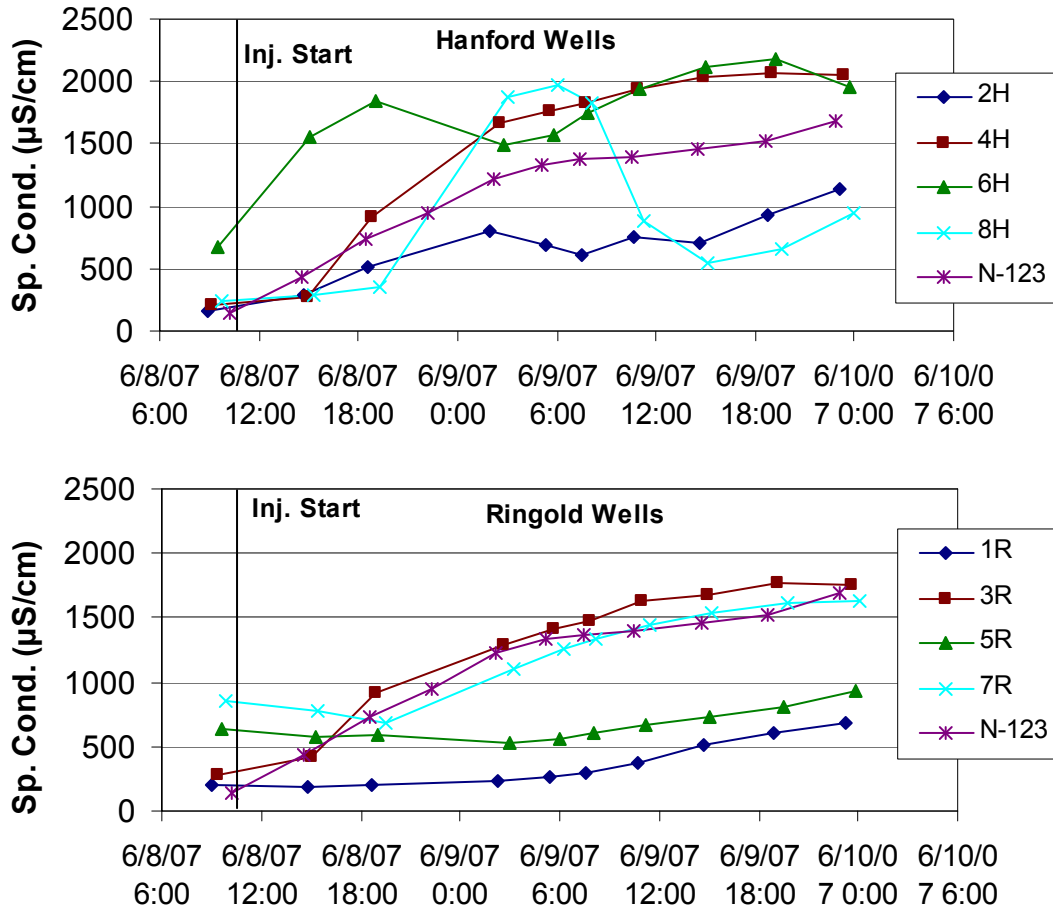


Figure A.9. Arrival Curves in Available Monitoring Wells During Treatment of 199-N-138

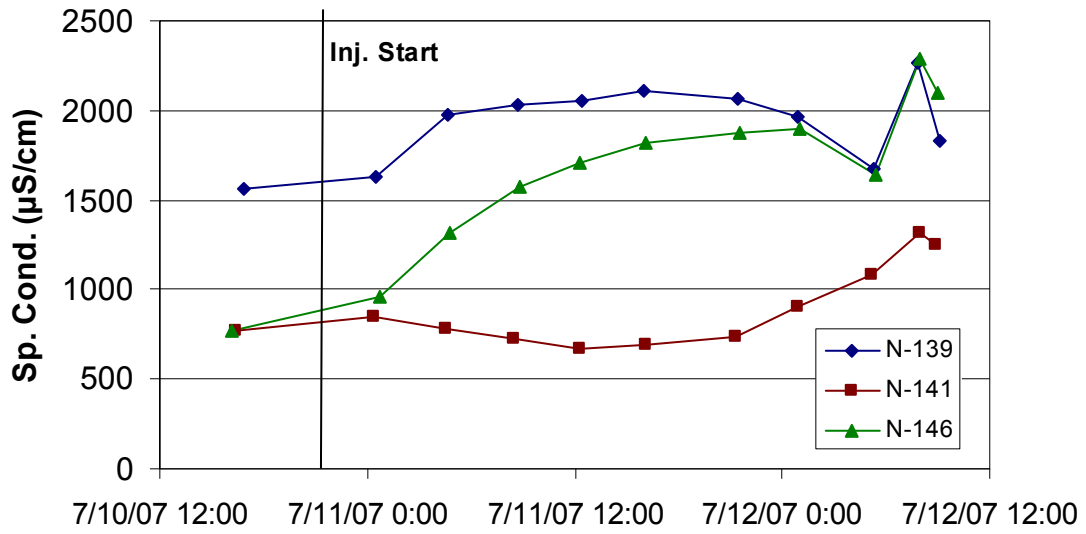


Figure A.10. Arrival Curves in Available Monitoring Wells During Treatment of 199-N-140

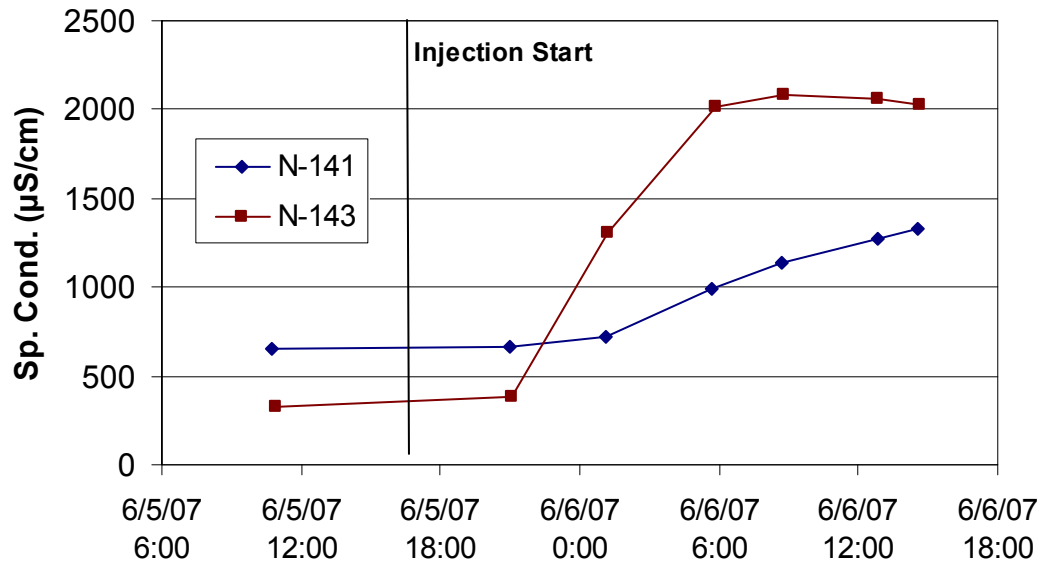


Figure A.11. Arrival Curves in Available Monitoring Wells During Treatment of 199-N-142

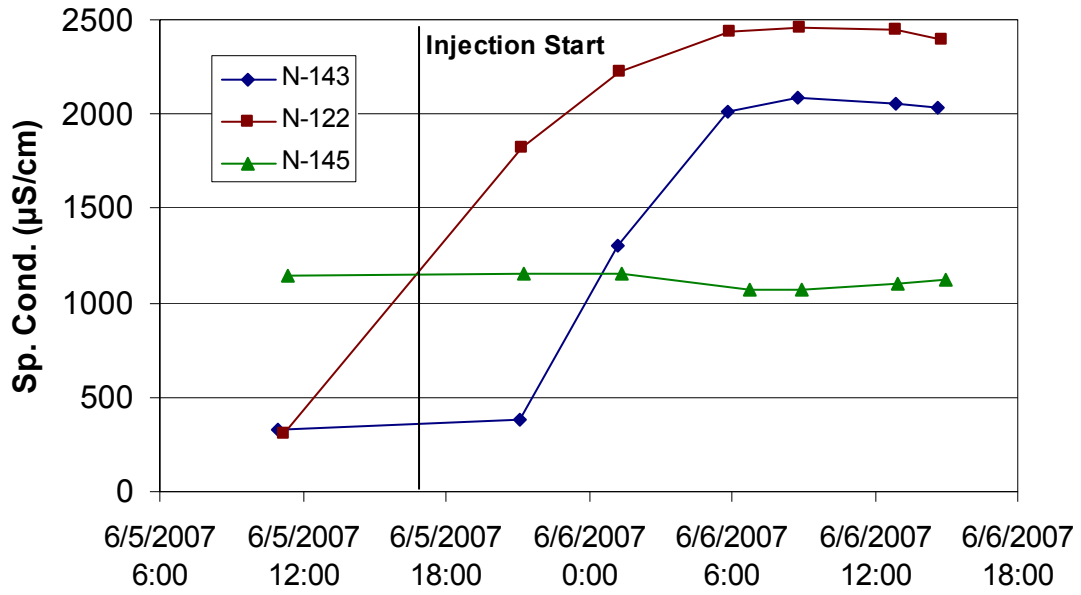


Figure A.12. Arrival Curves in Available Monitoring Wells During Treatment of 199-N-144

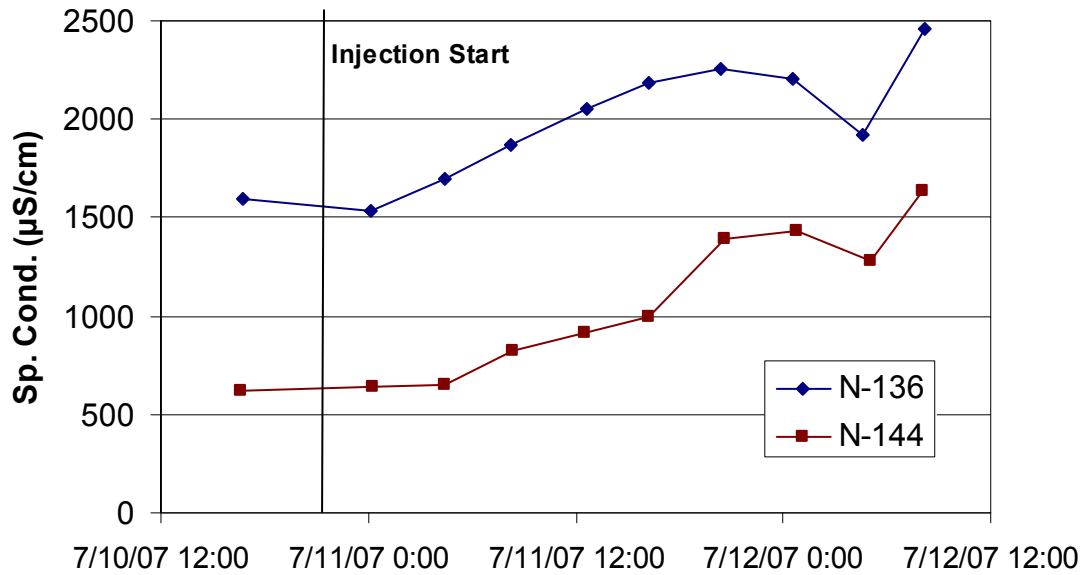


Figure A.13. Arrival Curves in Available Monitoring Wells During Treatment of 199-N-145

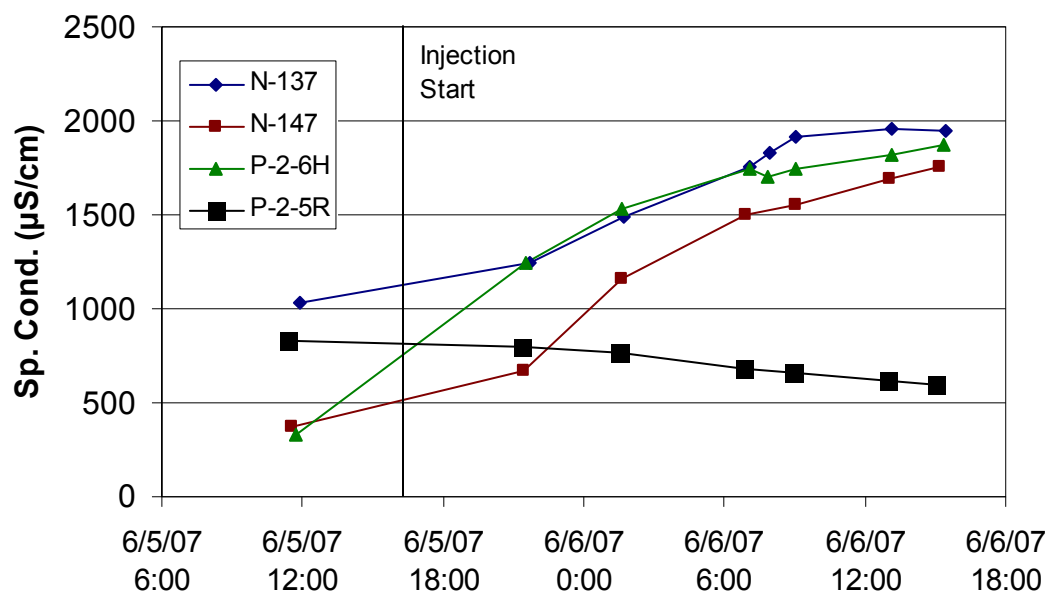


Figure A.14. Arrival Curves in Available Monitoring Wells During Treatment of 199-N-136

Appendix B

Pilot Test Performance Monitoring Figures

Appendix B

Pilot Test Performance Monitoring Figures

B.1 Pilot Test Site #1 Performance Monitoring Figures

The pilot test #1 performance monitoring plots for ^{90}Sr are shown in Figures B.1 through B.10. The pilot test #1 performance monitoring plots for calcium, phosphate, and SpC are shown in Figures B.11 through B.20. See Section 8.2.1 for additional discussion.

B.2 Pilot Test Site #2 Performance Monitoring Figures

The pilot test #2 performance monitoring plots for ^{90}Sr are shown in Figures B.21 through B.27. The pilot test #2 performance monitoring plots for calcium, phosphate, and SpC are shown in Figures B.28 through B.34. See Section 8.2.2 for discussion.

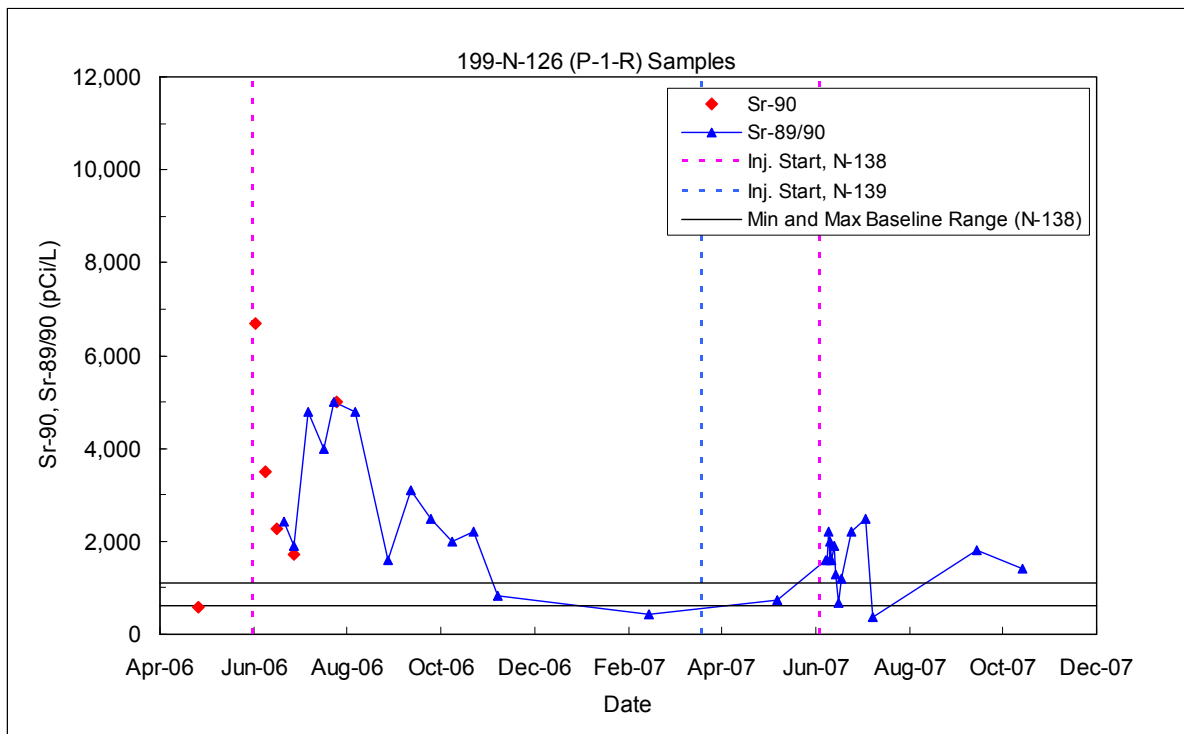


Figure B.1. ^{90}Sr Performance Monitoring Plots for Pilot Test #1 Well 199-N-126

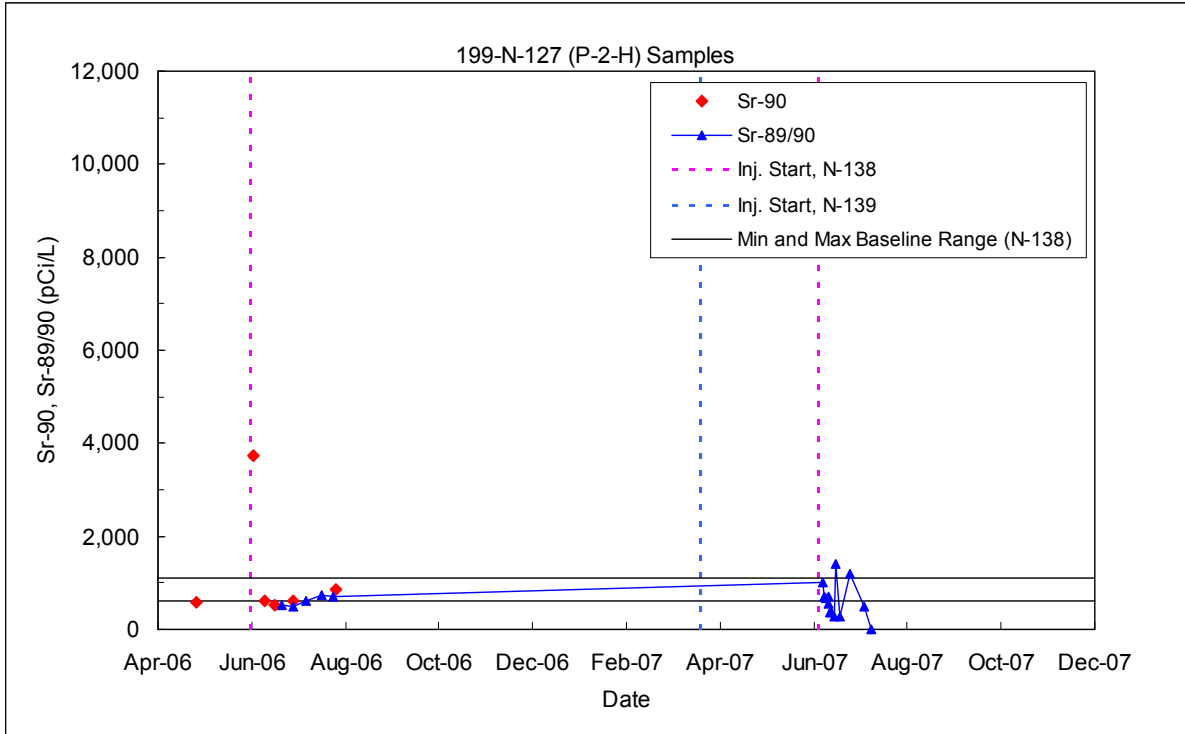


Figure B.2. ⁹⁰Sr Performance Monitoring Plots for Pilot Test #1 Well 199-N-127

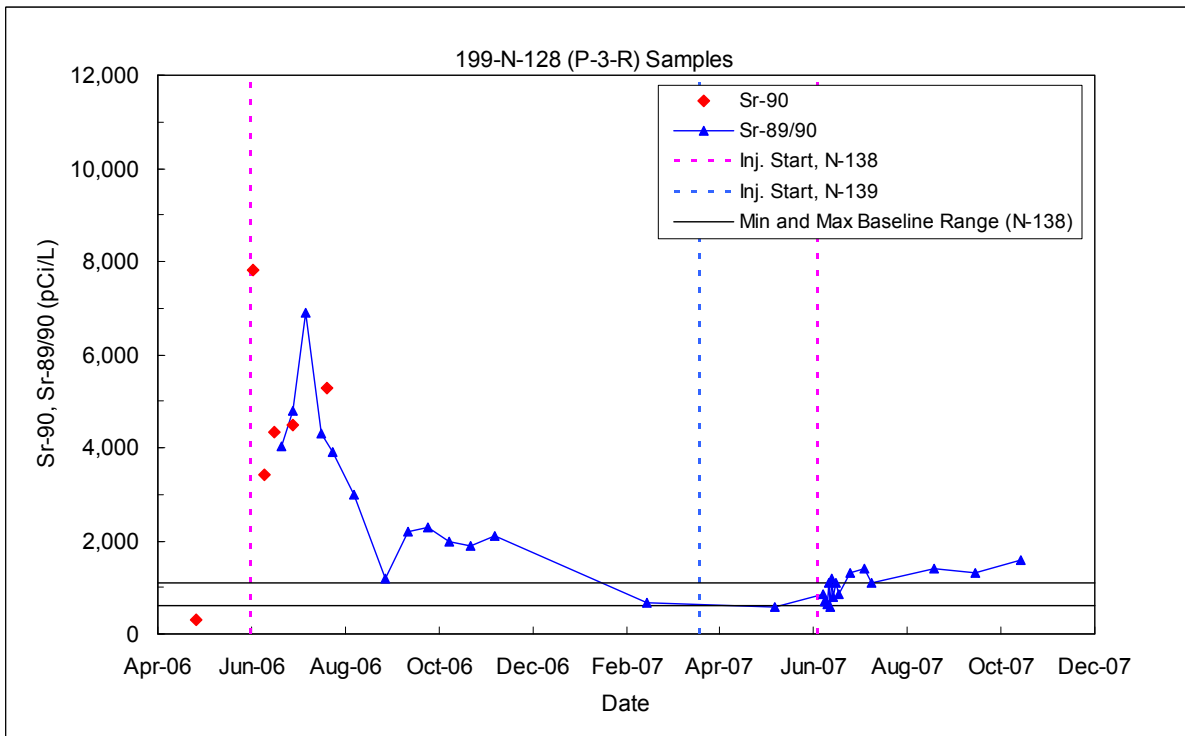


Figure B.3. ⁹⁰Sr Performance Monitoring Plots for Pilot Test #1 Well 199-N-128

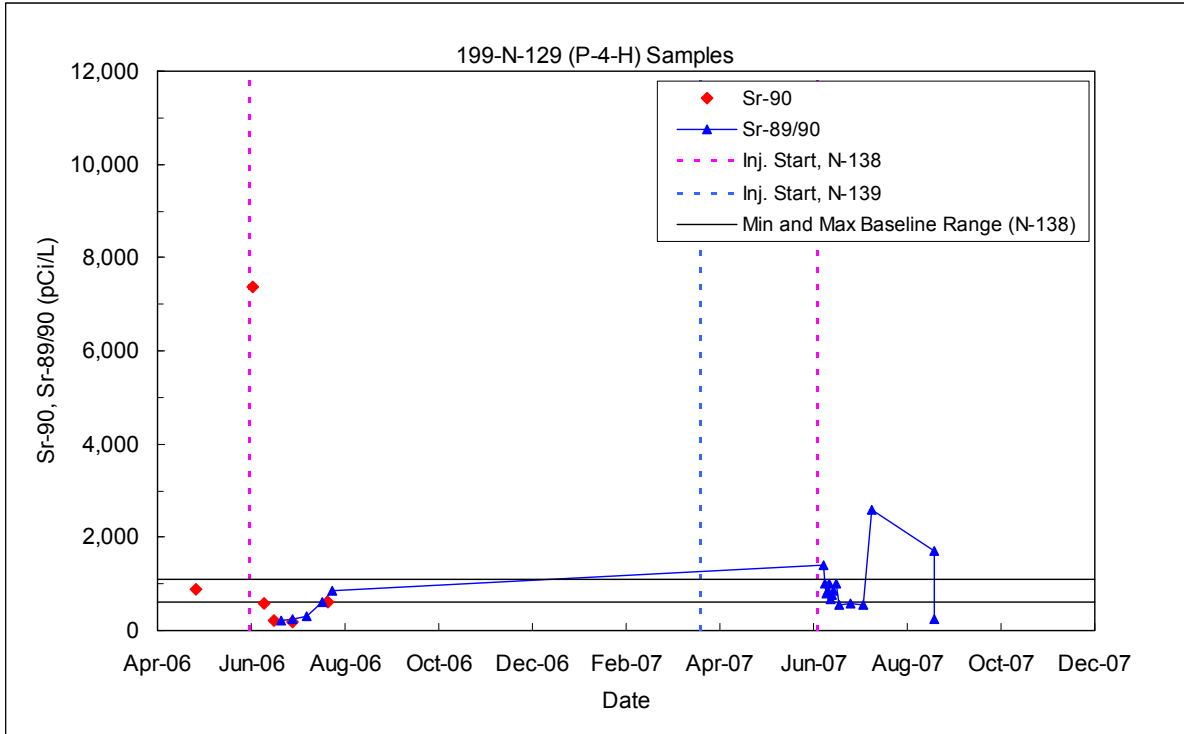


Figure B.4. ⁹⁰Sr Performance Monitoring Plots for Pilot Test #1 Well 199-N-129

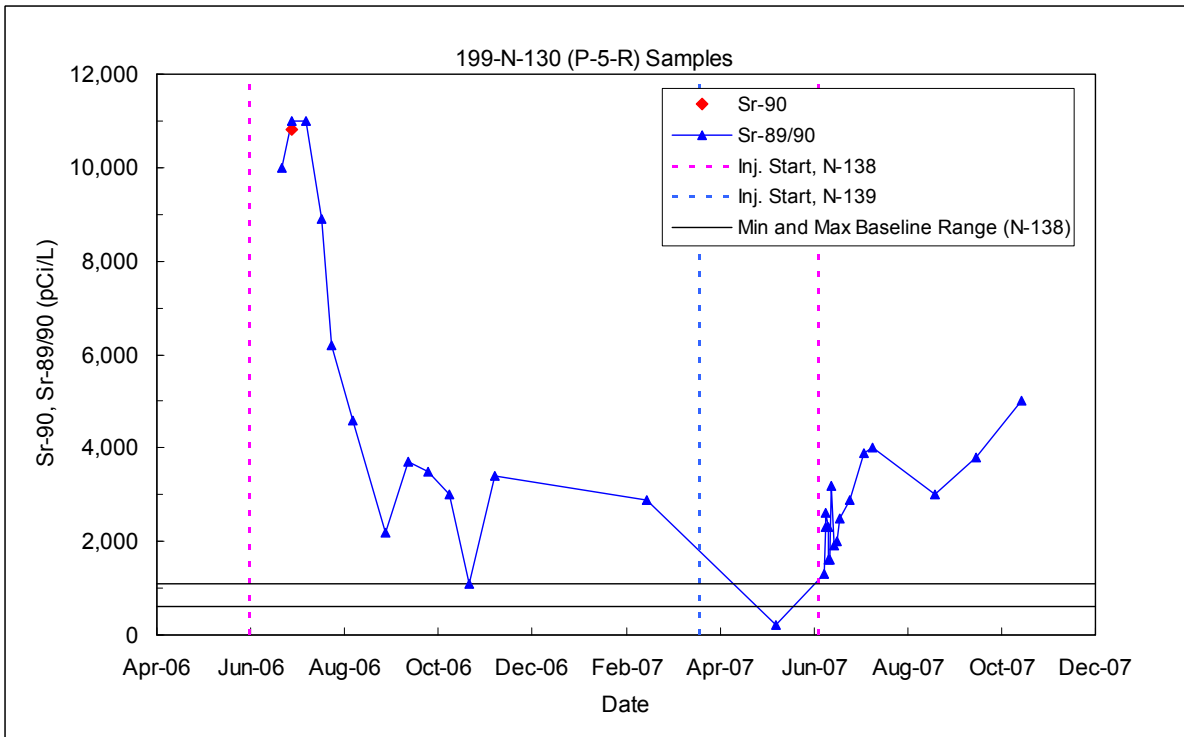


Figure B.5. ⁹⁰Sr Performance Monitoring Plots for Pilot Test #1 Well 199-N-130

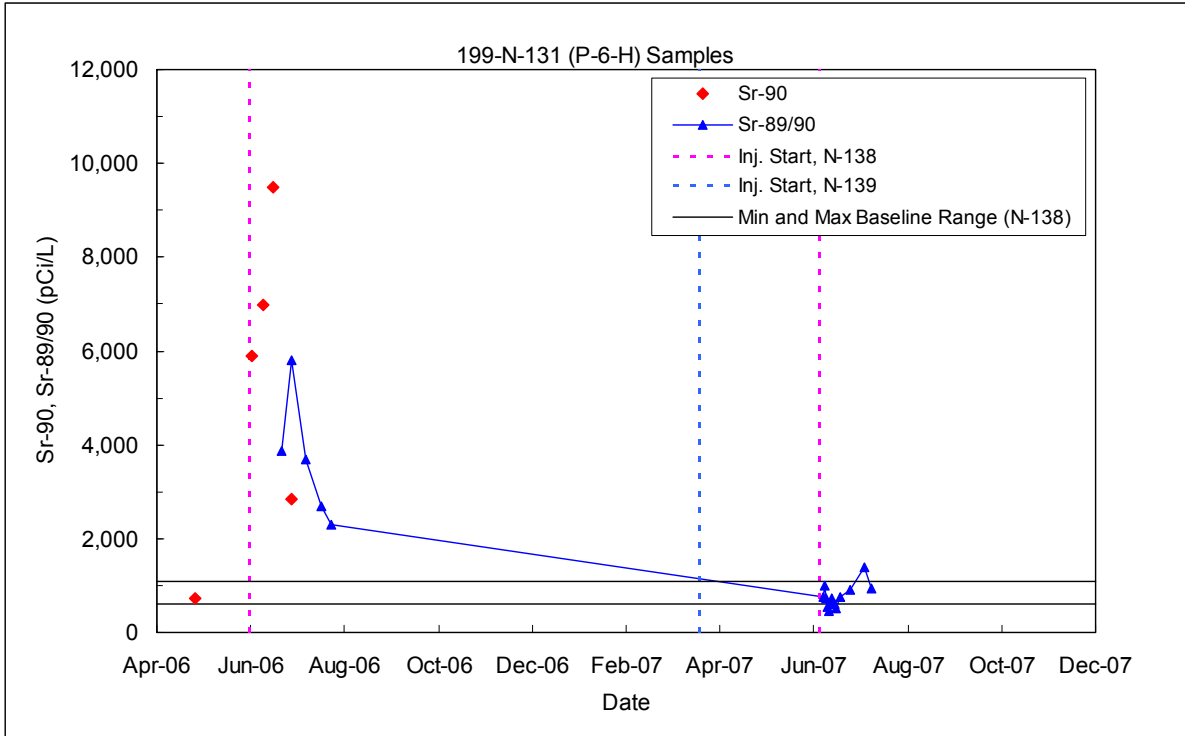


Figure B.6. ⁹⁰Sr Performance Monitoring Plots for Pilot Test #1 Well 199-N-131

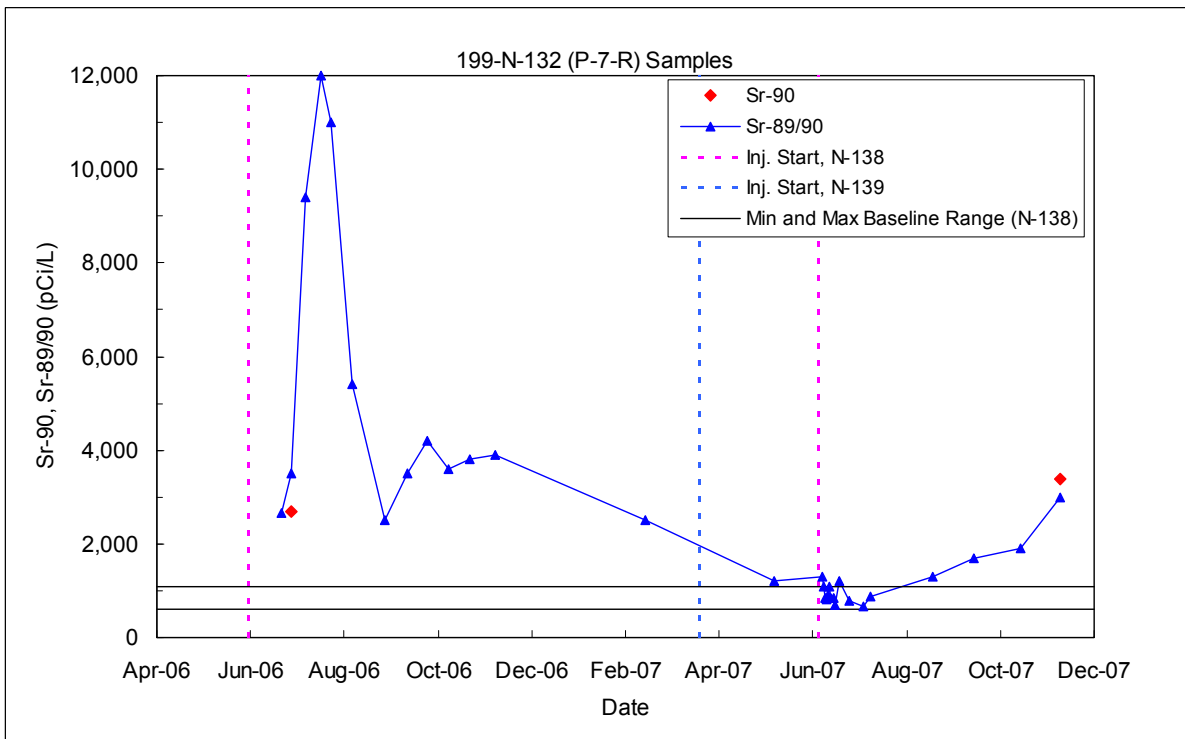


Figure B.7. ⁹⁰Sr Performance Monitoring Plots for Pilot Test #1 Well 199-N-132

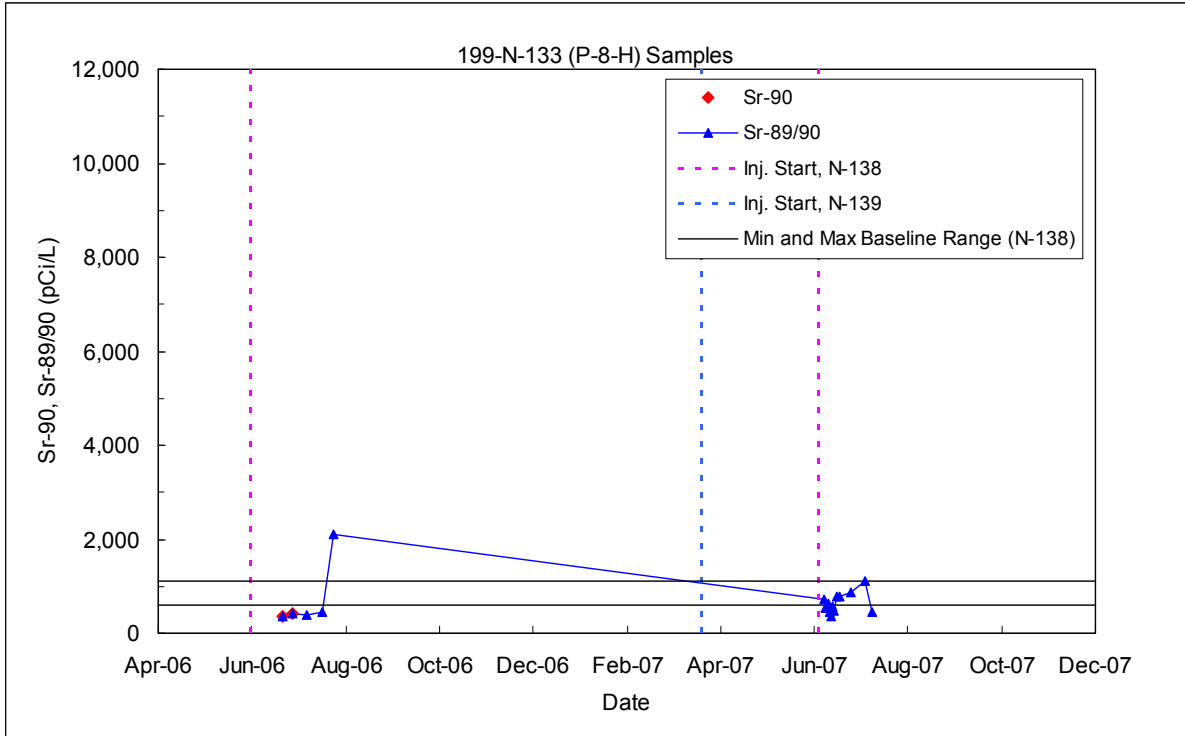


Figure B.8. ⁹⁰Sr Performance Monitoring Plots for Pilot Test #1 Well 199-N-133

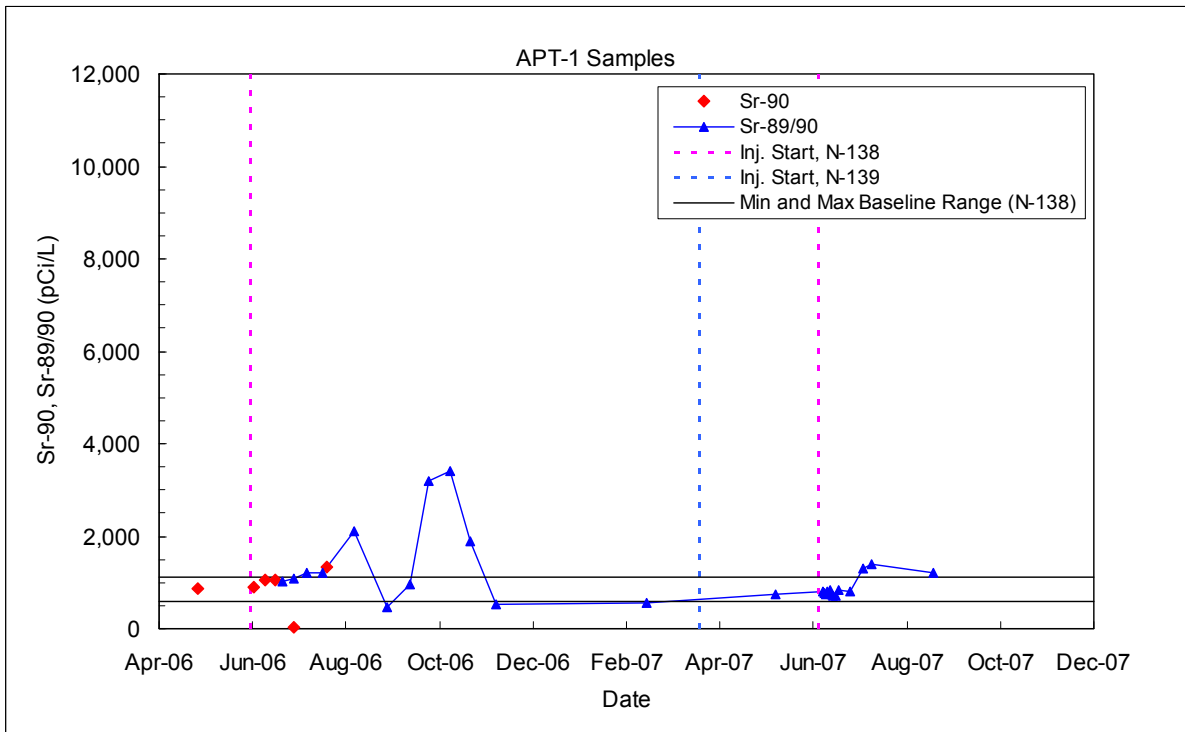


Figure B.9. ⁹⁰Sr Performance Monitoring Plots for Pilot Test #1 Aquifer Tube APT-1

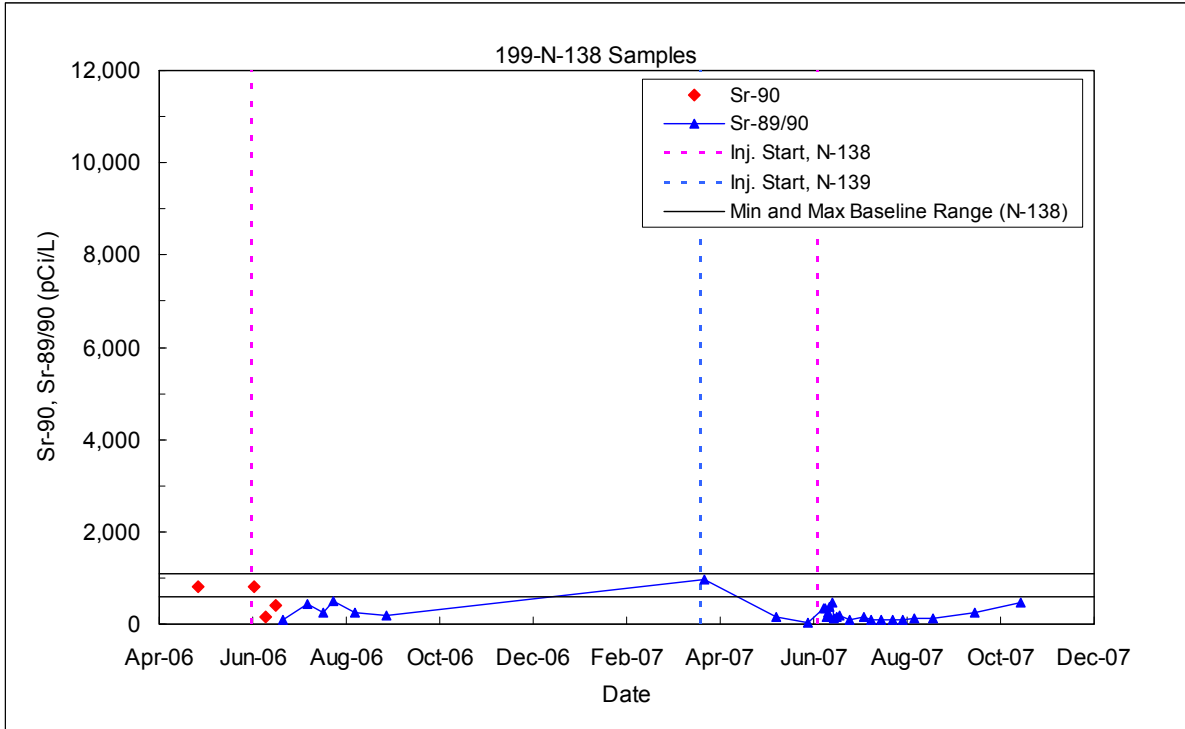


Figure B.10. ⁹⁰Sr Performance Monitoring Plots for Pilot Test #1 Injection Well 199-N-138

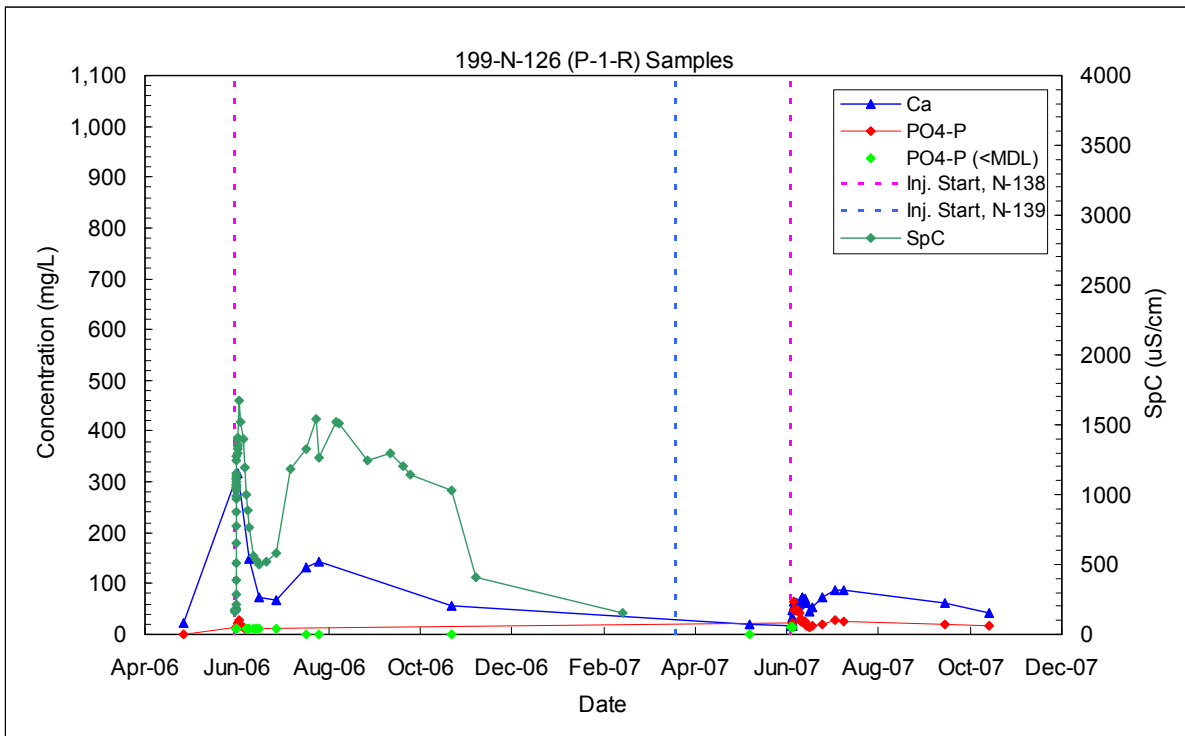


Figure B.11. Calcium, Phosphate, and Specific Conductance Performance Monitoring Plots for Pilot Test #1 Well 199-N-126

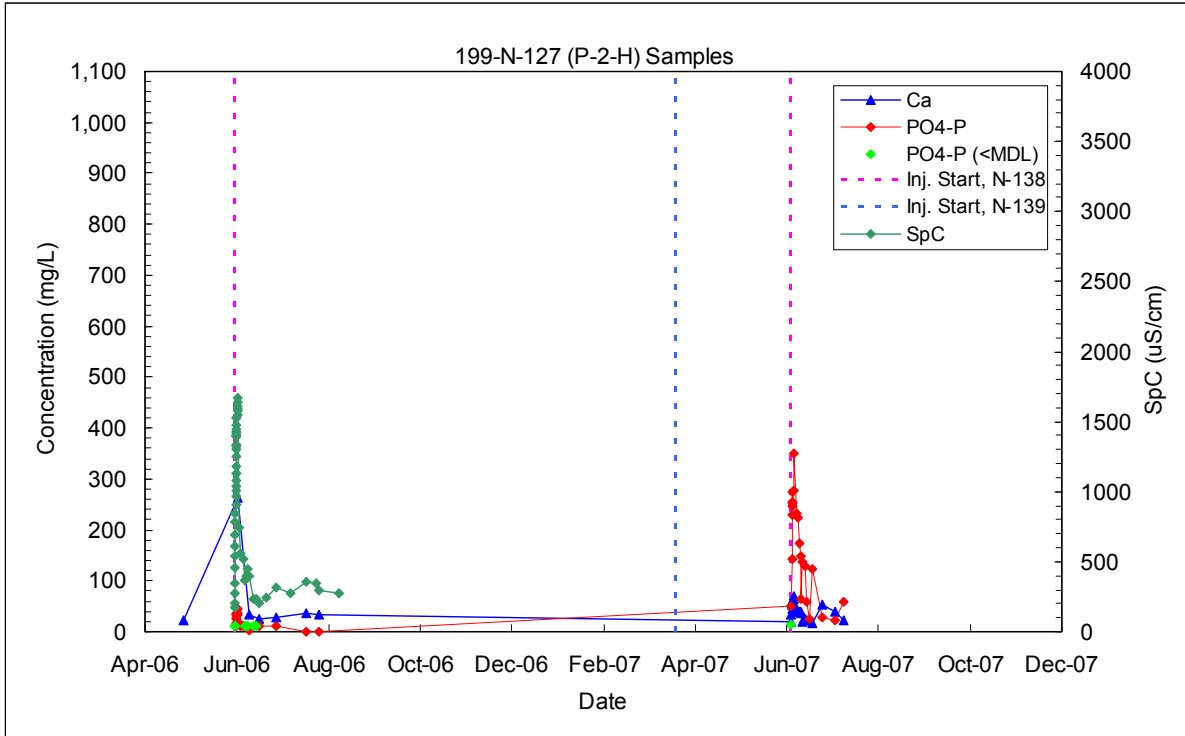


Figure B.12. Calcium, Phosphate, and Specific Conductance Performance Monitoring Plots for Pilot Test #1 Well 199-N-127

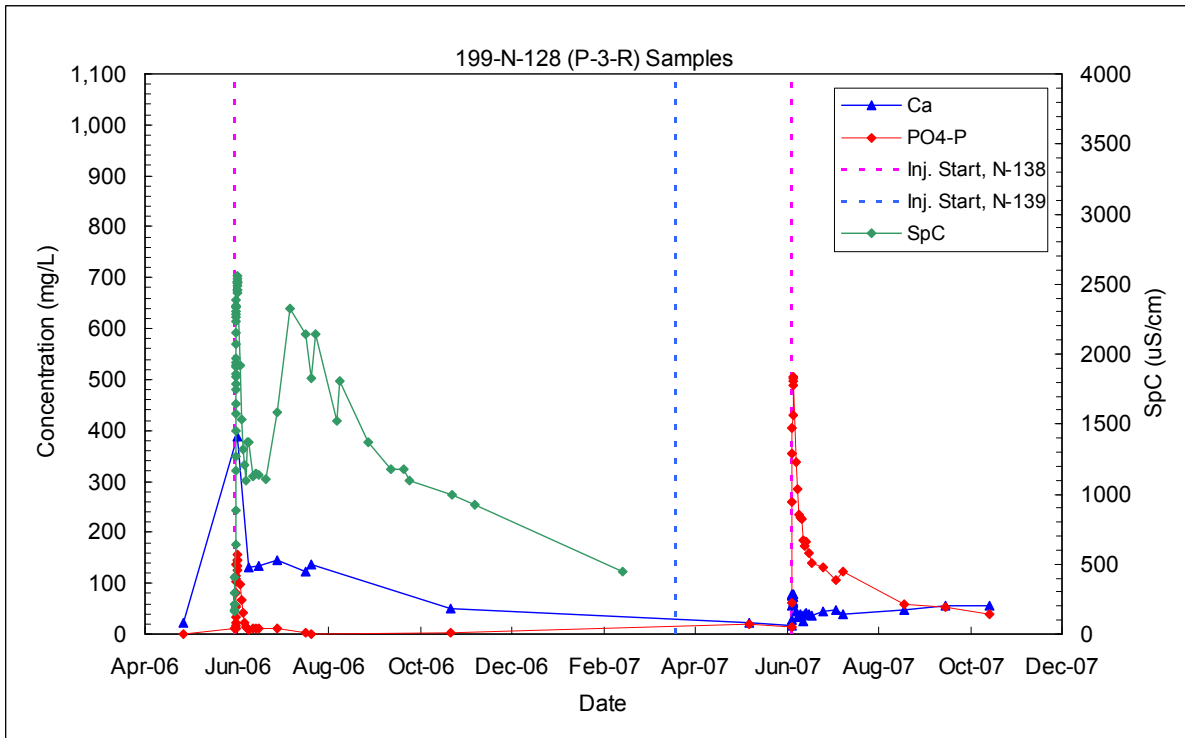


Figure B.13. Calcium, Phosphate, and Specific Conductance Performance Monitoring Plots for Pilot Test #1 Well 199-N-128

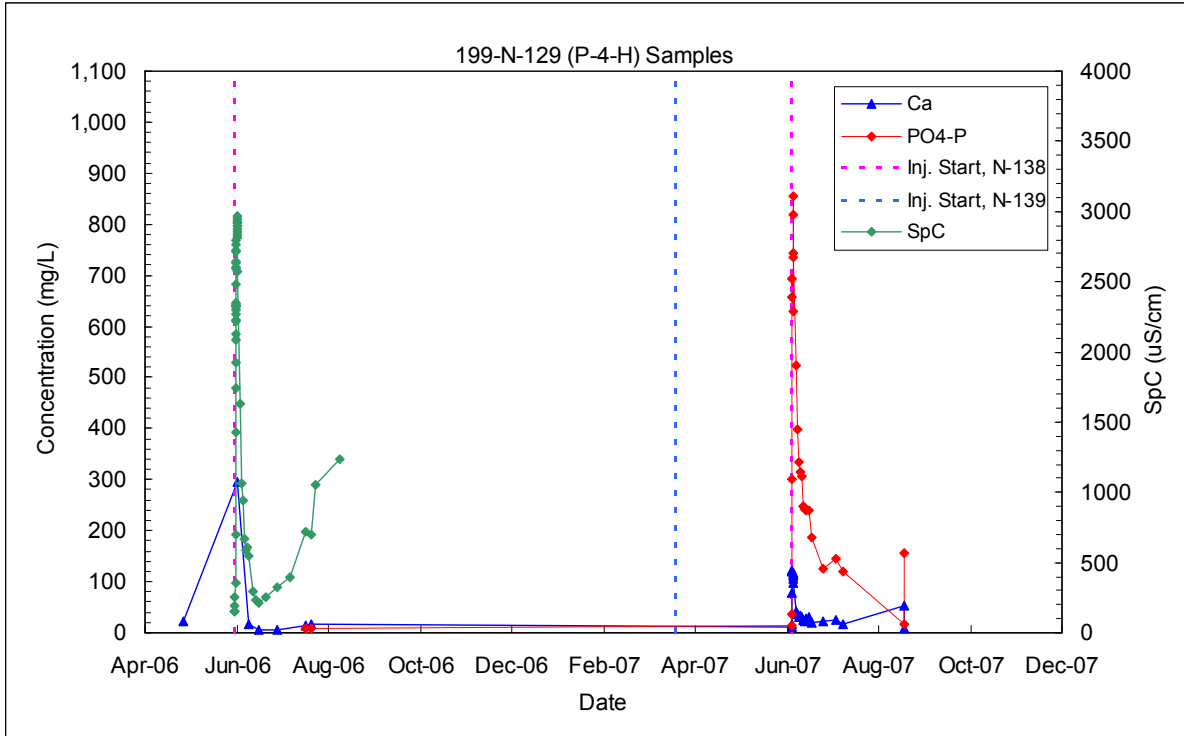


Figure B.14. Calcium, Phosphate, and Specific Conductance Performance Monitoring Plots for Pilot Test #1 Well 199-N-129

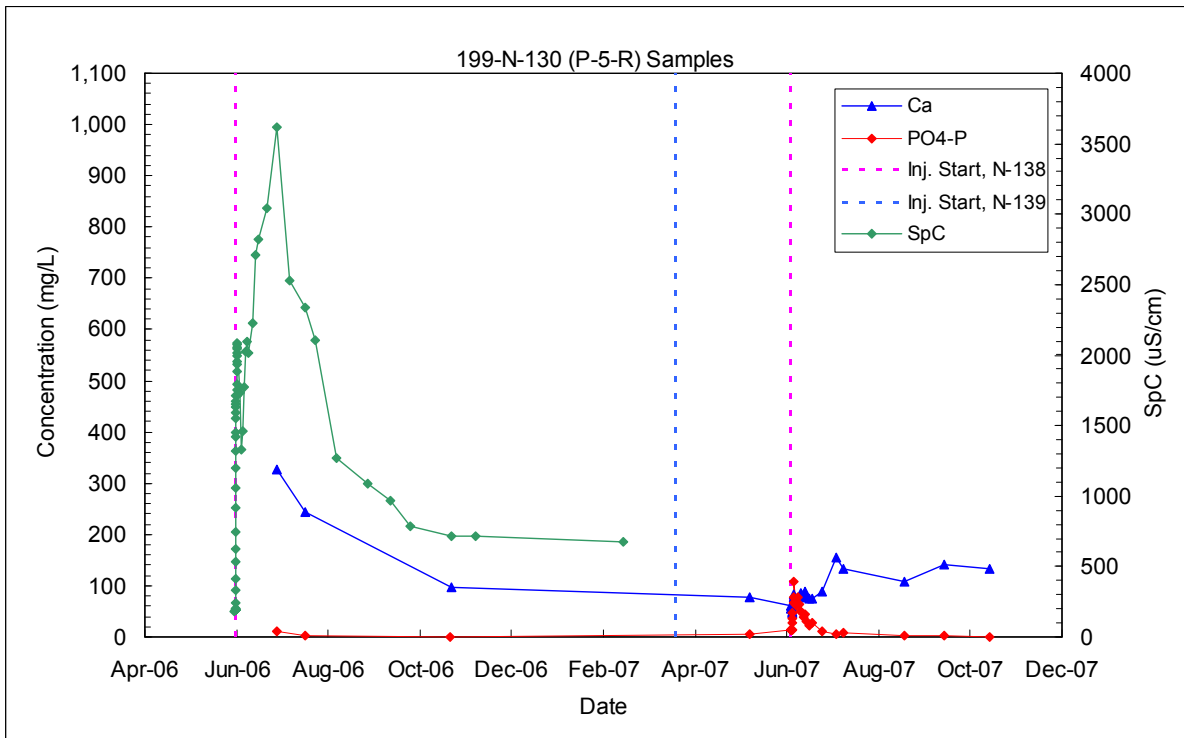


Figure B.15. Calcium, Phosphate, and Specific Conductance Performance Monitoring Plots for Pilot Test #1 Well 199-N-130

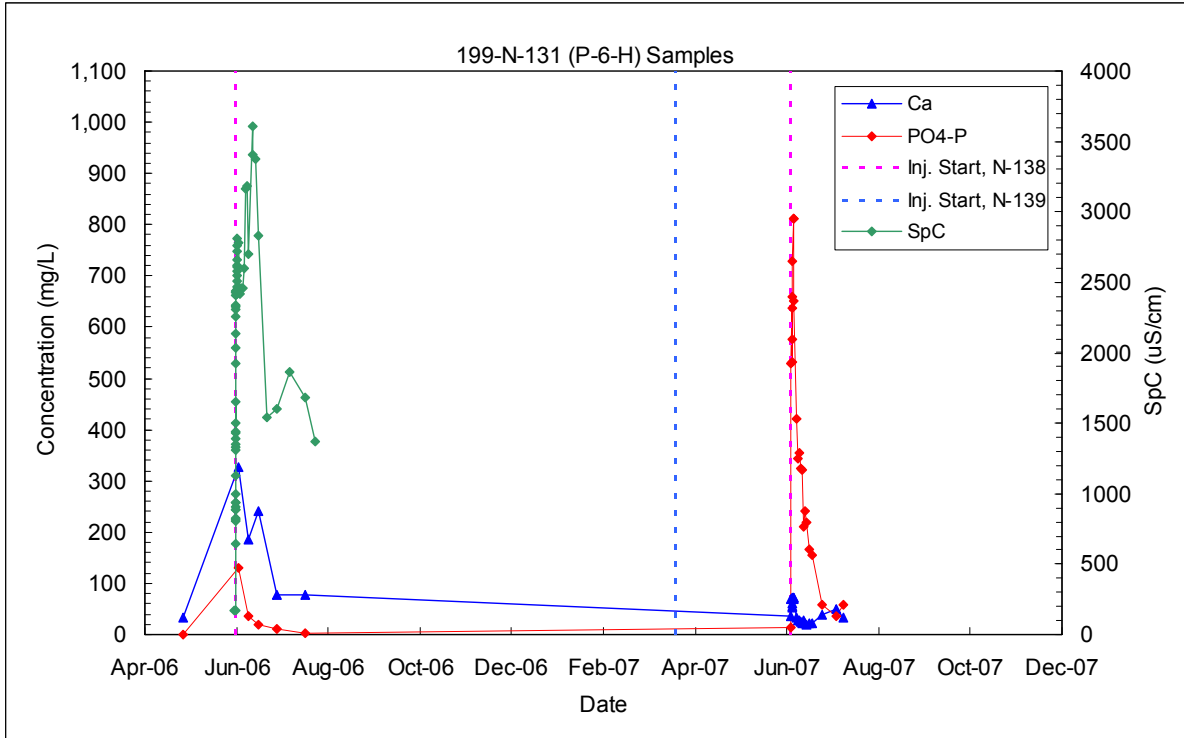


Figure B.16. Calcium, Phosphate, and Specific Conductance Performance Monitoring Plots for Pilot Test #1 Well 199-N-131

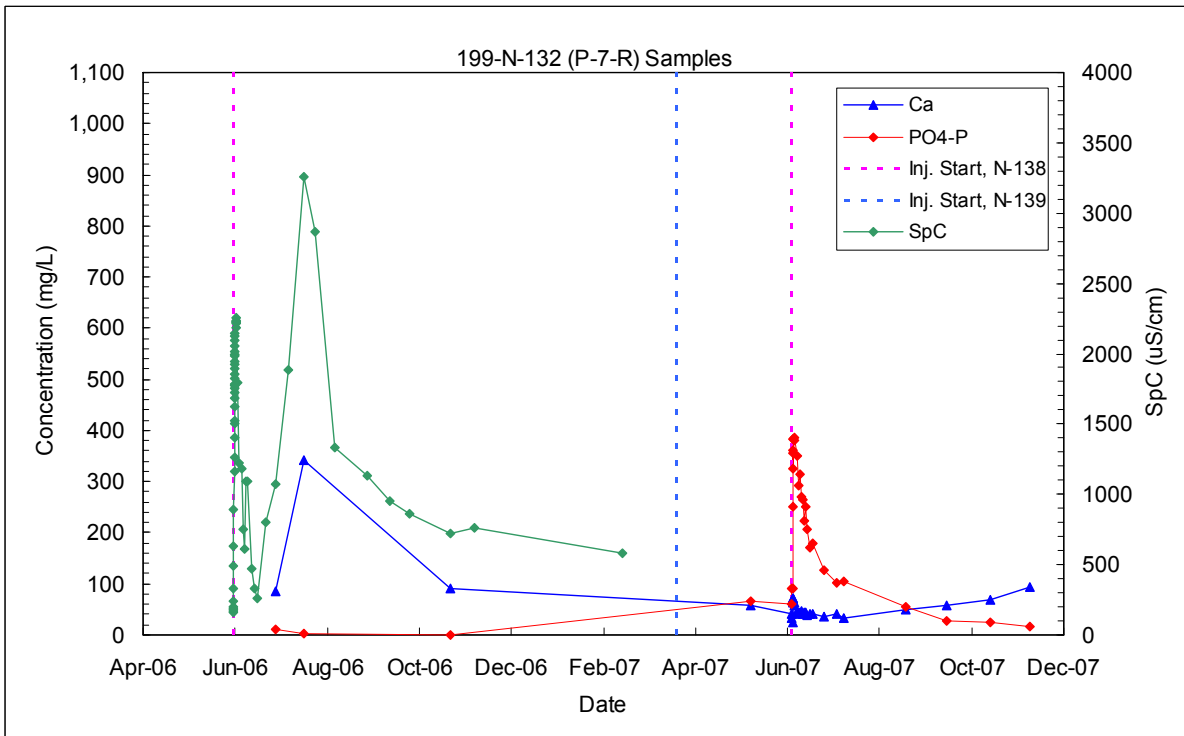


Figure B.17. Calcium, Phosphate, and Specific Conductance Performance Monitoring Plots for Pilot Test #1 Well 199-N-132

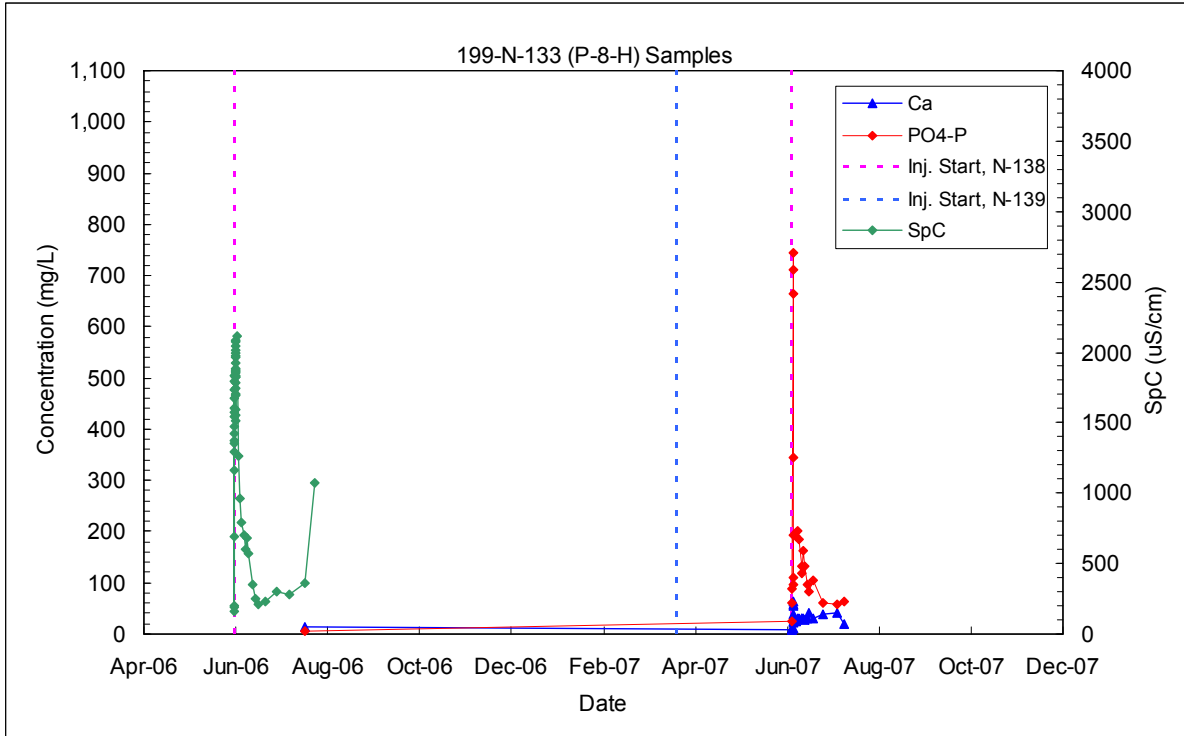


Figure B.18. Calcium, Phosphate, and Specific Conductance Performance Monitoring Plots for Pilot Test #1 Well 199-N-133

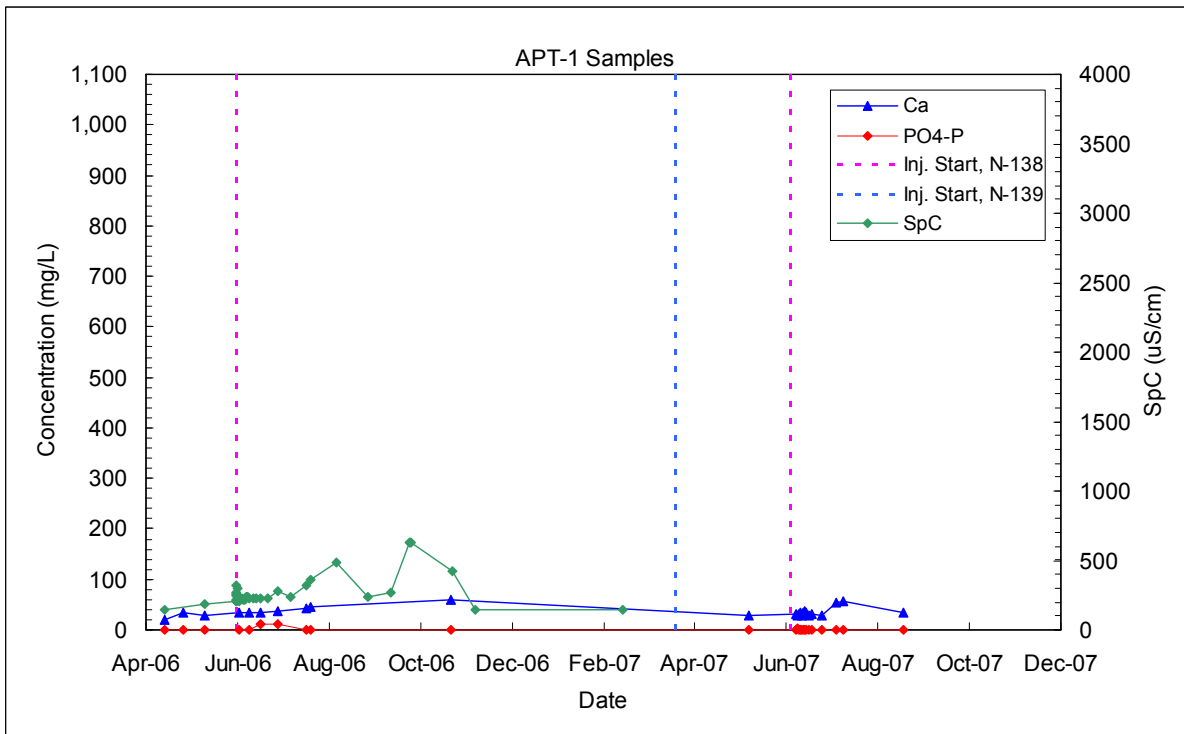


Figure B.19. Calcium, Phosphate, and Specific Conductance Performance Monitoring Plots for Pilot Test #1 Aquifer Tube APT-1

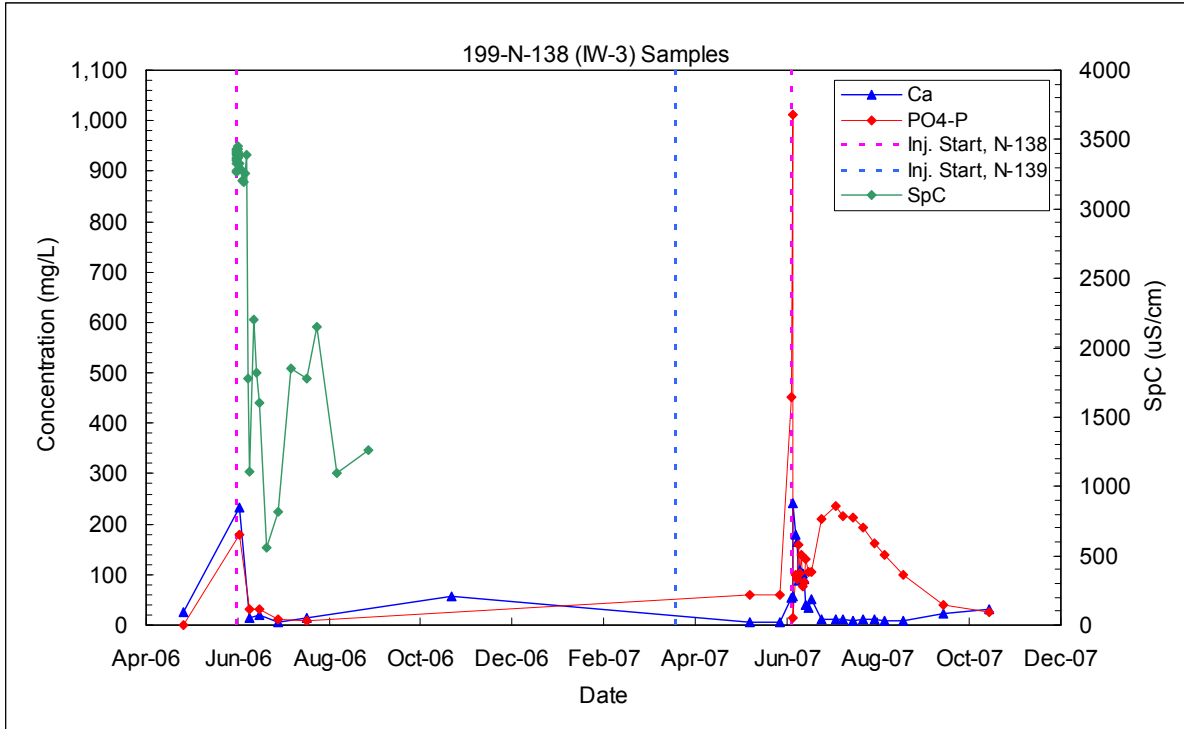


Figure B.20. Calcium, Phosphate, and Specific Conductance Performance Monitoring Plots for Pilot Test #1 Injection Well 199-N-138

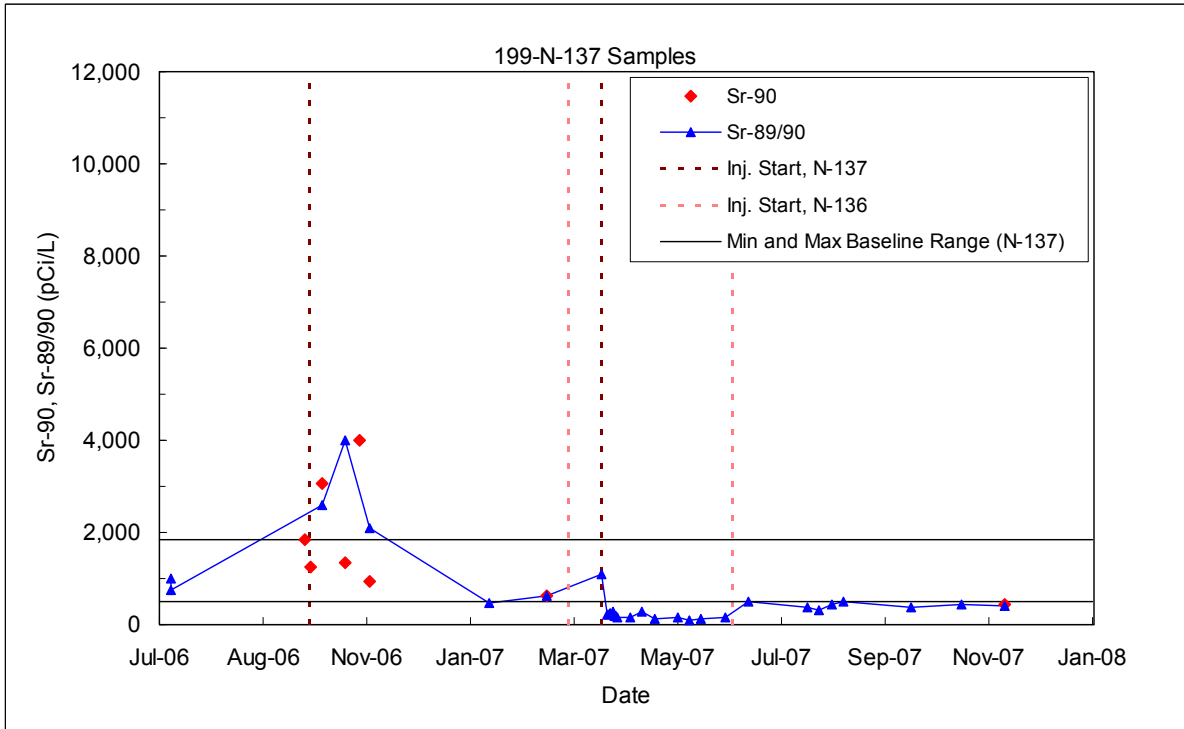


Figure B.21. ⁹⁰Sr Performance Monitoring Plots for Pilot Test #2 Injection Well 199-N-137

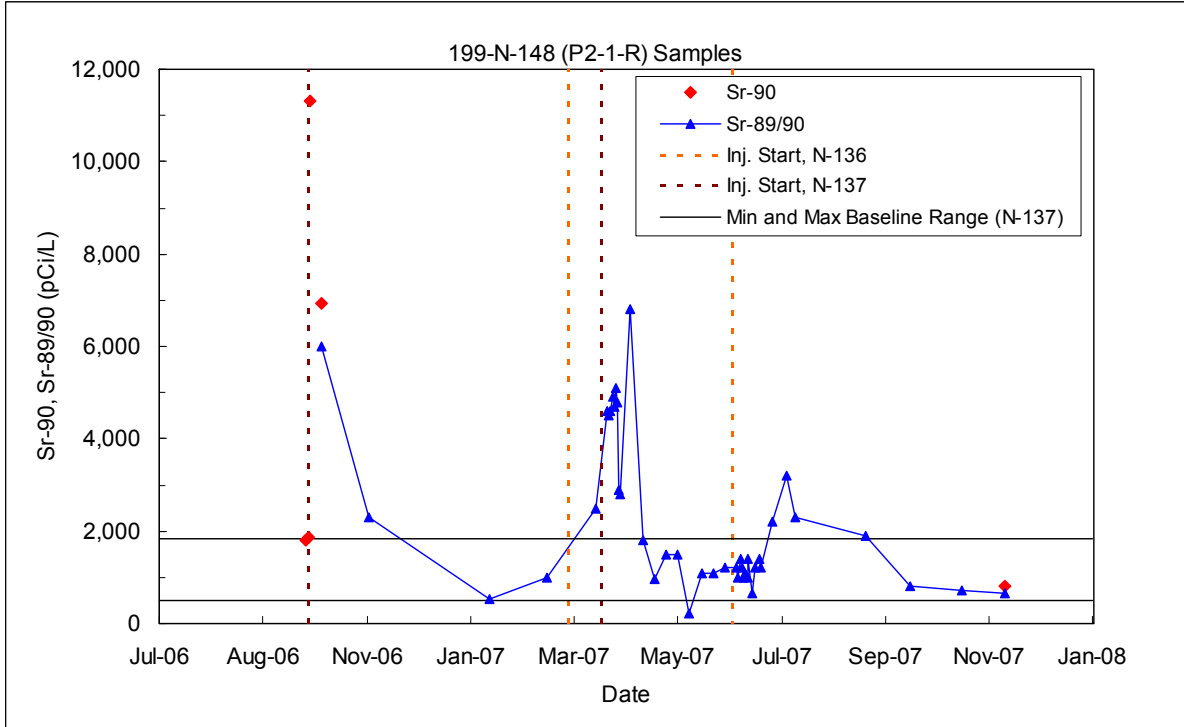


Figure B.22. ⁹⁰Sr Performance Monitoring Plots for Pilot Test #2 Well 199-N-148

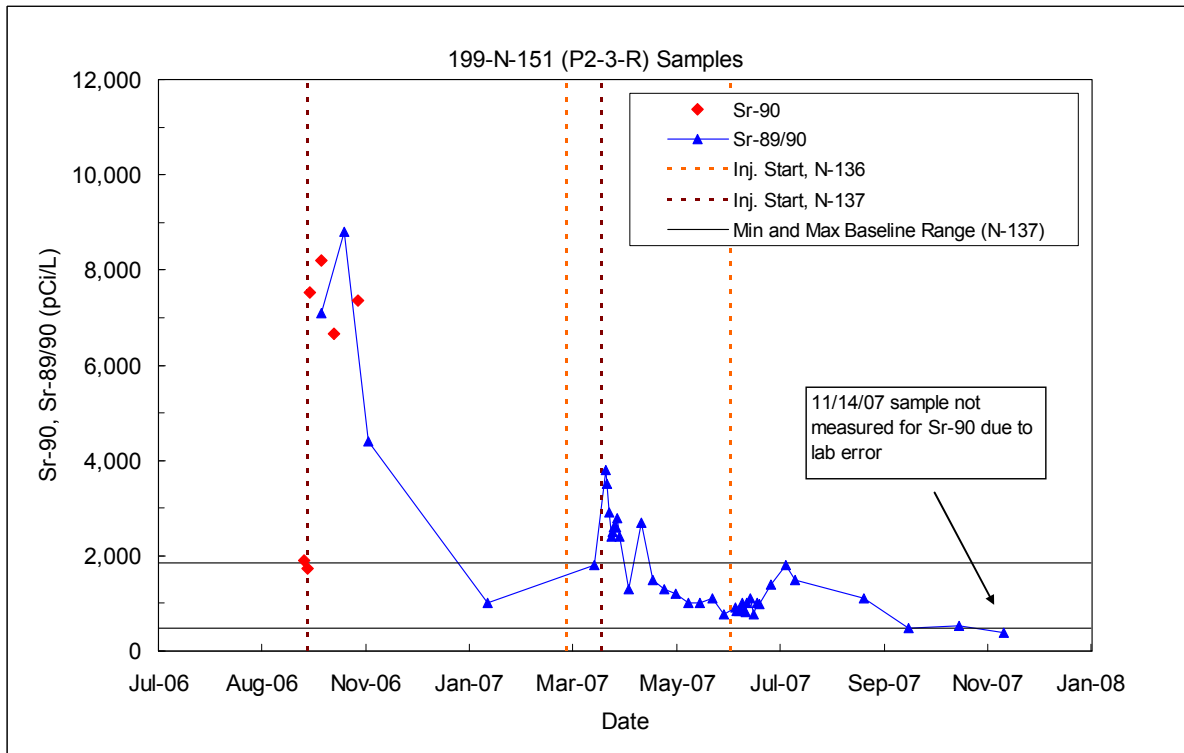


Figure B.23. ⁹⁰Sr Performance Monitoring Plots for Pilot Test #2 Well 199-N-151

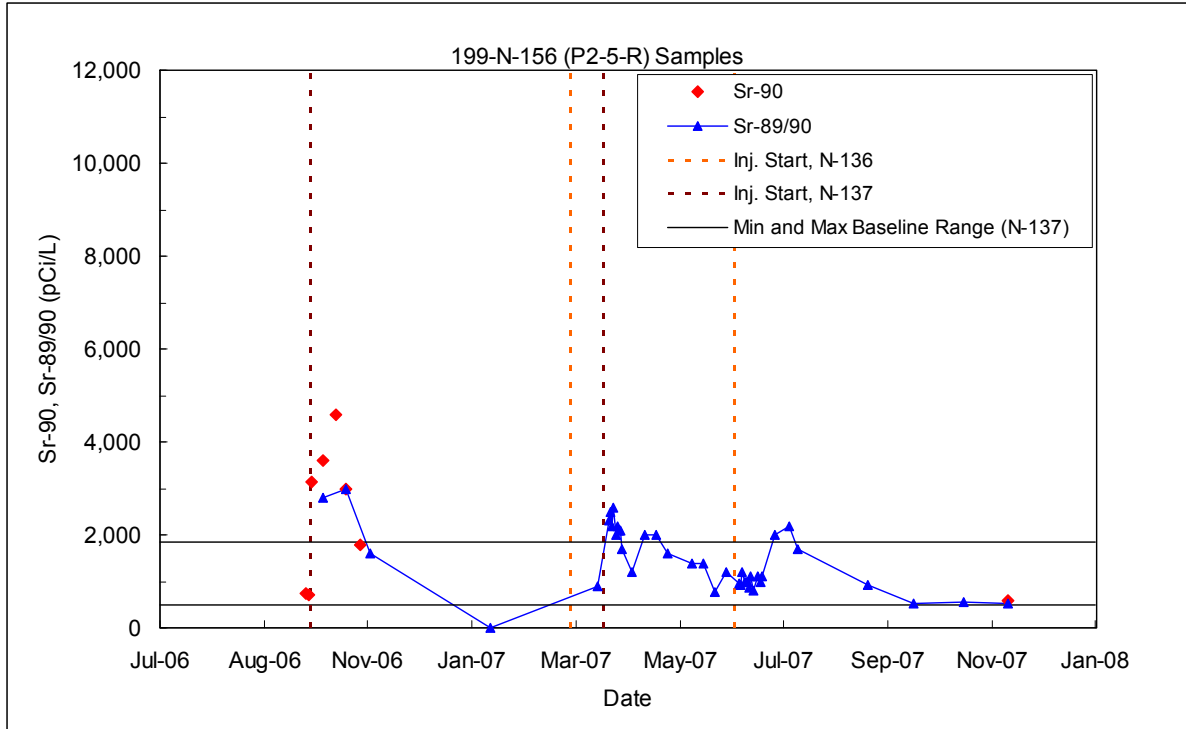


Figure B.26. ⁹⁰Sr Performance Monitoring Plots for Pilot Test #2 Well 199-N-156

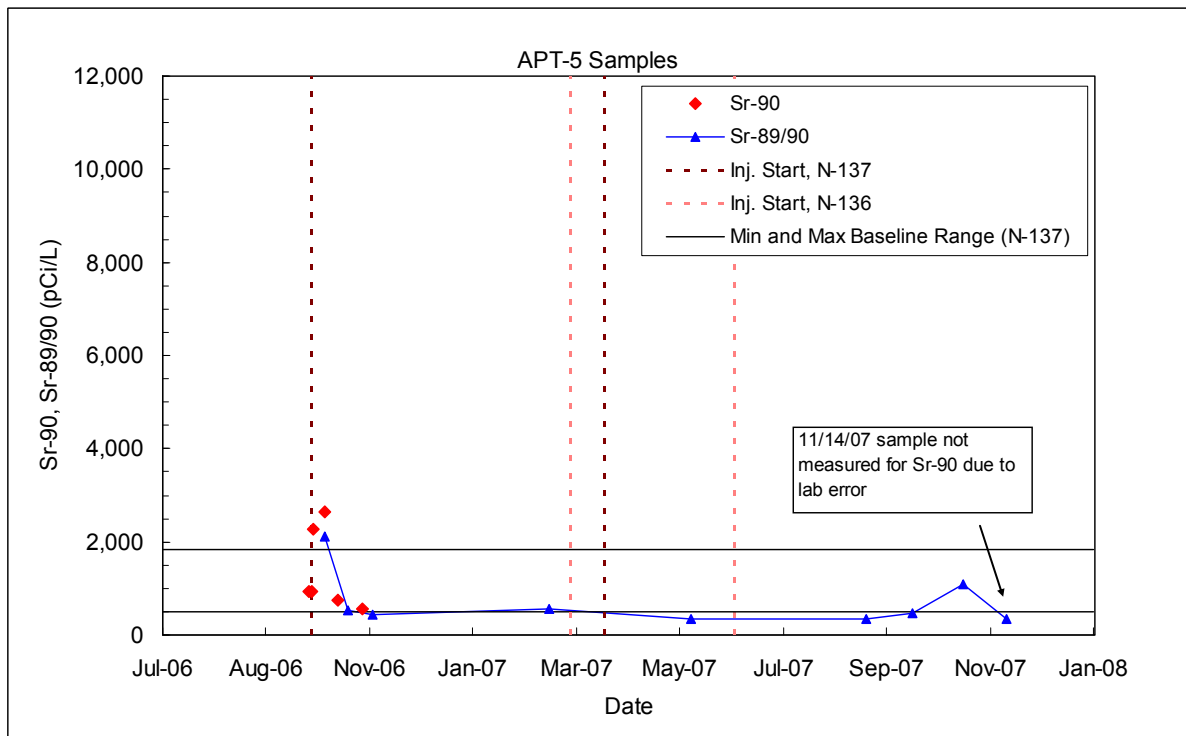


Figure B.27. ⁹⁰Sr Performance Monitoring Plots for Pilot Test #2 Aquifer Tube APT-5

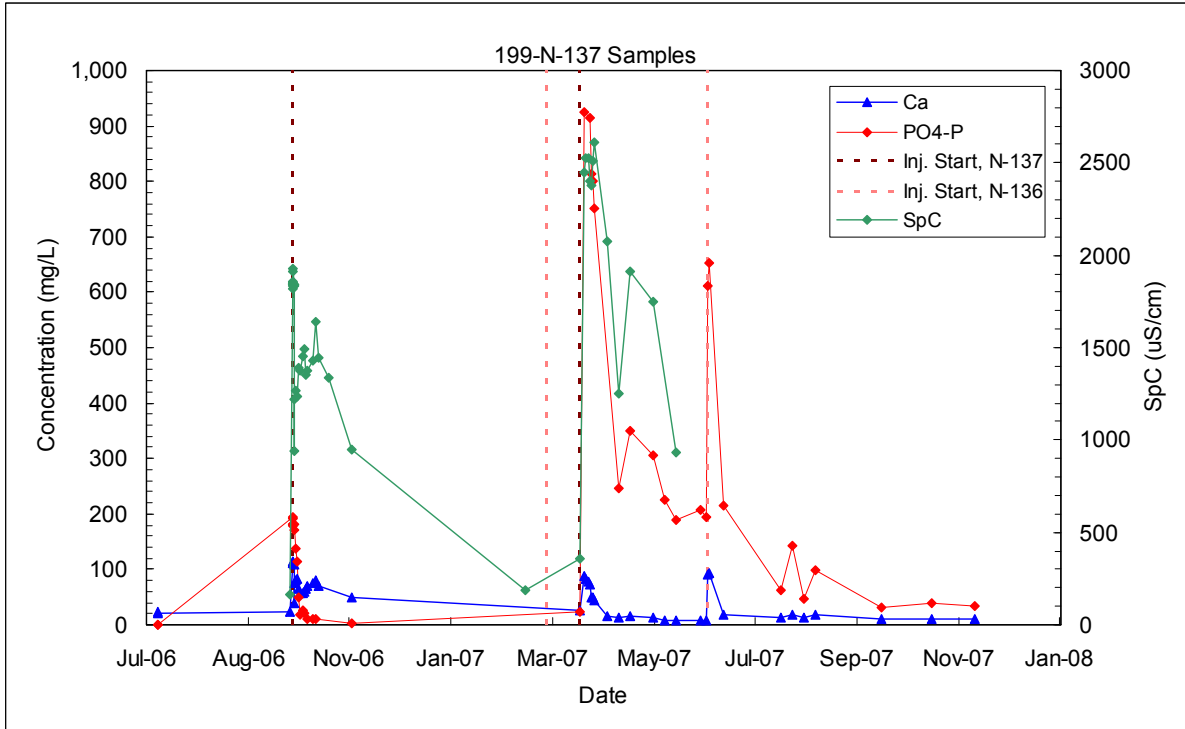


Figure B.28. Calcium, Phosphate, and Specific Conductance Performance Monitoring Plots for Pilot Test #2 Injection Well 199-N-137

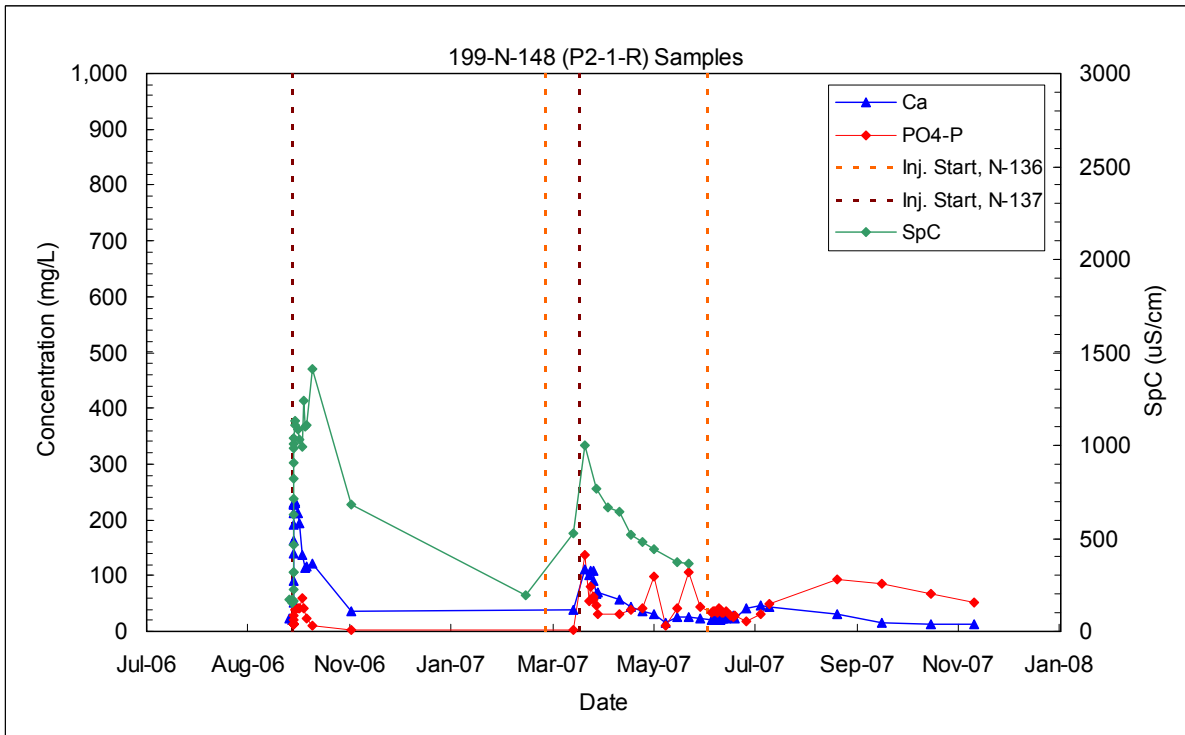


Figure B.29. Calcium, Phosphate, and Specific Conductance Performance Monitoring Plots for Pilot Test #2 Well 199-N-148

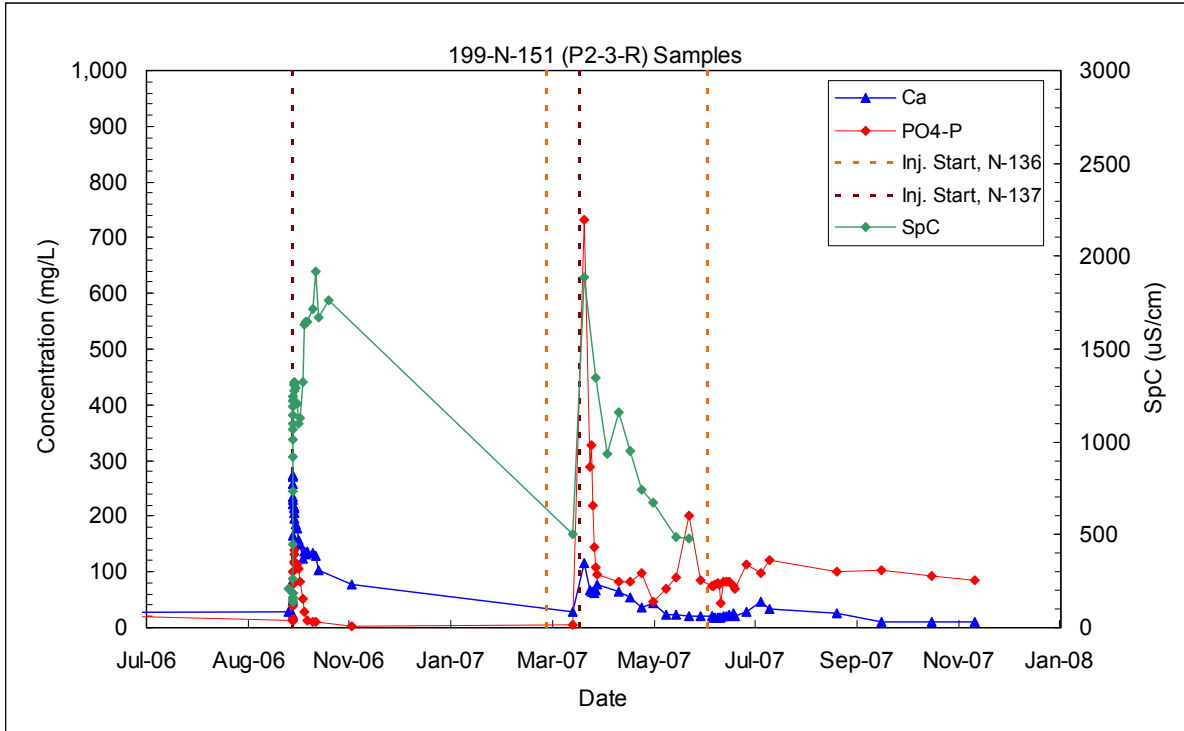


Figure B.30. Calcium, Phosphate, and Specific Conductance Performance Monitoring Plots for Pilot Test #2 Well 199-N-151

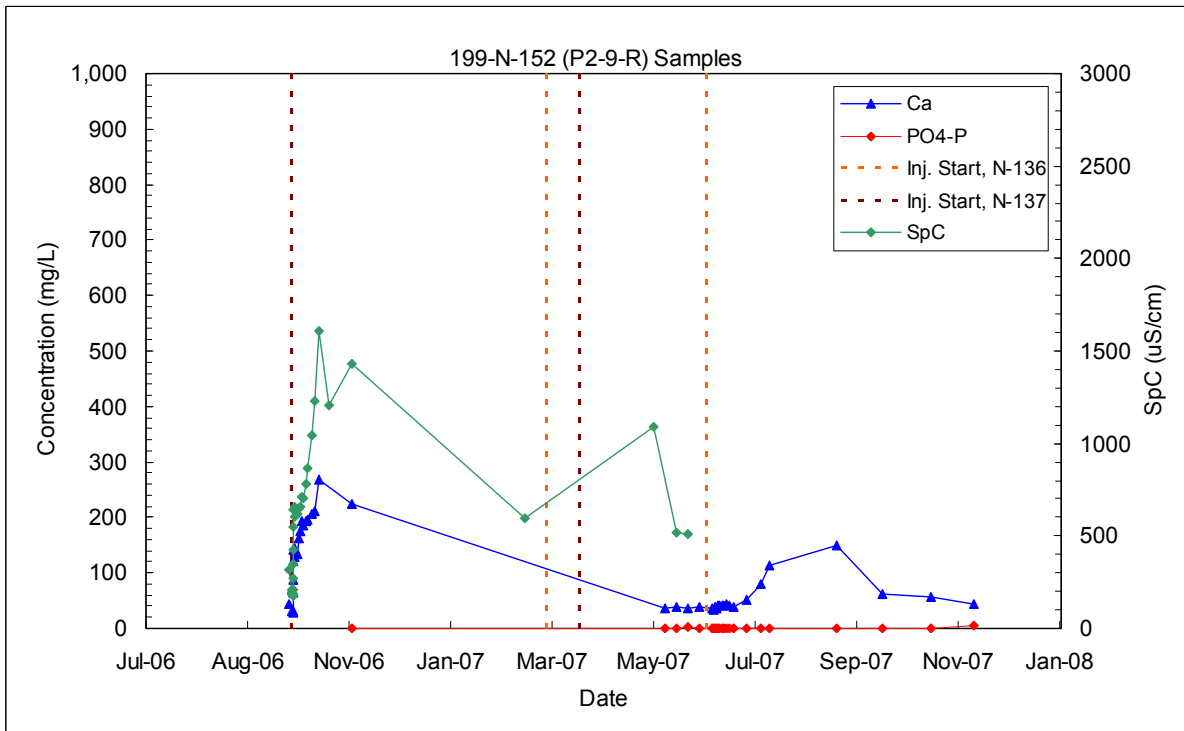


Figure B.31. Calcium, Phosphate, and Specific Conductance Performance Monitoring Plots for Pilot Test #2 Well 199-N-152

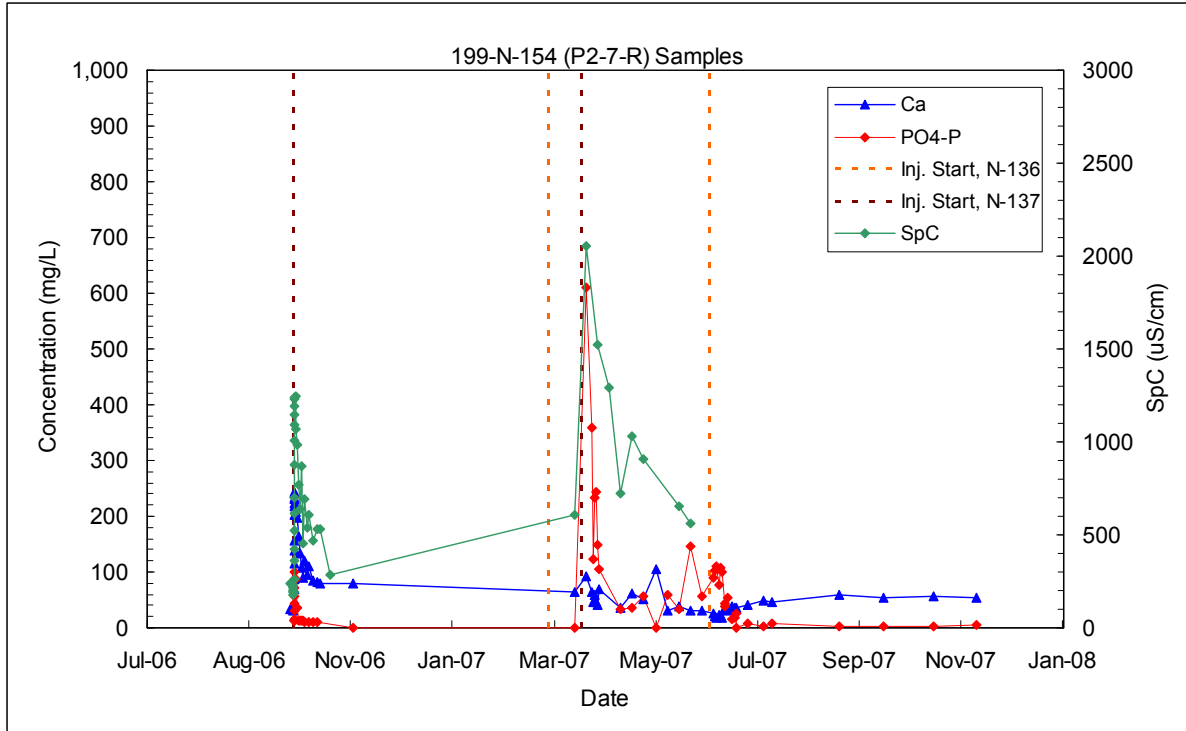


Figure B.32. Calcium, Phosphate, and Specific Conductance Performance Monitoring Plots for Pilot Test #2 Well 199-N-154

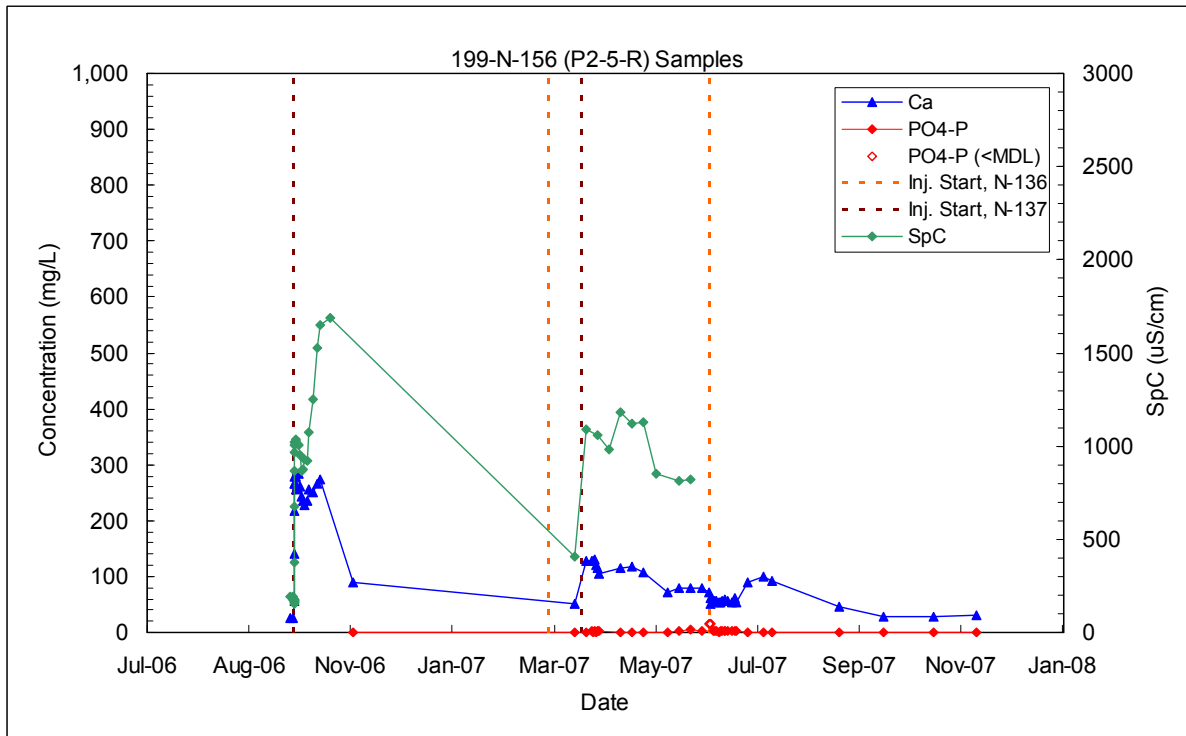


Figure B.33. Calcium, Phosphate, and Specific Conductance Performance Monitoring Plots for Pilot Test #2 Well 199-N-156

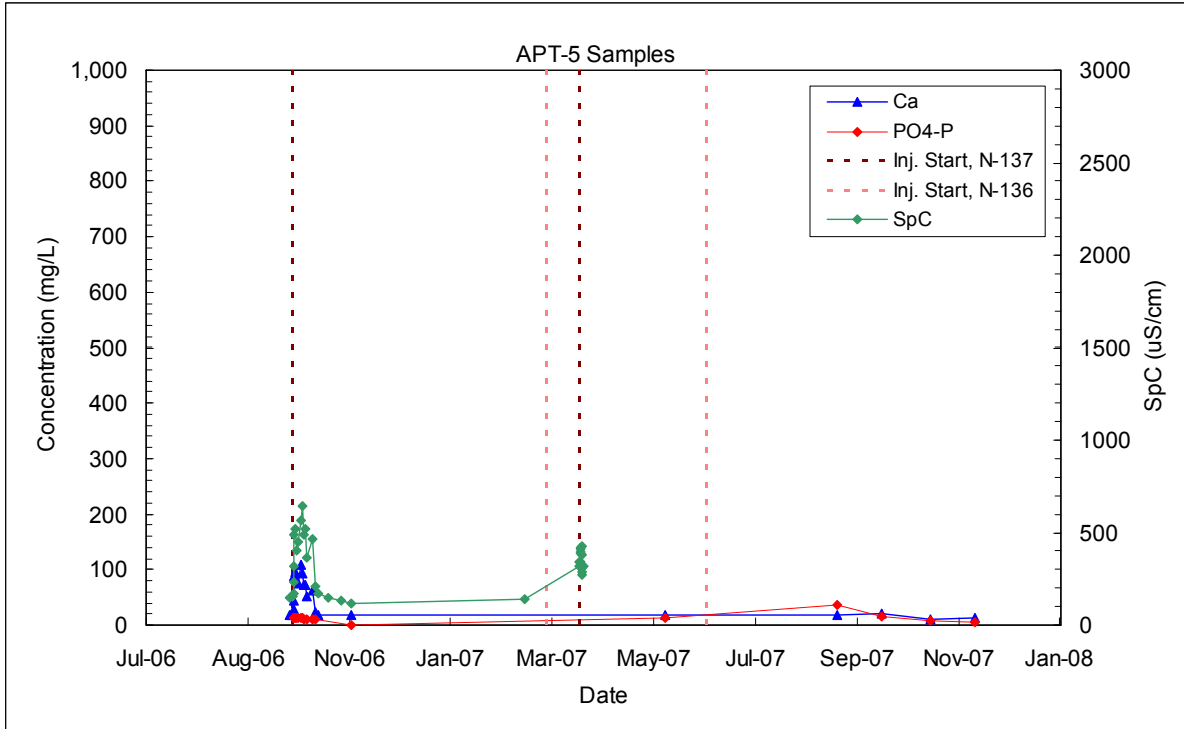


Figure B.34. Calcium, Phosphate, and Specific Conductance Performance Monitoring Plots for Pilot Test #2 Aquifer Tube APT-5

Appendix C

Well Information for Pilot Test #2 Site

Appendix C

Well Information for Pilot Test #2 Site

This section contains well information for the monitoring wells at pilot test site #2 that were installed in September 2006. A plan-view diagram of these wells is shown in Figure 4.3. The injection well for pilot test site #2, 199-N-137, is described in the *2006 100-NR-2 Borehole Completion Report* (FH 2006). Table C.1 shows the horizontal coordinates for the monitoring wells (a vertical survey was not conducted on these wells). Figures C.1 to C.18 contain the well construction sheets and the well summary diagrams. Additional details are provided in Section 4.1.3.

Table C.1. Survey Coordinates for 100-N Apatite Pilot Test #2 Monitoring Wells (to center of casing). Monitoring wells were surveyed on 11/28/2006 (data from Hanford Well Information System [HWIS]).

Well_ID	Well_Name	NORTHING (m)	EASTING (m)
C5043	199-N-137	149946.3	571344.43
C5316	199-N-148	149949.44	571341.01
C5317	199-N-149	149949.86	571341.48
C5318	199-N-150	149948.66	571342.87
C5319	199-N-151	149949.17	571343.21
C5320	199-N-152	149949.54	571343.62
C5321	199-N-153	149949.92	571347.41
C5322	199-N-154	149949.45	571347.82
C5323	199-N-155	149943.78	571340.68
C5324	199-N-156	149943.07	571341.00

WELL CONSTRUCTION SUMMARY REPORT				Start Date: 9-19-2006			
				Finish Date: 9-19-2006			
				Page 1 of 1			
Well ID: C5316		Well Name: 199-N-148		Approximate Location: 8' NE of 199-N-137			
Project: NR-2 OV Small diameter wells			Other Companies: Freestone Environmental Services				
Drilling Company: Pro sonic			Geologist(s): Greg Kasza Erika Rincon				
Driller: Aaron Adams		License #: 2831T					
TEMPORARY CASING AND DRILL DEPTH			DRILLING METHOD	HOLE DIAMETER (in.) / INTERVAL (ft)			
*Size/Grade/Lbs. Per FL	Interval	Shoe O.D./I.D.	Auger:	Diameter _____ From _____ to _____			
5"	0 - 27'	5" OD	Cable Tool:	Diameter _____ From _____ to _____			
			Air Rotary:	Diameter _____ From _____ to _____			
			A.R. w/Sonic:	Diameter _____ From _____ to _____			
			sonic	Diameter 5" From 0 to 27'			
				Diameter _____ From _____ to _____			
				Diameter _____ From _____ to _____			
*Indicate Welded (W) - Flush Joint (FJ) Coupled (C) & Thread Design				Diameter _____ From _____ to _____			
27.00 GS 1/4107			Drilling Fluid: none				
Total Drilled Depth: 27.00		Hole Dia @ TD: 5"		Total Amt. Of Water Added During Drilling: _____			
Well Straightness Test Results: not required per SOW			Static Water Level: 14.18' TDC Date: 9/21/2006				
GEOPHYSICAL LOGGING							
Sondes (type)	Interval	Date	Sondes (type)	Interval	Date		
NA			NA				
COMPLETED WELL							
Size/WL/Material	Depth	Thread	Slot Size	Type	Interval	Volume	Mesh Size
2" SCH 40 PVC	0 - 25.05'	✓	2" NA	Silica Sand	27.0 - 18.0		10-20
2" PVC screen	19.7' - 24.7'		0.020"	Granular Bentonite	18.0 - 3.0		
PVC endcap	24.7 - 25.05'	✓	NA	Portland cement	3.0 - 0		
OTHER ACTIVITIES							
Aquifer Test: NA	Date:	Well Decommission: NA		Yes:	No:	Date:	
Description:				Description:			
WELL SURVEY DATA (if applicable) not yet surveyed							
Washington State Plane Coordinates:				Protective Casing Elevation: at this time			
				Brass Survey Marker Elevation:			
COMMENTS / REMARKS							
ecology well tag: ALT-808							
Reported By: Erika Rincon		Title: geologist		Signature: Erika R		Date: 9-21-06	

A-6003-658 (04/03)

Figure C.1. Well Construction Summary Report for Well 199-N-148

WELL CONSTRUCTION SUMMARY REPORT				Start Date: 9-19-2006			
				Finish Date: 9-19-2006			
				Page 1 of 1			
Well ID: C5317		Well Name: 199-N-149		Approximate Location: 8' NE of 199-N-137			
Project: NR-2 OU small diameter wells			Other Companies: Freestone Environmental Services				
Drilling Company: Prosonic			Geologist(s): Greg Kasza Erika Rincon				
Driller: Aaron Adams		License #: 2831T					
TEMPORARY CASING AND DRILL DEPTH			DRILLING METHOD	HOLE DIAMETER (in.) / INTERVAL (ft)			
*Size/Grade/Lbs. Per Ft.	Interval	Shoe O.D./I.D.	Auger:	Diameter _____ From _____ to _____			
5"	0 - 17	5" OD	Cable Tool:	Diameter _____ From _____ to _____			
			Air Rotary:	Diameter _____ From _____ to _____			
			A.R. w/Sonic:	Diameter _____ From _____ to _____			
			Sonic	Diameter 5" From 0 to 17			
				Diameter _____ From _____ to _____			
				Diameter _____ From _____ to _____			
*Indicate Welded (W) - Flush Joint (FJ) Coupled (C) & Thread Design				Diameter _____ From _____ to _____			
			Drilling Fluid: none				
Total Drilled Depth: 17		Hole Dia @ TD: 5"		Total Amt. Of Water Added During Drilling: none			
Well Straightness Test Results: not required per SOW			Static Water Level: 14.12' rad Date: 9-21-06				
GEOPHYSICAL LOGGING							
Sondes (type)	Interval	Date	Sondes (type)	Interval	Date		
NA							
COMPLETED WELL							
Size/WL/Material	Depth	Thread	Slot Size	Type	Interval	Volume	Mesh Size
2" sch 40 PVC	0 - 16.35'	✓	20/44	Silica Sand	17.0 - 19.0		10-20
2" PVC screen	11.0' - 16.0'		0.020-in	Granular Bentonite	10.0 - 3.0		
2" PVC endcap	16.0' - 16.35'		NA	Portland Cement	3.0 - 0		
OTHER ACTIVITIES							
Aquifer Test: NA		Date:	Well Decommission: NA		Yes: No: Date:		
Description:			Description:				
WELL SURVEY DATA (if applicable)							
Washington State Plane Coordinates:			Protective Casing Elevation: Not yet measured at this time				
			Brass Survey Marker Elevation:				
COMMENTS / REMARKS							
ecology well tag: ALS-807							
Reported By: Erika Rincon		Title: geologist	Signature: Erika Rincon		Date: 9-21-06		

A-6003-658 (04/03)

Figure C.3. Well Construction Summary Report for Well 199-N-149

WELL SUMMARY SHEET		Start Date: 9-19-06	Page 1 of 1
		Finish Date: 9-19-06	
Well ID: C5317		Well Name: 199-N-149	
Location: 100-NR-2 OU N-Springs		Project: NR-2 OU Small Diameter Wells	
Prepared By: Erika Rincon	Date: 11/21/06	Reviewed By: <i>L. D. Walker</i>	Date: 12/7/06
Signature: <i>Erika Rincon</i>		Signature: <i>L. D. Walker</i>	
CONSTRUCTION DATA		GEOLOGIC/HYDROLOGIC DATA	
Description	Diagram	Depth in Feet	Lithologic Description/Groundwater Sample Depths (ft bgs)
Flush-Mount Concrete Surface Seal Portland Cement: 0 - 3.0 ft 2-in I.D. Schedule 40 PVC Casing: 0 - 11.0 ft Granular Bentonite: 3.0 - 10.0 ft Static Water Level: 14.52 ft bgs (9-21-2006) 2-in I.D. Schedule 40 PVC, 20 Slot (.020-in) Screen: 11.0 - 16.0 ft Primary Filter Pack 10-20 Mesh Colorado Silica Sand: 10.0 - 17.0 ft		0 5 10 15 20 25 30 35 40 BOREHOLE NOT LOGGED	17.0 Total Depth Drilled (9-19-2006)
All depths are in feet below ground surface. Borehole drilled with 5-in O.D. wall casing. All temporary casing removed from ground.			
PVC = Polyvinyl Chloride			

Figure C.4. Well Summary Sheet for Well 199-N-149

WELL CONSTRUCTION SUMMARY REPORT					Start Date: 9-20-06	
					Finish Date: 9-20-06	
					Page 1 of 1	
Well ID: C5318		Well Name: 199-N-150		Approximate Location: 10' NE of 199-N-137		
Project: 100-NR-2 OU small diameter wells				Other Companies: Freestone Environmental Service		
Drilling Company: Prosonic				Geologist(s): Greg Kosza Erika Rincon		
Driller: Aaron Adams		License #: 2831T				
TEMPORARY CASING AND DRILL DEPTH			DRILLING METHOD	HOLE DIAMETER (in.) / INTERVAL (ft)		
*Size/Grade/Lbs. Per Ft.	Interval	Shoe O.D./I.D.	Auger:	Diameter _____ From _____ to _____		
5"	0 - 18	5" OD	Cable Tool:	Diameter _____ From _____ to _____		
			Air Rotary:	Diameter _____ From _____ to _____		
			A.R. w/Sonic:	Diameter _____ From _____ to _____		
			Sonic	Diameter 5" From 0 to 18		
				Diameter _____ From _____ to _____		
				Diameter _____ From _____ to _____		
*Indicate Welded (W) - Flush Joint (FJ) Coupled (C) & Thread Design				Diameter _____ From _____ to _____		
			Drilling Fluid: none			
Total Drilled Depth: 18	Hole Dia @ TD: 5"		Total Amt. Of Water Added During Drilling: _____			
Well Straightness Test Results: not required per SOW			Static Water Level: 13.77' B.C.		Date: 9-21-06	
GEOPHYSICAL LOGGING						
Sondes (type)	Interval	Date	Sondes (type)	Interval	Date	
NA						
			NA			
COMPLETED WELL						
Size/WL/Material	Depth	Thread	Slot Size	Type	Interval	Mesh Size
2" SCH 40 PVC	0 - 16.35	✓	2 3/8"	Silica Sand	18.0 - 10.0	10-20
2" PVC Screen	11.0 - 16.0		0.020"	Granular Bentonite	10.0 - 3.0	
2" PVC end cap	16.0 - 16.35		NA	Portland Cement	3.0 - 0	
OTHER ACTIVITIES						
Aquifer Test: NA	Date:	Well Decommission: NA	Yes:	No:	Date:	
Description:	Description:					
WELL SURVEY DATA (if applicable)						
Washington State Plane Coordinates:			Protective Casing Elevation:			
			Brass Survey Marker Elevation:			
COMMENTS / REMARKS						
ecology well tag: AT ALJ-806 EPA-200						
Reported By: Erika Rincon	Title: geologist	Signature: Erika R		Date: 9-21-06		

A-6003-658 (04/03)

Figure C.5. Well Construction Summary Report for Well 199-N-150

WELL SUMMARY SHEET		Start Date: 9-20-06	Page 1 of 1
		Finish Date: 9-20-06	
Well ID: C5318		Well Name: 199-N-150	
Location: 100-NR-2 OU N-Springs		Project: NR-2 OU Small Diameter Wells	
Prepared By: Erika Rincon	Date: 11/21/06	Reviewed By: L.D. Walker	Date: 12/2/06
Signature: <i>Erika Rincon</i>		Signature: <i>L.D. Walker</i>	
CONSTRUCTION DATA		GEOLOGIC/HYDROLOGIC DATA	
Description	Diagram	Depth in Feet	Lithologic Description/Groundwater Sample Depths (ft bgs)
Flush-Mount Concrete Surface Seal Portland Cement: 0 - 3.0 ft 2-in I.D. Schedule 40 PVC: Casing: 0 - 11.0 ft Granular Bentonite: 3.0 - 10.0 ft Static Water Level: 14.47 ft bgs (9-21-2006) 2-in I.D. Schedule 40 PVC, 20 Slot (.020-in) Screen: 11.0 - 16.0 ft Primary Filter Pack 10-20 Mesh Colorado Silica Sand: 10.0 - 18.0 ft		0 5 10 15 20 25 30 35 40	BOREHOLE NOT LOGGED 18.0 Total Depth Drilled (9-20-2006)
All depths are in feet below ground surface. Borehole drilled with 5-in O.D. wall casing. All temporary casing removed from ground.			
PVC = Polyvinyl Chloride			

Figure C.6. Well Summary Sheet for Well 199-N-150

WELL CONSTRUCTION SUMMARY REPORT				Start Date: 9-20-06			
				Finish Date: 9-20-06			
				Page 1 of 1			
Well ID: C5320		Well Name: 199-N-152		Approximate Location: 5' NE of 199-N-137.			
Project: 100-NR-2 small diameter wells		Other Companies: Freestone Environmental Services					
Drilling Company: Prosonic		Geologist(s): Greg Kasza Erika Rincon					
Driller: Aaron Adams		License #: 2831T					
TEMPORARY CASING AND DRILL DEPTH			DRILLING METHOD	HOLE DIAMETER (in.) / INTERVAL (ft)			
*Size/Grade/Lbs. Per Ft.	Interval	Shoe O.D./I.D.	Auger:	Diameter _____ From _____ to _____			
5" casing	0 - 33.55	5" OD	Cable Tool:	Diameter _____ From _____ to _____			
			Air Rotary:	Diameter _____ From _____ to _____			
			A.R. w/Sonic:	Diameter _____ From _____ to _____			
			Sonic	Diameter 5" From 0 to 33.55			
				Diameter _____ From _____ to _____			
*Indicate Welded (W) - Flush Joint (FJ) Coupled (C) & Thread Design				Diameter _____ From _____ to _____			
			Drilling Fluid: none				
Total Drilled Depth: 33.55'		Hole Dia @ TD: 5"		Total Amt. Of Water Added During Drilling: _____			
Well Straightness Test Results: not required per SOW			Static Water Level: 14.00' TWC Date: 9-21-06				
GEOPHYSICAL LOGGING							
Sondes (type)	Interval	Date	Sondes (type)	Interval	Date		
NA							
COMPLETED WELL							
Size/WL/Material	Depth	Thread	Slot Size	Type	Interval Annular Seal/Filter Pack	Volume	Mesh Size
2" SCH 40 PVC	0 - 33.55	✓	NA	Silica Sand	33.55 - 27.0		10-20
2" PVC screen	28.2 - 33.2		0.020-in	Granular Bent.	27.0 - 3.0		
2" PVC endcap	33.2 - 33.35		NA	Portland Cement	3.0 - 0		
OTHER ACTIVITIES							
Aquifer Test: NA		Date:	Well Decommission: NA		Yes:	No:	Date:
Description:				Description:			
WELL SURVEY DATA (if applicable)							
				Not Yet Measured			
				Protective Casing Elevation: at this time			
Washington State Plane Coordinates:				Brass Survey Marker Elevation:			
COMMENTS / REMARKS							
ecology well tag: ALJ-804							
Reported By: Erika Rincon		Title: geologist		Signature: Erika Rincon		Date: 9-21-06	

A-6003-658 (04/03)

Figure C.9. Well Construction Summary Report for Well 199-N-152

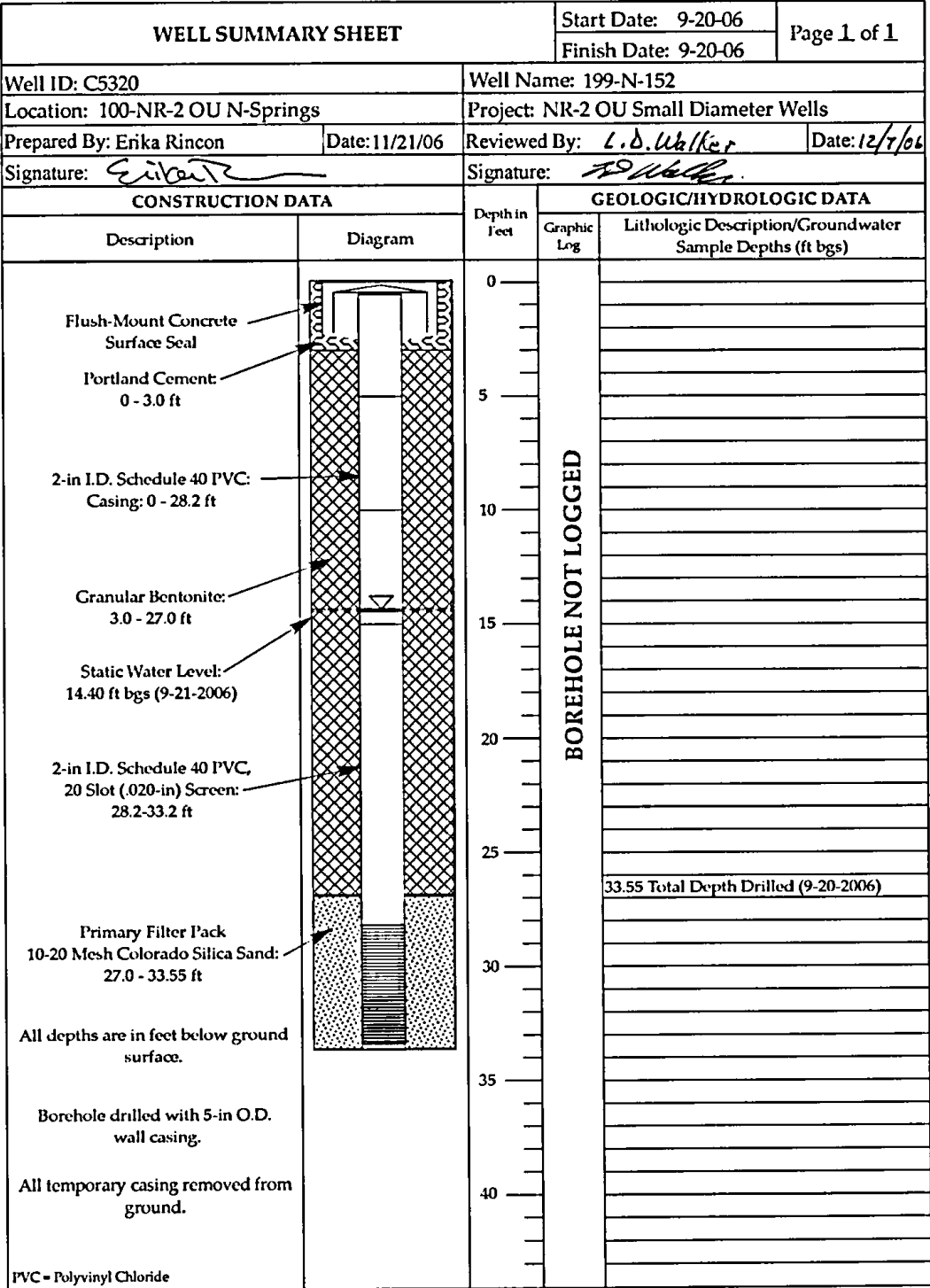


Figure C.10. Well Summary Sheet for Well 199-N-152

WELL CONSTRUCTION SUMMARY REPORT					Start Date: 9-19-06	
					Finish Date: 9-19-06	
					Page 1 of 1	
Well ID: C5321		Well Name: 199-N-153		Approximate Location: 10' NE of 199-N-137		
Project: 100-NR-2 00 small well diameters				Other Companies: Freestone Environmental Services		
Drilling Company: ProSonic		Geologist(s): Greg Kosza Erika Rincon				
Driller: Aaron Adams		License #: 2831T				
TEMPORARY CASING AND DRILL DEPTH			DRILLING METHOD	HOLE DIAMETER (in.) / INTERVAL (ft)		
*Size/Grade/Lbs. Per Ft.	Interval	Shoe O.D./I.D.	Auger:	Diameter _____ From _____ to _____		
5"	0 - 17	5" OD	Cable Tool:	Diameter _____ From _____ to _____		
			Air Rotary:	Diameter _____ From _____ to _____		
			A.R. w/Sonic:	Diameter _____ From _____ to _____		
			Sonic	Diameter 5" From 0 to 17		
				Diameter _____ From _____ to _____		
*Indicate Welded (W) - Flush Joint (FJ) Coupled (C) & Thread Design				Diameter _____ From _____ to _____		
			Drilling Fluid: none			
Total Drilled Depth: 17		Hole Dia @ TD: 5"		Total Amt. Of Water Added During Drilling: _____		
Well Straightness Test Results: not required per SQW			Static Water Level: 13.6' TOC		Date: 9-21-06	
GEOPHYSICAL LOGGING						
Sondes (type)	Interval	Date	Sondes (type)	Interval	Date	
NA						
COMPLETED WELL						
Size/Wt./Material	Depth	Thread	Slot Size	Type	Interval	Mesh Size
2" SCH 40 PVC	0 - 10.25	✓	70 ^{µm}	Silica Sand	17.0' - 10.0'	10-20
2" PVC Screen	10.9 - 15.9		0.020-in	Granular Ref.	10.0' - 3.0'	
2" PVC endcap	15.9 - 16.25		NA	Portland Cement	3.0' - 0'	
OTHER ACTIVITIES						
Aquifer Test: NA		Date:	Well Decommission: NA		Yes:	No:
Description:		Description:				
WELL SURVEY DATA (if applicable)						
			Not Yet measured			
			Protective Casing Elevation: at this time			
Washington State Plane Coordinates:			Brass Survey Marker Elevation:			
COMMENTS / REMARKS						
ecology well tag: ALJ-803						
Reported By: Erika Rincon		Title: geologist		Signature: Erika R		Date: 9-21-06

A-6003-658 (04/03)

Figure C.11. Well Construction Summary Report for Well 199-N-153

WELL SUMMARY SHEET		Start Date: 9-19-06	Page 1 of 1
		Finish Date: 9-19-06	
Well ID: C5321		Well Name: 199-N-153	
Location: 100-NR-2 OU N-Springs		Project: NR-2 OU Small Diameter Wells	
Prepared By: Erika Rincon	Date: 11/21/06	Reviewed By: L.D. Walker	Date: 12/7/06
Signature: <i>Erika Rincon</i>		Signature: <i>L.D. Walker</i>	
CONSTRUCTION DATA		GEOLOGIC/HYDROLOGIC DATA	
Description	Diagram	Depth in Feet	Lithologic Description/Groundwater Sample Depths (ft bgs)
Flush-Mount Concrete Surface Seal Portland Cement: 0 - 3.0 ft 2-in I.D. Schedule 40 PVC: Casing: 0 - 10.9 ft Granular Bentonite: 3.0 - 10.0 ft Static Water Level: 13.91 ft bgs (9-21-2006) 2-in I.D. Schedule 40 PVC, 20 Slot (.020-in) Screen: 10.9 - 15.9 ft Primary Filter Pack 10-20 Mesh Colorado Silica Sand: 10.0 - 17.0 ft		0 5 10 15 20 25 30 35 40	BOREHOLE NOT LOGGED 17.0 Total Depth Drilled (9-19-2006)
All depths are in feet below ground surface. Borehole drilled with 5-in O.D. wall casing. All temporary casing removed from ground.			
PVC = Polyvinyl Chloride			

Figure C.12. Well Summary Sheet for Well 199-N-153

WELL CONSTRUCTION SUMMARY REPORT				Start Date: 9-19-06			
				Finish Date: 9-19-06			
				Page 1 of 1			
Well ID: C5322		Well Name: 199-N-154		Approximate Location: 10' NE of 199-N-137			
Project: 100-NR-2 OU small diameter wells				Other Companies: Freestone Environmental Services			
Drilling Company: ProSonic				Geologist(s): Greg Kasza Erika Rincon			
Driller: Aaron Adams		License #: 28317					
TEMPORARY CASING AND DRILL DEPTH			DRILLING METHOD	HOLE DIAMETER (in.) / INTERVAL (ft)			
*Size/Grade/Lbs. Per Ft.	Interval	Shoe O.D./I.D.	Auger:	Diameter _____ From _____ to _____			
5"	0 - 27	5" OD	Cable Tool:	Diameter _____ From _____ to _____			
			Air Rotary:	Diameter _____ From _____ to _____			
			A.R. w/Sonic:	Diameter _____ From _____ to _____			
			Sonic	Diameter 5" From 0 to 27			
				Diameter _____ From _____ to _____			
*Indicate Welded (W) - Flush Joint (FJ) Coupled (C) & Thread Design				Diameter _____ From _____ to _____			
Drilling Fluid: none							
Total Drilled Depth: 27		Hole Dia @ TD: 5"		Total Amt. Of Water Added During Drilling: _____			
Well Straightness Test Results: not required per SOW				Static Water Level: 13.48' TGL Date: 9-21-06			
GEOPHYSICAL LOGGING							
Sondes (type)	Interval	Date	Sondes (type)	Interval	Date		
NA							
COMPLETED WELL							
Size/WL/Material	Depth	Thread	Slot Size	Type	Interval Annular Seal/Filter Pack	Volume	Mesh Size
2" SCH 40 PVC	0 - 24.45	✓	20 ^{NA}	Silica Sand	27.0' - 18.0'		10-20
2" PVC Screen	19.1 - 24.1		0.020 in	Granular bentonite	18.0 - 3.0'		
2" PVC endcap	24.1 - 24.45		NA	Portland cement	3.0 - 0'		
OTHER ACTIVITIES							
Aquifer Test: NA		Date:	Well Decommission: NA		Yes:	No:	Date:
Description:			Description:				
WELL SURVEY DATA (if applicable)							
Washington State Plane Coordinates:			Protective Casing Elevation:				
			Brass Survey Marker Elevation:				
COMMENTS / REMARKS							
ecology well tag: ALJ-802							
Reported By: Erika Rincon		Title: geologist		Signature: Erika Rincon			
				Date: 9-21-06			

A-6003-658 (04/03)

Figure C.13. Well Construction Summary Report for Well 199-N-154

WELL CONSTRUCTION SUMMARY REPORT				Start Date: 9-19-06			
				Finish Date: 9-19-06			
				Page 1 of 1			
Well ID: C5323		Well Name: 199-N-155		Approximate Location: 10' NW of 199-N-137			
Project: 100-NR-200 small diameter wells				Other Companies: Freestone Environmental Services			
Drilling Company: Prosonic				Geologist(s): Greg Kasza Erika Rincon			
Driller: Aaron Adams		License #: 2831T					
TEMPORARY CASING AND DRILL DEPTH			DRILLING METHOD	HOLE DIAMETER (in.) / INTERVAL (ft)			
*Size/Grade/Lbs. Per Ft.	Interval	Shoe O.D./I.D.	Auger:	Diameter _____ From _____ to _____			
5" casing	0 - 17	5" OD	Cable Tool:	Diameter _____ From _____ to _____			
			Air Rotary:	Diameter _____ From _____ to _____			
			A.R. w/Sonic:	Diameter _____ From _____ to _____			
			Sonic	Diameter 5" From 0 to 17			
				Diameter _____ From _____ to _____			
*Indicate Welded (W) - Flush Joint (FJ) Coupled (C) & Thread Design				Diameter _____ From _____ to _____			
			Drilling Fluid: none				
Total Drilled Depth: 17'		Hole Dia @ TD: 5"		Total Amt. Of Water Added During Drilling: _____			
Well Straightness Test Results: Not required per SOW				Static Water Level: 13.98' TD Date: 9-21-06			
GEOPHYSICAL LOGGING							
Sondes (type)	Interval	Date	Sondes (type)	Interval	Date		
NA							
COMPLETED WELL							
Size/WL/Material	Depth	Thread	Slot Size	Type	Interval	Volume	Mesh Size
2" sch 40 PVC	0 - 16.0	✓	20 ^{NA}	Silica Sand	17.0 - 10.0		10-20
2" PVC Screen	11.0 - 16.0		0.020 ^{NA}	Granular Bentonite	10.0 - 3.0		
2" PVC endcap	16.0 - 16.35		NA	Portland Cement	3.0 - 0'		
OTHER ACTIVITIES							
Aquifer Test: NA		Date:	Well Decommission: NA		Yes: No: Date:		
Description:			Description:				
WELL SURVEY DATA (if applicable)							
Washington State Plane Coordinates:			Protective Casing Elevation:				
			Brass Survey Marker Elevation:				
COMMENTS / REMARKS							
ecology well tag: ALJ-809							
Reported By: Erika Rincon		Title: geologist		Signature: Erika Rincon			
				Date: 9-21-06			

A-6003-658 (04/03)

Figure C.15. Well Construction Summary Report for Well 199-N-155

WELL SUMMARY SHEET		Start Date: 9-19-06	Page 1 of 1
		Finish Date: 9-19-06	
Well ID: C5323		Well Name: 199-N-155	
Location: 100-NR-2 OU N-Springs		Project: NR-2 OU Small Diameter Wells	
Prepared By: Erika Rincon	Date: 11/21/06	Reviewed By: L.D. Walker	Date: 12/7/06
Signature: <i>Erika Rincon</i>		Signature: <i>L.D. Walker</i>	
CONSTRUCTION DATA		GEOLOGIC/HYDROLOGIC DATA	
Description	Diagram	Depth in Feet	Lithologic Description/Groundwater Sample Depths (ft bgs)
Flush-Mount Concrete Surface Seal Portland Cement: 0 - 3.0 ft 2-in I.D. Schedule 40 PVC Casing: 0 - 11.0 ft Granular Bentonite: 3.0 - 10.0 ft Static Water Level: 14.28 ft bgs (9-21-2006) 2-in I.D. Schedule 40 PVC, 20 Slot (.020-in) Screen: 11.0 - 16.0 ft Primary Filter Pack 10-20 Mesh Colorado Silica Sand: 10.0 - 17.0 ft		0 5 10 15 20 25 30 35 40	BOREHOLE NOT LOGGED 17.0 Total Depth Drilled (9-19-2006)
All depths are in feet below ground surface. Borehole drilled with 5-in O.D. wall casing. All temporary casing removed from ground.			
PVC = Polyvinyl Chloride			

Figure C.16. Well Summary Sheet for Well 199-N-155

WELL CONSTRUCTION SUMMARY REPORT				Start Date: 9-18-06			
				Finish Date: 9-18-06			
				Page 1 of 1			
Well ID: C5324		Well Name: 199-N-156		Approximate Location: 10' NW of 199-N-07			
Project: NR 200 Small Diameter Wells			Other Companies: FROSTBONE ENVIRONMENTAL SERVICES				
Drilling Company: PZO SONIC			Geologist(s): GORDA KASZA, ERINA RINCON				
Driller: AARON ADAMS		License #:					
TEMPORARY CASING AND DRILL DEPTH			DRILLING METHOD		HOLE DIAMETER (in.) / INTERVAL (ft)		
*Size/Grade/Lbs. Per Ft.	Interval	Shoe O.D./I.D.	Auger:	Diameter _____ From _____ to _____			
5"	0 - 27	5 5/8"	Cable Tool:	Diameter _____ From _____ to _____			
			Air Rotary:	Diameter _____ From _____ to _____			
			A.R. w/Sonic:	Diameter _____ From _____ to _____			
			Sonic	Diameter 5" From 0 to 27-0			
				Diameter _____ From _____ to _____			
				Diameter _____ From _____ to _____			
*Indicate Welded (W) - Flush Joint (FJ) Coupled (C) & Thread Design				Diameter _____ From _____ to _____			
			Drilling Fluid: None				
Total Drilled Depth: 27-0		Hole Dia @ TD: 5"		Total Amt. Of Water Added During Drilling: _____			
Well Straightness Test Results: Not Run (per SOL)			Static Water Level: 13.71' TOC		Date: 9-21-06		
GEOPHYSICAL LOGGING							
Sondes (type)	Interval	Date	Sondes (type)	Interval	Date		
NA							
COMPLETED WELL							
Size/Wt./Material	Depth	Thread	Slot Size	Type	Interval Annular Seal/Filter Pack	Volume	Mesh Size
2" SCH 40 PVC	0' - 19.0'	✓	NA	Silica Sand	27.0' - 18.0'		10-20
2" PVC Screen	19.0 - 24.0		0.020-in	Granular bentonite	18.0' - 3.0'		
2" PVC endcap	24.0 - 24.35		NA	Portland Cement	3.0' - 0'		
OTHER ACTIVITIES							
Aquifer Test: NA		Date:	Well Decommission: NA		Yes:	No:	Date:
Description:			Description:				
WELL SURVEY DATA (if applicable) Not Yet Measured							
Washington State Plane Coordinates:				Protective Casing Elevation: at this time			
				Brass Survey Marker Elevation:			
COMMENTS / REMARKS							
ecology well tag: ALJ-810							
Reported By: GORDA L. KASZA		Title: Geologist		Signature: [Signature]		Date: 9-29-06	

A-6003-658 (04/03)

Figure C.17. Well Construction Summary Report for Well 199-N-156

WELL SUMMARY SHEET		Start Date: 9-20-06	Page 1 of 1
		Finish Date: 9-20-06	
Well ID: C5324		Well Name: 199-N-156	
Location: 100-NR-2 OU N-Springs		Project: NR-2 OU Small Diameter Wells	
Prepared By: Erika Rincon	Date: 11/21/06	Reviewed By: <i>L.D. Walker</i>	Date: 12/7/06
Signature: <i>Erika Rincon</i>		Signature: <i>L.D. Walker</i>	
CONSTRUCTION DATA		GEOLOGIC/HYDROLOGIC DATA	
Description	Diagram	Depth in Feet	Lithologic Description/Groundwater Sample Depths (ft bgs)
Flush-Mount Concrete Surface Seal Portland Cement: 0 - 3.0 ft 2-in I.D. Schedule 40 PVC: Casing: 0 - 19.0 ft Granular Bentonite: 3.0 - 18.0 ft Static Water Level: 14.01 ft bgs (9-21-2006) 2-in I.D. Schedule 40 PVC 20 Slot (.020-in) Screen: 19.0 - 24.0 ft Primary Filter Pack 10-20 Mesh Colorado Silica Sand: 18.0 - 27.0 ft		0 5 10 15 20 25 30 35 40 BOREHOLE NOT LOGGED	27.0 Total Depth Drilled (9-18-2006)
All depths are in feet below ground surface. Borehole drilled with 5-in O.D. wall casing. All temporary casing removed from ground.			
PVC = Polyvinyl Chloride			

Figure C.18. Well Summary Sheet for Well 199-N-156

Distribution

<u>No. of</u>		<u>No. of</u>	
<u>Copies</u>		<u>Copies</u>	
21 U.S. Department of Energy		27 Pacific Northwest National Laboratory	
J. P. Hanson	A5-11	B. N. Bjornstad	K6-81
M. Thompson (20)	A6-38	M. D. Freshley	K9-33
		B. G. Fritz	K6-75
8 Fluor Hanford, Inc.		J. S. Fruchter	K6-96
J. V. Borghese	E6-44	T. J. Gilmore	K6-96
R. J. Fabre (5)	E6-44	R. D. Mackley	K6-96
M. J. Hartman	E6-35	D. McFarland	K6-75
S. W. Petersen	E6-35	D. P. Mendoza	K6-81
		D. R. Newcomer	K6-75
		G. W. Patton	K6-75
		R. E. Peterson	K6-75
		M. L. Rockhold	K9-36
		J. E. Szecsody	K3-61
		P. D. Thorne	K6-96
		V. R. Vermeul (5)	K6-96
		M. D. Williams (5)	K6-96
		Y. Xie	K6-81
		Hanford Technical Library (2)	P8-55